Subversion of Rho GTPases by WxxxE Effectors of Attaching and Effacing Pathogens

Richard Bulgin

Imperial College London
Department of Cell and Molecular Biology

This thesis is presented for the degree of Doctor of Philosophy of Imperial College London and the Dipolma of Imperial College London 2009.

The copyright of this thesis rests with the author and no quotation from it or information derived from it maybe published without the prior written consent of the author.

Candidate's Declaration

I, Richard Bulgin, hereby confirm that this thesis represents my own work, and that any external contributions to the research are duely acknowledged.

Richard Bulgin 05/10/2009

Abstract

Enteropathogenic *E. coli* (EPEC), Enterohaemorhagic *E. coli* (EHEC) and *Citrobacter rodentium* are constituent members of the attaching and effacing (A/E) pathogens. The A/E group of bacteria are considered to be extracellular pathogens which form characteristic lesions by intimately adhering to host enterocytes and directing the effacement intestinal brush border. EPEC and EHEC are diarrhoeal pathogens, which are a global health burden in developing and industrialised countries respectively. *Citrobacter rodentium* is a murine pathogen which is an excellent animal model for EPEC and EHEC infection.

EPEC, EHEC and *C. rodentium* conserve a genomic region termed the locus of enterocyte effacement (LEE) which encodes a type 3 secretion system (T3SS), a core set of type 3 secreted effector proteins and the outer membrane adhesin intimin, which are essential for A/E lesion formation. A/E pathogens utilise their T3SSs to translocate dozens of effector proteins directly from the bacteria into host cells. Once translocated these effector proteins modulate a range of eukaryotic signalling pathways including those which regulate the host cell cytoskeleton. An example of this is the T3SS effector Tir which localises to the mammalian plasma membrane, acts as a receptor for intimin and subsequently directs the polymerisation of actin rich pedestals beneath adherent bacteria.

Subversion of the eukaryotic cytoskeleton is a strategy employed by a range of bacterial pathogens. Due to the pivotal role of Rho GTPases in regulating actin dynamics they are commonly targeted by bacterial virulence factors. Recently a family of type 3 secreted effector proteins has been defined based on their homology around an invariant tryptophan and glutamic acid residue separated by three variable amino acids (WxxxE).

In this study we have identified the EspM family of proteins and EspT as novel WxxxE effectors in the A/E pathogens. We demonstrate that the EspM proteins and EspT are translocated into host cells in a T3SS dependent manner. Once translocated, EspM proteins direct the nucleation of actin stress fibres, while EspT drives the formation of lamellipodia and membrane ruffles. Furthermore, we found that the cytoskeletal re-arrangements associated with the WxxxE proteins are dependent on the activation of the small Rho GTPases. EspM proteins activate RhoA while EspT induces the activity of both Rac1 and Cdc42.

A more detailed structural and function analysis of the mechanism by which EspM2 activates RhoA revealed that EspM2 binds RhoA in a concentration dependent manner and subsequently promotes RhoA nucleotide exchange from a GDP to GTP bound form. We also show that EspM2 adopts a structure similar to that of the previously reported *Salmonella* T3SS Rho GEF SopE despite their limited sequence homology. Although the catalytic domain of SopE was not conserved in EspM2 we identified a novel loop which is essential for EspM2 RhoA GEF activity.

As expression of EspT resulted in the formation of membrane ruffles which are often associated with the invasion of bacterial pathogens we investigated whether EspT dependent cytoskeletal remodelling could facilitate the internalisation of the canonically non-invasive A/E pathogens. Interestingly, we found that EPEC strains expressing EspT were significantly more invasive than those which did not and furthermore that this invasion was dependent upon the activity of Rac1 and Wave2. Additionally, we demonstrate that once internalised EPEC is maintained within a vacuole (ECV) and is capable of surviving and replicating intracellularly. We also report that EPEC translocates Tir into the vacuolar membrane where it can nucleate actin in an analogous manner to the formation of pedestals by extracellular bacteria. This is the first time an

intracellular bacterial pathogen has been shown to polymerise actin tails across a vacuolar membrane.

Together the results presented in this study demonstrate that the EspM and EspT families of WxxxE effector proteins are potent modulators of eukaryotic GTPase signalling cascades and as a result convey novel virulence attributes to the A/E pathogen group.

Acknowledgements

I dedicate this thesis to the memory of my mother, Elizabeth Bulgin, who sadly passed away during its completion. Mum, you are always in my thoughts and prayers, you gave me so much love and support without you none of this would have been possible. I love you now and always and miss you every single day.

I would firstly like to acknowledge the people without whom this thesis would not have been possible. Thanks go to my supervisor Professor Gadi Frankel for allowing me the opportunity to work in his laboratory, for mentoring me and for his enthusiasm, guidance and support thoughout my PhD. I would also like to thank Dr. Ana Arbeloa for her day to day teaching, advice and help in all aspects of this thesis. Thanks also go to Valerie Crepin, Cedric Berger, Benoit Raymond and Eric Martinez for their friendship and the assistance and expertise which they provided me in various aspects of this work. Thanks also go to Alex Wong for his camaraderie and his contribution of reagents to help with my project. I would also like to thank Dr. Niki Gounaris and Professor Steve Mathews for their guidance and encouragement in their role as my PhD advisors. Thanks also go to Dr. Francis Girard for his role as lab manager and also for training me to use the SEM. Thanks also to Anthony Fitzgerald for his role as lab manager in the first years of my PhD.

I would also like to thank our collaborators Professors Steve Mathews (Imperial College) and Susan Lea (Oxford University) for their excellent contribution to the structural and functional data presented in this thesis. Thanks also to Professor Gordon Dougan and Dr. David Goulding (Sanger Centre, University of Cambridge) for providing the TEM pictures presented in this thesis. I would also like to thank Jade Chung, Leanna Jones, Silvia Colucci, Clare Harding and Georgina McKenzie for their various contributions to my PhD project. Thanks also go to Professors David Holden, Mark Jepsom, Mark Stevens, Chihiro Sasakawa, Laura Machesky and Dr. Rey Carabeo for providing various strains, plasmids and antibodies.

I would also like to thank all past and present members of the Frankel lab and first floor CMMI for their hospitality, help, support and friendship over the years.

Thanks also go to my friends both new and old for all their help and support.

Special thanks to my girlfriend Cordula, for her love, support, encouragement and interest both inside and outside the lab. Without you this thesis would not have been possible.

Huge thanks also to my parents, Elizabeth and Donald for their support, encouragement, belief, love and for providing me the basis to undertake this PhD. Thanks also to my sister Nicola and her husband Allan for all their support and friendship. Thanks also to my late Papi for his encourangement and love and to whom I can finally say “I am now a doctor”.

Finally I would like to thank the Wellcome trust and their committee at Imperial College for the financial support throughout this PhD and for affording me the opportunity to be a part of their programme.

Table of Contents

CANDIDATE'S DECLARATION **2**

ABSTRACT **3**

ACKNOWLEDGEMENTS **6**

TABLE OF CONTENTS **7**

LIST OF FIGURES **11**

LIST OF TABLES **12**

ABBREVIATIONS **13**

CHAPTER 1 - INTRODUCTION **15**

1.0 Escherichia coli 16

1.1. Intestinal Pathogenic E.coli (InPEC) 16

1.1.1 Enteroinvasive E.coli (EIEC) 17

1.1.2 Enteroaggregative E.coli (EAEC) and Diffusely Adhering E.coli (DAEC) 17

1.1.4 Enterotoxigenic E.coli (ETEC) 18

1.1.5 Enteropathogenic E.coli (EPEC), Enterohemorrhagic E.coli (EHEC): Attaching and Effacing Pathogens 19

1.2 Bacterial Secretion Systems 23

1.2.1 The General Secretory Pathway 23

1.2.2 The Chaperone Usher Pathway. 25

1.2.3 Type 2 Secretion System (T2SS) 26

1.2.4 Type 4 secretion systems (T4SS) 27

1.2.5 Type 5 secretion (T5S) 27

1.2.6 Type 1 Secretion System (T1SS). 28

1.2.7 Type 6 Secretion Systems (T6SS) 29

1.2.8 Type 3 Secretion Systems (T3SS) 29

1.3 The A/E pathogen T3SS and LEE Pathogenicity Island. 31

1.4 A/E Lesion and Pedestal Formation 34

1.5 Subversion of Eukaryotic Signalling by A/E Pathogen Effectors 36

1.6 The Actin Cytoskeleton 39

1.6.1 Actin nucleators 40

1.6.2 Actin recycling factors 44

1.6.3 Elongation factors 44

1.7 Rho GTPases 46

1.8 Regulation of Rho GTPases 47

1.8.1 GEFs 47
1.8.2 GAPs 49
1.8.3 GDIs and GDFs 50
1.9 RhoA, Rac1 and Cdc42 51
1.9.1 RhoA 52
1.9.2 Rac1 53
1.9.3 Cdc42 54
1.10 Bacterial Virulence and Rho GTPases 55
1.10.1 Bacterial Enzymes which Chemically Modify Rho GTPases 56
1.10.2 Bacterial Mimics of Host Rho GTPase Regulatory Factors 58
1.10.3 Bacterial Factors which Indirectly Modulate GTPase Activity 59
1.11 The WxxxE Family of Effectors. 60
1.11.1Map 62
1.11.2 TrcA 63
1.11.3 IpgB1 63
1.11.4 IpgB2 64
1.11.5 SifA 64
1.11. 6 SifB 65
1.12 The EspM Family of Effectors and EspT. 66
1.13 Aims 66

CHAPTER 2 – EXPERIMENTAL PROCEDURES 67
2.0 Bacteria Strains 68
2.1 Bioinformatics 68
2.2 Constructs and Cloning 69
2.3 Site Directed Mutagenesis 70
2.4 Cell Culture 70
2.5 In Vitro Infections 71
2.6 β Lactamase (TEM) T3SS Dependent Translocation Assay 71
2.7 Immunofluorescence Staining and Microscopy 72
2.8 Differential Staining 73
2.9 Gentamycin Protection Invasion Assay 74
2.10 Confocal Microscopy 74
2.11 Scanning Electron Microscopy (SEM) 74
2.12 Transmission Electron Microscopy (TEM) 75
2.13 Transfection 76
2.14 siRNA 76
2.15 Pharmacology 77
2.16 GTP Activation GST Pulldown Assays 77
2.17 Detection of Cofilin Phosphorylation 78
2.18 Preparation of Recombinant Proteins 79
2.19 Surface Plasmon Resonance 80
2.19 Guanine nucleotide exchange analysis 81
2.20 NMR sample preparation and backbone assignment of $EspM2^{29-196}$ 81
2.21 NMR titration of RhoA against $EspM2^{29-196}$ 82
2.22 Screening of Clinical Isolates 82

CHAPTER 3: THE ESPM FAMILY OF PROTEINS ARE WXXXE EFFECTORS WITH RHOA GUANINE NUCLEOTIDE EXCHANGE FACTOR ACTIVITY..... 90
3.1 Identification of Novel IpgB2-Like WxxxE Effectors in the A/E {athogen Group. 91
3.2 Genomic Context of the EspM Effectors..... 93
3.3 The EspM Effectors are Translocated into host Cells in a T3SS Dependent Manner..... 94
3.4 The EspM Effectors Trigger Formation of Stress Fibres with Subtly Different Architectures..... 95
3.5 The Effect of Site Directed Mutagenesis of the WxxxE motif of EspM2 and EspM3..... 98
3.6 Stress Fibre Induction by EspM2 and EspM3 is Inhibited by Expression of a RhoA Dominant Negative. 100
3.7 EspM2 and EspM3 Activate RhoA to Induce Stress Fibre Formation..... 102
3.8 Stress Fibres Induced by EspM2 and EspM3 are ROCK-Dependent..... 103
3.9 EspM2 and EspM3 Induce an Increase in the level of Phospho-Cofilin..... 104
3.10 EspM2 Binds RhoA..... 105
3.11 EspM2 is a Guanine Exchange Factor for RhoA..... 108
3.12 Mapping the EspM2 Interface of the EspM2-RhoA Complex..... 111
3.13 Site Directed Mutagenesis of the EspM2 Catalytic Loop..... 114
3.14 Distribution of EspM in EPEC and EHEC Strains..... 116
3.15 Discussion..... 120

CHAPTER 4 - ESPT IS A NOVEL WXXXE EFFECTOR WHICH ACTIVATES RAC1 AND CDC42..... 126
4.1 Identification of the Novel WxxxE Effector EspT..... 127
4.2 EspT is Translocated into Host Cells in a T3SS Dependent Manner..... 128
4.3 EspT Induces Formation of Lamellipodia and Membrane Ruffles on Swiss 3T3 and HeLa Cells Respectively..... 129
4.4 Ultrastructure Analysis of the EspT-Induced Membrane Protrusions..... 131
4.5 Ectopic Expression of EspT Results in Characteristic Actin Cytoskeletal Reorganisations 133
4.6 EspT Triggered Lamellipodia Formation is Inhibited by Dominant Negative Rac1 and Cdc42. 134
4.7 EspT Activates Rac1 and Cdc42 to Trigger Formation of Lamellipodia and Membrane Ruffles..... 137
4.8 Ectopic Expression of ELMO in Swiss 3T3 Cells Infected with E2348/69 Expressing EspT Causes a Shift from Lamellipodia to Membrane Ruffles..... 139
4.9 EspT Induced Cytoskeletal Rearrangements are Independent of ELMO or Dock180 Activity. 141
4.10 EspT Triggered Lamellipodia are Not Inhibited by Agonists of Canonical Rac1 Activation Signalling Pathways..... 143
4.11 EspT Induces the Phosphorylation of Cofilin..... 145
4.12 Distribution of espT Among Clinical EPEC and EHEC Strains..... 146
4.13 Discussion..... 149

CHAPTER 5 - ESPT IS A NOVEL A/E PATHOGEN INVASIN..... 153
5.1 EspT-Induced Membrane Ruffles Surround Adherent Bacteria..... 154
5.2 EspT Dependent Lamellipodia Formation is Independent of N-WASP..... 157

5.3 Wave2 and Abi1 are Localized to Membrane Ruffles and Lamellipodia Induced by EspT 159
5.4 IRSp53 is Recruited to EspT Induced Membrane Ruffles but not Lamellipodia 160
5.5 Wave2 is Essential for EspT-Induced Membrane Remodeling 161
5.6 Wave2 WHD and VCA Domains are Required for EspT-Induced Membrane Remodeling 163
5.7 EspT Facilitates EPEC Invasion 165
5.8 The Conserved WxxxE Motif is Essential for EspT Mediated Membrane Remodelling and Invasion. 168
5.9 Ectopic Expression of EspT Induces Membrane Ruffles which Facilitate the Invasion of T3SS Null Mutants. 170
5.10 Rac1 and Wave2 are Essential for EspT Mediated Bacterial Cell Invasion 171
5.11 Internalized EPEC Bacteria are Enclosed Within a Vacuole 173
5.12 The ECV Matures to Become Lamp1 Positive at Late Time Points of Infection 175
5.13 Internalized EPEC are Associated with Actin Comets 177
5.14 Internalized EPEC Bacteria Incorporate Tir into the Vacuolar Membrane which Nucleates Intracellular Actin Pedestals. 178
5.15 Intracellular Pedestal Formation is Tir Dependent. 180
5.16 Internalised EPEC Bacteria can Replicate within Host Cells. 181
5.17 Discussion 183

CHAPTER 6 – GENERAL DISCUSSION 188
6.1 Attaching and Effacing Pathogens and the Eukaryotic Cytoskeleton 189
6.2 Bacterial Pathogens and GTPases 190
6.3 Evolution of the Mechanism of WxxxE Effectors 191
6.4 Other Factors which Contribute to WxxxE Mediated Activation of GTPases 194
6.5 WxxxE Effectors Contribution to Pathogenesis 195
6.6 EPEC as an Intracellular Pathogen 196
6.7 The distribution of EspM and EspT proteins 200
6.8 Concluding Remarks 201
References 203

APPENDIX 1 – PUBLICATIONS 221

List of Figures

Figure 1.1 Virulence strategies of the Intestinal Pathogenic *E.coli* Pathovars (InPEC).. 22
Figure 1.2 Gram Negative Bacterial secretion systems (T1SS-T6SS). 31
Figure 1.3 A. The LEE operon anf T3SS of A/E pathogens. 33
Figure 1.4 A/E pathogen mediated pedestal and lesion formation.. 35
Figure 1.5 Mechanism of actin pedestal formation by EPEC, EHEC and a sub group of atypical EPEC strains.. 36
Figure 1.6 T3SS effector protein distribution. 37
Figure 1.7 Factors involved in the assembly and turnover of the actin cytoskeleton.. 45
Figure 1.6 The Regulatory Cycle of Rho GTPases. 51
Figure 1.7 Regulation of the host cell cytoskeleton by RhoA, Rac1 and Cdc42. 55
Figure 1.8 Alignment of the WxxxE region of the founding members of the WxxxE family of effectors. 61
Figure 3.1 Identification of novel IpgB2 like WxxxE Effectors in the A/E Pathogen Group. 92
Figure 3.2 Genomic context of EspM family members. 94
Figure 3.3 EspM2 and EspM3 are translocated into host cells in a T3SS dependent manner. 95
Figure 3.4 IpgB2 like A/E effectors induce formation of actin stress fibres in Swiss 3T3 cells upon infection.. 97
Figure 3.5 Site directed mutagenesis on the WxxxE motif of EspM2 and EspM3 99
Figure 3.6 EspM2 and EspM3 dependent stress fibre formation is dependent of the small GTPase RhoA. 101
Figure 3.7 EspM2 and EspM3 activate RhoA.. 102
Figure 3.8. EspM2 and EspM3 trigger the RhoA-ROCK pathway.. 103
Figure 3.9 EspM2 and EspM3 induce an increase in cofilin phosphorylation.. 104
Figure 3.10 EspM2 binds to RhoA.. 107
Figure 3.11 EspM2 is a guanine exchange factor for RhoA. 110
Figure 3.12 Model of $EspM2^{29-196}$ and the $EspM2^{29-196}$-RhoA complex. 113
Figure 3.13 Site directed mutagenesis of the EspM2 catalytic loop. 115
Table 3.14 Distribution of *espM* among 151 non-O157 clinical EHEC strains. 117
Table 3.16 Distribution of *espM* among 602 aEPEC strains. 118
Figure 4.1 Phylogeny of the novel WxxxE effector EspT. 127
Figure 4.2 EspT is translocated into host cells in a T3SS dependent manner. 128
Figure 4.3 EspT induces lamellipodia and membrane ruffles on Swiss 3T3 and HeLa cells respectively 130
Figure 4.4 Ultrastructure analysis of the EspT-Induced membrane protrusions. . 132
Figure 4.5 Ectopic expression of EspT and EspM2 induces characteristic cytoskeletal rearrangement in Swiss 3T3 cells. 134
Figure 4.6 EspT-induced cytoskeletal rearrangements are dependent on Rac1 and Cdc42. 136
Figure 4.7 EspT activates Rac1 and Cdc42. 138
Figure 4.8 Expression of ELMO1 causes a shift from lamellipodia to membrane ruffles. 140
Figure 4.9 EspT induced cytoskeletal rearrangements are independent of ELMO or Dock180 activity. 142
Figure 4.10 EspT triggered lamellipodia are not inhibited by agonists of canonical Rac1 activation signalling pathways.. 144
Figure 4.11 EspT induces a phosphorylation of cofilin. 146

Figure 4.12 Prevalence and sequence of EspT in Clinical EPEC and EHEC Isolates. 148
Figure 5.1 EspT-induced membrane ruffles surround adherent bacteria..... 156
Figure 5.2 EspT dependent formation of lamellipodia is independent of N-WASP.. 158
Figure 5.3 Wave2 and Abi1 are localized to membrane ruffles and lamellipodia induced by ectopically expressed EspT. 160
Figure 5.4 IRSp53 is enriched in membrane ruffles induced by EspT. 161
Figure 5.5 Wave2 is essential for EspT induced membrane remodeling and invasion. 162
Figure 5.6 Wave2 WHD and VCA domains are needed for EspT membrane remodeling. 164
Figure 5.7. EspT-dependent actin remodeling facilitates bacterial invasion of epithelial cells. 167
Figure 5.8 EspT mediated membrane remodeling and invasion is dependent on the conserved WxxxE motif. 169
Figure 5.9 Ectopic expression of EspT can facilitate invasion of epithelial cells by a T3SS null mutant. 170
Figure 5.10 Rac1 and Wave2 are essential for EspT-mediated bacterial invasion. 172
Figure 5.11 Internalized EPEC bacteria are enclosed within a vacuole. 174
Figure 5.12 The ECV matures to become Lamp1 positive at late time points of infection.....176
Figure 5.13 Intracellular EPEC are associated with actin comets. 177
Figure 5.14 Internalized EPEC bacteria incorporate Tir into the vacuolar membrane which nucleates intracellular actin pedestals.. 179
Figure 5.15 Tir is essential for the formation of intracellular pedestals. 180
Figure 5.16 Internalized A/E pathogens survive and replicate in epithelial cells. 182

List of Tables

Table 1 Primers used in this study 83
Table 2 Plasmids used in this study 85
Table 3 Strains used in this study 88
Table 4 Primary antibodies used in this study 89
Table 5 Secondary antibodies used in this study 89

Abbreviations

actin related proteins 2/3: Arp2/3
adenosine 5' mono-phosphate: AMP
adenosine triposphatase: ATPase
adhesins involved in diffuse adherence: AIDA
aggregative adherence fimbriae: AAF
ATP Binding Cassette: ABC
attaching and effacing: A/E
atypical EPEC: aEPEC
bovine serum albumin: BSA
bundle forming pili: BFP
Cdc42 and Rac1 interacting domain: CRIB
c-Jun N terminal Kinase: JNK
Cytotoxic necrotizing factor: CNF
Dbl Homology: DH
Dermonecrotizing toxin: DNT
diffuse adherent *E. coli*: DAEC
Dock Homology Region: DHR
Endosome Antigen 1: EEA1
Engulfment and Motility protein: ELMO
enteroaggregative *E.coli*: EAEC
enterohemorrhagic *E.coli*: EHEC
enteroinvasive *E.coli*: EIEC
enteropathogenic *E.coli*: EPEC
enterotoxigenic *E.coli*: ETEC
EPEC adherence factor: EAF
EPEC containing vacuole: ECV
Extraintestinal Pathogenic *E.coli*: ExPEC
ezrin-radixin-moesin: ERM
filamentous actin: F-actin
filamentous T3SS: FT3SS
Fluorescence Actin Staining: FAS
G Protein Coupled Receptors: GPCR
GDI displacement factor: GDF
general secretory pathway: Sec
global parallel stress fibres: GP-SF
GTPase Activating Proteins: GAP
Guanine Exchange Factors: GEF
Haemolytic Uremic Syndrome: HUS
haemorrhagic colitis: HC
Inhibitory Guanine nucleotide Dissociation Inhibitors: GDI
Intestinal Pathogenic *E.coli*: InPEC
IRSp53/MIM homology domain: IMD
Leiomodin: Lmod
LIM kinase: LIMK
local parallel stress fibres: LP-SF
local radial stress fibres: LR-SF
Locus of Enterocyte Effacement: LEE
Luria–Bertani: LB
magnesium: Mg^{2+}
mitochondrial associated protein: Map
Mitochondrial Rho: Miro
Myosin Binding Subunit: MBS
Myosin Light Chain: MLC
Nictotinamide Adenine Di-nucleotide: NAD
non sorbitol fermenting: nsf
Nuclear Magnetic Resonance: NMR
nucleation promoting factors: NPF
P21 activating kinases: PAK
Paraformaldehyde: PFA
Phosphoinositide 3-kinase: PI3K
plasmid encoded toxin: pet
proline rich region: PRR
PSD-95/Sap90, Disc large and Zonal occludin1/ZO1: PDZ
pullulanase: PulA
Rac1 binding motif: RBM
Ras related C3 substrate 1: Rac1
Rho coiled coil p160 serine/threonine kinase: ROCK
Salmonella Containing Vacuole: SCV
Scanning Electron Microscopy: SEM
Shiga toxin: Stx
Shigella enterotoxin 1: shET1
SifA and Kinesin Interacting Protein (SKIP): SKIP
sorbitol fermenting: sf
surface plasmon resonance: SPR
translocated intimin receptor: Tir
transmission electron microscopy: TEM
Twin Arginine transport system: Tat
Type 1 secretion system: T1SS
Type 2 secretion system: T2SS
Type 3 secretion system: T3SS
Type 4 secretion systems: T4SS
Type 5 secretion system: T5SS

Type 6 secretion system: T6SS
typical EPEC: tEPEC
Uropathogenic *E. coli*: UPEC,
Vacuolar ATPase: VATPase
WASP-like Verprolin-homologous protein 2: Wave2
Wave homology domain: WHD
Wiskott-Aldrich syndrome protein: N-WASP

Chapter 1 - Introduction

1.0 Escherichia coli

Escherichia coli is the most abundant facultative anaerobic Gram negative bacterial commensal of the intestinal microflora. For more than half a century after its discovery, in 1885, *E. coli* was considered to be avirulent. However, accumulating evidence linking the bacterium with infection, particularly of the gastro-intestinal tract, led to the realisation that *E. coli* can cause disease. As well as diarrhoeal disease caused by Intestinal Pathogenic *E.coli* (InPEC) other pathogenic *E. coli* strains categorised as Extraintestinal Pathogenic *E.coli* (ExPEC) are associated with other conditions including urinary tract infections, neonatal meningitis and septicaemia (Kaper et al., 2004; Smith et al., 2007). Currently, InPEC are recognised as a major cause of diarrhoeal infections worldwide and is considered to be a serious public health problem particularly in developing nations (Chen and Frankel 2005). Pathogenic *E. coli* were first grouped according to the serology of their surface characteristics in a method described by Kauffmann in 1947 (Kauffmann, 1947). A modified version of the Kauffmann's serological approach is still used today to classify *E. coli* isolates based on their somatic (O), flagellar (H) and Capsular (K) antigens (Orskov et al., 1984). InPEC isolates are not normally encapsulated and are therefore grouped based on their somatic and flagellar antigens (Nataro and Kaper, 1998).

1.1. Intestinal Pathogenic E.coli (InPEC)

At present there are six pathotypes of diarrhoeagenic InPEC which are recognised and grouped based on their virulence attributes and genetic features (Figure 1). Currently accepted groups are: enteroinvasive *E.coli* (EIEC), enteroaggregative *E.coli* (EAEC), diffuse adherent *E. coli* (DAEC), enterotoxigenic *E.coli* (ETEC) and enteropathogenic *E.coli* (EPEC), enterohemorrhagic *E.coli* (EHEC).

1.1.1 Enteroinvasive E.coli (EIEC)

The EIEC pathovar is currently comprised of fourteen distinct O antigens including O112ac, O124, and O152 which are identical to *Shigella boydii* and *Shigella dysenteriae* (Reviewed in (Parsot, 2005)). EIEC infection is most commonly associated with the onset of dysentery in a very similar manner to *Shigella* species (Kotloff et al., 1999). Both EIEC and *Shigella* harbour a 220 kb plasmid referred to generally as pINV which is the primary locus required to bring about bacterial invasion of non-phagocytic cells. The pINV plasmid encodes a type 3 secretion system (T3SS), gene regulators, chaperones and around twenty four effectors proteins which are translocated into host cells. pINV also encodes the outer membrane protein IcsA which is involved in actin based intracellular movement (Reviewed in (Parsot, 2005)). EIEC and *Shigella* species share an almost identical virulence strategy centred on the invasion of host cells and subsequent cell to cell spread resulting in severe watery diarrhoea. Colonisation of the gut by *Shigella* and EIEC species is characterised by destruction of the host colonic epithelium and a subsequent inflammatory response (Schroeder and Hilbi, 2008). Until now, EIEC is the only InPEC pathovar for which invasion of the host cell is the main virulence strategy; the rest of the pathovars are considered as extracellular.

1.1.2 Enteroaggregative E.coli (EAEC) and Diffusely Adhering E.coli (DAEC)

The EAEC and DAEC pathotypes are defined on the basis of their adherence patterns. EAEC serogroups commonly include O3, O7, O15, O44, O77, O86, O111, O126 and O127 (Stenutz et al., 2006). EAEC is most commonly associated with infantile diarrhoea and is one of the most prevalent pathogens associated with adult traveller's diarrhoea (Araujo et al., 2007; Huang et al., 2008) . EAEC pathogenesis is resultant from the formation of a mucoid biofilm on the intestinal epithelium and the delivery of bacterial toxins into host cells. EAEC aggregation and biofilm

formation is dependent on the aggregative adherence fimbriae (AAF) or the hdaA pilin which are both regulated by the AggR regulatory protein (Boisen et al., 2008; Farfan et al., 2008). Another secreted protein called dispersin is associated with a relief of the aggregative phenotype and is thought to allow dispersal of the EAEC aggregates and infection of new intestinal sites (Velarde et al., 2007). So far three toxins have been identified in EAEC; *Shigella* enterotoxin 1 (shET1), a serine protease plasmid encoded toxin (pet) and the heat stable toxin EAST (reviewed in (Flores and Okhuysen, 2009))

The DAEC pathotype is defined by a diffuse pattern of bacteria adherence on cultured epithelial cells (Nataro and Kaper, 1998). The DAEC are a heterogeneous group and are divided into two sub groups; the first class of DAEC strains harbour Afa/Dr adhesins (Afa/DrDAEC) and are primarily associated with urinary tract infections and sometimes with gastrointestinal disease (Le Bouguenec and Servin, 2006). The second class of DAEC express adhesins involved in diffuse adherence (AIDA) and share a variety of virulence factors with the intestinal pathogens EPEC and EHEC (Le Bouguenec and Servin, 2006).

1.1.4 Enterotoxigenic E.coli (ETEC)

ETEC is associated with infantile and traveller's diarrhoea particularly in regions associated with poor sanitation (Okoh and Osode, 2008). In a similar manner to EAEC and DAEC, ETEC colonises the gut via adhering to enterocytes using specialised outer membrane colonisation factors. To date more than 20 ETEC colonisation factors have been identified (reviewed in (Turner et al., 2006)). Once ETEC has established a tight adherence to host cells it secretes one or more toxins which have a cytopathic effect on host cells. These toxins include heat stable STa and STb enterotoxins which bind host receptors and synergistically mediate the influx of fluid into the gut by modifying host cell calcium homeostasis (Turner et al., 2006). ETEC also

elaborates heat liable toxins which are members of the A_1B_5 family of toxins, once secreted the B subunits bind the host cell membrane to direct the internalisation of the A subunit. Once in the cytoplasm the A subunit modifies host cell adenylate cyclase signalling (Nataro and Kaper, 1998). ETEC also secretes various other toxigenic factors including the EatA serine protease autotransporter, the CylA pore forming toxin and EAST (reviewed in (Turner et al., 2006)).

1.1.5 Enteropathogenic E.coli (EPEC), Enterohemorrhagic E.coli (EHEC): Attaching and Effacing Pathogens

EPEC, EHEC and the mouse pathogen *Citrobacter rodentium* comprise a group of closely related extracellular diarrhoeal pathogens which are characterised by their ability to colonise the gut epithelium by intimately adhering to enterocytes and producing distinctive attaching and effacing (A/E) lesions (Knutton et al., 1987). A/E lesions are characterised by disruption of the local intestinal brush border and distension of the microvili (Figure 1.3). A pathogenicity island referred to as the Locus of Enterocyte Effacement (LEE) is the genetic determinant required in order to induce the formation of A/E lesions (McDaniel et al., 1995). The LEE island encodes the functional and structural components of a type 3 secretion system (T3SS), associated chaperones and seven T3SS effector proteins which are translocated into host cells (McDaniel et al., 1995).

EHEC is comprised of a range of serogroups including O26, O55, O111 and O145, however the most prevalent and virulent EHEC serotype is O157. EHEC O157s are often segregated based on their ability to ferment sorbitol, conventionally non sorbitol fermenting (nsf) O157 EHEC were associated with severe disease however in recent times there has been an increase in the prevalence of infections attributed to sorbitol fermenting (sf) O157 serovars (Eklund et al., 2006). EHEC strains carry two isoforms of a potent phage encoded Shiga toxin (Stx1 and Stx2)

similar to that of *Shigella dysenteriae* (Herold et al., 2004). EHEC is associated with acute gastroenteritis which can progress to more serious conditions such as haemorrhagic colitis (HC) and Haemolytic Uremic Syndrome (HUS), a common cause of acute renal failure in children and the elderly in the developed world (Thorpe, 2004). EHEC is considered to be an important pathogen in developed countries and in 2006 there were 1003 cases of O157:H7 related infections in England and Wales (HPA). Sporadic outbreaks of EHEC are reported worldwide and are normally linked to contaminated bovine products, salads or drinks. The largest outbreak reported to date occurred in Osaka, Japan in 1996 causing 9000 cases and 11 deaths (WHO).

EPEC is also comprised of a variety of serogroups, most commonly, O26, O55, O111, O119, O127 and O142. EPEC strains can be classified as typical EPEC (tEPEC) and atypical EPEC (aEPEC) based on the presence or absence of a large virulence plasmid called EPEC adherence factor (EAF), respectively (Kaper et al., 2004). The EAF plasmid encodes the components necessary for the assembly of long bundle forming pili (BFP) which promote the aggregation of EPEC bacteria into tight microcolonies (Giron et al., 1991). tEPEC are divided in to two distinct evolutionary lineages: EPEC1 and EPEC2. EPEC1 is characterised by expression of the flagellar antigens H6 or H34 (Whittmen et al 1993) and encodes intimin subtype α (Adu-Bobie 1998). EPEC2 has the H2 or H- flagellar antigens (Whittmen et al 1993) and the β subtype of intimin (Adu-Bobie 1998). The archetypal stain of EPEC1 is E2348/69 an O127:H6 strain which has a very compact genome only encoding a fraction of the virulence genes associated with EPEC2 strains such as B171 O111:NM. Infectious diarrhoea is one of the world's leading causes of morbidity and mortality with an estimated 2 million deaths attributed to it annually (WHO). EPEC is the single most important bacterial pathogen contributing to infantile mortality in the

developing world (Chen and Frankel 2005). EPEC infections are most commonly linked to contaminated water supplies and poor sanitation.

Citrobacter rodentium is naturally occurring mouse pathogen which isgenetically highly similar to EPEC and EHEC strains and is the aetiological agent of transmissible murine colonic hyperplasia. *Citrobacter rodentium* shares many of the virulence factors previously described for EPEC and EHEC stains including the LEE pathogencity island and associated T3SS alond with an extensive repetiore of T3SS effectors (Petty *et al* 2009). Following ingestion *C. rodentium* colonizes the intestines of mice, residing predominantly in the cecum and colon (Wiles *et al* 2004) where in some inbred strains it can cause serious morbidity and mortality. Infection of the mouse intestinal tract with *C.rodentium* results in the formation of A/E lesions with associated distension of microvili and disruption of the host cell actin cytoskeleton indistinguishable from that of EPEC and EHEC (Mundy *et al* 2002). Due to its high degree of similarity to EPEC and EHEC it is used as a model *in vivo* system to study A/E pathogens.

The pathogenesis of the A/E pathogen group is reliant upon a functional T3SS and the associated repertoire of effector proteins.

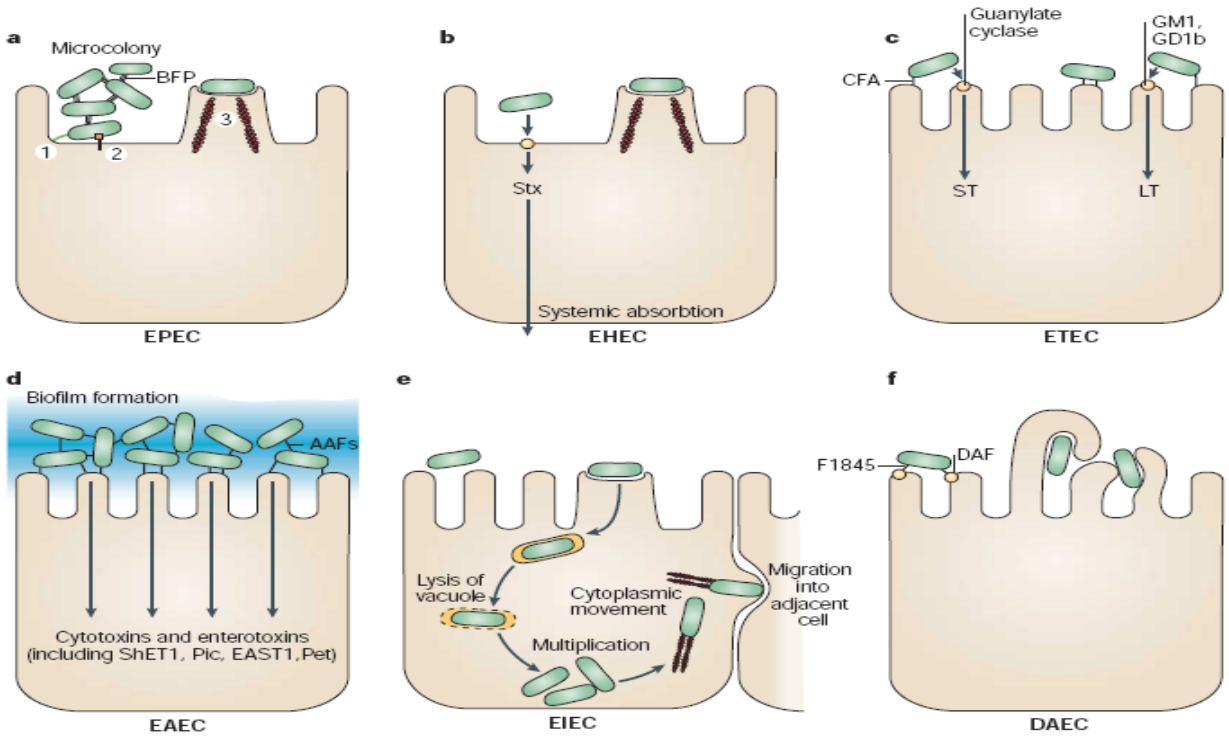


Figure 1.1 Virulence strategies of the Intestinal Pathogenic *E.coli* Pathovars (InPEC). Each InPEC pathovar has unique virulence attributes which contribute to their interaction with host cells. A. EPEC express bundle forming pili (BFP) which contribute to initial host association and EPEC microcolony formation (1). EPEC mediates the effacement of host cell microvili and utilises the T3SS in conjunction with the outer membrane adhesin intimin to establish an intimate adherence to host cells (2). EPEC then continues to secrete effector proteins through the T3SS which subvert a variety of host cell processes (3). B. EHEC colonisation of the host enterocyte is similar to that of EPEC except that EHEC strains do not posses BFP and so do not form microcolonies. In addition to translocating T3SS effector proteins EHEC also secretes a potent Shiga toxin which mediates further cytopathic effects. C. Adhesion of ETEC stains to host enterocytes is mediated by outer membrane colonisation factors. Once adhered, ETEC strains elaborate a range of toxins which subvert host cell calcium homeostasis as well as other processes. D. EAEC colonise the host gut epithelium by forming a mucoid biofilm by virtue of their Aggregative Adherence Factors (AAF). Once a microcolony has been established EAEC elaborate a range of enterotoxins including ShET1, Pic, Pet and EAST. E. EIEC unlike the other InPEC pathovars does not remain extracellular. EIEC encodes a virulence plasmid known as pINV which codes for a T3SS and effector proteins which mediate bacterial invasion of host cells. Once internalised EIEC quickly escape from their vacuole, multiply in the cytoplasm and use the specialised outer membrane protein IcsA to mediate actin dependent motility and subsequent cell to cell spread. F. DAEC utilise the AIDA adhesin factor to adhere to host enterocytes in a diffuse pattern and induce the formation of finger like extensions from the host cell membrane which wrap around the adherent bacteria. Reproduced from (Kaper et al., 2004).

1.2 Bacterial Secretion Systems

Bacteria are often subdivided into the categories Gram positive or negative based on characteristics of their cell envelope. Gram positive bacteria posses a single plasma membrane which is linked via lipoteichoic acids to a thick peptidoglycan layer. Protein transport in Gram positive bacteria is a relatively simple process as the substrates only have to traverse one membrane. Gram negative bacteria are comprised of an inner cytosolic membrane and an outer membrane enriched with lipopolysaccharides separated by a periplasmic space with a thin pedtidoglycan layer. Consequently protein secretion in Gram negative bacteria is a complex process as a secreted substrate which is destined to be incorporated into the outer membrane or secreted into extracellular milieu must first be translocated across the bacterial inner membrane, periplasm and outer membrane. Moreover, some Gram negative bacteria can translocate proteins directly into the cytoplasm of the host cell, and in this case the substrate must also traverse the eukaryotic plasma membrane. Thus Gram negative bacteria have evolved a plethora of specialised transport systems designed to traffic proteins across the inner and outer bacterial membranes, to the extracellular milieu or even directly into host cells. Currently six types of secretion system have been described in Gram negative bacteria and are designated type 1 to 6 (Figure 1.2).

1.2.1 The General Secretory Pathway

The primary system utilised by Gram positive and Gram negative bacteria to translocate proteins across the bacterial inner membrane is the general secretory pathway (Sec) (Driessen and Nouwen, 2008). The unfolded pre-proteins translated by ribosomes are recognised by trigger factor (TF) and or signal recognition particle (SRP) which prevent abberant folding of the pre-potriens prior to secretion via the Sec system. Trigger factor binds nascent polypedtides at the

ribosome independently of an N terminal signal sequence and plays a role in directing the newly synthesised polypedtides to the other chaperones which drive their proper folding (Valent et al., 1995). Proteins which are secereted via the Sec system have an N terminal signal sequences which are regognised by the signal recognition particle (SRP). The interaction of SRP with the nascent secretory proteins directs them to the membrane in a secretion competent state (reviewed in (Luirink et al., 2005)). After translocation of the prtotein across or into the inner membrane the N terminal signal sequence is cleaved to produce the mature protein which is either released into the periplasm or incorporated into the inner bacterial membrane. The Sec system consists of several key elements including a membrane spanning translocase constructed by three integral membrane proteins SecY, SecE and SecG (Brundage et al., 1990) and the multifunctional protein SecA (Economou, 1998). SecA recognises and binds substrates of Sec system and subsequently guides them to the SecYEG translocase. SecA then acts as an ATPase which performs several rounds of ATP binding and hydrolysis associated with conformational shifts which drive the translocation of substrate proteins across the bacterial inner membrane (Economou and Wickner, 1994). In addition to the Sec system, folded proteins can be transported across the bacterial inner membrane via the Twin Arginine transport system (Tat) which is powered via the proton motive force (reviewed in (Natale et al., 2008)).

Once a protein has reached the periplasm it can be sorted into any of three distinct routes (i) The protein can utilise the chaperone usher pathway which is one of the terminal branches of the Sec system. (ii) The protein can be secreted to the extracellular milieu via a complex interaction with components of a type 2 secretion system (T2SS) which constitutes the main terminal branch of the Sec pathway. (iii) The protein may have an auto-transporter activity and may facilitate its own passage across the bacterial outer membrane this is an example of a type 5 secretion system

(T5SS). (reviewed in (Gerlach and Hensel, 2007)). T5SSs can also operate in a two partner system where 1 protein encodes the β barrel domain whilst the other is the secreted passenger (Jacob-Dubuisson et al., 2004).

1.2.2 The Chaperone Usher Pathway.

Following translocation via the secYEG translocase the secreted pilins are bound by a periplasmic chaperone and directed towards an outer membrane usher protein, which allows the translocation of folded proteins through a large central pore. The best characterised example of this chaperone usher system is the assembly of the Uropathogenic *E. coli* (UPEC) type 1 pili. In this system the periplasmic chaperone FimC binds the prepilins FimA,F,G,H in a one to one ratio and prevents premature assembly while directing the immature pilins to the outer membrane usher FimD which acts as both an outer membrane translocase and an assembly platform for the pili (Saulino et al., 2000). Pilus extension and polymerisation is generated via a cycle of donor strand complementation and exchange (Sauer et al., 2004). In donor strand complementation FimC interacts with the newly synthesised prepilins to stabilise them via completing an Immunoglobulin like fold by donating its G1 strand (Thanassi et al., 1998). The FimC and prepilin complex then diffuses to the FimD usher, upon interaction with the exposed N terminus of FimD the chaperone then dissociates and the prepilin is incorporated into the nascent pilus stand and stabilised via an interaction with the previously incorporated prepilins in a process referred to as donor strand exchange (Sauer et al., 1999).

1.2.3 Type 2 Secretion System (T2SS)

Proteins which are secreted via the T2SS first utilise the Sec pathway in order to be translocated to the periplasm. The T2SS is used by Gram negative bacteria to secrete proteins and toxins into the extracellular milieu (reviewed in (Pugsley, 1993)). The T2SS is composed of a complex of inner membrane proteins some of which also contain cytoplasmic domains. The inner membrane components of the T2SS exhibit homology to Type IV pilins so have been labelled as pseudo-pilins. Due to the hydrophobic nature of the T2SS pseudopillins they are often co-translationally incorporated into the membrane via in interaction between their N-terminal signal sequences and the signal recognition particle (SRP). The signal regonition particle of *E. coli* is composed of 4.5S RNA and a polypeptide chain termed Ffh or P48. Upon translation of the psuedopillins the nascent poly peptide chain containg the N terminal signal sequence is bound by Ffh while still associated with the ribosome and subsequently transported to the membrane bound SRP receptor FtsY where it interacts with SecYEG (reviewed in (Luirink et al., 2005)). Once incorporated in or transported across the inner membrane there is speculation that the pseudo-pilins may be able to form a pilus like structure in the periplasm but there is no direct evidence for such an occurrence. Once a protein is translocated to the periplasm it has to fold to its tertiary or even quaternary structure before it is recognised by components of the T2SS (Pugsley, 1993). The outer membrane component of the T2SS is typically composed of a ring like structure consisting of 12-14 oligomerised monomers of a secretin stabilised in a one to one ratio with an outer membrane anchored lipoprotein (Nouwen et al., 1999). Perhaps the best characterised example of T2SS is the secretion of the pullulanase (PulA) by *Klebsiella oxytoca* (Pugsley et al., 1997).

1.2.4 Type 4 secretion systems (T4SS)

Type 4 secretion systems (T4SS) are conserved across a wide range of Gram negative pathogens including *Legionella*, *Helicobacter*, *Brucella* and *Agrobacter.* The T4SS is comprised of around 12 proteins and is capable of transporting proteins as well as DNA (Reviewed in (Li et al., 2005)). The archetypal T4SS is encoded by *Agrobacter tumefaciens* and consists of eleven VirB proteins (VirB1 to VirB11) and VirD4 (Christie et al., 2005). The T4SS forms a multi protein complex which is thought to span both bacterial membranes and the periplasm (Fronzes et al., 2009). The T4SS has three ATPases (VirB4, VirB11 and VirD4 in *Agrobacter*) which are involved in substrate recognition and secretion as well as assembly of the T4SS apparatus (Krall et al., 2002). VirB6, VirB8 and VirB10 are hypothesised to form an inner-membrane pore (Ward et al., 2002). The composition of the outer-membrane complex is yet to be established but may involve VirB7 and VirB9 components (Fronzes et al., 2009). VirB4, VirB7, VirB9 and VirB10 form the minimum complex which is still functional (Harris et al., 2001). Some T4SSs also have pili like extensions, in the case of *Agrobacter* these extensions are composed of the VirB2 and VirB5 subunits (Li et al., 2005). T4SS can traslocate proteins directly from the bacterial cytosol or act as one of the terminal brunches of the Sec system by interacting with substrates in the periplasm (Fronzes et al., 2009).

1.2.5 Type 5 secretion (T5S)

Type 5 secretion is a relatively simple process which is conserved thoughout Gram negative bacteria and is often referred to as autotransportation (Dautin and Bernstein, 2007). Autotransporters are typically large proteins which consist of N terminal passenger domain which is translocated across the bacterial outer membrane by a C terminal transporter domain. Initial transport across the inner membrane is directed by the general secretory pathway

(Brandon et al., 2003). Once the autotransporter reaches the periplasm the transporter domain inserts in the outer-membrane into a β barrel conformation allowing a threading of the passenger domain though the outer-membrane (Reviewed in (Dautin and Bernstein, 2007)). Other type 5 systems referred to as T5cSS contain a trimeric polypeptide where all of the components are involved in constructing the β barrel (Tseng et al., 2009). After translocation through the outer-membrane the passenger domain might be cleaved from the β barrel (Skillman et al., 2005) the mechanism of cleavage is not well conserved between bacterial species. Other T5SSs known as two partner systems rely on two independent polypeptides in order to direct secretion, one protein forms the β barrel while the other carries the passenger domain and is secreted (Jacob-Dubuisson et al., 2004).

1.2.6 Type 1 Secretion System (T1SS).

Type 1 secretion system (T1SS) is composed of a heterotrimeric complex consisting of a cytoplasmic ATPase, a membrane fusion protein and an outer membrane translocator. This secretion system is often referred to as an ABC (ATP Binding Cassette) transporter. The cytoplasmic ATPase provides substrate specificity and hydrolyses ATP in order to power protein translocation, the membrane fusion protein spans the periplasmic space to nullify the requirement for a periplasmic chaperone and the outer membrane protein creates a pore which allows protein secretion (reviewed in (Gerlach and Hensel, 2007)). Perhaps the best characterised example of a T1SS is the secretion of haemolysin by some UPEC strain. The HlyD membrane fusion protein has a large periplasmic domain and a short cytoslolic region linked by one transmembrane helix. Using various truncations of HlyD it was demonstrated that its cytoplasmic region is specifically required to bind the substrate and that this interaction directs the formation of a complex which recruits the outer membrane TolC to induce pore formation

(Balakrishnan et al., 2001). The structure of homotrimeric TolC demonstrated that the outer membrane pore consists of twelve tunnel forming helices which in the closed state form tight ionic interactions resulting in a closed conformation. Disruption of the ionic interaction leads to a relaxation in packing of the helices resulting in an opening of the channel in an iris like manner (Andersen et al., 2002).

1.2.7 Type 6 Secretion Systems (T6SS)

A novel secretion system, known as the type 6 secretion system (T6SS), has recently been described in a variety of bacterial species. The T6SS was first defined based on the identification of a protein homologous to the *Legionella pneumophila* T4SS protein IcmF within clusters of genes which did not share homology to T4SSs (Das and Chaudhuri, 2003). T6SSs commonly consist of between 15 and 25 genes which have been identified based on their contribution to virulence or secretion (Pukatzki et al., 2009). The substrates of the T6SS are poorly defined, only the Hcp and VgrG components have been demonstrated to be secreted in the majority of organisms encoding a T6SS. The remaining proteins encoded within the T6SS clusters are thought to be involved in structural aspects of the secretion apparatus (Mougous et al., 2006). A definitive model for the secretion system is yet to be elucidated but recent evidence has suggested the VgrG component may adopt a phage tail like structure which is capped by Hcp monomers which could create a pore through the outer membrane (Leiman et al., 2009).

1.2.8 Type 3 Secretion Systems (T3SS)

Type 3 secretions systems are complex macromolecular machines which are capable of translocating effector proteins directly from the bacteria into the host cell cytoplasm. A wide range of Gram negative pathogens encode a T3SS apparatus including EPEC, EHEC, *C.*

rodentium, *Shigella*, *Yersinia* and *Pseudomonas* (Reviewed in (Moraes et al., 2008)). *Salmonella* species encode two independent T3SS, Spi1 and Spi2, which are expressed at different stages during infection and have distinct substrate repertoires (Gerlach and Hensel, 2007). The T3SS apparatus is composed of approximately 20-25 distinct proteins which form a basal body, a needle complex and a translocation pore (Reviewed in (Cornelis, 2006)). The basal body spans both the bacterial inner and outer membranes and is composed of two ring like structures. The inner-membrane ring is anchored in the membrane and is associated with a cytoplasmic ATPase which provided the energy required for protein translocation (Yip et al., 2005). The outer-membrane secretin is first exported to the periplasm where it required the assistance of a lipoprotein for proper assembly and orientation (Crago and Koronakis, 1998). The assembled basal body is then involved in the secretion and assembly of a stiff needle extension composed of several hundred YscF family monomers linked via their coiled coil domains (Cordes et al., 2003). The needle is tipped with a hollow extension which extends towards the eukaryotic membrane and directs the proper insertion of translocator proteins. The final component of the T3SS secretion is system is a pair of translocator proteins which direct the formation of a pore in the eukaryotic plasma membrane to allow injection of T3SS effector proteins directly into the host cell (Moraes et al., 2008). The correct assembly of the T3SS apparatus is orchestrated by a series of bacterial cytoplasmic chaperones. Class III chaperones bind to the structural components of the T3SS and maintain them in secretion competent state whilst masking their oligomerisation domains to prevent premature assembly (Yip et al., 2005). Class II chaperones are involved in maintaining the translocator proteins in a partially unfolded state to prevent toxic effects to bacterial cell (Creasey et al., 2003b). The substrates of the T3SS, called effectors, have an un-cleaved N-terminal chaperone recognition sequences which are not yet full defined and do

not appear well conserved from genus to genus (Galan and Wolf-Watz, 2006). Class I chaperone bind to substrates of the T3SS maintaining them in a secretion competent state whilst directing them to the injectisome where they dissociate (Creasey et al., 2003a).

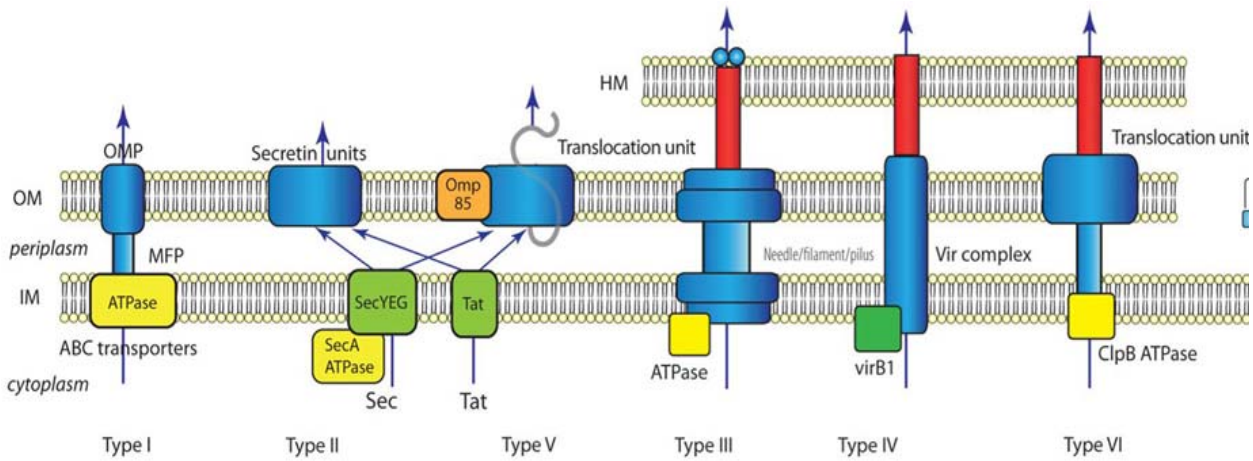


Figure 1.2 Gram Negative Bacterial secretion systems (T1SS-T6SS). TISSs are also referred to as ABC transporters and protein translocation across both bacterial membranes is powered by ATP hydrolysis. T3SS and T4SS are more complex multi component protein translocation machines which are also powered by ATP hydrolysis and can translocate effector proteins across both bacterial membranes and also directly into host cells. The T2SS and T5SS require a two step process in order to secrete proteins to the extracellular milieu. T2SS requires periplasmic chaperones and an outer membrane usher protein to export proteins whereas T5S is mediated by the formation of a translocation pore in the outermembrane by the C terminus of its autotransporter substrates. The mechanism of T6SS is yet to be fully understood but the structure resembles a phage tail spike composed of its VgrG and Hcp components and secretion is powered by an ATPase. Adapted from (Tseng et al., 2009).

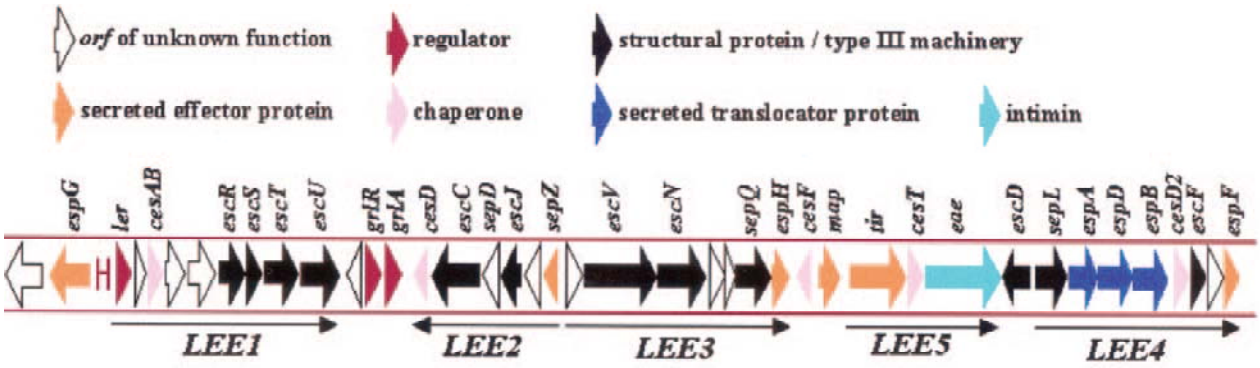
1.3 The A/E pathogen T3SS and LEE Pathogenicity Island.

Central to their virulence strategies, EPEC, EHEC and *Citrobacter rodentium* encode a T3SS in order to translocate effector proteins directly from the bacterial cell in to the host cell cytoplasm. The T3SS of EPEC, EHEC and *Citrobacter rodentium* is encoded on a region of the genome referred to as the Locus of Enterocyte Effacement (LEE) which is required for A/E lesion formation (McDaniel et al., 1995) (Figure 1.3). The 5′ end of the LEE island encodes the structural components of the T3SS. The central region encodes the outer-membrane adhesin intimin (Jerse et al., 1990) and the translocated intimin receptor (Tir) (Kenny et al., 1997). The 3′

end of the Lee locus codes for additional T3SS structural, translocator and effector proteins (Figure 1.3). In EPEC, EHEC and *Citrobacter rodentium* the fundamental components resemble other bacterial T3SS's with EscC, EscR, EscS, EscT, EscU and EscV forming the basal body, and EscJ linking the inner and outer membrane complexes. EscF forms the needle structure with EspD and EspB forming the translocation pore (Figure 1.3). The unique feature of the EPEC/EHEC and *Citrobacter rodentium* T3SS is the presence of the filamentous extension to the needle complex provided by polymerisation of EspA monomers. This forms a hollow conduit between the bacterial cell and the host membrane and constitutes a novel class of filamentous T3SS (FT3SS) (Daniell et al., 2001). There are several elements of the type 3 secretion apparatus which can be used to manipulate the T3SS to enhance or null secretion for the characterisation of putative effectors. One such example of this is EscN, the ATPase essential for powering type 3 secretion which when deleted renders the T3SS inactive (Gauthier et al., 2003).

Pathogenic *E. coli* and *Citrobacter rodentium* use the T3SS to translocate a range of effector proteins which allow them to subvert the host cell cytoskeleton in order to induce A/E lesion formation and to hijack several other key eukaryotic signalling pathways.

A



B

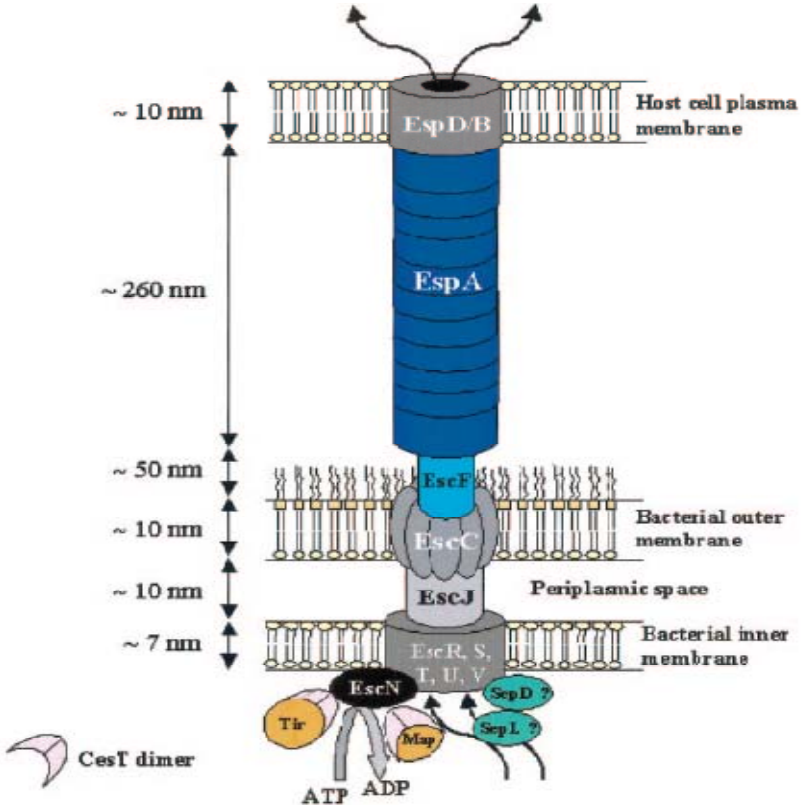


Figure 1.3 A. The LEE operon of A/E pathogens. The 5' region of LEE encodes the outer membrane adhesion intimin, its translocated receptor Tir and other T3SS effectors, while the central region encodes the structural components of the T3SS and the 3' region encodes additional effector proteins and translocators. B. The Type 3 secretion apparatus of the A/E group. Schematic diagram of the EPEC/EHEC and *Citrobacter* type 3 secretion apparatus. The basal body of the T3SS is composed of EscC, inner membrane proteins EscR, EscS, EscT, EscU and EscV, and the lipoprotein EscJ connect the inner and outer membrane. EscF makes up the needle structure, while EspA subunits polymerise to form the EspA filament. The translocation pore in the host plasma membrane is formed by EspB and EspD, connecting the bacteria and host through the EspA filaments. EscN, the cytoplasmic ATPase hydrolyzes ATP molecules into ADP, providing energy for the system. Reproduced from (Garmendia et al., 2005)

1.4 A/E Lesion and Pedestal Formation

The adherence of EPEC, EHEC and *C. rodentium* to intestinal epithelial cells results in the formation of characteristic A/E lesions from which the pathogens derive their name. A/E lesions are characterised by the effacement of brush border and distension of microvili at sites proximal to bacterial adherence (Figure 1.3). After initial association with host cells A/E pathogens utilise their T3SSs to translocate a plethora of effector proteins including the translocated intimin receptor (Tir) (Kenny et al., 1997). Tir is transloctaed from the bacterial cytoplasm to the host plasma membrane where it acts as a receptor for the bacterial outer membrane adhesion intimin (Frankel et al., 2001). The interaction between Tir and intimin results in a clustering of Tir and the polymerisation of actin beneath adherent bacteria which during *in vitro* cell culture results in the formation of a raised pedestal upon which the extracellular bacteria rest (Reviewed in (Frankel and Phillips, 2008)) (Figure 1.4). EPEC and EHEC employ similar approaches to direct actin pedestal formation but with some major differences, this is in part due to variations within their respective Tir proteins. During EPEC infection the clustering of Tir into lipid rafts results in its phosphorylation on tyrosine Y474 by c-Fyn (Hayward et al., 2009; Phillips et al., 2004). This phosphorylation allows the direct recruitment of the mammalian adaptor protein Nck (Campellone et al., 2002; Gruenheid et al., 2001), which in turn binds the ubiquitous form of Wiskott-Aldrich syndrome protein (N-WASP) resulting in an activation of N-WASP and subsequent recruitment of Actin related protein 2/3 (Arp2/3) complex which mediates actin polymerisation (Lommel et al., 2001) (Figure 1.5)**.** In contrast, the Tir protein encoded by EHEC does not possess a tyrosine at position 474 and instead utilises the non LEE encoded T3SS effector TccP/EspF_U which is associates with Tir via members of the IRSp53/MIM homology domain (IMD) family of adaptor proteins (Vingadassalom et al., 2009; Weiss et al., 2009).

TccP/EspF$_U$ then binds and activates N-WASP directly (Campellone et al., 2004; Garmendia et al., 2004) (Figure 1.5). TccP/EspF$_U$ homolog's have recently been identified in a group of atypical EPEC strains which would allow these strains to utilise both the Nck dependent and TccP/EspF$_U$ mediated pathway to polymerise actin pedestals (Whale et al., 2006) (Figure 1.5). Pedestals can be detected by immuno-fluorescence microscopy using the fungal toxin phalliodin coupled to a fluorophore. This technique is referred to as Fluorescence Actin Staining (FAS) and is utilised as a diagnostic test for EPEC and EHEC infections (Knutton et al., 1991). However, it was recently demonstrated using *in vivo* and *ex vivo* models of infection that A/E lesion formation can occur independently of both Nck and TccP/EspF$_U$ mediated actin polymerisation (Frankel and Phillips, 2008). This result suggests that pedestal formation and A/E lesion formation can be uncoupled from each other (Frankel and Phillips, 2008).

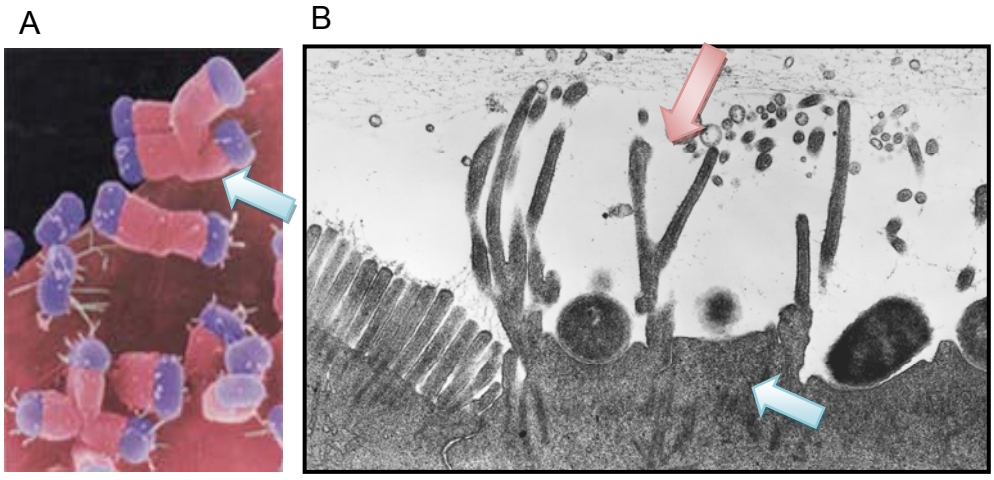


Figure 1.4 A/E pathogen mediated pedestal and lesion formation. A. Typical pedestal induced by EPEC and EHEC bacteria after initial adherence to host epithelial cell *in vitro* highlighted by the blue arrow. Pedestals are actin based membrane protrusions triggers via the interaction of the EPEC T3SS secreted effector tir and the bacterial outer membrane protein intimin and subsequent host cell actin polymerisation. B. Transmission electron micrograph of a bovine explant displaying typical A/E lesion formation. Bacteria are adhered to a cuplike pedestal structure (blue arrow) on the host enterocyte with disruption of the host brush border and distension of microvili in the proximal region highlighted by the red arrow

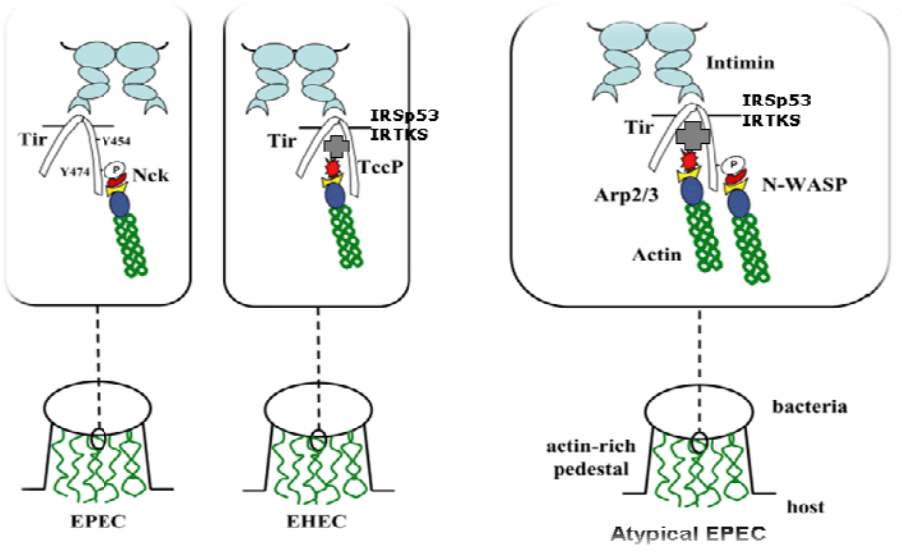


Figure 1.5 Mechanism of actin pedestal formation by EPEC, EHEC and a sub group of atypical EPEC strains. EPEC mediated pedestal formation is resultant from the tyrosine phosphorylation of Tir by c-Fyn on Y474 which subsequently recruits the adaptor protein Nck and in turn activates N-WASP dependent actin polymerisation. EHEC Tir does not conserve Y474 and instead utilises the effector protein TccP/EspFU which binds directly to N-WASP resulting in an activation of N-WASP and subsequent actin polymerisation. TccP/EspF$_U$ is coupled to Tir via members of the IRSp53/MIM homology domain. Homolog's of TccP/EspF$_U$ have recently been identified in a subset of atypical EPEC stains which can utilise both the Y474 and TccP/EspF$_U$ dependent mechanisms to induce pedestal formation. Adapted from (Whale et al., 2006).

1.5 Subversion of Eukaryotic Signalling by A/E Pathogen Effectors

Seven of the effector proteins involved in EPEC, EHEC and *Citrobacter* pathogenesis are encoded within the LEE island (Frankel et al., 1998). However, in recent years the genome of EPEC, EHEC and *Citrobacter rodentium* have been found to be enriched by novel genetic elements which encode a plethora of additional putative virulence factors. A recent paper by Tobe et al (Tobe et al., 2006) identified 50 proteins in EHEC O157 to be T3SS effectors including EspM2 (Sakai) and EspM1 (Sakai) which are further characterised in this study. In comparison EPEC E2348/69 encodes 21 T3SS effector proteins (Iguchi et al., 2009) and *C. rodentium* has a repertoire of 29 T3SS effector proteins (Figure 1.6).

Effector	*C. rodentium*	O127:H6 E2348/69	O111:NM B171	O157:H7 Sakai	O111:H9 E110019
Cif	0	1 (1)	1	0	0
EspB	1	1	1	1	1
EspF	1	1	1	1	2
EspG	1	2	1	1	1
EspH	1	1	1	1	1
EspJ	1	1	0	1	-
EspK	1	0	0	1	-
EspL	1	3 (2)	1	4 (1)	-
EspM	3 (1)	0	3 (1)	2	1
EspN	3 (2)	0	1	1	-
EspO	1	1 (1)	0	2	1(1)
EspR	0	0	0	4 (1)	-
EspT	1	0	0	0	1
EspV	1	0	1 (1)	1 (1)	-
EspW	0	0	1	1	-
EspX	1	0	0	6 (1)	3(1)
EspY	0	0	0	5 (1)	-
EspZ	1	1	1	1	1
Map	1	1	1	1	1
NleA	1	1	1	1	1
NleB	2 (1)	3 (1)	3 (2)	3 (1)	1
NleC	1	1	2 (2)	1	0
NleD	2	1	0	1	0
NleE	1	2	1	1	-
NleF	1	1	1	1	1
NleG	5 (2)	1	6	14 (5)	1(2)
NleH	1	3 (1)	2 (1)	2	(4)
Ibe	1	0	2(1)	0	1
TccP	0	0	1	2 (1)	-
Tir	1	1	1	1	1
	35 (6)	27 (6)	40 (12)	62 (12)	25 (8)

Figure 1.6 T3SS effector protein distribution in *C. rodentium*, EPEC E2348/69 (O127:H6), EPEC B171 (O111:NM), EHEC Sakai (O157:H7) and EPEC E110019 (O111:H9). The genome of E110019 is not yet published so effector number cannot be confrimed.

Once translocated these effector proteins subvert a variety of host cell processes including vesicle trafficking, apoptosis, the immune response and cytoskeletal signalling. The effector EspF is known to localise to the mitochondria triggering cell death (Nougayrede and Donnenberg, 2004) and to disrupt tight junctions (McNamara et al., 2001). EspF also perturbs host cell vesicle trafficking and induce membrane remodelling by interacting with Snx9 and N-WASP (Alto et al., 2007). NleA/EspI is a non LEE encoded effector of the A/E pathogens which inhibits protein transport from the endoplasmic reticulum via inhibiting the function of CopII (Kim et al., 2007). The effector EspJ is known to inhibit the opsono-phagocytosis of EHEC by macrophages (Marches et al., 2008). The NleH family of effectors have been demonstrated to induce the activation of NF-kappaB and TNF alpha (Hemrajani et al., 2008). More recently NleH has been demonstrated to inhibit host cell apoptosis through its interaction with the endoplasmic reticulum protein Bax inhibitor-1 (Hemrajani *et al*., unpublished). One of the major targets of A/E pathogen effectors is the eukaryotic cytoskeleton. In addition to Tir and TccP/EspF$_U$ mediated pedestal formation, the LEE encoded effector Map activates the small GTPase Cdc42 in order to induce the formation of filopodia at early times during infection (Berger et al., 2009; Huang et al., 2009; Kenny and Jepson, 2000). The LEE encoded effector EspG and it non LEE encoded homolog EspG2 are known to induce the formation of stress fibres by liberating GEFH1 via the depolymerisation of microtubules (Matsuzawa et al., 2004). The prophage encoded T3SS effector EspL2 has recently been demonstrated to enhance the cross linking of actin filaments via an activation of the host cell protein annexin 2 (Miyahara et al., 2009). Annexin 2 is a membrane protein which under normal physiological conditions is enriched at actin assembly sites on the plasma membrane and vesicles and is involved in coupling membrane and cytoskeletal dynamics.

1.6 The Actin Cytoskeleton

The eukaryotic cytoskeleton is a dynamic scaffold composed of microtubules, intermediate filaments and actin (reviewed in (Desai and Mitchison, 1997; Goldman et al., 2008; Millard et al., 2004)). Within the cytoskeleton actin polymerisation and depolymerisation drives the formation of dynamic structures which are tailored to respond to a diverse range of cellular and environmental cues. The actin cytoskeleton is integral to a plethora of cellular processes including maintenance of cell shape, integrity and polarity, cell migration and division (reviewed in (Barr and Gruneberg, 2007; Thery and Bornens, 2006)), vesicle trafficking (Girao et al., 2008), cell death (Franklin-Tong and Gourlay, 2008) and membrane dynamics (Lanzetti, 2007; McMahon and Gallop, 2005). Within eukaryotic cells actin is primarily found in its globular form (G-actin) which is one of the most abundant cellular proteins. G-actin is a adenosine triposphatase (ATPase) which can self associate and assemble into helical filaments which are referred to as filamentous actin (F-actin) (Welch and Mullins, 2002). Actin filament assembly is characterised by the presence of a slow growing pointed end and a fast growing barbed end (reviewed in (Millard et al., 2004)). The assembly of an F-actin filament is driven by association of G-actin monomers bound to ATP, as the filament grows in length the ATP is hydrolysed to ADP. The barbed end of the filament has an increased affinity for ATP bound G-actin which drives growth and extension of the filament. Meanwhile at the pointed end ADP bound G-actin is gradually lost creating a treadmilling of free G-actin subunits which can subsequently bind ATP to reconstitute to the free ATP-bound G-actin pool (reviewed in (Cooper and Schafer, 2000; Pollard et al., 2001)). This treadmilling of G-actin subunits allows the filament to be highly dynamic and responsive.

The process of self association and filament assembly or disassembly is controlled by a variety of other eukaryotic nucleation promoting factors (NPFs), adaptor proteins and actin binding proteins (Figure 1.7).

1.6.1 Actin nucleators

Despite the ability of G-actin monomers to self associate, spontaneous F-actin filament nucleation is prohibited by the inherent instability of actin dimers and trimers. This instability is no longer inhibitory in larger F-actin polymers which are capable of rapid self association and assembly (Millard et al., 2004). This necessitates the activity of actin nucleators which promote early actin polymer formation by stabilising actin dimers and trimers and promoting filament growth (Chesarone and Goode, 2009). To date there have been 3 classes of actin nucleators defined.

Class 1: WASP superfamily members contain a C-terminal WH2 domain which is used to recruit G-actin monomers and it veropolin (V), central (C) and acidic (A) domain to activate the actin related proteins 2/3 (Arp2/3) complex (Takenawa and Miki, 2001). The Arp2/3 complex is a heptameric arrangement of five Arp2/3 complex components (Arc 1-5) and two actin like subunits (Arp2 and Arp3). Arp2/3 does not possess basal actin nucleation activity, however when it is bound to NPFs such as WASP family members it is thought that the Arp2/3 complex acts a stable dimer or trimer which promotes the association of additional actin monomers in a manner similar to GTP loaded G-actin binding to a barbed end on a growing actin filament. It is also thought the Arp2/3 complex in association with NPFs can generate branching of existing F-actin filaments by binding three subunits from the mother filament and nucleating a new branch at a 70° angle (reviewed in (Chesarone and Goode, 2009; Goley and Welch, 2006; Takenawa and Miki, 2001)). WASP and Arp2/3 generated actin structures such as filopodia and

lamellipodia are generated by assembly of highly dynamic branched actin filaments. WASP is only encoded within haematopoietic cells but its near identical homolog N-WASP is ubiquitous and is particularly enriched in neuronal cells (Ochs and Thrasher, 2006). Other WASP family members include the Wave isoforms 1-3, WASH and WHAMM each of these proteins conserve the Arp2/3 and actin binding C terminus of WASP but have divergent N terminal domains (Campellone et al., 2008; Linardopoulou et al., 2007; Takenawa and Miki, 2001). Wave proteins are potent actin nucleation promoting factors involved in the formation of lamellipodia and membrane ruffles (Innocenti et al., 2004; Steffen et al., 2004; Suetsugu et al., 2006; Suetsugu et al., 1999). WASH, was first identified as a WASP family member encoded in the sub-telomeric region of chromosomes (Linardopoulou et al., 2007). More recently WASH has been shown to act as a downstream effector of Drosophila Rho where it acts as an actin and microtubule cross-linking and bundling agent (Liu et al., 2009). It has also been shown to play a role in a large multiprotein complex containing components of the retromer complex, where is has a role in endosome fission (Derivery et al., 2009) (Gomez *et al.*, 2009). WHAMM is another WASP homolog which has been described to have microtubule binding capacity, and this in conjunction with its actin nucleation activity regulates Golgi stability, anterograde vesicle transport and membrane tubulation (Campellone et al., 2008)

Class 2: The second class of actin nucleators, formins, nucleate unbranched linear actin filaments. Formins lack any detectable ability to bind actin monomer so it has been postulated that they may stabilise spontaneously formed actin dimers and trimers. The FH2 domain of the formin binds to the barbed end of nascent actin polymers and remains bound to the barbed end of the growing actin filament (Goode and Eck, 2007).

Class 3: The most recently identified class of actin nucleator includes Spire, Cordon bleu (Cobl), Leiomodin (Lmod) and JMY. Spire proteins have four dual WASP homology domains which are capable of binding four actin monomers in a chain which acts as a template for the addition of further actin monomers (Quinlan et al., 2005). The post nucleation activity of spire proteins is yet to be elucidated. Cobl nucleates actin filaments via a similar mechanism to spire proteins using three WASP homology domains to bind actin monomers. The arrangement of the actin monomers nucleated by Cobl is hypothesised to be a linear dimer with one perpendicular G-actin monomer. Cobl is thought to remain associated with the pointed end of the growing F-actin filament (Ahuja et al., 2007). Lmod has a single WASP homology domain and two tropomodulin like actin binding sites. Little is known of the mechanism by which Lmod nucleates actin but it is thought a nucleation seed of three actin monomers is formed and subsequently stabilised at the pointed end (Chereau et al., 2008). JMY was first identified as a cofactor of p53 but has subsequently been demonstrated to involved in cell migration and shown to nucleate actin via a spire like mechanism (Zuchero et al., 2009).

Regulation of Nucleation promoting factors.

Nucleation promoting factors are regulated via a plethora of physiological interactions, subcellular localisation, autoinhibition, degradation and phosphorylation (reviewed in (Bompard and caron 2004)). Inactive N-WASP is present in cells in a closed autoinhibitory conformation in which its GTPase binding domain (GBD) and the central (C) region of the VCA module mediate a interprotein interaction. This autoinhibitoy conformation is relieved by the binding of Cdc42 to the GBD domain of N-WASP resulting resulting in the VCA module being liberated and able to bind and activate the Arp2/3 complex (Higgs and Pollard 2001). The Wave family of proteins are

regulated via protein protein interaction. Under resting conditions Wave is complexed with PIR121(Sra1), Nap1, Abi1 and HSPC300 (Kunda et al., 2003). This complex has been demonstrated to prevent Wave2 degradation and to enhance its membrane localisation (Innocenti et al., 2004). Interaction of Rac1 with PIR121 (Sra1) enhances the actin polymerisation activity of the wave complex (Steffen et al., 2004). This suggests that unlike N-WASP Wave proteins are constitutively active and are regulated via localisation rather than autoinhibition. The interaction between the conserved VCA domain of WASP and Wave proteins and Phosphatidylinositol (3,4,5)-trisphosphates strongly enhances the actin polymerisation activity of this family of NPFs at the membrane (Oikawa et al., 2004). Both WASP and Wave family proteins are also regulated through phosphorylation my multiple cellular kinases including MAP Kinases. Abl and Src (reviewed in (Bompard and Caron 2004)).

Similarly to N-WASP the diaphanous related formins (Drf's) including MDia under resting conditions are present in an autoinhibitory conforamtion mediated by an interaction between their N terminal GTPase activating domain and their C terminal Diaphanous-autoregulatory domain (DAD). This inhibition is relieved via the binding of RhoA and related GTPases (Lammers et al., 2005). Formins can also be regulated by phosphorylation mediated by a variety of kinases as exemplified by the activation of FHOD1 and MDia via the phosphorylation of Rho associated coiled coil kinase (ROCK) (Takeya et al., 2008). Formins can also be regulated via homo-oligomerisation which greatly enhances their in vivo actin polymerisation activity (Copeland et al., 2004).

Little is currently understood regarding the regulation of Spire proteins and related actin nucleation promoting factors including JMY and LMod.

1.6.2 Actin recycling factors

Actin polymerisation and depolymerisation is a dynamic and reciprocal process which allows cells to respond to environmental and cellular cues with speed and plasticity. The number of actin monomers within a cell is a self limiting factor which governs the number of nascent actin filaments which may be nucleated or extended. This necessitates the rapid turnover of existing actin filaments to provide monomers to retain the dynamic nature of the actin cytoskeleton via the process of treadmilling (reviewed (Carlier et al., 1999b; Pollard et al., 2001)). ADF/cofilin has been demonstrated to bind both G and F–actin and in its un-phosphorylated state severs actin filaments at the pointed end which leads to a pool of G-actin monomers and also creates free barbed ends which can then be re-polymerised (Carlier et al., 1999b). After ADP-bound G-actin subunits have dissociated form the pointed end or been severed by ADF/cofilin they must be recycled to an ATP bound form to be competent for polymerisation. Profilin binds to ADP bound G-actin and catalyses the nucleotide exchange to the ATP-bound form of G-actin (Witke, 2004).

1.6.3 Elongation factors

Ena/Vasp proteins are recruited to sites of dynamic actin polymerisation but do not themselves under physiological conditions nucleate actin filaments (Bear et al., 2000) (reviewed in (Krause et al., 2003)). Ena/Vasp proteins have been demonstrated to delay the capping of the barbed end of actin filaments and subsequently promoting elongation (Bear et al., 2002). It has also been proposed that Ena/Vasp proteins play a role in inhibiting the branching activity of the Arp2/3 complex and debranching previously nucleated filaments (Krause et al., 2003). Ena/Vasp proteins are also known to bind profilin and this sequestration of profilin is postulated to enhance the recruitment of newly recycled ATP bound G-actin which can then be added to the uncapped barbed ends of growing actin filaments (Jonckheere et al., 1999).

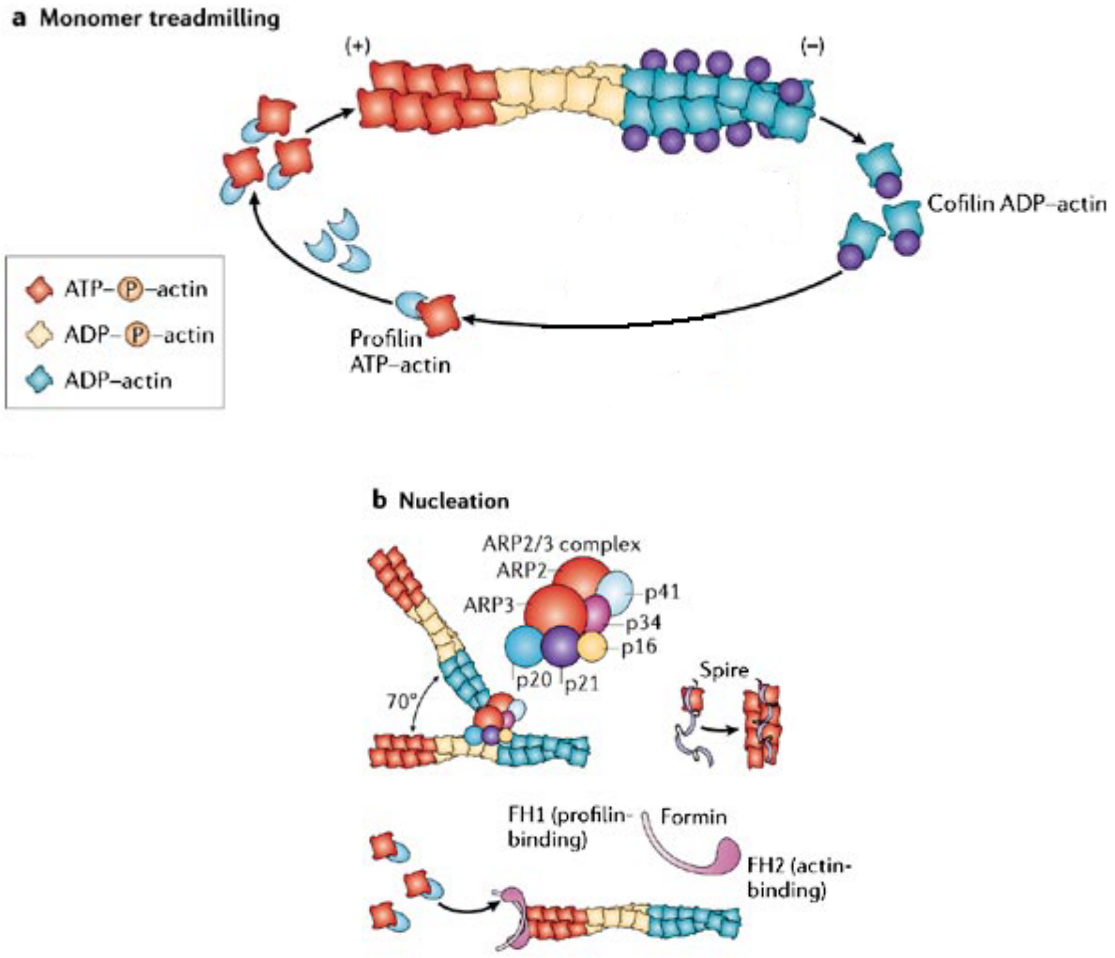


Figure 1.7 Factors involved in the assembly and turnover of the actin cytoskeleton. Actin polymerisation and depolymerisation drives the formation of dynamic structures able to respond to a range of cellular and environmental cues. A. In order to retain its dynamic nature filamentous actin is constantly being treadmilled in order to generate free monomers which can be reassembled into new filaments. Actin treadmilling is mediated by the slow intrinsic ATP hydrolysis generated by the ATPase activity of actin monomers and the depolymerisation and severing activity of actin recycling factors such as ADF cofilin family members. Depolymerisation of actin filaments ocurrs at the pointed (-) end of the filament. Actin filament growth is mediated by the addition of fresh ATP bound actin monomers at the babrbed end pf the filaments. Subsequent to ADP actin dissociating from the pointed end or being severed by coflin it is bound by profilin family members which mediate the regeneration of ADP actin monomers to their ATP bound form which can then be incorporated at the barbed end of the filament. B. Schematic representation of the mechanism utilised by the three classes of actin nucleators which have been identified to date. Adapted from (Baum et al., 2006). Although actin filaments are capable of rapid self assembly and turnover, the nucleation of nascent filaments is an energetically unfavourable process due to the inherent instability of actin dimmers and trimers, this necessitates the the role of actin nucleation promoting factors. Currently there are three major classes of actin nucleation promoting factors 1. ARP2/3 complex which, when activated in complex with Wasp family proteins, mimics a stable actin trimer which promotes rapid filament assembly. 2. Spire proteins which contain multiple actin monomer binding sequences which recruit ATP bound actin into chains of 4 to act as a templat for subsequent monomer addition. 3. Formins which bind to the barbed end of nascent actin filaments and enhance profilin binding and increasing the rate of ATP bound actin monomer addition to the filament facilitating their rapid growth.

1.7 Rho GTPases

The mammalian cytoskeleton is subject to an intricate and complex regulatory network regulated by kinases such as Src (Frame, 2004), Abl (Woodring et al., 2003), LimK (Bernard, 2007) and Phosphoinositide 3-kinase (PI3K) (Cain and Ridley, 2009), adaptor proteins including Nck (Buday et al., 2002), amphiphysin (Aspenstrom, 2009) and Grb2 (Giubellino et al., 2008), G Protein Coupled Receptors (GPCR) (Cotton and Claing, 2009), ezrin-radixin-moesin (ERM) proteins (Niggli and Rossy, 2008) and small Rho family GTPases (Etienne-Manneville and Hall, 2002) to name but a few.

The Rho GTPases are often referred to as "master regulators of the actin cytoskeleton" due to their pivotal role in almost all aspects of actin dynamics. Rho family GTPases are a distinct subgroup of within the Ras superfamily of GTPases. Currently 22 Rho Family GTPases were indentified in mammalian cells including RhoA, RhoB, RhoC, RhoD, RhoE, RhoG, RhoH, RhoBTB1, RhoBTB2, Rac1, Rac2, Rac3, Cdc42, Rnd1, Rnd2, TC10, TCL, Chp, Wrch1, Rif, Miro1, Miro2 (reviewed in (Jaffe and Hall, 2005)). The best characterised Rho family GTPases are RhoA, Rac1 and Cdc42.

Rho GTPases are molecular switches which cycle between an inactive GDP bound form and an active GTP bound form (Etienne-Manneville and Hall, 2002). As their names suggest Rho GTPases have an intrinsic GTPase activity which acts as an internal regulatory system which slowly hydrolyses the GTP of the active form to GDP of the inactive form and subsequently limiting the longevity of the activation (Jaffe and Hall, 2005). Activation of Rho GTPases requires the binding of GTP instead of GDP which results in a subsequent conformational shift of the proteins. Rho GTPases contain several key regions including the switch 1 and 2 regions and the P-loop which are involved in the activity and regulation of the proteins (Jaffe and Hall,

2005). During nucleotide exchange from GDP to GTP the conformation of the switch regions change dramatically altering the structure of the GTPases allowing them to interact with downstream effector proteins and signalling molecules which mediate the cellular events such as actin polymerisation and membrane protrusion (Bishop and Hall, 2000; Etienne-Manneville and Hall, 2002). Misregulation of Rho GTPases is associated with a range of developmental abnormalities, immunological diseases, physiological conditions. Most importantly aberrant GTPases signalling is linked to almost every aspect of oncogenesis and metastasis (reviewed in (Jaffe and Hall, 2002; Li and Lim, 2003; Toksoz and Merdek, 2002). As such, Rho GTPase are subjected to tight and elaborate networks of regulation which includes activating Guanine Exchange Factors (GEFs), inactivating GTPase Activating Proteins (GAPs) and Inhibitory Guanine nucleotide Dissociation Inhibitors (GDIs) as well as numerous kinases, adaptor proteins and ubiquitinases (reviewed in (Etienne-Manneville and Hall, 2002; Jaffe and Hall, 2005)) (Figure 1.6). Rho family GTPases can also be regulated spatially via the prenylation of C-terminal motifs which allow then to be anchored in the membrane (Zhang and Casey, 1996).

1.8 Regulation of Rho GTPases

1.8.1 GEFs

Rho GTPases have a nucleotide binding groove which can be loaded with GTP or GDP depending on the activation status of the GTPase. As well as having the capacity to bind guanine nucleotides Rho GTPases also have a magnesium (Mg^{2+}) binding pocket which acts as a lock to stabile the bound nucleotide (Jaffe and Hall, 2005). GEFs binds to GTPases and facilitate the switch from a nucleotide and Mg^{2+} loaded GTPase to an unbound intermediate which remains associated with the GEF. Due to the relative abundance of cellular GTP compared to GDP the GEF then mediates the binding of GTP to the GTPase nucleotide binding pocket by stabilising

the intermediate nucleotide free GTPase. Following the reacquisition of a Mg^{2+} ion the GEF then normally dissociates leaving the GTP bound GTPase to interact with its downstream effectors (reviewed in (Schmidt and Hall, 2002)). It has however been reported that some Rho GEFs such as Intersectin-1 can form a trimeric complex with GTPases and their downstream effector which can enhance the activity of the GEF (Hussain et al., 2001). The majority of Rho GTPases GEFs belong to the Dbl superfamily and are characterised by the presence of a Dbl Homology (DH) domain. The DH motif comprises 10-15 alpha helices which have 3 conserved regions (CR1-3) (Rossman et al., 2005). The CR1 and CR3 regions along with some additional amino acids at the C terminus of the DH domain contribute the majority of the GTPase binding motif (Soisson et al., 1998). DH domains interact with the switch regions of Rho GTPase and mediate a significant restructuring of the nucleotide binding pocket. The switch 1 region moves along the nucleotide binding groove to disturb nucleotide and Mg^{2+} binding while the switch 2 region rotates to occlude the Mg^{2+} binding site (Rossman et al., 2005). Almost all Rho GEFs also contain Pleckstrin Homology (PH) domains which are a one hundred amino acid motif which bind phosphoinositols of the plasma membrane and are thought to provide localisation of the GEF and or GEF GTPase complex to the membrane (Olson et al., 1997). Some Rho GEFs also contain C terminal PSD-95/Sap90, Disc large and Zonal occludin1/ZO1 (PDZ) domains which are thought to aid in localising and retaining the GEF in specific cellular localisations (Garcia-Mata and Burridge, 2007). Other atypical GEFs such as Dock180 have recently been described which do not contain DH domains but rather utilise Dock Homology Region (DHR) domains in order to GEF Rho GTPases (Cote and Vuori, 2007). Dock180 has been demonstrated to interact with another cellular protein, named Engulfment and Motility protein (ELMO), which by virtue of its PH domain stabilises the nucleotide free GTPase and Dock180 complex to enhance the GEF

activity of the DHR domains (Lu et al., 2004). Little is known about how GEFs are turned on and off, however autoinhibition and localised activation models have been proposed as mechanisms for GEF regulation (reviewed in (Schmidt and Hall, 2002)).

1.8.2 GAPs

Rho family GTPase have a slow intrinsic GTPase activity however this rate is not sufficient to provide the tight regulation required when turning off GTPase signalling. GAP proteins are required to enhance the intrinsic GTPase activity to provide tight temporal regulation of GTPase activity. The repertoire of human GAP proteins is predicted to be around 70 proteins which all contain the conserved GAP motif along with various other less well conserved domains (Peck et al., 2002). The RhoGAPs can be separated into around 23 sub-families based on different structural and physiological variations (reviewed in (Tcherkezian and Lamarche-Vane, 2007). GAPs bind GTPases and enhance their intrinsic GTPases activity by inserting an arginine finger motif into the nucleotide binding pocket which is essential for the hydrolysis of GTP to GDP (Fidyk and Cerione, 2002). The arginine acts as electron acceptor during the hydrolysis reaction (Leonard et al., 1998). It has also been proposed that binding of GAPs to Rho family GTPase results in a stabilisation of the normally flexible switch regions creating a stable catalytic centre for GTP hydrolysis (Scheffzek et al., 1997). After GTP hydrolysis GAPs dissociate from the GTPase. Rho GAPs are regulated through a combination of phosphorylation, localisation, protein protein interaction and degradation (reviewed in (Tcherkezian and Lamarche-Vane, 2007) (Roof et al., 1998).

1.8.3 GDIs and GDFs

To date only three human GDI proteins have been identified: RhoGDI which is ubiquitously expressed, GDI1β which is present in hematopoietic cell lineages and GDI3 which is only expressed in lung, brain and testis (reviewed in (DerMardirossian and Bokoch, 2005)). Rho GDIs function by associating with GTPases in their GDP bound form to prevent nucleotide exchange by GEFs resulting in the GTPase remaining in an inactive conformation (Olofsson, 1999). GDIs are also capable of binding to GTP bound form of Rho GTPase and prevent GTP hydrolysis mediated intrinsically or aided by GAPs whilst preventing the active GTPase from interacting with its downstream effectors (DerMardirossian and Bokoch, 2005; Scheffzek et al., 2000). Rho GDIs are also thought to function by preventing localisation of active Rho GTPases to the plasma membrane and removing GTP-bound GTPase from the membrane by burying their prenylated membrane anchor thus sequestering them away from activating membrane bound GEFs (Olofsson, 1999). Rho GDIs can be dissociated from GTPase by GDI displacement factors (GDFs) including the ERM proteins (Takahashi et al., 1997), lipids and the tyrosine kinase Etk (Kim et al., 2002). GDIs may also be regulated via direct phosphorylation (DerMardirossian and Bokoch, 2005).

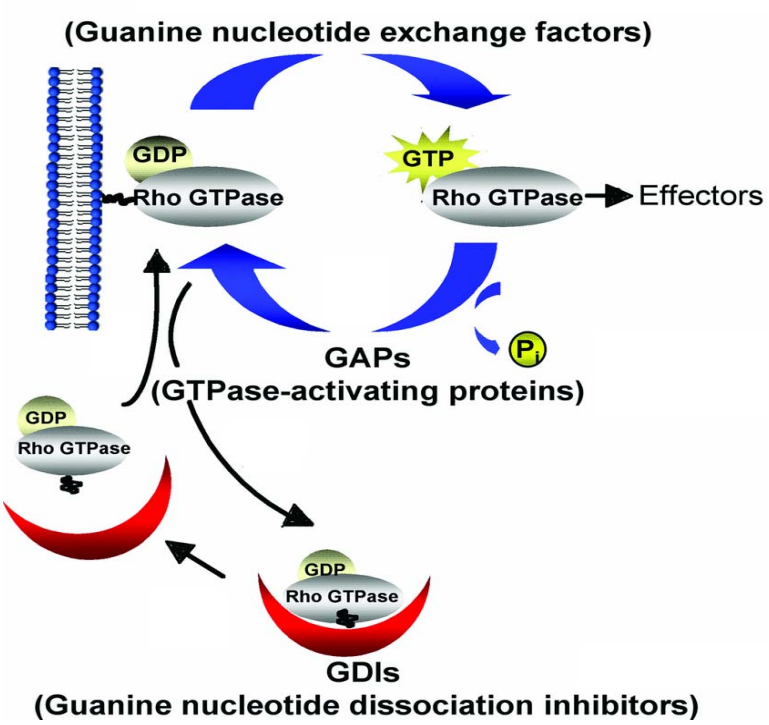


Figure 1.6 The Regulatory Cycle of Rho GTPases. The Rho family of GTPases are tightly regulated by three major classes of protein. Activating Guanine Exchange Factors (GEFs), Inactivating GTPase Activating Proteins (GAPs) and Inhibitory Guanine nucleotide Dissociation Inhibitors (GDIs). GEFs interact with Rho GTPases and promote the nucleotide exchange of GDP for GTP resulting in an activation of the GTPase. GAPs stimulate the intrinsic GTP hydrolysis activity of GTPases resulting in accumulation of the GDP bound inactive forms. GDIs bind to GTPases and inhibit their association with their effectors and GEFs. Adapted from (Tcherkezian and Lamarche-Vane, 2007)

1.9 RhoA, Rac1 and Cdc42

The best characterised members of the Rho family of small GTPases are RhoA, Rac1 and Cdc42 which are involved in the formation of stress fibres, lamellipodia and filopodia respectively. Studies conducted on these GTPase have clearly defined the mechanisms by RhoA, Rac1 and Cdc42 mediate the formation of these three different actin based phenotypes (Jaffe and Hall, 2005). (Figure 1.7)

1.9.1 RhoA

RhoA induces actomyosin contractibility and the subsequent formation of stress fibres in fibroblasts (Ridley and Hall, 1992). In addition RhoA induces cell rounding in other cell lines which is has been demonstrated also to be due to actomyosin contraction (reviewed in (Ridley, 2001)) and is essential for retraction of the tail end of cells during cell migration (Ridley et al., 2003).

Stress fibres are specific arrangements of actin monomers into long polymers. These fibres are involved in structural aspects of the cell architecture. Stress fibres form at focal adhesions which link the actin cytoskeleton at the plasma membrane with the extracellular matrix. Contraction of these fibres allows the cell to exert tension on the surrounding extracellular matrix, a process which is essential for maintaining structural integrity and also in facilitating cell migration (reviewed in (Ridley, 1999)). RhoA exerts its effect by interacting with the Rho coiled coil p160 serine/threonine kinase (ROCK) and the formin mDia. ROCK phosphorylates the Myosin Light Chain (MLC) and the Myosin Binding Subunit (MBS) of the MLC phosphatase (Amano et al., 1996; Kawano et al., 1999). This results in an increase in MLC phosphorylation and formation of actomyosin filaments which can exert a mechanical force on the cell (reviewed in (Bishop and Hall, 2000)). ROCK also phosphorylates Lim Kinase (LimK) which subsequently phosphorylates cofilin, resulting in an inactivation of cofilin mediated actin filament severing (Maekawa et al., 1999). RhoA also interacts with the formin mDia which nucleates and directs the polymerisation of linear actin filaments as described previously. The result of RhoA co-ordination of ROCK and mDia is the formation of actin stress fibres which are coupled to cell contraction.

1.9.2 Rac1

Ras related C3 substrate 1 (Rac1) was first identified based on its sensitivity to the C3 botulinum toxin (Didsbury et al., 1989). The C3 toxin was identified to transfer a ribosyl moiety to the asparagines residue at position 63 leading to its inactivation. Rac1 activation is coupled with the formation of membrane ruffles and lamellipodia which are predominantly associated with cell movement (Etienne-Manneville and Hall, 2002; Ridley et al., 1992). Lamellipodia are actin rich extensions which project from the leading edge of cells. These structures are thought to provide the motor for the crawling movement of cell. The actin at the leading edge of the lamellipodia is constantly treadmilling to allow dynamic movement (reviewed in (Fukata et al., 2003)). Membrane ruffles are sheet like membrane structures which are induced by mammalian cells in order to facilitate crawling movement, macro-pinocitosis and receptor recycling (reviewed in (Buccione et al., 2004)). Rac1 activation is also linked to superoxide production, microtubule stability, MAP kinase signalling and regulation of transcription factors (reviewed in (Bosco et al., 2009)). The major effectors of Rac1 are WASP-like Verprolin-homologous protein 2 (Wave2, also known as Scar) and the P21 activating kinases (PAK). Wave proteins are members of the WASP superfamily of protein and have the conserved C terminal WH2 domain and VCA Arp2/3 binding module through which they can nucleate branched actin filaments. Wave proteins also have a N terminal Wave homology domain (WHD) and a central proline rich region (PRR) (reviewed in (Takenawa and Miki, 2001)). Wave2 does not bind to Rac1 directly but interacts in a complex together with the GTPase in order to induce membrane ruffling and lamellipodia formation; there are two different mechanisms which have been proposed to describe how a Wave2-Rac1 complex can be formed. Innocenti et al and Steffen et al demonstrate that Wave2 binds to Abi1 and two accessory proteins PIR121 and Nap1 which

mediate Rac1 binding (Innocenti et al., 2004; Steffen et al., 2004). Another study from Miki et al has proposed that IRSp53 is the protein which links Rac1 to Wave2 (Miki et al., 2000). The other major effector of Rac1, PAK, has several isoforms which are serine threonine kinases known to phosphorylate MLC kinase to decrease actomyosin contractibility (Sanders et al., 1999). PAK isoforms have also been demonstrated to inactivate cofilin by the phosphorylation of LimK (Edwards et al., 1999). Rac1 has also been shown to signal to growth receptor pathway involved in transformation via c-Jun N terminal Kinase (JNK) in a PAK dependent manner (Westwick et al., 1997). Recently, Rac1 mediated PAK activation was shown to activate Erk1/2 in order to enhance lamellipodial stability (Smith et al., 2008). PAK has also been linked to an active role in the formation of lamellipodia as well as a subsidiary role in transporting the Wave complex to the membrane (Machuy et al., 2007) (Takahashi and Suzuki, 2009).

1.9.3 Cdc42

Cdc42 activation leads to the formation of finger like actin rich membrane protrusions from the cell known as filopodia. Filopodia are often found at the leading edge of cells where they contact the substratum during migration to generate the resistance required for the lamellipodia to drive the cell during migration (Faix and Rottner, 2006). Additionally filopodia are thought to play a role in sampling the local environment of the cell and also in contacting neighbouring cells (Ridley, 2001). The major effector of Cdc42 is the haematopoietic specific WASP and its ubiquitously expressed homolog N-WASP. As previously mention WASP and N-WASP have a conserved WH2 domain and VCA module involved in Arp2/3 binding as well as an N terminal WH1 motif and a proline rich region (Takenawa and Miki, 2001). WASP/N-WASP differ from their Wave homolog's in that they possess a Cdc42 interacting domain (CRIB). The CRIB motif facilitates the direct binding of Cdc42 which subsequently relieves the autoinhibitory

conformation of WASP/N-WASP. This allows WASP/N-WASP to promote actin nucleation in an Arp2/3 dependent manner. WASP/N-WASP also bind profilin which enhances their actin polymerisation activity (Takenawa and Miki, 2001). Cdc42 can also bind to PAK in a similar way to that described for Rac1. Cdc42 has also been proposed to play a role in maintaining stability of lamellipodia and membrane ruffles which are nucleated in a Rac1 dependent manner (Kurokawa et al., 2004).

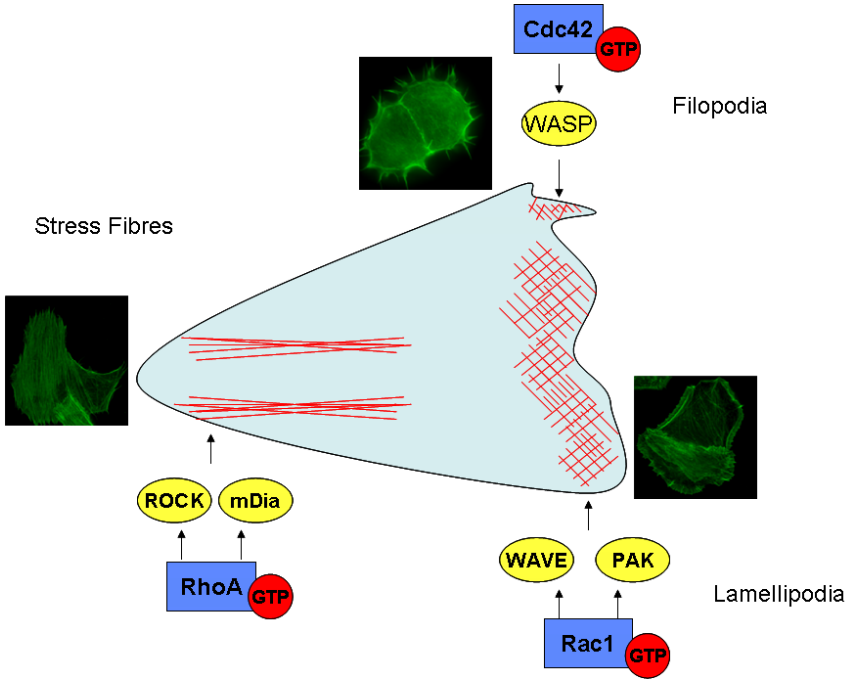


Figure 1.7 Regulation of the host cell cytoskeleton by RhoA, Rac1 and Cdc42. GTP bound RhoA induces the formation of stress fibres via the coordinated activation of Rho coiled coil p160 kinase (ROCK) and the formin mDia. Rock and mDia stimulate an increase in actomyosin contractibility and the nucleation of stress fibres respectively. Active Rac1 directs the formation of lamellipodia and membrane ruffles via its activation of the Wave complex and subsequent recruitment of the actin nucleator Arp2/3. Rac1 also activates the effector PAK which is proposed to play a role in maintaining lamellipodia stability as well as localising Wave to the membrane. GTP-bound CDc42 induces the formation of finger like extensions in the plasma membrane kwon as filopodia. Cdc42 dependent filopodia formation is mediated via the WASP proteins and Arp2/3.

1.10 Bacterial Virulence and Rho GTPases

Rho GTPases are common targets for bacterial toxins and secreted effector proteins due to their pivotal role in the control of cytoskeletal dynamics along with a wide range of other cellular

processes including: the NF-κB signalling cascade, progression through G1 of the cellular cycle and regulation of JNK and p38 cascades (Hall, 2005). To date, more than 30 bacterial effectors and toxins are known to interfere directly or indirectly with RhoA, Rac1 and Cdc42 (Finlay, 2005). Bacterial factors which modulate Rho GTPase signalling can be placed into three distinct groups: 1. Enzymes which chemically modify GTPase. 2. Proteins which are mimics of host Regulatory factors. 3. Factors which indirectly modulate GTPase activity.

1.10.1 Bacterial Enzymes which Chemically Modify Rho GTPases

One of the classic examples of bacterial modification of Rho GTPases are the Clostridial toxins (reviewed in (Aktories et al., 2000)). Toxin A and B from *Clostridium difficile* have a fold which is similar to that of type A glycoslytransferases. Toxin A and B can modify RhoA, Rac1 and Cdc42 along with many of the less well characterised Rho GTPases family (reviewed in (Jank et al., 2007)). Each Rho GTPase substrate of toxin A and B are modified on the same threonine residue (T37 for RhoA and T35 for Rac1 and Cdc42) (Just et al., 1995a; Just et al., 1995b). This threonine residue is located in the switch 1 region and is essential for coordinating the Mg^{2+} ion. Glycosylation of this residue by toxin A and B results in an inactivation of Rho GTPases. This inactivation is due to the inability of the glycosylated GTPase to interact with its effectors or GEFs (Herrmann et al., 1998).

In addition to Glycosyltransferases, other species of *clostridium* posses enzymes known as ADP ribosyltransferases which include the C3 toxin of *C. botulinum*. Ribosyltransferases catalyse the transfer of an ADP moiety from a cofactor such as Nictotinamide Adenine Di-nucleotide (NAD) to a donor amino acid. In the case of toxin C3 the ADP moiety is transferred to an asparagine residue at position 63 in Rho GTPases. Toxin C3 ribosyltransferase activity is specific to RhoA and other Rho GTPase are very poor targets for the enzyme. The functional consequence of

RhoA ribosylation by C3 is the inactivation of the GTPase by two distinct mechanisms, firstly the modification prevents RhoA from interacting with its GEFs and secondly the ribosylation can lock RhoA in an inactive complex with its GDI (reviewed in (Vogelsgesang et al., 2007).

The *Vibrio* T3SS effector VopS was recently described as having a novel ampylation activity towards RhoA, Rac1 and Cdc42. Ampylation involves the modification of the same conserved threonine targeted by *C. difficile* toxin A and B with the addition of a adenosine 5' mono-phosphate (AMP) moiety. The conserved Fic domain with its invariant histidine residue is essential for VopS mediated ampylation of Rho GTPases. The addition of the AMP moiety by VopS resulted in Rho GTPases being unable to bind their downstream effectors (Yarbrough et al., 2009).

As well as modifying Rho GTPases by the addition of glycosyl, ADP, or AMP groups several bacterial factors such as the T3SS YopT of *Yersinia* can post translationally modify GTPases by proteolytic cleavage. YopT is a member of a family of cysteine proteases and has been demonstrated to cleave RhoA, Rac1 and Cdc42. Cleavage of these GTPases by YopT has been shown to result in a loss of the CaaX box at the C terminal of the GTPases (Shao et al., 2002). The CaaX box is a eukaryotic motif which is a target for prenylation in host cells, addition of a prenyl group to Rho GTPases allows them to be anchored in the plasma membrane (Pereira-Leal et al., 2001). Cleavage of the GTPase prenylation site by YopT results in the removal of active GTPases from the membrane, additionally YopT can also cleave inactive GTPases inhibiting their translocation to the membrane even after activation (Shao et al., 2002; Shao et al., 2003).

In addition to inactivating Rho GTPases, bacterial toxin can also render GTPases constitutively active. Cytotoxic necrotizing factor 1 and 2 (CNF) and Dermonecrotizing toxin (DNT) are toxins delivered by *Escherichia* and *Bordetella* species respectively. CNF and DNT posses' deaminase

activity which results in the removal of the amine group from a target amino acid within the GTPase. CNF toxins deaminase activity targets glutamine 63 in RhoA, Rac1 and to a lesser extent Cdc42 (Aktories et al., 2000). Glutamine 63 is essential for the hydrolysis of GTP so modification of this residue by CNF toxins results in an inability of Rho GTPases or GAPs to hydrolyse GTP rendering them constitutively active (Flatau et al., 1997; Paduch et al., 2001). In addition to its deaminase activity DNT also posses' a transglutamase activity which also targets glutamine 63 to inactivate GTP hydrolysis and activate Rho GTPases (reviewed in (Aktories et al., 2000)).

1.10.2 Bacterial Mimics of Host Rho GTPase Regulatory Factors

Many secreted bacterial effectors have evolved functional or structural characteristics of GEFs, GAPs, and GDIs in order to mimic their cellular activities to subvert GTPase signalling to the benefit of the bacteria. Perhaps the most well studied example of bacterial functional mimicry of a GTPase regulatory factor is the T3SS effector SopE of *Salmonella* which mediates bacterial invasion of mammalian cells via the formation of membrane ruffles (Hardt et al., 1998). SopE acts as a GEF of Cdc42 and Rac1 in order to promote the invasion of the *Salmonella* bacteria (Hardt et al., 1998). SopE is dissimilar in structure to canonical Dbl family mammalian GEFs and does not possess DH or PH domains. However upon binding of Cdc42, SopE induces almost identical shifts in the Cdc42 Mg^{2+} binding pocket and switch 1 and 2 regions (Buchwald et al., 2002). It has been demonstrated that SopE utilises residues which are equivalent to those in Dbl family GEFs to interact with Cdc42 (Buchwald et al., 2002). However the catalytic mechanism by which SopE promotes nucleotide exchange on Cdc42 is unique and involves the insertion of the SopE GAGA loop between the switch 1 and 2 pocket of Cdc42 (Schlumberger et al., 2003).

Other bacterial mimics of GEFs include SopE2 and BopE (Stender et al., 2000; Upadhyay et al., 2008).

Other bacterial effectors such as the T3SS effector SptP, which down regulates ruffle formation after *Salmonella* invasion, have been demonstrated to have GAP activity towards Rho GTPases (Fu and Galan, 1999). Structural determination of the SptP-Rac1 complex revealed that SptP is structurally dissimilar from mammalian GAPs. However, SptP still binds Rac1 between the switch 1 and 2 regions and donates a catalytic arginine to facilitate GTP hydrolysis (Stebbins and Galan, 2000). One key difference between SptP and mammalian RhoGAPs is the placement of the catalytic arginine, in cellular RhoGAPs the arginine is on a flexible finger whereas SptP's donor arginine is confined within an alpha helix. Other bacterial GAPs such as *Yersinia* YopE have been demonstrated to have a similar fold to SptP (Evdokimov et al., 2002).

The Yersinia T3SS effector YpkA forms a complex with Rac1 which is similar to that of Rac1 in complex with mammalian GDI proteins (Prehna et al., 2006). YpkA inserts an alpha helix into the switch 1 and 2 regions of Rac1 stabilising the GDP bound form of the GTPase. Interestingly, YpkA forms an almost identical acidic amino acid contact with Thr35 of Rac1 as host GDIs which provides a stable network between Rac1, YpkA and the Mg^{2+} ion (Prehna et al., 2006). YpkA efficiently inhibits both host GEF and GDI interaction with Rac1 suggesting that the YpkA-Rac1 interaction is very stable (Prehna et al., 2006)

1.10.3 Bacterial Factors which Indirectly Modulate GTPase Activity

In addition to post translationally modifying Rho GTPases and mimicking their cellular regulators, bacteria can also influence their activity utilising a number of indirect strategies.

Instead of directly activating GTPases by acting as GEFs several bacterial effector proteins such as EspG of the A/E pathogens can activate endogenous mammalian Rho GEFs. EspG depolymerises microtubules resulting in the liberation of GEFH1 which subsequently activates RhoA resulting in the formation of stress fibres (Matsuzawa et al., 2004). As well as recruiting and activating GEFs other bacterial factor such as the Opa adhesins of *Neisseria gonorrhoeae* have been shown to bind the cellular CEACAM family of receptors to trigger Rac1 and Cdc42 activation (Billker et al., 2002).

Other bacterial factors such as *Staphylococcus* enterotoxin B (SEB) have been demonstrated to transcriptionally modulate Rho GTPase signalling. Expression of SEB unregulated the transcript level of RhoA whilst co-ordinately down regulating the transcript of the RhoA negative regulator Rnd3 resulting in a marked increase in the level of stress fibre production during *Staphylococci* infection (Ionin et al., 2008).

1.11 The WxxxE Family of Effectors.

WxxxE proteins were first described by Alto *et al* 2006 who grouped together 26 known effectors and named them after their conserved motif consisting of an invariant Tryptophan (W) and Glutamic acid (E) residue separated by three variable amino acids (Alto et al., 2006) (Figure 1.8). This new family of proteins includes effectors from EPEC, EHEC *Citrobacter rodentium*, *Shigella* and *Salmonella.* In this initial study it was demonstrated that ectopic expression of IpgB1 and IpgB2 of *Shigella* and Map of EHEC resulted in the induction of membrane ruffles, stress fibres and filopodia respectively (Alto et al., 2006). These phenotypes are reminiscent of those induced by constitutively active Rac1, RhoA and Cdc42 respectively (Etienne-Manneville and Hall, 2002). The WxxxE motif was subsequently shown to be essential for the biological activity of this novel effector family. Further work on IpgB2 demonstrated that inactivation of

RhoA via dominant negatives or the bacterial toxins YopT and C3 did not inhibit IpgB2 dependent stress fibre formation. Concordantly the authors demonstrated that IpgB2 binds to the RhoA effectors ROCK and mDia and stimulates the kinase activity of the former. This led the authors to propose that WxxxE effectors act as functional mimics of host Rho GTPases with IpgB2 mimicking RhoA, IpgB1 functioning as Rac1 and Map mimicking Cdc42 (Alto et al., 2006). However, a more recent study by Handa and colleagues reported that IpgB1 rather than mimicking Rac1 in fact utilises the mammalian bipartite ELMO-Dock180 GEF complex to activate Rac1 (Handa et al., 2007). Thus the mechanism by which WxxxE proteins exert their biological effect is in need of further clarification.

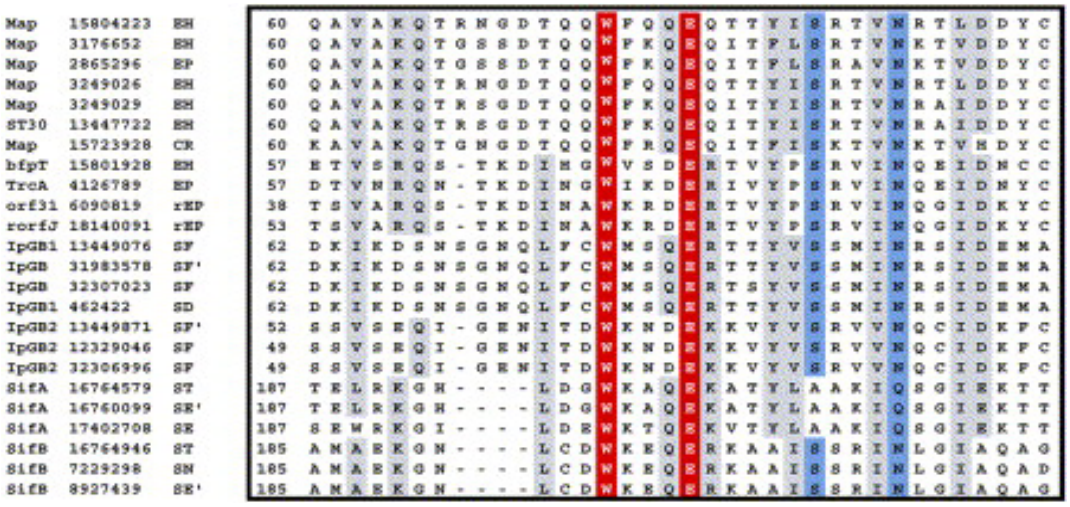


Figure 1.8 Alignment of the WxxxE region of the founding members of the WxxxE family of effectors. The conserved WxxxE motif after which this family of effectors is named is highlighted in red. Founding WxxxE family members included Map and TrcA from A/E pathogens, IpgB1 and IpgB2 from *Shigella* and SifA and SifB from *Salmonella*.

1.11.1Map

Map (mitochondrial associated protein) is encoded is a multifunctional T3SS effector protein encoded on the LEE pathogenicity island of the A/E pathogens upstream of the translocated intimin receptor Tir. Map was first demonstrated to localise to the mitochondria altering their morphology (Kenny and Jepson, 2000). Using mitochondria purified from yeast, Map was shown to gain access to the mitochondrial matrix using the TOM import machinery and the mitochondrial chaperone mtHsp70 resulting in a loss of mitochondrial membrane potential (Papatheodorou et al., 2006). Further work has demonstrated that expression of a GST-Map fusion in yeast results in a potent growth defect, mislocalisation of cortical actin and abnormal septin formation suggesting that map signalling may interfere with yeast polarity (Rodriguez-Escudero et al., 2005). Other studies have revealed that Map functions to induce formation of filopodia in a Cdc42 manner at early time points during EPEC and EHEC infection (Berger et al., 2009; Kenny et al., 2002). Map is also known to interact with EBP50/NHERF1 in a PDZ domain dependent manner. Deletion of the DTRL C-terminal region of Map which is a consensus PDZ binding motif resulted in a reduction in the longevity of filopodia (Berger et al., 2009) (Simpson et al., 2006). It has also been demonstrated that depletion of NHERF1 from cells can abolish Map mediated filopodia formation (Alto et al., 2006). Several studies have also implicated Map in disruption of tight junctions and inhibition of mitochondrial fission and fusion (Dean and Kenny, 2004; Papatheodorou et al., 2006). Interestingly, expression of a Map-GST construct which localised specifically to mitochondria lacked toxicity in yeast (Rodriguez-Escudero et al., 2005), suggesting that import of Map to the mitochondria may be represent a mechanism by which the cytoplasmic functions of Map, such as its ability to trigger Cdc42-dependent actin rearrangements and disruption of epithelial barrier function, may be regulated

(Dean and Kenny, 2004; Kenny et al., 2002) It has also been demonstrated that a *C. rodentium* map mutant is attenuated for virulence in a mouse model (Mundy et al., 2004).

1.11.2 TrcA

TrcA was first identified as a gene which responded to transcriptional regulation by the transcription initiator complex *bfpTVW* which is known to co-ordinately upregulate bundle forming pili (BFP) and intimin expression (Gomez-Duarte and Kaper, 1995; Tobe et al., 1996). TrcA was found to act as chaperone for the BfpA component of the BFP and deletion of TrcA results in a reduction of BFP expression and a decrease in size of EPEC microcolonies. Pulldown assays also detected an interaction between TrcA and Intimin within the bacterial cytoplasmic compartment (Tobe et al., 1999). More recently a homolog of TrcA in EHEC Sakai was demonstrated to be secreted in a T3SS dependent manner (Tobe et al., 2006).

1.11.3 IpgB1

Shigella is an invasive pathogen which gains entry to host cells in a T3SS dependent manner, after initial invasion *Shigella* species escape from the phagosome to the cytoplasm where they can replicate (Cossart and Sansonetti, 2004). Colonisation of the gut by *Shigella* species is characterised by destruction of the host colonic epithelium and a subsequent inflammatory response (Schroeder and Hilbi, 2008). IpgB1 was identified in two separate transponson mutagenesis screens to identify proteins involved in invasion of *Shigella* strains into HeLa cells and those involved in virulence (Maurelli et al., 1985; Sasakawa et al., 1988). The secretion of IpgB1 by the *Shigella* Mxi/Spa T3SS was then described by Buchrieser and colleagues (Buchrieser et al., 2000). Furthermore IpgB1 is translocated into host cells in a T3SS dependent manner (Ohya et al., 2005). The study of Ohya et al demonstrated that IpgB1 induced formation

of membrane ruffles in Rac1 and Cdc42 dependent manner which participate in invasion of non-phagocytic cells by *Shigella* (Ohya et al., 2005). A follow up study by Handa and co-workers has shown that IpgB1 binds to the mammalian protein ELMO which in turn is a binding partner for the atypical GEF Dock180. The IpgB1-ELMO-Dock180 tripartite complex activates Rac1 in an ELMO and Dock180 dependent manner resulting in formation of membrane ruffles (Handa et al., 2007).

1.11.4 IpgB2

IpgB2 is another substrate of the Shigella Mxi/Spa T3SS which is translocated into host cells (Hachani et al., 2008). Alto et al have reported that ectopic expression of IpgB2 induces formation of stress fibres in a RhoA independent manner. Furthermore IpgB2 was shown to interact with ROCK and mDia and to stimulate the kinase activity of ROCK *in vitro* (Alto et al., 2006). IpgB2 has also been implicated in triggering host cell NF-κB activation in response to *Shigella* infection (Fukazawa et al., 2008).

1.11.5 SifA

Salmonella is an intracellular pathogen that resides within a vacuole which is extensively modified by a range of T3SS effector proteins in order to allow the replication of *Salmonella* within epithelial and macrophage cells (Steele-Mortimer, 2008). SifA was first identified in a mutagenesis screen to determine virulence factors responsible for the formation of filaments rich in lysosomal glycoproteins induced by *Salmonella* infection. These structures are referred to as *Salmonella* Induced Filaments (Sifs) from where the gene derives its name. It was also shown that a *sifA* mutant was attenuated in a mouse model of infection (Stein et al., 1996). SifA was subsequently demonstrated to be secreted by the Spi2 T3SS (Miao and Miller, 2000). SifA is

also implicated in the maintenance of the *Salmonella* Containing Vacuole (SCV) as a *sifA* mutant loses its vacuole and is released into the cytoplasm (Beuzon et al., 2000). It has also been shown that SifA is essential for the replication of *Salmonella* within macrophages and that ectopic expression of SifA results in vacuolation of host cell Lamp1 rich compartments (Brumell et al., 2001). Interestingly, SifA posses a C-terminal CaaX box which is normally associated with prenylation and membrane anchoring and is commonly found in Rho GTPase. This C-terminal domain was found to be prenylated in host cells and is essential for SifA targeting to the host cell membranes and for the formation of Sifs (Boucrot et al., 2003; Reinicke et al., 2005). SifA has been shown to bind to the SifA and Kinesin Interacting Protein (SKIP). Interaction of SifA with SKIP results in a displacement of kinesin from the SCV (Boucrot et al., 2005). It has also been shown that SifA interacts with the Spi1 secreted effector SipA to modulate positioning and morphology of the SCV (Brawn et al., 2007). More recently SifA has been shown to be an agonist of Rab9 via its interaction with Skip which is also a Rab9 effector (Jackson et al., 2008).

1.11. 6 SifB

Although SifB is related by sequence homology to SifA little is known about its contribution to *Salmonella* virulence. SifB has been demonstrated to be secreted in conditions which are known to upregulate the Spi2 T3SS (Hansen-Wester et al., 2002). A *Salmonella* mutant in the *sifB* gene is not significantly attenuated for intracellular replication or in a mouse model (Ruiz-Albert et al., 2002). It has also been shown that SifB localises to the SCV and subsequently traffics away from the vacuole along Sifs (Freeman et al., 2003).

1.12 The EspM Family of Effectors and EspT.

Alto and colleagues identified the T3SS protein Map which is conserved in all A/E pathogens as one of the founding WxxxE effectors. TrcA was also reported to be a member of the WxxxE family (Alto et al., 2006). Interestingly, TrcA is encoded on a poorly conserved genomic loci which is present only in a subset of atypical *E. coli* including EPEC B171 O111:NM. In order to establish if the A/E pathogen group encodes other WxxxE effectors in discrete genomic loci we performed a BLAST analysis using Map and IpgB2 as reference proteins. Several IpgB2-like proteins were identified in EHEC O157:H7 strain Sakai, *C. rodentium* and EPEC B171 which we termed EspM1, EspM2 and EspM3. EspM1 and EspM2 from EHEC Sakai have previously been shown to be secreted in a T3SS dependent manner (Tobe et al., 2006). Additionally we identified a protein in *C. rodentium* and EPEC E110019 O111:H9 which we have named EspT which harbours the WxxxE motif but shares little homology with previously identified family members.

1.13 Aims

The EspM family of proteins and EspT have not been characterised. The current study was designed to determine if the EspM proteins and EspT are T3SS WxxxE effectors and to elucidate their mechanism of action and their effect on cellular signalling. In order to do this we aim to:

1. Confirm the status of the EspM proteins and EspT as T3SS effector proteins.
2. Establish if translocation or ectopic expression of the EspM and EspT proteins results in an alteration of the host cell cytoskeleton.
3. Elucidate the role of Rho GTPases in EspM and EspT mediated phenotypes.
4. Define the mechanism by which WxxxE proteins modulate Rho GTPase.
5. Determine the role of the EspM and EspT WxxxE effectors in A/E pathogen virulence strategies.

Chapter 2 – Experimental Procedures

2.0 Bacteria Strains

Bacterial strains used in this study are listed in Table 1. The E2348/69 Δ*escN* T3SS null mutant strain was constructed using the using the one-step PCR λ-red-mediated mutation protocol (Datsenko and Wanner, 2000) by Junkal Garmendia (Garmendia et al., 2004). The *C. rodentium* Δ*tir* and *C. rodentiun* Δ*espT* mutants were also constructed using the λ-red-mediated mutation protocol (Datsenko and Wanner, 2000) by Dr. Rosanna Mundy and Dr. Benoit Raymond respectively. The λ red phage mediated knock out protocol is based on the amplification of a chloramphenicol or kanamycin gene from pKD3 or pKD4 respecively flanked by regions of the gene which are targeted for knock out. The antibiotic resistance gene is then inseted into the genome in place of the tagetted gene via homologous recombination mediated by the λ red phage recombinase encoded on the pKD46 suicide vector. The O111:H2 E110019 strain was a kind gift from James Kaper and was isolated from an outbreak in Finland (Viljanen et al., 1990). *Salmonella enterica* Typhimurium strain SL1344 was kindly provided by Mark Stevens.

All strains were maintained on Luria–Bertani (LB) broth or agar supplemented with ampicilin (100μg/ml) or kanamycin (50μg/ml). Plates were grown for 16 hours at 37°C and liquid cultures were incubated at 37°C with agitation of 200 RPM for 16 hours. Bacterial strains used in this study as listed in Table 2.

2.1 Bioinformatics

A PSI-BLAST search (Altschul *et al.*, 1997) was performed under default conditions using IpgB2 from *Shigella flexneri* (gi:13448971) and Map from EPEC (gi:2865296) as query sequences to search the latest version of the NCBI NR database and combined with a library of peptide sequences derived from all coding sequences ≥50 codons in length from the genome sequences of *Citrobacter rodentium* ICC168, EPEC B171, E110019 and EPEC E2348/69.

Using the sequence alignment program ClustalW2 (Larkin *et al.,* 2007), a phenogram was constructed based upon hierarchical clustering of EspT, EspM2 and EspM3 form *C. rodentium*, EspM1 from EPEC B171, and IpgB1 and IpgB2 form *Shigella flexneri*.

2.2 Constructs and Cloning

Plasmids and primers used to construct them are listed in Table 2 and primer sequences are listed in Table 1. The genes encoding the effector proteins were amplified by PCR from genomic DNA and cloned into pSA10 with a C-terminal HA tag (YPYDVPDYA). *espM2* and *espM1* genes were amplified from EHEC O157:H7 strain Sakai, *trcA* and *espM1* genes were amplified from EPEC O111:H- strain B171 and *espM2*, *espM3* and *espT* genes were amplified from *Citrobacter rodentium* strain ICC169 to construct plasmids pICC398, pICC401, pICC402, pICC403, pICC400, pICC399 and pICC427 respectively. *espM2* from EHEC Sakai, *espT* from *C. rodentium* and *ipgB1* from *Shigella flexneri* were also cloned into pRK5 with an N terminal Myc Tag (EQKLISEEDL) to create pICC228, pICC320 and pICC429 respectively. *espM2 and* $espM2^{29\text{-}196}$ from EHEC O157:H7 Sakai in addition *sifA* from *S.* Typhimurium was inserted into the pET28a (Novagen) vector with a C terminal His tag (HHHHHH) for protein purification to create the plasmid pICC454. PCRs were performed using Platinum Taq (Invitrogen) using an initial temperature of 94°C followed by 30 cycles of denaturing 94°C for 45 seconds, annealing temperature of 55°C for 60 seconds and an extension of 68°C for 30 seconds per kilobase amplified. Annealing temperature was adjusted depending on the melting point of the primers used. PCRs were purified using the QIAquick® Gel Extraction Kit (QIAGEN). The vectors pSA10, pRK5 and pet28a were maintained in *E. coli* Top10 cells and extracted using the QIAprep Spin Miniprep Kit (QIAGEN). The Plasmids and PCR products were then digested with the appropriate restriction enzymes (NEB) overnight at 37°C. The digested products were

repurified using a QIAquick® PCR Purification Kit. All ligations were carried out overnight using T4 ligase (NEB) at 16°C.

The mammalian expression vector pRK5 containing one of Rho^{N19}, Rac^{N17} or $Cdc42^{N17}$ dominant negatives used in the transfection assays were generously provided by Nathalie Lamarche-Vane. The vector pGEX expressing the binding domain of Rhotekin fused to GST was kindly supplied by J. Bertoglio. The pDSRed Wave dominant negative constructs were provided by Laura Machesky via Rey Carabeo. The pEGFP-C1 mammalian expression vector containing the $RhoG^{N17}$ and $ELMO^{T625}$ dominant negatives and ELMO1 along with the pCXN2 vector with the FLAG tagged $Dock180^{ISP}$ were kindly supplied by Yutaka Handa and Chihiro Sasakawa (Handa et al., 2007). The vector pMW172-His expressing RhoA or Rac1 fused to a His Tag (HHHHHH) was a gift from Michael Way.

2.3 Site Directed Mutagenesis

Site directed mutagenesis was carried out using a Quickchange® II kit (Stratagene) according to the manufacturer's instructions. Primers were designed using the Quickchange mutagenic primer design program (Stratagene). Plasmids pRK5::*espM2*$^{29\text{-}196}$,pET28::*espM2*$^{29\text{-}196}$, pSA10::*espM2* and pSA10::*espT* were used as template for the mutagenic reactions. Colonies were screened by sequencing.

2.4 Cell Culture

Swiss 3T3 cells were maintained in DMEM with 4500mg/ml glucose and supplemented with 15% foetal calf serum (Gibco) and 4mM Glutamax (Gibco) with non-essential amino acids. HeLa cells were cultured in DMEM with 1000 mg/ml glucose and supplemented with 10% foetal calf serum (Gibco) and 4mM Glutamax (Gibco). Cells were passaged every two days and by

trypsination with EDTA supplemented with 2.5% trypsin. Cells were then re-suspended in the appropriate growth media and harvested at 1500 RPM for 3 minutes before re-suspension in an appropriate volume to achieve a confluence of 50-75% as required. Caco2 cells were grown in DMEM with 4500 mg/ml glucose and supplemented with 20% foetal calf serum (Gibco) and 4mM Glutamax (Gibco) with non-essential amino acids. The media was changed every day for 12 days until the cells had polarised. All cell lines were maintained in an incubator at 37°C in a 5% CO_2 atmosphere. Serially cultured cells were not used above a passage of 20.

2.5 *In Vitro* Infections

24 well plates were seeded with an autoclaved glass coverslip prior to addition of Swiss 3T3, HeLa or Caco2 cells which were split as described above in order to achieve a confluence of 50%, 70%, and 100% respectively in each well. 6 hours prior to infection the 24 well plates seeded with Swiss 3T3, HeLa and Caco2 cells were washed twice in sterile PBS and 500 µl serum free media was added to each well. Overnight cultures of the appropriate bacteria were inoculated 1:50 into DMEM and primed as described previously (Collington et al., 1998). Expression of proteins from pSA10 was induced by the addition of 500mM IPTG 30 minute prior to infection. 500µl of primed bacteria were added to the wells, and the plates were then centrifuged at 900 RPM for 5 min. Infections were carried out at 37°C in 5% CO_2 for the appropriate amount of time.

2.6 β Lactamase (TEM) T3SS Dependent Translocation Assay

HeLa cells were seeded on to glass coverslips for infection as previously described. EPEC E2348/69 wild type and the Δ*escN* T3SS null mutant were transformed with the pCX340 vector

encoding a TEM-1 fusion of EspM2, EspM and EspT from *C. rodentium* and an NleD positive control from EHEC O157:H7 Sakai. The bacteria were cultured overnight and primed as described previously. Expression of the fusion protein was induced by the addition of 500mM IPTG for 1 hour. The strains were then used to infect the HeLa cells for 90 minutes. After infection, cells were washed 3 times with PBS and loaded with the fluorescent substrate CCF2-AM (Invitrogen), and incubated at room temperature in the dark for 1.5 h. Cells were then washed 3 more times in PBS. The cells were then visualised using a Nikon Eclipse E600 fluorescence microscope using a UV-2A filter (330-380nm excitation). Cleavage of the CCF2-AM substrate by the TEM-1 β-lactamase fusion proteins was detected by an emission of blue fluorescence indicating translocation of the effector fusion protein. Conversely, green fluorescence due to the presence of uncleaved CCF2-AM substrate is indicative of an absence of translocated fusion protein within the eukaryotic cells (Charpentier and Oswald, 2004). Images were taken using a Nikon digital camera DXM1200 and processed using Adobe Illustrator.

2.7 Immuno-fluorescence Staining and Microscopy

Coverslips were washed 3 times in PBS and fixed with PBS supplemented with 3% paraformaldehyde (PFA) for 15 min before washing 3 more times in PBS. For immuno-staining, the cells were permeabilised for 5 min in PBS 0.5% Triton X100, washed 3 times in PBS and quenched for 30 min with 50mM NH_4Cl. The coverslips were then blocked in PBS supplemented with 2% bovine serum albumin (BSA) for 1 hour. Cover slips were incubated with primary antibodies diluted to the appropriate concentration in PBS with 1% BSA in a humidified chamber for 1 hour at room temperature. A list of primary antibodies and the working concentrations used in this study can be found in Table 4. The coverslips were then washed a

further 3 times in PBS. The cells were then incubated with secondary antibodies, phalliodin, and Dapi stain diluted in PBS with 1% BSA in a humidified chamber for 45 minutes at room temperature. A list of secondary antibodies and reagents along with the working concentration utilised in this study can be found in Table 5. The coverslips were then washed 3 times in PBS before a 10 min incubation in fresh PBS. The coverslips were then washed 1 more time in distilled deionised water before mounting on glass cover-slides with Prolong Gold Antifade mounting reagent (Invitrogen). Cells were visualized by Zeiss Axioimager immunofluorescence microscope (100X objective giving a total magnification of 1000X) using the following excitation wavelengths: Cy3 – 605nm, Cy5 – 690nm and Cy2– 525nm. All images were analysed using the Axiovision Rel 4.5 software and trimmed to 5 cm^2 (300 pixels) using Adobe Photoshop.

2.8 Differential Staining

Coverslips were fixed, washed and quenched as previously described. Pre-permeabilised samples were not treated with triton X100. The coverslips were then blocked for 1 h with PBS 1% BSA before incubation with a primary rabbit anti O127, O111 or a goat anti-LPS antibody to detect JPN15, E110019 and *S.* Typhimurium respectively. Secondary donkey anti rabbit and goat antibodies coupled to a Rhodamine (RRX) fluorophore as described above. Cells were then washed 6 times in PBS before permeablisation with Triton X100 as described previously. The post permeabilised coverslips were then stained with a primary rabbit anti O127, O111 or a goat anti-LPS antibody to detect JPN15, E110019 and *S.* Typhimurium respectively. Secondary Donkey anti-rabbit and -goat antibodies coupled to a Cy2 fluorophore as described previously. Other antibodies and phalloidin were added to the second round of primary and secondary

antibodies as outlined above. The coverslips were then mounted on coverslides in Prolong Gold antifade mounting reagent (Invitrogen). Cells were visulised as described in 2.6.

2.9 Gentamycin Protection Invasion Assay

Cells seeded into the wells of a 24 well plate were infected as described above for 3 to 6 h at 37°C in 5% CO_2. The pre-gentamycin plates were washed 5 times in PBS and then permeabilzed for 15 minutes with 1% saponin in sterile water before plating in triplicate on LB plates in dilutions ranging from 10^0 to 10^{-7}. The post gentamycin samples were washed 5 times with PBS after the final wash the PBS was replaced with serum free DMEM containing 200µg/ml of gentamycin and the cells incubated for 1 h at 37°C in 5% CO_2. The plates were then washed a further 5 times in PBS before permeabilisation and plating as described above. The pre and post gentamycin plates were then incubated for 15 h in a static 37°C incubator and the colony forming units (cfu) were counted. The percentage of invasion was calculated based on the ratio of cfu on the pre and post gentamycin plates.

2.10 Confocal Microscopy

Samples were immuno-stained as described in 2.7 with the addition of phalloidin coupled to a Cy5 fluorophore. The cells were then mounted as described previously and were then visualised with a Leica Sp2 upright confocal microscope. X stacks were then taken through cells and images were processed with Adobe Photoshop.

2.11 Scanning Electron Microscopy (SEM)

Glass coverslips were seeded with Swiss 3T3 HeLa or Caco2 cells and infected for 2 h with the appropriate strains as described above. The cells were washed 3 times in phosphate buffer pH7.2 and then fixed with 2.5% Gluteraldehyde (Agar) in phosphate buffer pH7.2 for 15 min. The

coverslips were then washed with phosphate buffer pH7.2 for a further 3 times before being post fixed in 1% Osmium Tetroxide (Agar) for 1 h. The cells were then washed 3 times in phosphate buffer before being washed for 15 min in graded ethanol solutions from 50% to 100% to dehydrate the samples. The cells were then transferred to an Emitech K850 Critical Point drier and processed according to the manufacturer's instructions. The coverslips were coated in gold/palladium mix using a Emitech Sc7620 minisputter to a thickness of approximately 370Å. Samples for scanning electron microscopy (SEM) were then examined blindly at an accelerating voltage of 25 kV using a Jeol JSM-6390.

2.12 Transmission Electron Microscopy (TEM)

6 well plates were seeded with HeLa or Swiss 3T3 cells and infected for 2 h with the appropriate strains. The cells were washed 3 times in phosphate buffer pH7.2 and then fixed with 2.5% Gluteraldehyde in phosphate buffer pH7.2 for 15 min. The plates were then washed with phosphate buffer pH7.2 a further 3 times before being removed from the plate using a Teflon scraper and subsequently harvested into in eppendorf tube. The eppendorfs were then centrifuged at 10,000 RPM to pellet the cells. The cell pellets were post fixed in 1% Osmium Tetroxide (Agar) for 1 h, followed by 1% buffered tannic acid for 30 min and then a 1% aqueous sodium sulphate rinse for 10 min. The sample was dehydrated using an ethanol-propylene oxide series (with 2% uranyl acetate added at the 30% step) and embedded in Epon-araldite for 24 h at 60°C. Ultrathin sections (60nm) were cut with a Leica EMUC6 ultramicrotome, contrasted with uranyl acetate and lead citrate, and viewed with an FEI 120-kV Spirit Biotwin TEM. Images were obtained with a Tietz F415 digital TemCam. The Post fixation stages and imaging were kindly performed by David Goulding (Sanger Centre, Cambridge).

2.13 Transfection

Swiss 3T3 and HeLa cells were seeded at a density of $5x10^6$ cells per well 24 hour prior to transfection so as to achieve a 70% confluence. 3 hours before transfection the cells were washed twice in PBS and 500µl of serum free media was added to each well. Swiss 3T3 cells or HeLa cells were transfected with pRK5 encoding $RhoA^{N19}$, Rac^{N17}, $Cdc42^{N17}$ dominant negatives fused to a Myc tag, pEGFP-C1 containing $RhoG^{N17}$, $ELMO^{T625}$ dominant negatives with a GFP tag, pCNX2 containing $Dock180^{ISP}$ dominant negative with a FLAG tag, pDSRed containing Wave2wt, Wave2ΔBP, Wave2 ΔA or pRK5 encoding EspT, IpgB1, EspM2 by lipofectamine 2000 (Invitrogen) at 1µl per well for HeLa cells and 1.5µl per well in Swiss 3T3 cells as per the manufacturer's recommendations. All plasmid constructs were transfected at 0.8µg of DNA per well. The DNA and lipofectamine were diluted in 50ul of Optimem media per well for 5 minutes. The lipofectamine was then added to the DNA for 15 minutes to allow complexes to form before addition to the wells. The cells were incubated at 37 °C in a humidified incubator with 5% CO_2 for 16 h, washed twice in PBS before having their media replaced with complete DMEM as described previously. The transfected cells were then fixed or infected with an appropriate strain as described above.

2.14 siRNA

Swiss 3T3 cells were seeded at a density of approximatetly $5x\ 10^6$ cells per well 24 h prior to transfection of either Wave2 siRNA pool or a non-targeting pool supplied by Dharmacon using HiPerFect (Qiagen) according to the manufacturers instructions. The media was changed 16 h after transfection and the cells were allowed to recover for 12 h before being trypsinated and seeded at a density of 5×10^6 cells. The siRNA procedure was repeated for a total of 3 rounds before the cells were used. Levels of Wave2 and tubulin were then detected by western blotting

using anti-wave2 (Santa Cruz) and anti-tubulin (Sigma) antibodies. Cells were then infected with the appropriate strain and processed for immuno-fluorescence microscopy as previously described.

2.15 Pharmacology

Swiss 3T3 or HeLa cells were seeded for infection as described previously. 2 hours prior to infection the cells were treated with the cell permeable PI-3K inhibitor Wortmannin at a concentration of 50 nM, the Src family kinase inhibitor PP2 and the control compound PP3 at concentration of 20 μM, the Rac1 GEF inhibitor NSC23766 at a 100μM concentration and the ROCK inhibitor Y-27362 at a concentration of 10μM per well. Cells were then infected with the appropriate strain as described previously.

2.16 GTP Activation GST Pulldown Assays

Overnight cultures of *E. coli* BL21 expressing pGEX encoding the RhoA binding domain of Rhotekin, the Cdc42 and Rac1 interacting domain (CRIB) of WASP and the Rac1 binding motif (RBM) of Pak were diluted 1:20 and cultured at 30°C until $O.D_{260nm}$ reached 0.7; the cultures was induced with 1 mM IPTG and incubated for a further 4 h. The bacterial cultures were then aliquoted into 50 ml falcon tubes and centrifuged for 15 min at 4600 rpm at 4°C and the pellets stored at -80°C. The pellets were re-suspended in lysis buffer (20% Saccharose, 10% glycerol, 50mM Tris pH 8, 200mM $Na_2S_2O_3$, 2mM $MgCl_2$, 2mM DTT and 1% of protease inhibitor cocktail (Sigma)) and sonicated 5 times for 10 seconds. The solutions were centrifuged for 30 min at 15,000 rpm at 4°C and the supernatants harvested and coupled to GST-glutathione S-transferase beads for 45 min at 4°C. 75 cm^2 cell culture flasks were seeded with Swiss 3T3 cells, infected as described above. The cells were then lysed in 750 μl of Mg^{2+} buffer (25 mM HEPES,

pH 7.5, 150 mM NaCl, 1% NP-40, 10 mM $MgCl_2$, 5% glycerol, 1mM EDTA and protease inhibitors (Sigma)). The lysate was transferred to a pre-chilled eppendorf tube and centrifuged at 14,000 RPM for 5 min at 4°C. The cleared lysate was transferred to a fresh pre-chilled eppendorf tube containing 30 µl of GST-Rhotekin-RBD, GST-WASP-CRIB or GST- Pak-RBM. The lysate was incubated with the beads for 1 h at 4°C. The suspension was washed 3 times in Mg^{2+} buffer spinning down at 14, 000 RPM at 4°C between each wash. The beads were eluted by the addition of 45 µl of 2 x protein loading buffer and the samples heated at 100°C for 5 min. The samples were loaded on 15% SDS PAGE gels. The gels were then transferred to PVDF membrane using wet transfer apparatus for 1 hour at 400V. The membranes were then blocked with 5% BSA in PBS 0.1% Tween for 1 hour. RhoA, Cdc42 or Rac1 were detected with monoclonal antibodies from Santa Cruz Biotechnology. Primary antibodies were diluted in TBS 0.1% Tween-20 supplemented with 3% BSA and incubated on the membrane with agitation for 1 hour. The membrane was then washed 3 times in TBS 0.1% Tween-20 with shaking. Secondary antibodies coupled to HRP were also diluted in TBS 0.1% Tween-20 supplemented with 3% BSA and incubated for 45 mins with agitation. The membrane was then washed a further 5 times before incubation with ECL reagents (GE healthcare). The Western blots were then detected using chemiluminescence in a LAS 3000 Fugi imager. Densitometry was performed using ImageJ software. Results shown are representative of at least 4 independent experiments.

2.17 Detection of Cofilin Phosphorylation

48 h prior to infection Swiss 3T3 cells were seeded onto 6 well plates to attain a confluent monolayer. Each well was infected as described above. After a 1.5 h infection cells were lysed by addition of 4 x protein SDS-PAGE loading buffer. The lysate was harvested and heated at 100°C for 5 min before loading in duplicate onto a 12% SDS PAGE gel. The proteins were then

transferred to PVDF by wet transfer as described previously. The PVDF membranes were blocked overnight in TBS, supplemented with 5% BSA at 4°C with gentle rocking. Each membrane was incubated in either monoclonal mouse anti-cofilin (Cell Signalling Technology) or mouse anti Phospho-cofilin (Cell Signalling Technology) at a dilution of 1:1000 in TBS 0.1% Tween-20 supplemented with 3% BSA for 1 h at room temperature with gentle rocking. The membranes were washed 5 times in TBS 0.1% Tween-20 for 5 min. and incubated for 45 min with 1:3000 dilution of Goat anti-Mouse (Invitrogen) secondary antibody coupled to HRP at room temperature diluted in TBS 0.1% Tween-20 supplemented with 3% BSA. The membranes were developed using ECL reagents (GE healthcare) before detection using chemiluminescence in a LAS 3000 Fugi imager. Western blots were analysed by densitometry using ImageJ software. Results presented are the average of 5 independent experiments.

2.18 Preparation of Recombinant Proteins

B834 cells containing pET28a (*Nde*1/*Bam*H1 inserted *espM2*$^{29\text{-}196}$ or *SifA*) were grown at 310 K in LB broth containing 25μg ml^{-1} kanamycin until an $A_{600\ nm}$ of 0.6 was reached. Protein overexpression was induced by the addition of 1.0 mM IPTG. Cells were harvested after incubation at 30°C overnight (4500g 20 min 4°C). Cell pellets were resuspended in lysis buffer (20mM Tris pH8, 500mM NaCl, 1mM DTT, Complete EDTA-free protease inhibitor cocktail (Roche) and homogenised . After centrifugation (14000 g, 30 minutes, 4°C), the soluble fraction was applied to a 5ml His trap FF Column (GE Healthcare) in a gradient of 0 – 300mM imidazole. EspM2 fractions were pooled and purified using a Superdex 75 26/60 equilibrated in 20 mM Tris pH 8, 500mM NaCl, 10mM DTT, high salt due to the instability of the protein. Protein was liquid Nitrogen flash cooled and frozen at -80°C on the same day, after experiencing protein precipitation in samples kept at 4°C over 2-3 days.

Preparation of His-RhoA and His-Rac1 was identical with the following exceptions: Expression was constitutive; cells were harvested after incubation at 37°C overnight. Lysis buffer was 20mM Tris, 500mM NaCl, 20mM imidazole, 5mM $MgCl_2$. Size exclusion buffer was 20mM Tris, 200mM NaCl, 3mM $MgCl_2$, 1mM DTT. Protein purification was conducted by Ana Arbeloa and James Garnett (Imperial College, London). Purified His-GTPases were stripped of nucleotides by incubating them for 10 min at room temperature in binding buffer (20 mM Tris-HCl [pH 7.5], 100 mM NaCl, 2.5 ng of bovine serum albumin per ml, 10 mM EDTA, 0.1% Triton X-100, 1 mM dithiothreitol, 10% glycerol) supplemented with a cocktail of protease inhibitors.

2.19 Surface Plasmon Resonance

Surface Plasmon resonance was carried out in collaboration with James Lillington and Prof. Susan Lea (Oxford University). Experiments were carried out using a BIAcore™ 2000 System (Biacore AB, Sweden) at 20˚C. $EspM2^{29-196}$ was coupled to a CM5 sensor chip leading to a rise of 2000 Response Units per minute using standard amine coupling protocols (BIAcore Amine Coupling Kit BR-1000-50). HEPES buffered saline containing 5mM $MgCl_2$ was flowed throughout the experiment at 50 μl min^{-1}. Samples of RhoA/Rac1 were injected (in the same buffer) for 180 seconds duration over the $EspM2^{29-196}$ channel and over a RhoA control channel. Dissociation was followed for 1000 s from the end of injection after which regeneration of the surface was carried out with 25 mM NaOH. No loss of activity was seen after regeneration. Experiments (repeated three times) were carried out with i) varying concentrations of RhoA (ε= 18825 $M^{-1}cm^{-1}$) and Rac1 (ε= 23295 $M^{-1}cm^{-1}$) (concentration determined by Nanodrop Spectrophotometer, 0.005 – 50 μM), and with ii) fixed 4μM RhoA but varying concentrations of GDP/GTP (0.5 – 8 μM) added to the buffer. RhoA control channel subtracted signals are

presented (BIAEvaluation software). The same conditions were used to analyse the SifA-RhoA interaction. BIAcore analysis was performed by James Lillington (Oxford University).

2.19 Guanine nucleotide exchange analysis

In vitro GEF activity assay was carried out using RhoGEF exchange assay biochem kit (Cytoskeleton Inc. Denver) according to the manufacturer's instructions. The assay is based on GTP coupled to the fluorescent substrate *N*-methylanthraniloyl which when unbound has a low intrinsic fluorescence. The binding of the *N*-methylanthraniloyl labelled GTP to the GTP binding pocket of the GTPase results in a conformational shift which increases the substrates fluorescence emission. When a GEF is present there is marked increase in the loading of the *N*-methylanthraniloyl GTP into the GTP binding pocked of the GTPases and the subsequent increase in fluorescence is monitored using as fluorometer. Briefly, exchange reaction assay mixtures contained 20mM Tris pH 7.5, 50mM NaCl, 10mM MgCl2, 50µg/ml bovine serum albumin (BSA), 0.75µM *N*-methylanthraniloyl(mant)-GTP, and 2µM of Rac1-His, Cdc42-His, HRas or RhoA-His GTPase. Fluorescence spectroscopic analysis of mant-GTP was carried out using Fluostar Optima spectrometer. The fluorescence measurements were taken every 30 s with excitation and emission wavelengths of 360nm and 440nm respectively. After 5 readings (150 s), purified EspM2$^{29\text{-}196}$ was added and the relative mant fluorescence was monitored every 30 s for a total time of 30 min. Experiments were performed in triplicate.

2.20 NMR sample preparation and backbone assignment of EspM2$^{29\text{-}196}$

All NMR experiments were carried out by Professor Steve Matthews and James Garnett, Imperial College London. Uniformly ^{15}N ^{13}C-labelled EspM2$^{29\text{-}196}$ was expressed in ^{15}N ^{13}C-labelled rich media (Cambridge isotopes). After purification as described above the sample was

dialysed against NMR buffer (50mM $NaPO_4$ pH 7.5, 150mM NaCl, 5mM DTT, 10% (*v*/*v*) D_2O) and concentrated to 0.9mM. Backbone assignment for ~65% of EspM2$^{29\text{-}196}$ was achieved using standard double- and triple-resonance assignment experiments (Sattler *et al*., 1999) at 20°C. Structural assignment and NMR was carried out by James Garnett and Steve Matthews (Imperial College, London)

2.21 NMR titration of RhoA against EspM2$^{29\text{-}196}$

^{15}N ^{13}C-labelled EspM2$^{29\text{-}196}$ was mixed with unlabelled His-RhoA (dialysed in NMR buffer) ranging from 0x to 7x molar excess and ^{15}N TROSY-HSQC experiments were performed at each increment at 25°C. 5mM GTP was added to the sample of EspM2$^{29\text{-}196}$ saturated with RhoA and a final ^{15}N TROSY-HSQC was carried out. NMR work was conducted by James Garnett and Steve Matthews (Imperial College, London).

2.22 Screening of Clinical Isolates

Screening experiments were carried out in collarboration with Prof. Jorge Blanco and Tania Gomes. Colonies from clinical isolates were streaked on a plate so as to achieve single colonies. Colony PCRs were performed using Taq polymerase (Invitrogen) using an initial temperature of 94°C for 5 minutes followed by 30 cycles of denaturing 94°C for 45 seconds, annealing temperature of 55°C for 60 seconds and an extension of 72°C for 30 seconds per kilobase amplified. Annealing temperature was adjusted depending on the melting point of the primers used (Table 1).

Table 1 Primers used in this study

Primer Number	Primer Name	Primer Sequence
1	EspM3-S9A_S12A-F	5'-ccagtgaatgttcaaggtttagcttttaatgcttttggtatcagctgccatc-3'
2	EspM3-S9A_S12A-R	5'-gatggcagctgataccaaaagcattaaaagctaaaccttgaacattcactgg-3'
3	EspM3-W66A-F	5'-gcagagtactaaagatattgatggagcgataaaagatgaacagaaagtgtat-3'
4	EspM3-W66A-R	5'-atacactttctgttcatcttttatcgctccatcaatatctttagtactctgc-3'
5	EspM3-H125A-F	5'-ggagcagctcaaagctccatcaatgctatgataataggaaatggtt-3'
6	EspM3-H125A-R	5'-aaccatttcctattatcatagcattgatggagctttgagctgctcc-3'
7	EspM3-Y188F-F	5'-gtatgattcctcgttatatgaggtttgctatatcgctgtacc-3'
8	EspM3-Y188F-R	5'-ggtacagcgatatagcaaacctcatataacgaggaatcatac-3'
9	EspM3-D115A-F	5'-ttatggcctggaacttgcttctggagcagctcaaa-3'
10	EspM3-D115A-R	5'-tttgagctgctccagaagcaagttccaggccataa-3'
11	EspM3-L114A-F	5'-tttcaaagcattatggcctggaagctgattctggagcagc-3'
12	EspM3-L114A-R	5'-gctgctccagaatcagcttccaggccataatgctttgaaa-3'
13	EspM2Cr-W66A-F	5'-ggcagagcactaaagatcttttagcagcgaaaaaagatgaaaaagtaatttatc-3'
14	EspM2Cr-W66A-R	5'-gataaattacttttttcatctttttttcgctgctaaaagatctttagtgctctgcc-3'
15	EspM2Cr-H125A-F	5'-gcccgctcagcacaaagttctataaatgctatcataaccggaaa-3'
16	EspM2Cr-H125A-R	5'-tttccggttatgatagcatttatagaactttgtgctgagcgggc-3'
17	EspM3-K149A-F	5'-cgaggggatgaccaggaatgtagcaaatcatacatcagattacatg-3'
18	EspM3-K149A-R	5'-catgtaatctgatgtatgatttgctacattcctggtcatcccctcg-3'
19	EspM3-W66Y-F	5'-gcagagtactaaagatattgatggatatataaaagatgaacagaaagtgtatcc-3'
20	EspM3-W66Y-R	5'-ggatacactttctgttcatcttttatatatccatcaatatctttagtactctgc-3'
21	EspM3-E70D-F	5'-tgatggatggataaaagatgatcagaaagtgtatccatcaagg-3'
22	EspM3-E70D-R	5'-ccttgatggatacactttctgatcatcttttatccatccatca-3'
23	EspM2-W70Y-F	5'-gcagagtactaaagatattgatgagtatataaaagatgaacggatagtatatcc-3'
24	EspM2-W70Y-R	5'-ggatatactatccgttcatcttttatatactcatcaatatctttagtactctgc-3'

25	EspM2-E74D-F	5'-taaagatattgatgagtggataaaagatgatcggatagtatatccctc-3'
26	EspM2-E74D-R	5'-gagggatatactatccgatcatcttttatccactcatcaatatcttta-3'
27	EspM1-pKK-F	5'-ttgaattcatgccagtaaatgcgacagg-3'
28	EspM1-pKK-R	5'-ccaatgcactgcagttaagcgtagtctgggacgtcgtatgggtacccctgtataacacgactca-3'
29	EspM2-pKK-F	5'-tttgaattcatgccgatgaatactacaggtatgt-3'
30	EspM2-pKK-R	5'-tttctgcagtcaagcgtagtctgggacgtcgtatgggtatccctgtatagcacgcatcaa-3'
31	EspM2 W70A-F	5'-gcagagtactaaagatattgatgaggcgataaaagatgaacggatagtatat-3'
32	EspM2 W70A-R	5'-atatactatccgttcatcttttatcgcctcatcaatatctttagtactctgc-3'
33	EspM3-pKK-F	5'-ttgaattcatgccagtgaatgttcaagg-3'
34	EspM3-pKK-R	5'-ttgcctgcagttaagcgtagtctgggacgtcgtatgggtacacgatatagcatacctca-3'
35	EspM2Cr-pKK-F	5'-ttgaattcatgccagcgaatatatcagg-3'
36	EspM2Cr-pKK-R	5'-ttgtcgacttaacttaagcgtagtctgggacgtcgtatgggtatgccgacatggcatttgcca-3'
37	TrcA-pKK-F	5'-ttgaattcatgccgatgaatactacaagtac-3'
38	TrcA-pKK-R	5'-aactgcagttaagcgtagtctgggacgtcgtatgggtatgcctgtatagcacacctca-3'
39	EspM1 B171-pKK-F	5'-tacccatacgacgtcccagactacgct-3'
40	EspM1 B171-pKK2-R	5'-ccaatgcactgcagttaagcgtagtctgggacgtcgtatgccgatatgacgctggcag-3'
41	EspT-HA-F	5'-ttgaattcatgccgggaacaataagctccag-3'
42	EspT-HA-R	5'-ttctgcagttaagcgtagtctgggacgtcgtatgggtaggttctctgagcctcctgaa-3'
43	EspT-pRK5-F	5'-cgcggatccatgccgggaacaataagctccag-3'
44	EspT-pRK5-R	5'-ccaatgcactgcagttaggttctctgagcctcctgaa-3'
45	EspM2-pRK5-F	5'-tttcgatccggatccggagcaatgcaaattctaaacaaaatac-3'
46	EspM2-pRK5-R	5'-tttgaattctcatccctgtatagcacgcatca-3'
47	IpgB1-pRK5-F	5'-tttggatccggagcaatgcaaattctaaacaaaatac-3'
48	IpgB1-pRK5-F	5'-ccaatgcattggttctgcagttaatttgtattgctttgac-3'
49	EspT-E110019-F	5'- ttgaattcatgccaggaacagtaaactcc-3'
50	EspT-E110019-R	5'- ccaatgcattggttctgcattaaacatattttaaatttctc -3'
51	espM2(29-196)-His F	5'-catgccatgggacatcatcatcatcatcacggaggagggaagaaggatatgaggtcgt-3'
52	espM2(29-196)-His R	5'-aagaattctcatccctgtatagcacgca-3'
53	sifA-His F	5'-ggaattccatatgatgccgattactataggga-3'
54	sifA-His R	5'-aaagaattcttataaaaaacaacataaacagccgc-3'
55	espM2(29-196)-myc F	5'-tttgaattcagggaagaatgatgaggtcgt-3'
56	espM2(29-196)-myc R	5'-ccaatgcattggttctgcagtcatccctgtatagcacgca-3'
57	espM2 W70A F	5'-gcagagtactaaagatattgatgaggcgataaaagatgaacggatagtatat-3'
58	espM2 W70A R	5'-atatactatccgttcatcttttatcgcctcatcaatatctttagtactctgc-3'
59	espM2 L118A F	5'-ccaggagaatcaactaaccgctgatgttaaggcagcacaa-3'
60	espM2 L118A R	5'-ttgtgctgccttaacatcagcggttagttgattctcctgg
61	espM2 Q124A F	5'-actaacccttgatgttaaggcagcagcaagttctattaatcatgtaataatg-3'
62	espM2 Q124A R	5'-cattattacatgattaatagaacttgctgctgccttaacatcaagggttagt-3'

63	espM2 I127A F	5'-gatgttaaggcagcacaaagttctgctaatcatgtaataatggggagtgc-3'
64	espM2 I127A R	5'-gcactccccattattacatgattagcagaactttgtgctgccttaacatc-3'
65	EspM-1 screening	5’-tctttcagctctttggtat-3’
66	EspM-2 screening	5’-ccaaaagaagcattccccattat-3’
67	EspM-3 screening	5’-tgatgaggtcatgaaatgttcaat-3’
68	EspM-4 screening	5’-atgattaatagaactttg-3’
69	EspTSc-1 screening	5’-aatctcattctcttatc-3’
70	EspTSc-2 screening	5’-tcatgtgatgagtggatg-3’
71	EspTSc-3 screening	5’-atagatggtttctttttagg-3’
72	EspTSc-4 screening	5’catccaacgagaaaccgcaat-3’
73	EspTSc-5 screening	5’-ccggaattcatgccgggaacaataagctccag-3’
74	EspTSc-6 screening	5’-gggaagcttttaggttctctgagcctc-3’
75	EspTSc-7 screening	5’-ttgaattcatgcatagcatgccagga-3’
76	EspTSc-8 screening	5’-ccaatgcactgcagggagcattaaacatattttaaatttctc-3’
77	EspTW63AF	5'-gaaaaacgaaggaaaaatgaatgaggcgatgagggaagaatgtatttgcttt-3'
78	EspTW63AR	5'-aaagcaaatacattcttccctcatcgcctcattcatttttccttcgtttttc-3'

Table 2 Plasmids used in this study

Name	Description	Primers	Reference
pSA10	pKK177-3 with Lac^q		(Schlosser-Silverman et al., 2000)
pICC398	pSA10::*espM2* O157: H7 Sakai fused to HA	29 + 30	(Arbeloa et al., 2008)
pICC399	pSA10::*espM3* *C. rodentium* ICC169 fused to HA	33 + 34	(Arbeloa et al., 2008)

pICC400	pSA10::*espM2 C.rodentium* ICC169 fused to HA	35 + 36	(Arbeloa et al., 2008)
pICC401	pSA10::*espM1* O157: H7 Sakai fused to HA	27 +28	(Arbeloa et al., 2008)
pICC402	pSA10::*trcA* O111:NM B171 fused to HA	37 + 38	(Arbeloa et al., 2008)
pICC403	pSA10::*espM1* O111:NM B171 fused to HA	38 + 40	(Arbeloa et al., 2008)
pICC404	pSA10::*espM2*-W70A fused to HA	31 +32	(Arbeloa et al., 2008)
pICC405	pSA10::*espM2*-W70Y fused to HA	23 + 24	(Arbeloa et al., 2008)
pICC406	pSA10::*espM2*-E74D fused to HA	25 + 26	(Arbeloa et al., 2008)
pICC407	pSA10::*espM3*-W66A fused to HA	3 + 4	(Arbeloa et al., 2008)
pICC408	pSA10::*espM3*-W66Y fused to HA	19 + 20	(Arbeloa et al., 2008)
pICC409	pSA10::*espM3*-S9A + S12A fused to HA	1 + 2	(Arbeloa et al., 2008)
pICC410	pSA10::*espM3*-L114A fused to HA	11 + 12	(Arbeloa et al., 2008)
pICC411	pSA10::*espM3*-D115A fused to HA	9 + 10	(Arbeloa et al., 2008)

pICC412	pSA10::*espM3*-H125A fused to HA	5 + 6	(Arbeloa et al., 2008)
pICC413	PSA10::*espM3*-K149A fused to HA	17 + 18	(Arbeloa et al., 2008)
pDEST53::*espM2*	EspM2 transfection vector	45 + 46	(Arbeloa et al., 2008)
pRK5::*myc-rhoA*^{N17}	Dominant negative RhoA		(Pelletier et al., 2005)
pRK5::*myc-rac1*^{N17}	Dominant negative Rac1		(Pelletier et al., 2005)
pRK5::*myc-cdc42*^{N17}	Dominant negative Cdc42		(Pelletier et al., 2005)
pGex::*gst-Rhotekin RBD*	pGex::*gst-Rhotekin RBD*		(Sander and Collard, 1999)
pEGFPC1::*GFP-rhoGN19*P	Dominant negative RhoG		(Handa et al., 2007)
pEGFPC1::*elmo*^{T625}	Dominant negative ELMO		(Handa et al., 2007)
pCXN2 ::*dock180*^{ISP}	Dominant negative Dock180		(Handa et al., 2007)
pGex ::*GST-CRIBWASP*	Cdc42 binding motif of WASP		(Sander and Collard, 1999)
pGex ::*GST-PAK*	Rac1 and Cdc42 binding domain of PAk		(Sander and Collard, 1999)
pEGFPC1::*elmo*	Elmo GFP tagged		(Handa et al., 2007)
pICC427	pSA10::*espT-HA*	41 + 42	(Bulgin et al., 2009)
pICC228	pRK5::*espT-Myc*	43 + 44	(Bulgin et al., 2009)
pICC429	pRK5::*IpgB1-Myc*	47 + 48	(Bulgin et al., 2009)
pICC320	pRK5::*EspM2-Myc*	45 + 46	(Bulgin et al., 2009)
pICC453	pET28::*espM2*$^{29\text{-}196}$	55 + 56	This work
pMW172-*His-RhoA* F25N	His Tagged RhoA		(Valderrama et al., 2006)
pMW172-*His-Rac1*	His tagged Rac1		(Valderrama et al., 2006)
pICC454	pET28::*sifA*	53 + 54	This work
pICC455	pRK5::*myc-espM2*	45 + 46	(Bulgin et al., 2009)
pICC456	pRK5::*myc-espM2*$^{29\text{-}196}$	55 + 56	This work
pICC457	pRK5::*myc-espM2*$^{29\text{-}196}$	57 + 58	This work

pICC458	W70A pRK5::*myc-espM2*$^{29-196}$	59 + 60	This work
pICC459	L118A pRK5::*myc-espM2*$^{29-196}$	61 + 62	This work
pICC460	Q124A pRK5::*myc-espM2*$^{29-196}$	63 + 64	This work
pRK5 :*myc-:wave2*	I127A Wave2 full length		Gifted by Laura Machesky
pDSRED ::*wave2ΔA*	Wave2 with truncated VCA		Gifted by Laura Machesky
pDSRED ::*wave2 ΔBP*	Wave2 with truncated WHD		Gifted by Laura Machesky
pICC461	pSA10 ::*espT* E110019	76 + 42	This work
pICC489	pACYC184 ::*espt* *C. rodentium*	76 + 42	This work

Table 3 Strains used in this study

Strain Name	Description	Reference
E69	E2348/69 Wild type EPEC O127:H6	(Levine et al., 1978)
	EHEC Sakai Wild type EHEC O157:H7	(Hayashi et al., 2001)
	EPEC B171 Wild type EPEC O111:NM	(Riley et al., 1987)
ICC168	*Citrobacter rodentium*	(Barthold et al., 1976)
	Salmonella Typhimurium strain SL1344	(Hueck et al., 1995)
ICC192	ICC192 EPEC E2348/69Δ*escN*	(Garmendia et al., 2004)
E110019	EPEC O111:H9 wild type	(Viljanen et al., 1990)
JPN15	EPEC O127:H6Δ*bfp*	(Jerse et al., 1990)
ICC306	*Citrobacter rodentium Δ*espT*	B. Raymond
ICC305	*Citrobacter rodentium Δtir*	R. Mundy
XL1blue	*Escherchia coli*	Stratagene
BL21	*Escherchia coli*	NEB
DH5α	*Escherchia coli*	Promega

Table 4 Primary antibodies used in this study

Antibody (species)	Application	Dilution	Source
0127 (E2348/69) (Rabbit)	IF	1:150	VLA
O111 (E110019) (Rabbit)	IF	1:150	VLA
CSA1 (Salmonella) (Goat)	IF	1:500	D. Holden
HA (Mouse)	IF/WB	1:500	Milipore
MYC (Mouse)	IF	1:200	Upstate
Tir (Rabbit)	IF	1:500	This Lab
IRSp53 (Mouse)	IF	1:100	L. Machesky
Wave2 (Rabbit)	IF	1:200	R. Carabeo
Abi1 (Mouse)	IF	1:250	Abcam
Vinculin (Mouse)	IF	1:300	Abcam
EEA1 (Mouse)	IF	1:150	BD Bioscience
Lamp1 (Mouse)	IF	1:100	DSHB University of Iowa
Cofilin (Mouse)	WB	1:1000	Cell Signalling Technology
P-Cofilin (Mouse)	WB	1:1000	Cell Signalling Technology
RhoA (Rabbit)	WB	1:200	Santa Cruz Biotechnology
Rac1 (Rabbit)	WB	1:200	Santa Cruz Biotechnology
Cdc42 (Rabbit)	WB	1:200	Santa Cruz Biotechnology
Tubulin (Mouse)	WB	1:1000	DSHB University of Iowa

Table 5 Secondary antibodies used in this study

Antibody	Application	Dilution	Source
Oregan Green Phalloidin	IF	1:150	Molecular Probes Invitrogen
Texas Red Phalloidin	IF	1:200	Molecular Probes Invitrogen
Cy5 Phalloidin	IF	1:100	Molecular Probes Invitrogen
Donkey anti Rabbit Cy2	IF	1:200	Jackson Immunology
Donkey anti Rabbit Cy5	IF	1:200	Jackson Immunology
Donkey anti Rabbit Cy3	IF	1:200	Jackson Immunology
Donkey anti Goat Cy2	IF	1:200	Jackson Immunology
Donkey anti Rabbit Cy3	IF	1:200	Jackson Immunology
Donkey anti Mouse Cy2	IF	1:200	Jackson Immunology
Donkey anti Mouse Cy5	IF	1:200	Jackson Immunology
Donkey anti Mouse Cy3	IF	1:200	Jackson Immunology
Rabbit anti Mouse HRP	WB	1:2000	Invitrogen
Swine anti Rabbit HRP	WB	1:3000	Invitrogen
Dapi	IF	1:1000	Molecular Probes Invitrogen
Mitotracker CmxROS	IF	125nM/well	Molecular Probes Invitrogen

Chapter 3: The EspM Family of Proteins are WxxxE Effectors with RhoA Guanine Nucleotide Exchange Factor Activity

Recently a study by Alto et al (Alto et al., 2006) grouped together several previously identified T3SS effector proteins into the novel WxxxE family based on their sequence similarity and the presence of a common motif consisting of an invariant tryptophan residue separated from a conserved glutamic acid by three variable amino acids. Alto et al also noted that the majority of T3SS effectors identified as WxxxE proteins induced cytoskeletal rearrangements reminiscent of active Rho family GTPases. It was also reported that mutation of either the conserved tryptophan or glutamic acid resulted in a loss of the biological activity of these proteins (Alto et al., 2006). Alto and colleagues identified IpgB1 and IpgB2 from *Shigella,* SifA and SifB from *Salmonella*, Map and TrcA from EPEC and EHEC as WxxxE effectors using a BLAST search based on the sequence of Map from EHEC (Alto et al., 2006).

3.1 Identification of Novel IpgB2-Like WxxxE Effectors in the A/E {athogen Group.

In collaboration with Mark Pallen (University of Birmingham) we utilised IpgB1 and IpgB2 from *Shigella flexneri* and Map from EPEC O127:H6 as index proteins in order to perform a series of PSI-BLAST searches (Altschul et al., 1997) on the available genomes of A/E pathogens. Using this approach we identified the putative effectors EspM1 and EspM2 from EHEC O157:H7 Sakai as sharing a considerable identity to the *Shigella* WxxxE effector IpgB2 (40 and 41 percent identity respectively) (Arbeloa et al., 2008) (Figure 3.1). Both EspM1 and EspM2 harbour an intact WxxxE motif and have previously been demonstrated to be secreted in a T3SS dependent manner (Tobe et al., 2006). Alto et al identified TrcA from EPEC B171 (O111:NM) as a putative WxxxE effector (Alto et al., 2006). Our search revealed an additional putative WxxxE effector, EspM1 (Accession#: AM910623), in EPEC B171 which shares

significant homology with EspM1 from EHEC Sakai O157:H7 (Arbeloa et al., 2008) (Figure 3.1). We next searched the unfinished genome of *Citrobacter rodentium* ICC168 and we identified two additional IpgB2-like proteins which we have termed EspM2 (Accession#: AM910622) and EspM3 (Accession#:AM910621) both of which also have a WxxxE motif (Figure 3.1).

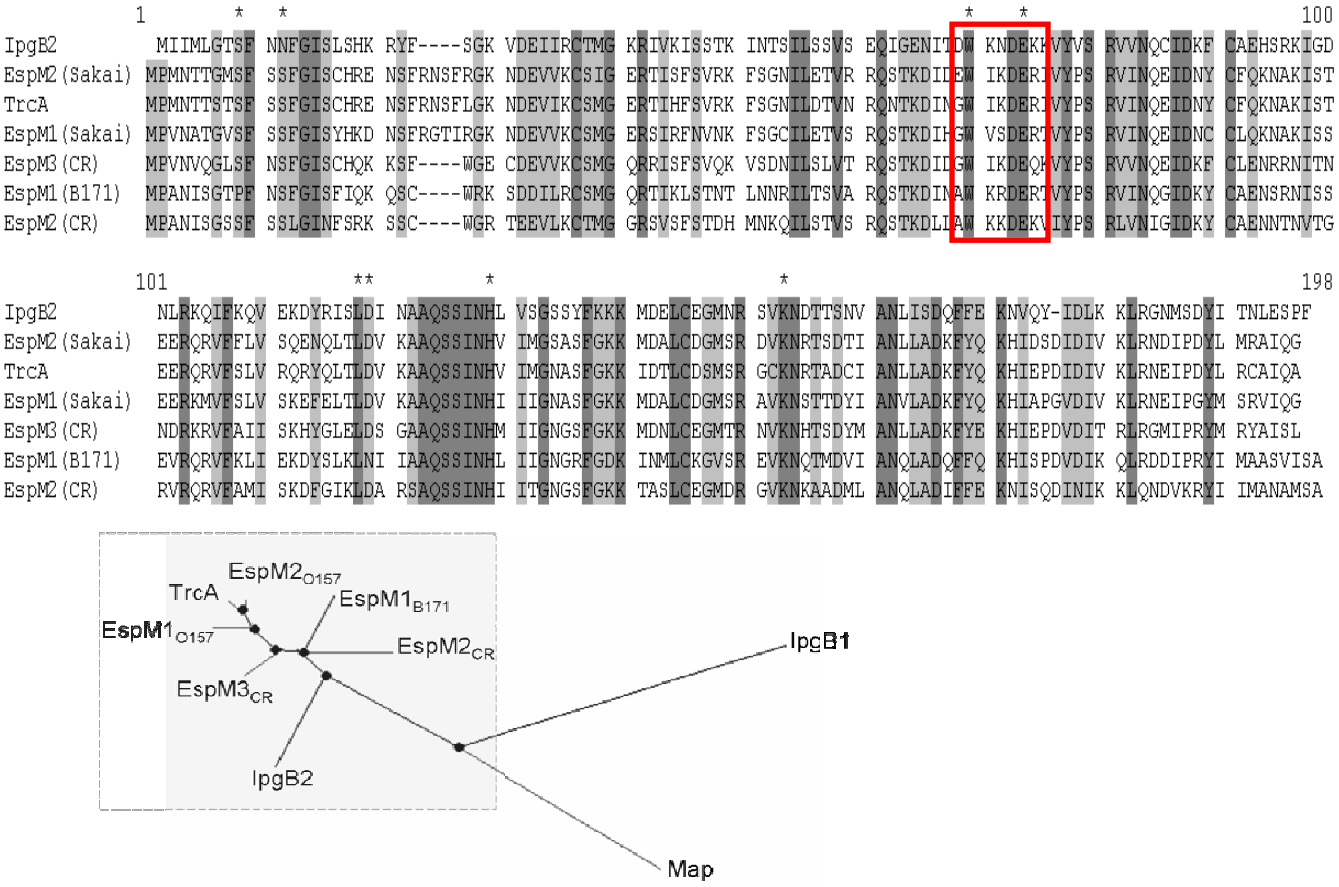


Figure 3.1 Identification of novel IpgB2-like WxxxE Effectors in the A/E Pathogen Group (A) Multiple sequence alignment with hierarchical clustering of *Shigella flexneri* IpgB2, EspM1 and EspM2 from EHEC O157:H7 Sakai, EspM2 and EspM3 from *C. rodentium and* TrcA and EspM1 from EPEC B171. The conserved motif WxxxE is boxed. (B) Radial phylogeny tree showing the sub-family of IpgB2-like WxxxE effectors in the A/E group, EPEC E2348/69 Map and *Shigella* IpgB1 and IpgB2.

Based on their homology and phylogeny we designated EspM1 and EspM2 from EHEC O157: H7 Sakai, TrcA and EspM1 from EPEC B171 and EspM2 and EspM3 from *Citrobacter rodentium* as the EspM family of effectors.

3.2 Genomic Context of the EspM Effectors

A/E pathogens conserve the LEE pathogenicity island which encodes a T3SS and several core secreted effector proteins (Elliott et al., 1998). In addition to the LEE encoded effectors A/E pathogens also encode several other genetic elements which encode T3SS effector proteins (reviewed in (Frankel et al., 1998)). The EspM family of proteins are encoded on distinct genomic loci in EHEC O157:H7 Sakai, EPEC B171 and *C. rodentium* suggesting that may have been acquired from divergent sources or at different times (Figure 3.2). Interestingly the EspM proteins are invariably positioned alongside at least one representative of the NleG family of proteins which have also been demonstrated to be T3SS effectors (Figure 3.2) (Tobe et al., 2006). In EHEC O157:H7 Sakai *espM1* is encoded on the same pathogenicity island as the T3SS effector *espO* (Figure 3.2) which has recently been shown to interact with integrin linked kinase (Kim et al., 2009). *espM2* is encoded in a distinct insertion element upstream of another T3SS effector (*hopW*) which is a homolog of an effector of unknown function from the plant pathogen *Pseudomonas syringae* (Tobe et al., 2006). Uniquely, *espM1* from EPEC B171 is encoded immediately downstream of the LEE pathogenicity island (Figure 3.2). The other EspM family member TrcA is encoded on an insertion element containing metabolic genes including an ABC transporter. In *C. rodentium espM2* is positioned on the same pathogenicity island as *espO* and another WxxxE effector *espT* (Figure 3.2) which is further discussed in chapters 4 and 5. EspM3 is encoded on the genomic backbone of *C. rodentium* and is positioned downstream of a *lifA* homolog (Figure 3.2). LifA (limphostatin) has been shown to contribute to the adherence of EPEC to epithelial cell (Badea et al., 2003), and to be essential in colonic colonisation and crypt cell hyperplasia which is associated with *C. rodentium* infection of the mouse colon (Babbin et al., 2009).

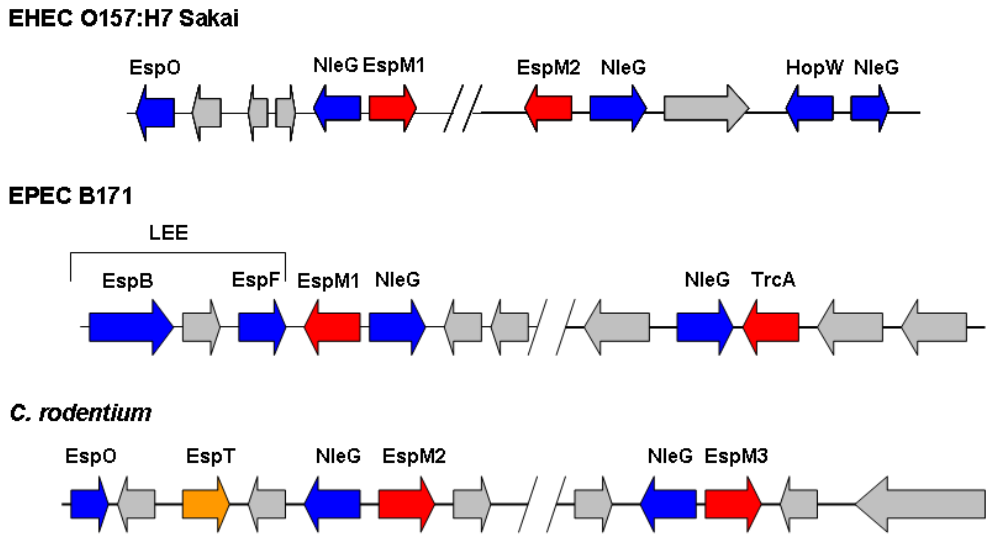


Figure 3.2 Genomic context of EspM family members. A graphical representation of the EspM family genomic loci in EHEC O157:H7 Sakai, EPEC B171 and *C. rodentium*. EspM family homolog's are labelled in red, the WxxxE effector EspT is labelled in orange and other putative T3SS effector proteins are marker in blue.

3.3 The EspM Effectors are Translocated into host Cells in a T3SS Dependent Manner

EspM1 and EspM2 from EHEC O157:H7 Sakai along with TrcA have previously been demonstrated to be T3SS effectors (Tobe et al., 2006; Tobe et al., 1999). In order to confirm the status of the new EspM proteins as T3SS effectors we performed trasnlocation assays using the TEM-1 (β–lactamase) reporter (Charpentier and Oswald, 2004). To this end EspM2 and EspM3 from *C. rodentium* were fused to TEM-1 in the pCX340 vector and transformed wild type and the T3SS null Δ*escN* EPEC E2348/69 and used these strains to infect HeLa cells which were pre-treated with the cell permeable CCF2/AM substrate. The CCF2/AM compound fluoresces green when uncleaved and blue when cleaved by β–lactamase. When the effector TEM-1 fusion protein is translocated into host cells via the T3SS of E2348/69 the CCF2/AM substrate is cleaved and the change in fluorescence is detected uising immuno-fluorescence microscopy. The T3SS effector NleD fused to TEM-1 was used as a positive control (Marches et al., 2005). This

assay was performed by Georgina MacKenzie (a rotation student in the lab) under my supervison. Both EspM2 and EspM3 from *C. rodentium* were found to be translocated into host cells from the wild type E2348/69 but not from the Δ*escN* mutant indicating that they are bone fide T3SS effectors.

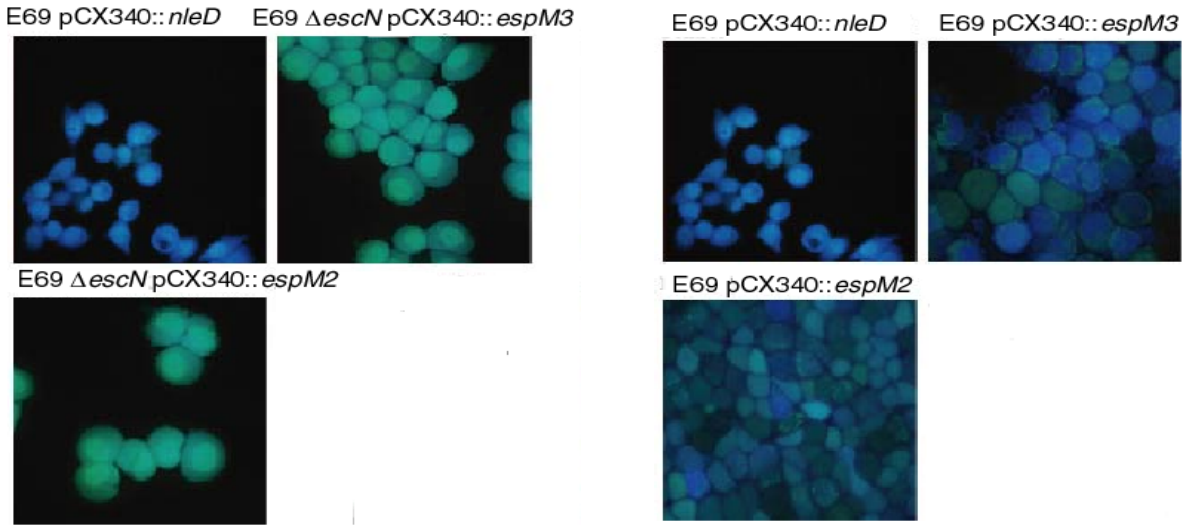


Figure 3.3 EspM2 and EspM3 are translocated into host cells in a T3SS dependent manner. HeLa cells were infected with E2348/69 (E69) or the E69 T3SS null mutant Δ*escN* containing the pCX340 β-lactamase fused to EspM2 or EspM3. Upon translocation the β-lactamase cleaves the CCF2/AM substrate, which fluoresces in green when uncleaved and in blue when cleaved, indicating translocation of the fusion protein. The previouslt identified T3SS effector NleD was used as a positive control.

3.4 The EspM Effectors Trigger Formation of Stress Fibres with Subtly Different Architectures

As the EspM effectors share significant homology with IpgB2, which induces formation of stress fibres (Alto et al., 2006), we tested the ability of EspM1, EspM2 from EHEC O157:H7 Sakai, EspM1 and TrcA from EPEC B171, EspM2 and EspM3 of *C. rodentium* to remodel the mammalian actin cytoskeleton. The genes were cloned into the expression vector pSA10 (Schlosser-Silverman et al., 2000) and expressed in EPEC E2348/69 which lacks any IpgB2 homologues. Recombinant E2348/69 were used to infect serum starved Swiss 3T3 cells, which generally lack stress fibres (Figure 3.4) and are capable of dynamic actin signalling. Control

infections with wild type EPEC E2348/69 trigger efficient Tir-dependent actin-rich pedestals (Figure 3.4) while stress fibres were seen only in a small percentage of infected cells (Figure 3.4). In contrast, infection of Swiss 3T3 cells with E2348/69 expressing EspM2 (Sakai) (Figure 3.4) EspM2 (*C. rodentium*) (data not shown as the phenotype is identical to that of EspM2 (Sakai)) induced simultaneous formation of actin pedestals (inset) and global parallel stress fibres (GP-SF), which were on different focal planes. These stress fibres were observed in ca. 90% of infected cells after 1.5 h infection (Figure 3.4). Using vinculin antibodies we observed intense distal staining of the GP-SF (Figure 3.4), suggesting that the GP-SF triggered by EspM2 are linked to the plasma membrane through focal adhesions (Ziegler et al., 2006).

Infection of Swiss 3T3 cells with E2348/69 expressing EspM1 (B171) (Figure 3.4), EspM1 (Sakai) and TrcA (B171) (data not shown as the stress fibres induced are indistinguishable from EspM1 (B171)) resulted in simultaneous formation of actin pedestals and localized parallel stress fibers (LP-SF), which were subtly different from those triggered by EspM2 as they were confined to the site of bacterial adhesion (Figure 3.4). Immuno-fluorescence using the anti-vinculin antibodies revealed intense staining at the tip of each of the LP-SF (Figure 3.4).

Infection of Swiss 3T3 with E2348/69 expressing EspM3 (*C. rodentium*) resulted in formation of actin pedestals and stress fibers with vinculin-rich tips in ca. 90% of the cells at 1.5 h post infection (Figure 3.4). EspM3-triggered formation of a distinct architecture of localized radial (3D) stress fibers (LR-SF) (Figure 3.4). The GP-SF, LP-SF and LR-SF appeared as soon as 30 min post infection and were stable for at least for 3 h. Taken together these results illustrate that the IpgB2-like WxxxE effectors from A/E pathogens subvert actin dynamics and trigger formation of GP-SF (EspM2), LP-SF (EspM1 and TrcA) or LR-SF (EspM3). We selected EspM2 (Sakai) and EspM3 as model effectors for further study.

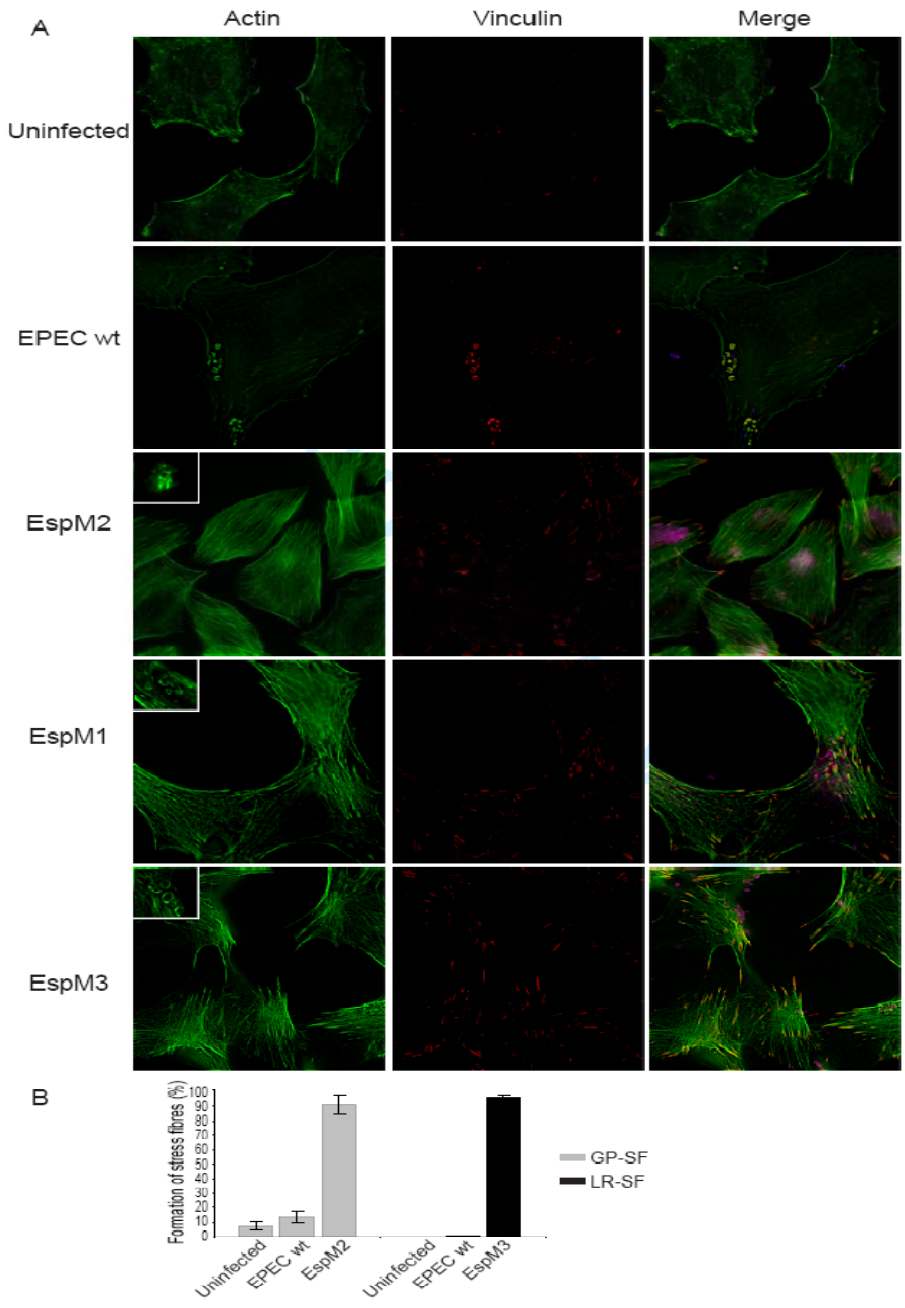


Figure 3.4 IpgB2 like A/E effectors induce formation of actin stress fibres in Swiss 3T3 cells upon infection. (A) Fluorescence microscopy of Swiss 3T3 cell uninfected or infected for 1h30 with primed EPEC 2348/69 wt (E69) and E69 pSA10 expressing EspM1, EspM2 and EspM3. Actin was stained with Oregon green phalloidin, EPEC were detected with rabbit anti 0127 antibody and vinculin was visualised using a monoclonal mouse antibody. Typical EPEC pedestals were observed underneath most the bacteria and strong stress fibres were only observed in cell infected with EPEC pSA10 harbouring the IpgB2 like effectors. EspM2 induces the formation of global parallel stress fibres (GP-SF), while EspM1 nucleates localised parallel stress fibres (LP-SF) which are confined to the site of bacterial attachment. EspM3 induces formation of local radial stress fibres (LR-SF) which are three dimensional in nature. (B) Quantification of parallel or radial stress fibre formation in uninfected Swiss cells or after 1h30 infection with E69 wt, E69 pSA10::espM2 or E69 pSA10::espM3. One hundred cells were counted in three independent experiments. Results are presented as mean±SEM.

3.5 The Effect of Site Directed Mutagenesis of the WxxxE motif of EspM2 and EspM3

Previous work by Alto and colleagues has demonstrated that the conserved tryptophan and glutamic acid residues are essential to the biological activity of WxxxE effectors (Alto et al., 2006). It was demonstrated that substitituon of either the tryptophan or glutamic acid residue to alanine resulted in a marked reduction in the ability of IpgB2 to nucleate actin stress fibres (Alto et al., 2006). In order to determine if the same was true of the EspM effectors we mutated the invariant tryptophan (W) of EspM2 (W70) and EspM3 (W66) to alanine. Swiss cells infected with E2348/69 expressing EspM2^{W70A} and EspM3^{W66A} triggered actin-rich pedestals with no evidence of GP-SF or LP-SF, respectively, and were indistinguishable from cell infected with wild type E2348/69 (Figure 3.5). In order to establish if conservative mutation of the invariant WxxxE residues also inhibited the biological activity of EspM2 and EspM3 we substituted the conserved tryptophan (W) and glutamic acid (E) residues with tyrosine (Y) or aspartic acid (D) respectively. Interestingly, conservative substitution of the W and E residues with a Y and D respectively did not result in any significant loss of stress fibre formation (Fig 3.5). These substitutions did however produce a shift in the architecture of stress fibers induced by EspM3 from a LR-SF morphology to a LP-SF arrangement. Taken together these results indicate that the conserved tryptophan and glutamic acid residues can be substituted by structurally related tyrosine and aspartic acid residues but not by alanine suggesting the invariant tryptophan and glutamic acid residues may play in role in maintaining the structure or function of WxxxE effectors.

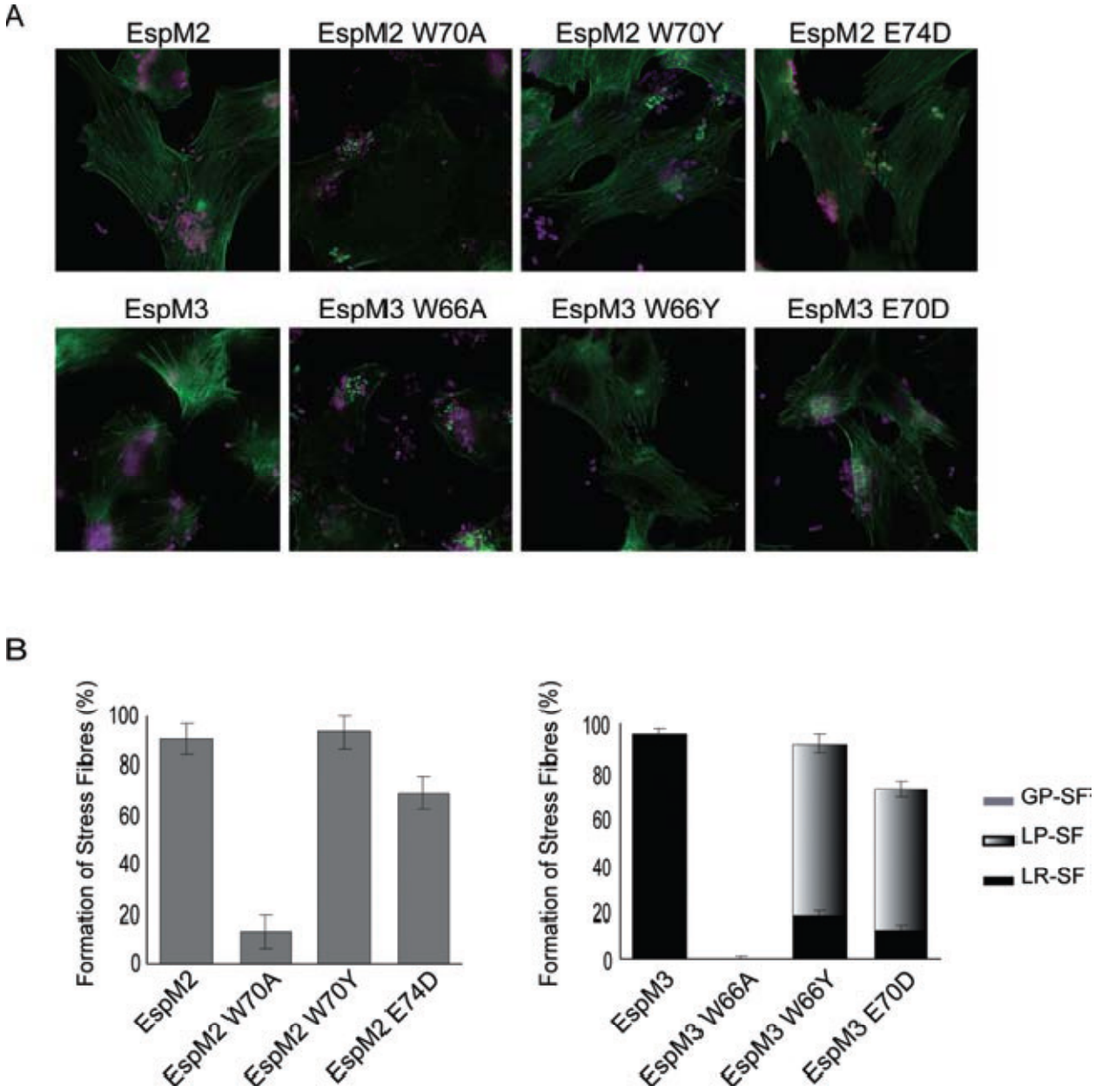


Figure 3.5 The effect of site directed mutagenesis on the WxxxE motif of EspM2 and EspM3. (A) Merged fluorescence microscopy of Swiss 3T3 cells infected for 90 min with primed E2348/69 expressing EspM2 (Sakai) and EspM3 (CR) wild type prtoteins or derivative mutants within the conserved WxxxE motif. Actin was stained with Oregon green phalloidin and EPEC were detected with rabbit anti 0127 antibody. The W70A mutant of EspM2 and the W66A mutant of EspM3 were significantly impaired in their ability to form stress fibres. Conversely the conservative W70Y and E74D mutant of EspM2 and the W66Y and E70D mutant of EspM3 were largely unaffected in their abilty to form stress fibres compared to the wild type proteins. (B) Quantification of stress fibers formation in Swiss cells after 90 min infection. One hundred infected cells were counted in triplicate from three independent experiments. Results are presented as mean ± SEM

3.6 Stress Fibre Induction by EspM2 and EspM3 is Inhibited by Expression of a RhoA Dominant Negative.

In mammalian cells formation of stress fibres is normally regulated by the small Rho family GTPase RhoA (reviewed in (Etienne-Manneville and Hall, 2002)). The recent study of Alto *et al* proposed that nucleation of stress fibres by the *Shigella* WxxxE effector IpgB2 was independent of the activity of RhoA leading to the hypothesis that IpgB2 was mimicking a Rho GTPase rather than activating endogenous RhoA (Alto et al., 2006). In order to determine if the EspM effectors, which also induce stress fibre formation (Figure 3.4), require the activity of cellular RhoA we utilised dominant negative RhoA ($RhoA_{N19}$) dominant negatives Cdc42 ($Cdc42_{N17}$) and Rac1 ($Rac1_{N17}$) were used as control. Infection of transfected cells with E2348/69 expressing EspM2 or EspM3 for 1.5 h revealed that formation of GP-SF and LR-SF, respectively, was not affected by inactivation of Cdc42 or Rac1 (Figure 3.6). In contrast, infection of cells expressing $RhoA_{N19}$ resulted in formation of typical actin-rich pedestals but with a marked reduction in formation of GP-SF or LR-SF, respectively (Figure 3.6). This result suggests that, unlike IpgB2, formation of stress fibres by EspM2 and EspM3 requires active RhoA.

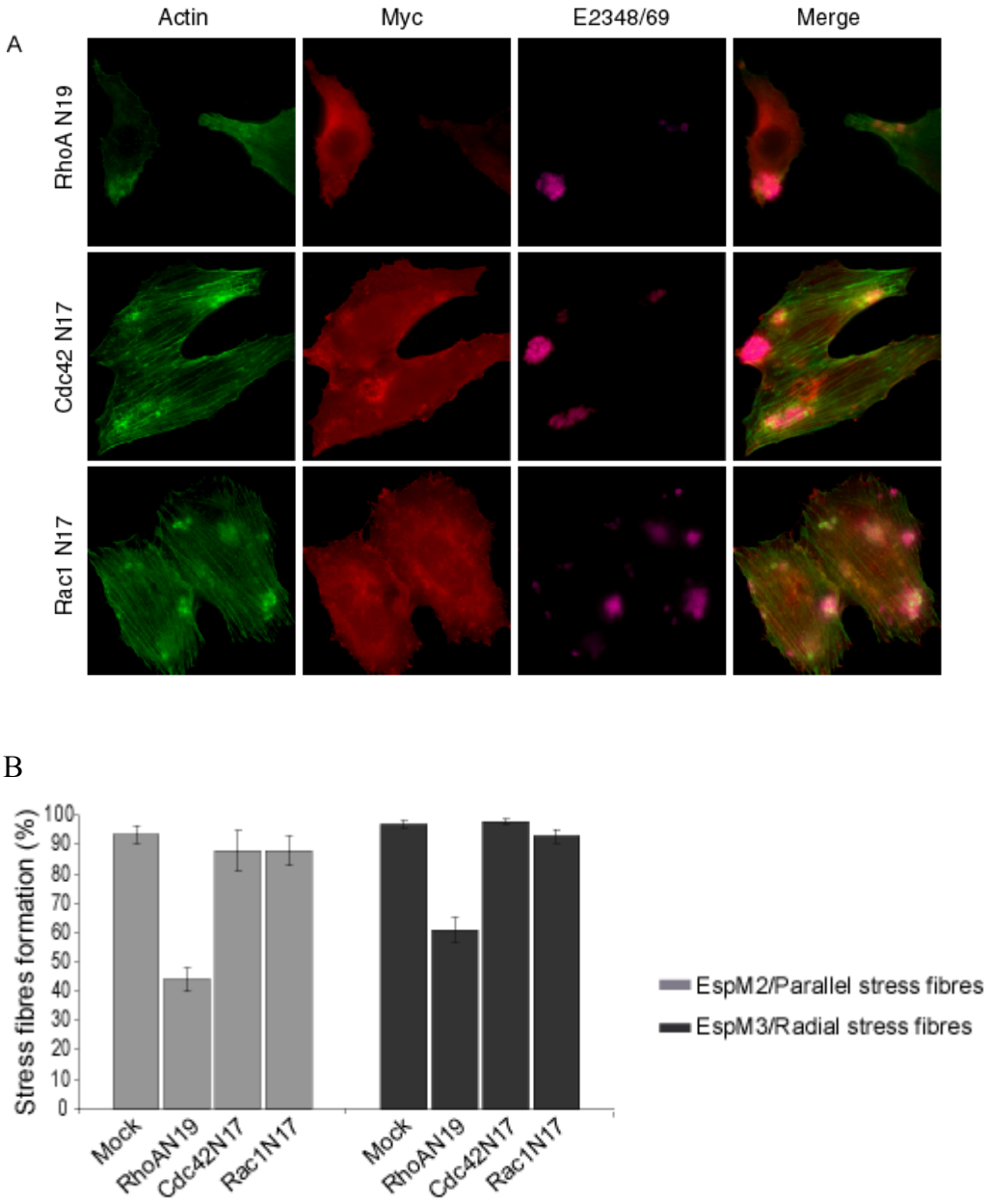


Figure 3.6 EspM2 and EspM3 dependent stress fibre formation is dependent of the small GTPase RhoA and independent on Cdc42 and Rac1. (A) Swiss 3T3 cells were transfected for 24h with the mammalian transfection vector pRK5 expressing a myc fusion of the Cdc42N19, Rac1N19 or RhoAN17 dominant negatives. The Swiss 3T3 cells were then infected 1h30 with EPEC pSA10::*espM2* or EPEC pSA10::*espM3*. Actin was stained with Oregon green phalloidin, Myc with anti-myc mouse antibody and EPEC with anti O127 rabbit antibody. (B) Formation of stress fibres in one hundred transfected infected cells were counted in three independent experiments. Results are presented as mean±SEM. Formation of stress fibres depending on EspM2 or EspM3 is inhibited by expression of RhoAN17, but not by expression of Cdc42N19 or RacN19.

3.7 EspM2 and EspM3 Activate RhoA to Induce Stress Fibre Formation

Rho GTPases act as molecular switches cycling between an inactive GDP bound form and an active GTP bound form (reviewed in (Jaffe and Hall, 2005)). When in the active GTP loaded conformation Rho GTPase can bind specific downstream signalling proteins known as effectors (Aspenstrom, 1999). In order to determine if translocation of EspM2 and EspM3 into mammalian cells results in an activation of RhoA, we performed pull down assays using GST-Rhotekin, which specifically binds the active GTP-bound form of RhoA. Cells infected with wild type E2348/69 were used as a negative control. Swiss 3T3 cells infected with E2348/69 expressing EspM2 or EspM3 exhibited a significantly higher level of activated RhoA compared with cells infected with wild type E2348/69 (Figure 3.7). These results suggest that EspM2 and EspM3 activate RhoA and that formation of GP-SF and LR-SF are dependent on RhoA signalling.

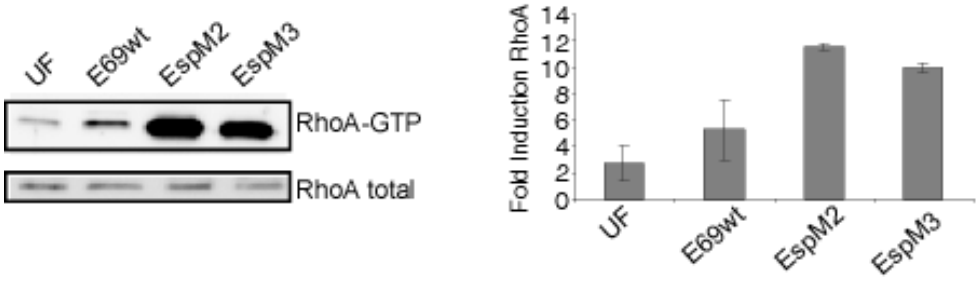


Figure 3.7 EspM2 and EspM3 activate RhoA. Swiss 3T3 cells were infected with wild type E2348/69 or E2348/69 expressing EspM2 or EspM3. Cells were lysed and a GST fusion of the Rho binding domain of Rhotekin was used to co-purify RhoA-GTP. Total RhoA in the lysates and RhoA-GTP were detected by Western blot with anti-RhoA antibodies. In cells infected with wild type E69 there was no significant iduction of RhoA GTP. In contrast cells infected with E2348/69 expressing EspM2 or EspM3 displayed a significant enrichment of GTP loaded RhoA compared to the cells infected with wild type E2348/69. The average level of RhoA enrichment from 6 independent experiments was calculated using densiometry. Quantified data are means ± S.D. of the results of three independent experiments.

3.8 Stress Fibres Induced by EspM2 and EspM3 are ROCK-Dependent.

ROCK is one of the major RhoA downstream effectors which mediates formation of stress fibres (Jaffe and Hall, 2005). To determine if EspM2 and EspM3 activate the RhoA-ROCK pathway, Swiss 3T3 cells were incubated with the ROCK inhibitor Y-27632 for 1 h prior to infection with E2348/69 expressing EspM2 or EspM3. Y-27632 is a highly specific inhibitor of ROCK-I and ROCK-II which competitively excludes ATP from the catalytic site (Yamaguchi et al., 2006). Pre-incubation with Y-27632 completely blocked formation of GP-SF and LR-SF by EspM2 and EspM3, respectively (Figure 3.8). The ROCK inhibitor did not affect formation of actin rich pedestals.

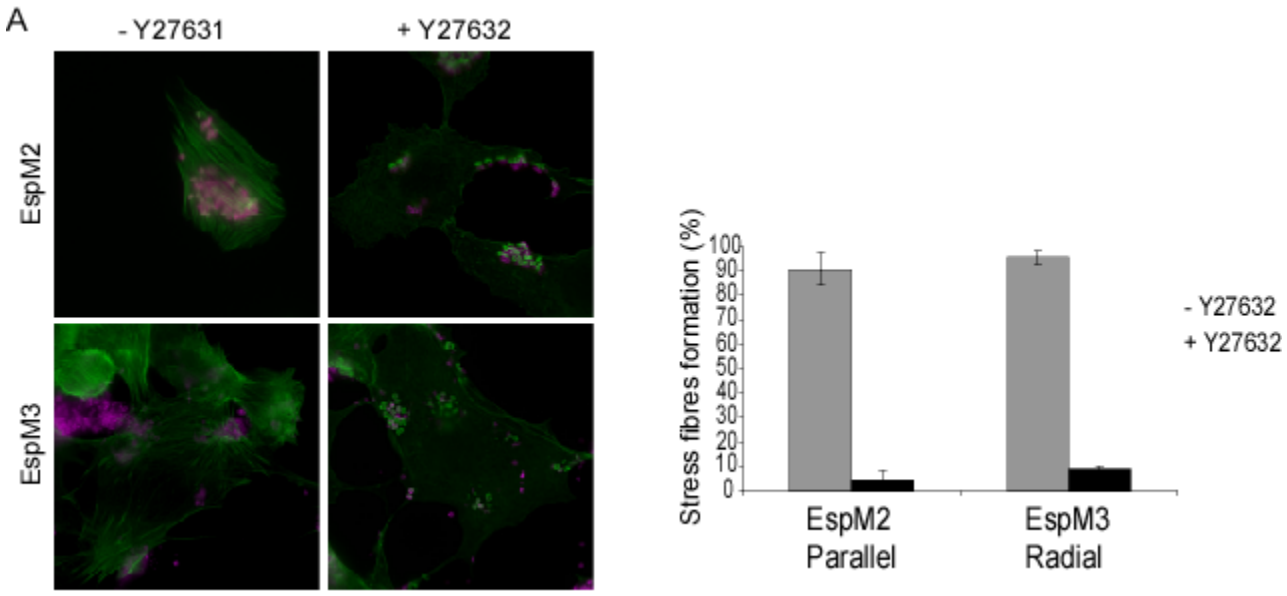


Figure 3.8 EspM2 and EspM3 trigger the RhoA-ROCK pathway. (A) Fluorescence microscopy of Swiss 3T3 cells incubated for 1 h in presence or absence of 10 µM of the ROCK inhibitor Y-27632 and infected for 90 min with E2348/69 expressing EspM2 or EspM3. Y-27632 did not affect formation of actin-rich pedestals, but abolished formation of stress fibers. (B) Percentage of Swiss 3T3 cells presenting stress fibers in the presence or absence of Y-27632. One hundred cells were counted in triplicate from three independent experiments. Results are presented as mean ± SEM.

3.9 EspM2 and EspM3 Induce an Increase in the level of Phospho-Cofilin

Lim kinase (LimK) is downstream effector of ROCK which is involved in stress fibres formation (Jaffe and Hall, 2005). It has been shown that phosphorylation of the LimK by ROCK and the consequent inactivation (by phosphorylation) of cofilin by LimK contributes to Rho-induced stress fibre formation (Maekawa et al., 1999). We examined the phosphorylation state of cofilin by immunoblot following infection of Swiss cell with E2348/69 expressing EspM2 or EspM3. When compared with uninfected or cells infected with the wild type E2348/69 higher level of phospho-cofilin was observed after translocation of EspM2 or EspM3 (Figure 3.9). These results suggest that EspM2 and EspM3 trigger stress fibre formation through the RhoA-ROCK- LimK-cofilin pathway.

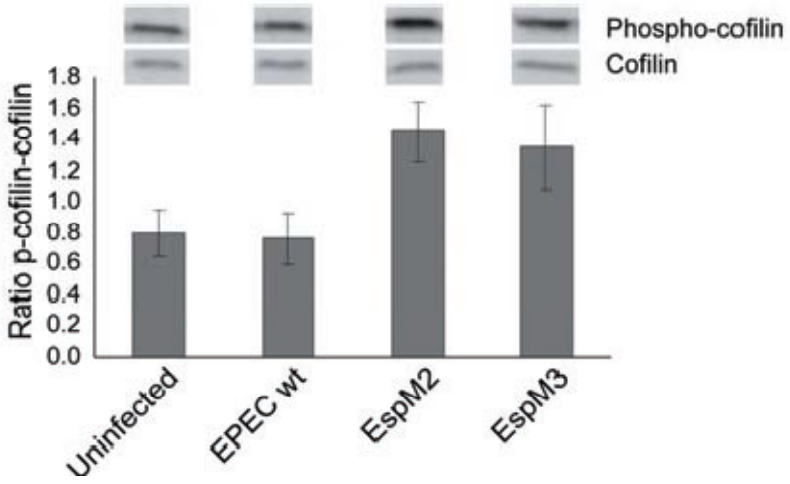


Figure 3.9 EspM2 and EspM3 induce an increase in cofilin phosphorylation. Swiss 3T3 cells were left uninfected or infected for 90 min with wild type E2348/69 carrying empty pSA10 vector or E2348/69 expressing EspM2 or EspM3. The levels of cofilin and phospho-cofilin were determined by Western blot using anti cofilin and anti phospho-cofilin antibodies. Quantification of densitometry was conducted using image J software and results presented here represent the mean ratio ± S.D of four independent experiments.

3.10 EspM2 Binds RhoA

The following figures and results were contributed by Ana Arbeloa, James Garnet, Steve Mathews, James Lillington and Susan Lea. In this section it was investigated if EspM2 can directly bind RhoA. To this end *espM2* was cloned in the bacterial expression vector pET28a and the protein was purified following induction. Purified His-EspM2 was soluble but appeared in two distinct bands corresponding to the full-length effector and a spontaneous degradation product; N-terminal sequencing reveal that the latter corresponds to EspM2 lacking the first 28 amino acids, which we have termed EspM2$^{29\text{-}196}$. Full length *espM2* and *espM2*$^{29\text{-}196}$ were cloned into the mammalian expression vector pRK5 fused to an N terminal Myc tag. Ectopic expression of EspM2 and EspM2$^{29\text{-}196}$ in Swiss 3T3 cells resulted in the formation of global parallel stress fibres which are identical to those observed when EspM2 is translocated from E2348/69 (Figure 3.4 and 3.10). Stres fibres induced by EspM2$^{29\text{-}196}$ were formed in a similar percentage of cells and were phenotipically indistiguishale from those envoked by EspM2 (Figure 3.10A). This result confirms that the truncated effector retained its biological activity. Consequently we have used EspM2$^{29\text{-}196}$ throughout the rest of this work.

In order to conduct protein interaction studies, surface plasmon resonance (SPR) was used to probe the interaction between His-EspM2$^{29\text{-}196}$ and His-RhoA. This technique allows binding to be observed in real time by the change in mass over the surface of a sensor chip. RhoA was flowed (sequential injections ranging from 0.05μM to 50μM) over an EspM2$^{29\text{-}196}$ bound surface and displayed an increased rate of binding with concentration confirming a specific interaction (Figure 3.10B).

As a negative control, Rac1 was flowed over the same EspM2$^{29\text{-}196}$ surface and for any given GTPase concentration showed substantially less binding (Figure 3.10C), confirming the

specificity of EspM2$^{29\text{-}196}$ for RhoA over other GTPases. Recent data suggested that the *Salmonella* WxxxE effector SifA can bind RhoA (Ohlson et al., 2008). In order to confirm this interaction we cloned *sifA* from *Salmonella enterica* serovar Typhimurium into pet28A to create a C terminal His tag fusion which was purified using a His bind nickel column. We found that His-SifA and His-RhoA also bound in a concentration dependent manner (Figure 3.10D).

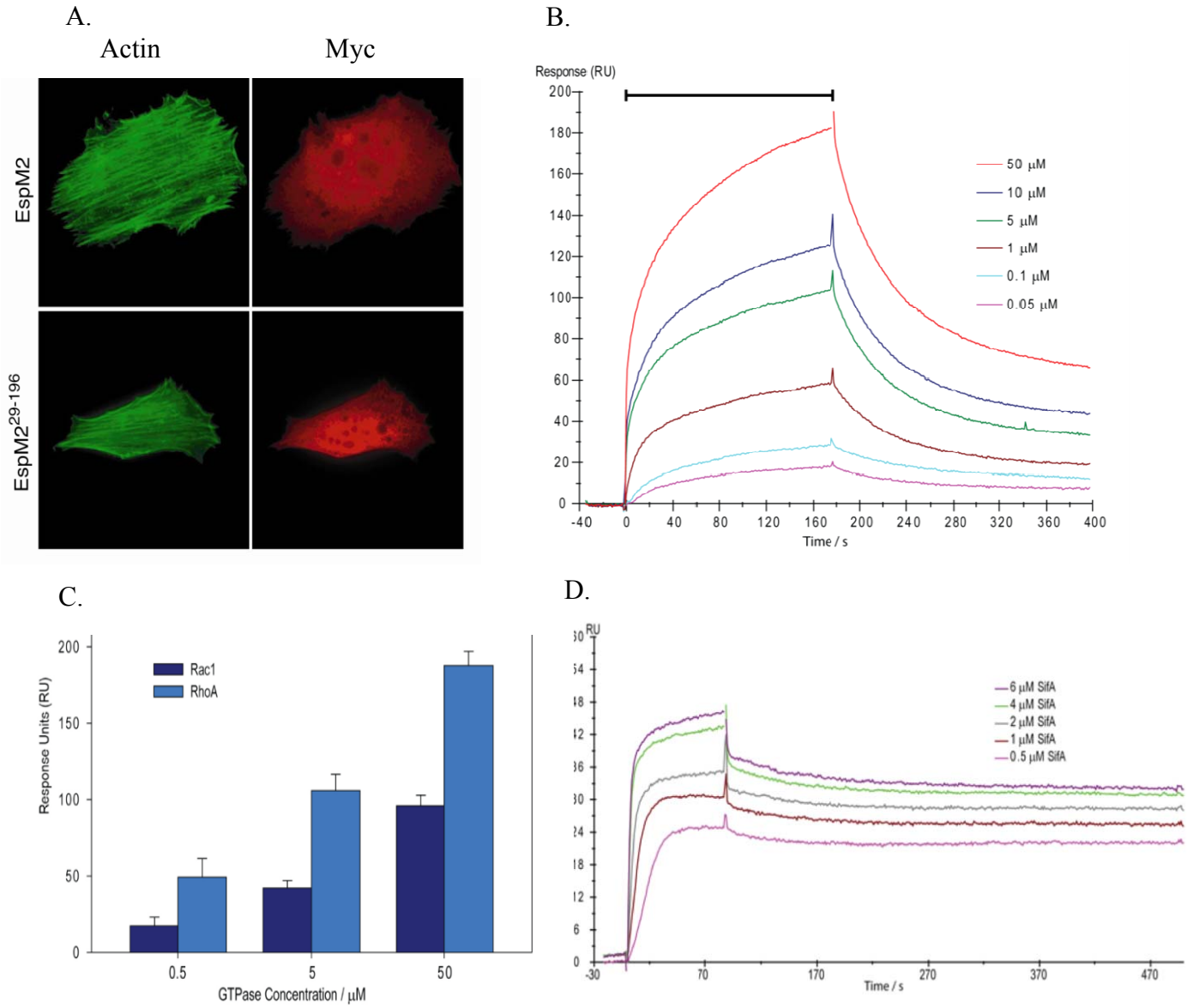
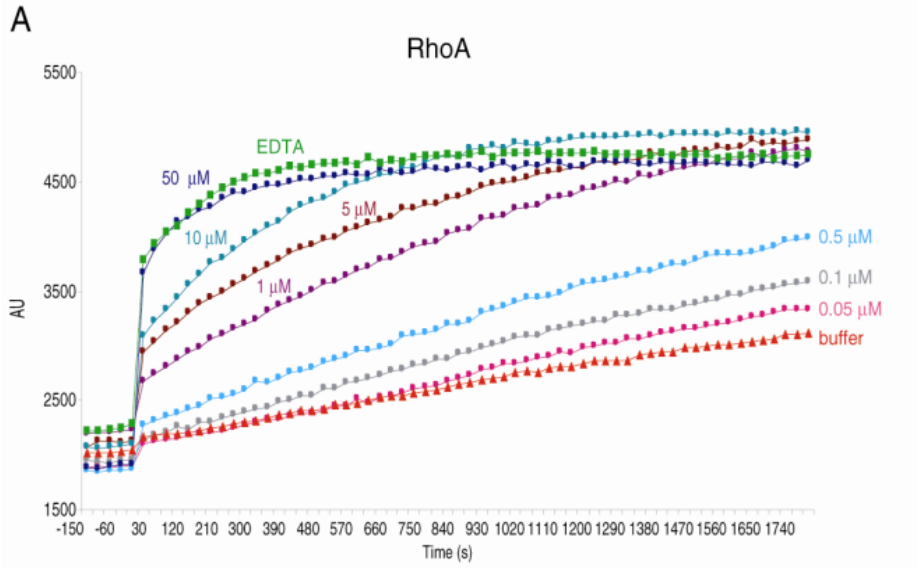
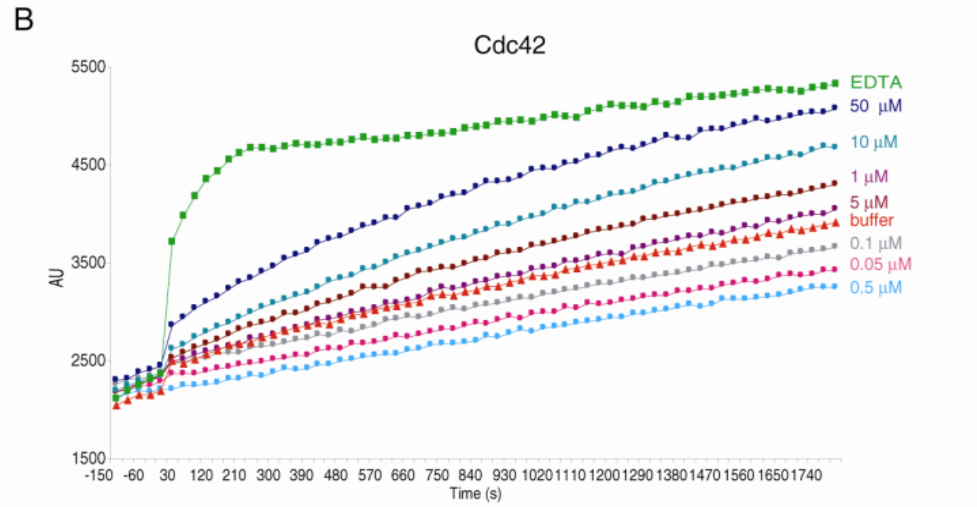


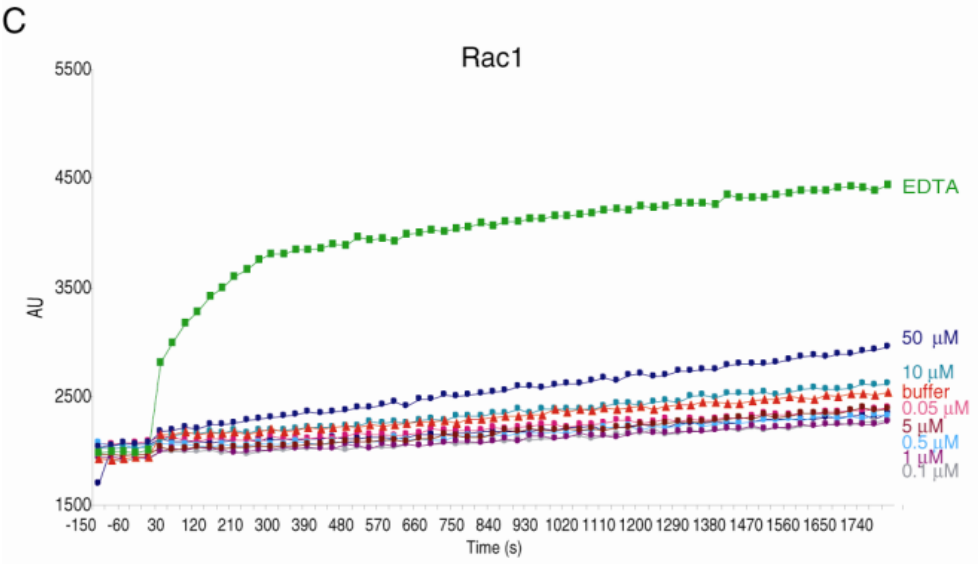
Figure 3.10 EspM2 binds to RhoA. (A) Swiss 3T3 cells were transfect with pRK5 encoding EspM2 and EspM2$^{29\text{-}196}$ fused to a myc tag. Actin was labelled in green with Oregon Green phalloidin and EspM2 and EspM2$^{29\text{-}196}$ were detected using a monoclonal Myc antibody in red. Both constructs produced stress fibres which were indistinguishable from each other. (B). Surface Plasmon resonance demonstrates RhoA concentration dependence for binding EspM2$^{29\text{-}196}$. Concentrations of RhoA varying from 0.05µM to 50µM were flowed at 50µl min^{-1} (duration indicated by black bar) over a CM5 sensor chip with EspM2$^{29\text{-}196}$ covalently bound to the surface. Control substituted signals are shown. (C.) Binding of EspM2$^{29\text{-}196}$ to RhoA and Rac1. Averaged response maxima for three representative concentrations compare the strength of EspM2 binding with the two GTPases. (D.) Surface Plasmon resonance demonstrates RhoA concentration dependence for binding SifA. Concentrations of SifA varying from 0.5 µM to 6 µM were flowed at 50 µl min^{-1} (duration indicated by black bar) over a CM5 sensor chip with RhoA covalently bound to the surface. Figure provided by James Lillington and Susan Lea

3.11 EspM2 is a Guanine Exchange Factor for RhoA

We next investigated the ability of EspM2$^{29-196}$ to stimulate guanine nucleotide exchange in RhoA *in vitro* using a RhoGEF exchange assay (Cytoskeleton, Inc., USA). The Rho GTPases Rac1 and Cdc42 in addition to the distantly related H-Ras GTPase were also used in this assay to determine the specificity of EspM2 activity. This spectroscopic assay measures fluorescent emission upon insertion of *N*-methylanthraniloyl(mant)-GTP into the nucleotide binding pocket of the GTPases. We utilised 250mM EDTA as a positive control in the assay as it induced efficient nucleotide exchange in RhoA, Cdc42, Rac1 and HRas, indicating that these proteins were biologically functional. A slow intrinsic nucleotide exchange activity was detected in the presence of buffer alone (negative control). The fluorescence intensity increased dramatically and in a dose dependent manner when increasing amounts of purified EspM2$^{29-196}$ were added to RhoA (Figure 3A). In contrast, EspM2$^{29-196}$ showed a weak exchange activity in Cdc42 (Figure 3.11), whereas it had no effect on Rac1 (Figure 3.11). Testing the GEF activity of SifA revealed that it cannot stimulate nucleotide exchange in any of the tested Rho GTPases or HRas (Figure 3.11). These results demonstrate that EspM2$^{29-196}$ is a specific RhoA GEF, and that although SifA can bind RhoA it cannot induce nucleotide exchange. It should be noted that the EDTA positive contol used in this is experiment does not represent a suitable control as the concentration is too high and most likely has a denaturing effect on the GTPases. Additionally the high concentration of EDTA present would prohibit the locking of new GTP moieties into the GTP binding groove.


A
RhoA
AU
Time (s)
EDTA
50 µM
10 µM
5 µM
1 µM
0.5 µM
0.1 µM
0.05 µM
buffer


B
Cdc42
AU
Time (s)
EDTA
50 µM
10 µM
1 µM
5 µM
buffer
0.1 µM
0.05 µM
0.5 µM


C
Rac1
AU
Time (s)
EDTA
50 µM
10 µM
buffer
0.05 µM
5 µM
0.5 µM
1 µM
0.1 µM

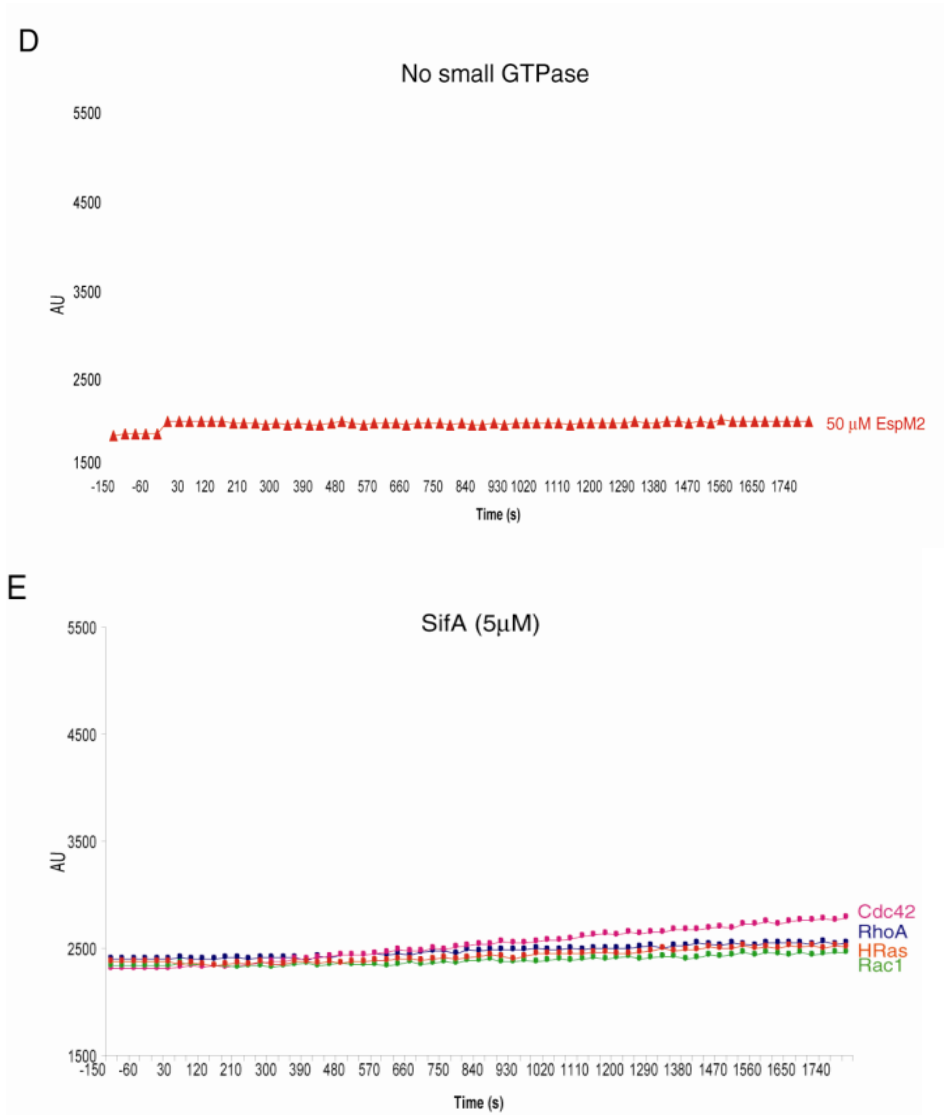


Figure 3.11 EspM2 is a guanine exchange factor for RhoA. A. EspM2 mediates loading of mant-GTP into RhoA. 0.5µM mant-GTP was incubated with 2 µM RhoA in presence of 250mM EDTA (squares), or 0.05-50 µM EspM2 (circles) or in presence of buffer only (triangles). The insertion of the mant-GTP into the nucleotide binding pocket of RhoA in presence of EspM2 detected by an increase in the fluorescent emission was found to be dose dependent. B. EspM2 weakly induces loading of mant-GTP into Cdc42. 0.5µM mant-GTP was incubated with 2µM Cdc42 in presence of 250mM EDTA (squares), or 0.05- 50µM EspM2 (circles) or in presence of buffer only (triangles). Slow loading of mant-GTP into Cdc42 was only detected when high concentrations of EspM2 were added. C. EspM2 does not induce nucleotide exchange for Rac1. 0.5µM mant-GTP was incubated with 2µM Rac1 in presence of 250mM EDTA (squares), or 0.05- 50µM EspM2 (circles) or in presence of buffer only (triangles). No efficient loading of man-GTP into Rac1 was observed after incubation with up to 50µM of EspM2. D. SifA does not induce nucleotide exchange on RhoA, Cdc42, Rac1 or HRas. 0.5µM mant-GTP was incubated with 2µM of RhoA (blue circles), Cdc42 (pink circles), Rac1 (green circles) or HRas (orange circles) in presence of 5µM SifA. No loading of man-GTP into any of the small GTPases tested was observed in these conditions. Results shown are the average of three independent experiments. E. Incubation of 50µM of EspM2 in the exchange buffer alone did not change the fluorescence intensity. The EDTA used in this experiment is not a suitable positive control.

3.12 Mapping the EspM2 Interface of the EspM2-RhoA Complex

In collaboration with Ana Arbeloa, James Garnett and Steve Mathews we utilised Nuclear Magnetic Resonance spectroscopy (NMR) to elucidate the structure of $EspM^{29-196}$. Although the protein was reasonably unstable we were able to assign ~65% of the backbone using heteronuclear multidimensional NMR spectroscopy. NMR was then used to monitor the titration of RhoA against $EspM2^{29-196}$ where at least a 1:1 molar ratio was needed to see any change within the ^{15}N-HSQC spectra, although at 4-fold molar excess RhoA it was possible to determine which of assigned EspM2 residues were within intimate proximity of RhoA upon complex formation (Figure 3.12). After the addition of 7-fold molar excess RhoA, peaks corresponding to structured regions of $EspM^{29-196}$ had broadened to such an extent that many were no longer visible indicating in an interaction between EspM and RhoA. Furthermore, addition of 5 mM GTP to the sample did not result in dissociation of the complex.

Secondary structure prediction with PSIPRED (Jones, 1999) and NMR data including the chemical shift index of $^{13}C^{\alpha}$ and $^{13}C^{'}$ (Wishart et al., 1993) show that EspM2 is primarily helical, (albeit for an unstructured ~30 residue region at the N-terminus) with a helical content similar to that of the C-terminal domain of SifA whose crystal structure has been determined (pdb:3cxb; (Ohlson et al., 2008). A primary sequence alignment was performed with $EspM^{229-196}$, Map, IpgB1 and IpgB2. This was then used along with the crystal structure of the C-terminal domain of SifA containing the WxxxE motif (pdb:3cxb; (Ohlson et al., 2008)) to create a homology model using SWISS-MODEL (Arnold et al., 2006) and the data from the RhoA titration was mapped onto it (Figure 3.12). A model of the complex with RhoA was created by superimposing the $EspM^{229-196}$ model and the crystal structure of RhoA (pdb:1xcg; (Derewenda et al., 2004)) onto the crystal structures of SopE and Cdc42, respectively, within the SopE-Cdc42 complex

(pdb:1gzs;(Buchwald et al., 2002)) (Figure 3.12). In this model of EspM2 bound to RhoA, almost all of the interactions derived from the titration experiments lie within the interface and are situated at both of the switch sites of RhoA giving validity to the EspM2 model. The structural data also demonstrated that EspM2 adopts an inverted V shape comprised of six alpha helices which is very similar to that of SopE (Figure 3.12 B). Interestingly, EspM2 also has a flexible loop, which although is unrelated on a sequence level, occupies a similar position to the catalytic GAGA loop of SopE. These results suggest that EspM2 may utilise a similar mechanism to SopE in order to GEF RhoA. In addition to its homology with SopE, EspM2 also shares a significant degree of structural similarity with the recently structed WxxxE effector Map (Huang *et al* 2009). Both Map and EspM2 adopt a very similar inverted V structure and share a common catalytic loop and GTPase interacting domain.

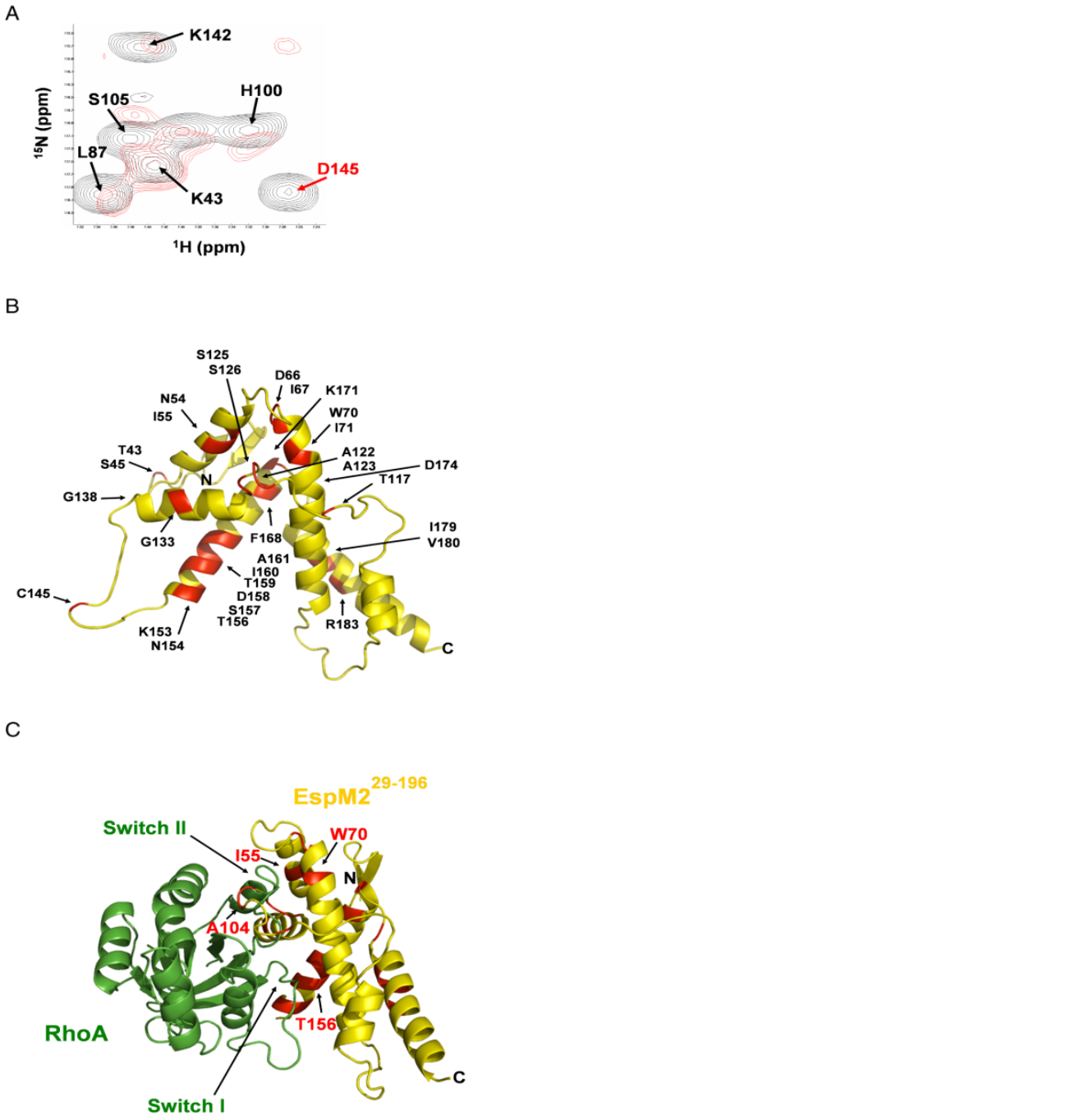


Figure 3.12 Model of EspM2$^{29\text{-}196}$ and the EspM2$^{29\text{-}196}$-RhoA complex. A. ^{15}N HSQC titration of RhoA against EspM2$^{29\text{-}196}$. Black peaks show no addition of RhoA whilst red peaks show 4-fold molar excess of RhoA. Chemical shift changes were deemed significant if the peak intensity was reduced by more than 80% (i.e. D145). B. Homology model of EspM2$^{29\text{-}196}$ created with SWISS-MODEL (Arnold *et al.*, 2006.) Data from the RhoA titration have been mapped onto the model and are coloured red with residues labelled. C. Model of the EspM2$^{29\text{-}196}$-RhoA complex created by superimposing the EspM2$^{29\text{-}196}$ model and the crystal structure of RhoA (pdb:1xcg; Derewenda *et al.*, 2004) onto the crystal structure of the SopE-Cdc42 complex (pdb:1gzs; Buchwald *et al.*, 2002). All residues identified by the RhoA titration appear at the interface except for those within the C-terminal helix. In this model the intimate contacts with EspM2 are through the switch regions I and II of RhoA.

3.13 Site Directed Mutagenesis of the EspM2 Catalytic Loop.

Based on the titration and modelling we selected three EspM2 residues for mutagenesis, the mutant W70A was used as a control. The three residues selected, L118, Q124 and I127, are located within the loop equivalent to the catalytic loop of SopE. The EspM2$^{29-196}$ derivatives were expressed ectopically in Swiss 3T3 cells and formation of stress fibres was determined microscopically (Figure 3.13). As shown in Figure 3.5 a W70A substitution completely abolished stress fibre formation (Figure 3.14). The other mutations had diverse effects on the capacity of EspM2 to induce stress fibres. We found that replacement Q124A had a mild effect on EspM2 activity, while I118 reduces the formation of stress fibres by 50% and L127A by 60% (Figure 3.14). These results show that I118, L127 and Q124 play an important role in induction of stress fibres by EspM2. Together with the structural shifts in EspM2 upon RhoA interaction demonstrated previously (Figure 3.12) these results indicate that I118, Q124 and L127 may be part of a catalytic loop analogous to that described for SopE and Cdc42 (Buchwald et al., 2002).

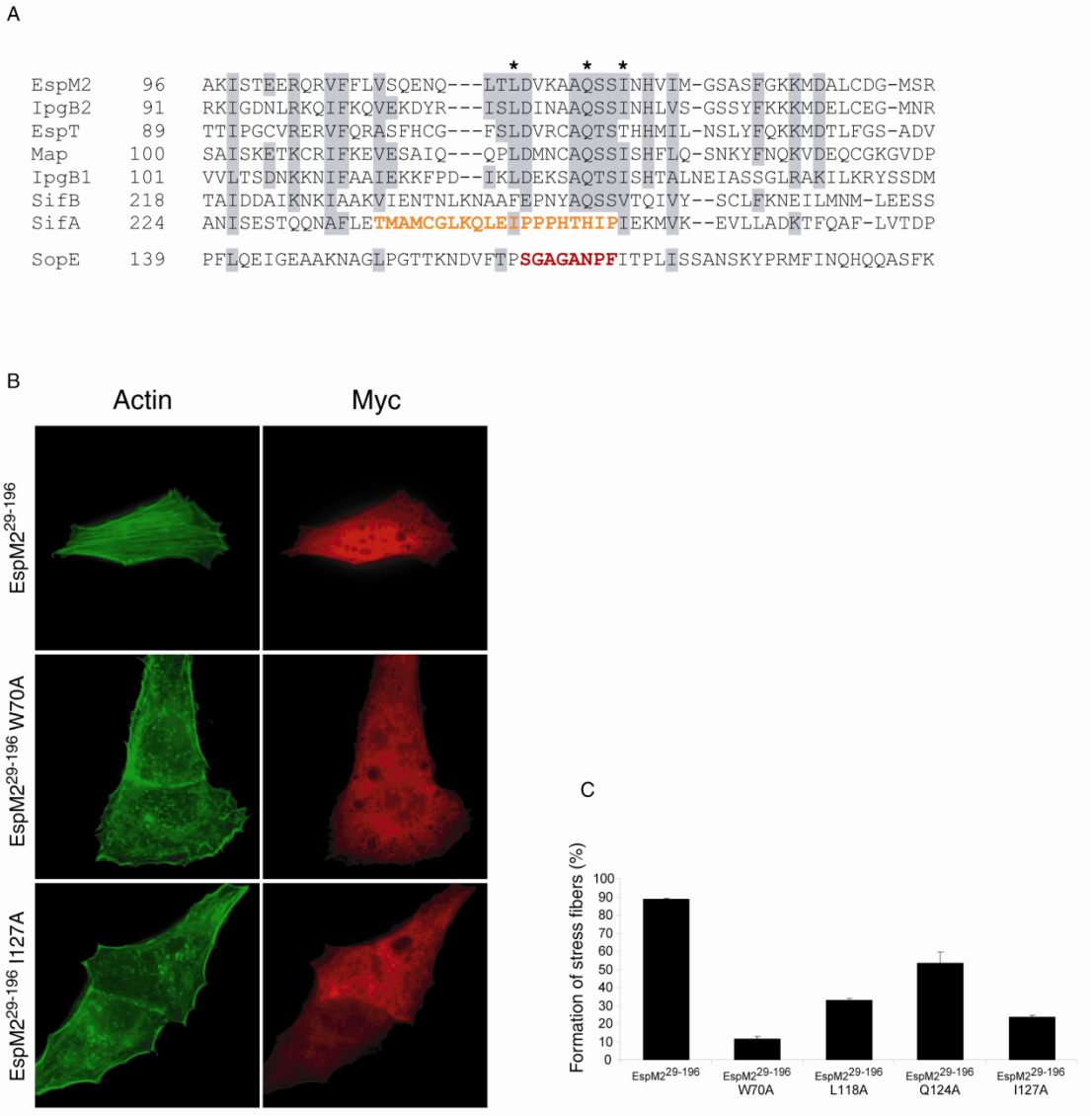


Figure 3.13 Site directed mutagenesis of the EspM2 catalytic loop. Serum-starved Swiss 3T3 cells were mock transfected or transfected with the mammalian expression vector pRK5 encoding myc-tagged EspM2, EspM2$^{29\text{-}196}$, EspM2$^{29\text{-}196}$ W70A and EspM2$^{29\text{-}196}$ I127A for 19 h. Actin was stained with Oregon green phalloidin and the myc tag was detected with monoclonal antibody. Transfection of EspM2 and EspM2$^{29\text{-}196}$ induces the formation of parallel stress fibers. Transfection of mutants EspM2$^{29\text{-}196}$ L118A, EspM2$^{29\text{-}196}$ Q124A and EspM2$^{29\text{-}196}$ I127A abolished to different extent the formation of stress fibers. B. Quantification of stress fibers on Swiss 3T3 after 19h transfection with EspM2, EspM2$^{29\text{-}196}$, EspM2$^{29\text{-}196}$ W70A, EspM2$^{29\text{-}196}$ L118A, EspM2$^{29\text{-}196}$ Q124A and EspM2$^{29\text{-}196}$ I127A. Fifty cells were counted in duplicate in three independent experiments. Results are displayed as mean ± SEM.

3.14 Distribution of EspM in EPEC and EHEC Strains

Among the WxxxE effectors, Map, which is encoded on the LEE region, is absolutely conserved in all EPEC and EHEC strains. However the EspM family of effectors are carried on cryptic prophages and as such it is not currently known how widespread these proteins are amongst clinical EPEC and EHEC. In order to address this and determine the prevelance of *espM* genes in EPEC and EHEC, in collaboration with Drs Tania Gomes, Jorge Blanco and Ana Arbeloa, we screened several sets of clinical EPEC and EHEC isolates from collections in Spain and South America.

In order to screen for *espM* by PCR we used the eight *espM* sequences identified in EHEC O157 strain Sakai, EPEC strains B171 and E22 and *C. rodentium*, to design common internal espM-F1 (5'-TCTTTCAGCTCTTTTGGTAT) and espM-F2 (5'-CCAAAAGAAGCATTCCCCATTAT) forward and reverse primers. The identity of representative PCR amplicons was confirmed by DNA sequencing. We screened by PCR 943 EHEC and EPEC strains for the presence of *espM*, EHEC O157:H7 Sakai and EPEC E2348/69 were used as positive and negative controls.

We first screened 45 non-sorbitol fermenting (nsf) EHEC O157:H7 (expressing Stx1 and Stx2) isolated in Spain, Canada and Bolivia and two SF EHEC O157:H- (expressing VT2), isolated in Germany for the presence of *espM* genes. *espM* was found in 43 of the non-SF O157 isolates (95%) and in the two sf isolates (Table 3.14). We then screened 151 non-O157 EHEC strains and *espM* was found in 60 of 62 (97%) of the non-O157 EHEC strains belonging to serogroups O26, O103, O111, O118 and O145 (Table 3.14). In contrast *espM* was found in only 17 of 89 (19%) strains belonging to the other non-O157 serogroups (Table 3.14).

We then screened a total of 132 tEPEC strains, isolated in Brazil, Bolivia, Burundi, Spain, Chile, Germany, UK and Uruguay and 602 aEPEC strains, isolated in Brazil, Bolivia, Chile and Spain for the presence of *espM*. *espM* was found in 91 tEPEC isolates (69%) belonging to 16 different serogroups (the O serogroup of 6 strains was non-typeable - ONT) (Table 3.15). *espM* was found in 259 aEPEC isolates (43%) belonging to 59 different serogroups (the O serogroup of 109 strains was ONT (Table 3.16). Of the 109 ONT aEPEC *espM* was found in 45 isolates (41%). Among the atypical EPEC which share serogroups with the some EHEC strains, *espM* was found in 23 of 31 (74%) O26, 4 of 12 (33%) O103, 2 of 4 (50%) O111, 25 of 33 (73%) O145 and 4 of 7 (57%) O157 isolates; in total 58 of 87 or 66%. Interestingly, *espM* was found in 100% (16 of 16) of the O55 strains, regardless of serotype.

Table 3.14: Distribution of *espM* among 151 non-O157 clinical EHEC strains.

Serotype (no. of strains)	Stx^+ type	*espM*
ONT (14):HND(7), H-(6), H11(1)	1,2	4
O5 :HND(3)	1,2	2
O14 :H-(1)	1	1
O26 (37): HND(17), H-(2), H8(1), H11(17)	1	36
O32 :H6 (1)	1	1
O69 :H21 (1)	1	1
O80 :HND (1)	1,2	1
O98 :H21 (1)	1	1
O103 (6):HND(1), H2(5)	1,2	6
O111 (10):HND(5), H-(3), H8(1), H10(1),	1,2	9
O118 (6):HND(3), H-(1), H16(2)	1	6
O121 (2):H19(1), H40(1)	2	2
O145 (3):HND(1), H-(2)	1,2	3
O146 :HND(10)	1,2	1
O156 :H25(2)	1	2
O139, O141 :HND(1)	1,2	1

***espM* negative strains :- ONT :HNT (2), ONT :H5 (1), ONT :H8(1),ONT :H18 (1), ONT :H39 (1), O2 :H27 (1), O8 :H2 (1), O8 :H19(1), O15 :H16 (1), O15:H28 (1), O18 :ND (2), O22:H42 (1), O55:H- (1), O63 :HND (2), O64:H21 (1), O76 :ND (2), O76:H19 (2) O84:HNT (1), O84 :HND (1), O91:H- (2), O98:H- (1), O104 (4), O113 :HND (2), O113:H21 (2), O117 :HND (1), O136 :HND (1), O141 :HND (1), O146:H- (1), O146:H21 (4), O148 :HND (2), O148:H8 (1), O165:H- (1), O166 :HND (1), O166:H28 (1), O168:H8 (1), O174:H21 (1), O183:H- (1)**

Table 3.15: Distribution of *espM* among 132 tEPEC strains.

Serotype (no. of strains)	Origin	*espM*
ONT (2) :H6(1), H10(1)	Bolivia	2
O23 (2) :HND(1), H8(1)	Spain	2
O49 :H10(5)	Spain, Bolivia	5
O55 (22) :H-(8), H6(6), H51(8)	Uruguay, Bolivia, Brazil, UK	19
O86 (6): H-(2), H34(4)	Bolivia, Brazil,	6
O88 (17) :H-(1), H6(1), H25(15)	Spain, Bolivia	3
O103 (3) : H-(1), H7(2)	Bolivia	3
O109 :H-(2)	Spain, Chile	1
O111 (20) :H-(12), H2(7), H25(1)	Spain, Bolivia, Brazil, Uruguay	19
O118 (4) : HND(1), H-(1), H5(2)	Spain, Germany	4
O119 (17) :H-(2), H6(15)	Bolivia, Brazil, Uruguay	16
O125 :H-(1)	Burundi	1
O127 :H6(3)	Bolivia, Brazil,	1
O132 :H8(1)	Bolivia	1
O142 (6) :H6(2), H34(4)	Brazil, Spain	4
O145 :H45(3)	Brazil	3
O153 :H11(1)	Spain	1

***espM* negative strains: ONT :HND (1), ONT :H1, H12 (1), ONT :H8 (1), ONT :H25 (1), O1 :H1, H12 (1), O55 :H8 (1), O86 :H8 (1), O88 :H5 (2), O98 :HND (1), O127 :H40 (3), O131 :H46 (2), O153 :H8 (1), O157 :H45 (1)**

Table 3.16 Distribution of *espM* among 602 aEPEC strains.

Serotype (no. of strains)	Origin	*espM*
ONT(92)* :	Spain, Brazil, Bolivia, Chile	45
O1 (3): H7(1),H40(1),H45(1)	Brazil, Spain	3
O2 (11) :ND(3), H40(8)	Spain	3
O4 (4) : ND(2), H-(1), H1(1)	Spain, Brazil	3
O5 :ND(7)	Spain	2
O6 (2) :ND(1), H19(1)	Spain	2
O8 (5): HND(3), H11(1), H19(1)	Spain	3
O10 (5): HN(3), H-(2)	Spain	4
O11 :HND(4)	Spain	4
O14 :H5(1)	Brazil	1
O15 (17): HND(9), H2(8)	Spain	12
O18 :HND(2)	Spain	2
O20 :HND(2)	Spain	2
O22 :HND(2)	Spain	2
O25 :H2(1)	Spain	1
O26 (30) :ND(20), H-(6), H11(4)	Spain, Brazil	23
O28 : H28(1)	Bolivia	1
O33 :HND(3)	Spain	1
O49 (12): HND(6),H-(3), H2(1), H10(2)	Spain, Brazil	6
O51 (16): HND(5), H-(2), H1(1), H40(6), H49(2)	Spain, Brazil	7

O52 : H10(1)	Spain	1
O57 : H7(3)	Spain	3
O55 (16) :HND(4), H-(1), H6(1), H7(9), H51(1)	Spain, Brazil, Bolivia	16
O56 :H-(1)	Spain	1
O63 (6) : H6(5), H33(1)	Spain, Brazil	2
O64 :H25(2)	Spain	1
O70 :H2(1)	Brazil	1
O76 :HND(3)	Spain	2
O80 (9): ND(5), H2(4)	Spain	4
O82 (2): HND(1), H10(1)	Spain	2
O85 (13) :HND(5), H-(2), H31(5), H43(1)	Spain	4
O101 (7): HND(2), H-(5)	Spain, Brazil	7
O103 (12): HND(11), H2 (1)	Spain	4
O104 (4) :HND(1), H2(2), H12(1)	Spain, Brazil	2
O109 :H9(1)	Brazil	1
O111 (2) :HND(1), H-(1)	Spain	2
O113 :H6(4)	Spain	1
O115 (4): HND(1), H8(3)	Spain	3
O117 :HND(4)	Spain	2
O119 :HND(2)	Spain	2
O120 :HND(2)	Spain	1
O123 :H-(2)	Brazil	2
O125 :H28(1)	Spain	1
O127 :H40(5)	Spain, Bolivia	1
O128 (4) : HND(1), H-(1), H2(1), H27(1)	Spain	4
O132 :H34(3)	Spain	3
O139 :H19(1)	Spain	1
O145 (33) : HND(19), H-(8), H4(1), H5(1), H28(4)	Spain, Germany	25
O146 :HND(1)	Spain	1
O153 :HND(15)	Spain	2
O154 :H9(1)	Brazil	1
O156 (8) : HND(6), H-(2)	Spain	4
O157 (5): ND(2), H7(3)	Spain	4
O162 (4) :H-(2), H21(1), H33(1)	Spain, Brazil	3
O166 :HND(1)	Spain	1
O167 (4) :ND(2), H9(1), H11(1)	Spain	3
O177 :H11(1)	Spain	1
O178 :H7(1)	Spain	1
O179 :H31(1)	Spain	1
O115, O152(15) : HND(13), H8(1), H10(1)	Spain	10
R (2): H11,21(1), H28(1)	Brazil	1

EspM **negative strains ONT :H2 (2), ONT :H6 (4), ONT:H9 (1), ONT:H10 (2), ONT : H11, 21, 34 (1), ONT :H19 (2), ONT : H21,39 (1), ONT:H34 (1), ONT :H40, 43 (2), ONT:H51 (1), O1:H2 (1), O1:H11 (1), O1 :H46 (1), O1 :H49 (1), O2ab : H45 (1), O2 : NT (1), O2 :H6 (1), O2 :H16 (1), O2 :H45 (1), O2 :H49 (2), O3 :H4 (1), O5 :H6 (1), O5 :H40 (1), O5 :H49 (1), O6 :H4 (1), O6 :H16 (1), O9 :HND (2), O11 :H16 (2), O12 :HND (1), O13 : H11 (1), O15 :H- (2), O15 :H7 (1), O16 :H- (1), O18 :H7 (1), O18 :H16 (1), O20 :H6 (1), O21 :HND (2), O21 :H15 (1), O23 :HND (1), O24 :H2 (1), O25 :HND (2), O25 :H1 (1), O26 :H2 (1), O28 :HND (1), O33 :HNT (1), O33 :H6 (1), O33 :H34 (1), O34 :H- (1), O41 :H- (1), O49 :H40 (1), O51 :H41 (1), O55 :H40 (1), O56 :H6 (1), O63 :HND (1), O64 :H40 (1), O71 :H1, H12 (2), O76 :H19 (1), O84 :HND (1), O84 :H- (2), O85 :H8 (1), O85 :H49 (1), O86 :HNT (1), O86 :HND(1), O88, O168:HND (1), O98 :H- (1), O98 : H8 (1), O101 :H33 (2), O103 :H- (3), O103 :H4 (1), O103 :H19 (1), O103 :H40 (1), O104 :H- (2), O105 :HND (1), O105 :H4 (2), O108 :HND (3), O110 :HND (5), O111 :H9 (1), O111 :H38 (1), O112 :H15 (1), O113 :HND (4), O113 :H- (1), O114 :HND (1), O117 :H11 (1), O117 :H40 (2), O121 :HND (1), O123 :HND (1), O123 :H19 (1), O123 :H45 (1), O125:H6 (3), O127 :HND (1), O127 :H6 (1), O128 :H40 (1), O129 :HND (1), O129 :H- (1), O132 :HND (3), O132 :H5 (3), O137:HND (3),**

3.15 Discussion

In 2006 Alto et al. (Alto et al., 2006) assembled several known T3SS effectors into a single family which share a common motif consisting of an invariant tryptophan and glutamic acid residue separated by three variable amino acids (WxxxE). The authors suggested that IpgB1, IpgB2 and Map (the founder WxxxE effectors) mimic, in a GTP independent mechanism, the activated form of Rac1, RhoA and Cdc42, respectively. In this chapter we report the discovery and characterization of an array of T3SS effector proteins in A/E pathogens which belong to the WxxxE family. These new effectors share a high degree of homology with each other (47-86% identity) and with the *Shigella* effector IpgB2 (40-47% identity). We have defined this novel family of A/E effectors as the EspM family of proteins. Map is encoded on the LEE pathogenicity island which is conserved by all A/E pathogens, however the EspM proteins identified in this study are found mainly on prohages or other insertion elements. While a core set of T3SS effectors are encoded on LEE, the genome of clinical isolates of EPEC and EHEC are often enriched by mobile genetic elements which carry novel virulence factors which can increase the T3SS effector repetiore. The number of T3SS effector proteins is highly variable between different A/E pathogen strains ranging from 26 in EPEC E2348/69 to over 50 in EHEC Sakai. In order to determine the prevelance of the *espM* family in the A/E pathogens we screened several collections of clinical isolates. Screening of EPEC and EHEC clinical isolates revealed that the *espM* family members are well represented in most clinical isolates suggesting this family of effectors may play an important role in the virulence of A/E pathogens.

The founder WxxxE effectors are potent modulators of the host actin cytoskeleton (Alto et al., 2006; Handa et al., 2007; Kenny et al., 2002). In order to determine if the new proteins we studied are true WxxxE effectors that can subvert actin dynamics, we utilised EPEC

EPEC234/69 as a vehicle for protein translocation into Swiss cells. EPEC234/69 is a suitable host as it only harbours the WxxxE effector Map, which only induces transient filopodia at early time points post infection (Kenny and Jepson, 2000).

Using this infection model, we demonstrate that over-expression EspM1, EspM2, EspM3 and TrcA in EPEC E2348/69 triggers formation of stress fibres; similar to those induced by the *Shigella* effector IpgB2 (Alto *et al.*, 2006). Importantly, the stress fibres triggered by these WxxxE effectors had distinct architectures. Althoughthe EspM homologues were expressed from isogenic plasmids, we cannot exclude the possibility that differences in expression levels or translocation efficiency may contribute to their distinct stress fibre morphologies which appear as global parallel stress fibres (GP-SF) throughout the cell for EspM2, and local parallel stress fibres (LP-SF) restricted to the site of bacterial attachment in the case of EspM1 and TrcA. Most striking was the phenotype associated with translocation of EspM3, which induced formation of local radial stress fibres (LR-SF), which are reminiscent of the phenotypes linked to constitutively active Rho Kinase and phorbal ester treatment such as TPA (Imamura et al., 1998). To our knowledge, this is the first time that such a phenotype has been described in an infection context. The fact that ectopic expression of EspM2 results in GP-SF formation confirms that EspM proteins are sufficient to induce stress fibre formation independently of other bacterial factors. Despite the global and localized stress fibres triggered by EspM2 and EspM1 and EspM3, respectively, all proteins were found diffusely in the cytsol. Vinculin was found at the tip of the EspM family effector-triggered stress fibres suggesting that they are linked to the plasma membrane via focal adhesins.

As EspM2 and EspM3 trigger the two extreme stress fibre phenotypes they were chosen for detailed functional analysis. We confirmed that the GP-SF and LR-SF triggered by EspM2 and

EspM3 are dependent on the conserved WxxxE motif via substitution of the conserved Trp with an Ala. However, using conservative substitutions, Tyr and Asp for the Trp and Glu respectively, we did not observe any significant loss in biological activity. Translocation of EspM2 YxxxE and EspM2 WxxxD resulted in global stress fibre formation, while translocation of EspM3 YxxxE and WxxxD resulted in formation of mainly LP-SF as compared to the LR-SF observed in the wild type phenotype. The reason for the change of morphology observed for EspM3 YxxxE and WxxxD is currently not known but may be resultant from a decreased efficiency of translocation or reduction in the stability of the mutant proteins. These results suggest that the biological activity of the WxxxE proteins does not require the presence of the conserved tryptophan or glutamic acid but rather the presence of a bulky aromatic residue and an amino acid carrying a carbocylic acid side group suffices. Carboxylic side groups are involved in a range of biological functions such as protease activity (Kakudo et al., 1992) and interactions particularly with positively charged moieties such as metal ions. Structural analysis of EspM2 reveled that the conserved W70 residue of EspM2$^{29\text{-}196}$, is situated at the junctional region of two three-helix bundles. Recombinant EspM2$^{29\text{-}196}$ W70A was completely unstable, demonstrating the essential structural role of this residue in EspM2$^{29\text{-}196}$. A recent study by Ohlson and colleagues (Ohlson et al., 2008) determined the structure of the WxxxE effector SifA, and in agreement with the proposed role of the WxxxE motif in protein stability, it was reported that the conserved tryptophan forms multiple hydrophobic contacts with neighbouring residues and that the glutamic acid residue forms a hydrogen bond with an adjacent alpha helix.

The Ras superfamily of the small GTPases is the target of many bacterial effectors and toxins due to its role in the control of a wide range of cellular processes including cytoskeletal dynamics, membrane trafficking and growth (Etienne-Manneville and Hall, 2002). Several T3SS

effectors, such as YopT from *Yersinia* spp. Which proteolytically cleaves RhoA, Rac1 and Cdc42, are known to directly modify the small GTPases (Shao et al., 2002). Other effectors can either modify or mimic GEFs or GAPs (reviewed in (Finlay, 2005)). Although IpgB1, IpgB2 and Map do not share any sequence homology with the Rho GTPases, Alto et al. suggested that they may mimic, in a GTP-independent mechanism, the activated form of Rac1, RhoA and Cdc42, respectively (Alto *et al.*, 2006). The authors showed that stress fibre formation was RhoA independent as IpgB2 was functional in the presence of RhoA inhibitors (e.g. C3 botulinum toxin) or dominant negative $RhoA^{T19N}$. Moreover, it was shown that IpgB2 interacts with two of the major effectors of RhoA namely mDIA and ROCK, activating the latter directly. Alto et al. also reported that transfection of IpgB1 stimulated formation of actin-rich membrane ruffles at the dorsal cell surface, which resembled membrane ruffles induced by Rac1 (Alto *et al.*, 2006). Dorsal ruffles were not produced by $IpgB1^{E80A}$. A recent study by Handa et al. (Handa *et al.*, 2007) has shown that IpgB1 mimics RhoG and triggers membrane ruffling by binding ELMO and recruiting the ELMO - Dock180 complex to the membrane where it functions as a GEF for Rac1.

In this chapter we found that EspM2 and EspM3 activate RhoA. Using dominant negative $RhoA^{T19N}$ we observed a 60% and 40% reduction in stress fibre formation after infection of Swiss cell with E2348/69 expressing EspM2 and EspM3, respectively. In agreement with Alto et al 2006 (Alto *et al.*, 2006), using the specific ROCK inhibitor Y27632 we showed that the stress fibres induced by EspM2 and EspM3 are totally dependent upon ROCK activity. Consistent with this we have shown that EspM2 and EspM3 trigger phosphorylation of cofilin, a classical downstream ROCK target. Further characterisation of EspM2 using surface plasmon resonance (BiaCore) showed that $EspM2^{29-196}$ forms a stable complex with nucleotide free RhoA. The

dissociation of the EspM2-RhoA complex was very slow and as a consequence we were unable to measure the dissociation rate constant. In order to induce the nucleotide exchange GEFs form an initial low affinity complex, through binding the Switch 1 and 2 regions of the GDP-bound Rho GTPase, which favours GDP and Mg^{2+} release. This is then rapidly converted into a high affinity GEF-GTPase binary complex; loading with free GTP leads to dissociation of the GEF and formation of a tight Rho GTPase-GTP complex, which binds downstream effectors. To test if EspM2 has a GEF activity we incubated RhoA with mant-GTP and increasing concentrations of $EspM2^{29-196}$. We found that $EspM2^{29-196}$ induced loading of GTP into RhoA in a dose dependent manner. This activity was specific for RhoA as $EspM2^{29-196}$ only induced weak nucleotide exchange in Cdc42, while no nucleotide exchange was seen for Rac1 and the distant related GTPase HRas. Interestingly, the *Salmonella* WxxxE effector SifA, which also binds RhoA did not exhibit a detectable GEF activity.

SopE from *Salmonella* was the first described T3SS effector GEF (Hardt et al., 1998). SopE activates Cdc42 and Rac1 leading to formation of membrane ruffles and bacterial invasion (Hardt et al., 1998). The crystal structure of the SopE-Cdc42 complex illuminated the mechanism by which SopE functions as GEF (Buchwald et al., 2002). SopE is composed of six α-helixes arranged in two three-helix bundles forming a V-shape (Buchwald et al., 2002). The junction connecting the two arms consists on small β sheet followed by a loop consisting of the GAGA motif, which is proposed to be the catalytic loop of SopE. Insertion of the GAGA motif between the switch regions of Cdc42 induces a push and pull type movement and release of GDP (Buchwald et al., 2002). Although SopE does not share sequence or structural similarity with eukaryotic GEFs, they induce similar conformational changes in the Rho GTPases. NMR analysis of $EspM2^{29-196}$ revealed that it also has six alpha helixes arranged in a V shape structure

similar to SopE and a loop connecting the two arms (Buchwald et al., 2002; Ohlson et al., 2008) Interestingly, the sequence of this putative catalytic loop is conserved between EspM2$^{29-196}$ and other WxxxE effectors, apart from SifA, which might provide an explanation to the inability of SifA to GEF RhoA. We substituted three residues located within the putative catalytic loop of EspM2$^{29-196}$, L118, Q124 and I127, with alanine, a W70A substitution was used as a control as it has previously been demonstrated to lack biological activity. While transfection of Swiss 3T3 cells with EspM2 L118A and I127A had a substantial effect on stress fibre formation, little effect was seen for Q124A. A recent study by Huang *et al* (Huang et al., 2009) has solved the crystal structure of Map in complex with Cdc42. In this study the authors demonstrate that Map binds the variable β2-3 inter-switch region of Cdc42 with a structure similar to that of SopE and EspM2 (Buchwald et al., 2002). Furthermore, Huang and colleagues demonstrate that the β2-3 region acts as the determining factor in WxxxE effector GTPases specificity, as substitution of the β2-3 region of Cdc42 with that of RhoA or Rac1 severely inhibits interaction with Map. It was also demonstrated that IpgB1and IpgB2 act as a GEF of Rac1 and RhoA respectively (Huang et al., 2009).

Together these results demonstrate that the EspM family of proteins and other WxxxE effectors act as GEFs of the Rho family of small G proteins rather than mimics of the small GTPases themselves. Although the WxxxE effectors do not share any significant homology with SopE at a sequence level they do adopt highly similar 3 dimensional structures when in complex with Rho GTPases suggesting a convergent evolution of bacterial mammalian GEF mimics.

Chapter 4 - EspT is a Novel WxxxE Effector Which Activates Rac1 and Cdc42

4.1 Identification of the Novel WxxxE Effector EspT

In addition to identifying the EspM family of proteins as WxxxE effectors (Arbeloa *et al.,* 2008) we also used a BLAST algorithm with Map as an index protein to search for additional WxxxE family members within the A/E pathogen group. We identified a new putative effector, whose encoding gene we have named *espT,* in *C. rodentium.* EspT is encoded within the same pathogenicity island as EspM2 which also encodes an EspO/OspE homologue (Figure 3.2). EspT shares 29% identity with EspM2, 27% identity with IpgB2, and 19% identity to IpgB1. A phylogram based upon multiple sequence alignment with hierarchical clustering (Mackey et al., 2002) shows that EspT is divergent from the EspM/IpgB2 group and does not cluster well with either IpgB1 or Map (Figure 4.1).

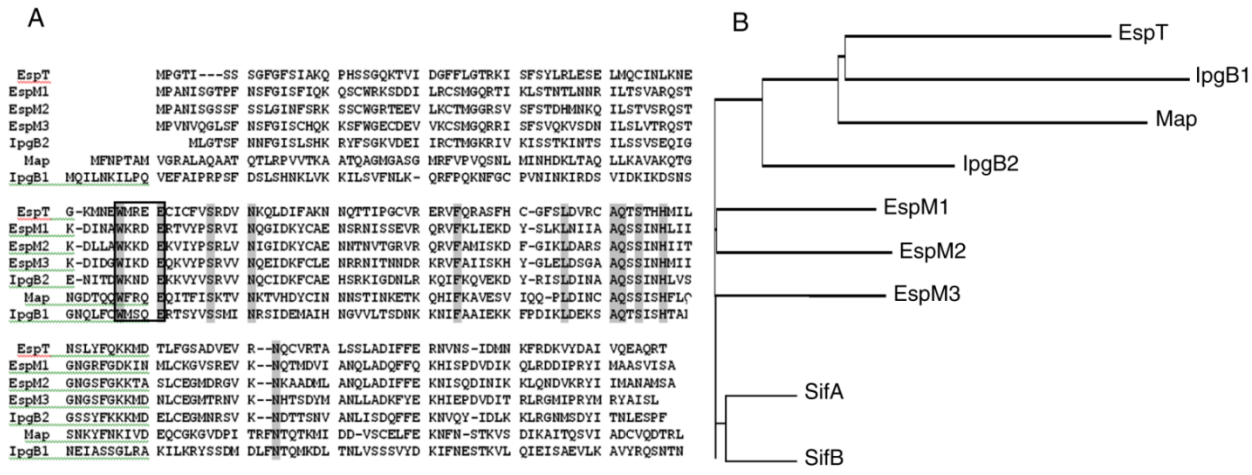


Figure 4.1 Phylogeny of the novel WxxxE effector EspT. (A) Multiple sequence alignment with hierarchical clustering of *Shigella flexneri* IpgB1 and IpgB2 along with Map, EspM2, EspM3 and EspT from *C. rodentium* and EspM1 from EPEC B171 O111:NM. Residues which are identical are highlighted in grey. The conserved WxxxE motif is boxed (B) Phenogram created using ClustalW2 showing the phylogeny of aligned WxxxE effectors in addition to SifA and SifB from *Salmonella.*

4.2 EspT is Translocated into Host Cells in a T3SS Dependent Manner

In order to confirm the status of the EspT as a WxxxE effector protein, we utilised a TEM β – lactamase fusion assay to detect translocation of the EspT into host cells as described for espM (Chapter 4). *espT* from *C. rodentium* was fused to a β – lactamase in the pCX340 vector which was transformed into wild type and the T3SS null Δ*escN* E2348/69. These strains were then used to infect HeLa cells which were pre-treated with CCF2/AM. The NleD-TEM fusion was used as a positive control (Marches et al., 2005). This assay was performed by Georgina MacKenzie (a student in the laboratory) under my supervision. EspT was found to be translocated into host cells from the wild type E2348/69 strain but not from the Δ*escN* strain indicating that EspT is translocated in a T3SS dependent manner.

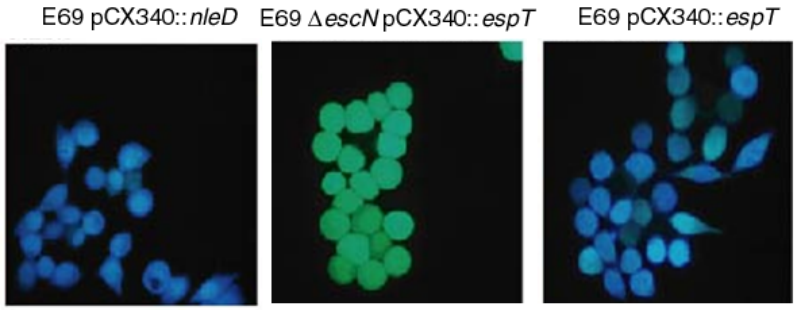


Figure 4.2 EspT is translocated into host cells in a T3SS dependent manner. HeLa cells were infected with E2348/69 (E69) containing the pCX340 β-lactamase fused to EspT. β-lactamase cleaves the CCF2/AM substrate, which fluoresces in green when uncleaved and in blue when cleaved, indicating translocation of the fusion protein. The previouslt identified T3SS effector NleD was used as a positive control. The Δ*escN* T3SS null derivative of E2348/69 was used as a negative contol for translocation.

4.3 EspT Induces Formation of Lamellipodia and Membrane Ruffles on Swiss 3T3 and HeLa Cells Respectively.

Previously characterised WxxxE effectors have been reported to induce a plethora of actin structures normally associated with activated Rho GTPases (Alto et al., 2006; Arbeloa et al., 2008; Handa et al., 2007). In order to determine if EspT has the ability to remodel actin within eukaryotic cells, *espT* was cloned into the expression vector pSA10 (Schlosser-Silverman et al., 2000) and expressed in EPEC E2348/69 which does not contain any WxxxE effectors other than Map (Arbeloa et al., 2008). E2348/69 with or without the vector encoding EspT was used to infect serum starved Swiss 3T3 and HeLa cells. E2348/69 with no plasmid or carrying empty pSA10 triggered formation of actin-rich pedestals beneath adherent bacteria on both Swiss 3T3 and HeLa cells, without any other major cytoskeletal rearrangements (Figure 4.3). In contrast, E2348/69 carrying pSA10 encoding EspT induced formation of pedestals on both cell lines and additionally triggered formation of lamellipodia on Swiss 3T3 cells and membrane ruffles on HeLa cells, which were not restricted to the site of bacterial attachment (Figure 4.3A and B). The lamellipodia induced by EspT have a strong leading edge, wide lamella, well defined microspikes and filopodia which extend beyond the cell periphery (Figure 4.3A). These lamellipodia and membrane ruffles were found in 90% and 80% of cells infected with E2348/69 respectively after 1.5 h (Figure 4.3C) and were still present at 3 h post infection. These results demonstrate that EspT is a T3SS effector that upon tranlocation triggers formation of lamellipodia and membrane ruffles and that the nature of actin rearrangement was cell type-specific.

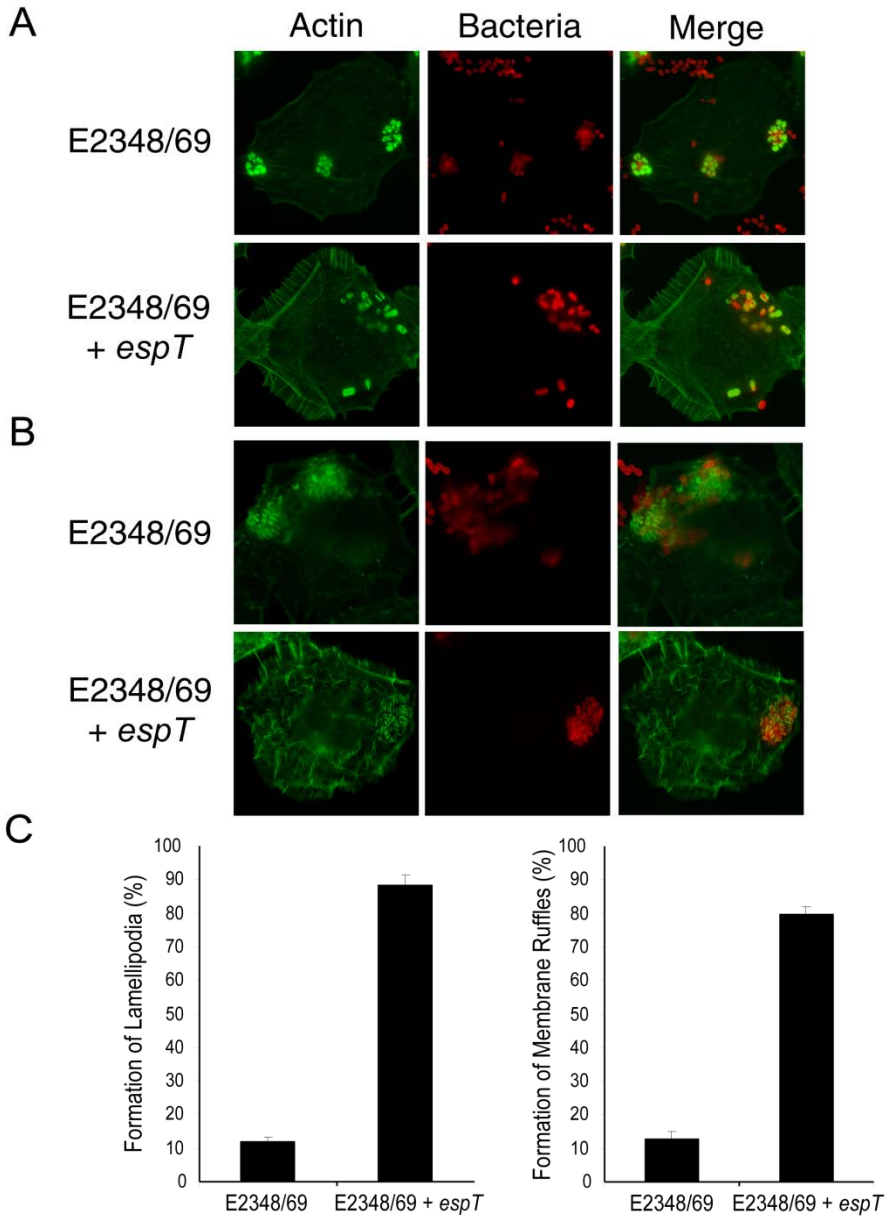


Figure 4.3 EspT induces lamellipodia and membrane ruffles on Swiss 3T3 and HeLa cells respectively. (A) Fluorescence microscopy of serum starved Swiss 3T3 cells uninfected or infected with wild type E2348/69 or E2348/69 expressing EspT for 90 min. Actin was stained with Oregon green phalloidin and E2348/69 was detected with a rabbit O127 antibody. Distinctive lamellipodia, which have a strong leading edge, wide lamella and well defined microspikes and filopodia which extend beyond the cell boundary, were observed on cells infected with E2348/69 expressing EspT but not in the wild type control. Both strains induced formation of actin rich pedestals beneath adherent bacteria. (B) Serum starved HeLa cells infected with E2348/69 expressing EspT exhibited membrane ruffles whereas those infected with wild type E2348/69 did not. Both strains formed actin pedestals. (C) Quantification of Lamellipodia and membrane ruffles on Swiss 3T3 and HeLa cells respectively after 90 min infection with wild type E2348/69 or E2348/69 expressing EspT. 100 cells were counted in triplicate in three independent experiments. Results are displayed as mean ± SEM

4.4 Ultrastructure Analysis of the EspT-Induced Membrane Protrusions

In order to further characterise the membrane protrusions triggered by expression of EspT we processed HeLa and Swiss 3T3 for Scanning Electron Microscopy (SEM). Serum starved HeLa and Swiss 3T3 cells were infected for 3 h with E2348/69 or E2348/9 expressing EspT. As in the immuno-fluorescence staining, SEM analysis revealed that HeLa and Swiss 3T3 cells infected with E2348/69 wild type did not display any significant membrane structure other than pedestals (Figure 4.4). HeLa cells infected with E2348/69 expressing EspT displayed wide spread ruffling over their entire surface, when these ruffles coincide with adherent E2348/69 they appear to form a pocket which can engulf the bacteria (Figure 4.4). Swiss 3T3 cells infected with E2348/69 expressing EspT have strong dorsal membrane ruffles and lamellipodia similar to those observed via immuno-fluorescence (Figure 4.4). Interestingly the SEM also shows that strong ruffles can be observed at the site of bacterial attachment which are not so apparent by fluorescence microscopy (Figure 4.4).

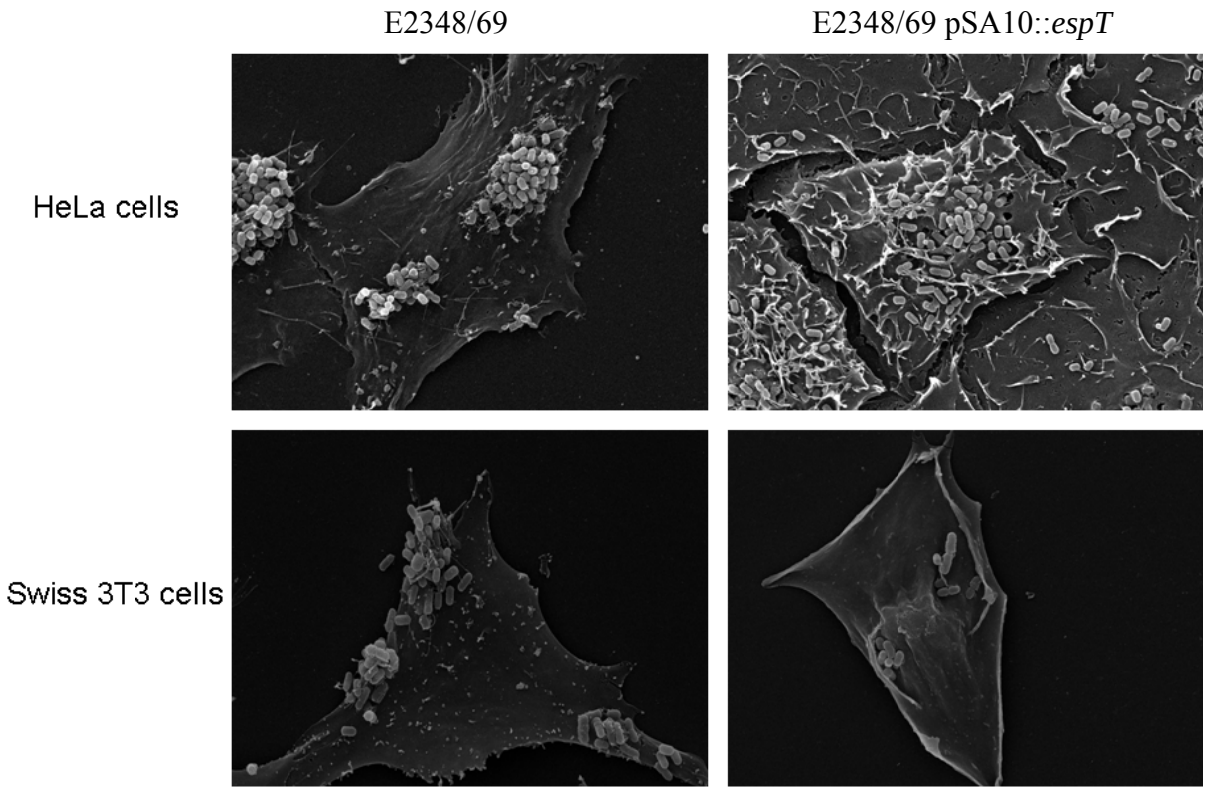


Figure 4.4 Ultrastructure analysis of the EspT-Induced membrane protrusions. Scanning electron microscopy of serum starved HeLa and Swiss 3T3 cells infected with wild type E2348/69 or E2348/69 expressing EspT for 3 hours. HeLa cells infected with E2348/69 expressing EspT display widespread membrane ruffling over their apical surface whereas the E2348/69 control did not. Lamellipodia, which have a strong leading edge, wide lamella which are distal to the site of bacterial attachment were observed on cells infected with E2348/69 expressing EspT but not in the wild type control. E2348/69 expressing EspT also induced the formation of membrane ruffles which were localised to adherent bacteria.

4.5 Ectopic Expression of EspT Results in Characteristic Actin Cytoskeletal Reorganisations

In order to determine if EspT alone is responsible for the observed lamellipodia, *espT* was cloned in the mammalian expression vector pRK5 to allow the ectopic expression of a Myc-tagged EspT. Transfection of Swiss 3T3 cells resulted in formation of lamellipodia that were indistinguishable from those visualised when EspT was delivered via infection with E2348/69 (Figure 4.5). Thus, EspT is necessary and sufficient for the re-arrangements of the actin cytoskeleton observed previously. It has been previously shown that ectopic expresion of the *Shigella* effector *IpgB1* induces formation of membrane ruffles in HeLa cells (Alto et al., 2006; Handa et al., 2007). As a control we cloned IpgB1 into pRK5 for expression as an N-terminal Myc tagged effector. Transfection of IpgB1 into Swiss 3T3 cells revealed that in contrast to EspT, IpgB1 induces membrane ruffles and not lamellipodia (Figure 4.5).

Additionally, we found that at 16 h post-transfection EspT and IpgB1 were targeted to the mitochondria, as shown by double staining with anti-Myc antibodies and Mitotracker CMXRos (Figure 4.5). Although the mitochondria appeared swollen and sometimes aggregated the fact that they were well-stained with Mitotracker CMXRos is indicative that they were metabolically active. Moreover, we did not observed any signs of apoptosis in EspT or IpgB1 transfected cells, indicating that the mitochondrial membrane has not been compromised. However, as EspT and IpgB1 contain no canonical mitochondrial targeting sequences, the mechanism involved in mitochondrial targeting remains unknown.

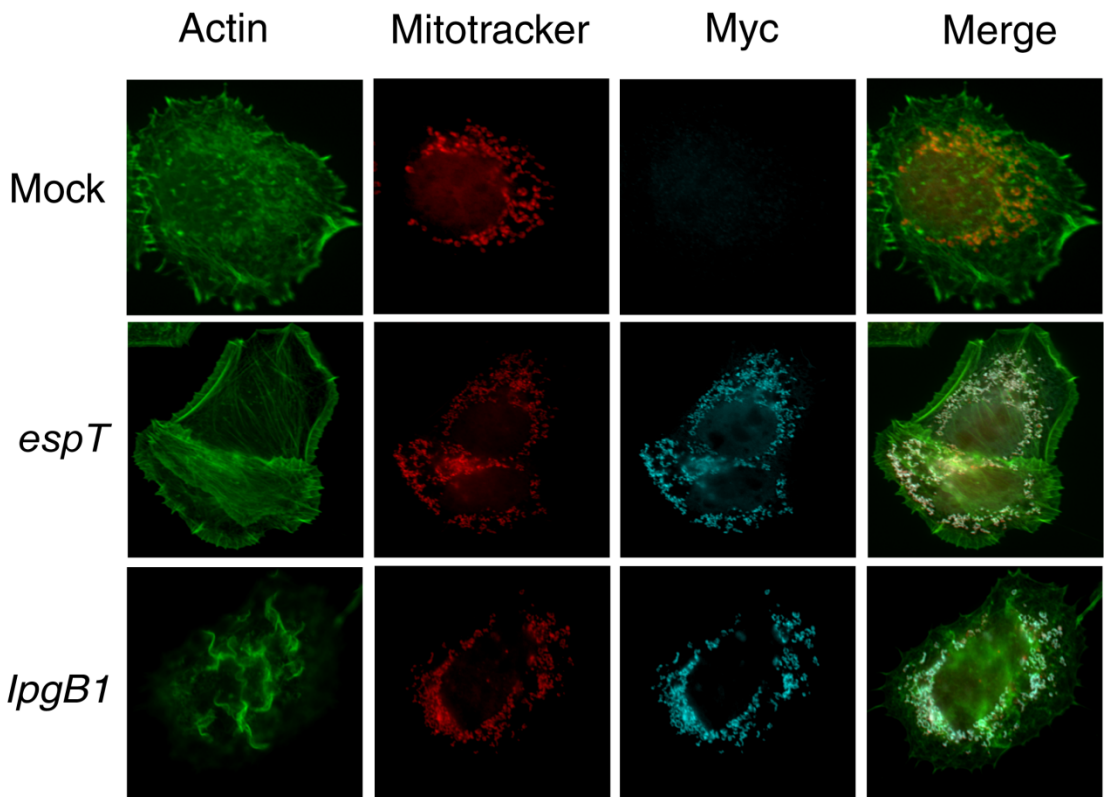


Figure 4.5 Ectopic expression of EspT induces characteristic cytoskeletal rearrangement in Swiss 3T3 cells. Serum starved Swiss 3T3 cells were mock transfected or transfected with the mammalian expression vector pRK5 encoding myc-tagged EspT, or IpgB1 for 16 h. Actin was stained with Alexifluor 633 phalloidin, the myc tag was detected with monoclonal antibody and mitochondria were stained with Mitotracker CMXRos. On transfection EspT induces the formation of lamellipodia identical to those observed during infection. Transfection of IpgB1 resulted in the induction of membrane ruffles. EspT and IpgB1 were found to be well colocalised with the mitochondrial marker Mitotracker.

4.6 EspT Triggered Lamellipodia Formation is Inhibited by Dominant Negative Rac1 and Cdc42.

WxxxE effectors have previously been demonstrated to act independently, as IpgB2, (Alto et al., 2006) or dependently, as the EspM (Arbeloa et al., 2008; Handa et al., 2007) (Figure 3.6) of the Rho GTPases. In order to determine if EspT activity was dependent on RhoA, Rac1, Cdc42 or RhoG we transfected the dominant negative forms of each of these GTPases ($RhoA^{N19}$, $Rac1^{N17}$, $Cdc42^{N17}$ and $RhoG^{N17}$), which competitively and specifically inhibit the wild type GTPase activation, into Swiss 3T3 cells. Additionally, we transfected the Cdc42 and Rac1 binding

domain (CRIB) of Pak which efficiently inhibits the downstream signalling of Rac1 and Cdc42 (Carreno et al., 2002). Transfected cells were subsequently infected with E2348/69 expressing EspT for 1.5 h and the presence of lamellipodia was assessed. Inactivation of either RhoA or RhoG had no affect on induction of lamellipodia by EspT on Swiss 3T3 (Figure 4.6). Conversely inhibition of Rac1 or Cdc42 significantly compromised the ability of EspT to form lamellipodia (Figure 4.6). The residual lamellipodia observed in the presence of the Rac1 and Cdc42 dominant negatives were shorter and less pronounced than those induced in mock transfected cells (Figure 4.6). Inhibition of both Rac1 and Cdc42 downstream signalling using the CRIB of Pak reduced the number and extent of EspT induced lamellipodia to a level comparable with the Rac1 dominant negative. This suggests that activation and subsequent downstream signalling of Rac1, Cdc42, or both is involved in the EspT signalling pathway.

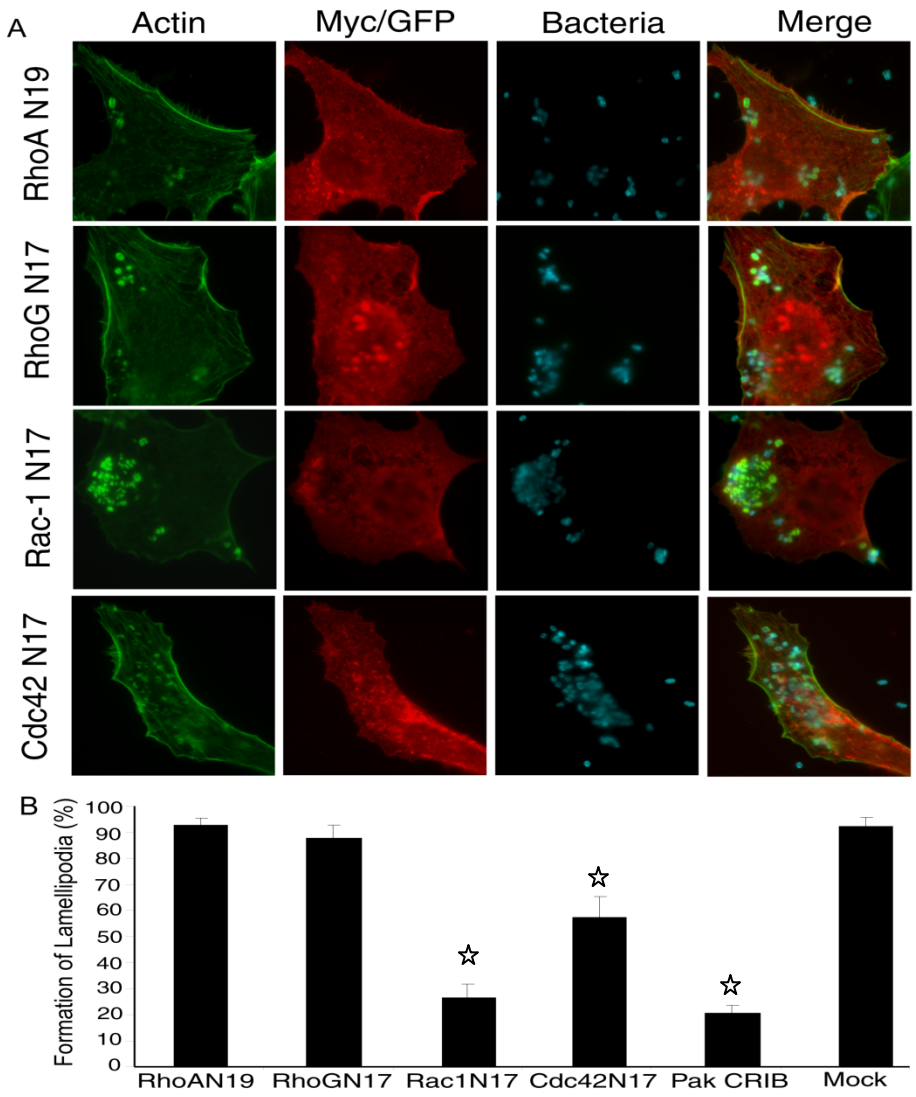


Figure 4.6 EspT-induced cytoskeletal rearrangements are dependent on Rac1 and Cdc42. (A) Swiss 3T3 cells were transfected with the dominant negative forms of RhoA, RhoG, Rac1 and Cdc42 18 h prior to infection for 90 min with E2348/69 expressing EspT. Actin was stained with Oregon green phalloidin, the Myc-tagged RhoA, Rac1 and Cdc42 dominant negatives were stained with a Myc tag monoclonal antibody, RhoG was detected via its GFP tag and E2348/69 was visualized using a rabbit O127 antibody. Actin pedestals were observed beneath all adherent bacteria. Lamellipodia were observed in cells transfected with dominant negative RhoA^{N19} and the RhoG^{N17}. The majority of cells transfected with dominant negative Rac1^{N17} did not display lamellipodia. Dominant negative Cdc42^{N17} reduced the number of cells expressing lamellipodia as well as reducing the extent of the lamellipodia compared to the mock or dominant negative RhoA^{N19} and RhoG^{N17}. (B) Quantification of lamellipodia in transfected Swiss 3T3 after 90 min infection with E2348/69 expressing EspT. 100 cells were counted in triplicate in three independent experiments. Results are displayed as mean ± SEM. Stars demonstrate the results are significant as demonstated by a student T test with p-value 0.01.

4.7 EspT Activates Rac1 and Cdc42 to Trigger Formation of Lamellipodia and Membrane Ruffles.

It has been previously demonstrated that EspM activates RhoA in order to induce formation stress fibres (Arbeloa et al., 2008) (Figure 3.7). In order to assess whether or not EspT activates Rac1 and Cdc42 we performed pulldown assays using the Cdc42 Rac1 interacting binding domain (CRIB) of Pak, which binds activated Rac1 and Cdc42 and the CRIB of WASP, which binds only activated Cdc42. Pull-downs were blotted with specific antibodies for Rac1 and Cdc42. Cells incubated with CNF1 toxin which activates Rho GTPases (Pei et al., 2001) were used as a positive control and E2348/69 containing empty pSA10 was used as a negative control. Swiss 3T3 cells infected with E2348/69 expressing EspT exhibited a marked increase in the level of activation of both Rac1 and Cdc42 compared to uninfected cells or those infected with the control E2348/69 strain (Figure 4.7). These results suggest that EspT-triggered actin rearrangements are dependent upon activation of the Rac1 and Cdc42 signalling cascades.

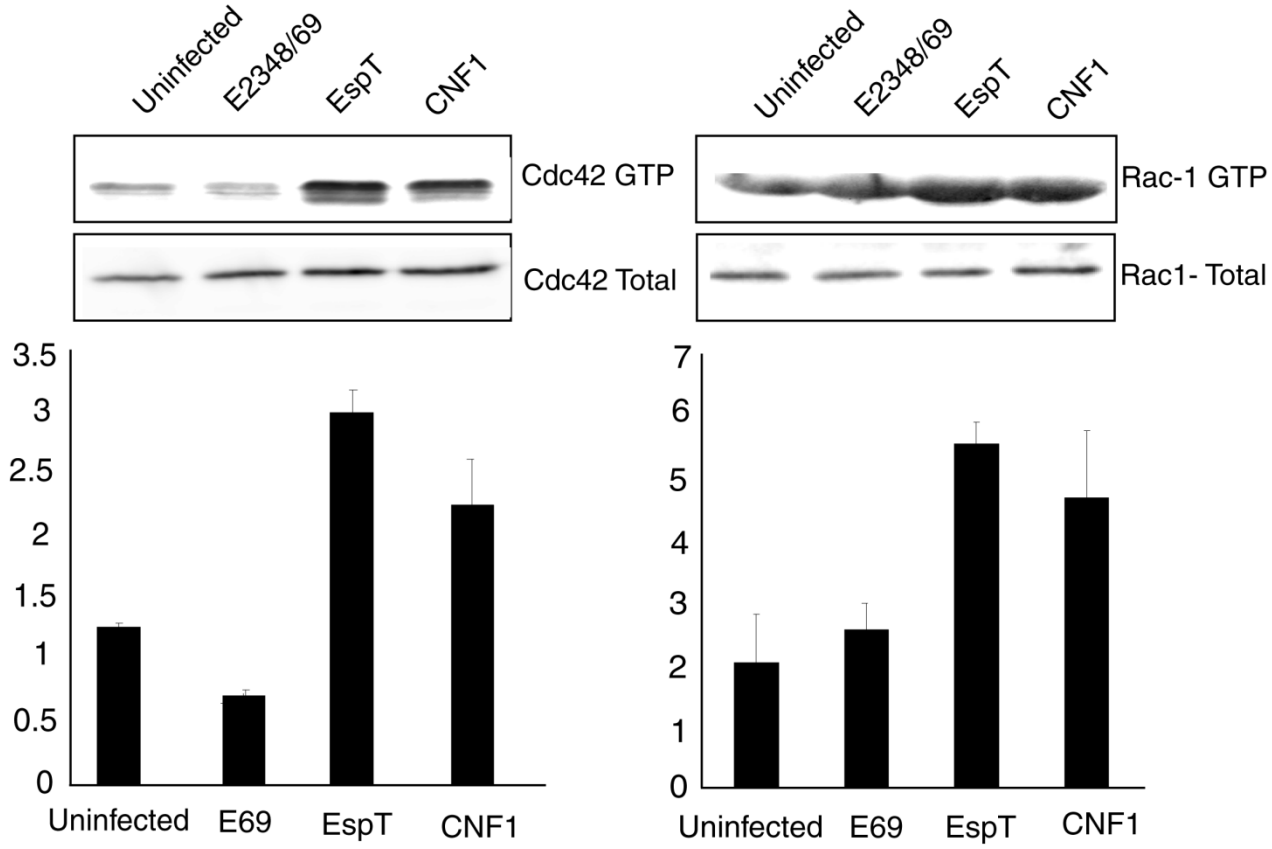


Figure 4.7 EspT activates Rac1 and Cdc42. Swiss 3T3 cells were left untreated or infected with wild type E2348/69 or E2348/69 expressing EspT. Cells treated with CNF1 toxin were used as a positive control. Cells were lysed and added to GST beads bound to either the CRIB of WASP or the Rac1 binding motif of Pak to capture active Cdc42 and Rac1 respectively. Total Cdc42 and Rac1 along with GTP bound Cdc42 and Rac1 were detected by western blotting with Cdc42 and Rac1 monoclonal antibodies. Quantified data are presented as mean ± SEM from three independent experiments.

4.8 Ectopic Expression of ELMO in Swiss 3T3 Cells Infected with E2348/69 Expressing EspT Causes a Shift from Lamellipodia to Membrane Ruffles

Despite the limited homology between EspT and IpgB1, the phenotype produced by the *Shigella* effector is reminiscent of the membrane ruffles induced by EspT in HeLa cells (Ohya et al., 2005). IpgB1 triggered membrane ruffles occur in a RhoG independent and Rac1 dependent manner (Handa et al., 2007). IpgB1 has been reported to interact with ELMO1 and ELMO2 and subsequently recruit DocK180 in order to activate Rac1 in a manner analogous to RhoG (Handa et al., 2007). Furthermore, Handa and co-workers show that ELMO is localised to the membrane ruffles produced during *Shigella* invasion (Handa et al., 2007). In order to determine if ELMO was also localised to EspT-induced dorsal ruffles and lamellipodia, we ectopically expressed ELMO1 from the mammalian expression vector pGFP. Surprisingly, when Swiss 3T3 cells expressing ELMO were infected with E2348/69 expressing EspT a shift from production of lamellipodia to membrane ruffles was observed with ELMO localized to these ruffles (Figure 4.8). These results suggest that while EspT may utilise a distinct mechanism to IpgB1 in order to induce lamellipodia in Swiss 3T3 cells that it may also be able to interact directly or indirectly with ELMO. Alternatively, over-expression of ELMO might interfere with the interaction between EspT and its typical partner proteins or affect the pathway normally used by EspT to activate Rac1 and Cdc42.

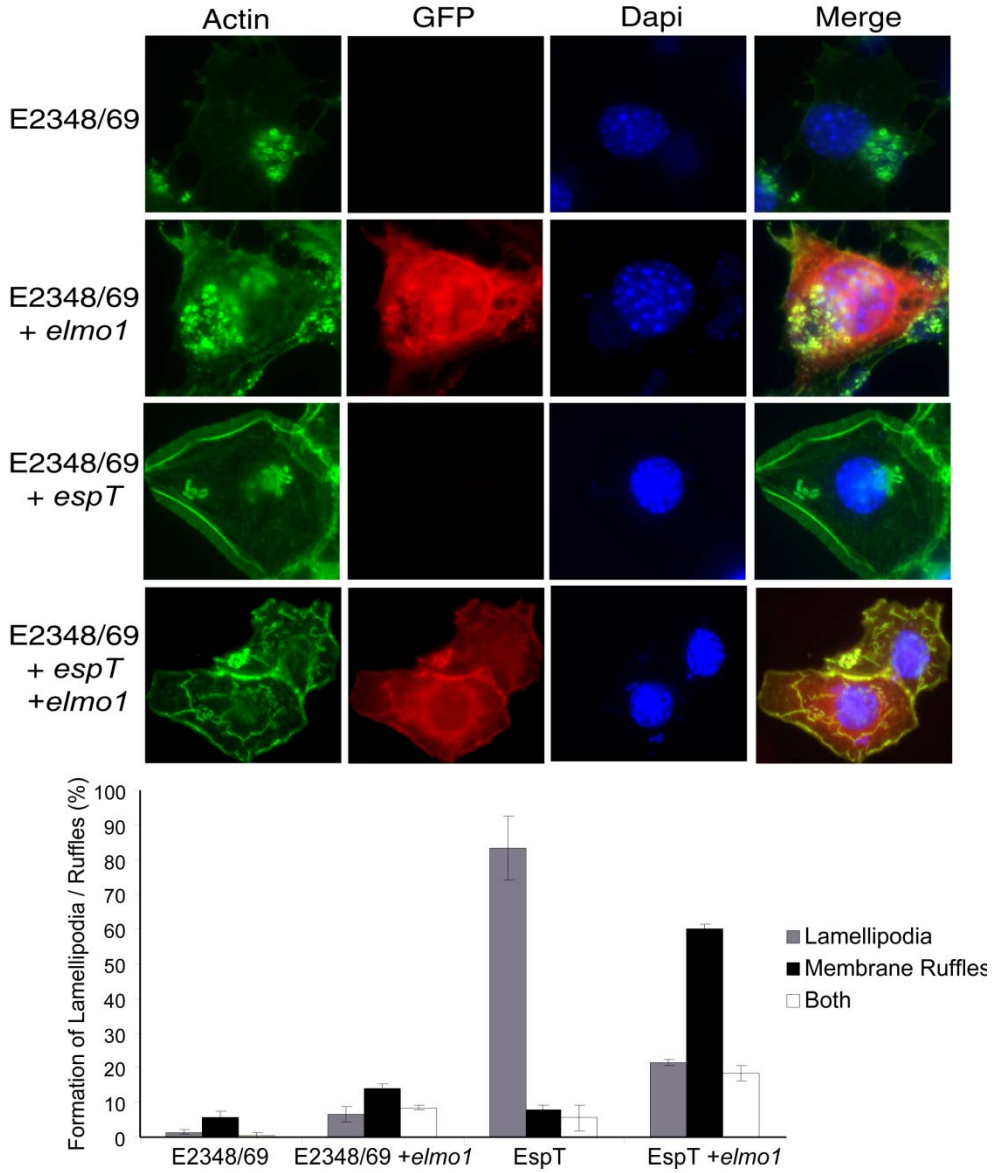


Figure 4.8 Expression of ELMO1 causes a shift from lamellipodia to membrane ruffles. (A) Swiss 3T3 cells were mock transfected or transfected with GFP tagged ELMO1 18 h prior to infection with wild type E2348/69 or E2348/69 expressing EspT. While wild type E2348/69 displayed only pedestal formation in mock transfected or cells transfected with ELMO1, E2348/69 expressing EspT induced formation of lamellipodia on mock transfected cells but in cells transfected with ELMO there was a shift from lamellipodia to membrane ruffles. (B) Quantification of lamellipodia and membrane ruffles on mock transfected Swiss 3T3 or Swiss 3T3 cells transfected with ELMO1 after 90 min infection with wild type E2348/69 or E2348/69 expressing EspT. 100 cells were counted in triplicate in three independent experiments. Results are displayed as mean ± SEM.

4.9 EspT Induced Cytoskeletal Rearrangements are Independent of ELMO or Dock180 Activity.

As EspT can induce membrane ruffles in HeLa cells and ectopically expressed ELMO induces a shift from lamellipodia to membrane ruffles in Swiss 3T3 cells (Figure 4.8) we utilized dominant negative constructs in order to investigate the role of ELMO and its binding partner Dock180 in the induction of lamellipodia and membrane ruffles by EspT on Swiss 3T3 and HeLa cells respectively. The ELMO-Dock180 complex is proposed to be a novel two part GEF which forms a trimeric complex with Rac1 where Dock180 recognises nucleotide free Rac1 and ELMO is involved in the nucleotide exchange (Brugnera et al., 2002). Handa and co-workers have previously demonstrated that IpgB1 hijacks the ELMO-Dock180 complex to activate Rac1 and induce membrane ruffles (Handa et al., 2007). In addition to its role in ELMO mediated Rac1 nucleotide exchange Dock-180 has also been shown to interact with other adaptor proteins such as CrkII and paxillin in order to mediate Rac1 activation (Valles et al., 2004). In order to determine if ELMO and Dock180 are required for EspT mediated activation of Rac1, cells were transfected with $ELMO^{T625}$ (a dominant negative of ELMO unable to interact with Dock180) or $Dock180^{ISP}$ (a dominant negative form of Dock180 incapable of interacting with Rac1) (Handa et al., 2007). Transfection of $ELMO^{T625}$ or $Dock180^{ISP}$ had no effect on the production of EspT dependent lamellipodia in Swiss 3T3 cells (Figure 4.9) or membrane ruffles in HeLa cells (Figure 4.9B). In contrast double transfection of $ELMO^{T625}$ or $Dock180^{ISP}$ with pRK5 expressing IpgB1 resulted marked reduction of membrane ruffles compared to mock transfected cells (Figure 4.9B). Together these results indicate that EspT induces lamellipodia and membrane ruffles via a mechanism which is distinct from IpgB1 and independent of ELMO or Dock180.

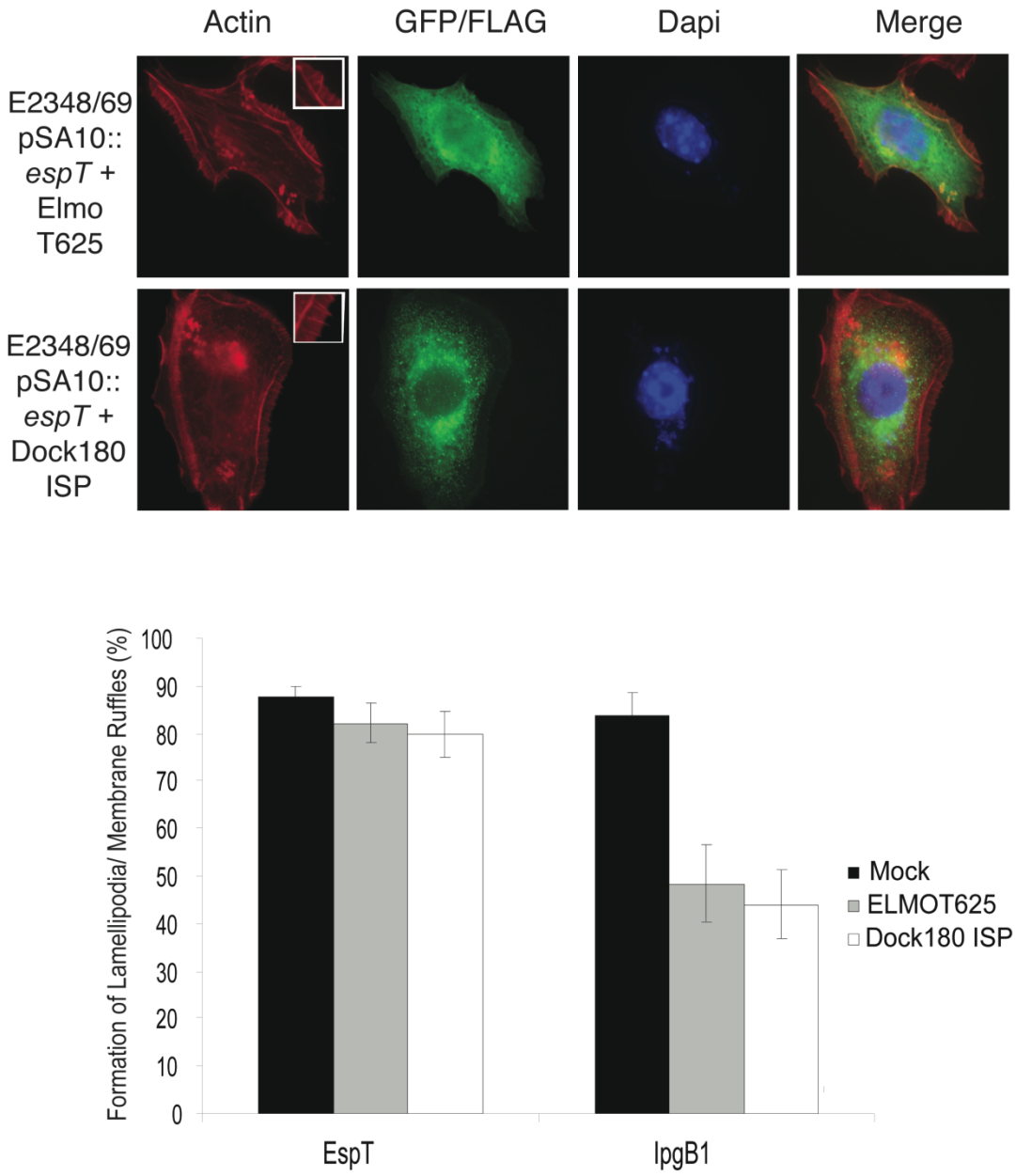


Figure 4.9 EspT induced cytoskeletal rearrangements are independent of ELMO or Dock180 activity. Swiss 3T3 were transfected with the dominant negative forms of ELMO and Dock180 18 h prior to infection with E2348/69 expressing EspT. Neither ELMO^{T625} nor Dock180^{ISP} had any effect on lamellipodia induction by EspT. (B) Quantification of lamellipodia or membrane ruffles in Swiss 3T3 and HeLa cells transfected with dominant negative ELMO^{T625} or Dock180^{ISP} and infected with E2348/69 expressing EspT or co-transfected with IpgB1 from *S. flexneri* as control. 100 cells were counted in triplicate from 3 independent experiments. Results are displayed as mean ± SEM.

4.10 EspT Triggered Lamellipodia are Not Inhibited by Antagonists of Canonical Rac1 Activation Signalling Pathways.

Rac1 activation is mediated by a complex signalling network of typical and atypical GEFs as well as kinases and other mammalian adaptor proteins (reviewed in (Bosco et al., 2009)). Typical Rac1 GEFs including Tiam and Trio bind a conserved region of Rac1 between the switch 1 and switch 2 region (Gao et al., 2001). This binding can be inhibited by addition of the NSC23766 compound which preferentially fits the Tiam/Trio recognition groove in Rac1 (Gao et al., 2004). Atypical Rac1 GEFs such as Vav proteins require upstream activation by Src family kinases before they can catalyse nucleotide exchange on Rac1 (Kawakatsu et al., 2005). In addition to GEFs, Rac1 can also be activated by phosphoinositol 3 kinase (PI3K) (Pan et al., 2005). As we have demonstrated that EspT mediated induction of membrane ruffles and lamellipodia are independent of RhoG (Figure 4.7), ELMO and Dock180 (Figure 4.9) we utilised inhibitors of the remaining canonical Rac1 activation pathways in order to determine the mechanism of EspT mediated Rac1 activation. NSC23766 was used to inhibit typical Rac1 GEFs such as Trio and Tiam, PP2 was utilised to inhibit Src kinase dependent activation of the Vav family of atypical GEFs and Wortmannin was used to inhibit PI3K. Swiss 3T3 cells were pretreated with inhibitory doses of the chemical inhibitors as described in the literature and then infected with E2348/69 expressing EspT for 90 min. Lamellipodia formation was unaffected by NSC23766, Wortmannin or PP2 treatment. These results suggest that EspT activates Rac1 in a manner which is independent of previously identified Rac1 regulatory factors.

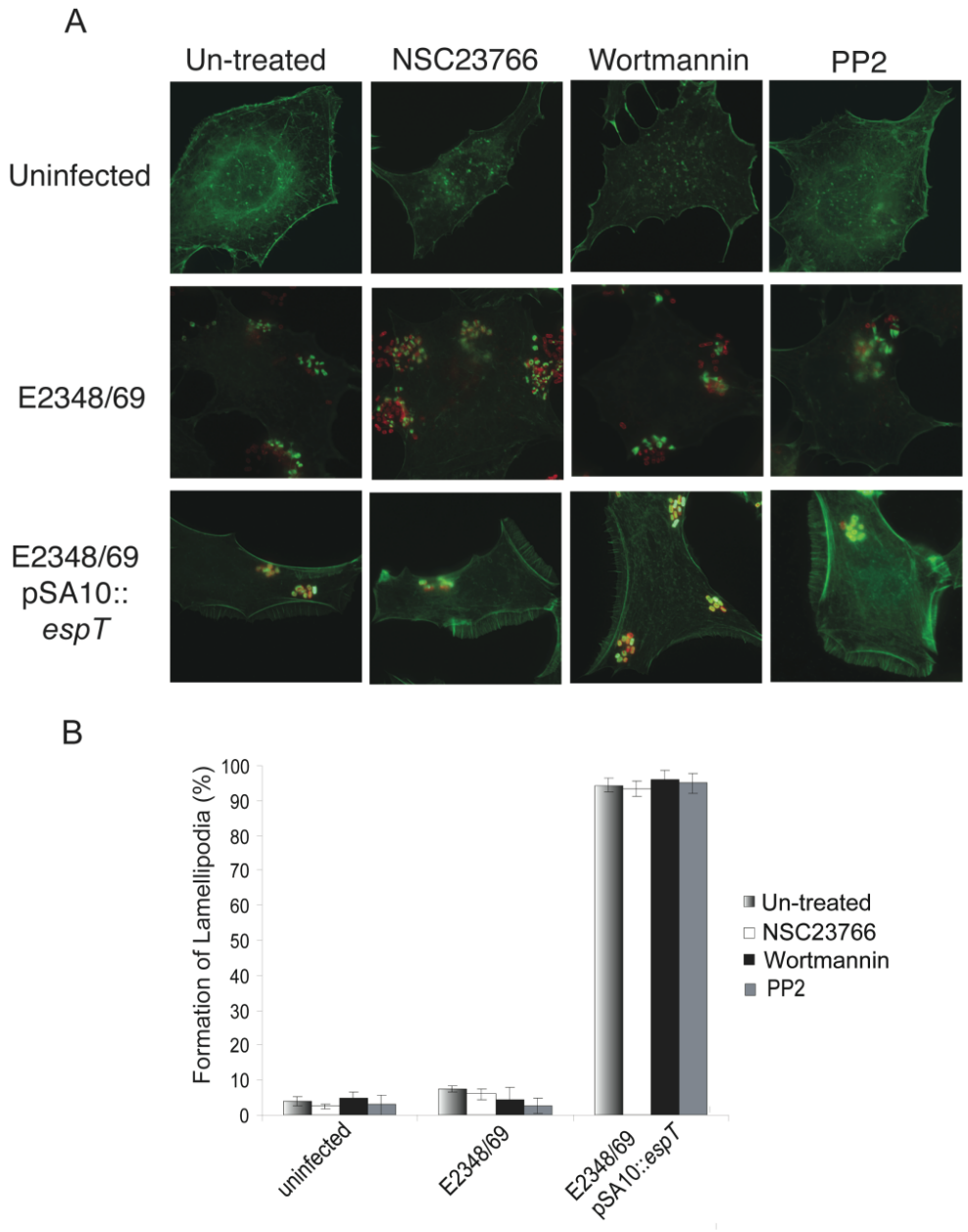


Figure 4.10 EspT triggered lamellipodia are not inhibited by agonists of canonical Rac1 activation signalling pathways. A Swiss 3T3 cells were left untreated or treated with the typical Rac1 GEF inhibitor NSC23766, the PI3K inhibitor Wortmannin and the Src kinase inhibitor PP2 at inhibitory concentrations. The cells were then left uninfected or infected with E2348/69 or E2348/69 expressing EspT. Cells treated with the chemical inhibitors and infected with E2348/69 or E2348/69 pSA10::*espT* formed typical actin rich pedestals which were indistinguishable for untreated cells. B. Cells infected with E2348/69 expressing EspT retained lamellipodia formation to a similar level as untreated cells in the presence of NSC23766, Wortmannin and PP2.

4.11 EspT Induces the Phosphorylation of Cofilin

As EspT mediated lamellipodia and membrane ruffles are stable for upward of 3 h after infection of Swiss 3T3 or HeLa cells respectively (Bulgin et al., 2009) we next investigated whether EspT inhibits the activity of the cofilin which is known to depolymerise actin filaments (reviewed in (Maciver, 1998)) and lamellipodia (Lai et al., 2008). Rac1 activates a plethora of downstream effectors including the PAK family of serine/threonine kinases (reviewed in (Bokoch, 2003)). It has been demonstrated that PAK isoforms can phosphorylate and activate LimK resulting in a downstream phosphorylation and inactivation of cofilin (Dan et al., 2001). In order to determine if Rac1 activated by EspT also stimulates the phosphorylation and subsequent inactivation of cofilin we left serum starved HeLa cells uninfected or infected them for 90 min with E2348/69 or E2348/69 expressing EspT. The cells were then lysed and a western blot was performed to detect total cofilin and phosphorylated cofilin (Figure 4.11). The western blots were then analysed by densitometry and a ratio between cofilin and phospho-cofilin was determined. Uninfected cells and cells infected with E2348/69 did not show any significant induction of cofilin phosphorylation. Cells infected with E234/69 expressing EspT exhibited a 2 fold increase in the levels of cofilin phosphorylation. These results demonstrate that EspT mediates lamellipodia stability by inducing the phosphorylation and subsequent inactivation of cofilin.

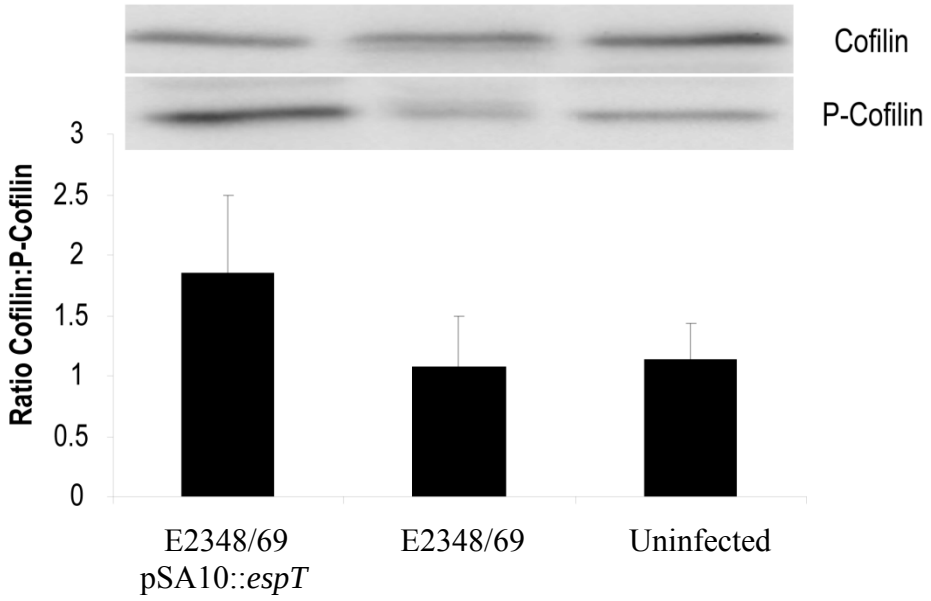


Figure 4.11 EspT induces a phosphorylation of cofilin. HeLa cells were left uninfected on infected with E2348/69 or E2348/69 expressing EspT. The cells were then then lysed and the lysate was run on an SDS PAGE gel before transfer to a PVDF membrane for western blotting. Cofilin and phospho-cofilin were detected using monoclonal antibodies. Densitometry was then utilised to generate a ratio of cofilin to phospho-cofilin for each sample. Quantification of densitometry was conducted using image J software and results presented here represent the mean ratio ± S.D of four independent experiments. Cells infected with E2348/69 expressing EspT induce a two fold induction of cofilin phosphorylation compared to the uninfected or E2348/69 infected cells.

4.12 Distribution of *espT* Among Clinical EPEC and EHEC Strains

In collaboration with Drs. Tania Gomes and Jorge Blanco we determined the prevalence of *espT* in range of circa 1000 EPEC and EHEC clinical isolates which were described in chapter 3 (Fig. 3.14). Using BLAST analysis of the unfinished genome of EPEC E110019 O111:H9, we identified an *espT* gene which shared around 78% homology with *espT* from *C. rodentium.* We used the *espT* sequences from *C. rodentium* and E110019 to design common internal espT-F1 (5'-AATCTCATTCTCTTATC) and espT-F2 (5'- TCATGTGATGAGTGGATG) primers to be used in a PCR screen. *C. rodentium* and EPEC E2348/69 were used as positive and negative controls respectively. All the O157 and non-O157 EHEC strains were *espT* negative. We also

used the additional primers EspTSc-1 to EspTSc-8 to confirm that all strains screened were truly *espT* negative (Table 1).

Among the 132 tEPEC and 602 aEPEC strains *espT* was found in only one (0.8%) tEPEC strain (O111:H-) isolated in Spain and in 12 of aEPEC strains (1.9%) (Figure 4.12). Sequencing of *espT* revealed high level of sequence conservation (Figure 4.12). In eight strains *espT* was identical to that of E110019, defined as group 1 EspT. In two strains we detected one single amino acid difference (group 2) and in 3 other strains we found 6 amino acids that differ from EspT of E110019 (group 3) (Figure 4.12).

A

Serotype (no. of strains)	Origin	Pathotype	*espM*
Group 1			
O111 : H9 (1)	Finland	aEPEC	+
ONT : H- (1)	Brazil	aEPEC	+
O49 : H- (1)	Brazil	aEPEC	+
O85 : H- (1)	Brazil	aEPEC	–
O109 : H9 (1)	Brazil	aEPEC	+
O111 : H- (1)	Spain	tEPEC	+
O123 : H- (2)	Brazil	aEPEC	+
O154 : H9 (1)	Brazil	aEPEC	+
Group 2			
O2 : H49 (1)	Spain	aEPEC	–
O2 : H49 (1)	Spain	aEPEC	–
Group 3			
ONT : H7 (1)	Brazil	aEPEC	+
O104 : H2 (1)	Spain	aEPEC	–
O104 : H2 (1)	Brazil	aEPEC	–

B

```
                7                                                   57
EspT 1/E110019  TVNSCGFGFS ITKAPYSSGQ KPVIDGFFLG ARRISFSYPR LESELIQCIN
       EspT 2   TVNSCGFGFS ITKAPYSSGQ KPVIDGFFLG ARRISFSYPR LESELIQCIN
       EspT 3   TVNSCGFGFS ITKAPYSSGQ KPFIDGFFLG ARKISFSYPR LESELIQCIN

               58                                                  107
EspT 1/E110019  LKNEGKKNEW MKEESICFVS RDVNKLLDMF AKNNQTNIPK GVRERVFQLA
       EspT 2   LKNEGKKNEW MKEESICFVS RDVNKLLDMF AKNNQTNIPK GVRERVFQLA
       EspT 3   LKNEGKKNEW MKEEGICFVS RDVNKLLDMF AKNNQTNIPE GVRERVFQLA

               108                                                 157
EspT 1/E110019  SFYCGFSLDA RCAQASTHHM ILNSQYFQKK MDTLLTSVDI NVRNQCVRTA
       EspT 2   SFYCGFSLDA RCAQTSTHHM ILNSQYFQKK MDTLLTSVDI NVRNQCVRTA
       EspT 3   SFYCGFSLDA RCAQTSTHHM ILNSQYFQKK MDTLLTSVDI NVRNQCVRTA

               158                             190
EspT 1/E110019  LSSLADTFFE NNVNNIDMNK LRDRVHNTIV QEV
       EspT 2   LSSLADTFFE NNVNNIDMNK LRDRVHNTIV QEV
       EspT 3   LSSLADTFFE NNVNNIDMNK FRDRVHNTIV QEV
```

Figure 4.12 Prevalence and sequence of EspT in clinical EPEC and EHEC Isolates. (A) Characteristics of EspT positive strains. (B) Multiple sequence alignment of representative EspT sequences. The conserved motif WxxxE is boxed. When compared with EspTE110019, eight of the 13 EspT showed 100% sequence identity (ONT:H-, O49:H-, O85:H-, O109:H9, O111:H-, O123:H- (2), O154:H9) as represented by sequence 1. Two strains belonging to serotype O2:H49 had one amino acid difference (sequence 2, shown in dark grey), while three strains (O104:H2 (2), ONT:H7) differed in six amino acids (sequence 3).

4.13 Discussion

In this chapter we have identified and characterised the *C. rodentium* effector protein EspT. Previously identified effectors, Map, EspM, IpgB1 and IpgB2, which are grouped together with EspT as WxxxE effectors have all been reported to be potent modulators of the host cell cytoskeleton (Handa et al., 2005, Alto et al., 2007, Kenny et al., 2002, Arbeloa et al., 2008). Consistent with this, using E2348/69 as a delivery system to translocate EspT along with ectopic expression we have shown that EspT also subverts host actin dynamics. Interestingly, the effect of EspT was cell-line specific. While expression in Swiss 3T3 led to formation of lamellipodia, EspT triggered membrane ruffles on HeLa cells. When EspT was delivered by infection via E2348/69 the lamellipodia and membrane ruffles appeared as early as 15 min post infection and were stable for over 3 h.

Based on the initial examination of IpgB1, IpgB2 and Map it was suggested that these effector proteins are molecular mimic of Rho GTPases and function in a GTP independent manner (Alto et al., 2006). More recently, Handa et al showed that IpgB1 activates Rac1 via the ELMO-Dock180 machinery (Handa et al., 2007). Despite EspT sharing limited sequence identity with other family members, the membrane ruffles observed on HeLa cells were reminiscent of those induced by IpgB1 (Ohya et al., 2005) except that the EspT induced ruffles were not restricted to the site of bacterial attachment. Interestingly, expressing EspT in Swiss cells led to formation of lamellipodia, which have a strong leading edge, wide lamella and well defined microspikes and filopodia which extend beyond the cell boundary. In contrast, IpgB1 expression induced membrane ruffles on Swiss cells.

Lamellipodia and membrane ruffles are normally regulated by interplay between Rac1, Cdc42, RhoG and RhoA (Sander et al., 1999, Kurokawa et al., 2004, Ladwein and Rottner., 2008). In order to determine the pathway by which EspT subverts the host cell cytoskeleton we utilized dominant negative forms of these GTPases to competitively inhibit the wild type proteins. In the presence of dominant negative $Rac1^{TN17}$ a 60% reduction in formation of lamellipodia was observed. Transfection of $Cdc42^{TN17}$ reduced lamellipodia formation by 30%. These dominant negative constructs attenuated EspT-induced membrane ruffles in HeLa cells to a similar magnitude. These results demonstrate that the actin re-arrangements induced by EspT are dependent on the activation of Rac1 and to a lesser extent Cdc42. Furthermore, using the CRIB domains of PAK and WASP which bind activated Rac1 and Cdc42 respectively, we demonstrate that EspT activates both Rac1 and Cdc42 during infection of Swiss 3T3 cells. These results are consistent with the report of Handa *et al* who have previously demonstrated that IpgB1 activates Rac1 (Handa et al., 2007).

Handa and co-workers also show that IpgB1 interacts with ELMO and subsequently recruits Dock180 to a trimeric complex which brings about the activation of Rac1 (Handa et al., 2007). As EspT induces a Rac1 dependent phenotype similar to IpgB1 in HeLa cells we investigated the role of ELMO during EspT triggered actin modulation. We transfected a GFP-tagged ELMO into Swiss 3T3 cells and infected these cells with wild type E2348/69 or E2348/69 expressing EspT. No ruffles were observed during E2348/69 infection. Surprisingly, when ELMO was transfected into Swiss 3T3 cells infected with E2348/69 expressing EspT we observed a shift from the lamellipodia to membrane ruffles similar to those induced by IpgB1. This result might suggest that EspT is able to interact with ELMO. Alternatively, over-expression of ELMO could have an effect on the typical downstream signalling pathway employed by EspT. To determine if the

lamellipodia observed in Swiss 3T3 cells or the membrane ruffles formed in HeLa cells are dependent upon the ELMO–Dock180 machinery we used the dominant negative forms of ELMO ($ELMO^{T625}$) and Dock180 ($Dock180^{ISP}$) which have been demonstrated to abolish IpgB1 induced membrane ruffles (Handa et al., 2007). As previously observed (Handa et al., 2007) these dominant negatives greatly reduced the formation of membrane ruffles induced by IpgB1. However, neither the $ELMO^{T625}$ nor $Dock180^{ISP}$ had any significant affect on the formation of lamellipodia or membrane ruffles induced by EspT. Further inhibition of typical Rac1 GEFs and activating pathways demonstrated that EspT activates Rac1 independently of canonical upstream signalling. Due to the insoluble nature of recombinant EspT we currently do not know whether the observed activation of Rac1 and Cdc42 is direct or indirect however given the recent evidence that the EspM, Map, IpgB1 and IpgB2 are GEFs it seems likely that EspT will also directly activate Rac1 and perhaps also Cdc42 (Arbeloa et al 2009) (Huang et al., 2009).

Map, which triggers filopodia formation via activation of Cdc42 (Berger et al., 2009; Huang et al., 2009), contains an N-terminus mitochondrial targeting sequence (Paptheodorou et al., 2006), while EspM2, IpgB1 and EspT do not have any obvious mitochondrial targeting sequences. EspM2, which triggers formation of parallel stress fibres upon transfection, localizes in the cytoplasm. In contrast, we found here that EspT and IpgB1 are targeted to mitochondria following 16 h ectopic expression. It is interesting to note that mitochondrial trafficking and morphology is regulated by the atypical Rho GTPases Mitochondrial Rho (Miro) 1 and 2 (Franson et al., 2006, Frederick et al., 2004). The mitochondrial localization of IpgB1 and EspT may suggest a role for these proteins in regulating mitochondrial dynamics as well as subversion of the host actin cytoskeleton. However, although ectopic expression of EspM leads to cytosolic localization, we cannot rule out the possibility that mitochondria targeting by EspT and IpgB1 is

an artefact due to the over-expression. Further studies are needed to determine if EspT and IpgB1 have a physiological mitochondrial function.

Interestingly, although *espT* is absent from the common EPEC strains (including the prototypes E2348/69 and B171) and EHEC O157, we recently found an *espT* homologue (78% identity) in the atypical EPEC strain E110019, which caused a particularly severe outbreak in Finland in 1987 which affected adults and children alike (Viljanen et al., 1990). However, the overall prevalence of *espT* among clinical EPEC and EHEC strains is very limited. This may suggest that EspT is an emerging effector which is still being acquired by A/E pathogens or that conversely it is an evolutionary remnant which is being lost.

Chapter 5 - EspT is a Novel A/E Pathogen Invasin

EPEC, EHEC and *C. rodentium* are generally considered extracellular pathogens and their attachment sites on epithelial cells are normally characterized by the assembly of an actin-rich pedestals rather than membrane ruffles (reviewed in (Frankel and Phillips, 2008)). However, in both rabbit and human biopsies EPEC have been visualized inside enterocytes and detected in the submucosa, mesenteric lymph nodes and spleen (Drucker et al., 1970) (reviewed in (Donnenberg and Kaper, 1992)). Recently, Hernandes et al has shown that the atypical EPEC strain 1551-2 is capable of invading cultured epithelial cells in an intimin omicron dependent manner (Hernandes et al., 2008). As EspT induces membrane ruffles similar to those triggered by IpgB1 (Ohya et al., 2005) we investigated whether EspT can mediate EPEC invasion into non-phagocytic cells.

5.1 EspT-Induced Membrane Ruffles Surround Adherent Bacteria

In order to investigate if EspT plays a role in cell invasion we selected to use the *espT* positive strain E110019; the *espT* negative strain JPN15 (Jerse et al., 1990), a derivative of E2348/69 lacking the EAF plasmid encoding BFP, was used as a control. Due to its lack of BFP expression, JPN15 does not form tight microcolnies which can hinder invasion assays and is more comparable to the atypical EPEC E110019. In addition, we generated a JPN15 clone that expresses EspT encoded by E110019 from the bacterial expression vector pSA10.

We infected serum starved HeLa, Swiss 3T3 and Caco2 cells with E110019, JPN15 and JPN15 expressing EspT; the cells were then fixed and processed for scanning electron microscopy (SEM). The JPN15-infected HeLa and Swiss 3T3 cells displayed characteristic diffuse bacterial adhesion without any noteworthy surface structures. Caco2 cells infected with JPN15 also show a diffuse pattern of bacterial adherence and a concordant localized effacement of microvili (Figure 5.1). HeLa cells infected with JPN15 expressing EspT or E110019 displayed extensive

membrane ruffling over the entire cell surface (Figure 5.1); in the vicinity of adherent bacteria the ruffles surrounded and wrapped individual bacterial cells forming structures which appear permissive for internalization. Swiss 3T3 cells infected with JPN15 expressing EspT or E110019 exhibited extensive dorsal ruffles and lamellipodia in addition to localized membrane ruffles at the site of bacterial attachment (Figure 5.1). Caco2 cells infected with JPN15 expressing EspT or E110019 displayed prominent membrane ruffles at the site of bacterial adherence in addition to effacement of micovili (Figure 5.1). These results show that EspT from E110019 can induce actin remodeling and surface structures identical to those induced by EspT from *C. rodentium*. Interesting the membrane remodeling induced by EspT expressing strains is strikingly similar to those associated with *Shigella* and *Salmonella* invasion (reviewed in (Cossart and Sansonetti, 2004))

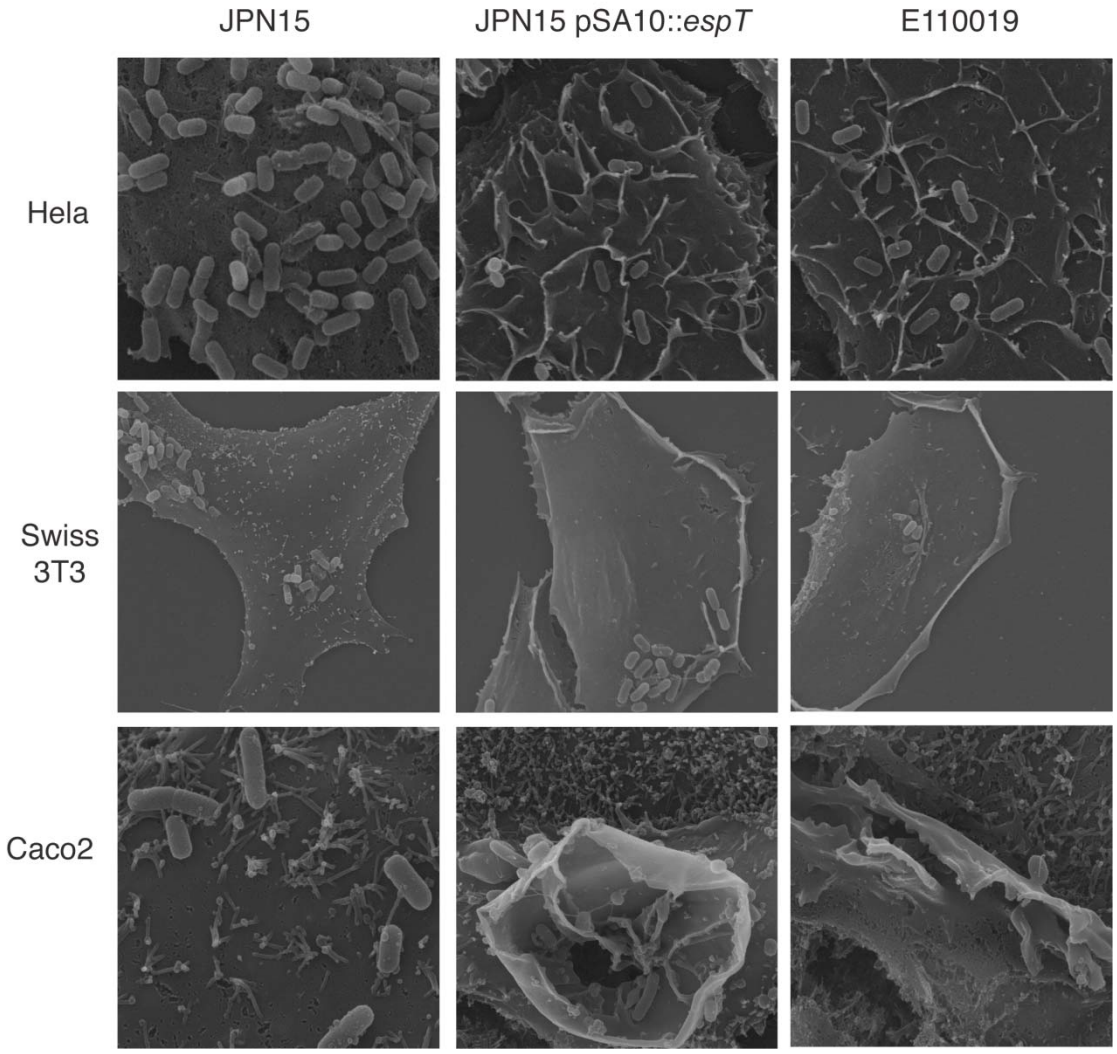


Figure 5.1 EspT-induced membrane ruffles surround adherent bacteria. Scanning electron microscopy of HeLa, Swiss 3T3 and polarized Caco2 cells infected with JPN15, JPN15 expressing EspT or E110019 for 2 h. JPN15 displayed a pattern of diffuse adherence on HeLa, Swiss 3T3 and Caco2 cells but did not induce any significant membrane remodeling. JPN15 expressing EspT and E110019 also adhered to HeLa, Swiss 3T3 and Caco2 cells in a diffuse pattern but induced membrane ruffles at the site of bacterial attachment, which were more pronounced on Caco2 cells. In addition to membrane ruffles JPN15 expressing EspT and E110019 also induced formation of lamellipodia and dorsal ruffles at locations distal from the site of bacterial attachment on Swiss 3T3 cells. Magnifications: HeLa cells X5000; Swiss 3T3 X3500; Caco2 X10000 and X6500 (middle)

5.2 EspT Dependent Lamellipodia Formation is Independent of N-WASP

We have shown that EspT activates both Rac1 and Cdc42 (Figure 4.7). However inhibition of Cdc42 using dominant negative constructs only reduces EspT mediated lamellipodia by approximately 30% compared to a 65% reduction when Rac1 is inhibited (Figure 4.6). Cdc42 is generally associated with membrane protrusions such as filopodia but is also considered to play a role in stabilising Rac1 dependent lamellipodia (Kurokawa et al., 2004). Consistently, we observed that inhibition of Cdc42 reduces the size and stability of EspT induced lamellipodia (Figure 4.6). Cdc42 dependent actin modulation occurs primarily through the WASP/N-WASP proteins which are activated by GTP bound Cdc42 and subsequently recruits and activates the Arp2/3 complex (Carlier et al., 1999a). N-WASP has also been implicated in formation of dorsal ruffles and lamellipodia in fibroblasts (Legg et al., 2007). In order to investigate the role of Cdc42 in lamellipodia formation we utilised N-WASP deficient fibroblasts. The N-WASP knockout fibrobalsts were infected with JPN15 and JPN15 expressing EspT from the pSA10 vector for 2 h. As pedestal formation is N-WASP dependent (Gruenheid et al., 2001; Lommel et al., 2001) no pedestals were observed upon infection with either JPN15 or JPN15 pSA10::*espT* (Figure 5.2). Knockout cells infected with JPN15 expressing EspT formed lamellipodia and dorsal ruffles at a similar rate as Swiss 3T3 cells (Figure 5.2). The lamellipodia formed on the N-WASP knockout cells were not as pronounced as those induced on Swiss 3T3 cells (Figure 5.2). These results further support the assertion that Cdc42 and N-WASP are not required for EspT mediated lamellipodia formation but may play a role in stabilising the lamellipodia after formation.

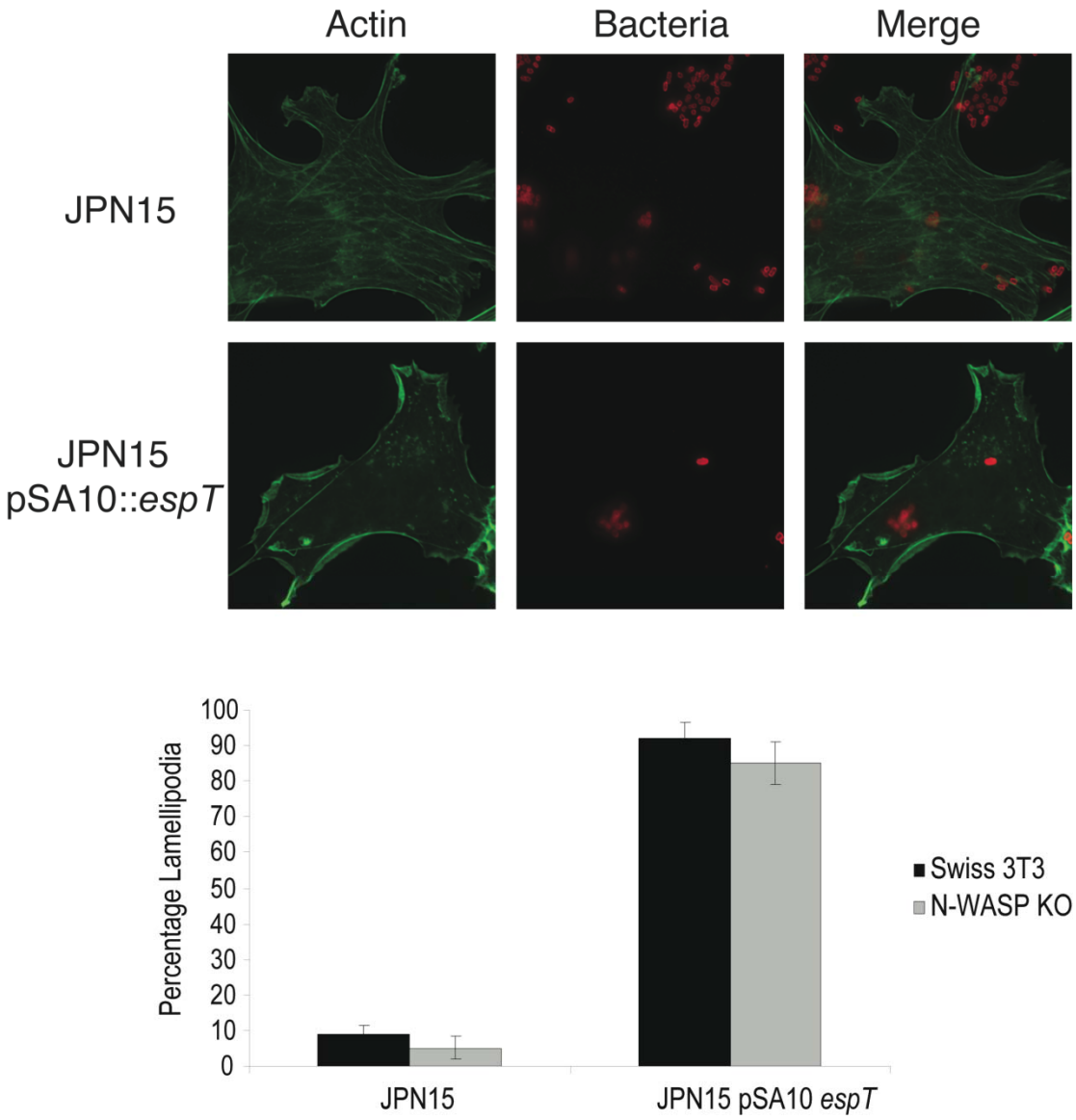


Figure 5.2 EspT dependent formation of lamellipodia is independent of N-WASP. Knockout N-WASP fibroblasts were infected with JPN15 or JPN15 expressing EspT for 2 hours. Actin is stained in green with phalloidin and JPN15 was detected with a rabbit polyclonal anti O127 antibody in Red. Neither JPN15 nor JPN15 pSA10::*espT* formed pedestals on the N-WASP knockout fibroblasts. JPN15 expressing EspT formed lamellipodia to a similar level to Swiss 3T3 fibroblasts although the lamellipodia were smaller. Quantified lamellipodia were counted in one hundred cells in three independent experiments. Results are presented as mean±SEM.

5.3 Wave2 and Abi1 are Localized to Membrane Ruffles and Lamellipodia Induced by EspT

Remodeling of the host cell actin cytoskeleton by EspT is mainly dependent on Rac1 (Figure 4.6, 4.7 and 5.2). Rac1 utilizes a plethora of downstream effectors in order to regulate cytoskeletal dynamics (reviewed in (Etienne-Manneville and Hall, 2002) and (Chhabra and Higgs, 2007)). Several GTPase effectors including IRSp53, N-WASP, Pak, Wave2 and Abi1 have been previously been implicated in formation of membrane ruffles (Innocenti et al., 2004; Legg et al., 2007; Machuy et al., 2007; Miki et al., 2000). N-WASP is not required for EspT induced lamellipodia formation (Figure 5.2). Wave2 is a member of the WASP superfamily of proteins and is a prominent downstream effector of Rac1 which can mediate activation of the Arp2/3 complex (reviewed in (Takenawa and Miki, 2001)). Wave2 cannot bind Rac1 directly; Innocenti et al and Steffen et al have proposed a model in which Wave2 binds to Abl Interactor 1 (Abi1) and two accessory proteins PIR121 and Nap1 which then mediate Rac1 binding (Innocenti et al., 2004; Steffen et al., 2004). We transfected Swiss 3T3 and HeLa cells with the mammalian ectopic expression vector pRK5 encoding EspT for 16 h. Using immuno-fluorescence microscopy we found that both Wave2 and Abi1 were present and co-localized with actin at membrane ruffles and the leading edge of lamellipodia induced by EspT (Figure 5.3).

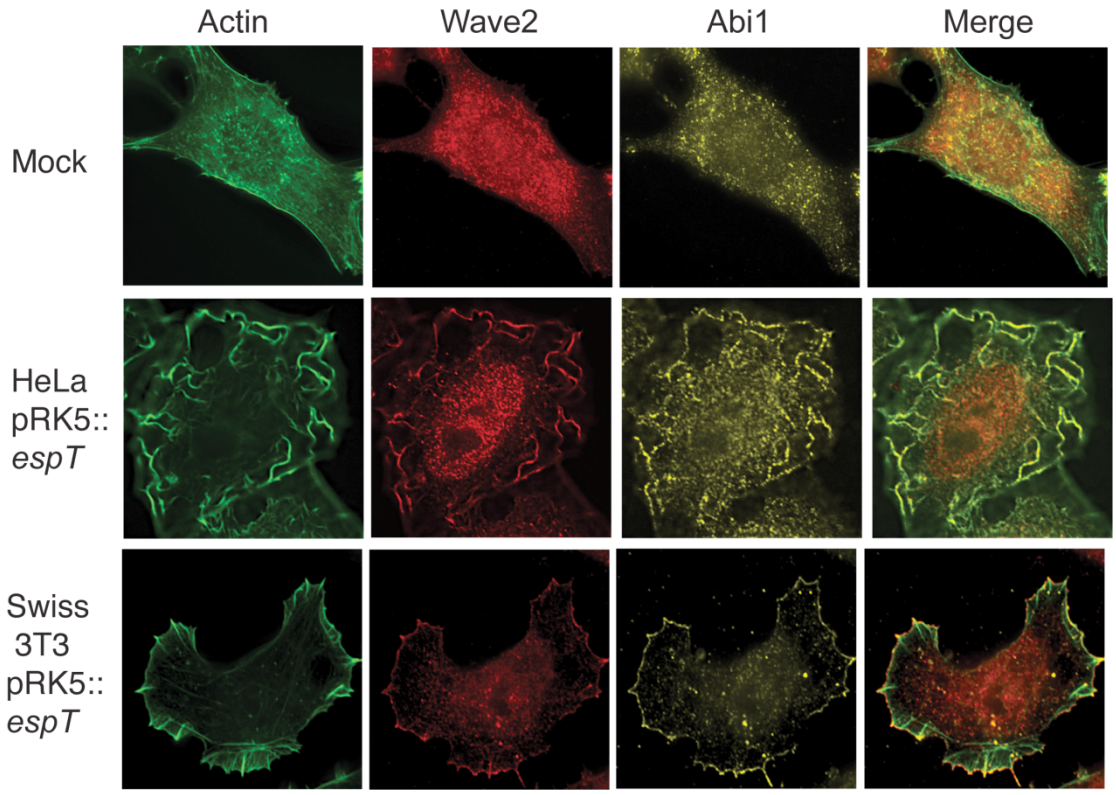


Figure 5.3 Wave2 and Abi1 are localized to membrane ruffles and lamellipodia induced by ectopically expressed EspT. Actin was stained with Oregon Green phalloidin (Green), Wave2 was detected with a polyclonal rabbit antibody (Red) and Abi1 was visualized using a mouse monoclonal antibody (Yellow). Mock transfected cells did not display any significant actin structures and Wave2 and Abi1 were localized diffusely in the cytoplasm. HeLa cells transfected with pRK5::*espT* exhibit prominent membrane ruffles on their apical surface which were enriched with Wave2 and Abi1. Ectopic expression of EspT in Swiss 3T3 cells resulted in formation of distinctive lamellipodia to which Wave2 and Abi1 were extensively recruited and co-localized.

5.4 IRSp53 is Recruited to EspT Induced Membrane Ruffles but not Lamellipodia

The signaling protein IRSp53 has been proposed to participate in Abi1-Wave2-Rac1 complex formation (Miki et al., 2000; Suetsugu et al., 2006). We transfected HeLa and Swiss 3T3 cells with the mammalian ectopic expression vector encoding EspT for 16 h. Interestingly, while we did not detect any significant enrichment of IRSp53 in lamellipodia, IRSp53 was localized to

membrane ruffles nucleated by EspT (Figure 5.4). This suggests that IRSp53 may play a subsidury role in EspT induced membrane remodeling.

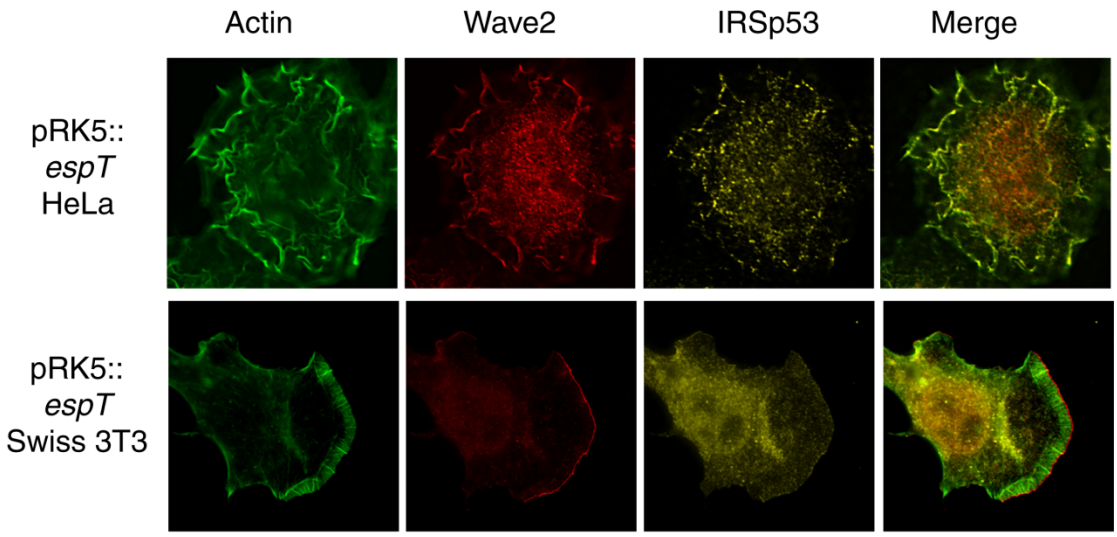


Figure 5.4 IRSp53 is enriched in membrane ruffles induced by EspT. HeLa and Swiss 3T3 cells were transfected with the ectopic expression vector pRK5 encoding EspT for 12 h. Actin was labeled with Oregon Green phalloidin (green), Wave2 was detected with polyclonal rabbit antisera and IRSp53 was detected using a monoclonal mouse antibody (Yellow). Transfection of EspT resulted in formation of membrane ruffles and lamellipodia in HeLa and Swiss 3T3 cells respectively. Wave2 was localized to membrane ruffles and lamellipodia induced by EspT. IRSp53 was recruited to EspT dependent ruffles in HeLa cells but was not present in lamellipodia induced on Swiss 3T3 cells.

5.5 Wave2 is Essential for EspT-Induced Membrane Remodeling

Wave2 is a ubiquitously expressed member of the WASP superfamily of actin regulators which potently activates the Arp2/3 complex (Suetsugu et al., 1999). Wave2 has been demonstrated to be required for the formation of membrane ruffles induced by *Salmonella* to invade epithelial cells (Shi et al., 2005). We utilized siRNA in order to determine if Wave2 is essential for formation of the EspT-dependent membrane ruffles. Depletion of endogenous Wave2 from Swiss 3T3 cells, confirmed by Western blotting (Fig. 5.5A), resulted in a marked decrease in

formation of membrane ruffles and lamellipodia induced by JPN15 expressing EspT or E110019, compared with cells treated with scrambled siRNA (Fig. 5.5B).

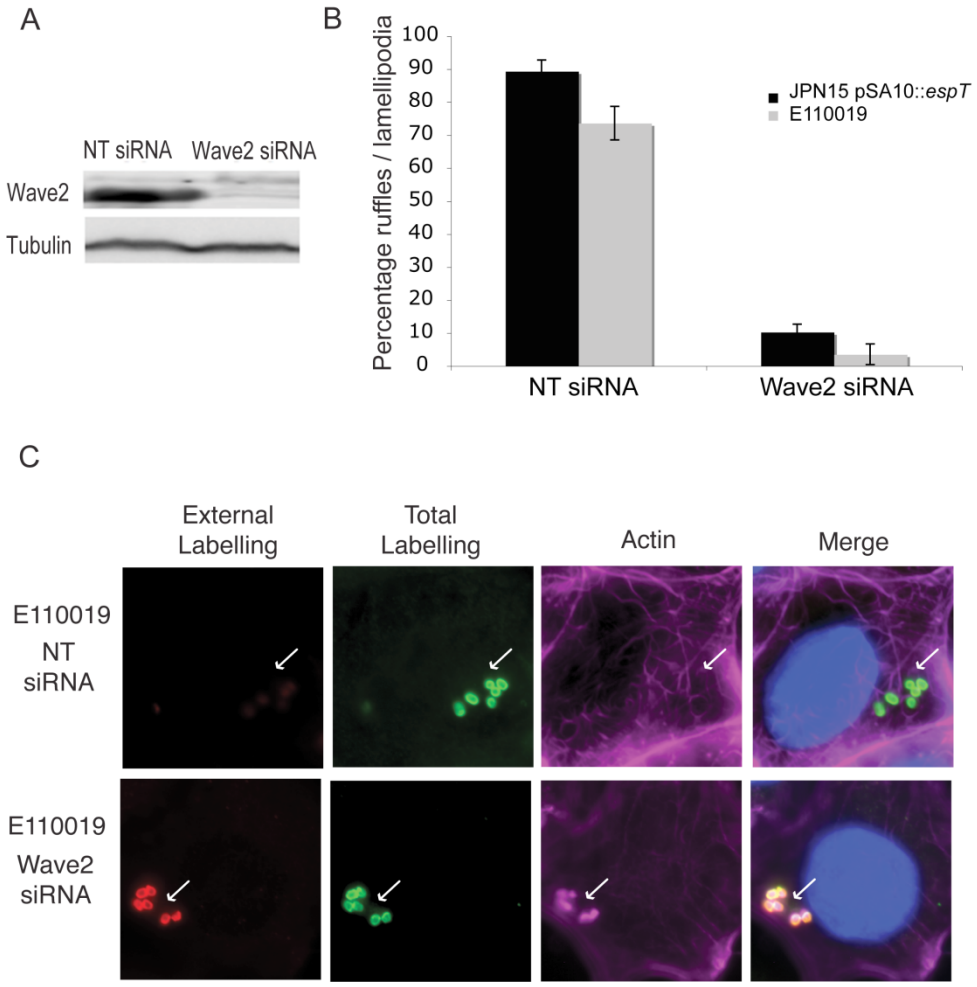


Figure 5.5 Wave2 is essential for EspT induced membrane remodeling and invasion. (A) Swiss 3T3 cells were treated with Non Targeting (NT) siRNA or siRNA targeted against Wave2. (A) Western blot with lysates from Swiss 3T3 cells treated with NT and Wave2 siRNA. Wave2 and Tubulin were detected with monoclonal antibodies. Non Targeting siRNA did not alter Wave2 expression whereas treatment with Wave2 siRNA depleted the protein. Protein levels in the lysates were normalized using anti tubulin antibodies. (B) Quantification of membrane remodeling induced by E110019 and JPN15 expressing EspT in Swiss 3T3 cells treated with NT and Wave2 siRNA after 3 h of infection. 100 cells were counted in triplicate resulted are presented as mean ± SEM. (C) Cells were infected with E110019 for 3 h were fixed and stained prior to permeabilization (extracellular labeling) (Red). The cells were then washed, permeabilized, re-labeled (Total labeling) (Green) along with Alexaflour 633 Phalloidin (Cyan) and Dapi (Blue). In cells treated with the NT siRNA E110019 induced formation of membrane ruffles and a large proportion of bacteria were labeled by the total stain which were absent from the extracellular labeling. Depletion of Wave2 using siRNA inhibited formation of membrane ruffles by E110019 and the majority of bacteria were detected by both the extracellular and total staining demonstrating that depletion of Wave2 inhibits EPEC invasion

5.6 Wave2 WHD and VCA Domains are Required for EspT-Induced Membrane Remodeling

The Wave family of proteins have a modular structure consisting of a N terminal Wave homology domain (WHD), a central proline rich region (PRR) and a C terminal Arp2/3 binding domain (VCA module) (reviewed in (Takenawa and Miki, 2001)). The WHD domain has been shown to bind Abi1 (Innocenti et al., 2004) and the PRR has been shown to interact with the SH3 domain of IRSp53 (Miki et al., 2000). In order to determine which regions of Wave2 were required for formation of lamellipodia and membrane ruffles by EspT Swiss 3T3 and HeLa cells were transfected with full length Wave2 or dominant negative forms of Wave2 lacking the WHD (ΔBP) which can no longer bind to wave2 or the Arp2/3 interacting domain (ΔA) which cannot interact with Arp2/3 and is so deficient in actin nucleation activity. Transfected cell were infected for 1.5 h with JPN15 expressing EspT and the presence of lamellipodia or membrane ruffles was assessed. Mock transfected cells or cells transfected with full length Wave2 had lamellipodia and membrane ruffles on 80 to 90 % of infected cells (Figure 5.6). Transfection with either the ΔBP or the ΔA Wave2 dominant negative constructs resulted in significant reduction in lamellipodia and membrane ruffle formation (Figure 5.6). This result demonstrates that binding of Arp2/3 and of Abi1 to Wave2 is essential for EspT-mediated formation of lamellipodia and membrane ruffles. Furthermore, the observation that the ΔBP construct, which is capable of binding IRSp53 but not Abi1, has a dominant negative effect further suggests that IRSp53 does not play a prominent role in EspT mediated signaling.

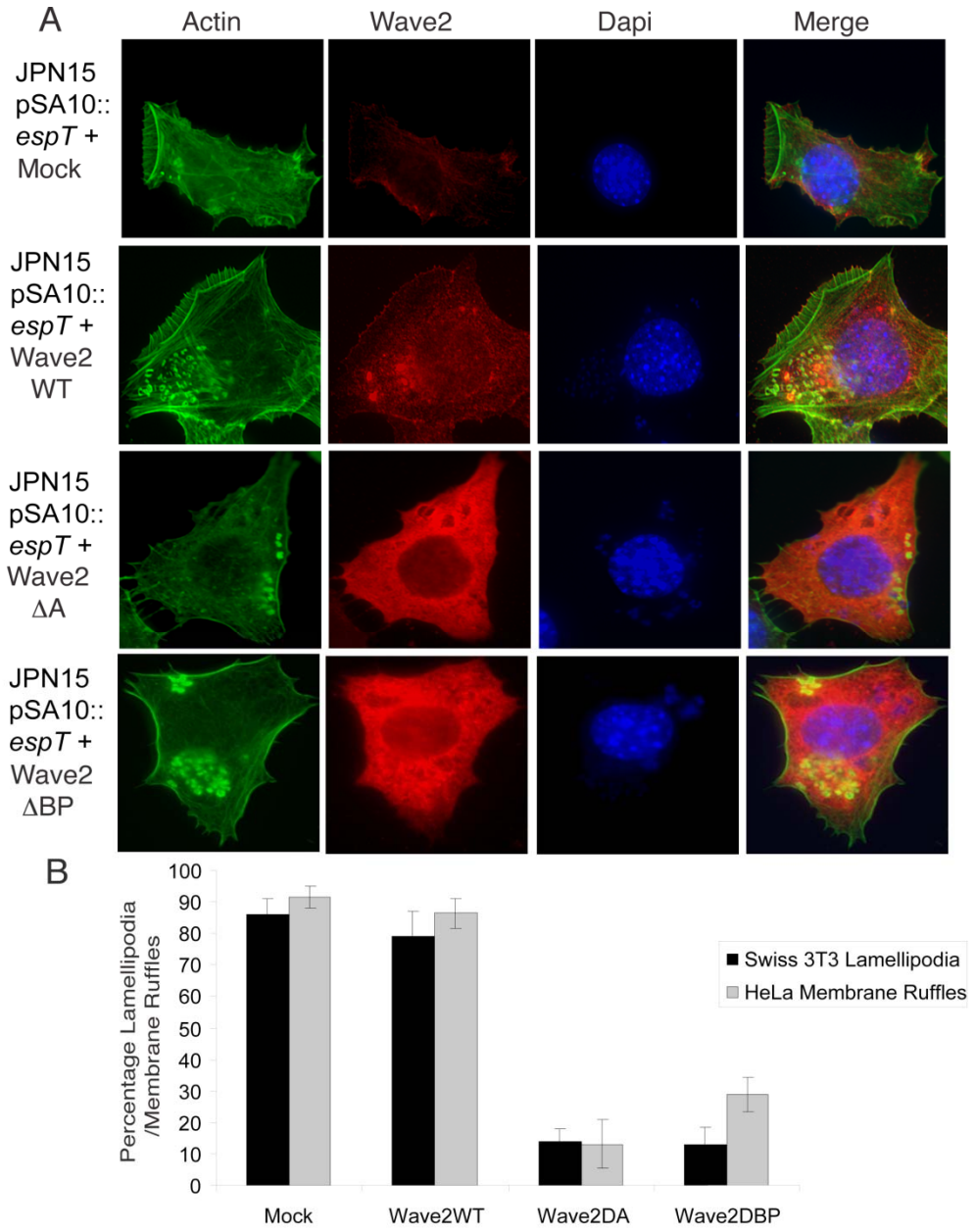


Figure 5.6 Wave2 WHD and VCA domains are needed for EspT-induced membrane remodeling. (A) Swiss cells were left untransfected or transfected with pDSRed encoding wild type Wave2 and Wave2ΔA (lacking the acidity Arp2/3 interacting region) or Wave2ΔBP (lacking the WHD needed for Abi1 binding). Transfected cells were infected with JPN15 expressing EspT for 2 h and processed for immuno-fluorescence microscopy. Actin was stained with Oregon green phalloidin (Green), the Wave constructs were detected with a polyclonal rabbit Wave2 antibody (Red) and JPN15 expressing EspT were visualized by Dapi. Mock transfected cells or cell transfected with wild type Wave2 displayed lamellipodia in 80-90% of transfected cells. Cells transfected with Wave2ΔA or Wave2ΔBP were severely attenuated in lamellipodia formation compared to the mock or Wave2 wild type transfected cells. (B) Quantification of lamellipodia and membrane ruffles on Swiss and HeLa cells respectively after 2 h infection with JPN15 expressing EspT. 100 cells were counted in triplicate in three independent experiments. Results are displayed as mean ± SEM.

5.7 EspT Facilitates EPEC Invasion

Induction of membrane ruffles is a mechanism employed by a range of pathogenic bacteria in order to facilitate cell invasion. This method of bacterial invasion is referred to as the trigger mechanism and relies upon induction of actin polymerization to form an entry foci and a macropinocytic pocket (reviewed in (Cossart and Sansonetti, 2004)). JPN15 expressing EspT and E110019 induce membrane remodeling which is reminiscent of entry foci and membrane ruffles induced by *Shigella* and *Salmonella* (reviewed in (Cossart and Sansonetti, 2004)) (Figure 5.1).

We used differential staining to visualize invasion of Swiss 3T3 cells by JPN15, JPN15 expressing EspT, and E110019; *Salmonella enterica* serovar Typhimurium strain SL1344 was used as a control. In addition, we conducted gentamycin protection assays to quantify cell invasion of Swiss 3T3, HeLa and Caco2 cells after 3 h infection. Differential immuno-fluorescence staining and gentamycin protection assays were also performed in HeLa and Swiss 3T3 cells infected for 6 h with wild type *C. rodentium*, *C. rodentium* Δ*espT* and complemented *C. rodentium* Δ*espT*. Prior to use in this infection the *C. rodentium* wild type *C. rodentium* Δ*espT* were tested and no significant differences were observed in cell adhesion, pedestal formation of growth rate were observed. Furthermore, testing via polymerase chain reaction demonstrated that the *C. rodentium* Δ*espT* mutation was unaffected via serial culturing or infection of mammalian cells and also that the complemented *C. rodentium* Δ*espT* pSa10:;*espT* maintained the plasmid thoughout. For immuno-fluorescence extracellular bacteria were stained prior to cell permeabilzation with primary anti-O127 (JPN15), anti-O111 (E110019) or anti-LPS (*S.* Typhimurium*)* antibodies and a secondary antibody coupled to a Cy3 fluorophore (red). The cells were then permeabilized and total bacteria were stained with the same primary antibodies

and a secondary antibody coupled to a Cy2 fluorophore (green), Alexafluor 633 phalloidin and Dapi were used to visualize actin and DNA respectively.

Adherent JPN15 bacteria were homogenously stained by both the extracellular and total bacterial probes, indicating that this strain is not significantly invasive (Fig. 5.7A). In cells infected with JPN15 expressing EspT or E110019 a significant proportion of the bacteria were labeled with the total bacterial stain but not by the extracellular probe (Fig. 5.7A). *S.* Typhimurium-infected cells exhibited characteristic membrane ruffling at the entry foci and a high proportion of bacteria were labeled only with the total bacterial probe (Fig. 5.7A).

The quantitative gentamycin protection assay revealed that JPN15 does not efficiently invade HeLa, Swiss 3T3 or Caco2 cells, exhibiting an invasion rate of less than 1.5% (Fig. 5.7B). JPN15 expressing EspT was significantly more invasive with an invasion rate of 15.5% in Swiss 3T3, 14.3% in HeLa and 7.2% in Caco2 cells (Fig. 5.7B). E110019 invaded Swiss 3T3, HeLa and Caco2 cells at a rate of 9.2%, 11.4% and 5.8% respectively. The invasive capacity of EPEC was significantly less than *S.* Typhimuriumin (Fig. 5.7B).

E110019 is multi drug resistant, which limits the ability to genetically modified the isolate. In order to determine if cell invasion is mediated by EspT, we infected Swiss 3T3 and HeLa cells for 6 h with wild type *C. rodentium* and *C. rodentium* Δ*espT* and *C. rodentium* Δ*espT* complemented with pACYC184::*espT*. Infection with wild type *C. rodentium* resulted in a moderate level of cell invasion, while the *espT* mutant exhibited little or no invasion (Fig. 5.7B). Complementing *C. rodentium* Δ*espT* with *espT* expressed from pACYC184 restored the invasiveness of the mutant to a level which was greater than the wild type strain (Fig. 5.7B).

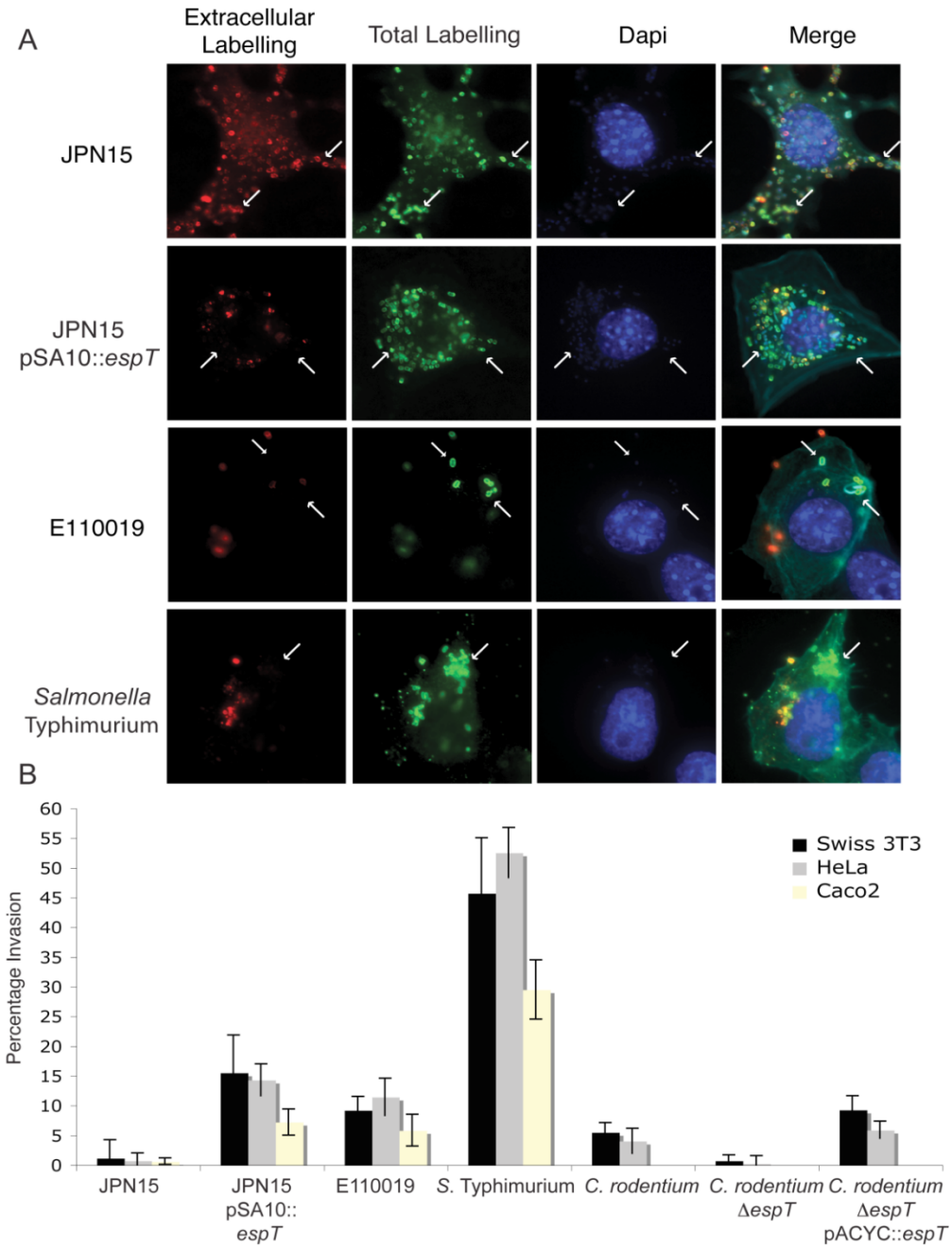


Figure 5.7. EspT-dependent actin remodeling facilitates bacterial invasion of epithelial cells. (A) Swiss 3T3 cells infected with JPN15, JPN15 expressing EspT, E110019 or *S.* Typhimurium for 3 h were fixed and stained prior to permeabilization (extracellular labeling) (Red). The cells were then washed, permeabilized, re-labeled (Total labeling) (Green) along with Alexaflour 633 Phalloidin (Cyan) and Dapi (Blue). In cells infected with JPN15 all the bacteria labeled by the total staining were also detected with the extracellular probe indicating that there was no significant invasion (highlighted with arrows). Significant numbers of bacteria labeled with the total stain, which were not represented in the extracellular staining, were seen in cells infected JPN15 expressing EspT, E110019 and *S.* Typhimurium indicating that there was a significant degree of bacterial invasion (highlighted with arrows). (B) Gentamycin protection assay of Swiss 3T3 and HeLa cells infected JPN15, JPN15 expressing EspT, E110019, *S.* Typhimurium, *C. rodentium*, *C. rodentium* Δ*espT* or complemented *C. rodentium* Δ*espT* and polarized Caco2 cells infected with JPN15, JPN15 expressing EspT , E110019 or *S.* Typhimurium. Results are representative of 3 independent experiments carried out in duplicate and are displayed as mean ± SEM.

5.8 The Conserved WxxxE Motif is Essential for EspT Mediated Membrane Remodelling and Invasion.

Previous studies have demonstrated that mutation of either the conserved typtophan or glutamic acid motif results in a loss of activity of WxxxE effectors (Alto et al., 2006, Arbeloa et al., 2008) (Figure 3.5). Thus we mutated the conserved tryptophan (W63) of EspT to alanine in order to create the plasmid pSA10::*espT*^{W63A}. HeLa cells were then infected with JPN15 pSA10::*espT* or JPN15 pSA10::*espT*^{W63A} in order to determine the role of the WxxxE motif during EspT induced membrane remodelling and invasion. Approximately 90% of HeLa cells infected with JPN15 pSA10::*espT* exhibited membrane ruffles which surrounded adherent bacteria in addition to pedestals. In contrast cells infected with JPN15pSA10::*espT*^{W63A} only induced ruffles in around 15% of cells whilst pedestal formation was unaffected (Figure 5.8). Quantitative gentamycin protection assays were used to quantify the invasiveness of JPN15 pSA10::*espT* and JPN15 pSA10::*espT*^{W63A} in HeLa cells infected for 3 h, JPN15 and *S.* Typhimurium were used as negative and positive controls respectively. We found that JPN15 expressing EspT^{W63A} was significantly less invasive that JPN15 expressing the wild type protein (Figure 5.8C).

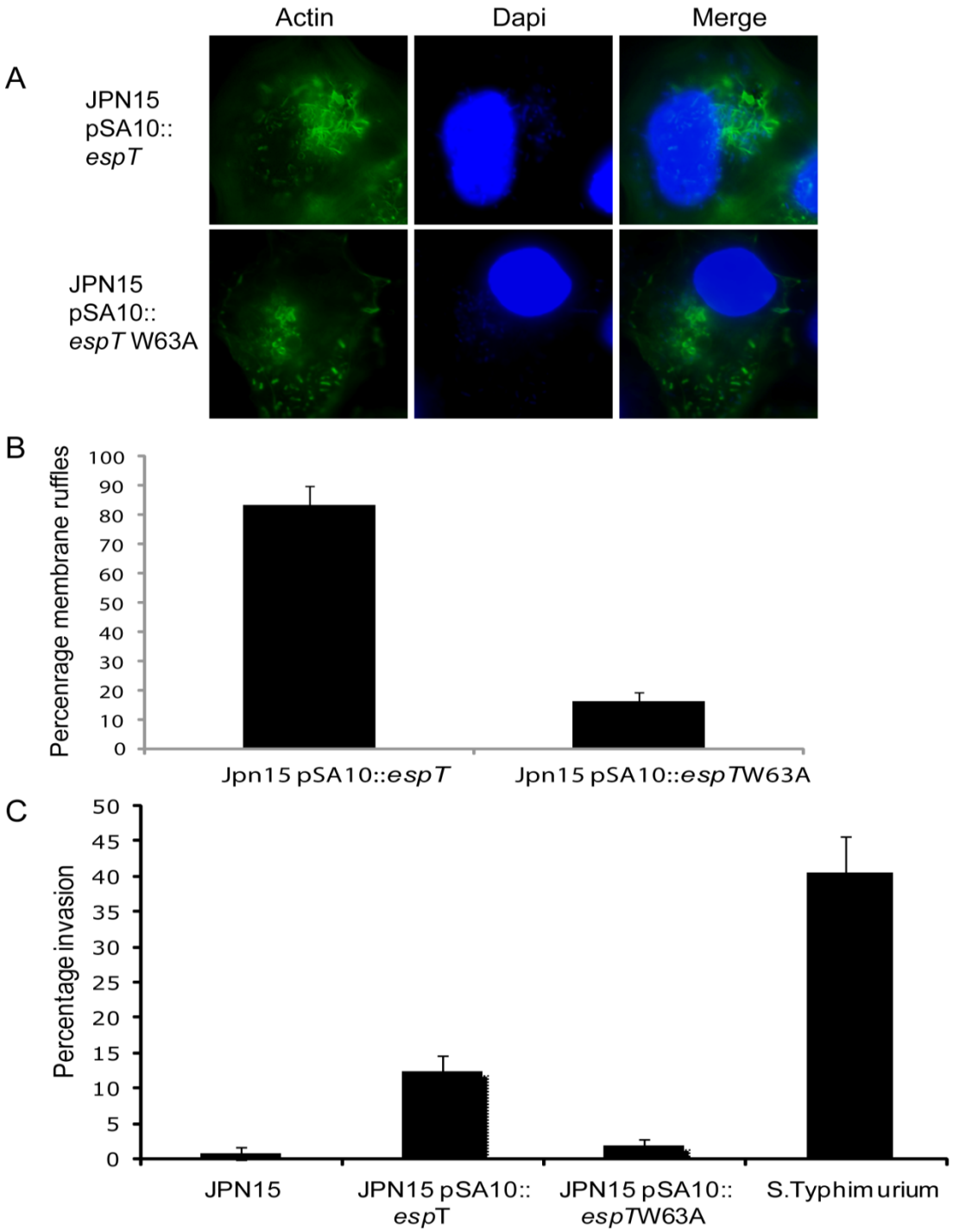


Fig.ure 5.8 EspT mediated membrane remodeling and invasion is dependent on the conserved WxxxE motif. HeLa cells infected with JPN15, JPN15 expressing wild type EspT, or JPN15 expressing EspT^{W63A} for 3 h were fixed and stained with phalliodin (green) to detect actin and Dapi stain to label bateria (blue). In cells infected with JPN15 and JPN15 expressing EspT^{W63A} there was no significant induction of membrane ruffling. Infection of HeLa cells with JPN15 expressing wild type EspT resulted in the formation of characteristic membrane ruffles. (B) Gentamycin protection assay of HeLa cells infected JPN15 and JPN15 expressing EspT or EspT^{W63A}. Results are representative of 3 independent experiments carried out in duplicate and are displayed as mean ± SEM.

5.9 Ectopic Expression of EspT Induces Membrane Ruffles which Facilitate the Invasion of T3SS Null Mutants.

A/E pathogens encode a plethora of T3SS effector proteins which can modulate the host cell cytoskeleton including; Map which activates Cdc42 to induce filopodia (Berger et al., 2009; Kenny and Jepson, 2000), EspM proteins which activate RhoA to induce stress fibres (Arbeloa et al., 2008) and Tir which mediates the formation of actin rich pedestals (Gruenheid et al., 2001). In order to confirm that EspT can promote EPEC invasion of non-phagocytic cells independently of other T3SS effectors we ectopically expressed EspT in HeLa cells prior to infection with EPEC Δ*escN*. Extracellular and intracellular bacteria were labeled as described above. Cells ectopically expressing EspT displayed membrane ruffling which facilitated the uptake of Δ*escN* bacteria (Figure 5.9). These results demonstrate that EspT is sufficient to induce the internalization of EPEC bacteria independently of other T3SS effectors.

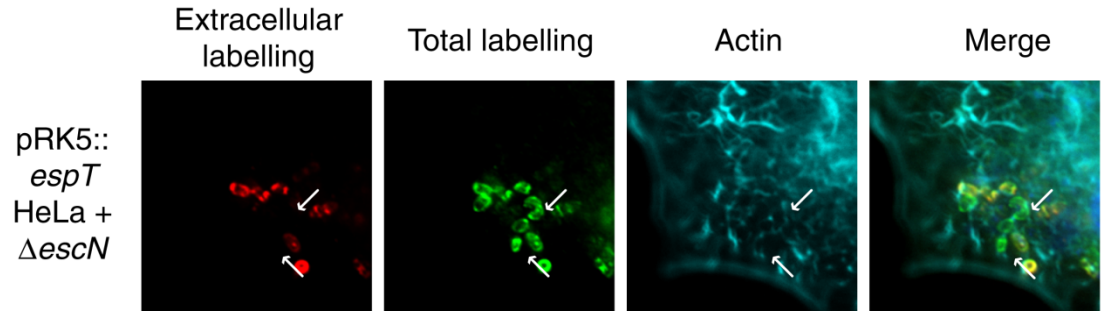


Figure 5.9 Ectopic expression of EspT can facilitate invasion of epithelial cells by a T3SS null mutant. HeLa cells were transfected with pRK5 encoding EspT for 12 h and subsequently infected with a Δ*escN* T3SS mutant for 1.5 h. The cells were then fixed and processed for immuno-fluorescence microscopy. Actin was stained using Alexafluor 633 phalloidin (Cyan), external and internal bacteria were labeled in red and green respectively. Ectopic expression of EspT led to the formation of actin rich membrane ruffles and a significant proportion of Δ*escN* bacteria became internalized (highlighted with arrows).

5.10 Rac1 and Wave2 are Essential for EspT Mediated Bacterial Cell Invasion

As actin remodeling by EspT is dependent on the activation of Rac1, Cdc42 (Figure 4.7) and Wave2 (Figure 5.5 and 5.6), we utilized dominant negative constructs of these signaling proteins and monitored the effect on invasion of JPN15 expressing EspT and E110019. HeLa cells transfected with dominant negative Rac1 ($Rac1^{N17}$), Cdc42 ($Cdc42^{N17}$), Wave2ΔA and Wave2ΔBP were infected for 3 h. The cells were fixed and stained for bacterial invasion as described above. Cells transfected with $Cdc42^{N17}$ were still permissive of bacterial invasion while cells transfected with the $Rac1^{N17}$, Wave2ΔA or Wave2ΔBP dominant negative constructs were not (Figure 5.10). Depletion of Wave2 using siRNA in Swiss 3T3 cells significantly reduced the invasive capacity of both JPN15 expressing EspT and E110019 compared to cells treated with non-targeting siRNA (Fig. 5.5C and 5.10B). Thus, Rac1, Wave2 and Abi1 are essential mediators of EspT-induced bacterial invasion.

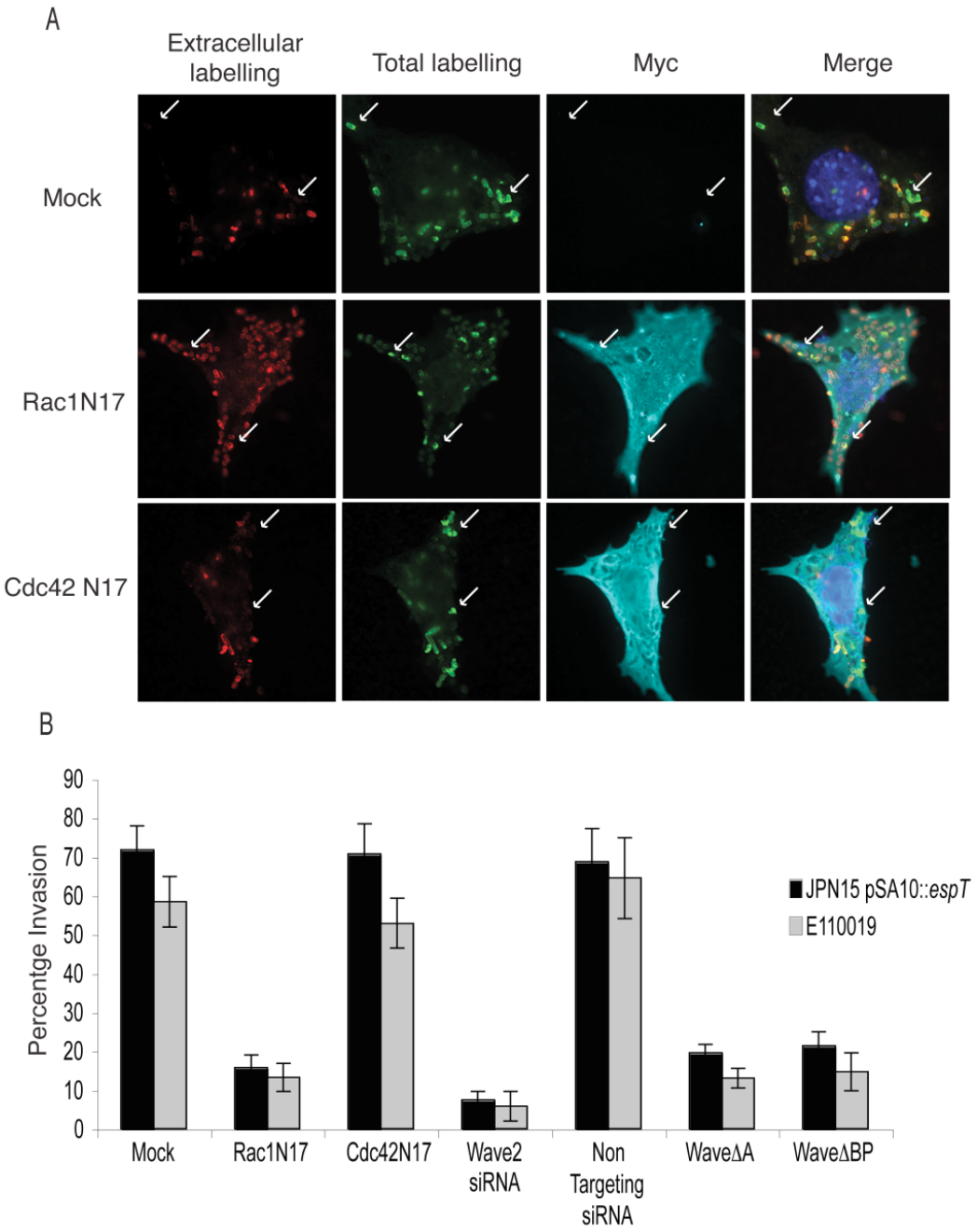


Figure 5.10 Rac1 and Wave2 are essential for EspT-mediated bacterial invasion. (A) Swiss 3T3 cells were left untransfected or transfected with Non Targeting (NT) or Wave2 siRNA oligos, the ectopic expression vector pDSRed encoding Wave2ΔA, Wave2ΔBP or pRK5 expressing dominant negative Rac1 and Cdc42 and infected with JPN15, JPN15 expressing EspT or E110019. Mock transfected cells or cells transfected with dominant negative Cdc42 were efficiently invaded by both JPN15 expressing EspT and E110019. Cells transfected with dominant negative Rac1 were significantly more resistant to bacterial invasion. The Wave2ΔA and Wave2ΔBP constructs also had a potent dominant negative effect on bacterial internalization. (B) Quantification of bacterial invasion; cells which had 3 or more internalized bacteria were scored as invaded. 100 cells were counted in triplicate in three independent experiments. Results are displayed as mean ± SEM.

5.11 Internalized EPEC Bacteria are Enclosed Within a Vacuole

After the initial invasion of host cells internalized bacteria are often bound within a vacuole which resembles early endosomes (reviewed in (Kumar and Valdivia, 2009)). Intracellular bacteria either remain within the vacuole or rapidly escape to the cytoplasm (Cossart and Sansonetti, 2004). In order to determine whether invasive EPEC are bound within a vacuole or free in the cytoplasm HeLa cells were infected with JPN15, JPN15 pSA10::*espT* and E110019 for 5 min up to 12 h and stained with various vacuolar markers including Early Endosome Antigen 1 (EEA1) and Vacuolar ATPase (VATPase). Internalized JPN15 pSA10:::*espT* and E110019 were labeled with EEA1 while external bacteria and JPN15 lacking EspT were not (Figure 5.11 shows staining at 45 min post infection). EEA1 staining was apparent after 5 min and persists up until 1 h post infection (data not shown). At 3 h and up to 12 h post infection the EPEC containing vacuole (ECV) was labeled with VATPase whilst external bacteria were not (Figure 5.14A). Unlike invasive *Salmonella*, at 12 h post infection we did not observe intracellular EPEC microcolonies. However, similarly to the *Salmonella* containing vacuole (SCV), ECVs appear to adopt a perinuclear localization (Figure 5.12).

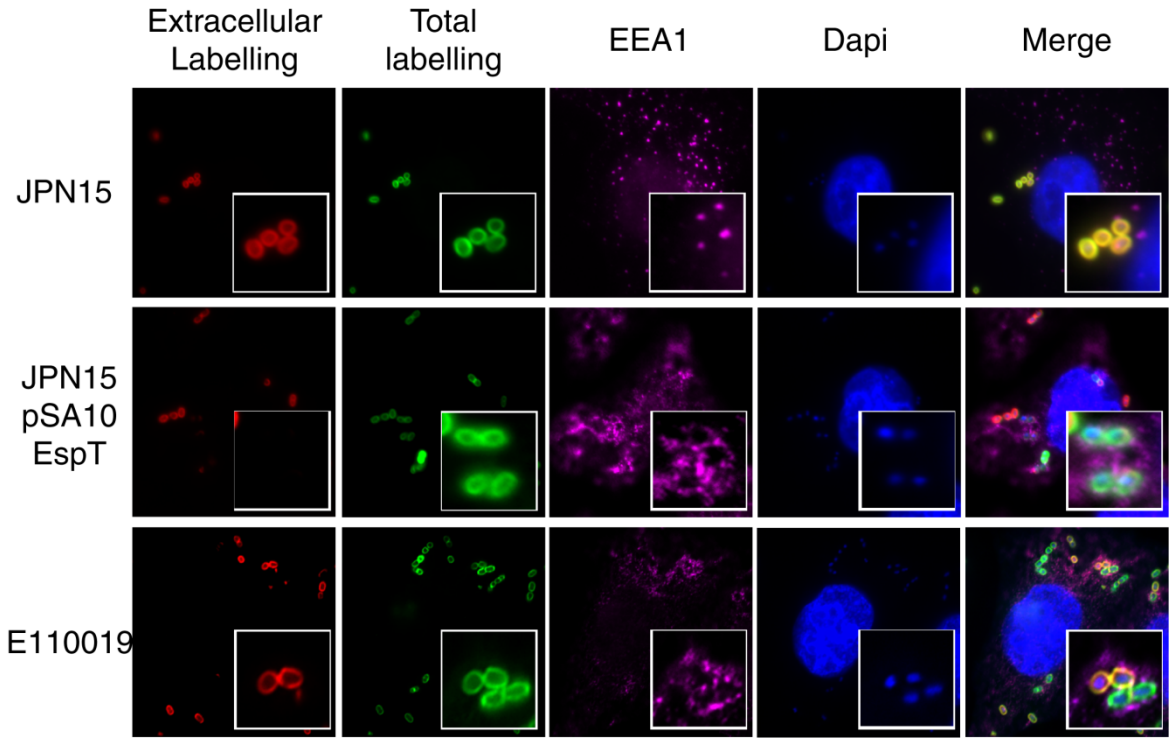


Figure 5.11 Internalized EPEC bacteria are enclosed within a vacuole. Internalized bacteria bound within a vacuole were detected by anti EEA1 and a secondary antibody coupled to a CY5 (magenta). DNA was detected using Dapi staining. Extracellular JPN15 bacteria which were detected by both the total stain and the extra-cellular probes were not co-localized with EEA1 staining. Intracellular JPN15 pSA10::*espT* and E110019 which were detected by the total bacterial probe but not by the pre permeabilization stain were contained within EEA1 rich structures indicative of early endosome like vacuoles.

5.12 The ECV Matures to Become Lamp1 Positive at Late Time Points of Infection.

Intracellular pathogens which are bound by a vacuolated must evade host cell lysosome mediated degradation and maintain the integrity of the vacuole. *Salmonella* is one such intracellular pathogen which after initial invasion of host cells is contained in a vacuole which resembles an early endosome before maturation and acquisition of late endosomal and lysosomal components such as VATPase and Lamp1 (Reviewed in (Kumar and Valdivia, 2009)). Other intracellular pathogens such as *Legionella* modify their vacuole by enriching it with membrane derived from the endoplasmic reticulum (Machner and Isberg, 2007). The vacuole containing *Chlamydia* species is devoid of typical endo-membrane components and instead disrupts the Golgi apparatus in order to scavenge lipids to maintain its vacuole (Heuer et al., 2009). In order to determine the longevity and membrane composition of the EPEC Containing Vacuole (ECV) we infected HeLa cells for 30 min with E110019 and then killed extracellular bacteria with a gentamycin wash before incubation for a further 16 or 24 h. We utilized immuno-fluorescence microscopy to stain for the late endosomal marker Lamp1. At 16 hours post infection the ECVs begins to acquire Lamp1 staining which progressed to label a sub-population of internalized bacteria after 24 h (Figure 5.12). Interestingly the ECV was found to be associated with actin around its boundary (Figure 5.12B). Where the actin staining is prominent there is no localization with the Lamp1 marker (Figure 5.12B).

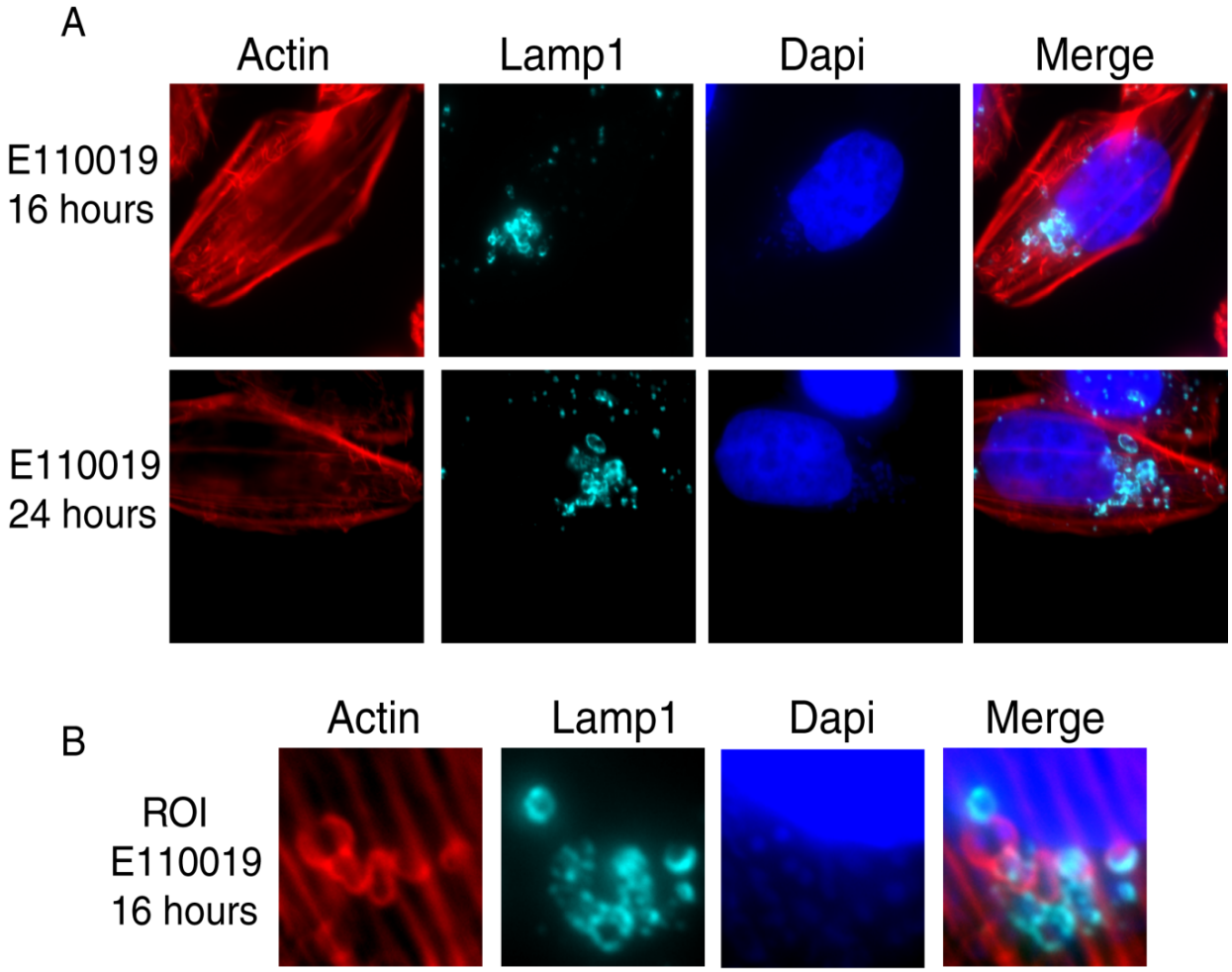


Figure 5.12 The ECV matures to become Lamp1 positive at late time points of infection. HeLa cells were infected for 30 min before extracellular bacteria were eliminated by a gentamycin wash. The cells were then incubated for a further 16 or 24 h. Actin was detected with phalloidin in Red, Lamp1 was detected with a monoclonal antibody in cyan and bacteria were detected with Dapi staining in blue (A) At 16 h post infection the ECV begins to acquire the Lamp1 marker. At 24 h almost all intracellular E110019 are associated with Lamp1. (B) The ECV is associated with actin and where the actin staining is prominent the Lamp1 marker is excluded.

5.13 Internalized EPEC are Associated with Actin Comets

After escaping from the vacuole many intracellular pathogens such as *Shigella* and *Listeria* utilize specialized outer membrane proteins to recruit actin nucleating factors in order to produce a propulsive force (reviewed in (Cossart and Sansonetti, 2004)). Extracellular EPEC is synonymous with actin nucleation which leads to formation of Tir-dependent actin rich pedestals (Frankel et al., 2001). During the course of this study we observed that invasive EPEC contained within the ECV were associated with filamentous actin comets reminiscent of pedestals. In order to confirm that intracellular bacteria are associated with actin we infected Swiss 3T3 cells for 3 h with E110019. We utilized Confocal X-stacks and observed that the intracellular EPEC bacteria were associated with pedestal-like filamentous actin structures (Figure 5.13).

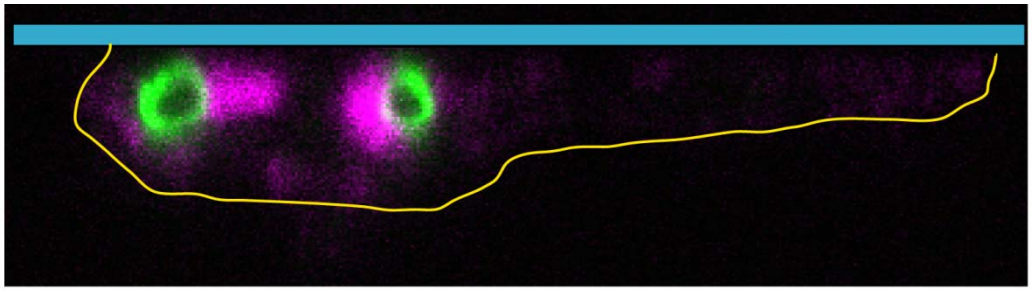


Figure 5.13 Intracellular EPEC are associated with actin comets. Swiss 3T3 cells were infected with E110019 and processed for immuno-fluorescence confocal microscopy. A series of confocal X-stacks were taken through the infected cells. The cell boundaries are defined by a yellow line and the coverslip is represented by the blue bar. The staining shows intracellular E110019 (green) associated with actin comet-like structures (magenta). The cell boundary was defined using actin staining.

5.14 Internalized EPEC Bacteria Incorporate Tir into the Vacuolar Membrane which Nucleates Intracellular Actin Pedestals.

In order to determine if intracellular EPEC actin recruitment was mediated by Tir, we infected HeLa cells for 30 min with JPN15, JPN15 pSA10::*espT* and E110019; following washes the cells were incubated in the presence of gentamycin for a further 8 h. The cells were then stained with anti-VATPase and anti-Tir antisera in conjunction with phalloidin and Dapi staining. In HeLa cells infected with JPN15 pSA10::*espT* and E110019 internalized bacteria were labeled with anti-VATPase and were associated with filamentous actin (Figure 5.14A). In contrast, JPN15 formed pedestals which were associated with Tir but not with VATPase staining (Figure 5.14A). Interestingly, internalized bacteria, which were co-localized with VATPase, were also associated with Tir. Additionally, intracellular EPEC Δ*escN,* internalized by cells ectopically expressing EspT, were not associated with actin pedestals (Figure 5.9). These results suggest that the actin filaments associated with EPEC contained within the ECV is nucleated in a Tir-dependent mechanism analogous to pedestal formation by extracellular bacteria.

In order to confirm this assertion we infected HeLa cells with E110019 for 2 h and processed the cells for transmission electron microscopy (TEM). The TEM confirmed that E110019 bacteria are internalized via ruffle formation (Figure 5.14B). E110019 can also be seen forming multiple pedestals with the membrane on opposing surfaces during ruffle formation and closure (Figure 5.14C). Moreover, internalized EPEC bacteria contained within the ECV are associated actin pedestals, which are strikingly similar to those normally associated with extracellular EPEC (Figure 5.14B-D). Interestingly, bacteria bound within ECVs can form multiple pedestals around their circumference (Figure 5.14D).

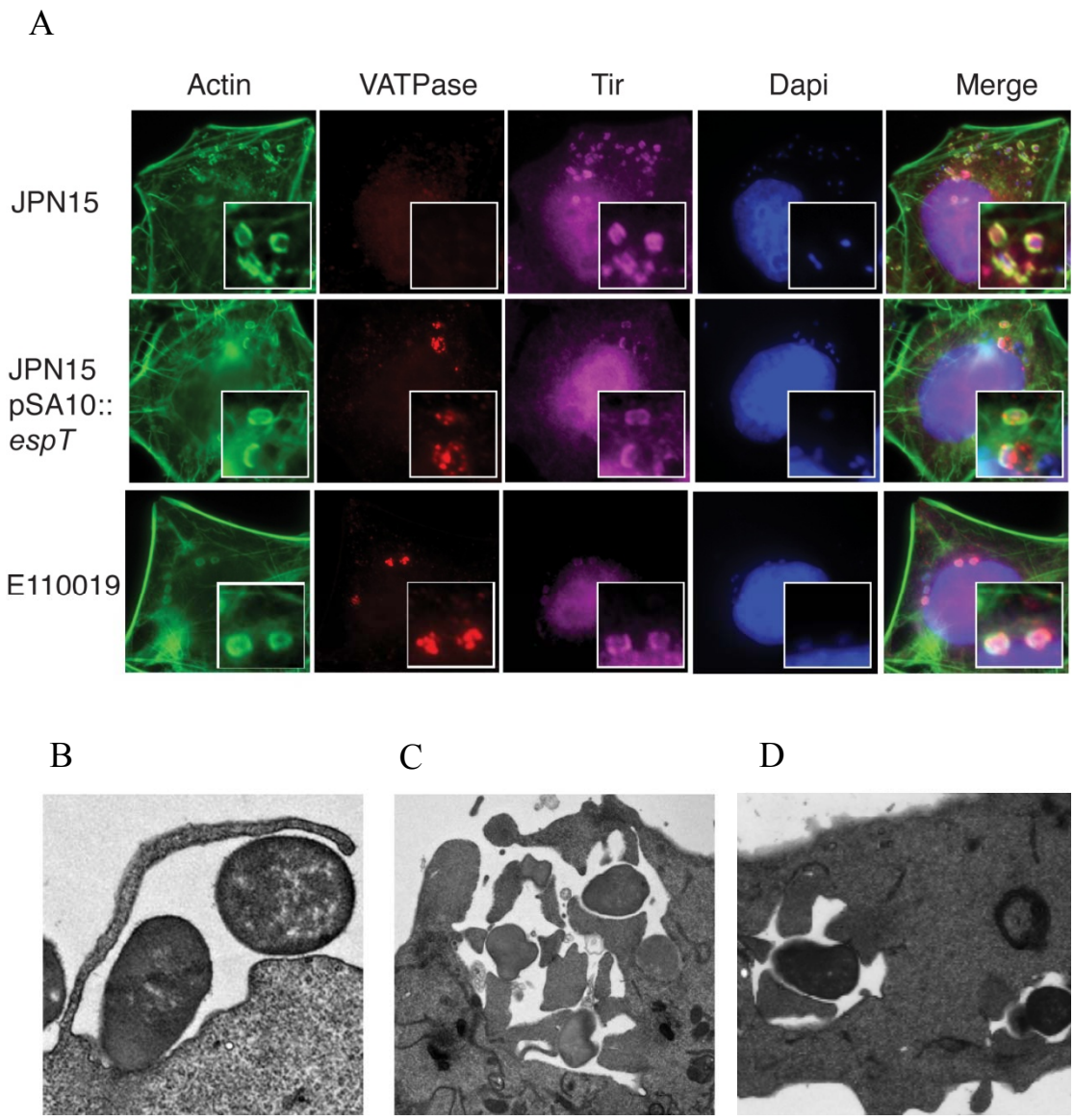


Figure 5.14 Internalized EPEC bacteria incorporate Tir into the vacuolar membrane which nucleates intracellular actin pedestals. (A) HeLa cells were infected for 30 min with JPN15, JPN15pSA10::*espT*, and E110019 were processed for immuno-fluorescence microscopy after 8 h gentamycin treatment. Actin was stained using Oregon Green phalloidin (Green), Tir was detected using polyclonal Tir antisera (Magenta), Vacuolar ATPase (VATPase) was detected using a monoclonal antibody (Red) and bacteria were detected using Dapi staining. Cells infected JPN15 recruited Tir to the site of bacterial attachment and form canonical actin rich pedestals but do not display any bacterial co-localization with the VATPase vacuolar marker. In cells infected with JPN15 pSA10::*espT* or E110019 a proportion of bacteria were co-localized with VATPase, Tir and actin. (B) A TEM micrograph showing membrane ruffles engulfing E110019. (C) E110019 has the capacity to form multiple pedestals during ruffle formation and closure. (D) E110019 bacteria bound within a vacuole with intracellular pedestals formed around its circumference.

5.15 Intracellular Pedestal Formation is Tir Dependent.

As E110019 is multi-antibiotic resistant and as a result difficult to genetically modify we utilised *Citrobacter rodentium* which encodes a genomic copy of *espT* in order to determine if Tir is required for the formation of intracellular pedestals. Swiss 3T3 cells were infected with *C. rodentium* or *C. rodentium* Δ*tir* for 1 h and extracellular bacteria did not form pedestals at this time (data not shown). Extracellular bacteria were eliminated using a gentamycin wash, and the infected cells were then incubated for a further 16 h. We observed that wild type *C. rodentium* formed intracellular pedestals at a similar rate to that observed for E110019 whereas *C. rodentium* Δ*tir* failed to accumulate any actin around ECVs (Figure 5.15). Interestingly, in the *C. rodentium* Δ*tir* mutant all of the intracellular bacteria were homogenously labelled with Lamp1 wheras the wild type had a sub-population associated with actin which was Lamp negative. These results demonstrate that intracellular pedestal formation by invasive A/E pathogens is a Tir dependent process.

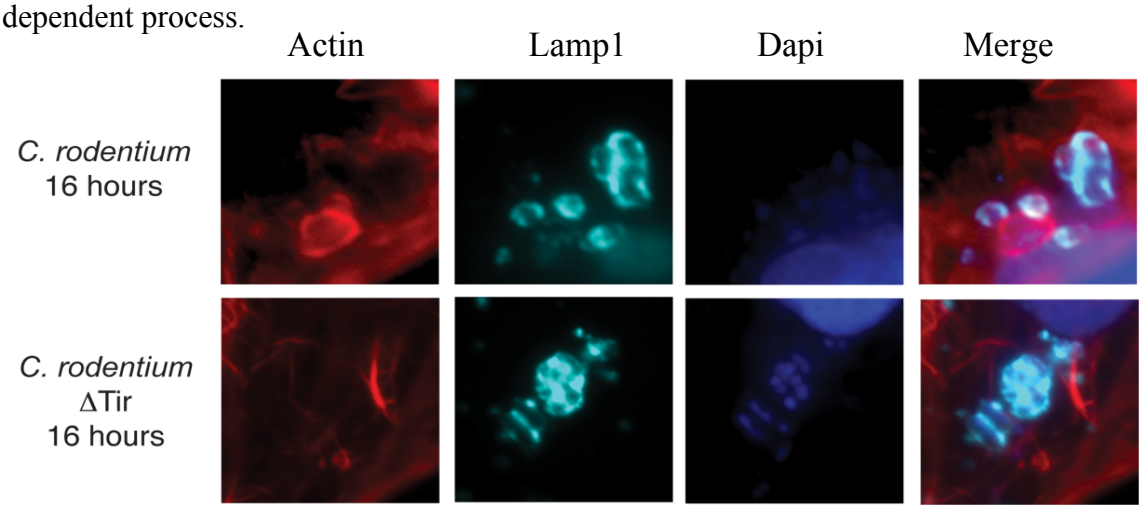


Figure 5.15. Tir is essential for the formation of intracellular pedestals. HeLa cells were infected for 1 h with *C. rodentium* and *C. rodentium* Δ*tir* , before extracellular bacteria were killed with a gentamycin wash. The cells were then incubated for a further 16 h in the presence of gentamycin and fixed for immuno-fluorescence microscopy. Actin was labeled with phalliodin (Red), Lamp1 was detected with a monoclonal antibody (Blue) and bacteria were detected with Dapi stain. *C. rodentium* formed intracellular pedestals whereas *C. rodentium* Δ*tir* did not.

5.16 Internalised EPEC Bacteria can Replicate within Host Cells.

The majority of intracellular bacterial pathogens have the ability to survive and replicate within host cells (Kumar and Valdivia, 2009). In order to determine if E110019 can replicate with host cells we infected HeLa cells for 90 min, killed extracellular bacteria with a gentamycin wash and then incubated the HeLa cells in the presence of gentamycin for a further 2, 8, 16 and 24 h. We found that the number of E110019 bacteria within host cells increased in a time dependent manner consistent with bacterial replication (Figure 5.16). The rate of replication observed for internalised E110019 was significantly lower than what has been previously reported for *Salmonella* or *Shigella* species. Furthermore, HeLa cells infected with E110019 for 8, 16 and 24 h display a substantial amount of actin rich blebbing (Figure 5.16). However, the nuclei were not condensed and the cells do not display any other signs of apoptosis (Figure 5.16).

In order to determine if the formation of intracellular pedestals by A/E pathogens plays a role in bacterial replication and survival within host cells we infected Swiss cells with wild type *C. rodentium* and *C. rodentium* Δ*tir* for 1.5 h and with E110019 for 30 min. Extracellular bacteria were then killed by a gentamycin wash and the cells incubated for a further 6, 12 or 24 h. We observed that both wild type *C. rodentium* and E110019 were capable of intracellular replication whereas the *C. rodentium* Δ*tir* mutant failed to replicate and instead exhibited a slow decline in bacterial numbers over time (Figure 5.16B). These results demonstrate that formation of pedestals by invasive A/E pathogens may play a functional role during intracellular survival.

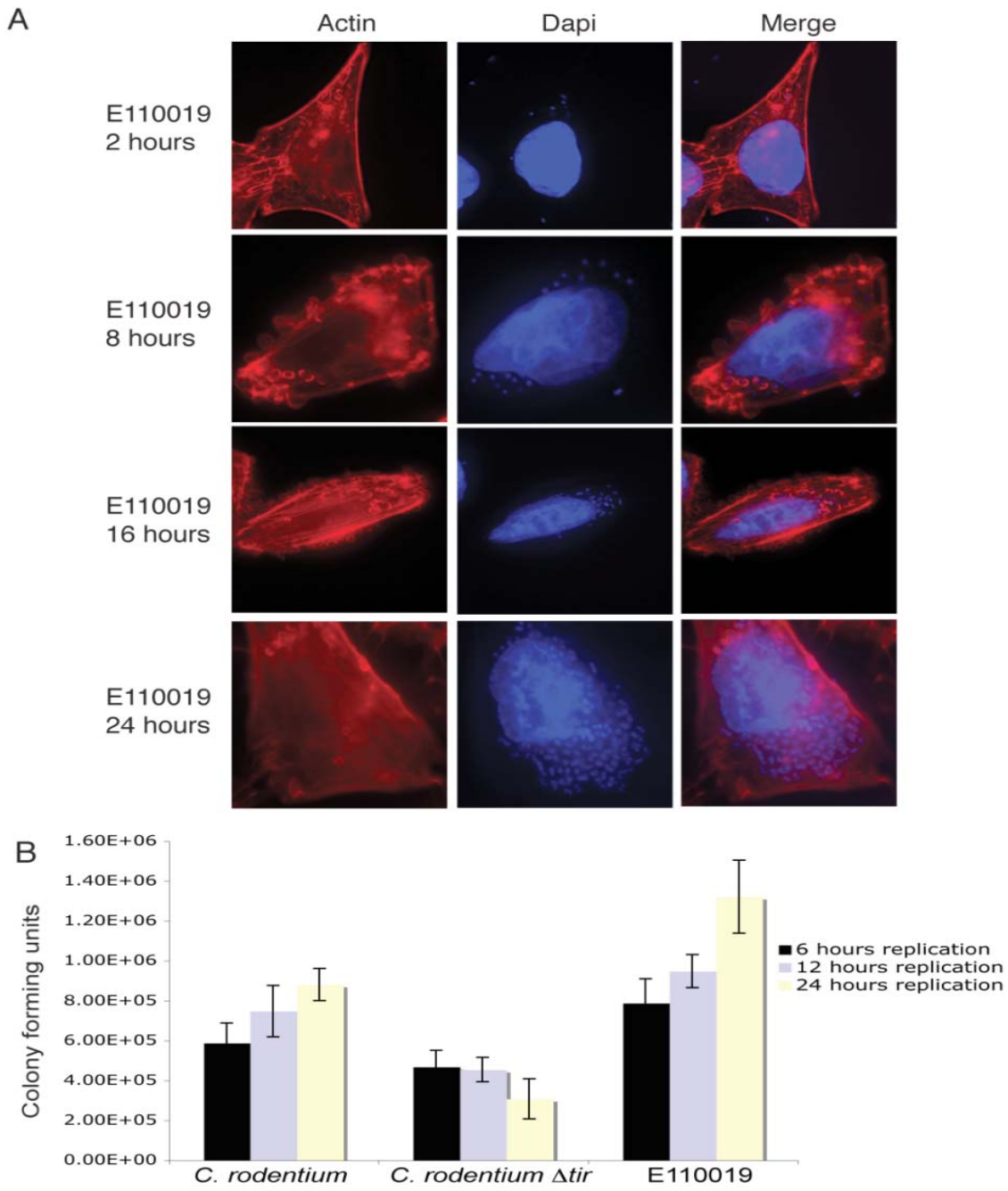


Figure 5.16 (A) Internalized A/E pathogens survive and replicate in epithelial cells. HeLa cells were infected with E110019 for 30 min before the cells were washed with gentamycin to eliminate non invasive-bacteria. The cells were then incubated for 2, 8, 16 and 24 h in the presence of gentamycin. Cells were processed for immuno-fluorescence microscopy, bacteria were detected with Dapi (Dlue) and actin was labeled with phalliodin (Red). There was a time dependent increase in the level of intracellular bacteria. (B) Quantitative gentamycin protection assay of intracellular growth. HeLa cells were infected for 3 h with *C. rodentium, C. rodentium* Δ*tir* and E110019 before extracellualr bacteria were eliminated with gentamycin. Cells were then incubated in the presence of gentamycin for 6, 12 or 24 h before the cells were lysed and plated for CFU counting. Results are representative of 3 independent experiments and are presents as mean ± SEM.

5.17 Discussion

A/E pathogens have been long considered to be extracellular bacteria which do not invade mammalian cells (Celli et al., 2000). However, sporadic reports have shown that atypical EPEC strains can invade non-phagocytic cells (Donnenberg et al., 1989; Hernandes et al., 2008). The invasive ability has been linked to the adherence pattern and tight association of EPEC with the host cell membrane which is hypothesized to produce a passive push effect by which the intimate association of the bacteria with the host cell results in the formation of an invagination which of the membrane leading to internalization (Donnenberg and Kaper, 1992; Hernandes et al., 2008). In this chapter we have demonstrated for the first time that EPEC can actively invade non-phagocytic cells by inducing formation of membrane ruffles, defining a new category of invasive EPEC. Furthermore, we demonstrate that this phenomenon is dependent on the T3SS effector EspT which we have shown activates Rac1 and Cdc42 (Bulgin et al., 2009).

Intracellular pathogens have evolved a variety of mechanisms to promote invasion of mammalian cells, including the trigger (employed by *Salmonella* and *Shigella*) and zipper (employed by *Yersinia* and *Listeria*) mechanisms (reviewed in (Cossart and Sansonetti, 2004)). The trigger invasion mechanism is characterized by formation of actin rich membrane ruffles at the site of bacterial attachment, which are regulated by Rho GTPases, particularly Rac1 and Cdc42 and other cytoskeletal regulators such as PI3K (Ladwein and Rottner, 2008). *Shigella* and *Salmonella* utilize T3SS effector and translocator proteins such as IpgB1 and IpaC and SopB and SopE/2 to hijack host cell GTPase and phospho-inositol signaling to modulate membrane ruffling and formation of the macropinocytic pocket (Hardt et al., 1998; Ohya et al., 2005; Patel and Galan, 2006; Tran Van Nhieu et al., 1999). Importantly, although both IpgB1 and EspT belong to the WxxxE family of effectors and play a prominent role in bacterial invasion by

inducing membrane ruffles, we have recently shown that they activate Rac1 by distinct mechanisms (Bulgin et al., 2009).

Downstream of Rho GTPase signaling, membrane ruffle formation is nucleated by the WASP superfamily proteins including N-WASP and Wave2. *Salmonella* invasion has been demonstrated to be at least in part dependent upon the Arp2/3 binding activity of Wave2 and also the association of Wave2 with Abi1 (Shi et al., 2005). Wave2 cannot bind Rac1 directly; two different mechanisms have been proposed to describe how a Wave2-Rac1 complex is formed. Innocenti et al and Steffen et al demonstrate that Wave2 binds to Abi1 and two accessory proteins PIR121 and Nap1 which mediate Rac1 binding (Innocenti et al., 2004; Steffen et al., 2004). A report by Miki et al proposed that IRSp53 is the protein which links Rac1 to Wave2 (Miki et al., 2000). In this study we demonstrate that EspT activation of Rac1 leads to a downstream recruitment of Wave2, Abi1 and IRSp53 to membrane ruffles. Depletion of endogenous Wave2 using siRNA resulted in a significant reduction in both the level of membrane ruffles induced by strains expressing EspT and their associated invasive capacity. We also show that the Arp2/3 and Abi1 binding regions of Wave2 are required for EspT-induced membrane ruffles. Furthermore, a construct of Wave2 which retained the IRSp53 and Arp2/3 binding regions but lacked the Abi1 interacting domain had a dominant negative effect on membrane ruffle formation, suggesting that IRSp53 is not required for, but may play an accessory role in, EspT-mediated actin rearrangements. Additionally we demonstrate that inhibition of Rac1, depletion of Wave2 or expression of Wave2 constructs lacking the Arp2/3 or Abi1 binding regions abolishes the invasion capacity of EPEC strains expressing EspT.

Once internalized *Shigella* and *Listeria* quickly escape the vacuole (reviewed in (Schroeder and Hilbi, 2008)). In contrast, *Salmonella* remains vacuole bound and utilizes different virulence

factors to modify the vacuolar environment, position and interaction with the host endomembrane system in order to create an intracellular replicative SCV (reviewed in (Steele-Mortimer, 2008)). In this study we demonstrated that after invasion EPEC is bound within a vacuole (ECV) and remains vacuolated until at least 12 h post infection. We found that the ECV is EEA1 positive for up to 1 h post infection and progresses to being VATPase positive from 3 h to 12 h post infection and eventually becoming enriched in the lysosomal glycolprotein Lamp1. Furthermore, 12 h after infection the ECV appears to adopt a peri-nuclear position, which resembles the properties of the SCV. Importantly, we found that the ECV is associated with filamentous actin tails which are reminiscent of the actin-rich pedestals that are induced by extracellular adherent EPEC.

Formation of extracellular pedestals is dependent upon the T3SS effector Tir (Kenny *et al* 1997). The interaction of Tir with intimin triggers recruitment of the mammalian adaptor Nck which in turn recruits and activates N-WASP leading to Arp2/3 recruitment and actin polymerization (Campellone et al., 2002; Gruenheid et al., 2001; Kenny et al., 1997; Lommel et al., 2001). In this study we found that internalized EPEC can translocate Tir to the vacuolar membrane in a T3SS dependent manner and that the localization of Tir can promote actin nucleation. Additionally, we found that a *C. rodentium* Δ*tir* mutant is still invasive but does not form intracellular pedestals, demonstrating that pedestal formation by internalized bacteria is a Tir-dependent process analogous to that of extracellular bacteria. Furthermore, using TEM we found that invasive EPEC bound within a vacuole are associated with intracellular pedestals around the circumference of the bacteria. Interestingly, membrane ruffles seen engulfing invading EPEC were occasionally associated with pedestals, suggesting the pedestals can be formed during or after internalization.

Canonically actin is recruited to the surface of intracellular pathogens which are non-vacuolated and this recruitment is mediated by outer-membrane proteins which are free to interact with host cell signaling molecules present in the cytoplasm. For example following escape from the vacuole *Shigella* and *Listeria* utilize IcsA/VirG and ActA, respectively, to trigger actin polymerization and motility (reviewed in (Cossart, 1995)). The Vaccinia virus uses the viral membrane protein A36R in order to generate actin based motility in a similar manner to the extracellular EPEC pedestals (Frischknecht et al., 1999). Importantly, the SCV is also associated with an actin nest which is required to maintain the integrity of the vacuole and support the intracellular replication of *Salmonella* (reviewed in (Guiney and Lesnick, 2005)).

Due to the positioning of the actin extensions around the entire circumference of EPEC it is unlikely these intracellular pedestals are involved in classical actin-based motility. However, there are reports suggesting that actin polymerization and depolymerization around the periphery of E-cadherin-coated beads can lead to directional movement in process referred to as flashing (Yam and Theriot, 2004); for this reason at this stage we cannot rule out the possibility that intracellular pedestals confer actin based motility. Furthermore, formation of intracellular pedestals by invasive EPEC may play a role in maintaining the vacuole integrity in a similar way to that described for other vacuolated pathogens (Guiney and Lesnick, 2005). To the best of our knowledge the current study demonstrates for the first time that an intracellular bacteria is able to recruit filamentous actin comets to the pathogen cell surface whilst encapsulated in a vacuole.

In order to survive within an intracellular niche vacuolated bacteria must evade host cell lysosome mediated degradation. In this study we provide evidence that internalised EPEC bacteria can survive and replicate for at least 24 h post infection. Furthermore, we also report that a *C. rodentium* Δ*tir* mutant was attenuated for intracellular replication. We propose that

formation of actin rich intracellular pedestals around the circumference of the ECV by invasive EPEC may constitute a physical barrier to lysosome fusion. A similar phenomenon has been described for the trafficking of endosomes and lysosomes to wounded sites of plasma membrane. At sites of plasma membrane disruption lysosomes and endosomes are recruited to seal the breach, this process is inhibited if the cortical actin meshwork is stabilized and enhanced when it is disrupted (Miyake et al., 2001). Similarly the lysosome dependent internalization of *Trypanosoma cruzi* requires a depolymerization of the cortical actin network to allow lysosome transit to the plasma membrane (Rodriguez et al., 1995).

Recently, while screening ca. 1000 clinical EPEC and EHEC isolates we found that none of the EHEC strains and only 1.8% of the EPEC strains contain *espT* (Arbeloa et al., 2009). Interestingly, *espT* was found in EPEC E110019 which was linked to a particularly severe outbreak of gastroenteritis in Finland (Viljanen et al., 1990). E110019 was found to be particularly infectious and unusually for EPEC was associated with person to person spread and adult disease (Viljanen et al., 1990). Although we have no clinical data of the other *espT* positive isolates it is tempting to speculate that the expression of EspT could be at least in part responsible for the hyper virulence of the E110019 strain. Further studies of the invasive EPEC category are needed to assess the risk they pose to human health.

Chapter 6 – General Discussion

6.1 Attaching and Effacing Pathogens and the Eukaryotic Cytoskeleton

Attaching and effacing bacteria are a group of related pathogens which mediate gastroenteritis and other more serious conditions such as hemolytic uremic syndrome (HUS) and hemorrhagic colitis (Kaper et al., 2004). The pathogenesis of A/E pathogens is dependent upon their tight adherence to the host cell gut epithelium and subsequent subversion of host cell signaling networks. Intimate adherence to host enterocytes and the modulation of eukaryotic cell processes by A/E pathogens is dependent upon their conserved T3SS. EPEC, EHEC and *Citrobacter rodentium* utilize their T3SS to translocate anywhere between twenty five to fifty effector proteins directly from the bacterial cell to the host cytosol. These effector proteins then interact with a plethora of eukaryotic proteins in order to usurp host cell signaling to mediate bacterial survival and proliferation. A common theme in A/E pathogen subversion of host signaling is the modulation of the eukaryotic cytoskeleton. Uniquely, A/E pathogens translocate their own receptor, Tir, into host cells (Kenny et al., 1997). Upon translocation to the cytoplasm, Tir is phosphorylated and targeted to the host cell plasma membrane where it acts as a docking receptor for the bacterial outer membrane adhesin intimin. The interaction between Tir and intimin results in a recruitment and activation of N-WASP either through the eukaryotic adaptor Nck or the bacterial T3SS effector TccP resulting in actin polymerization and the assembly of pedestal structures on which extracellular bacteria rest (reviewed in (Frankel and Phillips, 2008)) Interestingly, although TccP can bind and activates N-WASP directly it requires members of the IRSp53/MIM homology domain proteins in order to interact with Tir (Vingadassalom et al., 2009; Weiss et al., 2009). Other A/E pathogen T3SS effectors such as EspG mediate the depolymerisation of microtubules and consequent formation of stress fibres (Matsuzawa et al., 2004), EspL interacts with the eukaryotic protein annexin2 to mediate crosslinking of actin

(Miyahara et al., 2009) and TccP interacts with N-WASP to relieve its auto-inhibitory confirmation and allow actin polymerization (Cheng et al., 2008). Subversion of the eukaryotic cytoskeleton by T3SSs is not limited to the A/E pathogen effectors and is in fact utilized by an array of bacterial pathogens. *Salmonella* utilises the kinase SteC to aid in the formation of an F-actin meshwork in proximity to the SCV (Poh et al., 2008), SipA enhances *Salmonella* invasion and vacuole maturation by both stimulating actin polymerisation and protecting already polymerized actin filaments from disassembly (McGhie et al., 2004) (Brawn et al., 2007). Another *Salmonella* effector SipC has been demonstrated to posses both actin nucleating and bundling properties (Hayward and Koronakis 1999). Similarly, *Vibrio* species translocate the effector VopL which contains homologs of eukaryotic actin binding domains which can mediate actin polymerization (Liverman et al., 2007). The *Shigella* translocator IpaC can mediate membrane ruffle formation via the subversion of eukaryotic Src kinase signaling (Mounier et al., 2009; Tran Van Nhieu et al., 1999) to name but a few.

6.2 Bacterial Pathogens and GTPases

Small GTPases are a common target of bacterial toxins and effector proteins due to their pivotal role in eukaryotic cell biology (Etienne-Manneville and Hall, 2002). The Rho family of GTPases are fundamental regulators of the host cell cytoskeleton and as such act as an "achilles heel" which is often targeted by pathogens in order to promote adherence, invasion and evasion of the host immune response (Finlay, 2005). Some bacterial toxins modify GTPases by adding carbohydrate moieties or by chemically altering constituent amino acids in order to activate or inactivate small G proteins signaling (Aktories et al., 2000; Yarbrough et al., 2009). The T3SS effector YopT has been demonstrated to cleave the membrane retention sequences from active Rho GTPases in order to inhibit their function (Shao et al., 2002). Other T3SS effectors have

been shown to mimic Rho GTPase regulator factors including activating GEFs, Inactivating GAPs and Inhibitory GDIs (Fu and Galan, 1999; Hardt et al., 1998; Prehna et al., 2006).

6.3 Evolution of the Mechanism of WxxxE Effectors

In 2006 Alto and colleagues grouped 26 previously identified effectors into a family based on their conservation of a motif comprising an invariant tryptophan and glutamic acid residue separated by three variable amino acids (Alto et al., 2006). Alto et al also noted that several of the effector proteins within this group were capable of inducing phenotypes which were reminiscent of active Rho GTPases including IpgB2, IpgB1 and Map which induce the formation of stress fibres, membrane ruffles and filopodia respectively. In the same study the authors demonstrate formation of stress fibres by IpgB2 was independent of the activity of RhoA. Furthermore, it was found that IpgB2 was capable of binding the canonical GTP bound RhoA partners ROCK and mDia and activating the former *in vitro*. This led the authors to propose that WxxxE effectors act as functional mimics of Rho GTPases (Alto et al., 2006). This mechanism of WxxxE effectors was augmented by a report from Handa *et al* who provided evidence that the WxxxE effectors IpgB1 can mimic RhoG by binding its partner proteins ELMO and Dock180 which act as a bipartite GEF of Rac1 (Handa et al., 2007). This mechanism differs from that proposed by Alto et al who suggested that IpgB1 would act as a functional mimic of Rac1.

In the current study we identify a family of IpgB2 homologues within the A/E pathogens which we have defined as the EspM family of effectors. In contrast to the data reported in Alto et al., (Alto et al., 2006) for IpgB2, our results indicate that EspM triggered formation of stress fibres is dependent on RhoA. Furthermore, we have demonstrated that EspM proteins significantly activate RhoA when translocated into mammalian cells (Arbeloa et al., 2008). We also identified the novel effector EspT which induces membrane ruffles and lamellipodia similar to those

formed by expression of IpgB1. In an analogous manner to reliance of EspM proteins on RhoA to induce stress fibres we demonstrated that membrane ruffle and lamellipodia formation by EspT requires the activity of Rac1 and to a lesser extent Cdc42. Concurrently, we show that EspT activates both Rac1 and Cdc42. Interestingly, we report here that EspT can activate Rac1 and form membrane ruffles and lamellipodia independently of ELMO or Dock180. Furthermore, we demonstrate that EspT mediated induction of actin protrusions is also independent of other canonical Rac1 activation pathways including typical mammalian GEFs, Src family kinases and PI3K (Bulgin et al., 2009). Together these results challenge the model by which WxxxE effector would act as functional mimics of Rho GTPases and lends weight to the hypothesis that WxxxE effectors stimulate the activity of endogenous Rho family GTPases. The fact that EspT can activate Rac1 independently of ELMO, Dock180, Src kinases and Pi3K further suggests that WxxxE mediated activation of Rho GTPases may be direct.

In 2008 the structure of the WxxxE effector SifA was solved; interestingly it was demonstrated that the carboxy terminus of SifA which harbors its WxxxE motif adopts a fold which is similar to the bacterial Rho GEF SopE (Ohlson et al., 2008). Further characterisation of EspM family of proteins, in collaboration with Professors Steve Mathews and Susan Lea, demonstrated that EspM2 is capable of binding in a dose dependent manner to RhoA favoring its nucleotide free form. This interaction is similar to that of a mammalian GEF with its partner GTPases. In order to determine if EspM2 posses GEF activity we performed a nucleotide exchange assay on RhoA, Rac1, Cdc42 and H-Ras. We report that EspM acts specifically as a GEF of RhoA with only residual activity towards the other GTPases. The structure of EspM2 confirms that it too adopts an inverted V shape consisting of 6 alpha helixes which is similar to that of SopE (Arbeloa et al unpublished information). Several regions of EspM2 were found to move when in contact with

RhoA, one of these regions was predicted to be a flexible loop in an analogous position to the functional GAGA loop of SopE which is required for its nucleotide exchange activity. Although the regions do not share any sequence homology mutagenesis of the loop in EspM2 resulted in a severe attenuation of stress fibre formation (Arbeloa et al unpublished information). A study by Huang et al has also demonstrated that the WxxxE effector Map binds directly to Cdc42 in a SopE like conformation (Huang et al., 2009). In the same study it was also reported that IpgB1, IpgB2 and Map acts as GEFs of Rac1, RhoA and Cdc42 respectively (Huang et al., 2009). Thus it has become clear that rather than mimicking Rho GTPases WxxxE effectors act as GEFs. Interestingly, although there is very little sequence similarity between the WxxxE effectors and SopE their 3D structures are strikingly similar suggesting they have arisen through convergent evolution. The catalytically active loop is similarly positioned in SopE and the WxxxE effectors but is dissimilar in respect to its constituent residues. The flexible loop region of IpgB1, IpgB2, Map, EspT and the EspM are very well conserved the corresponding region of SifA is divergent from the other WxxxE effectors. Although SifA has been demonstrated to bind RhoA (Ohlson et al., 2008) we did not detect any GEF activity of SifA towards RhoA in the nucleotide exchange assay. This demonstrates that the interaction of WxxxE effectors with Rho GTPase can be uncoupled from their GEF activity and may represent a regulatory mechanism. Huang et al have also demonstrated that the variable β2-3 inter-switch region of the Rho GTPase determines the specificity of WxxxE effector binding (Huang et al., 2009), the authors also identified residues within alpha helix 4 and 6 of the WxxxE effectors which interact with the β2-3 region of Rho GTPases and are predicted to generate WxxxE effector GTPase targeting (Huang et al., 2009). In this study we report that conservative substitution of the WxxxE motif's invariant tryptophan or glutamic acid residues, with tyrosine or aspartic acid respectively, allows retention of the

biological activity of EspM2. This data is in agreement with the positioning of the WxxxE motif within core region of EspM2, SifA and Map (Huang et al., 2009) (Ohlson et al., 2008). The WxxxE motif contributes many hydrophobic interactions involved in stabilizing the catalytic loop and alpha helices 3, 4 and 6. In addition the conserved glutamic acid residue of the WxxxE motif contributes two hydrogen bonds to the interface of Map and the switch 2 region of Cdc42 (Huang et al., 2009).

6.4 Other Factors which Contribute to WxxxE Mediated Activation of GTPases

Although the mechanism by which WxxxE effectors activate RhoA GTPases has now been elucidated there are still several open questions which need to be addressed. Although IpgB1 is capable of acting as a GEF *in vitro* it has been demonstrated that in a cellular environment it requires the ELMO-Dock180 complex for efficient formation of membrane ruffles (Handa et al., 2007). We have also demonstrated that although EspT activity is independent of the ELMO-Dock180 complex over-expression of ELMO in conjunction with translocation of EspT results in a shift from lamellipodia to membrane ruffle sin Swiss 3T3 fibroblasts. IpgB2 has been found to bind ROCK and mDia as well as acting as a GEF for RhoA (Alto et al., 2006). This may represent the formation of a tripartite complex between the WxxxE proteins, Rho GTPases and their downstream effctors which may have a role in enhancing or regulating the biological activities of the WxxxE effectors. The A/E pathogen effector Map has a C terminal PDZ binding domain which is required for its interaction with the membrane associated NHERF proteins (Simpson et al., 2006) (Berger et al., 2009). It is also interesting to note the presence of a CaaX motif at the C-terminus of SifA which is found in many host GTPases and is recognition site for host cell prenylation which is required for membrane anchoring (Boucrot et al., 2003). Together

these results suggest that there is a further layer of complexity in WxxxE effector signaling which is generated by additional interactions with cellular partners other than there cognate GTPases. These interactions may be required for the proper localization, regulation or cell line specific activities of WxxxE effectors.

6.5 WxxxE Effectors Contribution to Pathogenesis

The complete functional significance of WxxxE effectors in the virulence strategies of their respective pathogens is still relatively poorly understood. Several reports have demonstrated that WxxxE effectors can circumvent more than just the eukaryotic cytoskeleton. Map is trafficked to cellular mitochondria where it has been shown to induce a loss of membrane potential and to limit mitochondrial damage induced by other A/E pathogen T3SS effectors (Kenny et al., 2002; Papatheodorou et al., 2006). A recent study has implicated IpgB2 in a signalling cascade which via activation of RhoA, RiP2 and ROCK results in an activation of NF-kB (Fukazawa et al., 2008). SifA has been reported to induce the formation of membranous tubular filaments rich in lysosomal glycoproteins which are required for *Salmonella* intracellular replication and survival (Beuzon et al., 2000; Brumell et al., 2001; Stein et al., 1996). However, the most striking and apparent effect of the majority of WxxxE effectors is their GTPase dependent reorganisation of the actin cytoskeleton. Perhaps the most well studied example of cytoskeletal rearrangement in respect to virulence is the membrane ruffle formation induced by IpgB1. The entry of *Shigella* into non-phagocytic cells is largely dependent upon the trigger mechanism of invasion generated by the engulfment of bacteria by membrane ruffles induced by IpgB1 (Handa et al., 2007; Ohya et al., 2005). The membrane ruffle mediated engulfment of *Shigella* results in the formation of a maco-pinocytic pocket which leads to bacterial internalisation. *Salmonella* also utilises the

trigger mechanism of invasion which is mediated via the action of SopE1/2 effectors which act as GEFs of Rac1 and Cdc42 (Buchwald et al., 2002; Hardt et al., 1998; Patel and Galan, 2006). Attaching and effacing pathogens are generally considered to be extracellular pathogens although sporadic reports have linked then with invasion cultured cells in a passive adherence pattern dependent manner (Donnenberg et al., 1989; Hernandes et al., 2008). In this study we have identified the WxxxE effector EspT in *C. rodentium*, EPEC E110019 and a small percentage of atypical EPEC clinical isolates (Arbeloa et al., 2009; Bulgin et al., 2009). EspT has been demonstrated to activate Rac1 and Cdc42 to promote formation of membrane ruffles (Bulgin et al., 2009). Further characterisation of EspT, EPEC E110019 and *C. rodentium* in this study has revealed that EspT dependent subversion of host cell Rho GTPases and subsequent re-organisation of the actin cytoskeleton facilitates invasion of A/E pathogens into eukaryotic cells. This shows for first time that EPEC and *C. rodentium* can invade host cells in a T3SS dependent manner. Additional insights into the mechanism by which EspT mediated membrane ruffles and lamellipodia are formed revealed that Wave2 and its interacting partner Abi1 are essential downstream signalling proteins required for cytoskeletal organisation. These results demonstrate that the WxxxE effectors EspT and IpgB1 in addition to sharing mechanistic similarities also have a common role in the virulence strategies of their respective bacteria. It will prove interesting to carry out *in vivo* studies using *C. rodentium* in order to establish the contribution of EspT to virulence in an animal model of infection.

6.6 EPEC as an Intracellular Pathogen

Once internalised bacterial pathogens are contained within a membrane bound vacuole. The bacteria then either escape to the cytosol or remain within the vacuole (Kumar and Valdivia, 2009). Intracellular pathogens such as *Shigella* and EIEC quickly escape from the initial

phagosome using components of their T3SS allowing them access to the mammalian cytoplasm (Cossart and Sansonetti, 2004). Once in the cytosol *Shigella* and EIEC species encode a protein called IcsA/VirG which directs recruitment of N-WASP which subsequently triggers actin polymerisation (Suzuki et al., 2002). This actin polymerisation at the surface of the bacteria facilitates movement and intracellular spread of the pathogens. In contrast *Salmonella, Legionella* and *Mycobacterium* species are examples of intracellular bacteria which remain encapsulated within a vacuole. These vacuoles are often extensively modified by the pathogens which are bound within them in order to promote bacterial survival and replication ((reviwed in Kumar and Valdivia, 2009)).

The best studied example of an intracellular bacteria which resides within a vacuole is *Salmonella.* After invasion of host cells *Salmonella* translocates a plethora of T3SS effectors from two independent secretion apparatus which modify and direct the maturation of the *Salmonella* containing vacuole (SCV). The SCV matures from an early endosome like vacuole characterised by EEA1 and transferrin receptor enrichment, through intermediate stages characterised by Rab5, Rab7 and VATPase towards a late endosomal/lysosomal compartment which is marked by the lysosomal glycoproteins Lamp1 and Lamp2 (reviewed in (Steele-Mortimer, 2008)). Interestingly, although the SCV is associated with lysosomal proteins such as lamps it is rarely labelled Mannose 6-phosphate receptor or hydrolases which are also normally associated with degradative lysosomes (Garcia-del Portillo and Finlay, 1995). This data suggests that salmonella can inhibit the fusion of degradative lysosomes whilst recruiting other components of the endomembrane network. In this study we have demonstrated that after EspT mediated invasion, EPEC are also contained within a vacuole which we have termed ECV for EPEC containing vacuole. The ECV also matures in a similar pattern to the SCV moving from

an early endosome like structure to an intermediate VATPase rich compartment and a subgroup of ECVs also become enriched in lysosomal glycoproteins.

Although invasive EPEC encoding EspT were found to be vacuolated, we noted that the internalised bacteria were still associated with filamentous actin. As mentioned previously EPEC is generally considered to be an extracellular pathogen which intimately associates with host cells via the interaction between the bacterial outer membrane protein intimin and the T3SS effector protein Tir. Tir is translocated into the plasma membrane and acts as a receptor for intimin. Interaction between intimin and Tir results in a Tir mediated recruitment of the mammalian adaptor protein Nck which subsequently activates N-WASP resulting in actin polymerisation and the formation of pedestal like structures upon which extracellular bacteria rest. Further examination of the actin structures associated with the ECV demonstrated that Tir was present in the vacuolar membrane at sites of actin polymerisation, this suggests that intracellular EPEC can form pedestals in an analogous manner to extracellular bacteria. Transmission electron microscopy images confirmed that EPEC which are contained within a vacuole are capable of forming actin rich pedestals around the circumference of the bacteria. Furthermore, these images indicate that EPEC may form pedestals both during and after the internalisation process. This to the best of our knowledge is the first time an intracellular pathogen has been shown recruit actin to the bacterial surface across a vacuolar membrane. It has yet to be determined if internalised EPEC can utilise their intracellular pedestal to drive movement through the cytoplasm, although the presence of pedestals around the entire bacterial surface would seem to preclude with idea.

After internalisation EPEC strains encoding EspT were found to remain bound within a vacuole for at least 24 hours post infection. Intracellular vacuolated pathogens must overcome a serious

of hurdles in order to successfully survive and replicate within the host cell including membrane and nutrient acquisition, avoidance of the host degradative lysosome fusion and maintenance of the vacuole.

Upon closer examination we found that ECVs which had strong pedestal formation around the circumference of the vacuole were lamp negative whilst those which had irregular or weak actin polymerisation were lamp positive. We also often observed an accmulatuion of unfused lamp1 rich vesicles in close proximity to ECVs which had strong actin staining. These results lead us to hypothesis that the dense actin network found in pedestals may constitute a physical barrier to lysosome fusion. The observation that a *C. rodentim* Δ*tir* mutant, which did not form intracellular pedestals, was attenuated for intracellular survival adds further weight to this theory. Similar physical inhibition of lysosome movement has been described in the cell cortex where the cortical actin meshwork must first be depolymerised to allow vesicle trafficking to the cell periphery (Miyake et al., 2001). Further work is required in order to establish other factors which may contribute to stability and longevity of the ECV.

Maturation of the SCV is a highly dynamic and active process (Steele-Mortimer 2008) and so it is likely that EPEC factors which act downstream of internalisation may play a role in ECV maintenance and evolution. The fact that we observed Tir in the vacuolar membrane, which mediates the formation of intracellular pedestals, suggests that EPEC can traslocate T3SS effectors across the vacuolar membrane in an analogous manner to *Salmonella.* EPEC secretes several factors such as EspF, EspI and EspG which have been demonstrated to affect various aspects of vesicle trafficking (Alto et al., 2007; Kim et al., 2007, Matsuzawa et al., 2004). It would be interesting to investigate further the role of these and other EPEC T3SS effectors on intracellular bacterial survival and replication as well as in the maturation of the ECV.

6.7 The distribution of EspM and EspT proteins

The distribution of EspM proteins and EspT is markedly different, EspM appears to be relatively widespread whereas EspT is found only in a small percentage of strains. This suggests that while EspM proteins are established T3SS effectors, EspT may be an emerging virulence factor of A/E pathogens. However the fact that we found EspT in an outbreak strain first described in 1987 may preclude this idea. Another possibility is that EspT is a remnant of a time when EPEC may have been an intracellular pathogen. The effect of EspM proteins and EspT on the virulence of A/E pathogen strains which harbour these WxxxE effector is not yet clearly defined. However, our results show that *espM* is found predominantly in the major EPEC and EHEC serogroups associated with severe disease outbreaks including: O26, O103, O111, O118, O145 and O157. These results suggest that *espM* is more commonly found in EPEC and EHEC serogroups that are linked to severe human infections. Due to the poor conservation of EspT in screened EPEC and EHEC strains it is difficult to ascertain the role of EspT in A/E pathogen infection at the current time. However, the presence of EspT in the E110019 strain which was linked with a particularly virulent outbreak of EPEC mediated gastroenteritis which uncharacteristically of EPEC infection was capable of person to person spread provides anecdotal evidence for a role of EspT during EPEC infection (Viljanen et al., 1990). This increase in infectivity and severity of infection attributed to this strain may be linked to the invasive qualities provided by EspT mediated actin rearrangements. Further work will be required on E110019 and other EspT positive strains in order to fully establish the role of EspT during EPEC infection.

6.8 Concluding Remarks

In this study we have characterised two novel families of WxxxE effector proteins encoded by the A/E pathogen group. We have demonstrated that both EspM and EspT mediate the reorganisation of the host cell cytoskeleton in a GTPase dependent manner. Furthermore, we have shown that these novel WxxxE effectors activate host cell Rho GTPases in cells. Detailed examination of the mechanism by which EspM2 activates RhoA has demonstrates that EspM2 is able to bind and GEF RhoA. Additionally structural determination of an EspM2-RhoA complex has shown that EspM2 although sharing little homology with SopE (19% protein identity) adopts a similar fold to the *Salmonella* GEF effector. Mutagenesis of the putative catalytic loop of EspM2 which is similarly positioned to that of SopE led to a drastic reduction in the formation of stress fibres by EspM2. Similarly we demonstrate that EspT mediated activation of Rac1 and Cdc42 is independent of ELMO, Dock180, typical mammalian Rac1 GEFs, Pi3K and Src kinases. We also show that EspT mediated formation of membrane ruffles and lamellipodia facilitates the invasion of epithelial cells by EPEC strains which harbour this effector. This is the first time EPEC has been shown to mediate its own internalisation in a T3SS dependent manner. Furthermore, we describe for the first time the polymerisation of actin to a bacterial cell surface across a vacuolar membrane as internalised EPEC bacteria are capable of forming intracellular Tir dependent pedestals after and during EspT mediated uptake. Together these results increase the WxxxE effector protein repertoire of A/E pathogens and demonstrate novel functions of these effectors in EPEC virulence. Structural and functional analysis of EspM2 has also provided novel insights into the mechanism of action of WxxxE effectors. The role of EspT in mediating EPEC invasion of epithelial cells has contributed significantly to breaking the dogma of EPEC as strictly extracellular pathogens. Further *in vivo* studies will be required in order to fully

determine the effects of EspM and EspT proteins in A/E pathogen virulence strategies. It will also prove interesting to investigate the role of these novel effectors in other cell lines such as polarised epithelial cells and macrophages. Finally a more stringent screening and examination of EspM and EspT positive strains is required in order to fully understand their contribution to the clinical outcome of disease caused by the A/E pathogens.

In conclusion we have demonstrated that the novel A/E pathogen WxxxE effectors EspM and EspT are complex modulators of host cell GTPases which contribute to A/E pathogen virulence strategies by mediating a plethora of cellular signalling events particularly those associated with cytoskeletal re-arrangement.

References

Ahuja, R., Pinyol, R., Reichenbach, N., Custer, L., Klingensmith, J., Kessels, M. M., and Qualmann, B. (2007). Cordon-bleu is an actin nucleation factor and controls neuronal morphology. Cell *131*, 337-350.

Aktories, K., Schmidt, G., and Just, I. (2000). Rho GTPases as targets of bacterial protein toxins. Biol Chem *381*, 421-426.

Alto, N. M., Shao, F., Lazar, C. S., Brost, R. L., Chua, G., Mattoo, S., McMahon, S. A., Ghosh, P., Hughes, T. R., Boone, C., and Dixon, J. E. (2006). Identification of a bacterial type III effector family with G protein mimicry functions. Cell *124*, 133-145.

Alto, N. M., Weflen, A. W., Rardin, M. J., Yarar, D., Lazar, C. S., Tonikian, R., Koller, A., Taylor, S. S., Boone, C., Sidhu, S. S., *et al.* (2007). The type III effector EspF coordinates membrane trafficking by the spatiotemporal activation of two eukaryotic signaling pathways. J Cell Biol *178*, 1265-1278.

Altschul, S. F., Madden, T. L., Schaffer, A. A., Zhang, J., Zhang, Z., Miller, W., and Lipman, D. J. (1997). Gapped BLAST and PSI-BLAST: a new generation of protein database search programs. Nucleic Acids Res *25*, 3389-3402.

Amano, M., Ito, M., Kimura, K., Fukata, Y., Chihara, K., Nakano, T., Matsuura, Y., and Kaibuchi, K. (1996). Phosphorylation and activation of myosin by Rho-associated kinase (Rho-kinase). J Biol Chem *271*, 20246-20249.

Araujo, J. M., Tabarelli, G. F., Aranda, K. R., Fabbricotti, S. H., Fagundes-Neto, U., Mendes, C. M., and Scaletsky, I. C. (2007). Typical enteroaggregative and atypical enteropathogenic types of Escherichia coli are the most prevalent diarrhea-associated pathotypes among Brazilian children. J Clin Microbiol *45*, 3396-3399.

Arbeloa, A., Blanco, M., Moreira, F. C., Bulgin, R., Lopez, C., Dahbi, G., Blanco, J. E., Mora, A., Alonso, M. P., Mamani, R. C., *et al.* (2009). Distribution of espM and espT among enteropathogenic and enterohaemorrhagic Escherichia coli. J Med Microbiol *58*, 988-995.

Arbeloa, A., Bulgin, R. R., MacKenzie, G., Shaw, R. K., Pallen, M. J., Crepin, V. F., Berger, C. N., and Frankel, G. (2008). Subversion of actin dynamics by EspM effectors of attaching and effacing bacterial pathogens. Cell Microbiol *10*, 1429-1441.

Arnold, K., Bordoli, L., Kopp, J., and Schwede, T. (2006). The SWISS-MODEL workspace: a web-based environment for protein structure homology modelling. Bioinformatics *22*, 195-201.

Aspenstrom, P. (1999). Effectors for the Rho GTPases. Curr Opin Cell Biol *11*, 95-102.

Aspenstrom, P. (2009). Roles of F-BAR/PCH proteins in the regulation of membrane dynamics and actin reorganization. Int Rev Cell Mol Biol *272*, 1-31.

Babbin, B. A., Sasaki, M., Gerner-Schmidt, K. W., Nusrat, A., and Klapproth, J. M. (2009). The bacterial virulence factor lymphostatin compromises intestinal epithelial barrier function by modulating rho GTPases. Am J Pathol *174*, 1347-1357.

Badea, L., Doughty, S., Nicholls, L., Sloan, J., Robins-Browne, R. M., and Hartland, E. L. (2003). Contribution of Efa1/LifA to the adherence of enteropathogenic Escherichia coli to epithelial cells. Microb Pathog *34*, 205-215.

Barr, F. A., and Gruneberg, U. (2007). Cytokinesis: placing and making the final cut. Cell *131*, 847-860.

Barthold, S. W., Coleman, G. L., Bhatt, P. N., Osbaldiston, G. W., and Jonas, A. M. (1976). The etiology of transmissible murine colonic hyperplasia. Lab Anim Sci *26*, 889-894.

Baum, J., Papenfuss, A. T., Baum, B., Speed, T. P., and Cowman, A. F. (2006). Regulation of apicomplexan actin-based motility. Nat Rev Microbiol *4*, 621-628.
Bear, J. E., Loureiro, J. J., Libova, I., Fassler, R., Wehland, J., and Gertler, F. B. (2000). Negative regulation of fibroblast motility by Ena/VASP proteins. Cell *101*, 717-728.
Bear, J. E., Svitkina, T. M., Krause, M., Schafer, D. A., Loureiro, J. J., Strasser, G. A., Maly, I. V., Chaga, O. Y., Cooper, J. A., Borisy, G. G., and Gertler, F. B. (2002). Antagonism between Ena/VASP proteins and actin filament capping regulates fibroblast motility. Cell *109*, 509-521.
Berger, C. N., Crepin, V. F., Jepson, M. A., Arbeloa, A., and Frankel, G. (2009). The mechanisms used by enteropathogenic Escherichia coli to control filopodia dynamics. Cell Microbiol *11*, 309-322.
Bernard, O. (2007). Lim kinases, regulators of actin dynamics. Int J Biochem Cell Biol *39*, 1071-1076.
Beuzon, C. R., Meresse, S., Unsworth, K. E., Ruiz-Albert, J., Garvis, S., Waterman, S. R., Ryder, T. A., Boucrot, E., and Holden, D. W. (2000). Salmonella maintains the integrity of its intracellular vacuole through the action of SifA. Embo J *19*, 3235-3249.
Billker, O., Popp, A., Brinkmann, V., Wenig, G., Schneider, J., Caron, E., and Meyer, T. F. (2002). Distinct mechanisms of internalization of Neisseria gonorrhoeae by members of the CEACAM receptor family involving Rac1- and Cdc42-dependent and -independent pathways. Embo J *21*, 560-571.
Bishop, A. L., and Hall, A. (2000). Rho GTPases and their effector proteins. Biochem J *348 Pt 2*, 241-255.
Boisen, N., Struve, C., Scheutz, F., Krogfelt, K. A., and Nataro, J. P. (2008). New adhesin of enteroaggregative Escherichia coli related to the Afa/Dr/AAF family. Infect Immun *76*, 3281-3292.
Bokoch, G. M. (2003). Biology of the p21-activated kinases. Annu Rev Biochem *72*, 743-781.
Bosco, E. E., Mulloy, J. C., and Zheng, Y. (2009). Rac1 GTPase: a "Rac" of all trades. Cell Mol Life Sci *66*, 370-374.
Boucrot, E., Beuzon, C. R., Holden, D. W., Gorvel, J. P., and Meresse, S. (2003). Salmonella typhimurium SifA effector protein requires its membrane-anchoring C-terminal hexapeptide for its biological function. J Biol Chem *278*, 14196-14202.
Boucrot, E., Henry, T., Borg, J. P., Gorvel, J. P., and Meresse, S. (2005). The intracellular fate of Salmonella depends on the recruitment of kinesin. Science *308*, 1174-1178.
Brandon, L. D., Goehring, N., Janakiraman, A., Yan, A. W., Wu, T., Beckwith, J., and Goldberg, M. B. (2003). IcsA, a polarly localized autotransporter with an atypical signal peptide, uses the Sec apparatus for secretion, although the Sec apparatus is circumferentially distributed. Mol Microbiol *50*, 45-60.
Brawn, L. C., Hayward, R. D., and Koronakis, V. (2007). Salmonella SPI1 effector SipA persists after entry and cooperates with a SPI2 effector to regulate phagosome maturation and intracellular replication. Cell Host Microbe *1*, 63-75.
Brugnera, E., Haney, L., Grimsley, C., Lu, M., Walk, S. F., Tosello-Trampont, A. C., Macara, I. G., Madhani, H., Fink, G. R., and Ravichandran, K. S. (2002). Unconventional Rac-GEF activity is mediated through the Dock180-ELMO complex. Nat Cell Biol *4*, 574-582.
Brumell, J. H., Rosenberger, C. M., Gotto, G. T., Marcus, S. L., and Finlay, B. B. (2001). SifA permits survival and replication of Salmonella typhimurium in murine macrophages. Cell Microbiol *3*, 75-84.

Brundage, L., Hendrick, J. P., Schiebel, E., Driessen, A. J., and Wickner, W. (1990). The purified E. coli integral membrane protein SecY/E is sufficient for reconstitution of SecA-dependent precursor protein translocation. Cell *62*, 649-657.
Buccione, R., Orth, J. D., and McNiven, M. A. (2004). Foot and mouth: podosomes, invadopodia and circular dorsal ruffles. Nat Rev Mol Cell Biol *5*, 647-657.
Buchrieser, C., Glaser, P., Rusniok, C., Nedjari, H., D'Hauteville, H., Kunst, F., Sansonetti, P., and Parsot, C. (2000). The virulence plasmid pWR100 and the repertoire of proteins secreted by the type III secretion apparatus of Shigella flexneri. Mol Microbiol *38*, 760-771.
Buchwald, G., Friebel, A., Galan, J. E., Hardt, W. D., Wittinghofer, A., and Scheffzek, K. (2002). Structural basis for the reversible activation of a Rho protein by the bacterial toxin SopE. Embo J *21*, 3286-3295.
Buday, L., Wunderlich, L., and Tamas, P. (2002). The Nck family of adapter proteins: regulators of actin cytoskeleton. Cell Signal *14*, 723-731.
Bulgin, R. R., Arbeloa, A., Chung, J. C., and Frankel, G. (2009). EspT triggers formation of lamellipodia and membrane ruffles through activation of Rac1 and Cdc42. Cell Microbiol *11*, 217-229.
Cain, R. J., and Ridley, A. J. (2009). Phosphoinositide 3-kinases in cell migration. Biol Cell *101*, 13-29.
Campellone, K. G., Giese, A., Tipper, D. J., and Leong, J. M. (2002). A tyrosine-phosphorylated 12-amino-acid sequence of enteropathogenic Escherichia coli Tir binds the host adaptor protein Nck and is required for Nck localization to actin pedestals. Mol Microbiol *43*, 1227-1241.
Campellone, K. G., Robbins, D., and Leong, J. M. (2004). EspFU is a translocated EHEC effector that interacts with Tir and N-WASP and promotes Nck-independent actin assembly. Dev Cell *7*, 217-228.
Carlier, M. F., Ducruix, A., and Pantaloni, D. (1999a). Signalling to actin: the Cdc42-N-WASP-Arp2/3 connection. Chem Biol *6*, R235-240.
Carlier, M. F., Ressad, F., and Pantaloni, D. (1999b). Control of actin dynamics in cell motility. Role of ADF/cofilin. J Biol Chem *274*, 33827-33830.
Carreno, S., Caron, E., Cougoule, C., Emorine, L. J., and Maridonneau-Parini, I. (2002). p59Hck isoform induces F-actin reorganization to form protrusions of the plasma membrane in a Cdc42- and Rac-dependent manner. J Biol Chem *277*, 21007-21016.
Celli, J., Deng, W., and Finlay, B. B. (2000). Enteropathogenic Escherichia coli (EPEC) attachment to epithelial cells: exploiting the host cell cytoskeleton from the outside. Cell Microbiol *2*, 1-9.
Charpentier, X and Oswald, E. (2004). Identification of the secretion and translocation domain of the enteropathogenic and enterohemorrhagic Escherichia coli effector Cif, using TEM-1 beta-lactamase as a new fluorescence-based reporter. J Bacteriol 86(16) 5486-95
Cheng, H. C., Skehan, B. M., Campellone, K. G., Leong, J. M., and Rosen, M. K. (2008). Structural mechanism of WASP activation by the enterohaemorrhagic E. coli effector EspF(U). Nature *454*, 1009-1013.
Chereau, D., Boczkowska, M., Skwarek-Maruszewska, A., Fujiwara, I., Hayes, D. B., Rebowski, G., Lappalainen, P., Pollard, T. D., and Dominguez, R. (2008). Leiomodin is an actin filament nucleator in muscle cells. Science *320*, 239-243.
Chesarone, M. A., and Goode, B. L. (2009). Actin nucleation and elongation factors: mechanisms and interplay. Curr Opin Cell Biol *21*, 28-37.

Chhabra, E. S., and Higgs, H. N. (2007). The many faces of actin: matching assembly factors with cellular structures. Nat Cell Biol *9*, 1110-1121.
Christie, P. J., Atmakuri, K., Krishnamoorthy, V., Jakubowski, S., and Cascales, E. (2005). Biogenesis, architecture, and function of bacterial type IV secretion systems. Annu Rev Microbiol *59*, 451-485.
Collington, G. K., Booth, I. W., Donnenberg, M. S., Kaper, J. B., and Knutton, S. (1998). Enteropathogenic Escherichia coli virulence genes encoding secreted signalling proteins are essential for modulation of Caco-2 cell electrolyte transport. Infect Immun *66*, 6049-6053.
Cooper, J. A., and Schafer, D. A. (2000). Control of actin assembly and disassembly at filament ends. Curr Opin Cell Biol *12*, 97-103.
Cordes, F. S., Komoriya, K., Larquet, E., Yang, S., Egelman, E. H., Blocker, A., and Lea, S. M. (2003). Helical structure of the needle of the type III secretion system of Shigella flexneri. J Biol Chem *278*, 17103-17107.
Cornelis, G. R. (2006). The type III secretion injectisome. Nat Rev Microbiol *4*, 811-825.
Cossart, P. (1995). Actin-based bacterial motility. Curr Opin Cell Biol *7*, 94-101.
Cossart, P., and Sansonetti, P. J. (2004). Bacterial invasion: the paradigms of enteroinvasive pathogens. Science *304*, 242-248.
Cote, J. F., and Vuori, K. (2007). GEF what? Dock180 and related proteins help Rac to polarize cells in new ways. Trends Cell Biol *17*, 383-393.
Cotton, M., and Claing, A. (2009). G protein-coupled receptors stimulation and the control of cell migration. Cell Signal *21*, 1045-1053.
Crago, A. M., and Koronakis, V. (1998). Salmonella InvG forms a ring-like multimer that requires the InvH lipoprotein for outer membrane localization. Mol Microbiol *30*, 47-56.
Creasey, E. A., Delahay, R. M., Bishop, A. A., Shaw, R. K., Kenny, B., Knutton, S., and Frankel, G. (2003a). CesT is a bivalent enteropathogenic Escherichia coli chaperone required for translocation of both Tir and Map. Mol Microbiol *47*, 209-221.
Creasey, E. A., Friedberg, D., Shaw, R. K., Umanski, T., Knutton, S., Rosenshine, I., and Frankel, G. (2003b). CesAB is an enteropathogenic Escherichia coli chaperone for the type-III translocator proteins EspA and EspB. Microbiology *149*, 3639-3647.
Crowther, L. J., Whale, A., Carlier, M.F., Plomann, M., Garmendia, J. and Frankel, G. (2007). PACSIN 3 links the enterohemorrhagic E. coli O157:H7 effector proteins Tir and TccP to the actin polymerisation cascade. Under review.
Dan, C., Kelly, A., Bernard, O., and Minden, A. (2001). Cytoskeletal changes regulated by the PAK4 serine/threonine kinase are mediated by LIM kinase 1 and cofilin. J Biol Chem *276*, 32115-32121.
Daniell, S. J., Takahashi, N., Wilson, R., Friedberg, D., Rosenshine, I., Booy, F. P., Shaw, R. K., Knutton, S., Frankel, G., and Aizawa, S. (2001). The filamentous type III secretion translocon of enteropathogenic Escherichia coli. Cell Microbiol *3*, 865-871.
Das, S., and Chaudhuri, K. (2003). Identification of a unique IAHP (IcmF associated homologous proteins) cluster in Vibrio cholerae and other proteobacteria through in silico analysis. In Silico Biol *3*, 287-300.
Datsenko, K. A., and Wanner, B. L. (2000). One-step inactivation of chromosomal genes in Escherichia coli K-12 using PCR products. Proc Natl Acad Sci U S A *97*, 6640-6645.
Dautin, N., and Bernstein, H. D. (2007). Protein secretion in gram-negative bacteria via the autotransporter pathway. Annu Rev Microbiol *61*, 89-112.

De Brabander, M. J., Van de Veire, R. M., Aerts, F. E., Borgers, M., and Janssen, P. A. (1976). The effects of methyl (5-(2-thienylcarbonyl)-1H-benzimidazol-2-yl) carbamate, (R 17934; NSC 238159), a new synthetic antitumoral drug interfering with microtubules, on mammalian cells cultured in vitro. Cancer Res *36*, 905-916.
Dean, P., and Kenny, B. (2004). Intestinal barrier dysfunction by enteropathogenic Escherichia coli is mediated by two effector molecules and a bacterial surface protein. Mol Microbiol *54*, 665-675.
Derewenda, U., Oleksy, A., Stevenson, A. S., Korczynska, J., Dauter, Z., Somlyo, A. P., Otlewski, J., Somlyo, A. V., and Derewenda, Z. S. (2004). The crystal structure of RhoA in complex with the DH/PH fragment of PDZRhoGEF, an activator of the Ca(2+) sensitization pathway in smooth muscle. Structure *12*, 1955-1965.
DerMardirossian, C., and Bokoch, G. M. (2005). GDIs: central regulatory molecules in Rho GTPase activation. Trends Cell Biol *15*, 356-363.
Desai, A., and Mitchison, T. J. (1997). Microtubule polymerization dynamics. Annu Rev Cell Dev Biol *13*, 83-117.
Didsbury, J., Weber, R. F., Bokoch, G. M., Evans, T., and Snyderman, R. (1989). rac, a novel ras-related family of proteins that are botulinum toxin substrates. J Biol Chem *264*, 16378-16382.
Donnenberg, M. S., Donohue-Rolfe, A., and Keusch, G. T. (1989). Epithelial cell invasion: an overlooked property of enteropathogenic Escherichia coli (EPEC) associated with the EPEC adherence factor. J Infect Dis *160*, 452-459.
Donnenberg, M. S., and Kaper, J. B. (1992). Enteropathogenic Escherichia coli. Infect Immun *60*, 3953-3961.
Driessen, A. J., and Nouwen, N. (2008). Protein translocation across the bacterial cytoplasmic membrane. Annu Rev Biochem *77*, 643-667.
Drucker, M. M., Polliack, A., Yeivin, R., and Sacks, T. G. (1970). Immunofluorescent demonstration of enteropathogenic Escherichia coli in tissues of infants dying with enteritis. Pediatrics *46*, 855-864.
Economou, A. (1998). Bacterial preprotein translocase: mechanism and conformational dynamics of a processive enzyme. Mol Microbiol *27*, 511-518.
Economou, A., and Wickner, W. (1994). SecA promotes preprotein translocation by undergoing ATP-driven cycles of membrane insertion and deinsertion. Cell *78*, 835-843.
Edwards, D. C., Sanders, L. C., Bokoch, G. M., and Gill, G. N. (1999). Activation of LIM-kinase by Pak1 couples Rac/Cdc42 GTPase signalling to actin cytoskeletal dynamics. Nat Cell Biol *1*, 253-259.
Eklund, M., Leino, K., Siitonen, A. (2006). Clinical *Escherichia coli* Strains Carrying *stx* Genes: *stx* Variants and *stx*-Positive Virulence Profiles. J Clin Microbiol.
Elliott, S. J., Wainwright, L. A., McDaniel, T. K., Jarvis, K. G., Deng, Y. K., Lai, L. C., McNamara, B. P., Donnenberg, M. S., and Kaper, J. B. (1998). The complete sequence of the locus of enterocyte effacement (LEE) from enteropathogenic Escherichia coli E2348/69. Mol Microbiol *28*, 1-4.
Etienne-Manneville, S., and Hall, A. (2002). Rho GTPases in cell biology. Nature *420*, 629-635.
Evdokimov, A. G., Tropea, J. E., Routzahn, K. M., and Waugh, D. S. (2002). Crystal structure of the Yersinia pestis GTPase activator YopE. Protein Sci *11*, 401-408.
Faix, J., and Rottner, K. (2006). The making of filopodia. Curr Opin Cell Biol *18*, 18-25.

Farfan, M. J., Inman, K. G., and Nataro, J. P. (2008). The major pilin subunit of the AAF/II fimbriae from enteroaggregative Escherichia coli mediates binding to extracellular matrix proteins. Infect Immun *76*, 4378-4384.
Fidyk, N. J., and Cerione, R. A. (2002). Understanding the catalytic mechanism of GTPase-activating proteins: demonstration of the importance of switch domain stabilization in the stimulation of GTP hydrolysis. Biochemistry *41*, 15644-15653.
Finlay, B. B. (2005). Bacterial virulence strategies that utilize Rho GTPases. Curr Top Microbiol Immunol *291*, 1-10.
Flatau, G., Lemichez, E., Gauthier, M., Chardin, P., Paris, S., Fiorentini, C., and Boquet, P. (1997). Toxin-induced activation of the G protein p21 Rho by deamidation of glutamine. Nature *387*, 729-733.
Flores, J., and Okhuysen, P. C. (2009). Enteroaggregative Escherichia coli infection. Curr Opin Gastroenterol *25*, 8-11.
Frame, M. C. (2004). Newest findings on the oldest oncogene; how activated src does it. J Cell Sci *117*, 989-998.
Frankel, G., and Phillips, A. D. (2008). Attaching effacing Escherichia coli and paradigms of Tir-triggered actin polymerization: getting off the pedestal. Cell Microbiol *10*, 549-556.
Frankel, G., Phillips, A. D., Rosenshine, I., Dougan, G., Kaper, J. B., and Knutton, S. (1998). Enteropathogenic and enterohaemorrhagic Escherichia coli: more subversive elements. Mol Microbiol *30*, 911-921.
Frankel, G., Phillips, A. D., Trabulsi, L. R., Knutton, S., Dougan, G., and Matthews, S. (2001). Intimin and the host cell--is it bound to end in Tir(s)? Trends Microbiol *9*, 214-218.
Franklin-Tong, V. E., and Gourlay, C. W. (2008). A role for actin in regulating apoptosis/programmed cell death: evidence spanning yeast, plants and animals. Biochem J *413*, 389-404.
Freeman, J. A., Ohl, M. E., and Miller, S. I. (2003). The Salmonella enterica serovar typhimurium translocated effectors SseJ and SifB are targeted to the Salmonella-containing vacuole. Infect Immun *71*, 418-427.
Frischknecht, F., Moreau, V., Rottger, S., Gonfloni, S., Reckmann, I., Superti-Furga, G., and Way, M. (1999). Actin-based motility of vaccinia virus mimics receptor tyrosine kinase signalling. Nature *401*, 926-929.
Fronzes, R., Schafer, E., Wang, L., Saibil, H. R., Orlova, E. V., and Waksman, G. (2009). Structure of a type IV secretion system core complex. Science *323*, 266-268.
Fu, Y., and Galan, J. E. (1999). A salmonella protein antagonizes Rac1 and Cdc42 to mediate host-cell recovery after bacterial invasion. Nature *401*, 293-297.
Fukata, M., Nakagawa, M., and Kaibuchi, K. (2003). Roles of Rho-family GTPases in cell polarisation and directional migration. Curr Opin Cell Biol *15*, 590-597.
Fukazawa, A., Alonso, C., Kurachi, K., Gupta, S., Lesser, C. F., McCormick, B. A., and Reinecker, H. C. (2008). GEF-H1 mediated control of NOD1 dependent NF-kappaB activation by Shigella effectors. PLoS Pathog *4*, e1000228.
Galan, J. E. (2001). Salmonella interactions with host cells: type III secretion at work. Annu Rev Cell Dev Biol *17*, 53-86.
Galan, J. E., and Wolf-Watz, H. (2006). Protein delivery into eukaryotic cells by type III secretion machines. Nature *444*, 567-573.

Gao, Y., Dickerson, J. B., Guo, F., Zheng, J., and Zheng, Y. (2004). Rational design and characterization of a Rac GTPase-specific small molecule inhibitor. Proc Natl Acad Sci U S A *101*, 7618-7623.
Gao, Y., Xing, J., Streuli, M., Leto, T. L., and Zheng, Y. (2001). Trp(56) of rac1 specifies interaction with a subset of guanine nucleotide exchange factors. J Biol Chem *276*, 47530-47541.
Garcia-del Portillo, F., and Finlay, B. B. (1995). Targeting of Salmonella typhimurium to vesicles containing lysosomal membrane glycoproteins bypasses compartments with mannose 6-phosphate receptors. J Cell Biol *129*, 81-97.
Garcia-Mata, R., and Burridge, K. (2007). Catching a GEF by its tail. Trends Cell Biol *17*, 36-43.
Garmendia, J., Frankel, G., and Crepin, V. F. (2005). Enteropathogenic and enterohemorrhagic Escherichia coli infections: translocation, translocation, translocation. Infect Immun *73*, 2573-2585.
Garmendia, J., Phillips, A. D., Carlier, M. F., Chong, Y., Schuller, S., Marches, O., Dahan, S., Oswald, E., Shaw, R. K., Knutton, S., and Frankel, G. (2004). TccP is an enterohaemorrhagic Escherichia coli O157:H7 type III effector protein that couples Tir to the actin-cytoskeleton. Cell Microbiol *6*, 1167-1183.
Gauthier, A., Puente, J. L., and Finlay, B. B. (2003). Secretin of the enteropathogenic Escherichia coli type III secretion system requires components of the type III apparatus for assembly and localization. Infect Immun *71*, 3310-3319.
Gerlach, R. G., and Hensel, M. (2007). Protein secretion systems and adhesins: the molecular armory of Gram-negative pathogens. Int J Med Microbiol *297*, 401-415.
Girao, H., Geli, M. I., and Idrissi, F. Z. (2008). Actin in the endocytic pathway: from yeast to mammals. FEBS Lett *582*, 2112-2119.
Giron, J. A., Ho, A. S., and Schoolnik, G. K. (1991). An inducible bundle-forming pilus of enteropathogenic Escherichia coli. Science *254*, 710-713.
Giubellino, A., Burke, T. R., Jr., and Bottaro, D. P. (2008). Grb2 signaling in cell motility and cancer. Expert Opin Ther Targets *12*, 1021-1033.
Goldman, R. D., Grin, B., Mendez, M. G., and Kuczmarski, E. R. (2008). Intermediate filaments: versatile building blocks of cell structure. Curr Opin Cell Biol *20*, 28-34.
Goley, E. D., and Welch, M. D. (2006). The ARP2/3 complex: an actin nucleator comes of age. Nat Rev Mol Cell Biol *7*, 713-726.
Gomez-Duarte, O. G., and Kaper, J. B. (1995). A plasmid-encoded regulatory region activates chromosomal eaeA expression in enteropathogenic Escherichia coli. Infect Immun *63*, 1767-1776.
Goode, B. L., and Eck, M. J. (2007). Mechanism and function of formins in the control of actin assembly. Annu Rev Biochem *76*, 593-627.
Gruenheid, S., DeVinney, R., Bladt, F., Goosney, D., Gelkop, S., Gish, G. D., Pawson, T., and Finlay, B. B. (2001). Enteropathogenic E. coli Tir binds Nck to initiate actin pedestal formation in host cells. Nat Cell Biol *3*, 856-859.
Guiney, D. G., and Lesnick, M. (2005). Targeting of the actin cytoskeleton during infection by Salmonella strains. Clin Immunol *114*, 248-255.
Hachani, A., Biskri, L., Rossi, G., Marty, A., Menard, R., Sansonetti, P., Parsot, C., Van Nhieu, G. T., Bernardini, M. L., and Allaoui, A. (2008). IpgB1 and IpgB2, two homologous effectors secreted via the Mxi-Spa type III secretion apparatus, cooperate to mediate polarized cell invasion and inflammatory potential of Shigella flexenri. Microbes Infect *10*, 260-268.

Hall, A. (2005). Rho GTPases and the control of cell behaviour. Biochem Soc Trans *33*, 891-895.
Handa, Y., Suzuki, M., Ohya, K., Iwai, H., Ishijima, N., Koleske, A. J., Fukui, Y., and Sasakawa, C. (2007). Shigella IpgB1 promotes bacterial entry through the ELMO-Dock180 machinery. Nat Cell Biol *9*, 121-128.
Hansen-Wester, I., Stecher, B., and Hensel, M. (2002). Type III secretion of Salmonella enterica serovar Typhimurium translocated effectors and SseFG. Infect Immun *70*, 1403-1409.
Hardt, W. D., Chen, L. M., Schuebel, K. E., Bustelo, X. R., and Galan, J. E. (1998). S. typhimurium encodes an activator of Rho GTPases that induces membrane ruffling and nuclear responses in host cells. Cell *93*, 815-826.
Harris, R. L., Hombs, V., and Silverman, P. M. (2001). Evidence that F-plasmid proteins TraV, TraK and TraB assemble into an envelope-spanning structure in Escherichia coli. Mol Microbiol *42*, 757-766.
Hayashi, T., Makino, K., Ohnishi, M., Kurokawa, K., Ishii, K., Yokoyama, K., Han, C. G., Ohtsubo, E., Nakayama, K., Murata, T., *et al.* (2001). Complete genome sequence of enterohemorrhagic Escherichia coli O157:H7 and genomic comparison with a laboratory strain K-12. DNA Res *8*, 11-22.
Hemrajani, C., Marches, O., Wiles, S., Girard, F., Dennis, A., Dziva, F., Best, A., Phillips, A. D., Berger, C. N., Mousnier, A., *et al.* (2008). Role of NleH, a Type III Secreted Effector from Attaching and Effacing Pathogens, in Colonization of the Bovine, Ovine, and Murine Gut. Infect Immun *76*, 4804-4813.
Hernandes, R. T., Silva, R. M., Carneiro, S. M., Salvador, F. A., Fernandes, M. C., Padovan, A. C., Yamamoto, D., Mortara, R. A., Elias, W. P., da Silva Briones, M. R., and Gomes, T. A. (2008). The localized adherence pattern of an atypical enteropathogenic Escherichia coli is mediated by intimin omicron and unexpectedly promotes HeLa cell invasion. Cell Microbiol *10*, 415-425.
Herold, S., Karch, H., Schmidt, H. Shiga toxin-encoding bacteriophages--genomes in motion.J Med Int Microbiol 2004 Sep;294(2-3):115-21.
Herrmann, C., Ahmadian, M. R., Hofmann, F., and Just, I. (1998). Functional consequences of monoglucosylation of Ha-Ras at effector domain amino acid threonine 35. J Biol Chem *273*, 16134-16139.
Heuer, D., Lipinski, A. R., Machuy, N., Karlas, A., Wehrens, A., Siedler, F., Brinkmann, V., and Meyer, T. F. (2009). Chlamydia causes fragmentation of the Golgi compartment to ensure reproduction. Nature *457*, 731-735.
Huang, D. B., Brown, E. L., DuPont, H. L., Cerf, J., Carlin, L., Flores, J., Belkind-Gerson, J., Nataro, J. P., and Okhuysen, P. C. (2008). Seroprevalence of the enteroaggregative Escherichia coli virulence factor dispersin among USA travellers to Cuernavaca, Mexico: a pilot study. J Med Microbiol *57*, 476-479.
Huang, Z., Sutton, S. E., Wallenfang, A. J., Orchard, R. C., Wu, X., Feng, Y., Chai, J., and Alto, N. M. (2009). Structural insights into host GTPase isoform selection by a family of bacterial GEF mimics. Nat Struct Mol Biol.
Hueck, C. J., Hantman, M. J., Bajaj, V., Johnston, C., Lee, C. A., and Miller, S. I. (1995). Salmonella typhimurium secreted invasion determinants are homologous to Shigella Ipa proteins. Mol Microbiol *18*, 479-490.

Hussain, N. K., Jenna, S., Glogauer, M., Quinn, C. C., Wasiak, S., Guipponi, M., Antonarakis, S. E., Kay, B. K., Stossel, T. P., Lamarche-Vane, N., and McPherson, P. S. (2001). Endocytic protein intersectin-l regulates actin assembly via Cdc42 and N-WASP. Nat Cell Biol *3*, 927-932.
Iguchi, A., Thomson, N. R., Ogura, Y., Saunders, D., Ooka, T., Henderson, I. R., Harris, D., Asadulghani, M., Kurokawa, K., Dean, P.*, et al.* (2009). Complete genome sequence and comparative genome analysis of enteropathogenic Escherichia coli O127:H6 strain E2348/69. J Bacteriol *191*, 347-354.
Imamura, H., Takaishi, K., Nakano, K., Kodama, A., Oishi, H., Shiozaki, H., Monden, M., Sasaki, T., and Takai, Y. (1998). Rho and Rab small G proteins coordinately reorganize stress fibers and focal adhesions in MDCK cells. Molecular Biology of the Cell *9*, 2561-2575.
Innocenti, M., Zucconi, A., Disanza, A., Frittoli, E., Areces, L. B., Steffen, A., Stradal, T. E., Di Fiore, P. P., Carlier, M. F., and Scita, G. (2004). Abi1 is essential for the formation and activation of a WAVE2 signalling complex. Nat Cell Biol *6*, 319-327.
Ionin, B., Hammamieh, R., Shupp, J. W., Das, R., Pontzer, C. H., and Jett, M. (2008). Staphylococcal enterotoxin B causes differential expression of Rnd3 and RhoA in renal proximal tubule epithelial cells while inducing actin stress fiber assembly and apoptosis. Microb Pathog *45*, 303-309.
Jackson, L. K., Nawabi, P., Hentea, C., Roark, E. A., and Haldar, K. (2008). The Salmonella virulence protein SifA is a G protein antagonist. Proc Natl Acad Sci U S A *105*, 14141-14146.
Jaffe, A. B., and Hall, A. (2002). Rho GTPases in transformation and metastasis. Adv Cancer Res *84*, 57-80.
Jaffe, A. B., and Hall, A. (2005). Rho GTPases: biochemistry and biology. Annu Rev Cell Dev Biol *21*, 247-269.
Jank, T., Giesemann, T., and Aktories, K. (2007). Rho-glucosylating Clostridium difficile toxins A and B: new insights into structure and function. Glycobiology *17*, 15R-22R.
Jerse, A. E., Yu, J., Tall, B. D., and Kaper, J. B. (1990). A genetic locus of enteropathogenic Escherichia coli necessary for the production of attaching and effacing lesions on tissue culture cells. Proc Natl Acad Sci U S A *87*, 7839-7843.
Jonckheere, V., Lambrechts, A., Vandekerckhove, J., and Ampe, C. (1999). Dimerization of profilin II upon binding the (GP5)3 peptide from VASP overcomes the inhibition of actin nucleation by profilin II and thymosin beta4. FEBS Lett *447*, 257-263.
Jones, D. T. (1999). Protein secondary structure prediction based on position-specific scoring matrices. J Mol Biol *292*, 195-202.
Just, I., Selzer, J., Wilm, M., von Eichel-Streiber, C., Mann, M., and Aktories, K. (1995a). Glucosylation of Rho proteins by Clostridium difficile toxin B. Nature *375*, 500-503.
Just, I., Wilm, M., Selzer, J., Rex, G., von Eichel-Streiber, C., Mann, M., and Aktories, K. (1995b). The enterotoxin from Clostridium difficile (ToxA) monoglucosylates the Rho proteins. J Biol Chem *270*, 13932-13936.
Kakudo, S., Kikuchi, N., Kitadokoro, K., Fujiwara, T., Nakamura, E., Okamoto, H., Shin, M., Tamaki, M., Teraoka, H., Tsuzuki, H., and et al. (1992). Purification, characterization, cloning, and expression of a glutamic acid-specific protease from Bacillus licheniformis ATCC 14580. J Biol Chem *267*, 23782-23788.
Kaper, J. B., Nataro, J. P., and Mobley, H. L. (2004). Pathogenic Escherichia coli. Nat Rev Microbiol *2*, 123-140.

Kawakatsu, T., Ogita, H., Fukuhara, T., Fukuyama, T., Minami, Y., Shimizu, K., and Takai, Y. (2005). Vav2 as a Rac-GDP/GTP exchange factor responsible for the nectin-induced, c-Src- and Cdc42-mediated activation of Rac. J Biol Chem *280*, 4940-4947.
Kawano, Y., Fukata, Y., Oshiro, N., Amano, M., Nakamura, T., Ito, M., Matsumura, F., Inagaki, M., and Kaibuchi, K. (1999). Phosphorylation of myosin-binding subunit (MBS) of myosin phosphatase by Rho-kinase in vivo. J Cell Biol *147*, 1023-1038.
Kenny, B. (1999). Phosphorylation of tyrosine 474 of the enteropathogenic Escherichia coli (EPEC) Tir receptor molecule is essential for actin nucleating activity and is preceded by additional host modifications. Mol Microbiol *31*, 1229-1241.
Kenny, B., DeVinney, R., Stein, M., Reinscheid, D. J., Frey, E. A., and Finlay, B. B. (1997). k. Cell *91*, 511-520.
Kenny, B., Ellis, S., Leard, A. D., Warawa, J., Mellor, H., and Jepson, M. A. (2002). Co-ordinate regulation of distinct host cell signalling pathways by multifunctional enteropathogenic Escherichia coli effector molecules. Mol Microbiol *44*, 1095-1107.
Kenny, B., and Jepson, M. (2000). Targeting of an enteropathogenic Escherichia coli (EPEC) effector protein to host mitochondria. Cell Microbiol *2*, 579-590.
Kim, J., Thanabalasuriar, A., Chaworth-Musters, T., Fromme, J. C., Frey, E. A., Lario, P. I., Metalnikov, P., Rizg, K., Thomas, N. A., Lee, S. F., *et al.* (2007). The bacterial virulence factor NleA inhibits cellular protein secretion by disrupting mammalian COPII function. Cell Host Microbe *2*, 160-171.
Kim, M., Ogawa, M., Fujita, Y., Yoshikawa, Y., Nagai, T., Koyama, T., Nagai, S., Lange, A., Fassler, R., and Sasakawa, C. (2009). Bacteria hijack integrin-linked kinase to stabilize focal adhesions and block cell detachment. Nature.
Kim, O., Yang, J., and Qiu, Y. (2002). Selective activation of small GTPase RhoA by tyrosine kinase Etk through its pleckstrin homology domain. J Biol Chem *277*, 30066-30071.
Knutton, S., Lloyd, D. R., and McNeish, A. S. (1987). Adhesion of enteropathogenic Escherichia coli to human intestinal enterocytes and cultured human intestinal mucosa. Infect Immun *55*, 69-77.
Knutton, S., Phillips, A. D., Smith, H. R., Gross, R. J., Shaw, R., Watson, P., and Price, E. (1991). Screening for enteropathogenic Escherichia coli in infants with diarrhea by the fluorescent-actin staining test. Infect Immun *59*, 365-371.
Kotloff, K. L., Winickoff, J. P., Ivanoff, B., Clemens, J. D., Swerdlow, D. L., Sansonetti, P. J., Adak, G. K., and Levine, M. M. (1999). Global burden of Shigella infections: implications for vaccine development and implementation of control strategies. Bull World Health Organ *77*, 651-666.
Krall, L., Wiedemann, U., Unsin, G., Weiss, S., Domke, N., and Baron, C. (2002). Detergent extraction identifies different VirB protein subassemblies of the type IV secretion machinery in the membranes of Agrobacterium tumefaciens. Proc Natl Acad Sci U S A *99*, 11405-11410.
Krause, M., Dent, E. W., Bear, J. E., Loureiro, J. J., and Gertler, F. B. (2003). Ena/VASP proteins: regulators of the actin cytoskeleton and cell migration. Annu Rev Cell Dev Biol *19*, 541-564.
Kumar, Y., and Valdivia, R. H. (2009). Leading a sheltered life: intracellular pathogens and maintenance of vacuolar compartments. Cell Host Microbe *5*, 593-601.
Kurokawa, K., Itoh, R. E., Yoshizaki, H., Nakamura, Y. O., and Matsuda, M. (2004). Coactivation of Rac1 and Cdc42 at lamellipodia and membrane ruffles induced by epidermal growth factor. Mol Biol Cell *15*, 1003-1010.

Ladwein, M., and Rottner, K. (2008). On the Rho'd: the regulation of membrane protrusions by Rho-GTPases. FEBS Lett *582*, 2066-2074.
Lai, F. P., Szczodrak, M., Block, J., Faix, J., Breitsprecher, D., Mannherz, H. G., Stradal, T. E., Dunn, G. A., Small, J. V., and Rottner, K. (2008). Arp2/3 complex interactions and actin network turnover in lamellipodia. Embo J *27*, 982-992.
Lanzetti, L. (2007). Actin in membrane trafficking. Curr Opin Cell Biol *19*, 453-458.
Le Bouguenec, C., and Servin, A. L. (2006). Diffusely adherent Escherichia coli strains expressing Afa/Dr adhesins (Afa/Dr DAEC): hitherto unrecognized pathogens. FEMS Microbiol Lett *256*, 185-194.
Legg, J. A., Bompard, G., Dawson, J., Morris, H. L., Andrew, N., Cooper, L., Johnston, S. A., Tramountanis, G., and Machesky, L. M. (2007). N-WASP involvement in dorsal ruffle formation in mouse embryonic fibroblasts. Mol Biol Cell *18*, 678-687.
Leiman, P. G., Basler, M., Ramagopal, U. A., Bonanno, J. B., Sauder, J. M., Pukatzki, S., Burley, S. K., Almo, S. C., and Mekalanos, J. J. (2009). Type VI secretion apparatus and phage tail-associated protein complexes share a common evolutionary origin. Proc Natl Acad Sci U S A *106*, 4154-4159.
Leonard, D. A., Lin, R., Cerione, R. A., and Manor, D. (1998). Biochemical studies of the mechanism of action of the Cdc42-GTPase-activating protein. J Biol Chem *273*, 16210-16215.
Levine, M. M., Bergquist, E. J., Nalin, D. R., Waterman, D. H., Hornick, R. B., Young, C. R., and Sotman, S. (1978). Escherichia coli strains that cause diarrhoea but do not produce heat-labile or heat-stable enterotoxins and are non-invasive. Lancet *1*, 1119-1122.
Li, J., Wolf, S. G., Elbaum, M., and Tzfira, T. (2005). Exploring cargo transport mechanics in the type IV secretion systems. Trends Microbiol *13*, 295-298.
Li, X., and Lim, B. (2003). RhoGTPases and their role in cancer. Oncol Res *13*, 323-331.
Liverman, A. D., Cheng, H. C., Trosky, J. E., Leung, D. W., Yarbrough, M. L., Burdette, D. L., Rosen, M. K., and Orth, K. (2007). Arp2/3-independent assembly of actin by Vibrio type III effector VopL. Proc Natl Acad Sci U S A *104*, 17117-17122.
Lommel, S., Benesch, S., Rottner, K., Franz, T., Wehland, J., and Kuhn, R. (2001). Actin pedestal formation by enteropathogenic Escherichia coli and intracellular motility of Shigella flexneri are abolished in N-WASP-defective cells. EMBO Rep *2*, 850-857.
Lu, M., Kinchen, J. M., Rossman, K. L., Grimsley, C., deBakker, C., Brugnera, E., Tosello-Trampont, A. C., Haney, L. B., Klingele, D., Sondek, J.*, et al.* (2004). PH domain of ELMO functions in trans to regulate Rac activation via Dock180. Nat Struct Mol Biol *11*, 756-762.
Machner, M. P., and Isberg, R. R. (2007). A bifunctional bacterial protein links GDI displacement to Rab1 activation. Science *318*, 974-977.
Machuy, N., Campa, F., Thieck, O., and Rudel, T. (2007). c-Abl-binding protein interacts with p21-activated kinase 2 (PAK-2) to regulate PDGF-induced membrane ruffles. J Mol Biol *370*, 620-632.
Maciver, S. K. (1998). How ADF/cofilin depolymerizes actin filaments. Curr Opin Cell Biol *10*, 140-144.
Mackey, A. J., Haystead, T. A., and Pearson, W. R. (2002). Getting more from less: algorithms for rapid protein identification with multiple short peptide sequences. Mol Cell Proteomics *1*, 139-147.
Maekawa, M., Ishizaki, T., Boku, S., Watanabe, N., Fujita, A., Iwamatsu, A., Obinata, T., Ohashi, K., Mizuno, K., and Narumiya, S. (1999). Signaling from Rho to the actin cytoskeleton through protein kinases ROCK and LIM-kinase. Science *285*, 895-898.

Marches, O., Covarelli, V., Dahan, S., Cougoule, C., Bhatta, P., Frankel, G., and Caron, E. (2008). EspJ of enteropathogenic and enterohaemorrhagic Escherichia coli inhibits opsono-phagocytosis. Cell Microbiol *10*, 1104-1115.
Marches, O., Wiles, S., Dziva, F., La Ragione, R. M., Schuller, S., Best, A., Phillips, A. D., Hartland, E. L., Woodward, M. J., Stevens, M. P., and Frankel, G. (2005). Characterization of two non-locus of enterocyte effacement-encoded type III-translocated effectors, NleC and NleD, in attaching and effacing pathogens. Infect Immun *73*, 8411-8417.
Matsuzawa, T., Kuwae, A., Yoshida, S., Sasakawa, C., and Abe, A. (2004). Enteropathogenic Escherichia coli activates the RhoA signaling pathway via the stimulation of GEF-H1. Embo J *23*, 3570-3582.
Maurelli, A. T., Baudry, B., d'Hauteville, H., Hale, T. L., and Sansonetti, P. J. (1985). Cloning of plasmid DNA sequences involved in invasion of HeLa cells by Shigella flexneri. Infect Immun *49*, 164-171.
McDaniel, T. K., Jarvis, K. G., Donnenberg, M. S., and Kaper, J. B. (1995). A genetic locus of enterocyte effacement conserved among diverse enterobacterial pathogens. Proc Natl Acad Sci U S A *92*, 1664-1668.
McGhie E.J,, Hayward R,D,, Koronakis V. (2004). Control of actin turnover by a salmonella invasion protein. Mol Cell 13(4):497-510.
McMahon, H. T., and Gallop, J. L. (2005). Membrane curvature and mechanisms of dynamic cell membrane remodelling. Nature *438*, 590-596.
McNamara, B. P., Koutsouris, A., O'Connell, C. B., Nougayrede, J. P., Donnenberg, M. S., and Hecht, G. (2001). Translocated EspF protein from enteropathogenic Escherichia coli disrupts host intestinal barrier function. J Clin Invest *107*, 621-629.
Miao, E. A., and Miller, S. I. (2000). A conserved amino acid sequence directing intracellular type III secretion by Salmonella typhimurium. Proc Natl Acad Sci U S A *97*, 7539-7544.
Miki, H., Yamaguchi, H., Suetsugu, S., and Takenawa, T. (2000). IRSp53 is an essential intermediate between Rac and WAVE in the regulation of membrane ruffling. Nature *408*, 732-735.
Millard, T. H., Sharp, S. J., and Machesky, L. M. (2004). Signalling to actin assembly via the WASP (Wiskott-Aldrich syndrome protein)-family proteins and the Arp2/3 complex. Biochem J *380*, 1-17.
Miyahara, A., Nakanishi, N., Ooka, T., Hayashi, T., Sugimoto, N., and Tobe, T. (2009). Enterohemorrhagic Escherichia coli effector EspL2 induces actin microfilament aggregation through annexin 2 activation. Cell Microbiol *11*, 337-350.
Miyake, K., McNeil, P. L., Suzuki, K., Tsunoda, R., and Sugai, N. (2001). An actin barrier to resealing. J Cell Sci *114*, 3487-3494.
Moraes, T. F., Spreter, T., and Strynadka, N. C. (2008). Piecing together the type III injectisome of bacterial pathogens. Curr Opin Struct Biol *18*, 258-266.
Mougous, J. D., Cuff, M. E., Raunser, S., Shen, A., Zhou, M., Gifford, C. A., Goodman, A. L., Joachimiak, G., Ordonez, C. L., Lory, S., *et al.* (2006). A virulence locus of Pseudomonas aeruginosa encodes a protein secretion apparatus. Science *312*, 1526-1530.
Mounier, J., Popoff, M. R., Enninga, J., Frame, M. C., Sansonetti, P. J., and Van Nhieu, G. T. (2009). The IpaC carboxyterminal effector domain mediates Src-dependent actin polymerization during Shigella invasion of epithelial cells. PLoS Pathog *5*, e1000271.
Mundy, R., Petrovska, L., Smollett, K., Simpson, N., Wilson, R. K., Yu, J., Tu, X., Rosenshine, I., Clare, S., Dougan, G., and Frankel, G. (2004). Identification of a novel Citrobacter rodentium

type III secreted protein, EspI, and roles of this and other secreted proteins in infection. Infect Immun *72*, 2288-2302.
Natale, P., Bruser, T., and Driessen, A. J. (2008). Sec- and Tat-mediated protein secretion across the bacterial cytoplasmic membrane--distinct translocases and mechanisms. Biochim Biophys Acta *1778*, 1735-1756.
Nataro, J. P., and Kaper, J. B. (1998). Diarrheagenic *Escherichia coli*. Clin Microbiol Rev *11*, 142-201.
Niggli, V., and Rossy, J. (2008). Ezrin/radixin/moesin: versatile controllers of signaling molecules and of the cortical cytoskeleton. Int J Biochem Cell Biol *40*, 344-349.
Nougayrede, J. P., and Donnenberg, M. S. (2004). Enteropathogenic Escherichia coli EspF is targeted to mitochondria and is required to initiate the mitochondrial death pathway. Cell Microbiol *6*, 1097-1111.
Nouwen, N., Ranson, N., Saibil, H., Wolpensinger, B., Engel, A., Ghazi, A., and Pugsley, A. P. (1999). Secretin PulD: association with pilot PulS, structure, and ion-conducting channel formation. Proc Natl Acad Sci U S A *96*, 8173-8177.
Ogura, Y., Abe, H., Katsura, K., Kurokawa, K., Asadulghani, M., Iguchi, A., Ooka, T., Nakayama, K., Yamashita, A., Hattori, M.*, et al.* (2008). Systematic identification and sequence analysis of the genomic islands of the enteropathogenic Escherichia coli strain B171-8 by the combined use of whole-genome PCR scanning and fosmid mapping. J Bacteriol *190*, 6948-6960.
Ohlson, M. B., Huang, Z., Alto, N. M., Blanc, M. P., Dixon, J. E., Chai, J., and Miller, S. I. (2008). Structure and function of Salmonella SifA indicate that its interactions with SKIP, SseJ, and RhoA family GTPases induce endosomal tubulation. Cell Host Microbe *4*, 434-446.
Ohya, K., Handa, Y., Ogawa, M., Suzuki, M., and Sasakawa, C. (2005). IpgB1 is a novel Shigella effector protein involved in bacterial invasion of host cells. Its activity to promote membrane ruffling via Rac1 and Cdc42 activation. J Biol Chem *280*, 24022-24034.
Okoh, A. I., and Osode, A. N. (2008). Enterotoxigenic Escherichia coli (ETEC): a recurring decimal in infants' and travelers' diarrhea. Rev Environ Health *23*, 135-148.
Olofsson, B. (1999). Rho guanine dissociation inhibitors: pivotal molecules in cellular signalling. Cell Signal *11*, 545-554.
Olson, M. F., Sterpetti, P., Nagata, K., Toksoz, D., and Hall, A. (1997). Distinct roles for DH and PH domains in the Lbc oncogene. Oncogene *15*, 2827-2831.
Paduch, M., Jelen, F., and Otlewski, J. (2001). Structure of small G proteins and their regulators. Acta Biochim Pol *48*, 829-850.
Pan, J., Kao, Y. L., Joshi, S., Jeetendran, S., Dipette, D., and Singh, U. S. (2005). Activation of Rac1 by phosphatidylinositol 3-kinase in vivo: role in activation of mitogen-activated protein kinase (MAPK) pathways and retinoic acid-induced neuronal differentiation of SH-SY5Y cells. J Neurochem *93*, 571-583.
Papatheodorou, P., Domanska, G., Oxle, M., Mathieu, J., Selchow, O., Kenny, B., and Rassow, J. (2006). The enteropathogenic Escherichia coli (EPEC) Map effector is imported into the mitochondrial matrix by the TOM/Hsp70 system and alters organelle morphology. Cell Microbiol *8*, 677-689.
Parsot, C. (2005). Shigella spp. and enteroinvasive Escherichia coli pathogenicity factors. FEMS Microbiol Lett *252*, 11-18.
Patel, J. C., and Galan, J. E. (2006). Differential activation and function of Rho GTPases during Salmonella-host cell interactions. J Cell Biol *175*, 453-463.

Peck, J., Douglas, G. t., Wu, C. H., and Burbelo, P. D. (2002). Human RhoGAP domain-containing proteins: structure, function and evolutionary relationships. FEBS Lett *528*, 27-34.
Pei, S., Doye, A., and Boquet, P. (2001). Mutation of specific acidic residues of the CNF1 T domain into lysine alters cell membrane translocation of the toxin. Mol Microbiol *41*, 1237-1247.
Pelletier, S., Julien, C., Popoff, M. R., Lamarche-Vane, N., and Meloche, S. (2005). Cyclic AMP induces morphological changes of vascular smooth muscle cells by inhibiting a Rac-dependent signaling pathway. J Cell Physiol *204*, 412-422.
Pereira-Leal, J. B., Hume, A. N., and Seabra, M. C. (2001). Prenylation of Rab GTPases: molecular mechanisms and involvement in genetic disease. FEBS Lett *498*, 197-200.
Poh, J., Odendall, C., Spanos, A., Boyle, C., Liu, M., Freemont, P., and Holden, D. W. (2008). SteC is a Salmonella kinase required for SPI-2-dependent F-actin remodelling. Cell Microbiol *10*, 20-30.
Pollard, T. D., Blanchoin, L., and Mullins, R. D. (2001). Actin dynamics. J Cell Sci *114*, 3-4.
Prehna, G., Ivanov, M. I., Bliska, J. B., and Stebbins, C. E. (2006). Yersinia virulence depends on mimicry of host Rho-family nucleotide dissociation inhibitors. Cell *126*, 869-880.
Pugsley, A. P. (1993). The complete general secretory pathway in gram-negative bacteria. Microbiol Rev *57*, 50-108.
Pugsley, A. P., Francetic, O., Hardie, K., Possot, O. M., Sauvonnet, N., and Seydel, A. (1997). Pullulanase: model protein substrate for the general secretory pathway of gram-negative bacteria. Folia Microbiol (Praha) *42*, 184-192.
Pukatzki, S., McAuley, S. B., and Miyata, S. T. (2009). The type VI secretion system: translocation of effectors and effector-domains. Curr Opin Microbiol *12*, 11-17.
Quinlan, M. E., Heuser, J. E., Kerkhoff, E., and Mullins, R. D. (2005). Drosophila Spire is an actin nucleation factor. Nature *433*, 382-388.
Reinicke, A. T., Hutchinson, J. L., Magee, A. I., Mastroeni, P., Trowsdale, J., and Kelly, A. P. (2005). A Salmonella typhimurium effector protein SifA is modified by host cell prenylation and S-acylation machinery. J Biol Chem *280*, 14620-14627.
Ridley, A. J. (1999). Stress fibres take shape. Nat Cell Biol *1*, E64-66.
Ridley, A. J. (2001). Rho family proteins: coordinating cell responses. Trends Cell Biol *11*, 471-477.
Ridley, A. J., and Hall, A. (1992). The small GTP-binding protein rho regulates the assembly of focal adhesions and actin stress fibers in response to growth factors. Cell *70*, 389-399.
Ridley, A. J., Paterson, H. F., Johnston, C. L., Diekmann, D., and Hall, A. (1992). The small GTP-binding protein rac regulates growth factor-induced membrane ruffling. Cell *70*, 401-410.
Ridley, A. J., Schwartz, M. A., Burridge, K., Firtel, R. A., Ginsberg, M. H., Borisy, G., Parsons, J. T., and Horwitz, A. R. (2003). Cell migration: integrating signals from front to back. Science *302*, 1704-1709.
Riley, L. W., Junio, L. N., Libaek, L. B., and Schoolnik, G. K. (1987). Plasmid-encoded expression of lipopolysaccharide O-antigenic polysaccharide in enteropathogenic Escherichia coli. Infect Immun *55*, 2052-2056.
Rodriguez, A., Rioult, M. G., Ora, A., and Andrews, N. W. (1995). A trypanosome-soluble factor induces IP3 formation, intracellular Ca2+ mobilization and microfilament rearrangement in host cells. J Cell Biol *129*, 1263-1273.
Roof, R. W., Haskell, M. D., Dukes, B. D., Sherman, N., Kinter, M., and Parsons, S. J. (1998). Phosphotyrosine (p-Tyr)-dependent and -independent mechanisms of p190 RhoGAP-p120

RasGAP interaction: Tyr 1105 of p190, a substrate for c-Src, is the sole p-Tyr mediator of complex formation. Mol Cell Biol *18*, 7052-7063.
Rossman, K. L., Der, C. J., and Sondek, J. (2005). GEF means go: turning on RHO GTPases with guanine nucleotide-exchange factors. Nat Rev Mol Cell Biol *6*, 167-180.
Ruiz-Albert, J., Yu, X. J., Beuzon, C. R., Blakey, A. N., Galyov, E. E., and Holden, D. W. (2002). Complementary activities of SseJ and SifA regulate dynamics of the Salmonella typhimurium vacuolar membrane. Mol Microbiol *44*, 645-661.
Sander, E. E., and Collard, J. G. (1999). Rho-like GTPases: their role in epithelial cell-cell adhesion and invasion. Eur J Cancer *35*, 1302-1308.
Sanders, L. C., Matsumura, F., Bokoch, G. M., and de Lanerolle, P. (1999). Inhibition of myosin light chain kinase by p21-activated kinase. Science *283*, 2083-2085.
Sasakawa, C., Kamata, K., Sakai, T., Makino, S., Yamada, M., Okada, N., and Yoshikawa, M. (1988). Virulence-associated genetic regions comprising 31 kilobases of the 230-kilobase plasmid in Shigella flexneri 2a. J Bacteriol *170*, 2480-2484.
Saulino, E. T., Bullitt, E., and Hultgren, S. J. (2000). Snapshots of usher-mediated protein secretion and ordered pilus assembly. Proc Natl Acad Sci U S A *97*, 9240-9245.
Scheffzek, K., Ahmadian, M. R., Kabsch, W., Wiesmuller, L., Lautwein, A., Schmitz, F., and Wittinghofer, A. (1997). The Ras-RasGAP complex: structural basis for GTPase activation and its loss in oncogenic Ras mutants. Science *277*, 333-338.
Scheffzek, K., Stephan, I., Jensen, O. N., Illenberger, D., and Gierschik, P. (2000). The Rac-RhoGDI complex and the structural basis for the regulation of Rho proteins by RhoGDI. Nat Struct Biol *7*, 122-126.
Schlosser-Silverman, E., Elgrably-Weiss, M., Rosenshine, I., Kohen, R., and Altuvia, S. (2000). Characterization of Escherichia coli DNA lesions generated within J774 macrophages. J Bacteriol *182*, 5225-5230.
Schlumberger, M. C., Friebel, A., Buchwald, G., Scheffzek, K., Wittinghofer, A., and Hardt, W. D. (2003). Amino acids of the bacterial toxin SopE involved in G nucleotide exchange on Cdc42. J Biol Chem *278*, 27149-27159.
Schmidt, A., and Hall, A. (2002). Guanine nucleotide exchange factors for Rho GTPases: turning on the switch. Genes Dev *16*, 1587-1609.
Schmitt, L., Benabdelhak, H., Blight, M. A., Holland, I. B., and Stubbs, M. T. (2003). Crystal structure of the nucleotide-binding domain of the ABC-transporter haemolysin B: identification of a variable region within ABC helical domains. J Mol Biol *330*, 333-342.
Schroeder, G. N., and Hilbi, H. (2008). Molecular pathogenesis of Shigella spp.: controlling host cell signaling, invasion, and death by type III secretion. Clin Microbiol Rev *21*, 134-156.
Shao, F., Merritt, P. M., Bao, Z., Innes, R. W., and Dixon, J. E. (2002). A Yersinia effector and a Pseudomonas avirulence protein define a family of cysteine proteases functioning in bacterial pathogenesis. Cell *109*, 575-588.
Shao, F., Vacratsis, P. O., Bao, Z., Bowers, K. E., Fierke, C. A., and Dixon, J. E. (2003). Biochemical characterization of the Yersinia YopT protease: cleavage site and recognition elements in Rho GTPases. Proc Natl Acad Sci U S A *100*, 904-909.
Shi, J., Scita, G., and Casanova, J. E. (2005). WAVE2 signaling mediates invasion of polarized epithelial cells by Salmonella typhimurium. J Biol Chem *280*, 29849-29855.
Simpson, N., Shaw, R., Crepin, V. F., Mundy, R., FitzGerald, A. J., Cummings, N., Straatman-Iwanowska, A., Connerton, I., Knutton, S., and Frankel, G. (2006). The enteropathogenic

Escherichia coli type III secretion system effector Map binds EBP50/NHERF1: implication for cell signalling and diarrhoea. Mol Microbiol *60*, 349-363.
Skillman, K. M., Barnard, T. J., Peterson, J. H., Ghirlando, R., and Bernstein, H. D. (2005). Efficient secretion of a folded protein domain by a monomeric bacterial autotransporter. Mol Microbiol *58*, 945-958.
Smith, J. L., Fratamico, P. M., and Gunther, N. W. (2007). Extraintestinal pathogenic Escherichia coli. Foodborne Pathog Dis *4*, 134-163.
Smith, S. D., Jaffer, Z. M., Chernoff, J., and Ridley, A. J. (2008). PAK1-mediated activation of ERK1/2 regulates lamellipodial dynamics. J Cell Sci *121*, 3729-3736.
Soisson, S. M., Nimnual, A. S., Uy, M., Bar-Sagi, D., and Kuriyan, J. (1998). Crystal structure of the Dbl and pleckstrin homology domains from the human Son of sevenless protein. Cell *95*, 259-268.
Stebbins, C. E., and Galan, J. E. (2000). Modulation of host signaling by a bacterial mimic: structure of the Salmonella effector SptP bound to Rac1. Mol Cell *6*, 1449-1460.
Steele-Mortimer, O. (2008). The Salmonella-containing vacuole: moving with the times. Curr Opin Microbiol *11*, 38-45.
Steffen, A., Rottner, K., Ehinger, J., Innocenti, M., Scita, G., Wehland, J., and Stradal, T. E. (2004). Sra-1 and Nap1 link Rac to actin assembly driving lamellipodia formation. Embo J *23*, 749-759.
Stein, M. A., Leung, K. Y., Zwick, M., Garcia-del Portillo, F., and Finlay, B. B. (1996). Identification of a Salmonella virulence gene required for formation of filamentous structures containing lysosomal membrane glycoproteins within epithelial cells. Mol Microbiol *20*, 151-164.
Stender, S., Friebel, A., Linder, S., Rohde, M., Mirold, S., and Hardt, W. D. (2000). Identification of SopE2 from Salmonella typhimurium, a conserved guanine nucleotide exchange factor for Cdc42 of the host cell. Mol Microbiol *36*, 1206-1221.
Stenutz, R., Weintraub, A., and Widmalm, G. (2006). The structures of Escherichia coli O-polysaccharide antigens. FEMS Microbiol Rev *30*, 382-403.
Suetsugu, S., Kurisu, S., Oikawa, T., Yamazaki, D., Oda, A., and Takenawa, T. (2006). Optimization of WAVE2 complex-induced actin polymerization by membrane-bound IRSp53, PIP(3), and Rac. J Cell Biol *173*, 571-585.
Suetsugu, S., Miki, H., and Takenawa, T. (1999). Identification of two human WAVE/SCAR homologues as general actin regulatory molecules which associate with the Arp2/3 complex. Biochem Biophys Res Commun *260*, 296-302.
Suzuki, T., Mimuro, H., Suetsugu, S., Miki, H., Takenawa, T., and Sasakawa, C. (2002). Neural Wiskott-Aldrich syndrome protein (N-WASP) is the specific ligand for Shigella VirG among the WASP family and determines the host cell type allowing actin-based spreading. Cell Microbiol *4*, 223-233.
Takahashi, K., Sasaki, T., Mammoto, A., Takaishi, K., Kameyama, T., Tsukita, S., and Takai, Y. (1997). Direct interaction of the Rho GDP dissociation inhibitor with ezrin/radixin/moesin initiates the activation of the Rho small G protein. J Biol Chem *272*, 23371-23375.
Takahashi, K., and Suzuki, K. (2009). Membrane transport of WAVE2 and lamellipodia formation require Pak1 that mediates phosphorylation and recruitment of stathmin/Op18 to Pak1-WAVE2-kinesin complex. Cell Signal *21*, 695-703.
Takenawa, T., and Miki, H. (2001). WASP and WAVE family proteins: key molecules for rapid rearrangement of cortical actin filaments and cell movement. J Cell Sci *114*, 1801-1809.

Tcherkezian, J., and Lamarche-Vane, N. (2007). Current knowledge of the large RhoGAP family of proteins. Biol Cell *99*, 67-86.
Thery, M., and Bornens, M. (2006). Cell shape and cell division. Curr Opin Cell Biol *18*, 648-657.
Thorpe, C. M. (2004). Shiga toxin-producing Escherichia coli infection. Clin Infect Dis *38*, 1298-1303.
Tobe, T., Beatson, S. A., Taniguchi, H., Abe, H., Bailey, C. M., Fivian, A., Younis, R., Matthews, S., Marches, O., Frankel, G., *et al.* (2006). An extensive repertoire of type III secretion effectors in Escherichia coli O157 and the role of lambdoid phages in their dissemination. Proc Natl Acad Sci U S A *103*, 14941-14946.
Tobe, T., Schoolnik, G. K., Sohel, I., Bustamante, V. H., and Puente, J. L. (1996). Cloning and characterization of bfpTVW, genes required for the transcriptional activation of bfpA in enteropathogenic Escherichia coli. Mol Microbiol *21*, 963-975.
Tobe, T., Tatsuno, I., Katayama, E., Wu, C. Y., Schoolnik, G. K., and Sasakawa, C. (1999). A novel chromosomal locus of enteropathogenic Escherichia coli (EPEC), which encodes a bfpT-regulated chaperone-like protein, TrcA, involved in microcolony formation by EPEC. Mol Microbiol *33*, 741-752.
Toksoz, D., and Merdek, K. D. (2002). The Rho small GTPase: functions in health and disease. Histol Histopathol *17*, 915-927.
Tran Van Nhieu, G., Caron, E., Hall, A., and Sansonetti, P. J. (1999). IpaC induces actin polymerization and filopodia formation during Shigella entry into epithelial cells. Embo J *18*, 3249-3262.
Tseng, T. T., Tyler, B. M., and Setubal, J. C. (2009). Protein secretion systems in bacterial-host associations, and their description in the Gene Ontology. BMC Microbiol *9 Suppl 1*, S2.
Turner, S. M., Scott-Tucker, A., Cooper, L. M., and Henderson, I. R. (2006). Weapons of mass destruction: virulence factors of the global killer enterotoxigenic Escherichia coli. FEMS Microbiol Lett *263*, 10-20.
Upadhyay, A., Wu, H. L., Williams, C., Field, T., Galyov, E. E., van den Elsen, J. M., and Bagby, S. (2008). The guanine-nucleotide-exchange factor BopE from Burkholderia pseudomallei adopts a compact version of the Salmonella SopE/SopE2 fold and undergoes a closed-to-open conformational change upon interaction with Cdc42. Biochem J *411*, 485-493.
Valderrama, F., Cordeiro, J. V., Schleich, S., Frischknecht, F., and Way, M. (2006). Vaccinia virus-induced cell motility requires F11L-mediated inhibition of RhoA signaling. Science *311*, 377-381.
Valles, A. M., Beuvin, M., and Boyer, B. (2004). Activation of Rac1 by paxillin-Crk-DOCK180 signaling complex is antagonized by Rap1 in migrating NBT-II cells. J Biol Chem *279*, 44490-44496.
Velarde, J. J., Varney, K. M., Inman, K. G., Farfan, M., Dudley, E., Fletcher, J., Weber, D. J., and Nataro, J. P. (2007). Solution structure of the novel dispersin protein of enteroaggregative Escherichia coli. Mol Microbiol *66*, 1123-1135.
Viljanen, M. K., Peltola, T., Junnila, S. Y., Olkkonen, L., Jarvinen, H., Kuistila, M., and Huovinen, P. (1990). Outbreak of diarrhoea due to Escherichia coli O111:B4 in schoolchildren and adults: association of Vi antigen-like reactivity. Lancet *336*, 831-834.
Vingadassalom, D., Kazlauskas, A., Skehan, B., Cheng, H. C., Magoun, L., Robbins, D., Rosen, M. K., Saksela, K., and Leong, J. M. (2009). Insulin receptor tyrosine kinase substrate links the

E. coli O157:H7 actin assembly effectors Tir and EspF(U) during pedestal formation. Proc Natl Acad Sci U S A *106*, 6754-6759.
Vogelsgesang, M., Pautsch, A., and Aktories, K. (2007). C3 exoenzymes, novel insights into structure and action of Rho-ADP-ribosylating toxins. Naunyn Schmiedebergs Arch Pharmacol *374*, 347-360.
Ward, D. V., Draper, O., Zupan, J. R., and Zambryski, P. C. (2002). Peptide linkage mapping of the Agrobacterium tumefaciens vir-encoded type IV secretion system reveals protein subassemblies. Proc Natl Acad Sci U S A *99*, 11493-11500.
Weiss, S. M., Ladwein, M., Schmidt, D., Ehinger, J., Lommel, S., Stading, K., Beutling, U., Disanza, A., Frank, R., Jansch, L.*, et al.* (2009). IRSp53 links the enterohemorrhagic E. coli effectors Tir and EspFU for actin pedestal formation. Cell Host Microbe *5*, 244-258.
Welch, M. D., and Mullins, R. D. (2002). Cellular control of actin nucleation. Annu Rev Cell Dev Biol *18*, 247-288.
Westwick, J. K., Lambert, Q. T., Clark, G. J., Symons, M., Van Aelst, L., Pestell, R. G., and Der, C. J. (1997). Rac regulation of transformation, gene expression, and actin organization by multiple, PAK-independent pathways. Mol Cell Biol *17*, 1324-1335.
Whale, A. D., Garmendia, J., Gomes, T. A., and Frankel, G. (2006). A novel category of enteropathogenic *Escherichia coli* simultaneously utilizes the Nck and TccP pathways to induce actin remodelling. Cell Microbiol *8*, 999-1008.
Wishart, D. S., Sykes, B. D., and Richards, F. M. (1993). Improved synthetic methods for the selective deuteration of aromatic amino acids: applications of selective protonation towards the identification of protein folding intermediates through nuclear magnetic resonance. Biochim Biophys Acta *1164*, 36-46.
Witke, W. (2004). The role of profilin complexes in cell motility and other cellular processes. Trends Cell Biol *14*, 461-469.
Woodring, P. J., Hunter, T., and Wang, J. Y. (2003). Regulation of F-actin-dependent processes by the Abl family of tyrosine kinases. J Cell Sci *116*, 2613-2626.
Yam, P. T., and Theriot, J. A. (2004). Repeated cycles of rapid actin assembly and disassembly on epithelial cell phagosomes. Mol Biol Cell *15*, 5647-5658.
Yamaguchi, H., Miwa, Y., Kasa, M., Kitano, K., Amano, M., Kaibuchi, K., and Hakoshima, T. (2006). Structural basis for induced-fit binding of Rho-kinase to the inhibitor Y-27632. J Biochem *140*, 305-311.
Yarbrough, M. L., Li, Y., Kinch, L. N., Grishin, N. V., Ball, H. L., and Orth, K. (2009). AMPylation of Rho GTPases by Vibrio VopS disrupts effector binding and downstream signaling. Science *323*, 269-272.
Yip, C. K., Finlay, B. B., and Strynadka, N. C. (2005). Structural characterization of a type III secretion system filament protein in complex with its chaperone. Nat Struct Mol Biol *12*, 75-81.
Zhang, F. L., and Casey, P. J. (1996). Protein prenylation: molecular mechanisms and functional consequences. Annu Rev Biochem *65*, 241-269.
Ziegler, W. H., Liddington, R. C., and Critchley, D. R. (2006). The structure and regulation of vinculin. Trends Cell Biol *16*, 453-460.

Appendix 1 – Publications

Cellular Microbiology (2008) **10**(7), 1429–1441
doi:10.1111/j.1462-5822.2008.01136.x
First published online 26 March 2008

Subversion of actin dynamics by EspM effectors of attaching and effacing bacterial pathogens

OnlineOpen: This article is available free online at www.blackwell-synergy.com

Ana Arbeloa,[1†] Richard R. Bulgin,[1†] Georgina MacKenzie,[1] Robert K. Shaw,[2] Mark J. Pallen,[2] Valerie F. Crepin,[1] Cedric N. Berger[1] and Gad Frankel[1*]

[1]*Division of Cell and Molecular Biology, Imperial College London, London SW7 2AZ, UK.*

[2]*Division of Immunity and Infection, School of Medicine, University of Birmingham, Birmingham B15 2TT, UK.*

Summary

Rho GTPases are common targets of bacterial toxins and type III secretion system effectors. IpgB1 and IpgB2 of *Shigella* and Map of enteropathogenic (EPEC) and enterohemorrhagic (EHEC) *Escherichia coli* were recently grouped together on the basis that they share a conserved WxxxE motif. In this study, we characterized six WxxxE effectors from attaching and effacing pathogens: TrcA and EspM1 of EPEC strain B171, EspM1 and EspM2 of EHEC strain Sakai and EspM2 and EspM3 of *Citrobacter rodentium*. We show that EspM2 triggers formation of global parallel stress fibres, TrcA and EspM1 induce formation of localized parallel stress fibres and EspM3 triggers formation of localized radial stress fibres. Using EspM2 and EspM3 as model effectors, we report that while substituting the conserved Trp with Ala abolished activity, conservative Trp to Tyr or Glu to Asp substitutions did not affect stress-fibre formation. We show, using dominant negative constructs and chemical inhibitors, that the activity of EspM2 and EspM3 is RhoA and ROCK-dependent. Using Rhotekin pull-downs, we have shown that EspM2 and EspM3 activate RhoA; translocation of EspM2 and EspM3 triggered phosphorylation of cofilin. These results suggest that the EspM effectors modulate actin dynamics by activating the RhoA signalling pathway.

Received 4 January, 2008; revised 21 February, 2008; accepted 21 February, 2008. *For correspondence. E-mail g.frankel@imperial.ac.uk; Tel. (+44) 20 7594 5253; Fax (+44) 20 7594 3069. †These authors are equal contributors.

Re-use of this article is permitted in accordance with the Creative Commons Deed, Attribution 2.5, which does not permit commercial exploitation.

© 2008 The Authors
Journal compilation © 2008 Blackwell Publishing Ltd

Introduction

Colonization, invasion and transversion of mucosal surfaces are alternative strategies used by pathogenic bacteria to cause infectious diseases. Many Gram-negative bacteria employ a type III secretion system (T3SS) to inject effector proteins into the cytosol of their mammalian host (reviewed in Galan and Wolf-Watz, 2006), which facilitate their unique infection strategies. T3SS effectors are targeted to different subcellular compartments and affect diverse signalling pathways and physiological processes. For example, enteropathogenic (EPEC) and enterohemorrhagic (EHEC) *Escherichia coli* belong to a family of medically important extracellular diarrhoegenic pathogens (reviewed in Kaper *et al*., 2004) that colonize the gut mucosa by the attaching and effacing (A/E) mechanism (Knutton *et al*., 1987). EHEC and EPEC inject dozens of T3SS effector proteins (Tobe *et al*., 2006), including EspG and EspG2 which disrupt the microtubule network which may lead to formation of stress fibres at late stages of the infection via an indirect activation of RhoA (Matsuzawa *et al*., 2004; Shaw *et al*., 2005), Map which induces transient formation of filopodia (Kenny and Jepson, 2000), Tir which triggers extensive localized actin polymerization leading to formation of pedestal-shaped structures under adherent bacteria (Kenny *et al*., 1997) and TccP/EspF_U which connects Tir to the actin cytoskeleton (Campellone *et al*., 2004; Garmendia *et al*., 2004).

The actin cytoskeleton (reviewed in Cossart and Sansonetti, 2004) and Rho GTPases (reviewed in Jaffe and Hall, 2005) are prominent targets of T3SS effectors (Finlay, 2005). There are 22 Rho GTPases in man which regulate various cellular processes, including actin polymerization, microtubule dynamics and cell cycle, morphogenesis and migration (reviewed in Jaffe and Hall, 2005). GTPases act as molecular switches cycling between GTP-bound (active) and GDP-bound (inactive) conformations. Switching a GTPase on and off is mediated by guanine nucleotide exchange factors (GEFs) and GTPase-activating proteins (GAPs) respectively. The Rho GTPases transmit signals in a GTP-dependent manner by activating and/or recruiting downstream effector proteins to their sites of action (reviewed in Jaffe and Hall, 2005).

Recently, Alto *et al.* (2006) assembled several known T3SS effectors into a single family that share the common motif Trp-xxx-Glu (WxxxE). This family includes the

Salmonella effectors SifB and SifA, which is involved in intracellular survival and replication by maintaining the integrity of the *Salmonella*-containing vacuole (Beuzon *et al.*, 2000), the *Shigella* effectors IpgB2 and IpgB1, which is involved in bacterial cell invasion (Ohya *et al.*, 2005), the EPEC and EHEC effector Map (Kenny and Jepson, 2000) and the EPEC protein TrcA (bfpT-regulated chaperone-like protein gene) (Tobe *et al.*, 1999; Alto *et al.*, 2006). Although sharing no sequence homology with the Rho GTPases, Alto *et al.* (2006) suggested that IpgB1, IpgB2 and Map mimic, in a GTP-independent mechanism, the activated form of Rac-1, RhoA and Cdc42 respectively. It was shown that ectopic expression of IpgB2 induces formation of new stress fibres, while IpgB2^{W62A} and IpgB2^{E66A} were not biologically active; stress-fibre formation was RhoA-independent as IpgB2 was functional in the presence of RhoA inhibitors (e.g. C3 botulinum toxin) or dominant negative RhoA^{T19N}. In addition, IpgB2 was shown to directly stimulate the activity of Rho-associated kinase (ROCK) and to interact with mDIA, two downstream effectors of RhoA.

The completed and ongoing genome projects of the A/E pathogens EHEC O157:H7 (strains Sakai and EDL933), EPEC O127:H6 (strain E2348/69), EPEC O111:NM (strain B171) and the mouse pathogen *Citrobacter rodentium* (strain ICC168) have revealed that the number of T3SS effector proteins encoded by this family has been greatly underestimated. A comprehensive study of the T3SS repertoire of EHEC O157:H7 has shown that among the dozens of T3SS effectors are two new putative members of the WxxxE proteins, EspM1 and EspM2 (Tobe *et al.*, 2006). Using Map and IpgB2 as index genes, we identified additional putative WxxxE effectors in the A/E pathogens, including EspM1 in EPEC B171 and EspM2 and EspM3 in *C. rodentium*. The aim of this study was to investigate the function and mechanism of cell signalling triggered by the A/E pathogen WxxxE effectors.

Results

Identification of novel WxxxE effectors in the A/E pathogen group

EspM1 and EspM2 of EHEC O157 are putative WxxxE effectors (Tobe *et al.*, 2006), sharing 76% identity (Fig. 1). EspM1 and EspM2 are closely related to the *Shigella* WxxxE effector IpgB2 (40% and 41% identity respectively) while sharing only 23% and 22% identity, respectively, with Map of EPEC E2348/69 (Fig. 1).

In order to define the repertoire of WxxxE proteins in EPEC strains E2348/69 and B171 and *C. rodentium*, we searched their genomes using the BLAST algorithm with IpgB2 and Map as index proteins. In EPEC B171, one homologue, TrcA, had already been identified (Tobe *et al.*, 1999; Alto *et al.*, 2006). Here we report an additional putative WxxxE effector, EspM1 (Accession #: AM910623) (Fig. 1), which is closely related to proteins encoded in the LEE of rabbit EPEC and EHEC O103:H2. We demonstrated that HA-tagged TrcA and EspM1 (B171) are translocated in a T3SS-dependent mechanism (data not shown). TrcA and EspM1 (B171) exhibit 41% and 46% identity, respectively, with IpgB2 (Fig. 1). Importantly, the BLAST searches revealed that EPEC E2348/69 harbours no other functional WxxxE effector than Map.

Searching the *C. rodentium* ICC168 genome sequence, we identified two putative WxxxE effectors, EspM2 (Accession #: AM910622) and EspM3 (Accession #: AM910621), which share 42% and 47% identity, respectively, with IpgB2. Using a TEM-1-β-lactamase fusion assay (Charpentier and Oswald, 2004), we demonstrated that EspM2 (CR) and EspM3 are translocated in a T3SS-dependent mechanism (data not shown). BLAST hits that we did not follow up include one open reading frame (ROD40861) that has a frame shift deletion upstream of the WxxxE motif and a distantly related IpgB2 homologue.

A radial phylogenetic tree, created based upon multiple sequence alignment with hierarchical clustering (Corpet, 1988), showed that all the IpgB2-like A/E effectors indeed cluster with IpgB2 and are distant from IpgB1 and Map (Fig. 1B). The nomenclature of the A/E WxxxE effectors was based on functional homology rather than sequence identity (see below).

The WxxxE A/E effectors trigger formation of three distinct actin stress fibre architectures

In order to determine if similarly to IpgB2, the EspM1, EspM2, TrcA and EspM3 homologues can remodel actin in the mammalian host cells, the genes were cloned into the expression vector pSA10 (Schlosser-Silverman *et al.*, 2000) and expressed in wild-type EPEC E2348/69 (lacking any of the IpgB2 homologues). Recombinant E2348/69 were used to infect serum-starved Swiss 3T3 cells, which generally lack stress fibres (Fig. 2) and are capable of dynamic actin signalling. Control infections with wild-type EPEC E2348/69 (Fig. 2) or EPEC E2348/69 carrying the empty pSA10 vector (results not shown) trigger efficient Tir-dependent actin-rich pedestals, while stress fibres were seen only in a small percentage of infected Swiss 3T3 cells (Fig. 2). In contrast, infection of Swiss 3T3 cells with E2348/69 expressing EspM2 (Sakai) (Fig. 2) and EspM2 (CR) (data not shown) induced simultaneous formation of actin pedestals and global parallel stress fibres (GP-SF), which were on different focal planes. These stress fibres were observed in *c.* 90% of cells after 1.5 h infection (Fig. 2). Applying anti-HA antibodies, we could only detect

© 2008 The Authors
Journal compilation © 2008 Blackwell Publishing Ltd,

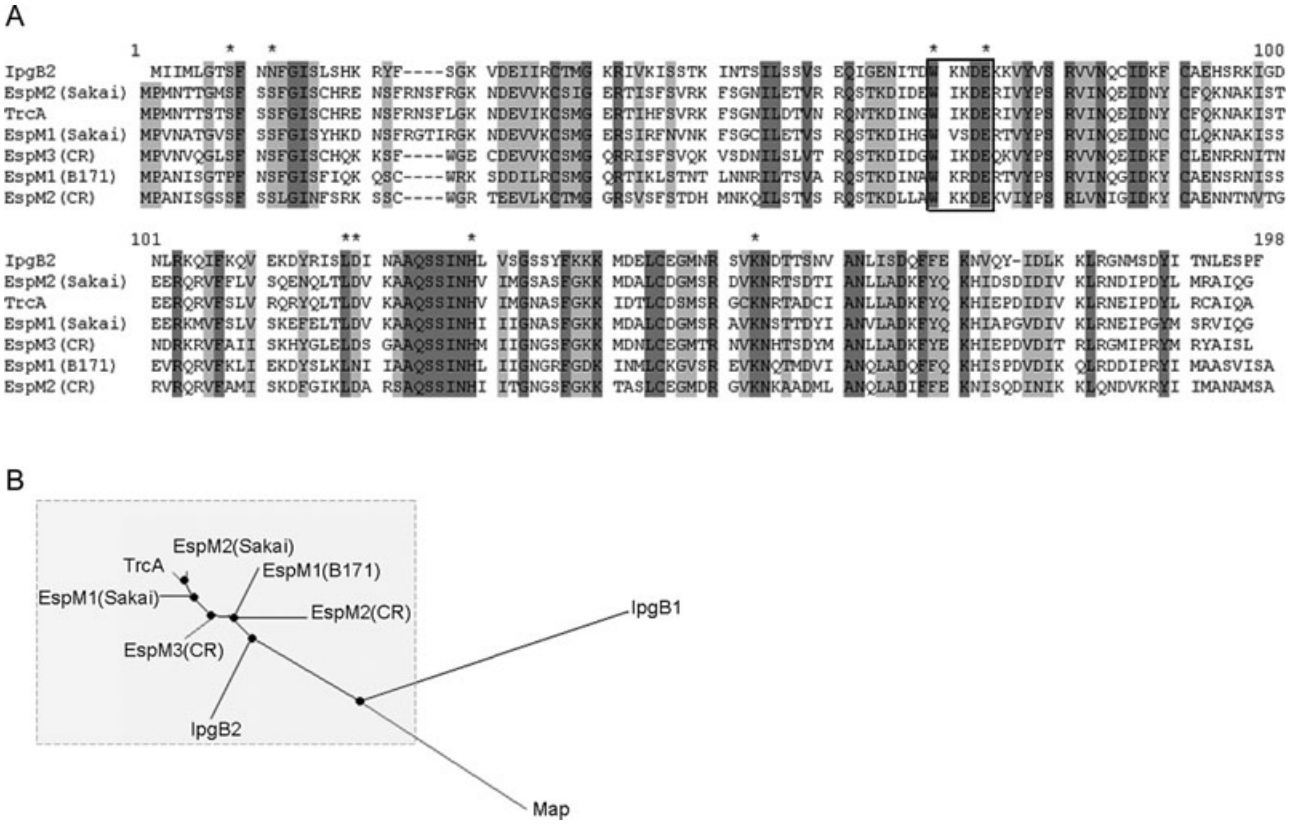


Fig. 1. The EspM WxxxE effector proteins in A/E pathogen group.
A. Multiple sequence alignment with hierarchical clustering of *S. exneri* IpgB2, EspM1 and EspM2 from EHEC O157:H7 Sakai, EspM2 and EspM3 from *C. rodentium* (CR) and TrcA and EspM1 from EPEC B171. Similar and identical residues are highlighted in bright and dark grey respectively. The conserved motif WxxxE is boxed. Conserved residues subjected to mutagenesis in this study are tagged with a star.
B. Radial phylogeny tree showing the subfamily of IpgB2-like WxxxE effectors in the A/E group, EPEC E2348/69 Map and *Shigella* IpgB1 and IpgB2.

diffuse cytosolic EspM2 staining (data not shown) while, using vinculin antibodies, we observed intense distal staining of the GP-SF (Fig. 2), suggesting that the GP-SF triggered by EspM2 are linked to the plasma membrane through focal adhesions (Ziegler *et al*., 2006).

Infection of Swiss 3T3 cells with E2348/69 expressing EspM1 (B171) (Fig. 2), EspM1 (Sakai) and TrcA (data not shown) resulted in simultaneous formation of actin pedestals and localized parallel stress fibres (LP-SF), which were subtly different from those triggered by EspM2 as they were confined to the site of bacterial adhesion (Fig. 2). Inmunofluorescence using the anti-vinculin antibodies revealed intense staining at the tip of each of the LP-SF (Fig. 2). Swiss cells infected with wild-type B171 for 90 min exhibited widespread stress fibres of the LP-SF morphology alongside well-developed actin pedestals (data not shown).

Infection of Swiss 3T3 with E2348/69 expressing EspM3 (CR) resulted in simultaneous formation of actin pedestals and stress fibres with vinculin-rich tips in *c.* 90% of the cells at 1.5 h post infection (Fig. 2). EspM3 triggered formation of a distinct architecture of localized radial (3D) stress fibres (LR-SF) (Fig. 2); despite the localized nature of the stress fibres, using anti-HA antibodies we only observed a diffuse cytosolic EspM3 straining (data not shown). To our knowledge, LR-SF have not been previously described in an infection context, but are reminiscent of cells treated with phorbal esters such as TPA (Imamura *et al*., 1998).

The GP-SF, LP-SF and LR-SF appeared as soon as 30 min post infection and were stable for at least 3 h (data not shown). In control experiments, Swiss 3T3 cells were infected with E2348/69Δ*escN* (T3SS mutant), E2348/69Δ*map*, E2348/69Δ*tir* and E2348/69Δ*espG*/*espG2* expressing EspM2 (Sakai). While no GP-SF or actin pedestal structures were seen after infection with the E2348/69Δ*escN* mutant, GP-SF and actin pedestals, similar to those seen after infection with wild-type E2348/69, were seen after infection with all other mutant strains. In addition, ectopic expression of EspM2 in transfected cells also triggers formation of GP-SF (data not shown).

© 2008 The Authors
Journal compilation © 2008 Blackwell Publishing Ltd,

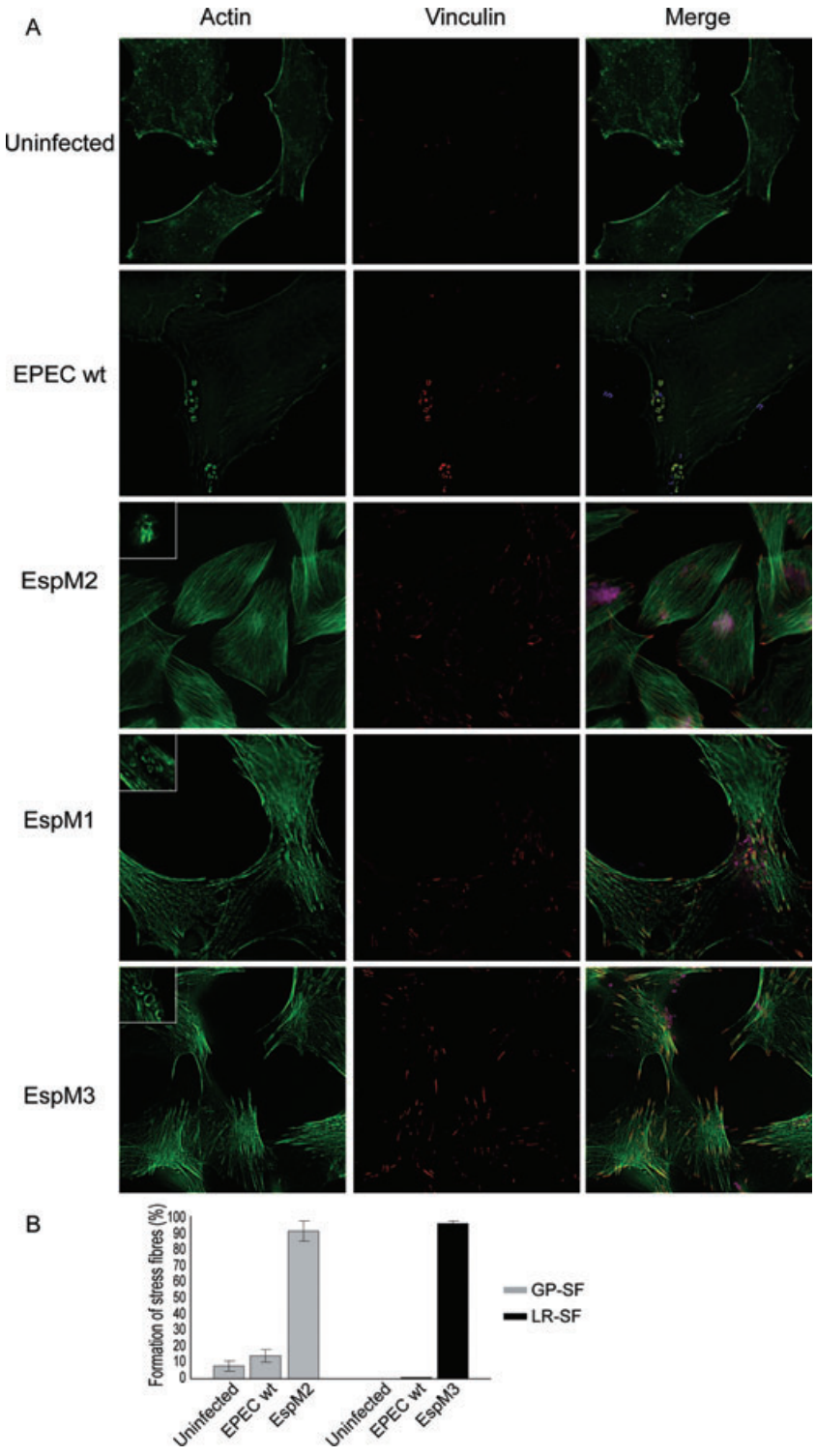


Fig. 2. The EspM A/E effectors trigger formation of actin stress fibres in infected Swiss 3T3 cells.
A. Fluorescence microscopy of uninfected Swiss 3T3 cell or cells infected for 90 min with wild-type E2348/69 and E2348/69 expressing EspM2 (Sakai), EspM1 (B171) and EspM3 (CR). Actin was stained with Oregon green phalloidin, EPEC were detected with rabbit anti-0127 antibody (merged column) and vinculin was visualised using a monoclonal mouse antibody. GP-SF, LP-SF and LR-SF were observed in cell infected with EPEC expressing EspM2, EspM1 and EspM3 respectively. All the recombinant strains also induced formation of actin pedestals (insets).
B. Quantification of parallel and radial stress-fibre formation in uninfected Swiss cells or after 90 min infection with wild-type E2348/69 and E2348/69 expressing EspM2 and EspM3. One hundred cells were counted in triplicate in three independent experiments. Results are presented as mean ± SEM.

Taken together, these results illustrate that the A/E EspM WxxxE effectors subvert actin dynamics and trigger formation of GP-SF (EspM2), LP-SF (EspM1 and TrcA) or LR-SF (EspM3). We selected EspM2 (Sakai) and EspM3 as model effectors for further study.

The effect of site-directed mutagenesis on the activity of EspM2 and EspM3

The actin modulation activity of the WxxxE effectors Map, IpgB1 and IpgB2 were previously shown to be dependent

© 2008 The Authors
Journal compilation © 2008 Blackwell Publishing Ltd,

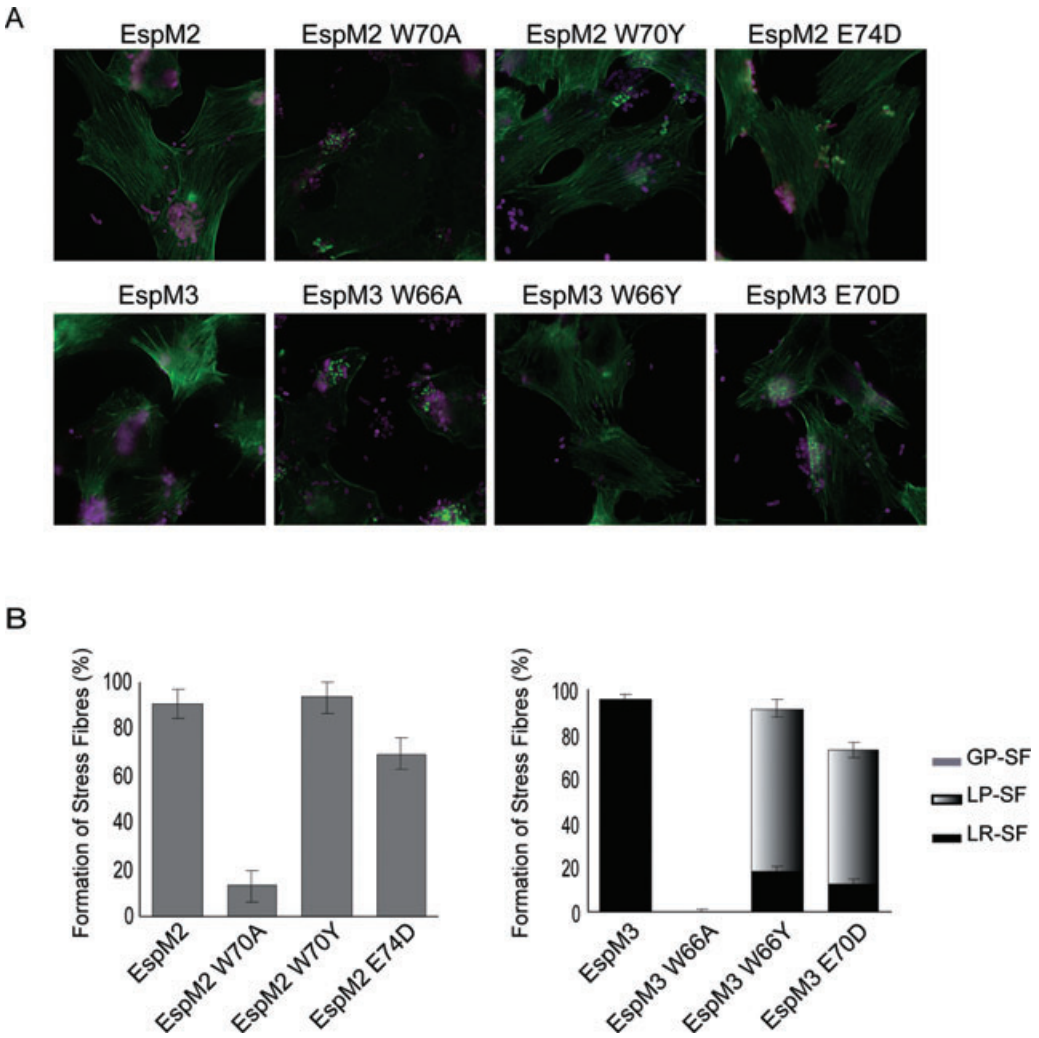


Fig. 3. Effect of site-directed mutagenesis on stress-fibre formation.
A. Merged fluorescence microscopy of Swiss 3T3 cells infected for 90 min with primed E2348/69 expressing EspM2 (Sakai) and EspM3 (CR) derivative mutants within the conserved WxxxE motif. Actin was stained with Oregon green phalloidin and EPEC were detected with rabbit anti-0127 antibody.
B. Quantification of stress-fibre formation in Swiss cells after 90 min infection. One hundred infected cells were counted in triplicate from three independent experiments. Results are presented as mean ± SEM.

on their invariant WxxxE motif (Alto *et al*., 2006). To determine if this is also true for EspM2 and EspM3, the conserved residues W70 and W66, respectively, were substituted by Ala. Swiss cells infected with E2348/69 expressing $EspM2_{W70A}$ and $EspM3_{W66A}$ triggered actin-rich pedestals with no evidence of GP-SF or LP-SF respectively, and were indistinguishable from cell infected with wild-type E2348/69 (Fig. 3). Conversely, conservative substitution of the Trp and Glu residues with a Tyr and Asp, respectively, did not result in any significant loss of stress-fibre formation (Fig. 3). These substitutions did, however, produce a shift in the architecture of stress fibres induced by EspM3 from a LR-SF morphology to a LP-SF arrangement. In addition, we mutated additional conserved residues located within the core region of the WxxxE effectors (Fig. 1). Mutagenesis of L114, D115 and H125 of EspM3 to Ala also resulted in a similar conformational change in the stress fibres (data not shown). Mutagenesis of other conserved residues within this group of effectors in EspM3 (Fig. 1) did not have any significant effect on stress-fibre formation or morphology (data not shown).

EspM2 and EspM3 activate RhoA

The formation of actin stress fibres in eukaryotic cells is regulated by the GTP-binding protein RhoA (Jaffe and Hall, 2005). However, IpgB2 has been shown to trigger formation of stress fibres through a mechanism which is independent of RhoA (Alto *et al*., 2006). In order to determine whether formation of GP-SF or LR-SF by EspM2

© 2008 The Authors
Journal compilation © 2008 Blackwell Publishing Ltd,

and EspM3 is dependent on activation of small Rho GTPases, we transfected Swiss cells with dominant negative Cdc42^{N17}, Rac1^{N17} and RhoA^{N19} (which competitively and specifically inhibit activation of the small GTPases). Infection of transfected cells with E2348/69 expressing EspM2 or EspM3 for 1.5 h revealed that formation of GP-SF and LR-SF, respectively, was not affected by inactivation of Cdc42 or Rac1 (Fig. 4A and B). In contrast, infection of cells expressing RhoA^{N19} resulted in formation of typical actin-rich pedestals, but with a marked reduction in formation of GP-SF or LR-SF respectively (Fig. 4A and B). This suggests that, unlike IpgB2, formation of stress fibres by EspM2 and EspM3 is RhoA-dependent.

In order to determine if EspM2 and EspM3 activate RhoA, we performed pull-down assays using GST-Rhotekin, which specifically binds the active GTP-bound form of RhoA. Cells incubated with 20 μM nocodazole, which destabilizes microtubules (DeBrabander *et al.*, 1976), for 40 min (data not shown), were used as a positive control and cell infected with wild-type E2348/69 were used as negative control. Swiss 3T3 cells infected with E2348/69 expressing EspM2 or EspM3 exhibited a significantly higher level of activated RhoA compared with cells infected with the wild-type E2348/69 (Fig. 4C). These results suggest that formation of GP-SF and LR-SF is dependent on RhoA signalling.

EspM2 and EspM3 stimulate the Rho-ROCK pathway

The p160 Rho-associated coiled-coil-containing protein kinase (ROCK) is one of the main RhoA downstream effectors which mediates the formation of stress fibres (Jaffe and Hall, 2005). To determine if EspM2 and EspM3 activate the RhoA-ROCK pathway, Swiss 3T3 cells were incubated with the ROCK inhibitor Y-27632 for 1 h prior to infection with E2348/69 expressing EspM2 or EspM3. Y-27632 is a highly specific inhibitor of ROCK-I and ROCK-II which competitively excludes ATP from the catalytic site (Yamaguchi *et al.*, 2006). Pre-incubation with Y-27632 completely blocked formation of GP-SF and LR-SF by EspM2 and EspM3 respectively (Fig. 5). The ROCK inhibitor did not affect formation of actin-rich pedestals.

LIM kinase (LIMK) is downstream effector of ROCK which is involved in stress-fibres formation (Jaffe and Hall, 2005). It has been shown that phosphorylation of the LIMK by ROCK and the consequent inactivation (by phosphorylation) of cofilin by LIMK contribute to Rho-induced formation of stress fibres (Maekawa *et al.*, 1999). We examined the phosphorylation state of cofilin by immunoblot following infection of Swiss cell with E2348/69 expressing EspM2 or EspM3. When compared with uninfected or cells infected with the wild-type E2348/69, higher level of phospho-cofilin was observed after translocation of EspM2 or EspM3 (Fig. 5). These results suggest that EspM2 and EspM3 trigger stress-fibre formation through the RhoA-ROCK-LIMK-cofilin pathway.

Discussion

In 2006, Alto *et al.* (2006) assembled several known T3SS effectors into a single family that share the common motif Trp-xxx-Glu (WxxxE). They suggested that IpgB1, IpgB2 and Map (the founder WxxxE effectors) mimic, in a GTP-independent mechanism, the activated form of Rac-1, RhoA and Cdc42 respectively. In this study, we report the discovery and characterization of an array of T3SS effector proteins in A/E pathogens which belong to the WxxxE family. These new effectors share a high degree of homology with each other (47–86% identity) and with the *Shigella* effector IpgB2 (40–47% identity).

The founder WxxxE effectors are potent modulators of the host actin cytoskeleton (Kenny *et al.*, 2002; Alto *et al.*, 2006; Handa *et al.*, 2007). In order to determine if the new proteins we studied are true WxxxE effectors that can subvert actin dynamics, we utilized EPEC EPEC234/69 as a vehicle for protein translocation into Swiss cells. EPEC234/69 is a suitable host as it only harbours the WxxxE effector Map, which induces transient filopdia at early time points post infection (Kenny and Jepson, 2000). Using this infection model, we demonstrated that overexpression of EspM1, EspM2, EspM3 and TrcA in EPEC E2348/69 triggers formation of stress fibres, related to those induced by the *Shigella* effector IpgB2 (Alto *et al.*, 2006). Importantly, the stress fibres triggered by these WxxxE effectors had distinct architectures. Although the EspM homologues were expressed from isogenic plasmids, we cannot exclude the possibility that differences in expression levels or translocation efficiency might contribute to their distinct stress fibre morphologies which appear as GP-SF throughout the cell cytosol for EspM, and LP-SF restricted to the site of bacterial attachment in the case of EspM1 and TrcA. Most striking was the phenotype associated with translocation of EspM3, which induced formation of LR-SF, which are reminiscent of the phenotypes linked to constitutively active Rho Kinase and phobal ester treatment such as TPA (Imamura *et al.*, 1998). To our knowledge, this is the first time that such a phenotype has been described in an infection context. Despite the global and localized stress fibres triggered by EspM2 and EspM1 and EspM3, respectively, all proteins were found diffusely in the cytsol. Vinculin was found at the tip of the WxxxE effector-triggered stress fibres, suggesting that they are linked to the plasma membrane via focal adhesion. The molecular basis for the different stress fibre architectures triggered by EspM1, EspM2, EspM3 and TrcA is not currently known. Of note is the fact that TrcA (bfpT-regulated chaperone-like protein gene)

© 2008 The Authors

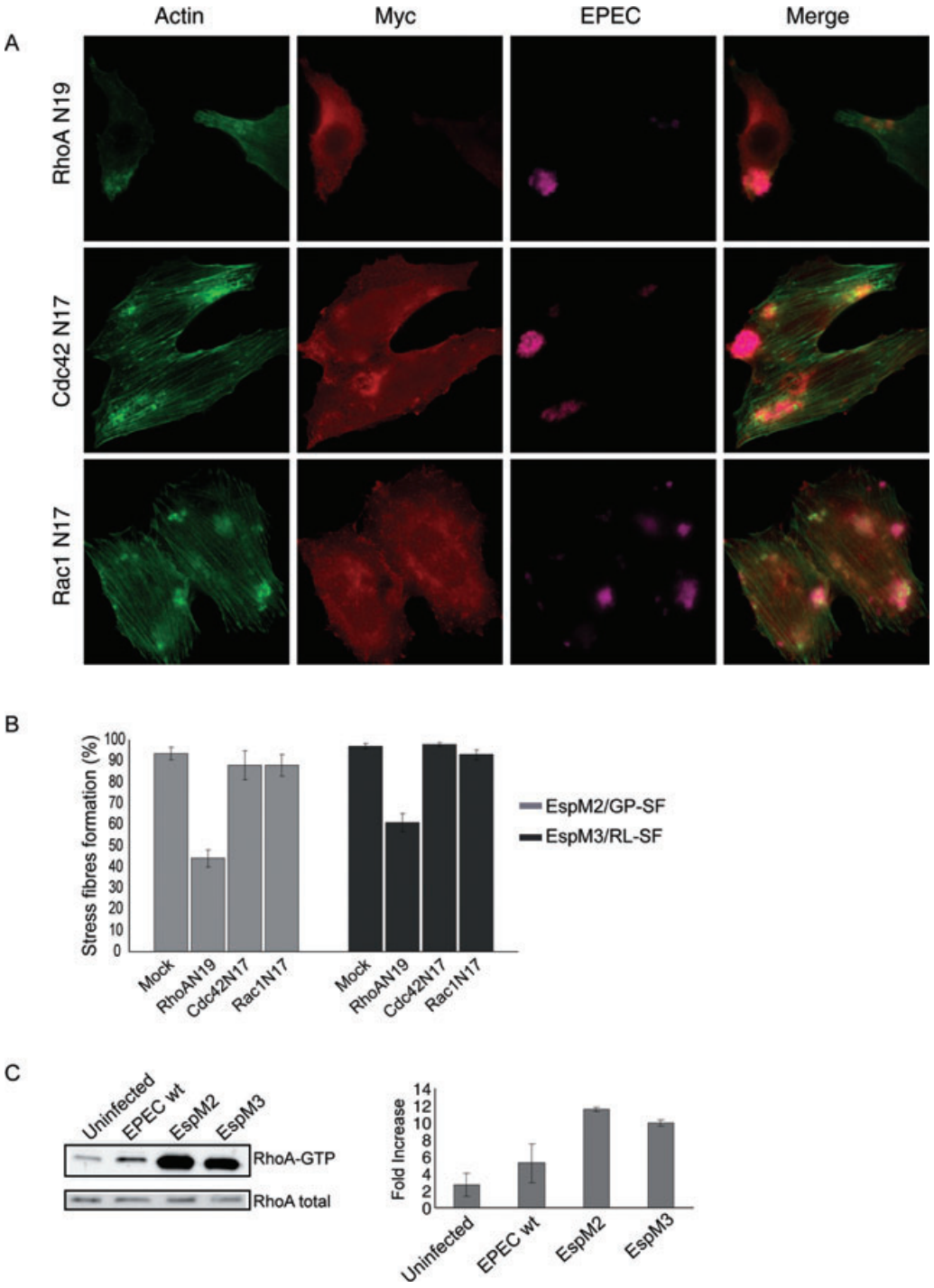


Fig. 4. Stress-fibre formation by EspM2 and EspM3 is RhoA-dependent.
A. Swiss 3T3 cells were transfected with dominant negative GTPase contracts 24 h prior to infection with E2348/69 expressing EspM2. Actin was stained with Oregon green phalloidin, the Myc-tagged GTPases with mouse anti-myc and EPEC with rabbit anti-O127. Actin-rich pedestals are observed under adherent bacteria in all transfected cells. GP-SF are observed, at the level of mock transfection, in cells transfected with dominant negatives $Cdc42^{N17}$ or $Rac1^{N17}$. In contrast, transfection with Rho^{N19} inhibited formation of GP-SF.
B. Quantification of stress-fibre formation in transfected Swiss 3T3 cells infected for 90 min with E2348/69 expressing EspM2 or EspM3. Formation of stress fibres in one hundred transfected infected cells were counted in triplicate from three independent experiments. Results are presented as mean ± SEM. Formation of stress fibres depending on EspM2 or EspM3 is affected by expression of $RhoA^{N19}$, but not by expression of $Cdc42^{N17}$ or Rac^{N17}.
C. Swiss 3T3 cells were infected with wild-type E2348/69 or E2348/69 expressing EspM2 or EspM3. Cells were lysed and a GST fusion of the Rho binding domain of Rhotekin was used to co-purify RhoA-GTP. Total RhoA in the lysates and RhoA-GTP were detected by Western blot with anti-RhoA antibodies. Quantified data are means ± SD of the results of three independent experiments.

© 2008 The Authors
Journal compilation © 2008 Blackwell Publishing Ltd,

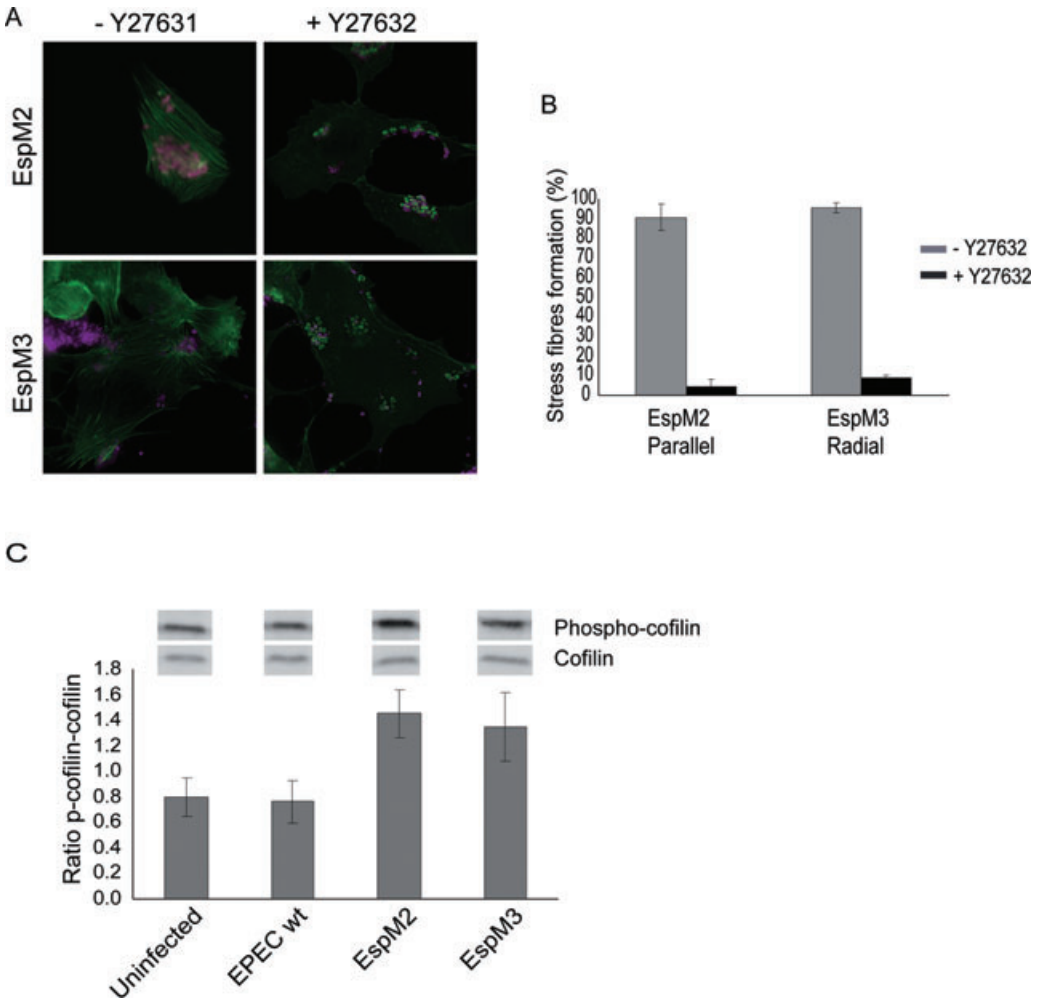


Fig. 5. EspM2 and EspM3 trigger the ROCK-LIMK-cofilin pathway.
A. Fluorescence microscopy of Swiss 3T3 cells incubated for 1 h in presence or absence of 10 μM of the ROCK inhibitor Y-27632 and infected for 90 min with E2348/69 expressing EspM2 or EspM3. Y-27632 did not affect formation of actin-rich pedestals, but abolished formation of stress fibres.
B. Percentage of Swiss 3T3 cells presenting stress fibres in the presence or absence of Y-27632. One hundred cells were counted in triplicate from three independent experiments. Results are presented as mean ± SEM.
C. Swiss 3T3 cells were infected for 90 min with wild-type E2348/69 or E2348/69 expressing EspM2 or EspM3. The levels of cofilin and phospho-cofilin were determined by Western blot using anti-cofilin and anti-phospho-cofilin antibodies. Quantification of densitometry was conducted using image J software and results presented here represent the mean ratio ± SD of four independent experiments.

was originally reported to bind the pilin protein BfpA and the outer membrane adhesion intimin (Tobe *et al*., 1999), suggesting that the TrcA might have a role in the bacterial cytosol prior to translocation into the host cell.

As EspM2 and EspM3 trigger the two extreme stress fibre phenotypes, they were chosen for detailed functional analysis. We confirmed that the GP-SF and LR-SF triggered by EspM2 and EspM3 are dependent on the conserved WxxxE motif via substitution of the conserved Trp with an Ala. However, using conservative substitutions, Tyr and Asp for the Trp and Glu, respectively, we did not observe any significant loss in biological activity. Translocation of EspM2 YxxxE and EspM2 WxxxD resulted in global stress-fibre formation, while translocation of EspM3 YxxxE and WxxxD resulted in formation of mainly LP-SF as compared with the LR-SF observed in the wild-type phenotype. The reason for the change of morphology observed for EspM3 YxxxE and WxxxD is currently not known.

These results suggest that the biological activity of the WxxxE proteins is not reliant upon the presence of the conserved tryptophan or glutamic acid, but rather the presence of a bulky aromatic residue and an amino acid carrying a carbocylic acid side group. Carboxylic side groups are involved in a range of biological functions such as protease activity (Kakudo *et al*., 1992) and interactions particularly with positively charged moieties such as metal ions.

© 2008 The Authors
Journal compilation © 2008 Blackwell Publishing Ltd,

Table 1. List of strains.

Strain	Description	Source/reference
E2348/69	Wild-type EPEC O127:H6	Levine *et al.* (1978)
ICC168	*C. rodentium*	Barthold *et al.* (1976); Wiles *et al.* (2004)
EHEC Sakai	Wild-type EHEC O157:H7 (RIMD 0509952)	Hayashi *et al.* (2001)
EPEC B171	Wild-type EPEC O111:NM	Riley *et al.* (1987)
ICC192	EPEC E2348/69Δ*escN*	Garmendia *et al.* (2004)
ICC202	EPEC E2348/69Δ*map*	Simpson *et al.* (2006)
ICC225	EPEC E2348/69Δ*tir*	Bai *et al.* (2008)
ICC243	EPEC E2348/69Δ*espG-espG2*	Marchès *et al.* (2008)

Further alanine substitutions of conserved residues did not abolish stress-fibre formation, suggesting that none of the selected residues on their own, other than the Typ and Glu, are essential for function. Structural data will be essential in order to gain further insights into the mechanism by which the conserved motif and surrounding residues lead to formation of the plethora actin structures associated with this family of effector proteins.

Using specific E2348/69 mutants, we have shown that stress-fibre formation was dependent on type III secretion but independent of other T3SS effectors, including Map, Tir, and EspG and EspG2. The later two were shown to induce late RhoA-dependent stress fibres by liberation of an active form of the RhoA-specific GEF, GEF-H1, as a result of disruption of the host cell microtubule network (Matsuzawa *et al*., 2004). This EspG activity might represent the small percentage (15%) of stress fibre seen in Swiss cells infected with wild-type E2348/69. The fact that EspM2 is necessary and sufficient for stress-fibre formation is supported by the fact that transfection of EspM2 into HeLa cells resulted in formation of characteristic GP-SF (data not shown).

The Ras superfamily of the small GTPases is the target of many bacterial effectors and toxins because of its role in the control of a wide range of cellular processes including cytoskeletal dynamics, membrane trafficking and growth. Several T3SS effectors, such as YopT from *Yersinia* spp., are known to directly modify the small GTPases (Wong and Isberg, 2005; Fueller *et al*., 2006). Other effectors can either modify or mimic GEFs or GAPs (Finlay, 2005). Although sharing no sequence homology with the Rho GTPases, Alto *et al.* (2006) suggested that IpgB1, IpgB2 and Map mimic, in a GTP-independent mechanism, the activated form of Rac1, RhoA and Cdc42, respectively. They showed that stress-fibre formation was RhoA-independent as IpgB2 was functional in the presence of RhoA inhibitors (e.g. C3 botulinum toxin) or dominant negative RhoA^{T19N}. Moreover, it was shown that IpgB2 interacts with two of the major effectors of RhoA, namely mDIA and ROCK, activating the latter directly.

Alto *et al.* (2006) reported that transfection of IpgB1 stimulated formation of actin-rich membrane ruffles at the dorsal cell surface, which resembled membrane ruffles induced by Rac-1. Dorsal ruffles were not produced by IpgB1^{E80A}. A recent study by Handa *et al.* (2007) has shown that IpgB1 mimics RhoG and triggers membrane ruffling by binding ELMO and recruiting the ELMO–Dock180 complex to the membrane where it functions as a GEF for Rac1.

In this investigation, we found that EspM2 and EspM3 activate RhoA. Using dominant negative RhoA^{T19N}, we observed a 60% and 40% reduction in stress-fibre formation after infection of Swiss cell with E2348/69 expressing EspM2 and EspM3 respectively. In agreement with Alto *et al.* (2006), using the specific ROCK inhibitor Y27632, we showed that the stress fibres induced by EspM2 and EspM3 are totally dependent upon ROCK activity. Consistent with this, we have shown that EspM2 and EspM3 trigger phosphorylation of cofilin, a classical downstream ROCK target. Although our data do not exclude the possibility that EspM2 and EspM3 are capable of mimicking RhoA to some degree, these effectors appear to contribute to stress-fibre production by activating endogenous RhoA. Alternatively, as was recently shown for IpgB1 (Handa *et al*., 2007), EspM might mimic GTPases upstream of RhoA activation. Further studies are needed to determine the mechanism of RhoA activation by EspM.

Experimental procedures

Bacterial strains, growth conditions and cell culture

The bacterial strains used in this study are listed in Table 1. Bacteria were grown from single colonies in Luria–Bertani (LB) broth in a shaking incubator at 37°C or maintained on LB plates. Culture media was supplemented with Ampicillin (100 μg ml^{-1}) as appropriate.

Bacterial cultures were primed prior to infection by growth in Dulbecco's modified Eagles media (DMEM) with 4500 mg ml^{-1} glucose supplemented with 1% mannose for 3 h (Collington *et al*., 1998) before addition of 1 mM IPTG to induce protein expression.

Swiss NIH 3T3 cells were maintained in DMEM with 4500 mg ml^{-1} glucose and supplemented with 10% fetal calf serum (Gibco) and 4 mM Glutamax (Gibco).

Bioinformatics

A PSI-BLAST search (Altschul *et al*., 1997) was performed under default conditions using IpgB2 from *Shigella flexneri*

© 2008 The Authors
Journal compilation © 2008 Blackwell Publishing Ltd,

Table 2. List of plasmids.

Name	Description	Reference
pSA10	pKK177-3 with Lac^q	Schlosser-Silverman *et al.* (2000)
pICC398	pSA10::*espM2* from O157:H7 Sakai fused to HA	This study
pICC399	pSA10::*espM3* from *C. rodentium* ICC169 fused to HA	This study
pICC400	pSA10::*espM2* from *C. rodentium* ICC169 fused to HA	This study
pICC401	pSA10::*espM1* from O157:H7 Sakai fused to HA	This study
pICC402	pSA10::*trcA* from O111:NM B171 fused to HA	This study
pICC403	pSA10::*espM1* from O111:NM B171 fused to HA	This study
pICC404	pSA10::*espM2*-W70A fused to HA	This study
pICC405	pSA10::*espM2*-W70Y fused to HA	This study
pICC406	pSA10::*espM2*-E74D fused to HA	This study
pICC407	pSA10::*espM3*-W66A fused to HA	This study
pICC408	pSA10::*espM3*-W66D fused to HA	This study
pICC409	pSA10::*espM3*-S9A + S12A fused to HA	This study
pICC410	pSA10::*espM3*-L114A fused to HA	This study
pICC411	pSA10::*espM3*-D115A fused to HA	This study
pICC412	pSA10::*espM3*-H125A fused to HA	This study
pICC413	PSA10::*espM3*-K149A fused to HA	This study
	pDEST53::*espM2*	Invitrogen, This study
	pRK5::*myc-rhoA*^{N17}	Pelletier *et al.* (2005)
	pRK5::*myc-rac1*^{N17}	Pelletier *et al.* (2005)
	pRK5::*myc-cdc42*^{N17}	Pelletier *et al.* (2005)
	pGex::*gst-RBD*	Sander *et al.* (1999)

(gi:13448971) and Map from EPEC (gi:2865296) as query sequence to search the latest version of the NCBI NR database and combined with a library of peptide sequences derived from all coding sequences ≥ 50 codons in length from the genome sequences of *C. rodentium* ICC168, EPEC B171 and EPEC E2348/69.

Multiple alignment and phylogenetic analysis of WxxxE effectors

Using the sequence alignment program Multalign, a radial phylogenetic tree was constructed based upon hierarchical clustering of the global sequence homology of the A/E pathogen group WxxxE proteins and IpgB1 compared with that of IpgB2. Protein sequences identified in the BLAST search that did not show near full-length homology to other EspM proteins were excluded from further analysis on the grounds that they are likely to represent non-functional pseudogenes.

Plasmids and molecular techniques

Plasmids used in this study are listed in Table 2; primers are listed in Table 3. The genes encoding effector proteins were amplified by PCR from genomic DNA and cloned into pSA10 with a C-terminal HA tag. *espM2* and *espM1* genes were amplified from EHEC O157:H7 strain Sakai, *trcA* and *espM1* genes were amplified from EPEC O111:NM strain B171 and *espM2* and *espM3* genes were amplified from *C. rodentium*. All constructs were verified by DNA sequencing.

The mammalian expression vector pRK5 containing one of Rho^{N19}, Rac^{N17} or Cdc42^{N17} dominant negatives used in the transfection assays was a gift from Nathalie Lamarche-Vane.The vector pGEX expressing the binding domain of Rhotekin fused to GST was a gift from J. Bertoglio.

Site-directed mutagenesis

Site-directed mutagenesis was carried out using a Quickchange II kit (Stratagene) according to the manufacturer's instructions. Primers were designed using the Quickchange mutagenic primer design program (Stratagene). Plasmids pSA10 containing *espM1*, *espM2*, *espM3 and trcA* were used as templates for the mutagenic reactions. Colonies were screened by sequencing and alignment to wild-type sequences to confirm mutagenesis.

Infection of Swiss 3T3 cells with EPEC E2348/69

Forty-eight hours prior to infection, Swiss 3T3 cells were seeded onto glass coverslips at a density of approximately 5×10^5 cells per well and maintained in DMEM 4500 supplemented with 10% FCS at 37°C in 5% CO_2. Three hours before infection, the cells were washed three times with PBS and the media replaced with fresh DMEM 4500 without FCS supplemented with 1% mannose. Overnight cultures of the appropriate bacteria were inoculated 1:50 into DMEM and primed as described previously (Collington *et al.*, 1998). Five hundred microlitres of primed bacteria was added to the wells and infections were carried out at 37°C in 5% CO_2 for 1.5 h.

Transfection

Swiss 3T3 cells were transfected with the mammalian expression vector pRK5 containing one of RhoA^{N19}, Rac^{N17} or Cdc42^{N17} dominant negatives fused to a Myc tag by lipofectamine2000 (Invitrogen) according to the manufacturer's recommendations. The cells were incubated at 37°C in a humidified incubator with 5% CO_2 for 24 h, washed twice in PBS before having their media replaced with DMEM as described previously. Transfected cells were infected with the appropriate strain as described above.

© 2008 The Authors
Journal compilation © 2008 Blackwell Publishing Ltd,

Table 3. List of primers.

Primer	Sequence
EspM3-S9A_S12A-F	5′-ccagtgaatgttcaaggtttagcttttaatgcttttggtatcagctgccatc-3′
EspM3-S9A_S12A-R	5′-gatggcagctgataccaaaagcattaaaagctaaaccttgaacattcactgg-3′
EspM3-W66A-F	5′-gcagagtactaaagatattgatggagcgataaaagatgaacagaaagtgtat-3′
EspM3-W66A-R	5′-atacactttctgttcatcttttatcgctccatcaatatctttagtactctgc-3′
EspM3-H125A-F	5′-ggagcagctcaaagctccatcaatgctatgataataggaaatggtt-3′
EspM3-H125A-R	5′-aaccatttcctattatcatagcattgatggagctttgagctgctcc-3′
EspM3-Y188F-F	5′-gtatgattcctcgttatatgaggtttgctatatcgctgtacc-3′
EspM3-Y188F-R	5′-ggtacagcgatatagcaaacctcatataacgaggaatcatac-3′
EspM3-D115A-F	5′-ttatggcctggaacttgcttctggagcagctcaaa-3′
EspM3-D115A-R	5′-tttgagctgctccagaagcaagttccaggccataa-3′
EspM3-L114A-F	5′-tttcaaagcattatggcctggaagctgattctggagcagc-3′
EspM3-L114A-R	5′-gctgctccagaatcagcttccaggccataatgctttgaaa-3′
EspM2Cr-W66A-F	5′-ggcagagcactaaagatcttttagcagcgaaaaaagatgaaaaagtaatttatc-3′
EspM2Cr-W66A-R	5′-gataaattacttttttcatctttttcgctgctaaaagatctttagtgctctgcc-3′
EspM2Cr-H125A-F	5′-gcccgctcagcacaaagttctataaatgctatcataaccggaaa-3′
EspM2Cr-H125A-R	5′-tttccggttatgatagcatttatagaactttgtgctgagcgggc-3′
EspM3-K149A-F	5′-cgaggggatgaccaggaatgtagcaaatcatacatcagattacatg-3′
EspM3-K149A-R	5′-catgtaatctgatgtatgatttgctacattcctggtcatcccctcg-3′
EspM3-W66Y-F	5′-gcagagtactaaagatattgatggatatataaaagatgaacagaaagtgtatcc-3′
EspM3-W66Y-R	5′-ggatacactttctgttcatcttttatatatccatcaatatctttagtactctgc-3′
EspM3-E70D-F	5′-tgatggatggataaaagatgatcagaaagtgtatccatcaagg-3′
EspM3-E70D-R	5′-ccttgatggatacactttctgatcatcttttatccatccatca-3′
EspM2-W70Y-F	5′-gcagagtactaaagatattgatgagtatataaaagatgaacggatagtatatcc-3′
EspM2-W70Y-R	5′-ggatatactatccgttcatcttttatatactcatcaatatctttagtactctgc-3′
EspM2-E74D-F	5′-taaagatattgatgagtggataaaagatgatcggatagtatatccctc-3′
EspM2-E74D-R	5′-gagggatatactatccgatcatcttttatccactcatcaatatcttta-3′
EspM1-pKK-F	5′-ttgaattcatgccagtaaatgcgacagg-3′
EspM1-pKK-R	5′-ccaatgcactgcagttaagcgtagtctgggacgtcgtatgggtacccctgtataacacgactca-3′
EspM2-pKK-F	5′-tttgaattcatgccgatgaatactacaggtatgt-3′
EspM2-pKK-R	5′-tttctgcagtcaagcgtagtctgggacgtcgtatgggtatccctgtatagcacgcatcaa-3′
EspM2 W70A-F	5′-gcagagtactaaagatattgatgaggcgataaaagatgaacggatagtatat-3′
EspM2 W70A-R	5′-atatactatccgttcatcttttatcgcctcatcaatatctttagtactctgc-3′
EspM3-pKK-F	5′-ttgaattcatgccagtgaatgttcaagg-3′
EspM3-pKK-R	5′-ttgcctgcagttaagcgtagtctgggacgtcgtatgggtacacgatatagcatacctca-3′
EspM2Cr-pKK-F	5′-ttgaattcatgccagcgaatatatcagg-3′
EspM2Cr-pKK-R	5′-ttgtcgacttaacttaagcgtagtctgggacgtcgtatgggtatgccgacatggcatttgcca-3′
TrcA-pKK-F	5′-ttgaattcatgccgatgaatactacaagtac-3′
TrcA-pKK-R	5′-aactgcagttaagcgtagtctgggacgtcgtatgggtatgcctgtatagcacacctca-3′
EspM1 B171-pKK-F	5′-tacccatacgacgtcccagactacgct-3′
EspM1 B171-pKK2-R	5′-ccaatgcactgcagttaagcgtagtctgggacgtcgtatgccgatatgacgctggcag-3′

Immunofluorescence staining and microscopy

Coverslips were washed three times in PBS and fixed with 3% Paraformaldehyde for 15 min before washing three more times in PBS. For immunostaining, the cells were permeabilized for 5 min in PBS 0.5%/Triton X-100, washed three times in PBS and quenched for 30 min with 50 mM NH_4Cl. The coverslips were then blocked for 1 h with PBS/0.5% BSA before incubation with primary and secondary antibodies. The primary antibody Mouse αVinculin (Abcam) and mouse anti-Myc (Millipore) were used at a dilution of 1:200, while Rabbit αO127 was used at a dilution of 1:150. Coverslips were incubated with the primary antibody for 1 h, washed three times in PBS and incubated with the secondary antibodies. Donkey anti-rabbit IgG conjugated to a Cy5 fluorophore or Donkey anti-mouse IgG conjugated to a Cy3 fluorophore (Jackson laboratories) was used at a 1:200 dilution. Actin was stained using Oregon Green phalloidin (Invitrogen) at a 1:100 dilution. All dilutions were in PBS/0.5% BSA. Coverslips were mounted on slides using ProLong Gold anti-fade reagent (Invitrogen) and visualized by Zeiss Axioimager immunofluorescence microscope (100× objective giving a total magnification of 1000×) using the following excitation wavelengths: Cy3 – 605 nm, Cy5 – 690 nm and Oregon Green – 525 nm. All images were analysed using the Axiovision Rel 4.5 software and trimmed to 5 cm^2 (300 pixels) using Adobe photoshop.

Chemical inhibition of ROCK activity

Coverslips were set up for infection as described above. One hour prior to infection, Y-27632 (Sigma) was added to cells to attain a final concentration of 10 μM per well. Coverslips were infected and processed for immunofluorescence.

Quantification of cofilin phosphorylation

Forty-eight hours prior to infection, Swiss 3T3 cells were seeded onto 6-well plates to attain confluent monolayer. Each well was infected as described above. After a 1.5 h infection, cells were lysed by addition of 4× protein SDS-PAGE loading buffer. The lysate was harvested and heated at 100°C for 5 min before loading in duplicate onto a 12% SDS-PAGE gel. The proteins were then transferred to PVDF by wet transfer. The PVDF mem-

© 2008 The Authors

branes were blocked overnight in TBS 5%/BSA at 4°C with gentle rocking. Each membrane was incubated in either monoclonal mouse anti-cofilin (Cell Signalling Technology) or mouse anti-Phospho-cofilin (Cell Signalling Technology) at a dilution of 1:1000 in TBS 5%/BSA for 1 h at room temperature with gentle rocking. The membranes were washed five times in TBS 1%/Tween for 5 min and incubated for 45 min with a 1:3000 dilution of Goat α Mouse (Invitrogen) secondary antibody coupled to HRP at room temperature. The membranes were developed using ECL reagents (GE healthcare) before detection using chemiluminescence in a LAS 3000 Fugi imager. Western blots were analysed by densitometry using ImageJ software. Results presented are the average of five independent experiments.

Preparation of GST-Rhotekin and RhoA-GTP pull-downs

An overnight culture of *E. coli* BL21 expressing pGEX encoding the RhoA binding domain of Rhotekin was diluted 1:20 and cultured at 30°C until OD_{260nm} reached 0.7; the culture was induced with 1 mM IPTG and incubated for a further 4 h. The bacterial culture was aliquoted into 50 ml falcon tubes and centrifuged for 15 min at 4600 r.p.m. at 4°C and the pellets stored at –80°C. The pellets were resuspended in lysis buffer [20% Saccharose, 10% glycerol, 50 mM Tris pH 8, 200 mM $Na_2S_2O_3$, 2 mM $MgCl_2$, 2 mM DTT and 1% protease inhibitor cocktail (Sigma)] and sonicated five times for 10 s. The solution was centrifuged for 30 min at 15 000 r.p.m. at 4°C and the supernatants harvested and coupled to GST-glutathione S transferase beads for 45 min at 4°C.

The 75 cm^2 cell culture flasks were seeded with Swiss 3T3 cells, infected as described above and the cells lysed in 750 µl of Mg^{++} buffer [25 mM Hepes, pH 7.5, 150 mM NaCl, 1% NP-40, 10 mM $MgCl_2$, 5% glycerol, 1 mM EDTA and protease inhibitors (Sigma)]. The lysate was transferred to a pre-chilled eppendorf tube and centrifuged at 14 000 r.p.m. for 5 min at 4°C. The cleared lysate was transferred to a fresh pre-chilled eppendorf tube containing 30 µl of GST-Rhotekin-RBD beads. The lysate was incubated with the beads for 1 h at 4°C. The suspension was washed three times in Mg^{++} buffer spinning down at 14 000 r.p.m. at 4°C between each wash. The beads were eluted by the addition of 45 µl of 2× protein loading buffer and the samples heated at 100°C for 5 min. The samples were loaded on a 15% SDS-PAGE gel. The gels were transferred to PVDF and blotted as previously described using monoclonal RhoA antibody (Santa Cruz).

Acknowledgements

We thank Francis Girard for editorial help. A.A. is supported by Becas de Formacion de Investigadores, Gobierno Vasco, Spain. The project was supported by the Wellcome Trust and the Medical Research Council.

References

Alto, N.M., Shao, F., Lazar, C.S., Brost, R.L., Chua, G., Mattoo, S., *et al.* (2006) Identification of a bacterial type III effector family with G protein mimicry functions. *Cell* **124:** 133–145.

Altschul, S.F., Madden, T.L., Schäffer, A.A., Zhang, J., Zhang, Z., Miller, W., and Lipman, D.J. (1997) Gapped BLAST and PSI-BLAST: a new generation of protein database search programs. *Nucleic Acids Res* **25:** 3389–3402.

Bai, L., Schüller, S., Whale, A., Mousnier, A., Marches, O., Wang, L., *et al.* (2008) Enteropathogenic *Escherichia coli* (EPEC) O125: H6 triggers attaching and effacing lesions on human intestinal biopsies independently of Nck and TccP/TccP2. *Infect Immun* **76:** 361–368.

Barthold, S.W., Coleman, G.L., Bhatt, P.N., Osbaldiston, G.W., and Jonas, A.M. (1976) The etiology of transmissible murine colonic hyperplasia. *Lab Anim Sci* **26:** 889–894.

Beuzon, C.R., Meresse, S., Unsworth, K.E., Ruiz-Albert, J., Garvis, S., Waterman, S.R., *et al.* (2000) *Salmonella* maintains the integrity of its intracellular vacuole through the action of SifA. *EMBO J* **19:** 3235–3249.

Campellone, K.G., Robbins, D., and Leong, J.M. (2004) $EspF_U$ Is a translocated EHEC effector that interacts with Tir and N-WASP and promotes Nck-independent actin assembly. *Dev Cell* **7:** 217–228.

Charpentier, X., and Oswald, E. (2004) Analysis of type III translocation signals of enteropathogenic and enterohemorrhagic *Escherichia coli* effectors using TEM-1 beta-lactamase as a fluorescence-based reporter. *J Bacteriol* **186:** 5486–5495.

Collington, G.K., Booth, I.W., and Knutton, S. (1998) Rapid modulation of electrolyte transport in Caco-2 cell monolayers by enteropathogenic *Escherichia coli* (EPEC) infection. *Gut* **42:** 200–207.

Corpet, F. (1988) Multiple sequence alignment with hierarchical clustering. *Nucleic Acids Res* **16:** 10881–10890.

Cossart, P., and Sansonetti, P.J. (2004) Bacterial invasion: the paradigms of enteroinvasive pathogens. *Science* **304:** 242–248.

DeBrabander, M.J., Van de Viere, F.E.M., Aerts, M., Borgers, P.A., and Jannsen, P.A. (1976) The effects of nocodazole, a new synthetic antitumoral drug interfering with microtubules, on mammalian cells cultured in vitro. *Cancer Res* **36:** 905–916.

Finlay, B.B. (2005) Bacterial virulence strategies that utilize Rho GTPases. *Curr Top Microbiol Immunol* **291:** 1–10.

Fueller, F., Bergo, M.O., Young, S.G., Aktories, K., and Schmidt, G. (2006) Endoproteolytic processing of RhoA by Rce1 is required for the cleavage of RhoA by *Yersinia enterocolitica* outer protein T. *Infect Immun* **74:** 1712–1717.

Galan, J.E., and Wolf-Watz, H. (2006) Protein delivery into eukaryotic cells by type III secretion machines. *Nature* **444:** 567–573.

Garmendia, J., Phillips, A., Chong, Y., Schuller, S., Marches, O., Dahan, S., *et al.* (2004) TccP is an enterohaemorrhagic *E. coli* O157:H7 type III effector protein that couples Tir to the actin-cytoskeleton. *Cell Microbiol* **6:** 1167–1183.

Handa, Y., Suzuki, M., Ohya, K., Iwai, H., Ishijima, N., Koleske, A.J., *et al.* (2007) *Shigella* IpgB1 promotes bacterial entry through the ELMO-Dock180 machinery. *Nat Cell Biol* **9:** 121–128.

Hayashi, T., Makino, K., Ohnishi, M., Kurokawa, K., Ishii, K., Yokoyama, K., *et al.* (2001) Complete genome sequence of enterohemorrhagic *Escherichia coli* O157:H7 and genomic comparison with a laboratory strain K-12. *DNA Res* **28:** 11–22.

© 2008 The Authors
Journal compilation © 2008 Blackwell Publishing Ltd,

Imamura, H., Takaishi, K., Nakano, K., Kodama, A., Oishi, H., Shiozaki, H., *et al.* (1998) Rho and Rab small G proteins coordinately reorganize stress fibers and focal adhesions in MDCK cells. *Mol Biol Cell* **9:** 2561–2575.

Jaffe, A.B., and Hall, A. (2005) Rho GTPases: biochemistry and biology. *Ann Rev Cell Dev Biol* **21:** 247–269.

Kakudo, S., Kikuchi, N., Kitadokoro, K., Fujiwara, T., Nakamura, E., Okamoto, H., *et al.* (1992) Purification, characterization, cloning, and expression of a glutamic acid-specific protease from *Bacillus licheniformis* ATCC 14580. *J Biol Chem* **267:** 23782–23788.

Kaper, J.B., Nataro, J.P., and Mobley, H.L. (2004) Pathogenic *Escherichia coli*. *Nat Rev Microbiol* **2:** 123–140.

Kenny, B., and Jepson, M. (2000) Targeting of an enteropathogenic *Escherichia coli* (EPEC) effector protein to host mitochondria. *Cell Microbiol* **2:** 579–590.

Kenny, B., DeVinney, R., Stein, M., Reinscheid, D.J., Frey, E.A., and Finlay, B.B. (1997) Enteropathogenic *E. coli* (EPEC) transfers its receptor for intimate adherence into mammalian cells. *Cell* **91:** 511–520.

Kenny, B., Ellis, S., Leard, A.D., Warawa, J., Mellor, H., and Jepson, M.A. (2002) Co-ordinate regulation of distinct host cell signalling pathways by multifunctional enteropathogenic *Escherichia coli* effector molecules. *Mol Microbiol* **44:** 1095–1107.

Knutton, S., Lloyd, D.R., and McNeish, A.S. (1987) Adhesion of enteropathogenic *Escherichia coli* to human intestinal enterocytes and cultured human intestinal mucosa. *Infect Immun* **55:** 69–77.

Levine, M.M., Bergquist, E.J., Nalin, D.R., Waterman, D.H., Hornick, R.B., Young, C.R., and Sotman, S. (1978) *Escherichia coli* that cause diarrhoea but do not produce heat-labile or heat-stable enterotoxins and are non-invasive. *Lancet* **i:** 119–122.

Maekawa, M., Ishizaki, T., Boku, S., Watanabe, N., Fujita, A., Iwamatsu, A., *et al.* (1999) Signaling from Rho to the actin cytoskeleton through protein kinases ROCK and LIM-kinase. *Science* **285:** 895–898.

Marchès, O., Covarelli, V., Dahan, S., Cougoule, C., Bhatta, P., Frankel, G., and Caron, E. (2008) EspJ of enteropathogenic and enterohaemorragic *Escherichia coli* inhibits opsono-phagocytosis. *Cell Microbiol* (epub ahead of print) doi:10.1111/j.1462-5822.2007.01112.x

Matsuzawa, T., Kuwae, A., Yoshida, S., Sasakawa, C., and Abe, A. (2004) Enteropathogenic *Escherichia coli* activates the RhoA signaling pathway via the stimulation of GEF-H1. *EMBO J* **23:** 3570–3582.

Ohya, K., Handa, Y., Ogawa, M., Suzuki, M., and Sasakawa, C. (2005) IpgB1 is a novel Shigella effector protein involved in bacterial invasion of host cells. Its activity to promote membrane ruffling via Rac1 and Cdc42 activation. *J Biol Chem* **280:** 24022–24034.

Pelletier, S., Julien, C., Popoff, M.R., Lamarche-Vane, N., and Meloche, S. (2005) Cyclic AMP induces morphological changes of vascular smooth muscle cells by inhibiting a Rac-dependent signaling pathway. *J Cell Physiol* **204:** 412–422.

Riley, L.W., Junio, L.N., Libaek, L.B., and Schoolnik, G.K. (1987) Plasmid-encoded expression of lipopolysaccharide O-antigenic polysaccharide in enteropathogenic *Escherichia coli*. *Infect Immun* **55:** 2052–2056.

Sander, E.E., ten Klooster, J.P., van Delft, S., van der Kammen, R.A., and Collard, J.G. (1999) Rac down-regulates Rho activity: reciprocal balance between both GTPases determines cellular morphology and migratory behavior. *J Cell Biol* **147:** 1009–1022.

Schlosser-Silverman, E., Elgrably-Weiss, M., Rosenshine, I., Kohen, R., and Altuvia, S. (2000) Characterization of *Escherichia coli* DNA lesions generated within J774 macrophages. *J Bacteriol* **182:** 5225–5230.

Shaw, R.K., Smollett, K., Cleary, J., Garmendia, J., Straatman-Iwanowska, A., Frankel, G., and Knutton, S. (2005) Enteropathogenic *E. coli* type III effectors EspG and EspG2 disrupt the microtubule network of intestinal epithelial cells. *Infect Immun* **73:** 4385–4390.

Simpson, N., Shaw, R., Mundy, R., Crepin, V., FitzGerald, A.J., Cummings, N., *et al.* (2006) The enteropathogenic *E. coli* type III secretion system effector Map binds EBP50/NHERF1: implication for cell signalling and diarrhoea. *Mol Microbiol* **60:** 349–363.

Tobe, T., Tatsuno, I., Katayama, E., Wu, C.Y., Schoolnik, G.K., and Sasakawa, C. (1999) A novel chromosomal locus of enteropathogenic *Escherichia coli* (EPEC), which encodes a bfpT-regulated chaperone-like protein, TrcA, involved in microcolony formation by EPEC. *Mol Microbiol* **33:** 741–752.

Tobe, T., Beatson, S.A., Taniguchi, H., Abe, H., Bailey, C.M., Fivian, A., *et al.* (2006) Extensive repertoire of type III secretion effectors in *Escherichia coli* O157 and the role of lambdoid phages in their dissemination. *Proc Natl Acad Sci USA* **103:** 14941–14946.

Wiles, S., Clare, S., Harker, J., Huett, A., Young, D., Dougan, G., *et al.* (2004) Organ-specificity, colonization and clearance dynamics *in vivo* following oral challenges with the murine pathogen *Citrobacter rodentium*. *Cell Microbiol* **6:** 963–972. Erratum. In: *Cell Microbiol* 2005, **7:** 459.

Wong, K.W., and Isberg, R.R. (2005) *Yersinia pseudotuberculosis* spatially controls activation and misregulation of host cell Rac1. *PloS Pathog* **1:** 125–136.

Yamaguchi, H., Miwa, Y., Kasa, M., Kitano, K., Amano, M., Kaibuchi, K., and Hakoshima, T. (2006) Structural basis for induced-fit binding of Rho-kinase to the inhibitor Y-27632. *J Biochem* **140:** 305–311.

Ziegler, W.H., Liddington, R.C., and Critchley, D.R. (2006) The structure and regulation of vinculin. *Trends Cell Biol* **16:** 453–460.

© 2008 The Authors
Journal compilation © 2008 Blackwell Publishing Ltd,

Cellular Microbiology (2009) **11**(2), 217–229
doi:10.1111/j.1462-5822.2008.01248.x
First published online 31 October 2008

EspT triggers formation of lamellipodia and membrane ruffles through activation of Rac-1 and Cdc42

Richard R. Bulgin,† Ana Arbeloa,† Jade C. S. Chung and Gad Frankel*
Centre for Molecular Microbiology and Infection, Division of Cell and Molecular Biology, Imperial College, London SW7 2AZ, UK.

Summary

Subversion of the eukaryotic cell cytoskeleton is a virulence strategy employed by many bacterial pathogens. Due to the pivotal role of Rho GTPases in actin dynamics they are common targets of bacterial effector proteins and toxins. IpgB1, IpgB2 (*Shigella*), SifA, SifB (*Salmonella*) and Map and EspM (attaching and effacing pathogens) constitute a family of type III secretion system effectors that subverts small GTPase signalling pathways. In this study we identified and characterized EspT from *Citrobacter rodentium* that triggers formation of lamellipodia on Swiss 3T3 and membrane ruffles on HeLa cells, which are reminiscent of the membrane ruffles induced by IpgB1. Ectopic expression of EspT and IpgB1, but not EspM, resulted in a mitochondrial localization. Using dominant negative constructs we found that EspT-induced actin remodelling is dependent on GTP-bound Rac-1 and Cdc42 but not ELMO or Dock180, which are hijacked by IpgB1 in order to form a Rac-1 specific guanine nucleotide exchange factor. Using pull-down assays with the Rac-1 and Cdc42 binding domains of Pak and WASP we demonstrate that EspT is capable of activating both Rac-1 and Cdc42. These results suggest that EspT modulates the host cell cytoskeleton through coactivation of Rac-1 and Cdc42 by a distinct mechanism.

Introduction

Subversion and modulation of host cell signalling networks is essential for effective invasion and colonization of a wide variety of bacterial pathogens. In order to facilitate the hijacking of essential host processes many bacterial pathogens employ one or a combination of secretion systems (reviewed in Filloux *et al*., 2008). These complex machines are capable of delivering a wide variety of toxins, colonization factors and effectors either in proximity to epithelium or directly into the host cell (reviewed in Gerlach and Hensel, 2007). A wide variety of Gram-negative pathogens utilize type III secretion systems (T3SS) in order to translocate effector proteins directly from the bacterial cell into the cytoplasm of the mammalian cell (reviewed in Galan and Wolf-Watz, 2006). The translocated effector proteins are directed to distinct cellular compartments where, by interacting with indigenous proteins, they form novel complexes that modulate a variety of signalling networks for the benefit of the bacterial cell.

The medically important enteropathogenic and entero-haemorrhagic *Escherchia coli* (EPEC and EHEC) (reviewed in Nataro and Kaper, 1998), along with the murine pathogen *Citrobacter rodentium* (reviewed in Mundy *et al*., 2005), are extracellular bacterial pathogens, which intimately adhere to host enterocytes causing distinctive attaching and effacing (A/E) lesions characterized by the local disruption of the brush border microvili (Knutton *et al*., 1987). Colonization and persistence of EPEC, EHEC and *C. rodentium* is dependent upon a T3SS-encoded within the locus of enterocyte effacement (LEE) (McDaniel *et al*., 1995). This T3SS translocates a plethora of effector proteins that are located both within the LEE and on a variety of other pathogenicity islands and prophages (Tobe *et al*., 2006). EPEC, EHEC and *C. rodentium* translocate their own receptor, Tir (Kenny *et al*., 1997), into mammalian cells that binds the bacterial outer membrane adhesisn intimin (reviewed in Frankel *et al*., 2001), resulting in Tir clustering and formation of actin-rich pedestals beneath adherent bacteria *in vitro* (reviewed in Frankel and Phillips, 2008). Other A/E bacterial effectors that target and modulate the host cell cytoskeleton include EspG and EspG2, which disrupt the host cell microtubule network (Matsuzawa *et al*., 2004; Shaw *et al*., 2005), Map, which induces transient filopodia formation (Kenny and Jepson, 2000) and EspM, which activates the small GTPase RhoA and induces formation of stress fibres (Arbeloa *et al*., 2008).

Small GTPases act as molecular switches that cycle between an inactive GDP bound form and an active GTP

Received 5 August, 2008; revised 30 September, 2008; accepted 3 October, 2008. *For correspondence. E-mail g.frankel@imperial.ac.uk; Tel. (+44) 2075 945 253; Fax (+44) 2075 943 069. †These authors are equal contributors.
Re-use of this article is permitted in accordance with the Creative Commons Deed, Attribution 2.5, which does not permit commercial exploitation.

© 2008 The Authors
Journal compilation © 2008 Blackwell Publishing Ltd

bound form. The switch from inactive to active forms of the GTPase results in a conformational change. This process is regulated by a variety of accessory proteins. Guanine exchange factors (GEFs) activate GTPases by promoting the dissociation of GDP and the binding of GTP, GTPase-activating proteins (GAPs) inactivate the small GTPases by stimulating their intrinsic GTPase activity. Guanine dissociation inhibitor (GDI) proteins cap the small GTPases preventing the dissociation of GDP and membrane localization (reviewed in Jaffe and Hall, 2005). Rho GTPases modulate a variety of host cell processes in a GTP-dependent manner by activating a plethora of downstream effectors at specific host cell compartments (Stebbins and Galan, 2001). The three best characterized Rho GTPases are RhoA, Rac-1 and Cdc42, which are implicated in formation of stress fibres, lamellipodia and filopodia respectively (Jaffe and Hall, 2005).

Recently, Alto and co-workers grouped together several previously known T3SS effector proteins which share a conserved WxxxE motif and induce the same actin structures as active Rho family GTPases (Alto *et al*., 2006). These effectors include IpgB1 and IpgB2, which are required during *Shigella* invasion (Ohya *et al*., 2005), SifA and SifB which are involved in maintenance of the *Salmonella* containing vacuole (Beuzon *et al*., 2000) and Map. In addition, we recently identified EspM effectors in EPEC, EHEC and *C. rodentium*, which share significant homology with IpgB2 (Arbeloa *et al*., 2008). Using IpgB1, IpgB2 and Map, Alto *et al*. (2006) showed that the activity of these proteins in modulating actin dynamics requires the conserved tryptophan and glutamic acid residues. They also demonstrated that the formation of stress fibres induced by IpgB2 and the filopodia nucleated by Map occurred independently of the activity of RhoA and Cdc42 respectively. It was suggested that IpgB1 mimics Rac-1, IpgB2 mimics RhoA and Map mimics Cdc42 (Alto *et al*., 2006). However, a recent report by Handa *et al*. (2007) demonstrated that IpgB1 binds to the RhoG effector ELMO which in turn recruits the GEF Dock180 and subsequently activates endogenous Rac-1 to produce the membrane ruffles, while we demonstrated that EspM-induced stress fibre formation is dependent on the activation of RhoA (Arbeloa *et al*., 2008). Browsing the ongoing genome sequencing projects of A/E pathogens we recently identified a novel WxxxE effector gene, we named *espT*, in *C. rodentium*. The aim of this study was to conduct phenotypic and functional analysis of EspT.

Results

Identification of EspT

Recently, we identified EspM1 and EspM2 in EHEC O157:H7 (strains Sakai and EDL933), TrcA and EspM1 in EPEC O111:NM (strain B171) and EspM2 and EspM3 in *C. rodentium* as members of the WxxxE family of effectors (Arbeloa *et al*., 2008). Using the BLAST algorithm with IpgB2 and Map as index proteins to search for new WxxxE family members within the A/E pathogen group, we identified a new putative effector, whose encoding gene we have named *espT*, in *C. rodentium* (Accession number: FM210026). EspT is encoded within the same pathogenicity island as EspM2, which also encodes an EspO/OspE homologue (Fig. 1A). OspE2 is a T3SS effector, which localizes to focal adhesions and regulate cell shape upon *Shigella sonnei* infection (Miura *et al*., 2006). EspT shares 29% identity with EspM2, 27% identity with IpgB2, and 19% identity with IpgB1. A phylogram based upon multiple sequence alignment with hierarchical clustering (Mackey *et al*., 2002) shows that EspT is divergent from the EspM/IpgB2 and does not cluster well with either IpgB1 or Map (Fig. 1C).

EspT triggers formation of lamellipodia and membrane ruffles

Previously characterized WxxxE effectors have been reported to induce a plethora of actin structures normally associated with activated Rho GTPases (Alto *et al*., 2006; Handa *et al*., 2007; Arbeloa *et al*., 2008). In order to determine if EspT has the ability to remodel actin within eukaryotic cells, *espT* was cloned into the expression vector pSA10 (Schlosser-Silverman *et al*., 2000) and expressed in EPEC E2348/69, which does not contain any WxxxE effectors other than Map (Arbeloa *et al*., 2008). T3SS-dependent translocation of EspT from E2348/69 into mammalian cells was confirmed using a β-lactamase fusion assay (data not shown). E2348/69 with or without the vector-encoding EspT was used to infect serum-starved Swiss 3T3 and HeLa cells. E2348/69 with no plasmid or carrying empty pSA10 triggered formation of actin-rich pedestals beneath adherent bacteria on both Swiss 3T3 and HeLa cells, without any other major cytoskeletal alterations (Fig. 2). In contrast, E2348/69 carrying pSA10-encoding EspT induced formation of pedestals on both cell lines and additionally triggered formation of lamellipodia on Swiss 3T3 cells and membrane ruffles on HeLa cells, which were not restricted to the site of bacterial attachment (Fig. 2A and B). The lamellipodia induced by EspT have a strong leading edge, wide lamella, well-defined microspikes and filopodia, which extend beyond the cell periphery (Fig. 2A). These lamellipodia and membrane ruffles were found in 90% and 80% of cells infected with E2348/69, respectively, after 1.5 h (Fig. 2C) and were still present at 3 h post infection. The E2348/69 type III secretion null mutant, Δ*escN*, carrying pSA10::*espT* did not produce actin-rich pedestals, lamellipodia or membrane ruffles (data not shown). These results demonstrate that

© 2008 The Authors

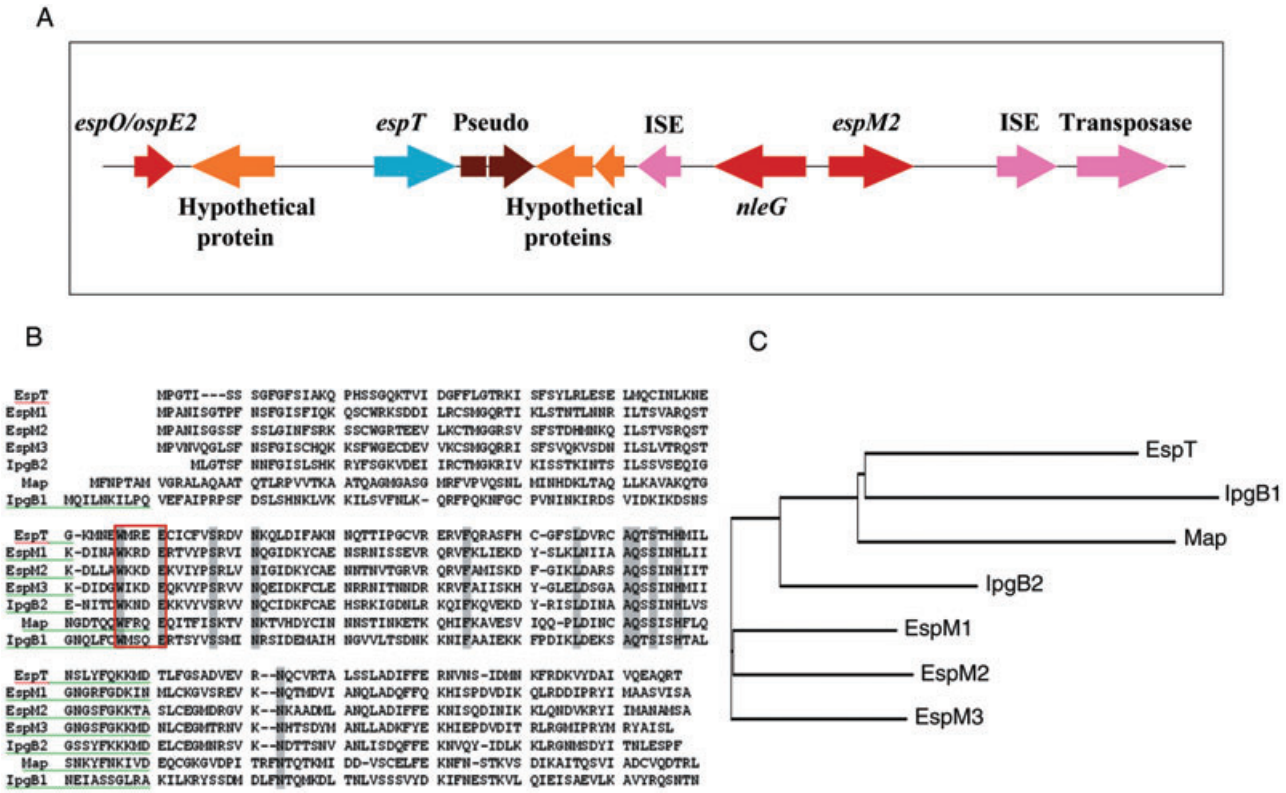


Fig. 1. A. A graphical representation of the *espT* pathogenicity island of *C. rodentium*.
B. Multiple sequence alignment with hierarchical clustering of *Shigella flexneri* IpgB1 and IpgB2 along with Map, EspM2, EspM3 and EspT from *C. rodentium* and EspM1 from EPEC B171 O111:NM. Residues that are identical are highlighted in grey. The conserved WxxxE motif is boxed.
C. Phenogram created using ClustalW2 showing the phylogeny of aligned WxxxE effectors.

EspT is a T3SS effector that upon tranlocation triggers formation of lamellipodia and membrane ruffles and that the nature of actin rearrangement was cell type-specific.

EspT is sufficient for lamellipodia and membrane ruffle formation

Ectopic expression of *espT*, fused to a myc tag, from the mammalian expression vector pRK5 in Swiss 3T3 cells resulted in formation of lamellipodia that were indistinguishable from those visualized when EspT was delivered by E2348/69 (Fig. 3). Tranfection of EspT into HeLa cells induced formation of membrane ruffles identical to those observed during infection (data not shown). Thus, EspT is necessary and sufficient for these re-arrangements of the actin cytoskeleton. It has been previously shown that ectopic expresion of the *Shigella* effector *IpgB1* induces formation of membrane ruffles in HeLa cells (Alto *et al*., 2006; Handa *et al*., 2007). As such we transfected IpgB1, fused to a N-terminal myc tag, into HeLa and Swiss 3T3 cells as a control. In agreement with previous data (Handa *et al*., 2007), we found that IpgB1 induce membrane ruffles on HeLa cells. However, in contrast to the result we obtained for EspT, we found that IpgB1 also induces membrane ruffles in Swiss 3T3 cells (Fig. 3).

Additionally, we found that at 16 h post transfection EspT was targeted to the mitochondria, as shown by double staining with anti-myc antibodies and Mitotracker CMXRos (Fig. 3). Similarly, 16 h post transfection IpgB1 was also found in the mitochondria, while EspM2 was uniformly distributed in the cytosol (Fig. 3). Although the mitochondria appeared swollen and sometimes aggregated, the fact that they were well-stained with Mitotracker CMXRos is indicative that they were metabolically active. Moreover, we did not observed any signs of apoptosis in EspT or IpgB1 transfected cells, indicating that the mitochondrial membrane has not been compromised (data not shown). However, as EspT and IpgB1 contain no canonical mitochondrial targeting sequences, the mechanism involved in mitochondrial targeting remains unknown.

Lamellipodia and membrane ruffles induced by EspT are dependent on activation of Rac-1 and Cdc42

WxxxE effectors have previously been demonstrated to act both independently (Alto *et al*., 2006) and dependently

© 2008 The Authors
Journal compilation © 2008 Blackwell Publishing Ltd,

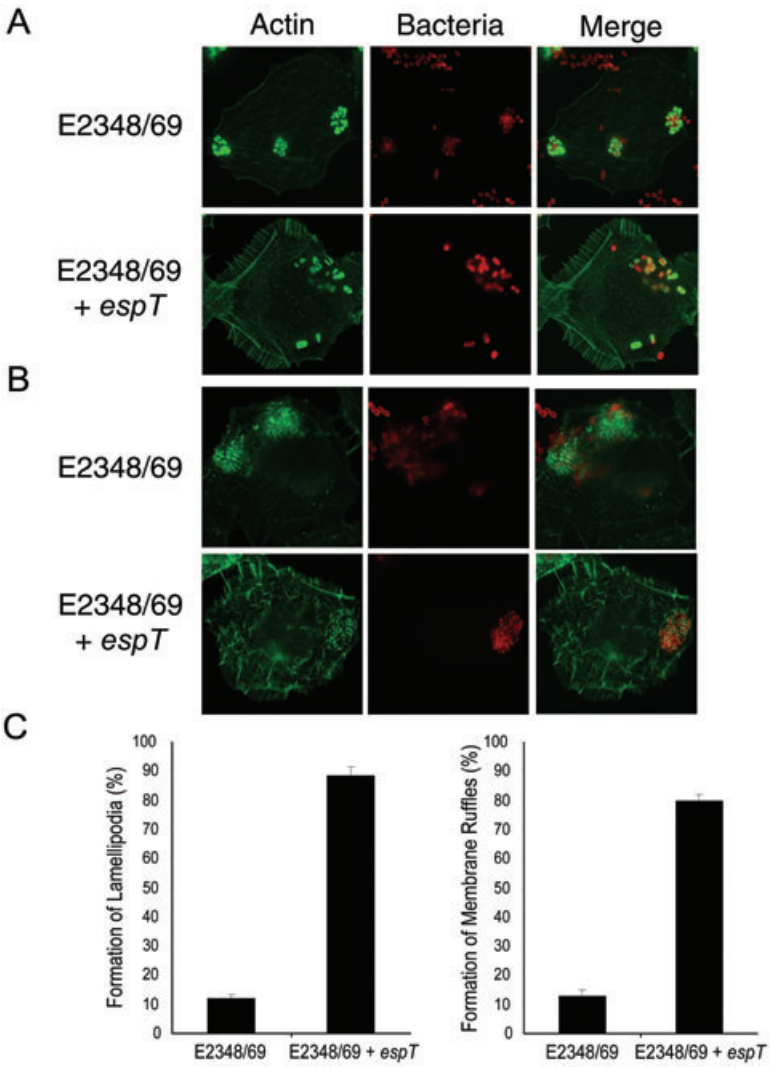


Fig. 2. A. Fluorescence microscopy of serum-starved Swiss 3T3 cells uninfected or infected with wild-type E2348/69 or E2348/69 expressing EspT for 90 min. Actin was stained with Oregon green phalloidin and E2348/69 was detected with a rabbit O127 antibody. Distinctive lamellipodia, which have a strong leading edge, wide lamella and well defined microspikes and filopodia that extend beyond the cell boundary, were observed on cells infected with E2348/69 expressing EspT but not in the wild-type control. Both strains induced formation of actin-rich pedestals beneath adherent bacteria.
B. Serum-starved HeLa cells infected with E2348/69 expressing EspT exhibited membrane ruffles whereas those infected with wild-type E2348/69 did not. Both strains formed actin pedestals.
C. Quantification of Lamellipodia and membrane ruffles on Swiss 3T3 and HeLa cells, respectively, after 90 min infection with wild-type E2348/69 or E2348/69 expressing EspT. One hundred cells were counted in triplicate in three independent experiments. Results are displayed as mean ± SEM.

(Handa *et al*., 2007; Arbeloa *et al*., 2008) of the Rho GTPases. In order to determine if EspT activity was dependent on RhoA, Rac-1, Cdc42 or RhoG, we transfected the dominant negative forms of each of these GTPases ($RhoA^{N19}$, $Rac\text{-}1^{N17}$, $Cdc42^{N17}$ and $RhoG^{N17}$), which competitively and specifically inhibit the wild-type GTPase activation, into both Swiss 3T3 and HeLa cells. Additionally, we transfected the Cdc42 and Rac1 binding domain (CRIB) of Pak, which efficiently inhibits the downstream signalling of Rac1 and Cdc42 (Carreno *et al*., 2002). Transfected cell were subsequently infected with E2348/69 expressing EspT from pSA10 for 1.5 h and the presence of lamellipodia or membrane ruffles was assessed. Inactivation of either RhoA or RhoG had no effect on the induction of lamellipodia or membrane ruffles by EspT on Swiss 3T3 and HeLa cells respectively (Fig. 4A). Conversely inhibition of Rac-1 or Cdc42 significantly compromised the ability of EspT to form either lamellipodia or membrane ruffles (Fig. 4B). The residual lamellipodia observed in the presence of the Rac-1 and Cdc42 dominant negatives were shorter and less pronounced than those induced in mock transfected cells (Fig. 4A). Inhibition of both Rac1 and Cdc42 downstream signalling using the CRIB of Pak reduced the number and extent of EspT-induced lamellipodia to a level comparable with the Rac1 dominant negative (Fig. 4B). This suggests that activation and subsequent downstream signalling of Rac-1, Cdc42, or both are involved in the EspT signalling pathway.

In order to assess whether or not EspT activates Rac-1 and Cdc42, we performed pull-down assays using the Cdc42 Rac-1 interacting binding domain (CRIB) of Pak, which binds activated Rac-1 and Cdc42 and the CRIB of WASP, which binds only activated Cdc42. Pull-downs were blotted with specific antibodies for Rac-1 and Cdc42. Cells incubated with CNF1 toxin that activates Rho GTPases (Pei *et al*., 2001) were used as a positive control, and E2348/69-containing empty pSA10 was used

© 2008 The Authors

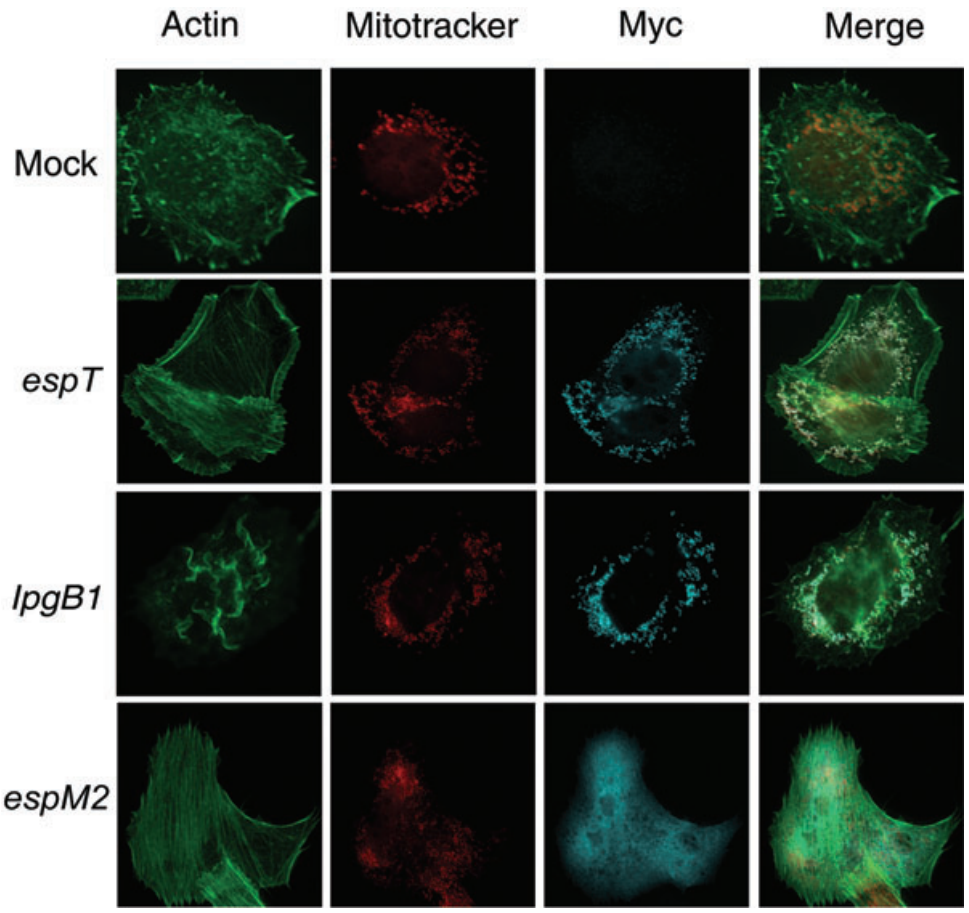


Fig. 3. Ectopic expression of EspT induces cytoskeletal rearrangement in Swiss 3T3 cells. Serum-starved Swiss 3T3 cells were mock transfected or transfected with the mammalian expression vector pRK5 encoding myc-tagged EspT, IpgB1 or EspM2 for 16 h. Actin was stained with Alexifluor 633 phalloidin, the myc tag was detected with monoclonal antibody and mitochondria were stained with Mitotracker CMXRos. On transfection EspT induces the formation of lamellipodia identical to those observed during infection. Transfection of IpgB1 and EspM2 resulted in the induction of membrane ruffles and stress fibres respectively. EspT and IpgB1 were found in the mitochondria while EspM2 remained cytoplasmic.

as a negative control. Swiss 3T3 cells infected with E2348/69 expressing EspT exhibited a marked increase in the level of activation of both Rac-1 and Cdc42 compared with uninfected cells or those infected with the control E2348/69 strain (Fig. 5B). These results suggest that EspT-triggered actin rearrangements are dependent upon activation of the Rac-1 and Cdc42 signalling cascades.

Ectopic expression of ELMO causes a shift from lamellipodia to membrane ruffles

Despite the limited homology between EspT and IpgB1, the phenotype produced by the *Shigella* effector is reminiscent of the membrane ruffles induced by EspT in HeLa cells (Ohya *et al*., 2005). Additionally, IpgB1-triggered membrane ruffles also occur in a RhoG-independent and Rac-1-dependent manner (Handa *et al*., 2007). IpgB1 has been reported to interact with ELMO1 and ELMO2 and subsequently recruit DOCK180 in order to activate Rac-1 in a manner analogous to RhoG (Handa *et al*., 2007). Furthermore, Handa and co-workers show that ELMO is localized to the membrane ruffles produced during *Shigella* invasion. In order to determine if ELMO was also localized to EspT-induced dorsal ruffles and lamellipodia, we ectopically expressed ELMO1 from the mammalian expression vector pGFP. Surprisingly, when Swiss 3T3 expressing ELMO were infected with E23348/69 carrying pSA10::*espT*, a shift from production of lamellipodia to membrane ruffles was observed with ELMO weakly localized to these ruffles (Fig. 6). These results suggest that while EspT may have a preferred binding partner in Swiss cells, it may also be able to interact directly or indirectly with ELMO. Alternatively, expression of ELMO might interfere with the pathway used by EspT to activate Rac-1 and Cdc42.

© 2008 The Authors
Journal compilation © 2008 Blackwell Publishing Ltd,

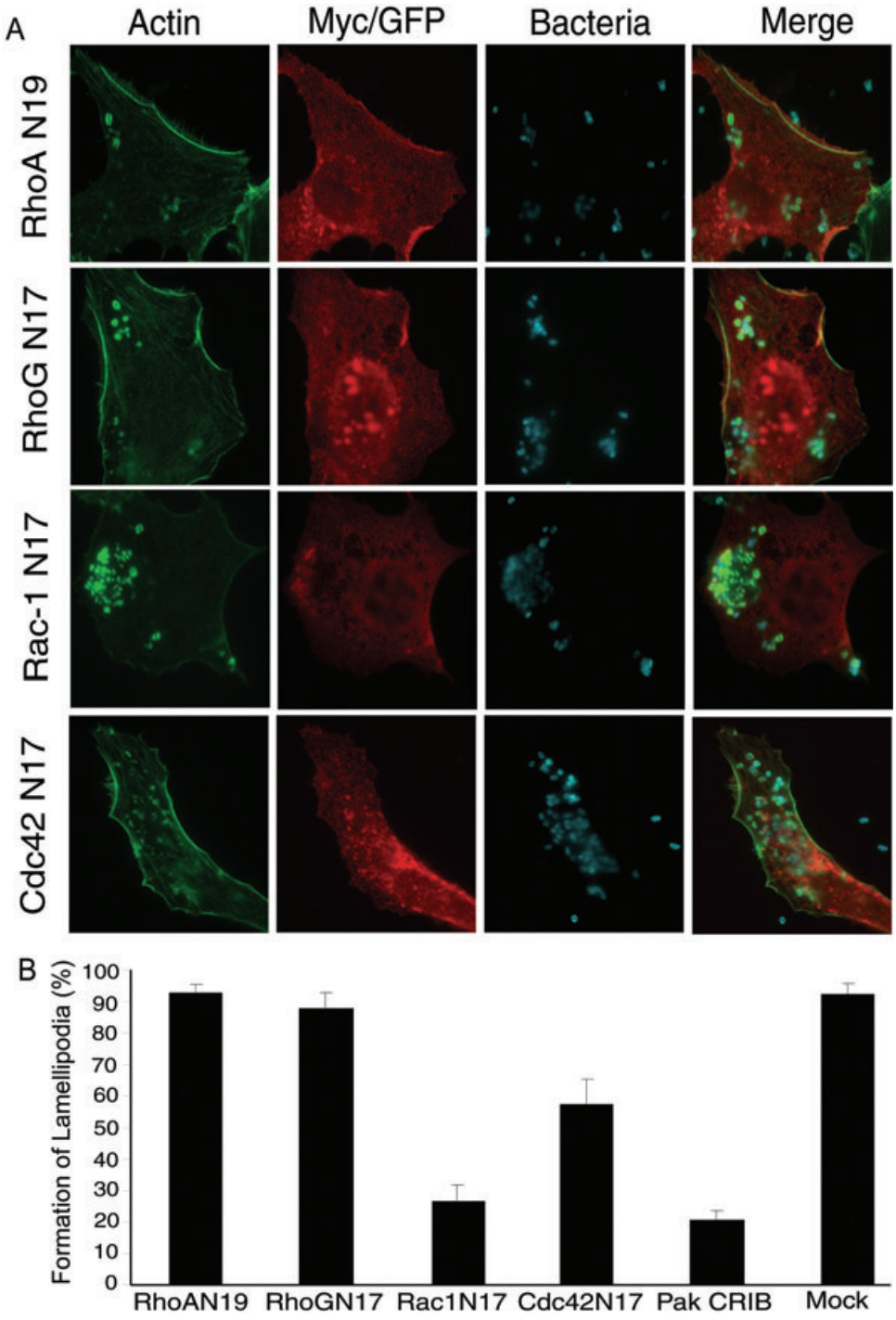


Fig. 4. EspT-induced cytoskeletal rearrangements are dependent on Rac-1 and Cdc42.
A. Swiss 3T3 cells were transfected with the dominant negative forms of RhoA, RhoG, Rac-1 and Cdc42 18 h prior to infection for 90 min with E2348/69 expressing EspT. Actin was stained with Oregon green phalloidin, the myc-tagged RhoA, Rac-1 and Cdc42 dominant negatives were stained with a myc tag monoclonal antibody, RhoG was detected via its GFP tag and E2348/69 was visualized using a rabbit O127 antibody. Actin pedestals were observed beneath all adherent bacteria. Lamellipodia were observed in cells transfected with dominant negative $RhoA^{N19}$ and the $RhoG^{N17}$. The majority of cells transfected with dominant negative $Rac\text{-}1^{N17}$ did not display lamellipodia. Dominant negative $Cdc42^{N17}$ reduced the number of cells expressing lamellipodia as well as reducing the extent of the lamellipodia compared with the mock or dominant negative $RhoA^{N19}$ and $RhoG^{N17}$.
B. Quantification of lamellipodia in transfected Swiss 3T3 after 90 min infection with E2348/69 expressing EspT. One hundred cells were counted in triplicate in three independent experiments. Results are displayed as mean ± SEM.

© 2008 The Authors

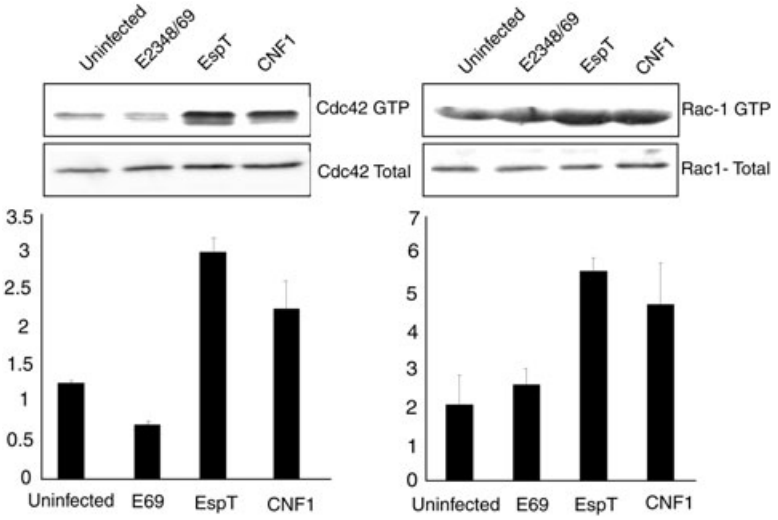


Fig. 5. EspT activates Rac-1 and Cdc42. Swiss 3T3 cells were left untreated or infected with wild-type E2348/69 or E2348/69 expressing EspT. Cells treated with CNF1 toxin were used as a positive control. Cells were lysed and added to GST beads bound to either the CRIB of WASP or the Rac-1 binding motif of Pak to capture active Cdc42 and Rac-1 respectively. Total Cdc42 and Rac-1 along with bound Cdc42 and Rac-1 were detected by Western blotting with Cdc42 and Rac-1 monoclonal antibodies. Quantified fold activation data are presented as mean ± SEM from three independent experiments.

EspT-induced cytoskeletal rearrangements are independent of ELMO or Dock180 activity

As ectopically expressed ELMO induces a shift from lamellipodia to membrane ruffles we utilized dominant negatives in order to investigate the role of the ELMO-Dock180 machinery in the induction of lamellipodia and membrane ruffles by EspT on Swiss 3T3 and HeLa cells respectively. Cells were transfected with ELMO^{T625} (a dominant negative of ELMO unable to interact with Dock180) or Dock180^{ISP} (a dominant negative form of Dock180 incapable of interacting with Rac-1) (Handa *et al*., 2007). Transfection of ELMO^{T625} or Dock180^{ISP} had no effect on the production of EspT-dependent lamellipodia in Swiss 3T3 cells (Fig. 7) or membrane ruffles in HeLa cells (data not shown). In contrast, double transfection of ELMO^{T625} or Dock180^{ISP} with pRK5 expressing IpgB1 resulted in a marked reduction of membrane ruffles compared with mock transfected cells (Fig. 7B). These results suggest that EspT induces lamellipodia and membrane ruffles via a mechanism that is distinct from IpgB1.

Discussion

In this study, we identified the *C. rodentium* effector protein EspT. Previously identified effectors, Map, EspM, IpgB1 and IpgB2, which are grouped together with EspT, have all been reported to be potent modulators of the host cell cytoskeleton (Kenny and Jepson, 2000; Alto *et al*., 2006; Handa *et al*., 2007; Arbeloa *et al*., 2008). Consistent with this, using E2348/69 as a delivery system to translocate EspT along with ectopic expression we have shown that EspT also subverts host actin dynamics. Interestingly, the effect of EspT was cell-line specific. While expression in Swiss 3T3 led to formation of lamellipodia, EspT-triggered membrane ruffles on HeLa cells. When EspT was delivered by infection via E2348/69, the lamellipodia and membrane ruffles appeared as early as 15 min post infection and were stable for over 3 h.

Based on the initial examination of IpgB1, IpgB2 and Map, it was suggested that these effector proteins are molecular mimics of Rho GTPases and function in a GTP-independent manner (Alto *et al*., 2006). More recently, Handa *et al*. showed that IpgB1 activates Rac-1 via the ELMO-Dock180 machinery (Handa *et al*., 2007). In addition, we recently identified a new subfamily in the A/E pathogen group, which share a high degree of similarity to IpgB2 named EspM. We have shown that EspM2 and EspM3 activate RhoA via a mechanism which is yet to be determined (Arbeloa *et al*., 2008).

Despite EspT sharing limited sequence identity with other family members, the membrane ruffles observed on HeLa cells were reminiscent of those induced by IpgB1 (Handa *et al*., 2007) except that the EspT-induced ruffles were not restricted to the site of bacterial attachment. As IpgB1 plays a role in *Shigella* cell invasion (Ohya *et al*., 2005), we tested if overexpression of EspT affects the level of E2348/69 cell entry. Invasion assay of wild-type E2348/69 and E2348/69 expressing EspT did not reveal any significant difference in the level of intracellular bacteria (data not shown). Interestingly, expressing EspT in Swiss cells led to formation of lamellipodia, which have a strong leading edge, wide lamella and well-defined microspikes and filopodia that extend beyond the cell boundary. In contrast, IpgB1 expression induced membrane ruffles on Swiss cells.

Lamellipodia and membrane ruffles are normally regulated by interplay between Rac-1, Cdc42, RhoG and RhoA (Sander and Collard, 1999; Kurokawa *et al*., 2004; Ladwein and Rottner, 2008). In order to determine the pathway by which EspT subverts the host cell cytoskeleton, we utilized dominant negative forms of these GTPases to competitively inhibit the wild-type proteins.

© 2008 The Authors
Journal compilation © 2008 Blackwell Publishing Ltd,

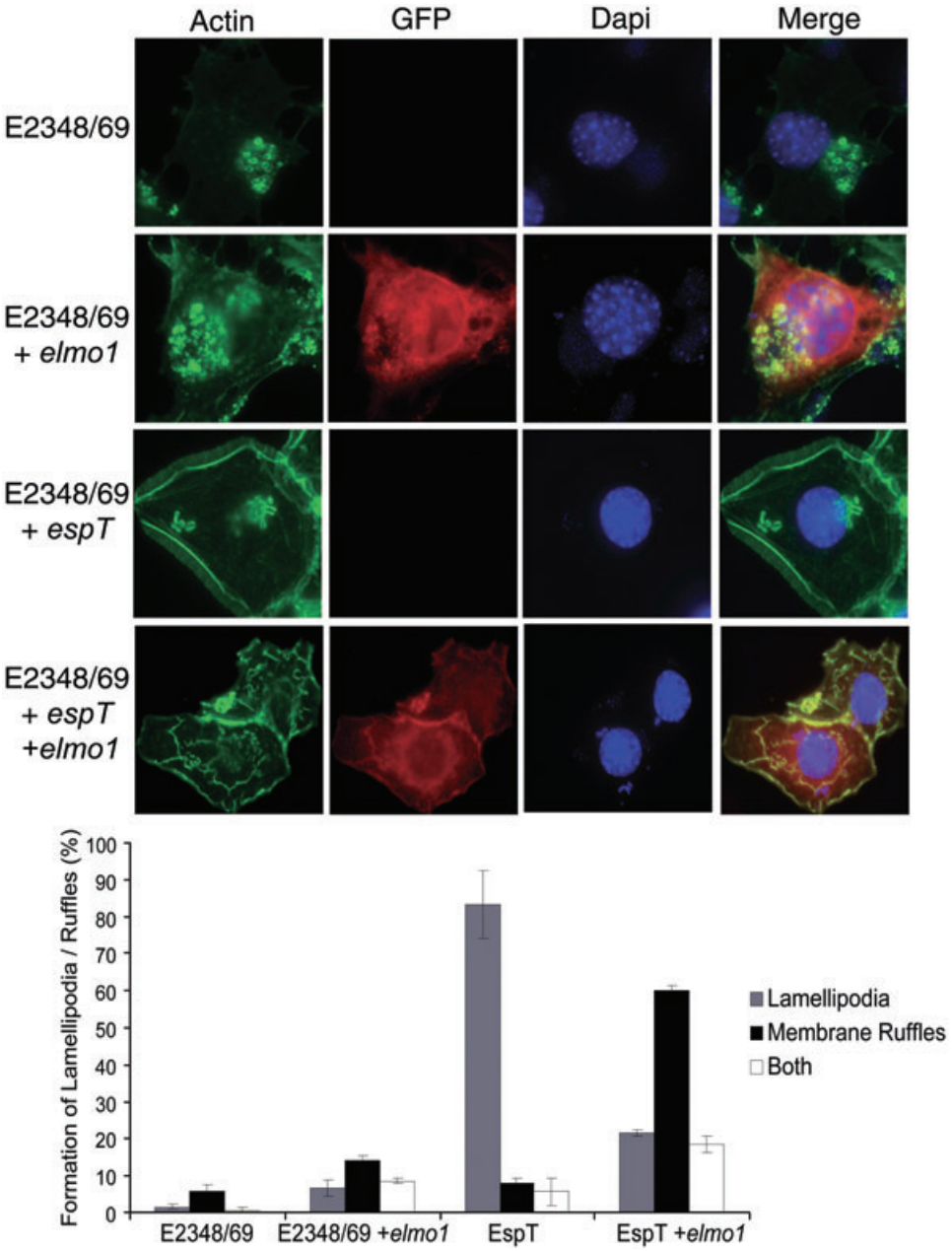


Fig. 6. Expression of ELMO1 causes a shift from lamellipodia to membrane ruffles.
A. Swiss 3T3 cells were mock transfected or transfected with GFP tagged ELMO1 18 h prior to infection with wild-type E2348/69 or E2348/69 expressing EspT. While wild-type E2348/69 displayed only pedestal formation in mock transfected or cells transfected with ELMO1, E2348/69 expressing EspT induced formation of lamellipodia on mock transfected cells but in cells transfected with ELMO there was a shift from lamellipodia to membrane ruffles.
B. Quantification of Lamellipodia and membrane ruffles on mock transfected Swiss 3T3 or Swiss 3T3 cells transfected with ELMO1 after 90 min infection with wild-type E2348/69 or E2348/69 expressing EspT. One hundred cells were counted in triplicate in three independent experiments. Results are displayed as mean ± SEM.

In the presence of dominant negative Rac-1^{TN17} a 60% reduction in formation of lamellipodia was observed. Transfection of Cdc42^{TN17} reduced lamellipodia formation by 30%. These dominant negative constructs attenuated EspT-induced membrane ruffles in HeLa cells to a similar magnitude. These results demonstrate that the actin re-arrangements induced by EspT are dependent on the activation of Rac-1 and to a lesser extent Cdc42. Furthermore, using the CRIB domains of PAK and WASP that bind activated Rac-1 and Cdc42, respectively, we demonstrate that EspT activates both Rac-1 and Cdc42 during infection of Swiss 3T3 cells. These results are consistent

© 2008 The Authors

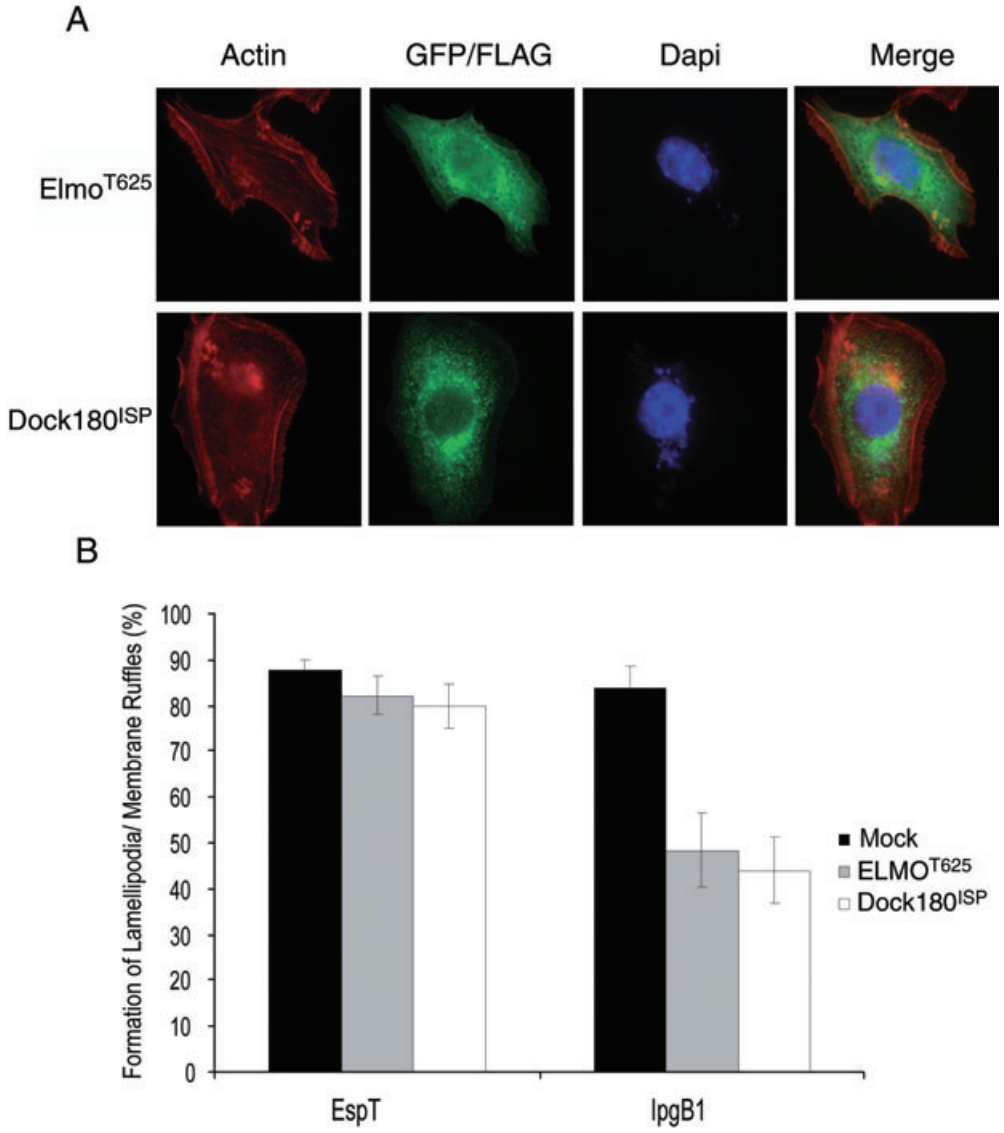


Fig. 7. A. EspT-induced cytoskeletal rearrangements are not dependent on ELMO or Dock180. Swiss 3T3 were transfected with the dominant negative forms of ELMO and Dock180 18 h prior to infection with E2348/69 expressing EspT. Neither ELMO^{T625} nor Dock180^{ISP} had any effect on lamellipodia induction by EspT.
B. Quantification of lamellipodia or membrane ruffles in Swiss 3T3 cells transfected with dominant negative ELMO^{T625} or Dock180^{ISP} and infected with E2348/69 expressing EspT or cotranfected with IpgB1 from *S. flexneri* as control. One hundred cells were counted in triplicate from three independent experiments. Results are displayed as mean ± SEM.

with the report of (Handa *et al*. (2007) who have previously demonstrated that IpgB1 activates Rac-1. We currently do not know whether EspT activates Rac-1 directly, via activation of Cdc42 or through a yet unknown GEF or adaptor.

Handa and co-workers also show that IpgB1 interacts with ELMO and subsequently recruits Dock180 to a trimeric complex which brings about the activation of Rac-1 (Handa *et al*., 2007). As EspT induces a Rac-1-dependent phenotype similar to IpgB1 in HeLa cells we investigated the role of ELMO during EspT-triggered actin modulation. We transfected a GFP-tagged ELMO into Swiss 3T3 cells and infected these cells with wild-type E2348/69 or E2348/69 expressing EspT. No ruffles were observed during E2348/69 infection. Surprisingly, when ELMO was transfected into Swiss 3T3 cells infected with E2348/69 expressing EspT, we observed a shift from the lamellipodia to membrane ruffles similar to those induced by IpgB1. This result might suggest that EspT is able to interact with ELMO. Alternatively, overexpression of ELMO could have an effect downstream of the signalling pathway employed by EspT. To determine if the lamellipodia observed in Swiss 3T3 cells or the membrane ruffles formed in HeLa cells are dependent upon the ELMO – Dock180

© 2008 The Authors
Journal compilation © 2008 Blackwell Publishing Ltd,

machinery, we used the dominant negative forms of ELMO (ELMO^{T625}) and Dock180 (Dock180^{ISP}), which have been demonstrated to abolish IpgB1 induced membrane ruffles (Handa *et al*., 2007). As previously observed (Handa *et al*., 2007) these dominant negatives greatly reduced the formation of membrane ruffles induced by IpgB1. However, neither the ELMO^{T625} nor Dock180^{ISP} had any significant affect on the formation of lamellipodia or membrane ruffles induced by EspT, suggesting that EspT activates Rac-1 and Cdc42 by a novel mechanism.

Map, which triggers filopodia formation via activation of Cdc42 (Berger *et al*., 2008), contains an N-terminus mitochondrial targeting sequence (Papatheodorou *et al*., 2006), while EspM2, IpgB1 and EspT do not have any obvious mitochondrial targeting sequences. EspM2, which triggers formation of parallel stress fibres upon transfection, localizes in the cytoplasm. In contrast, we found here that EspT and IpgB1 are targeted to mitochondria following 16 h ectopic expression. It is interesting to note that mitochondrial trafficking and morphology is regulated by the atypical Rho GTPases Mitochondrial Rho (Miro) 1 and 2 (Frederick *et al*., 2004; Fransson *et al*., 2006). The mitochondrial localization of IpgB1 and EspT may suggest a role for these proteins in regulating mitochondrial dynamics as well as subversion of the host actin cytoskeleton. However, although ectopic expression of EspM leads to cytosolic localization, we cannot rule out the possibility that mitochondria targeting by EspT and IpgB1 is due to the overexpression. Further studies are needed to determine if EspT and IpgB1 have a physiological mitochondrial function.

Further work is also required to elucidate the mechanism by which EspT activates Rac-1 and Cdc42. Interestingly, although *espT* is absent from the common EPEC strains (including the prototypes E2348/69 and B171) and EHEC O157, we recently found an *espT* homologue (78% identity) in the atypical EPEC strain E110019, which caused a particularly severe outbreak in Finland in 1987 (Viljanen *et al*., 1990). However, the overall prevalence of *espT* among clinical EPEC and EHEC strain is not yet known. Finally, additional studies are required to elucidate what role EspT plays *in vivo* during infection of A/E pathogens.

Experimental procedures

Bacterial strains, growth conditions and cell culture

The bacterial strains used in this study are listed in Table 1. Bacteria were grown in Luria–Bertani (LB) broth at 37°C or maintained on LB plates. Culture media were supplemented with Ampicillin (100 μg ml^{-1}) as appropriate.

Bacterial cultures were primed prior to infection by growth in Dulbecco's modified Eagle's media (DMEM) 4500 mg ml^{-1} glucose supplemented with 1% mannose for 3 h (Collington *et al*., 1998) before addition of 1 mM IPTG to induce protein expression.

Table 1. List of strains.

Strain	Description	Source/reference
E2348/69	EPEC O127:H6 wild-type	Levine *et al*. (1978)
ICC168	*Citrobacter rodentium*	Barthold *et al*. (1976)
ICC192	EPEC E2348/69Δ*escN*	Garmendia *et al*. (2004)

Swiss 3T3 cells were maintained in DMEM with 4500 mg ml^{-1} glucose and supplemented with 10% fetal calf serum (Gibco) and 4 mM Glutamax (Gibco). HeLa cells were cultured in DMEM with 1000 mg ml^{-1} glucose and supplemented with 10% fetal calf serum (Gibco) and 4 mM Glutamax (Gibco).

Bioinformatics

A PSI-BLAST search (Altschul *et al*., 1997) was performed under default conditions using IpgB2 from *Shigella flexneri* (gi:13448971) and Map from EPEC (gi:2865296) as query sequences to search the latest version of the NCBI NR database and combined with a library of peptide sequences derived from all coding sequences ≥50 codons in length from the genome sequences of *C. rodentium* ICC168, EPEC B171, E110019 and EPEC E2348/69.

Multiple alignment and phylogenetic analysis

Using the sequence alignment programme ClustalW2 (Larkin *et al*., 2007), a phenogram was constructed based upon hierarchical clustering of EspT, EspM2 and EspM3 form *C. rodentium*, EspM1 from EPEC B171, and IpgB1 and IpgB2 form *S. flexneri*.

Plasmids and molecular techniques

Plasmids used in this study are listed in Table 2; primers are listed in Table 3. The gene encoding the effector protein *espT* was amplified by PCR from *C. rodentium* genomic DNA and cloned into pSA10 with a C-terminal HA tag using primer pairs 1 and 2 (Table 3). The gene encoding the effector protein *espT* was amplified by PCR from *C. rodentium* genomic DNA and cloned into pRK5 with an N-terminal Myc tag using primer pair 3 and 4 (Table 3). The gene encoding the effector protein *IpgB1* was amplified by PCR from *S. flexneri* genomic DNA and cloned into pRK5 with a N-terminal Myc tag using primer pairs 7 and 8 (Table 3). All constructs were verified by DNA sequencing.

The mammalian expression vector pRK5 containing one of Rho^{N19}, Rac^{N17} or Cdc42^{N17} dominant negatives used in the transfection assays was a gift from Nathalie Lamarche-Vane. The pEGFP-C1 mammalian expression vector containing the RhoG^{N17} and ELMO^{T625} dominant negatives and Elmo1 along with the pCXN2 vector with the FLAG tagged Dock180^{ISP} were kindly supplied by Yutaka Handa and Chihiro Sasakawa (Handa *et al*., 2007). The vector pGEX expressing the Rac-1 binding domain of Pak, the CRIB of WASP and CNF1 toxin fused to GST were a gift from J. Bertoglio. The pRK5 vector encoding the CRIB of Pak fused to a myc tag was kindly provided by Dr Emmanuelle Caron (CMMI).

© 2008 The Authors

Table 2. List of Plasmids.

Name	Description	Source/reference
pSA10	pKK177-3 with LacP	Schlosser-Silverman *et al.* (2000)
pRK5::*myc-rhoA*^{N17}	Dominant negative RhoA	Pelletier *et al.* (2005)
pRK5::*myc-rac1*^{N19}	Dominant negative Rac1	Pelletier *et al.* (2005)
pRK5::*myc-cdc42*^{N19}	Dominant negative Cdc42	Pelletier *et al.* (2005)
pEGFPC1::*GFP-rhoG*^{N19}	Dominant negative RhoG	Handa *et al.* (2007)
pEGFPC1::*elmo*^{T625}	Dominant negative ELMO	Handa *et al.* (2007)
pCXN2::*dock180*^{ISP}	Dominant negative Dock180	Handa *et al.* (2007)
pGex::*GST-CRIBWASP*	Cdc42 binding motif of WASP	Sander and Collard (1999)
pGex::*GST-PAK*	Rac1 and Cdc42 binding domain of PAk	Sander and Collard (1999)
pEGFPC1::*elmo*	Elmo GFP tagged	Handa *et al.* (2007)
pICC427	pSA10::*espT-HA*	This study
pICC228	pRK5::*espT-Myc*	This study
pICC429	pRK5::*lpgB1-Myc*	This study
pICC320	pRK5::*EspM2-Myc*	This study

Infection of Swiss 3T3 and HeLa cells with EPEC E2348/69

48 h prior to infection cells were seeded onto glass coverslips at a density of approximately 5×10^5 cells per well and maintained in DMEM supplemented with 10% FCS at 37°C in 5% CO_2. Three hours before infection, the cells were washed three times with PBS, the media replaced with fresh DMEM without FCS supplemented with 1% mannose and 500 µl of primed bacteria were added to each well and infections were carried out at 37°C in 5% CO_2 for 1.5 h.

Transfection

Swiss 3T3 cells or Hela cells were transfected with pRK5 encoding RhoA^{N19}, Rac^{N17}, Cdc42^{N17} dominant negatives fused to a Myc tag, pEGFP-C1 containing RhoG^{N17} or ELMO^{T625} dominant negatives with a GFP tag, pCNX2 containing Dock180^{ISP} dominant negative with a FLAG tag or pRK5 encoding EspT, IpgB1, EspM2 or the CRIB of Pak fused to a Myc tag by lipofectamine 2000 (Invitrogen), according to the manufacturer's recommendations. The cells were incubated at 37°C in a humidified incubator with 5% CO_2 for 16 h, washed twice in PBS before having their media replaced with DMEM as described previously. Transfected cells were infected with the appropriate strain as described above.

Immunofluorescence staining and microscopy

Coverslips were washed three times in PBS and fixed with 3% paraformaldehyde for 15 min before washing three more times in PBS. For immunostaining, the cells were permeabilized for 5 min in PBS 0.5% Triton X-100, washed three times in PBS and quenched for 30 min with 50 mM NH_4Cl. The coverslips were then blocked for 1 h with PBS 0.5% BSA before incubation with primary and secondary antibodies. The primary antibody mouse αFLAG, mouse anti-HA (Cell Signalling Technology) and mouse anti-Myc (Millipore) were used at a dilution of 1:500, while rabbit anti-O127 (a gift from Dr Roberto La Ragione, VLA, UK) was used at a dilution of 1:150. Coverslips were incubated with the primary antibody for 1 h, washed three times in PBS and incubated with the secondary antibodies. Donkey anti-rabbit IgG conjugated to a Cy5 fluorophore or donkey anti-mouse IgG conjugated to a Cy3 fluorophore (Jackson laboratories) were used at a 1:200. Actin was stained using Oregon Green phalloidin or Rhodamine phalliodin (Invitrogen) at a 1:100 dilution. Mitochondria were visualized using Mitotracker CMX-Ros (Invitrogen) as recommended by the manufacturer. All dilutions were in PBS/0.5% BSA. Coverslips were mounted on slides using ProLong Gold antifade reagent (Invitrogen) and visualized by Zeiss Axioimager immunofluorescence microscope using the following excitation wavelengths: Cy3 – 550 nm, Cy5 – 650 nm and Oregon Green – 488 nm. All images were analysed using the Axiovision Rel 4.5 software.

GST-PAK and GST-WASP Rho GTPase pull-down

An overnight culture of *E. coli* BL21 expressing pGEX encoding the Rac-1 binding domain of Pak or the CRIB of WASP was diluted 1:20 and cultured at 30°C until OD_{260} reached 0.7; the culture was induced with 1 mM IPTG and incubated for a further 4 h. The bacterial culture was aliquoted into 50 ml falcon tubes

Table 3. List of primers.

Name	Sequence
EspT-HA-F	5′-TTGAATTCATGCCGGGAACAATAAGCTCCAG-3′
EspT-HA-R	5′-TTCTGCAGTTAAGCGTAGTCTGGGACGTCGTATGGGTAGGTTCTCTGAGCCTCCTGAA-3′
EspT-pRK5-F	5′-CGCGGATCCATGCCGGGAACAATAAGCTCCAG-3′
EspT-pRK5-R	5′-CCAATGCACTGCAGTTAGGTTCTCTGAGCCTCCTGAA-3′
EspM2-pRK5-F	5′-TTTGGATCCGGAGCAATGCAAATTCTAAACAAAATAC-3′
EspM2-pRK5-R	5′-TTTGAATTCTCATCCCTGTATAGCACGCATCA-3′
IpgB1-pRK5-F	5′-TTTGGATCCGGAGCAATGCAAATTCTAAACAAAATAC-3′
IpgB1-pRK5-F	5′-CCAATGCATTGGTTCTGCAGTTAATTTGTATTGCTTTGAC-3′

© 2008 The Authors
Journal compilation © 2008 Blackwell Publishing Ltd,

and centrifuged for 15 min at 4600 r.p.m. at 4°C and the pellets stored at –80°C. The pellets were re-suspended in lysis buffer [20% Saccharose, 10% glycerol, 50 Mm Tris pH 8, 200 mM $Na_2S_2O_3$, 2 mM $MgCl_2$, 2 mM DTT and 1% of protease inhibitor cocktail (Sigma)] and sonicated five times for 10 s. The lysate was centrifuged for 30 min at 15 000 r.p.m. at 4°C. The cleared lysate was coupled to GST-glutathione S transferase beads (GE healthcare) for 45 min at 4°C.

Cell culture flasks of 75 cm^2 were seeded with Swiss 3T3 cells, infected as described above and the cells lysed in 750 µl of Mg^{++} buffer [25 mM HEPES, pH 7.5, 150 mM NaCl, 1% NP-40, 10 mM $MgCl_2$, 5% glycerol, 1 mM EDTA and protease inhibitors (Sigma)]. The lysate was transferred to a pre-chilled eppendorf tube and centrifuged at 14 000 r.p.m. for 5 min at 4°C. The cleared lysate was transferred to a fresh pre-chilled eppendorf tube containing 30 µl of GST-Pak-RBD or GST-WASP-CRIB beads as appropriate. The lysate was incubated with the beads for 1 h at 4°C. The suspension was washed three times in Mg^{++} buffer spinning down at 14 000 r.p.m. at 4°C between each wash. The protein was eluted from the beads by the addition of 45 µl of 2× protein loading buffer and the samples heated at 100°C for 5 min. The samples were loaded on a 15% SDS-PAGE gel. The gels were transferred to PVDF by wet transfer. The PVDF membranes were blocked overnight in TBS, 5% BSA at 4°C with gentle rocking. Each membrane was incubated in either monoclonal rabbit anti-Rac-1 (Santa Cruz) or rabbit anti-Cdc42 (Santa Cruz) as appropriate at a dilution of 1:500 in TBS 5% BSA for 24 h at 4°C with gentle rocking. The membranes were washed five times in TBS 1% Tween for 5 min and incubated for 45 min with 1:10000 dilution of goat anti-rabbit (Invitrogen) secondary antibody coupled to HRP at room temperature. The membranes were developed using ECL reagents (GE healthcare) before detection using chemiluminescence in a LAS 3000 Fugi imager.

Acknowledgements

We thank Prof Chihiro Sasakawa and Dr Yutaka Handa for kindly providing the ELMO and Dock180 constructs along with the RhoG dominant negative. We also thank Dr Cedric Berger and Dr Emmanuelle Caron for their technical advice and support. This work was supported by grants from the MRC and the Wellcome Trust. Ana Arbeloa is supported by Becas de Formacion de Investigadores, Gobierno Vasco, Spain.

References

Alto, N.M., Shao, F., Lazar, C.S., Brost, R.L., Chua, G., Mattoo, S., *et al.* (2006) Identification of a bacterial type III effector family with G protein mimicry functions. *Cell* **124:** 133–145.

Altschul, S.F., Madden, T.L., Schaffer, A.A., Zhang, J., Zhang, Z., Miller, W., and Lipman, D.J. (1997) Gapped BLAST and PSI-BLAST: a new generation of protein database search programs. *Nucleic Acids Res* **25:** 3389–3402.

Arbeloa, A., Bulgin, R.R., MacKenzie, G., Shaw, R.K., Pallen, M.J., Crepin, V.F., *et al.* (2008) Subversion of actin dynamics by EspM effectors of attaching and effacing bacterial pathogens. *Cell Microbiol* **10:** 1429–1441.

Barthold, S.W., Coleman, G.L., Bhatt, P.N., Osbaldiston, G.W., and Jonas, A.M. (1976) The etiology of transmissible murine colonic hyperplasia. *Lab Anim Sci* **26:** 889–894.

Berger, C.N., Crepin, V.F., Jepson, M.A., Arbeloa, A., and Frankel, G. (2008) The mechanisms used by enteropathogenic E. coli to control filopodia dynamics. *Cell Microbiol* in press. doi: 10.1111/j.1462-5822.2008.01254.x

Beuzon, C.R., Meresse, S., Unsworth, K.E., Ruiz-Albert, J., Garvis, S., Waterman, S.R., *et al.* (2000) *Salmonella* maintains the integrity of its intracellular vacuole through the action of SifA. *EMBO J* **19:** 3235–3249.

Carreno, S., Caron, E., Cougoule, C., Emorine, L.J., and Maridonneau-Parini, I. (2002) p59Hck isoform induces F-actin reorganization to form protrusions of the plasma membrane in a Cdc42- and Rac-dependent manner. *J Biol Chem* **277:** 21007–21016.

Collington, G.K., Booth, I.W., Donnenberg, M.S., Kaper, J.B., and Knutton, S. (1998) Enteropathogenic *Escherichia coli* virulence genes encoding secreted signalling proteins are essential for modulation of Caco-2 cell electrolyte transport. *Infect Immun* **66:** 6049–6053.

Filloux, A., Hachani, A., and Bleves, S. (2008) The bacterial type VI secretion machine: yet another player for protein transport across membranes. *Microbiology* **154:** 1570–1583.

Frankel, G., and Phillips, A.D. (2008) Attaching effacing Escherichia coli and paradigms of Tir-triggered actin polymerization: getting off the pedestal. *Cell Microbiol* **10:** 549–556.

Frankel, G., Phillips, A.D., Trabulsi, L.R., Knutton, S., Dougan, G., and Matthews, S. (2001) Intimin and the host cell – is it bound to end in Tir(s)? *Trends Microbiol* **9:** 214–218.

Fransson, S., Ruusala, A., and Aspenstrom, P. (2006) The atypical Rho GTPases Miro-1 and Miro-2 have essential roles in mitochondrial trafficking. *Biochem Biophys Res Commun* **344:** 500–510.

Frederick, R.L., McCaffery, J.M., Cunningham, K.W., Okamoto, K., and Shaw, J.M. (2004) Yeast Miro GTPase, Gem1p, regulates mitochondrial morphology via a novel pathway. *J Cell Biol* **167:** 87–98.

Galan, J.E., and Wolf-Watz, H. (2006) Protein delivery into eukaryotic cells by type III secretion machines. *Nature* **444:** 567–573.

Garmendia, J., Phillips, A.D., Carlier, M.F., Chong, Y., Schuller, S., Marches, O., *et al.* (2004) TccP is an enterohaemorrhagic *Escherichia coli* O157: H7 type III effector protein that couples Tir to the actin-cytoskeleton. *Cell Microbiol* **6:** 1167–1183.

Gerlach, R.G., and Hensel, M. (2007) Protein secretion systems and adhesins: the molecular armory of Gram-negative pathogens. *Int J Med Microbiol* **297:** 401–415.

Handa, Y., Suzuki, M., Ohya, K., Iwai, H., Ishijima, N., Koleske, A.J., *et al.* (2007) *Shigella* IpgB1 promotes bacterial entry through the ELMO-Dock180 machinery. *Nat Cell Biol* **9:** 121–128.

Jaffe, A.B., and Hall, A. (2005) Rho GTPases: biochemistry and biology. *Annu Rev Cell Dev Biol* **21:** 247–269.

Kenny, B., and Jepson, M. (2000) Targeting of an enteropathogenic *Escherichia coli* (EPEC) effector protein to host mitochondria. *Cell Microbiol* **2:** 579–590.

Kenny, B., DeVinney, R., Stein, M., Reinscheid, D.J., Frey,

© 2008 The Authors

E.A., and Finlay, B.B. (1997) Enteropathogenic *E. coli* (EPEC) transfers its receptor for intimate adherence into mammalian cells. *Cell* **91:** 511–520.

Knutton, S., Lloyd, D.R., and McNeish, A.S. (1987) Adhesion of enteropathogenic *Escherichia coli* to human intestinal enterocytes and cultured human intestinal mucosa. *Infect Immun* **55:** 69–77.

Kurokawa, K., Itoh, R.E., Yoshizaki, H., Nakamura, Y.O., and Matsuda, M. (2004) Coactivation of Rac1 and Cdc42 at lamellipodia and membrane ruffles induced by epidermal growth factor. *Mol Biol Cell* **15:** 1003–1010.

Ladwein, M., and Rottner, K. (2008) On the Rho'd: the regulation of membrane protrusions by Rho-GTPases. *FEBS Lett* **582:** 2066–2074.

Larkin, M.A., Blackshields, G., Brown, N.P., Chenna, R., McGettigan, P.A., McWilliam, H., *et al.* (2007) Clustal W and Clustal X version 2.0. *Bioinformatics* **23:** 2947–2948.

Levine, M.M., Bergquist, E.J., Nalin, D.R., Waterman, D.H., Hornick, R.B., Young, C.R., and Sotman, S. (1978) *Escherichia coli* strains that cause diarrhoea but do not produce heat-labile or heat-stable enterotoxins and are non-invasive. *Lancet* **1:** 1119–1122.

McDaniel, T.K., Jarvis, K.G., Donnenberg, M.S., and Kaper, J.B. (1995) A genetic locus of enterocyte effacement conserved among diverse enterobacterial pathogens. *Proc Natl Acad Sci USA* **92:** 1664–1668.

Mackey, A.J., Haystead, T.A., and Pearson, W.R. (2002) Getting more from less: algorithms for rapid protein identification with multiple short peptide sequences. *Mol Cell Proteomics* **1:** 139–147.

Matsuzawa, T., Kuwae, A., Yoshida, S., Sasakawa, C., and Abe, A. (2004) Enteropathogenic *Escherichia coli* activates the RhoA signaling pathway via the stimulation of GEF-H1. *EMBO J* **23:** 3570–3582.

Miura, M., Terajima, J., Izumiya, H., Mitobe, J., Komano, T., and Watanabe, H. (2006) OspE2 of *Shigella sonnei* is required for the maintenance of cell architecture of bacterium infected cells. *Infect Immun* **74:** 2587–2595.

Mundy, R., MacDonald, T.T., Dougan, G., Frankel, G., and Wiles, S. (2005) *Citrobacter rodentium* of mice and man. *Cell Microbiol* **7:** 1697–1706.

Nataro, J.P., and Kaper, J.B. (1998) Diarrheagenic *Escherichia coli*. *Clin Microbiol Rev* **11:** 142–201.

Ohya, K., Handa, Y., Ogawa, M., Suzuki, M., and Sasakawa, C. (2005) IpgB1 is a novel *Shigella* effector protein involved in bacterial invasion of host cells. Its activity to promote membrane ruffling via Rac1 and Cdc42 activation. *J Biol Chem* **280:** 24022–24034.

Papatheodorou, P., Domanska, G., Oxle, M., Mathieu, J., Selchow, O., Kenny, B., and Rassow, J. (2006) The enteropathogenic *Escherichia coli* (EPEC) Map effector is imported into the mitochondrial matrix by the TOM/Hsp70 system and alters organelle morphology. *Cell Microbiol* **8:** 677–689.

Pei, S., Doye, A., and Boquet, P. (2001) Mutation of specific acidic residues of the CNF1 T domain into lysine alters cell membrane translocation of the toxin. *Mol Microbiol* **41:** 1237–1247.

Pelletier, S., Julien, C., Popoff, M.R., Lamarche-Vane, N., and Meloche, S. (2005) Cyclic AMP induces morphological changes of vascular smooth muscle cells by inhibiting a Rac-dependent signaling pathway. *J Cell Physiol* **204:** 412–422.

Sander, E.E., and Collard, J.G. (1999) Rho-like GTPases: their role in epithelial cell-cell adhesion and invasion. *Eur J Cancer* **35:** 1302–1308.

Schlosser-Silverman, E., Elgrably-Weiss, M., Rosenshine, I., Kohen, R., and Altuvia, S. (2000) Characterization of *Escherichia coli* DNA lesions generated within J774 macrophages. *J Bacteriol* **182:** 5225–5230.

Shaw, R.K., Smollett, K., Cleary, J., Garmendia, J., Straatman-Iwanowska, A., Frankel, G., and Knutton, S. (2005) Enteropathogenic *Escherichia coli* type III effectors EspG and EspG2 disrupt the microtubule network of intestinal epithelial cells. *Infect Immun* **73:** 4385–4390.

Stebbins, C.E., and Galan, J.E. (2001) Structural mimicry in bacterial virulence. *Nature* **412:** 701–705.

Tobe, T., Beatson, S.A., Taniguchi, H., Abe, H., Bailey, C.M., Fivian, A., *et al.* (2006) An extensive repertoire of type III secretion effectors in *Escherichia coli* O157 and the role of lambdoid phages in their dissemination. *Proc Natl Acad Sci USA* **103:** 14941–14946.

Viljanen, M.K., Peltola, T., Junnila, S.Y., Olkkonen, L., Jarvinen, H., Kuistila, M., and Huovinen, P. (1990) Outbreak of diarrhoea due to *Escherichia coli* O111:B4 in schoolchildren and adults: association of Vi antigen-like reactivity. *Lancet* **336:** 831–834.

© 2008 The Authors
Journal compilation © 2008 Blackwell Publishing Ltd,

Distribution of *espM* and *espT* among enteropathogenic and enterohaemorrhagic *Escherichia coli*

Ana Arbeloa,[1]† Miguel Blanco,[2]† Fabiana C. Moreira,[3] Richard Bulgin,[1] Cecilia López,[2] Ghizlane Dahbi,[2] Jesús E. Blanco,[2] Azucena Mora,[2] María Pilar Alonso,[4] Rosalia Ceferina Mamani,[2] Tânia A. T. Gomes,[3] Jorge Blanco[2] and Gad Frankel[1]

Correspondence
Jorge Blanco
jorge.blanco@usc.es
Gad Frankel
g.frankel@imperial.ac.uk

[1]Centre for Molecular Microbiology and Infection, Division of Cell and Molecular Biology, Imperial College London, London SW7 2AZ, UK

[2]Laboratorio de Referencia de *E. coli*, Departamento de Microbiología y Parasitología, Facultad de Veterinaria, Universidad de Santiago de Compostela, Lugo, Spain

[3]Departamento de Microbiologia, Imunologia e Parasitologia, Universidade Federal de São Paulo, São Paulo, Brazil

[4]Unidade de Microbioloxía Clínica, Complexo Hospitalario Xeral-Calde, Lugo, Spain

Enterohaemorrhagic *Escherichia coli* (EHEC) and enteropathogenic *E. coli* (EPEC) translocate dozens of type III secretion system effectors, including the WxxxE effectors Map, EspM and EspT that activate Rho GTPases. While *map*, which is carried on the LEE pathogenicity island, is absolutely conserved among EPEC and EHEC strains, the prevalence of *espM* and *espT* is not known. Here we report the results of a large screen aimed at determining the prevalence of *espM* and *espT* among clinical EPEC and EHEC isolates. The results suggest that *espM*, detected in 51 % of the tested strains, is more commonly found in EPEC and EHEC serogroups that are linked to severe human infections. In contrast, *espT* was absent from all the EHEC isolates and was found in only 1.8 % of the tested EPEC strains. Further characterization of the virulence gene repertoire of the *espT*-positive strains led to the identification of a new ζ2 intimin variant. All the *espT*-positive strains but two contained the *tccP* gene. *espT* was first found in *Citrobacter rodentium* and later *in silico* in EPEC E110019, which is of particular interest as this strain was responsible for a particularly severe diarrhoeal outbreak in Finland in 1987 that affected 650 individuals in a school complex and an additional 137 associated household members. Comparing the protein sequences of EspT to that of E110019 showed a high level of conservation, with only three strains encoding EspT that differed in 6 amino acids. At present, it is not clear why *espT* is so rare, and what impact EspM and EspT have on EPEC and EHEC infection.

Received 12 February 2009
Accepted 7 April 2009

INTRODUCTION

Enterohaemorrhagic *Escherichia coli* (EHEC) comprise a subgroup of Shiga-toxin producing *E. coli* that can cause bloody diarrhoea, haemorrhagic colitis and haemolytic-uraemic syndrome (reviewed by Tarr, 1995). EHEC O157 : H7 is the most common and virulent serotype that is implicated worldwide in human disease, although non-O157 EHEC serotypes, particularly O26, O103, O111, O118 and O145, are also prevalent (reviewed by Nataro & Kaper, 1998). Enteropathogenic *E. coli* (EPEC) is the leading cause of mortality due to infantile diarrhoea in the developing world (reviewed by Chen & Frankel, 2005). EPEC strains comprise a diverse group of serotypes that may be divided into typical EPEC (tEPEC) and atypical EPEC (aEPEC) based on the presence or absence of a large virulence plasmid (EAF), respectively (Kaper, 1996)

EPEC and EHEC, as well as the mouse pathogen *Citrobacter rodentium* (reviewed by Mundy *et al.*, 2005), colonize the gut mucosa via attaching and effacing (A/E)

†These authors contributed equally to this work.

Abbreviations: A/E, attaching and effacing; aEPEC, atypical enteropathogenic *Escherichia coli*; EHEC, enterohaemorrhagic *Escherichia coli*; EPEC, enteropathogenic *Escherichia coli*; SF, sorbitol fermenting; tEPEC, typical enteropathogenic *Escherichia coli.*

The GenBank/EMBL/DDBJ accession numbers for the *eae*-ζ2 variant gene sequences of E110019 and T2381-8 are FM872419 and FM872420, respectively.

 010231 © 2009 SGM *Printed in Great Britain*

lesions, which are characterized by the close association of the bacteria with the enterocyte plasma membrane and localized breakdown of the brush border microvilli (Knutton *et al.*, 1987; reviewed by Frankel & Phillips, 2008). The ability to induce A/E lesions is associated with the LEE pathogenicity island, which encodes gene regulators, intimin (Jerse *et al.*, 1990), a type III secretion system (Jarvis *et al.*, 1995), chaperones, translocator and effector proteins (reviewed by Garmendia *et al.*, 2005a). The principal effector protein needed for A/E lesion formation is Tir, which, once translocated, is integrated into the mammalian cell plasma membrane where it serves as a receptor for intimin (Kenny *et al.*, 1997). Recent studies have shown that different EPEC and EHEC strains encode distinct intimin and Tir types; currently there have been 27 intimin and 8 Tir types reported (Blanco *et al.*, 2006a, b; Garrido *et al.*, 2006; J. Blanco, unpublished data).

EPEC E2348/69, which is the prototype strain used worldwide to study EPEC infection, encodes 21 LEE and non-LEE effectors (Iguchi *et al.*, 2009). Other EPEC strains encode a greater number of T3SS effectors: 28 in EPEC B171 (Ogura *et al.*, 2008), 40 in EPEC E22 and 24 in EPEC E110019 (Iguchi *et al.*, 2009). EHEC O157 Sakai encodes 50 effectors, representing the most complex repertoire among A/E pathogens (Tobe *et al.*, 2006). This shows that the A/E pathogen class is much more heterogeneous than was previously thought, comprising strains expressing unique complements of T3SS effector proteins and as a result employing diverse infection strategies.

A novel family of T3SS effectors, known as the WxxxE proteins, was recently described (Alto *et al.*, 2006), which include IpgB1 and IpgB2 from *Shigella*, SifA and SifB from *Salmonella*, and Map (Kenny & Jepson, 2000), EspM (Arbeloa *et al.*, 2008) and EspT (Bulgin *et al.*, 2008) from EPEC and EHEC. Members of the WxxxE family are important virulence factors. For example, SifA is essential for intracellular *Salmonella* survival (Beuzon *et al.*, 2000) and IpgB1 is essential for *Shigella* cell invasion (Ohya *et al.*, 2005). Map, which is encoded on the LEE pathogenicity island and is absolutely conserved among EPEC and EHEC strains, plays a role in colonization *in vivo* (Mundy *et al.*, 2004) and triggers transient filopodia by activating the Rho GTPase Cdc42 (Kenny *et al.*, 2002; Berger *et al.*, 2009). The different EspM variants induce formation of stress fibres by activating RhoA (Arbeloa *et al.*, 2008), while EspT from the *C. rodentium* induces formation of extensive lamellipodia by activation of Rac-1 and Cdc42 (Bulgin *et al.*, 2009). By sequence homology searches we recently identified homologues of *espM* and *espT* in EPEC strain E110019 (Bulgin *et al.*, 2009), a clinical isolate from a diarrhoeal outbreak in

Table 1. Distribution of *espM* and *espT* among 151 non-O157 clinical EHEC strains (Spain)

The strains were isolated in Spain, except for strain FV10110 O111 : H8, which was isolated in Germany. *espM–espT* negative strains were: ONT : HNT (2), ONT : H5 (1), ONT : H8 (1), ONT : H18 (1), ONT : H39 (1), O2 : H27 (1), O8 : H2 (1), O8 : H19 (1), O15 : H16 (1), O15 : H28 (1), O18 : ND (2), O22 : H42 (1), O55 : H- (1), O63 : HND (2), O64 : H21 (1), O76 : ND (2), O76 : H19 (2), O84 : HNT (1), O84 : HND (1), O91 : H- (2), O98 : H- (1), O104 : HNT (4), O113 : HND (2), O113 : H21 (2), O117 : HND (1), O136 : HND (1), O141 : HND (1), O146 : H- (1), O146 : H21 (4), O148 : HND (2), O148 : H8 (1), O165 : H- (1), O166 : HND (1), O166 : H28 (1), O168 : H8 (1), O174 : H21 (1), O183 : H- (1).

Serotype (no. of strains)		VT type	*espM*	*espT*
O	H			
ONT (14)	HND (7), H- (6), H11 (1)	1, 2	4	0
O5	HND (3)	1, 2	2	0
O14	H- (1)	1	1	0
O26 (37)	HND (17), H- (2), H8 (1), H11 (17)	1	36	0
O32	H6 (1)	1	1	0
O69	H21 (1)	1	1	0
O80	HND (1)	1, 2	1	0
O98	H21 (1)	1	1	0
O103 (6)	HND (1), H2 (5)	1, 2	6	0
O111 (10)	HND (5), H- (3), H8 (1)*, H10 (1)	1, 2	9	0
O118 (6)	HND (3), H- (1), H16 (2)	1	6	0
O121 (2)	H19 (1), H40 (1)	2	2	0
O145 (3)	HND (1), H- (2)	1, 2	3	0
O146	HND (10)	1, 2	1	0
O156	H25 (2)	1	2	0
O139, O141	HND (1)	1, 2	1	0

VT, Verocytotoxin.

*Strain FV10110 O111 : H8 was isolated in Germany.

Finland in 1987 (Viljanen *et al.*, 1990). $EspM_{E110019}$ is 100 % identical to the EspM of EHEC O157 Sakai, while $EspT_{E110019}$ shares 79 % sequence homology with the *C. rodentium* EspT, including the WxxxE motif. The aim of this study was to determine the prevalence of *espM* and *espT* among clinical EPEC and EHEC isolates.

METHODS

Bacterial strains. The bacterial strains used in this study included EPEC strains E2348/69 (Levine *et al.*, 1978) and E110019 (Viljanen *et al.*, 1990), EHEC O157 : H7 strain Sakai (Hayashi *et al.*, 2001), *C. rodentium* strain ICC169 (Barthold *et al.*, 1976; Wiles *et al.*, 2004), and 932 clinical EHEC and EPEC isolates.

Serotyping. The determination of O and H antigens was carried out using the method described by Guinée *et al.* (1981) employing all available O (O1–O185) and H (H1–H56) antisera. All antisera were obtained and absorbed with the corresponding cross-reacting antigens to remove the non-specific agglutinins. The O antisera were produced in the Laboratorio de Referencia de *E. coli* and the H antisera were obtained from the Statens Serum Institut, Copenhagen, Denmark.

Prevalence of *espT* and *espM* among clinical EPEC and EHEC strains. In order to screen for *espM* by PCR we used the eight *espM* sequences identified in EHEC O157 strain Sakai, EPEC strains B171 and E22, and *C. rodentium* to design common internal espM-1 (5′-TCTTTCAGCTCTTTTGGTAT-3′) and espM-2 (5′-CCAAAAGAA-GCATTCCCCATTAT-3′) forward and reverse primers (30 cycles of 94 °C for 45 s, 48 °C for 1 min and 72 °C for 1 min). The identity of representative PCR amplicons was confirmed by DNA sequencing. A second round of PCR was employed to screen representative espM-1 and espM-2 PCR negative strains using primers espM-3 (5′-TGATGAGGTCATGAAATGTTCAAT-3′) and espM-4 (5′-ATGATT-AATAGAACTTTG-3′) (30 cycles of 94 °C for 45 s, 50 °C for 1 min and 72 °C for 1 min).

We used the *espT* sequences from *C. rodentium* and E110019 to design internal espT-1 (5′-AATCTCATTCTCTTATC-3′) and espT-2 (5′-TCATGTGATGAGTGGATG-3′) primers for PCR (30 cycles of 94 °C for 45 s, 55 °C for 1 min and 72 °C for 1 min).

A further three rounds of PCR were employed to screen representative espT-1 and espT-2 PCR-negative strains using additional common internal primers espT-3 (5′-ATAGATGGTTTCTTTTTAGG-3′) and espT-4 (5′-CATCCAACGAGAAACCGCAAT-3′), and primers espT-5 (5′-CCGgaattcATGCCGGGAACAATAAGCTCCAG-3′) and espT-6 (5′-GGGAAGCTTTTAGGTTCTCTGAGCCTC-3′) and espT-7 (5′-TTGAATTCATGCATAGCATGCCAGGA-3′) and espT-8 (5′-CCAA-TGCACTGCAGGGAGCATTAAACATATTTTAAATTTCTC-3′), which correspond to the 5′ and 3′ ends of the *C. rodentium* and E110019 *espT* homologue, respectively (30 cycles of 94 °C for 45 s, 52 °C for 1 min and 72 °C for 1 min).

EHEC O157 : H7 Sakai, *C. rodentium* and EPEC E2348/69 were used as positive and negative controls.

Intimin, Tir and TccP typing of the *espT*-positive strains. Intimin and Tir typing was performed by PCR and sequencing as previously described (Blanco *et al.*, 2006b; Garrido *et al.*, 2006). The nucleotide sequence of the amplification products purified using a QIAquick DNA purification kit (Qiagen) was determined by the dideoxynucleotide triphosphate chain-termination method of Sanger, with a BigDye terminator v3.1 cycle sequencing kit and an ABI 3100 genetic analyzer (Applied Biosystems). The new *eae* sequences of the strains analysed were deposited in the European Bioinformatics Institute EMBL nucleotide sequence database. The presence of *tccP2* was determined by PCR as described by Whale *et al.* (2007).

Table 2. Distribution of *espM* and *espT* among 132 tEPEC strains

espM–espT negative strains were: ONT : HND (1), ONT : H1, H12 (1), ONT : H8 (1), ONT : H25 (1), O1 : H1, H12 (1), O55 : H8 (1), O86 : H8 (1), O88 : H5 (2), O98 : HND (1), O127 : H40 (3), O131 : H46 (2), O153 : H8 (1), O157 : H45 (1).

Serotype (no. of strains)		Origin	*espM*	*espT*
O	H			
ONT (2)	H6 (1), H10 (1)	Bolivia	2	0
O23 (2)	HND (1), H8 (1)	Spain	2	0
O49	H10 (5)	Spain, Bolivia	5	0
O55 (22)	H- (8), H6 (6), H51 (8)	Uruguay, Bolivia, Brazil, UK	19	0
O86 (6)	H- (2), H34 (4)	Bolivia, Brazil	6	0
O88 (17)	H- (1), H6 (1), H25 (15)	Spain, Bolivia	3	0
O103 (3)	H- (1), H7 (2)	Bolivia	3	0
O109	H- (2)	Spain, Chile	1	0
O111 (20)	H- (12), H2 (7), H25 (1)	Spain, Bolivia, Brazil, Uruguay	19	1
O118 (4)	HND (1), H- (1), H5 (2)	Spain, Germany	4	0
O119 (17)	H- (2), H6 (15)	Bolivia, Brazil, Uruguay	16	0
O125	H- (1)	Burundi	1	0
O127	H6 (3)	Bolivia, Brazil	1	0
O132	H8 (1)	Bolivia	1	0
O142 (6)	H6 (2), H34 (4)	Brazil, Spain	4	0
O145	H45 (3)	Brazil	3	0
O153	H11 (1)	Spain	1	0

Table 3. Distribution of *espM* and *espT* among 602 aEPEC strains

espM–espT negative strains were: ONT : H2 (2), ONT : H6 (4), ONT : H9 (1), ONT : H10 (2), ONT : H11, 21, 34 (1), ONT : H19 (2), ONT : H21, 39 (1), ONT : H34 (1), ONT : H40, 43 (2), ONT : H51 (1), O1 : H2 (1), O1 : H11 (1), O1 : H46 (1), O1 : H49 (1), O2ab : H45 (1), O2 : NT (1), O2 : H6 (1), O2 : H16 (1), O2 : H45 (1), O2 : H49 (2), O3 : H4 (1), O5 : H6 (1), O5 : H40 (1), O5 : H49 (1), O6 : H4 (1), O6 : H16 (1), O9 : HND (2), O11 : H16 (2), O12 : HND (1), O13 : H11 (1), O15 : H- (2), O15 : H7 (1), O16 : H- (1), O18 : H7 (1), O18 : H16 (1), O20 : H6 (1), O21 : HND (2), O21 : H15 (1), O23 : HND (1), O24 : H2 (1), O25 : HND (2), O25 : H1 (1), O26 : H2 (1), O28 : HND (1), O33 : HNT (1), O33 : H6 (1), O33 : H34 (1), O34 : H- (1), O41 : H- (1), O49 : H40 (1), O51 : H41 (1), O55 : H40 (1), O56 : H6 (1), O63 : HND (1), O64 : H40 (1), O71 : H1, H12 (2), O76 : H19 (1), O84 : HND (1), O84 : H- (2), O85 : H8 (1), O85 : H49 (1), O86 : HNT (1), O86 : HND (1), O88, O168 : HND (1), O98 : H- (1), O98 : H8 (1), O101 : H33 (2), O103 : H- (3), O103 : H4 (1), O103 : H19 (1), O103 : H40 (1), O104 : H- (2), O105 : HND (1), O105 : H4 (2), O108 : HND (3), O110 : HND (5), O111 : H9 (1), O111 : H38 (1), O112 : H15 (1), O113 : HND (4), O113 : H- (1), O114 : HND (1), O117 : H11 (1), O117 : H40 (2), O121 : HND (1), O123 : HND (1), O123 : H19 (1), O123 : H45 (1), O125 : H6 (3), O127 : HND (1), O127 : H6 (1), O128 : H40 (1), O129 : HND (1), O129 : H- (1), O132 : HND (3), O132 : H5 (3), O137 : HND (3), O137 : H6 (2), O139 : HND (4), O139 : H2 (1), O141 : HND (10), O145 : H2 (1), O146 : H28 (1), O148 : H8 (1), O153 : H11 (1), O153 : H31 (1), O153 : H40 (1), O156 : H4 (1), O156 : H8 (3), O156 : H33 (1), O157 : H16 (2), O159 : HND (1), O164 : H- (1), O167 : H27 (1), O168 : H- (1), O171 : H19 (1), O173 : H- (1), O178 : H6 (1), O180 : HND (1), O180 : H2 (1), R : H28 (1).

Serotype (no. of strains)		Origin	*espM*	*espT*
O	**H**			
ONT (92)	HND (38), HNT (4), H- (24), H4 (3), H7 (4), H8 (3), H11 (4), H23 (1), H33 (2), H40 (6), H45 (3)	Spain, Brazil, Bolivia, Chile		
O1 (3)	H7 (1), H40 (1), H45 (1)	Brazil, Spain	3	0
O2 (11)	ND (3), H40 (8)	Spain	3	2
O4 (4)	ND (2), H- (1), H1 (1)	Spain, Brazil	3	0
O5	ND (7)	Spain	2	0
O6 (2)	ND (1), H19 (1)	Spain	2	0
O8 (5)	HND (3), H11 (1), H19 (1)	Spain	3	0
O10 (5)	HN (3), H- (2)	Spain	4	0
O11	HND (4)	Spain	4	0
O14	H5 (1)	Brazil	1	0
O15 (17)	HND (9), H2 (8)	Spain	12	0
O18	HND (2)	Spain	2	0
O20	HND (2)	Spain	2	0
O22	HND (2)	Spain	2	0
O25	H2 (1)	Spain	1	0
O26 (30)	ND (20), H- (6), H11 (4)	Spain, Brazil	23	0
O28	H28 (1)	Bolivia	1	0
O33	HND (3)	Spain	1	0
O49 (12)	HND (6), H- (3), H2 (1), H10 (2)	Spain, Brazil	6	1
O51 (16)	HND (5), H- (2), H1 (1), H40 (6), H49 (2)	Spain, Brazil	7	0
O52	H10 (1)	Spain	1	0
O57	H7 (3)	Spain	3	0
O55 (16)	HND (4), H- (1), H6 (1), H7 (9), H51 (1)	Spain, Brazil, Bolivia	15	0
O56	H- (1)	Spain	1	0
O63 (6)	H6 (5), H33 (1)	Spain, Brazil	2	0
O64	H25 (2)	Spain	1	0
O70	H2 (1)	Brazil	1	0
O76	HND (3)	Spain	2	0
O80 (9)	ND (5), H2 (4)	Spain	4	0
O82 (2)	HND (1), H10 (1)	Spain	2	0
O85 (13)	HND (5), H- (2), H31 (5), H43 (1)	Spain	4	1
O101 (7)	HND (2), H- (5)	Spain, Brazil	7	0
O103 (12)	HND (11), H2 (1)	Spain	4	0
O104 (4)	HND (1), H2 (2), H12 (1)	Spain, Brazil	2	2
O109	H9 (1)	Brazil	1	1
O111 (2)	HND (1), H- (1)	Spain	2	0
O113	H6 (4)	Spain	1	0
O115 (4)	HND (1), H8 (3)	Spain	3	0
O117	HND (4)	Spain	2	0

Table 3. cont.

Serotype (no. of strains)		Origin	*espM*	*espT*
O	H			
O119	HND (2)	Spain	2	0
O120	HND (2)	Spain	1	0
O123	H- (2)	Brazil	2	2
O125	H28 (1)	Spain	1	0
O127	H40 (5)	Spain, Bolivia	1	0
O128 (4)	HND (1), H- (1), H2 (1), H27 (1)	Spain	4	0
O132	H34 (3)	Spain	3	0
O139	H19 (1)	Spain	1	0
O145 (33)		Spain, Germany	25	0
O146	HND (1)	Spain	1	0
O153	HND (15)	Spain	2	0
O154	H9 (1)	Brazil	1	1
O156 (8)	HND (6), H- (2)	Spain	4	0
O157 (5)	ND (2), H7 (3)	Spain	4	0
O162 (4)	H- (2), H21 (1), H33 (1)	Spain, Brazil	3	0
O166	HND (1)	Spain	1	0
O167 (4)	ND (2), H9 (1), H11 (1)	Spain	3	0
O177	H11 (1)	Spain	1	0
O178	H7 (1)	Spain	1	0
O179	H31 (1)	Spain	1	0
O115, O152 (15)	HND (13), H8 (1), H10 (1)	Spain	10	0
R (2)	H11, 21 (1), H28 (1)	Brazil	1	0

RESULTS AND DISCUSSION

Screening O157 and non-O157 EHEC strains for the presence of *espM* and *espT*

We determined the prevalence of *espM* and *espT* among 45 non-sorbitol fermenting (non-SF) EHEC O157 : H7 (expressing VT1 and VT2), isolated in Spain, Canada and Bolivia, and two SF EHEC O157 : H- (expressing VT2), isolated in Germany. *espM* was found in 43 of the non-SF O157 isolates (96 %) and in the 2 SF isolates. We then screened 151 non-O157 EHEC strains. *espM* was found in 60 of the 62 (97 %) non-O157 EHEC strains belonging to

Table 4. Characterization of the *espT*-positive strains

Serotype (no. of strains)	Origin	Pathotype	*espM*	Intimin	Tir	Tccp2	GenBank accession no.
Group 1							
O111 : H9 (1)	Finland	aEPEC	+	ζ2	α1	+	
ONT : H- (1)	Brazil	aEPEC	+	ε2	α1	+	FM992854
O49 : H- (1)	Brazil	aEPEC	+	ζ2	α1	+	FM992855
O85 : H- (1)	Brazil	aEPEC	−	ι1	α1	+	FM992856
O109 : H9 (1)	Brazil	aEPEC	+	ε2	α1	+	FM992857
O111 : H- (1)	Spain	tEPEC	+	ζ2	α1	+	FM992858
O123 : H- (2)	Brazil	aEPEC	+	ε2	α1	+	FM992859
O154 : H9 (1)	Brazil	aEPEC	+	ζ2	α1	+	FM992860
Group 2							
O2 : H49 (1)	Spain	aEPEC	−	θ1	θ1	+	FM992862
O2 : H49 (1)	Spain	aEPEC	−	ι1	α1	−	FM992861
Group 3							
ONT : H7 (1)	Brazil	aEPEC	+	β1	β1	−	FM992863
O104 : H2 (1)	Spain	aEPEC	−	β1	β1	+	FM992864
O104 : H2 (1)	Brazil	aEPEC	−	β1	β1	+	FM992865

serogroups O26, O103, O111, O118 and O145 (Table 1). In contrast *espM* was found in only 17 of 89 (19 %) strains belonging to the other non-O157 serogroups (Table 1). All the O157 and non-O157 strains were *espT* gene negative.

In order to confirm the absence of *espM* and *espT* from the PCR gene-negative strains, we screened 50 O157 and non-O157 EHEC strains with a second set of conserved *espM* primers (espM-3 and espM-4) and three sets of *espT* primers (espT-3 and espT-4, espT-5 and espT-6, and espT-7 and espT-8). All the isolates remained *espM* and *espT* gene negative in these tests.

Screening tEPEC and aEPEC isolates for the presence of *espM* and *espT*

We screened a total of 132 tEPEC strains, isolated in Brazil, Bolivia, Burundi, Spain, Chile, Germany, the UK and Uruguay, and 602 aEPEC strains, isolated in Brazil, Bolivia, Chile and Spain, for the presence of *espM* and *espT*. *espM* was found in 91 tEPEC isolates (69 %) belonging to 16 different serogroups (the O serogroup of 6 strains was non-typable – ONT) (Table 2). *espM* was found in 258 aEPEC isolates (43 %) belonging to 59 different serogroups [the O serogroup of 109 strains was ONT and of 2 isolates was O rough (R)] (Table 3). Of the 109 ONT aEPEC, *espM* was found in 45 isolates (41 %). Among the aEPEC that shared a serogroup with the major EHEC strains, *espM* was found in 23 of 31 (74 %) O26, 4 of 12 (33 %) O103, 2 of 4 (50 %) O111, 25 of 33 (76 %) O145 and 4 of 7 (57 %) O157 isolates; in total 58 of 87 (67 %). Interestingly, *espM* was found in 94 % (15 of 16) of the O55 strains, regardless of serotype. *espT* was found in only 1 (0.8 %) tEPEC strain (O111 : H-) isolated in Spain and in 12 aEPEC strains (2 %) (Table 3).

In order to confirm the absence of *espM* and *espT* from the PCR gene-negative EPEC strains, we screened 50 tEPEC and 100 aEPEC strains with *espM* primers 3 and 4, and *espT* primers 3 and 4, 5 and 6, and 7 and 8. All the isolates remained *espM* and *espT* gene negative in these tests.

Further characterization of the *espT*-positive strains

Considering that *espT* was found in only 13 of the total 932 isolates tested, we sequenced their amplicons, and characterized their virulence genes implicated in colonization (e.g. intimin type) and pedestal formation (e.g. Tir type and TccP2) as described previously (Garmendia *et al.*, 2005b); strain E110019 was used as a reference strain. Sequencing of *espT* revealed a high level of sequence conservation (Table 4). In the eight strains EspT was identical to that of E110019, defined as group 1 EspT. In two strains we detected a single amino acid difference (group 2) and in three other strains we found 6 amino acids that differed from the EspT of E110019 (group 3) (Fig. 1). All the *espT*-positive strains encoded a Tir that can undergo tyrosine phosphorylation and thus trigger strong actin polymerization *in vitro* via the Nck-N-WASP pathway (Kenny, 1999; Gruenheid *et al.*, 2001). All the strains but two encoded TccP2, which can also activate the N-WASP actin-signalling pathway (Whale *et al.*, 2007). Eight of the *espT*-positive strains (as well as E110019) also encoded EspM.

Intimin typing was performed by sequencing the variable 3′ end of the *eae* gene from the 14 *espT*-positive strains (including E110019) (Table 4) (Blanco *et al.*, 2006b). This revealed known intimin types in 10 strains: β1 (3 strains), ε2 (4 strains), θ1 (1 strain) and ι1 (2 strains). Importantly, we identified a new intimin variant, ζ2, in 4 of the *espT* gene-positive strains (Table 4). We determined the complete nucleotide sequence of two of the new *eae*-ζ2 variant genes (accession numbers FM872419 and FM872420 for E110019 and T2381-8, respectively). Using CLUSTAL W software for optimal sequence alignment with the known 27 *eae* alleles, we found 98, 92 and 91 % sequence identity with the *eae*-ζ1 (AJ271407), *eae*-α1 (M58154) and *eae*-α2 (AF530555) genes, respectively.

Conclusions

Our results show that *espM* is found in approximately 96 % of the strains belonging to the major EHEC serogroups: O26, O103, O111, O118, O145 and O157, and in a

```
                7                                                   57
EspT 1/E110019  TVNSCGFGFS ITKAPYSSGQ KPVIDGFFLG ARRISFSYPR LESELIQCIN
       EspT 2   TVNSCGFGFS ITKAPYSSGQ KPVIDGFFLG ARRISFSYPR LESELIQCIN
       EspT 3   TVNSCGFGFS ITKAPYSSGQ KPFIDGFFLG ARKISFSYPR LESELIQCIN

               58                                                  107
EspT 1/E110019  LKNEGKKNEW MKEESICFVS RDVNKLLDMF AKNNQTNIPK GVRERVFQLA
       EspT 2   LKNEGKKNEW MKEESICFVS RDVNKLLDMF AKNNQTNIPK GVRERVFQLA
       EspT 3   LKNEGKKNEW MKEEGICFVS RDVNKLLDMF AKNNQTNIPE GVRERVFQLA

               108                                                 157
EspT 1/E110019  SFYCGFSLDA RCAQASTHHM ILNSQYFQKK MDTLLTSVDI NVRNQCVRTA
       EspT 2   SFYCGFSLDA RCAQTSTHHM ILNSQYFQKK MDTLLTSVDI NVRNQCVRTA
       EspT 3   SFYCGFSLDA RCAQTSTHHM ILNSQYFQKK MDTLLTSVDI NVRNQCVRTA

               158                                 190
EspT 1/E110019  LSSLADTFFE NNVNNIDMNK LRDRVHNTIV QEV
       EspT 2   LSSLADTFFE NNVNNIDMNK LRDRVHNTIV QEV
       EspT 3   LSSLADTFFE NNVNNIDMNK FRDRVHNTIV QEV
```

Fig. 1. Multiple sequence alignment of representative EspT sequences. The conserved motif WxxxE is boxed. When compared with $EspT_{E110019}$, 8 of the 13 EspT showed 100 % sequence identity (ONT : H-, O49 : H-, O85 : H-, O109 : H9, O111 : H-, O123 : H-(2), O154 : H9) as represented by sequence EspT 1. Two strains belonging to serotype O2 : H49 had 1 amino acid difference, indicated by dark grey (sequence EspT 2), while three strains O104 : H2 (2), ONT : H (7) differed in 6 amino acids, indicated by dark grey and light grey (sequence EspT 3).

significantly higher proportion than in other non-O157 EHEC strains ($P<0.05$). Similarly, *espM* was also more commonly found in EPEC serogroups O26, O55, O145 and O157 than in other aEPEC. Among the tEPEC strains *espM* was detected in approximately 69 % of the tested isolates. These results suggest that *espM* is more commonly found in EPEC and EHEC serogroups that are linked to severe human infections. In contrast, *espT* was found only infrequently and only among EPEC strains (1 tEPEC and 12 aEPEC isolates). *espT* was first found in *C. rodentium* and later *in silico* in EPEC E110019, which is of particular interest as it was responsible for a particularly severe diarrhoeal outbreak in Finland in 1987 that affected 650 individuals, including adults, in a school complex and an additional 137 associated household members (Viljanen *et al.*, 1990). Comparing the protein sequences of EspT to that of E110019 showed a high level of conservation, with only three strains encoding EspT that differed in 6 amino acids from the EspT of E110019. At present, it is not clear why *espT* is so rare and what impact EspM and EspT have on EPEC and EHEC infection.

ACKNOWLEDGEMENTS

We thank Jim Kaper for the E11001119 strain. A. Mora acknowledges the Ramón y Cajal programme from the Spanish Ministry of Education and Science. Work in the laboratory of Jorge Blanco was supported by grants from the Spanish Ministry of Health and Consumer Affairs [Fondo de Investigación Sanitaria, Spanish Network for the Research in Infectious Diseases (REIPI) RD06/0008-1018], Spanish Ministry of Education and Science (AGL-2008-02129) and the Autonomous Government of Galicia (Xunta de Galicia, PGIDIT065TAL26101P, 07MRU036261PR). Work in the laboratory of T. A. T. G. was supported by Fundação de Amparo à Pesquisa do Estado de São Paulo (FAPESP) grant 08/53812-4, and Programa de Apoio a Núcleos de Excelência - PRONEX MCT/CNPq/FAPERJ. F. C. M. received a fellowship from FAPESP. Work in the laboratory of Gad Frankel was supported by the MRC and the Wellcome Trust.

REFERENCES

Alto, N. M., Shao, F., Lazar, C. S., Brost, R. L., Chua, G., Mattoo, S., McMahon, S. A., Ghosh, P., Hughes, T. R. & other authors (2006). Identification of a bacterial type III effector family with G protein mimicry functions. *Cell* **124**, 133–145.

Arbeloa, A., Bulgin, R. R., MacKenzie, G., Shaw, R. K., Pallen, M. J., Crepin, V. F., Berger, C. N. & Frankel, G. (2008). Subversion of actin dynamics by EspM effectors of attaching and effacing bacterial pathogens. *Cell Microbiol* **10**, 1429–1441.

Barthold, S. W., Coleman, G. L., Bhatt, P. N., Osbaldiston, G. W. & Jonas, A. M. (1976). The etiology of transmissible murine colonic hyperplasia. *Lab Anim Sci* **26**, 889–894.

Berger, C. N., Crepin, V. F., Jepson, M. A., Arbeloa, A. & Frankel, G. (2009). The mechanisms used by enteropathogenic *Escherichia coli* to control filopodia dynamics. *Cell Microbiol* **11**, 309–322.

Beuzon, C. R., Meresse, S., Unsworth, K. E., Ruiz-Albert, J., Garvis, S., Waterman, S. R., Ryder, T. A., Boucrot, E. & Holden, D. W. (2000). *Salmonella* maintains the integrity of its intracellular vacuole through the action of SifA. *EMBO J* **19**, 3235–3249.

Blanco, M., Blanco, J. E., Dahbi, G., Alonso, M. P., Mora, A., Coira, M. A., Madrid, C., Juarez, A., Bernardez, M. I. & other authors (2006a). Identification of two new intimin types in atypical enteropathogenic *Escherichia coli*. *Int Microbiol* **9**, 103–110.

Blanco, M., Blanco, J. E., Dahbi, G., Mora, A., Alonso, M. P., Varela, G., Gadea, M. P., Schelotto, F., Gonzalez, E. A. & Blanco, J. (2006b). Typing of intimin (*eae*) genes from enteropathogenic *Escherichia coli* (EPEC) isolated from children with diarrhoea in Montevideo, Uruguay: identification of two novel intimin variants (*muB* and *xiR/beta2B*). *J Med Microbiol* **55**, 1165–1174.

Bulgin, R. R., Arbeloa, A., Chung, J. C. & Frankel, G. (2009). EspT triggers formation of lamellipodia and membrane ruffles through activation of Rac-1 and Cdc42. *Cell Microbiol* **11**, 217–229.

Chen, H. D. & Frankel, G. (2005). Enteropathogenic *Escherichia coli*: unravelling pathogenesis. *FEMS Microbiol Rev* **29**, 83–98.

Frankel, G. & Phillips, A. D. (2008). Attaching effacing *Escherichia coli* and paradigms of Tir-triggered actin polymerization: getting off the pedestal. *Cell Microbiol* **10**, 549–556.

Garmendia, J., Frankel, G. & Crepin, V. F. (2005a). Enteropathogenic and enterohemorrhagic *Escherichia coli* infections: translocation, translocation, translocation. *Infect Immun* **73**, 2573–2585.

Garmendia, J., Ren, Z., Tennant, S., Midolli Viera, M. A., Chong, Y., Whale, A., Azzopardi, K., Dahan, S., Sircili, M. P. & other authors (2005b). Distribution of *tccP* in clinical enterohemorrhagic and enteropathogenic *Escherichia coli* isolates. *J Clin Microbiol* **43**, 5715–5720.

Garrido, P., Blanco, M., Moreno-Paz, M., Briones, C., Dahbi, G., Blanco, J. & Parro, V. (2006). STEC-EPEC oligonucleotide microarray: a new tool for typing genetic variants of the LEE pathogenicity island of human and animal Shiga toxin-producing *Escherichia coli* (STEC) and enteropathogenic *E. coli* (EPEC) strains. *Clin Chem* **52**, 192–201.

Gruenheid, S., DeVinney, R., Bladt, F., Goosney, D., Gelkop, S., Gish, G. D., Pawson, T. & Finlay, B. B. (2001). Enteropathogenic *E. coli* Tir binds Nck to initiate actin pedestal formation in host cells. *Nat Cell Biol* **3**, 856–859.

Guinée, P. A. M., Jansen, W. H., Wadström, T. & Sellwood, R. (1981). *Escherichia coli* associated with neonatal diarrhoea in piglets and calves. *Curr Top Vet Anim Sci* **13**, 126–162.

Hayashi, T., Makino, K., Ohnishi, M., Kurokawa, K., Ishii, K., Yokoyama, K., Han, C. G., Ohtsubo, E., Nakayama, K. & other authors (2001). Complete genome sequence of enterohemorrhagic *Escherichia coli* O157 : H7 and genomic comparison with a laboratory strain K-12. *DNA Res* **8**, 11–22.

Iguchi, A., Thomson, N. R., Ogura, Y., Saunders, D., Ooka, T., Henderson, I. R., Harris, D., Asadulghani, M., Kurokawa, K. & other authors (2009). Complete genome sequence and comparative genome analysis of enteropathogenic *Escherichia coli* O127 : H6 strain E2348/69. *J Bacteriol* **191**, 347–354.

Jarvis, K. G., Girón, J. A., Jerse, A. E., McDaniel, T. K., Donnenberg, M. S. & Kaper, J. B. (1995). Enteropathogenic *Escherichia coli* contains a putative type III secretion system necessary for the export of proteins involved in attaching-effacing lesions formation. *Proc Natl Acad Sci U S A* **92**, 7996–8000.

Jerse, A. E., Yu, J., Tall, B. D. & Kaper, J. B. (1990). A genetic locus of enteropathogenic *Escherichia coli* necessary for the production of attaching and effacing lesions on tissue culture cells. *Proc Natl Acad Sci U S A* **87**, 7839–7843.

Kaper, J. B. (1996). Defining EPEC. *Rev Microbiol Sao Paulo* **27**, 130–133.

Kenny, B. (1999). Phosphorylation of tyrosine 474 of the enteropathogenic *Escherichia coli* (EPEC) Tir receptor molecule is essential

for actin nucleating activity and is preceded by additional host modifications. *Mol Microbiol* **31**, 1229–1241.

Kenny, B. & Jepson, M. (2000). Targeting of an enteropathogenic *Escherichia coli* (EPEC) effector protein to host mitochondria. *Cell Microbiol* **2**, 579–590.

Kenny, B., DeVinney, R., Stein, M., Reinscheid, D. J., Frey, E. A. & Finlay, B. B. (1997). Enteropathogenic *Escherichia coli* (EPEC) transfers its receptor for intimate adherence into mammalian cells. *Cell* **91**, 511–520.

Kenny, B., Ellis, S., Leard, A. D., Warawa, J., Mellor, H. & Jepson, M. A. (2002). Co-ordinate regulation of distinct host cell signalling pathways by multifunctional enteropathogenic *Escherichia coli* effector molecules. *Mol Microbiol* **44**, 1095–1107.

Knutton, S., Lloyd, D. R. & McNeish, A. S. (1987). Adhesion of enteropathogenic *Escherichia coli* to human intestinal enterocytes and cultured human intestinal mucosa. *Infect Immun* **55**, 69–77.

Levine, M. M., Bergquist, E. J., Nalin, D. R., Waterman, D. H., Hornick, R. B., Young, C. R. & Sotman, S. (1978). *Escherichia coli* strains that cause diarrhoea but do not produce heat-labile or heat-stable enterotoxins and are non-invasive. *Lancet* **1**, 1119–1122.

Mundy, R., Petrovska, L., Smollett, K., Simpson, N., Wilson, R. K., Yu, J., Tu, X., Rosenshine, I., Clare, S. & other authors (2004). Identification of a novel *Citrobacter rodentium* type III secreted protein, EspI, and roles of this and other secreted proteins in infection. *Infect Immun* **72**, 2288–2302.

Mundy, R., MacDonald, T. T., Dougan, G., Frankel, G. & Wiles, S. (2005). *Citrobacter rodentium* of mice and man. *Cell Microbiol* **7**, 1697–1706.

Nataro, J. P. & Kaper, J. B. (1998). Diarrheagenic *Escherichia coli*. *Clin Microbiol Rev* **11**, 142–201.

Ogura, Y., Abe, H., Katsura, K., Kurokawa, K., Asadulghani, M., Iguchi, A., Ooka, T., Nakayama, K., Yamashita, A. & other authors (2008). Systematic identification and sequence analysis of the genomic islands of the enteropathogenic *Escherichia coli* strain B171–8 by the combined use of whole-genome PCR scanning and fosmid mapping. *J Bacteriol* **190**, 6948–6960.

Ohya, K., Handa, Y., Ogawa, M., Suzuki, M. & Sasakawa, C. (2005). IpgB1 is a novel *Shigella* effector protein involved in bacterial invasion of host cells. Its activity to promote membrane ruffling via Rac1 and Cdc42 activation. *J Biol Chem* **280**, 24022–24034.

Tarr, P. I. (1995). *Escherichia coli* O157 : H7: clinical, diagnostic, and epidemiological aspects of human infection. *Clin Infect Dis* **20**, 1–8.

Tobe, T., Beatson, S. A., Taniguchi, H., Abe, H., Bailey, C. M., Fivian, A., Younis, R., Matthews, S., Marches, O. & other authors (2006). An extensive repertoire of type III secretion effectors in *Escherichia coli* O157 and the role of lambdoid phages in their dissemination. *Proc Natl Acad Sci U S A* **103**, 14941–14946.

Viljanen, M. K., Peltola, T., Junnila, S. Y., Olkkonen, L., Jarvinen, H., Kuistila, M. & Huovinen, P. (1990). Outbreak of diarrhoea due to *Escherichia coli* O111 : B4 in schoolchildren and adults: association of Vi antigen-like reactivity. *Lancet* **336**, 831–834.

Whale, A. D., Hernandes, R. T., Ooka, T., Beutin, L., Schuller, S., Garmendia, J., Crowther, L., Vieira, M. A., Ogura, Y. & other authors (2007). TccP2-mediated subversion of actin dynamics by EPEC 2 – a distinct evolutionary lineage of enteropathogenic *Escherichia coli*. *Microbiology* **153**, 1743–1755.

Wiles, S., Clare, S., Harker, J., Huett, A., Young, D., Dougan, G. & Frankel, G. (2004). Organ specificity, colonization and clearance dynamics in vivo following oral challenges with the murine pathogen *Citrobacter rodentium*. *Cell Microbiol* **6**, 963–972.

OPEN ACCESS Freely available online

PLoS PATHOGENS

The T3SS Effector EspT Defines a New Category of Invasive Enteropathogenic *E. coli* (EPEC) Which Form Intracellular Actin Pedestals

Richard Bulgin[1], Ana Arbeloa[1], David Goulding[2], Gordon Dougan[2], Valerie F. Crepin[1], Benoit Raymond[1], Gad Frankel[1]*

1 Centre for Molecular Microbiology and Infection, Division of Cell and Molecular Biology, Imperial College London, London, United Kingdom, **2** The Wellcome Trust Sanger Institute, Wellcome Trust Genome Campus, Hinxton, Cambridge, United Kingdom

Abstract

Enteropathogenic *Escherichia coli* (EPEC) strains are defined as extracellular pathogens which nucleate actin rich pedestal-like membrane extensions on intestinal enterocytes to which they intimately adhere. EPEC infection is mediated by type III secretion system effectors, which modulate host cell signaling. Recently we have shown that the WxxxE effector EspT activates Rac1 and Cdc42 leading to formation of membrane ruffles and lamellipodia. Here we report that EspT-induced membrane ruffles facilitate EPEC invasion into non-phagocytic cells in a process involving Rac1 and Wave2. Internalized EPEC resides within a vacuole and Tir is localized to the vacuolar membrane, resulting in actin polymerization and formation of intracellular pedestals. To the best of our knowledge this is the first time a pathogen has been shown to induce formation of actin comets across a vacuole membrane. Moreover, our data breaks the dogma of EPEC as an extracellular pathogen and defines a new category of invasive EPEC.

Citation: Bulgin R, Arbeloa A, Goulding D, Dougan G, Crepin VF, et al. (2009) The T3SS Effector EspT Defines a New Category of Invasive Enteropathogenic *E. coli* (EPEC) Which Form Intracellular Actin Pedestals. PLoS Pathog 5(12): e1000683. doi:10.1371/journal.ppat.1000683

Editor: Guy Tran Van Nhieu, Institut Pasteur, France

Received July 30, 2009; **Accepted** November 5, 2009; **Published** December 11, 2009

Copyright: © 2009 Bulgin et al. This is an open-access article distributed under the terms of the Creative Commons Attribution License, which permits unrestricted use, distribution, and reproduction in any medium, provided the original author and source are credited.

Funding: This work was supported by grants from the MRC and the Wellcome Trust. The funders had no role in study design, data collection and analysis, decision to publish, or preparation of the manuscript.

Competing Interests: The authors have declared that no competing interests exist.

* E-mail: g.frankel@imperial.ac.uk

Introduction

The human pathogens enteropathogenic *Escherichia coli* (EPEC) and enterohemorrhagic *E. coli* (EHEC) [1] and the mouse pathogen *Citrobacter rodentium* [2] are closely related extra-cellular diarrhoeal agents characterized by their ability to colonize the gut epithelium via attaching and effacing (A/E) lesion formation (reviewed in [3]) [4]. Similarly to other Gram-negative bacteria EPEC, EHEC and *C. rodentium* encode a type III secretion system (T3SS), which is central to their infection strategy (reviewed in [5]) [6]. This complex machinery translocate dozens of effector proteins [7,8] directly from the bacteria to the eukaryotic cell cytoplasm (reviewed in [9]). The translocated effectors are targeted to various sub-cellular compartments where they subvert a plethora of cell signaling pathways via interactions with a range of host cell proteins.

The host cell cytoskeleton is a common target of T3SS effectors [10]. EPEC, EHEC and *C. rodentium* translocate the effector Tir into the plasma membrane where it functions as a receptor for the bacterial outer membrane protein intimin [11]. Intimin:Tir interaction leads to activation of N-WASP and formation of actin rich pedestals on which the extracellular bacteria rest [12]. In addition to Tir, A/E pathogens translocate a variety of other effectors which also modulate the host cell cytoskeleton including EspG/EspG2, which induce depolymerization of the microtubule network [13], Map, which induces formation of transient filopodia early in infection [14] and EspM which directs formation of actin stress fibers [15]. Map and EspM are members of the WxxxE family [15,16,17], which was first grouped together based on conserved peptide motif consisting of an invariant tryptophan and glutamic acid residues separated by three variable amino acids and their shared ability to subvert host cell small GTPase signaling.

Small GTPases cycle between an inactive GDP bound and an active GTP bound form, allowing them to function as molecular switches in response to a variety of stimuli. The switch from inactive to active forms results in a conformational change, which allows the GTPase to bind downstream mammalian effectors. Small GTPases are regulated by guanine exchange factors (GEFs), GTPase activating proteins (GAPs) and guanine dissociation inhibitor (GDI) proteins (reviewed in [18,19]). The three best characterized Rho GTPases are RhoA, Rac1 and Cdc42 which are implicated in formation of stress fibers, lamellipodia and filopodia respectively (reviewed in [20]).

The WxxxE effectors were originally proposed to be functional mimics of mammalian small GTPases [16]. However, we have recently shown that EspM activates RhoA [15] whereas Map induces filopodia via activation of Cdc42 and RhoA [17]. In addition to Map and EspM we have recently discovered the novel WxxxE effector EspT, which is encoded by *C. rodentium* and a subset of EPEC strains [21], including EPEC E110019 which caused a sever outbreak in Finland in 1987 that affected children and adults alike [22]. We have shown that EspT induces formation of lamellipodia and membrane ruffles in epithelial cells via activation of Rac1 and Cdc42 [23].

Membrane ruffles are sheet like structures which are induced by mammalian cells in order to facilitate crawling movement, macro-

Author Summary

Enteropathogenic *E. coli* (EPEC) is an important diarrheal pathogen responsible for significant infant mortality in the developing world and is increasingly associated with sporadic outbreaks in the developed world. The virulence strategy of EPEC revolves around a conserved Type 3 secretion system (T3SS) which translocates bacterial effector proteins directly into host cells. EPEC is considered to be a non-invasive pathogen which intimately adheres to host cells and polymerizes actin rich pedestals on which extracellular bacteria rest. Recently we have identified the T3SS effector EspT which activates the mammalian Rho GTPases Rac1 and Cdc42, resulting in the formation of membrane ruffles and lamellipodia. In this study we dissect the signaling pathway utilized by EspT to nucleate membrane ruffles and demonstrate that these ruffles can promote EPEC invasion of host cells. Furthermore, we show that internalized EPEC are bound within a vacuole. We also report for the first time the ability of a bacterial pathogen to form actin comet tails across a vacuole membrane. In addition to providing novel insights into the subversion of cellular signaling by invasive pathogens, our study also breaks the long held dogma of EPEC as an extracellular pathogen and will have implications on how future EPEC infections are diagnosed and treated.

pinocitosis and receptor recycling (reviewed in [24]). These protrusion are regulated through activity of Rho family GTPases and their downstream effectors (reviewed in [25]). Importantly, a subset of invasive bacterial pathogens hijack and subvert mammalian signal transduction pathways which facilitate formation membrane ruffles in order to promote bacterial entry into mammalian cells. Perhaps the best studied of these pathogens are *Salmonella* and *Shigella* which induce extensive membrane ruffles at the site of bacterial attachment (reviewed in [26,27]). *Salmonella* invasion is dependent upon the activity of several T3SS effector proteins including SopE/E2 which act as GEFs for Rac1 and Cdc42 [28] and SopB which activates the RhoG GEF SGEF [29]. *Shigella* has also evolved several invasive mechanisms. For example the translocator IpaC has been shown to induce ruffles at the site of *Shigella* entry via the activation of Cdc42 [30], recruitment of Src kinase [31] and activation of Abl kinase [32]. The *Shigella* WxxxE effector IpgB1 has also been shown to induce membrane ruffles via interaction with the ELMO DOCK180 complex which results in activation of Rac1 [33].

EPEC, EHEC and *C. rodentium* are generally considered extracellular pathogens and their attachment sites on epithelial cells are normally characterized by the assembly of an actin rich pedestal rather than membrane ruffles (reviewed in [3]). However, in both rabbit and human biopsies EPEC have been visualized inside enterocytes and detected in the sub mucosa, mesenteric lymph nodes and spleen [34] (reviewed in [35]). Recently Hernandes *et al* has shown that the atypical EPEC strain 1551-2 is capable of invading cultured epithelial cells in an intimin omicron dependent manner [36]. As EspT induces membrane ruffles similar to those triggered by IpgB1 [37] the aim of this study was to investigate if expression of EspT leads to EPEC cell invasion and to define the underlying mechanism.

Results

EspT-induced membrane ruffles surround adherent bacteria

A large screen of clinical EPEC isolates for the presence of *espT*, a T3SS effector (Fig. S1), has shown that the gene is present in ca. 1.8% of the tested strains [21]. In order to investigate the role of EspT in cell invasion we selected to use the *espT* positive strains E110019 and *C. rodentum*; the *espT* negative EPEC, strain JPN15 [38], was used as a control. In addition, we generated a JPN15 clone that expresses EspT from the bacterial expression vector pSA10 (pICC461).

We infected serum starved HeLa, Swiss 3T3 and Caco2 cells with E110019, JPN15 and JPN15 expressing EspT; the cells were then fixed and processed for scanning electron microscopy (SEM). The JPN15-infected HeLa and Swiss 3T3 cells displayed characteristic diffuse bacterial adhesion without any noteworthy surface structures. Caco2 cells infected with JPN15 also show a diffuse pattern of bacterial adherence and a concordant localized effacement of microvili (Fig. 1). HeLa cells infected with JPN15 expressing EspT or E110019 displayed extensive membrane ruffling over the entire cell surface (Fig. 1); in the vicinity of adherent bacteria the ruffles surrounded and wrapped individual bacterial cells forming structures which appear permissive for internalization. Swiss 3T3 cells infected with JPN15 expressing EspT or E110019 exhibited extensive dorsal ruffles and lamellipodia in addition to localized membrane ruffles at the site of bacterial attachment (Fig. 1). Caco2 cells infected with JPN15 expressing EspT or E110019 displayed prominent membrane ruffles at the site of bacterial adherence in addition to effacement of micovili (Fig. 1). These results show that EspT can induce actin remodeling and surface structures, similar to those associated with *Shigella* and *Salmonella* invasion (reviewed in [26]).

Wave2 and Abi1 are localized to membrane ruffles and lamellipodia induced by EspT

We have recently shown that remodeling of the host cell actin cytoskeleton by EspT is dependent on Rac1 and to a lesser extent Cdc42 [23]. Rac1 and Cdc42 utilize a plethora of downstream effectors in order to regulate cytoskeletal dynamics (reviewed in [19] and [25]). Several GTPase effectors including IRSp53, N-WASP, Pak, Wave2 and Abi1 have been previously been implicated in formation of membrane ruffles [39,40,41,42]. By using immuno-fluorescence microscopy we found that both Wave2 and Abi1 were present and co-localized with actin at membrane ruffles and the leading edge of lamellipodia induced by EspT (Fig. 2), while N-WASP was not (data not shown). The signaling protein IRSp53 has been proposed to participate in Abi1-Wave2-Rac1 complex formation [39,43]. While we did not detect any significant enrichment of IRSp53 in lamellipodia, IRSp53 was localized to membrane ruffles nucleated by EspT (Fig. S2). Taken together these results show that Abi1 and Wave2 are localized to membrane ruffles and lamellipodia induced by EspT but IRSp53 is only recruited to EspT-induced membrane ruffles.

Wave2 is essential for EspT-induced membrane remodeling

Wave2 is a ubiquitously expressed member of the WASP super family of actin regulators which potently activates the Arp2/3 complex [44]. The Wave family of proteins have a modular structure consisting of a N terminal Wave homology domain (WHD), a central proline rich region (PRR) and a C terminal Arp2/3 binding domain (VCA module) (reviewed in [45]). The WHD domain has been shown to bind Abi1 [42] and the PRR has been shown to interact with the SH3 domain of IRSp53 [39]. We utilized siRNA in order to determine if Wave2 is essential for formation of the EspT-dependent membrane ruffles. Depletion of endogenous Wave2 from Swiss 3T3 cells, confirmed by Western blotting (Fig. 3A), resulted in a marked decrease in formation of

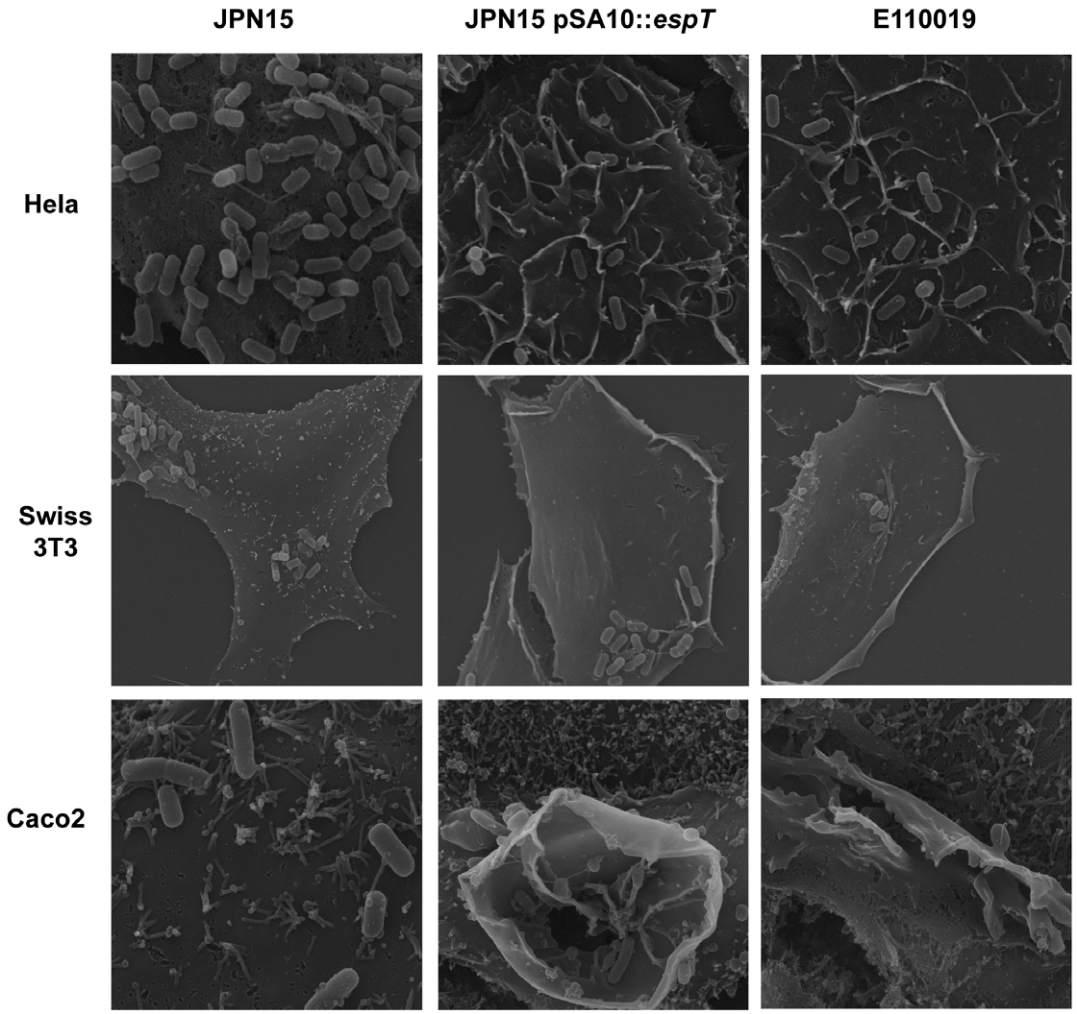


Figure 1. Scanning electron microscopy of HeLa, Swiss 3T3 and polarized Caco2 cells infected with JPN15, JPN15 expressing EspT or E110019 for 2 h. JPN15 displayed a pattern of diffused adherence on HeLa, Swiss 3T3 and Caco2 cells but did not induce any significant membrane remodeling. JPN15 expressing EspT and E110019 also adhered to HeLa, Swiss 3T3 and Caco2 cells in a diffuse pattern but induced membrane ruffles at the site of bacterial attachment, which were more pronounced on Caco2 cells. In addition to membrane ruffles JPN15 expressing EspT and E110019 also induced formation of lamellipodia and dorsal ruffles at locations distal from the site of bacterial attachment on Swiss 3T3 cells. Magnifications: HeLa cells X5000; Swiss 3T3 X3500; Caco2 X10000 and X6500 (middle).
doi:10.1371/journal.ppat.1000683.g001

membrane ruffles and lamellipodia induced by JPN15 expressing EspT or E110019, compared with cells treated with scrambled siRNA (Fig. 3B). In order to determine which of the Wave2 domains is required for formation of lamellipodia and membrane ruffles by EspT, we transfected Swiss 3T3 and HeLa cells with full length Wave2 or dominant negative forms of Wave2 lacking the WHD (ΔBP) or the acidic Arp2/3 interacting domain (ΔA). Transfected cell were infected for 1.5 h with JPN15 expressing EspT and the presence of lamellipodia or membrane ruffles was assessed. Mock transfected cells or cells transfected with full length Wave2 had lamellipodia and membrane ruffles on 80 to 90% of infected cells (Fig. S3). In contrast, transfection with either the ΔBP or the ΔA Wave2 dominant negative constructs resulted in significant reduction in lamellipodia and membrane ruffle formation (Fig. S3). This result demonstrates that binding of Arp2/3 to Wave2 is essential for EspT-mediated formation of lamellipodia and membrane ruffles. Furthermore, the observation that the N terminal truncated Wave2 ΔBP construct has a dominant negative effect suggests that the WHD motif is also required for EspT mediated cytoskeletal rearrangements. The fact that the Wave2 ΔBP construct, which is capable of binding IRSp53 but not Abi1, is not sufficient to induce EspT dependent actin remodeling further indicates that IRSp53 does not play a prominent role in EspT mediated signaling.

EspT facilitates EPEC invasion

Induction of membrane ruffles is a mechanism employed by a range of pathogenic bacteria in order to facilitate cell invasion. This method of bacterial invasion is referred to as the trigger mechanism and relies upon induction of actin polymerization to form an entry foci and a macropinocytic pocket (reviewed in [26]). JPN15 expressing EspT and E110019 induce host cell membrane remodeling which is reminiscent of entry foci and membrane ruffles induced by *Shigella* and *Salmonella* (reviewed in [26]) (Fig. 1).

We used differential staining to visualize invasion of Swiss 3T3 cells by JPN15, JPN15 expressing EspT, and E110019; *Salmonella enterica* serovar Typhimurium strain SL1344 was used as a control. In addition, we conducted gentamycin protection assays to quantify

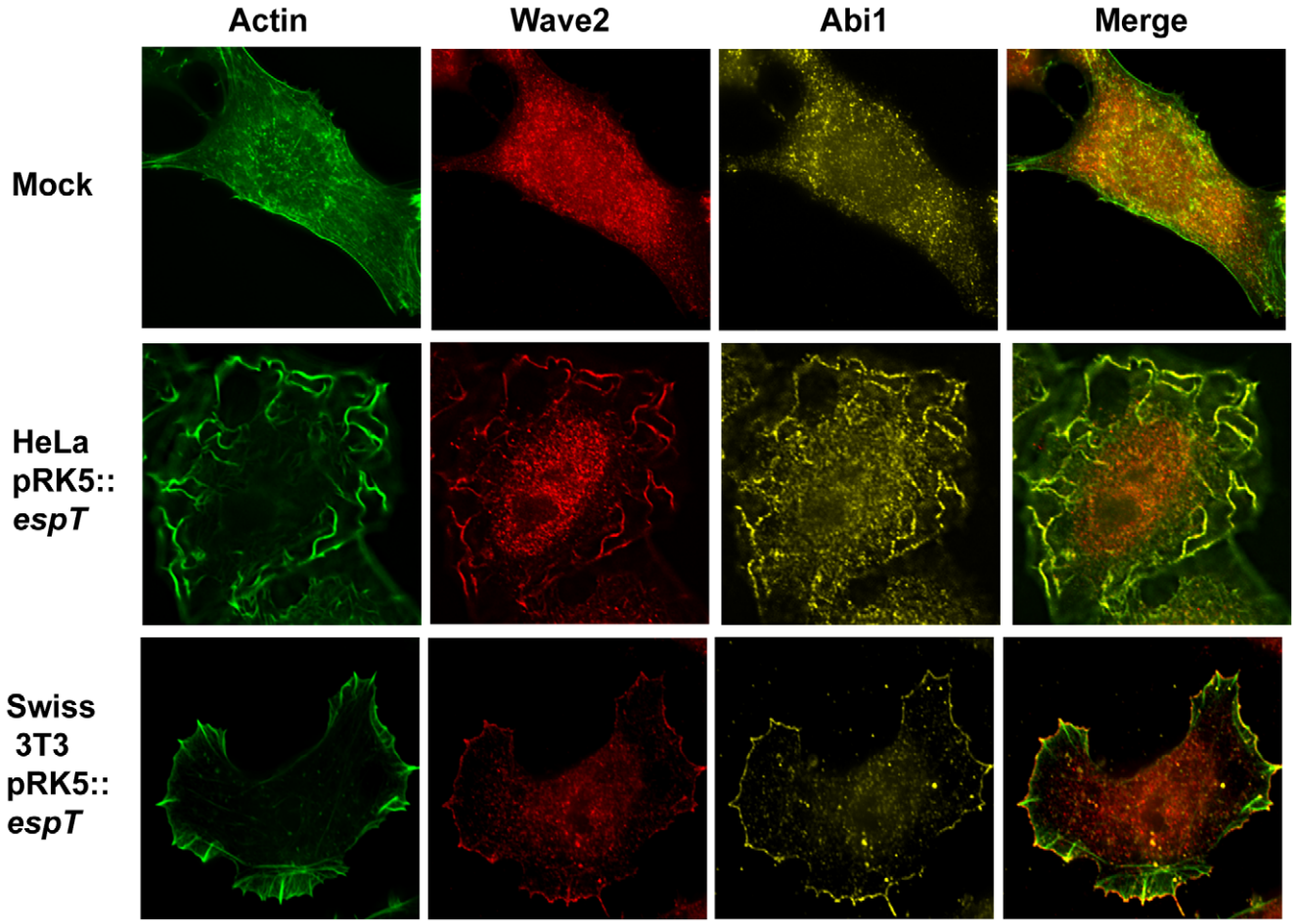


Figure 2. Wave2 and Abi1 are localized to membrane ruffles and lamellipodia induced by ectopically expressed EspT. Actin was stained with Oregon Green phalloidin (Green), Wave2 was detected with a polyclonal rabbit antibody (Red) and Abi1 was visualized using a mouse monoclonal antibody (Yellow). Mock transfected cells did not display any significant actin structures and Wave2 and Abi1 were localized diffusely in the cytoplasm. HeLa cells transfected with pRK5::*espT* exhibit prominent membrane ruffles on their apical surface which were enriched with Wave2 and Abi1. Ectopic expression of EspT in Swiss 3T3 cells resulted in formation of distinctive lamellipodia to which Wave2 and Abi1 were extensively recruited and co-localized.
doi:10.1371/journal.ppat.1000683.g002

cell invasion of Swiss 3T3, HeLa and Caco2 cells after 3 h infection. Differential immuno-fluorescence staining and gentamycin protection assays were also performed in HeLa and Swiss 3T3 cells infected for 6 h with wild type *C. rodentium*, *C. rodentium* Δ*espT* and complemented *C. rodentium* Δ*espT*. For immuno-fluorescence extracellular bacteria were stained pre cell permeabilzation with primary anti O127 (JPN15), anti O111 (E110019), anti O152 (*C. rodentium*) or anti LPS (*S.* Typhimurium) antibodies and a secondary antibody coupled to a Cy3 fluorophore (red). The cells were then permeabilized and total bacteria were stained with the same primary antibodies and a secondary antibody coupled to a Cy2 fluorophore (green), Alexafluor 633 phalloidin and Dapi were used to visualize actin and DNA respectively.

Adherent JPN15 bacteria were homogenously stained by both the extracellular and total bacterial probes, indicating that this strain is not significantly invasive (Fig. 4A). In cells infected with JPN15 expressing EspT or E110019 a significant proportion of the bacteria were labeled with the total bacterial stain but not by the extracellular probe (Fig. 4A). *S.* Typhimurium-infected cells exhibited characteristic membrane ruffling at the entry foci and a high proportion of bacteria were labeled only with the total bacterial probe (Fig. 4A).

The quantitative gentamycin protection assay revealed that JPN15 does not efficiently invade HeLa, Swiss 3T3 or Caco2 cells, exhibiting an invasion rate of less than 1.5% (Fig. 4B). JPN15 expressing EspT was significantly more invasive with an invasion rate of 15.5% in Swiss 3T3, 14.3% in HeLa and 7.2% in Caco2 cells (Fig. 4B). E110019 invaded Swiss 3T3, HeLa and Caco2 cells at a rate of 9.2%, 11.4% and 5.8% respectively. The invasive capacity of EPEC was significantly less than *S.* Typhimuriumin (Fig. 4B). Infection of HeLa cells with JPN15 expressing EspT^{W63A} for 3 h confirmed that the WxxxE motif plays a major role in membrane ruffling and cell invasion (Fig. S4).

E110019 is multi drug resistant, which limits the ability to genetically modified the isolate. In order to determine if cell invasion is mediated by EspT, we infected Swiss 3T3 cells for 6 h with wild type *C. rodentium* and *C. rodentium* Δ*espT*. Infection with wild type *C. rodentium* resulted in membrane ruffles and cell invasion, while the *espT* mutant exhibited neither (Fig. 4B). Complementing the mutant with *espT* expressed from pACYC184 (pICC489) restored membrane ruffle formation and cell invasion (Fig. 4B and S5).

In order to confirm that EspT can promote EPEC invasion of non-phagocytic cells independently of other T3SS effectors we ectopically expressed EspT in HeLa cells prior to infection with

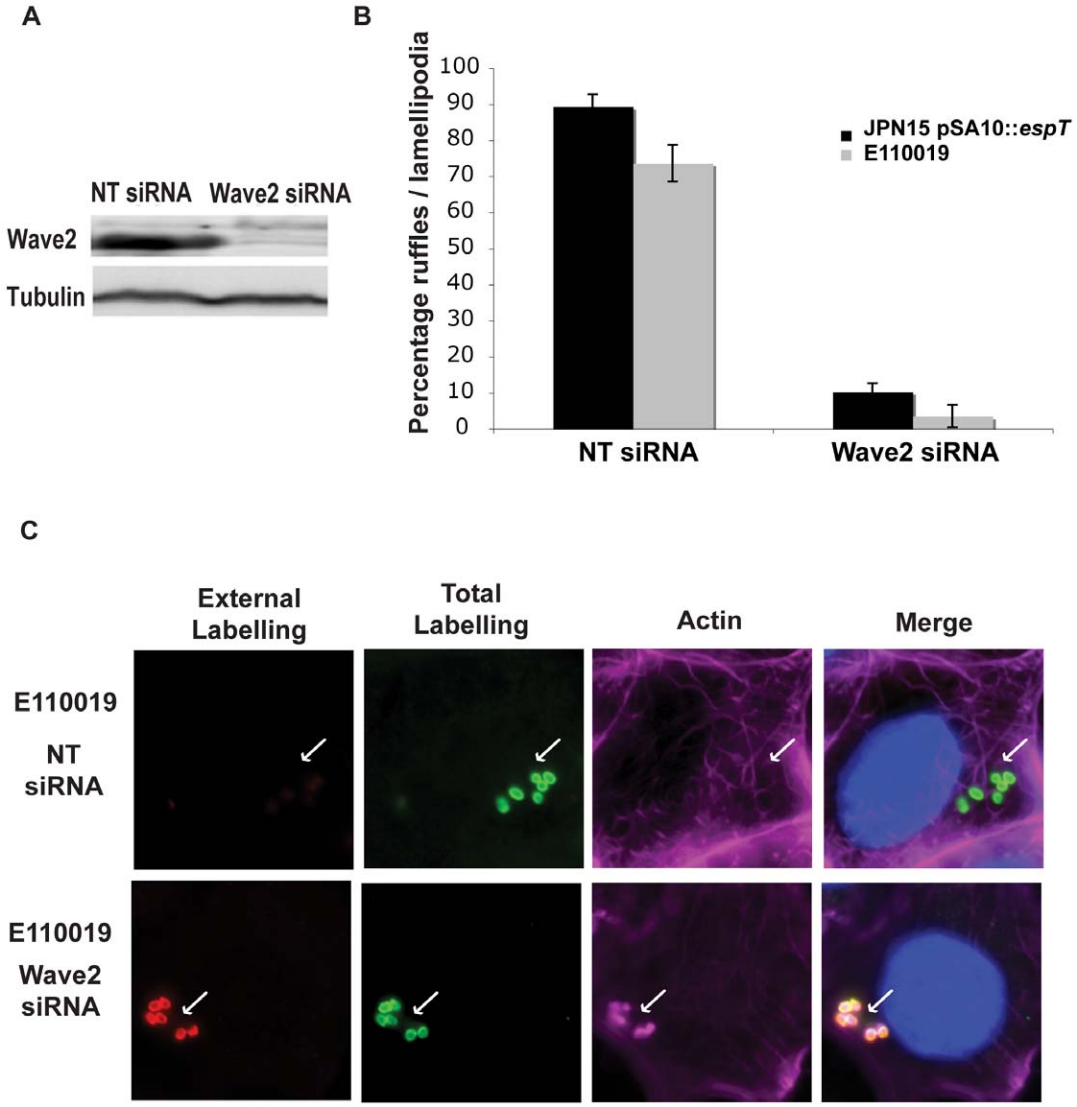


Figure 3. Wave2 is essential for EspT induced membrane remodeling and invasion. (A) Swiss 3T3 cells were treated with Non Targeting (NT) siRNA or siRNA targeted against Wave2. (A) Western blot with lysates from Swiss 3T3 cells treated with NT and Wave2 siRNA. Wave2 and Tubulin were detected with monoclonal antibodies. Non Targeting siRNA did not alter Wave2 expression whereas treatment with Wave2 siRNA depleted the protein. Protein levels in the lysates were normalized using anti tubulin antibodies. (B) Quantification of membrane remodeling induced by E110019 and JPN15 expressing EspT in Swiss 3T3 cells treated with NT and Wave2 siRNA after 3 h of infection. 100 cells were counted in triplicate resulted are presented as mean±SEM. Treatment with Wave2 siRNA oligos reduced the level of membrane remodeling induced by JPN15 pSA10::*espT* and E110019 to 10% and 5% respectively. This is comparable to the 9% of cells which display membrane ruffle and lamellipodia formation in cells infected with EPEC not expressing EspT. (C) Cells were infected with E110019 for 3 h were fixed and stained prior to permeabilization (extracellular labeling) (Red). The cells were then washed, permeabilized, re-labeled (Total labeling) (Green) along with Alexaflour 633 Phalloidin (Cyan) and Dapi (Blue). In cells treated with the NT siRNA E110019 induced formation of membrane ruffles and a large proportion of bacteria were labeled by the total stain which were absent from the extracellular labeling. Depletion of Wave2 using siRNA inhibited formation of membrane ruffles by E110019 and the majority of bacteria were detected by both the extracellular and total staining demonstrating that depletion of Wave2 inhibits EPEC invasion.
doi:10.1371/journal.ppat.1000683.g003

EPEC Δ*escN*, a T3SS null mutant. Cells ectopically expressing EspT displayed membrane ruffling which facilitated the uptake of Δ*escN* bacteria (Fig. S6). No membrane ruffles were observed in cells ectopically expressing EspTW63A (data not shown). These results show that EspT induces EPEC cell invasion by a trigger mechanism, analogous to that of *Shigella* and *Salmonella*.

Rac1 and Wave2 are essential for EspT mediated bacterial cell invasion

As actin remodeling by EspT is dependent on activation of Rac1, Cdc42 [23] and Wave2 (Fig. 3), we utilized dominant negative constructs of these signaling proteins and Wave2 siRNA to monitor the effect on invasion of JPN15 expressing EspT and E110019. Swiss 3T3 cells transfected with dominant negative Rac1 ($Rac1^{N17}$), Cdc42 ($Cdc42^{N17}$), Wave2ΔA truncated in the acidic Arp2/3 interacting region and Wave2ΔBP lacking the WHD were infected for 3 h. The cells were fixed and stained for bacterial invasion as described above. Cells transfected with $Cdc42^{N17}$ were still permissive of bacterial invasion while cells transfected with the $Rac1^{N17}$, Wave2ΔA or Wave2ΔBP dominant negative constructs were not (Fig. 5B). Depletion of Wave2 using siRNA in Swiss 3T3 cells significantly reduced the invasive

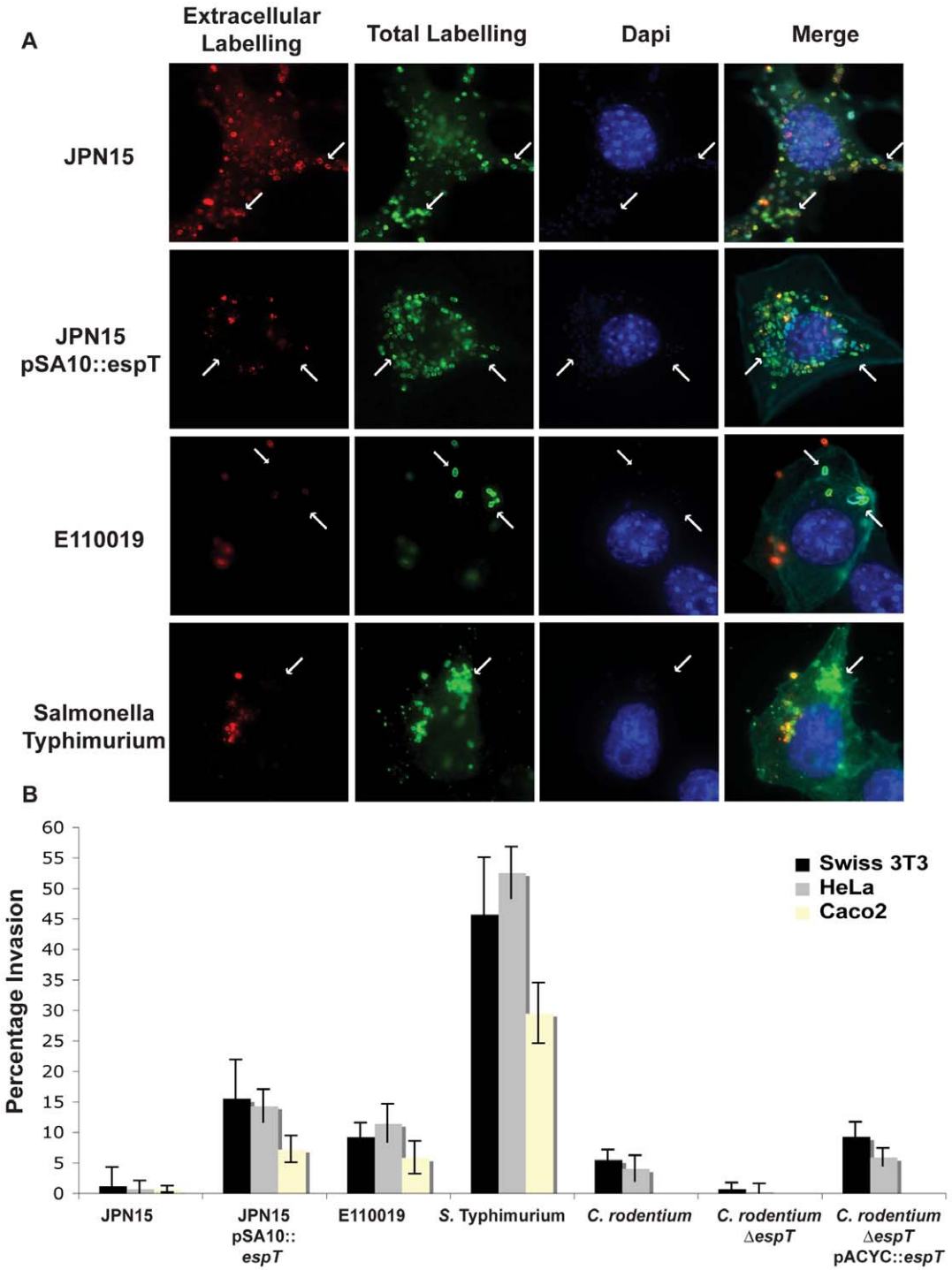


Figure 4. EspT-dependent actin remodeling facilitates bacterial invasion of epithelial cells. (A) Swiss 3T3 cells infected with JPN15, JPN15 expressing EspT, E110019 or *S.* Typhimurium for 3 h were fixed and stained prior to permeabilization (extracellular labeling) (Red). The cells were then washed, permeabilized, re-labeled (Total labeling) (Green) along with Alexaflour 633 Phalloidin (Cyan) and Dapi (Blue). In cells infected with JPN15 all the bacteria labeled by the total staining were also detected with the extracellular probe indicating that there was no significant invasion (highlighted with arrows). Significant numbers of bacteria labeled with the total stain, which were not represented in the extracellular staining, were seen in cells infected JPN15 expressing EspT, E110019 and *S.* Typhimurium indicating that there was a significant degree of bacterial invasion (highlighted with arrows). (B) Gentamycin protection assay of Swiss 3T3 and HeLa cells infected JPN15, JPN15 expressing EspT, E110019, *S.* Typhimurium, *C. rodentium*, *C. rodentium ΔespT* or complemented *C. rodentium ΔespT* and polarized Caco2 cells infected with JPN15, JPN15 expressing EspT, E110019 or *S.* Typhimurium. Results are representative of 3 independent experiments carried out in duplicate and are displayed as mean±SEM.

doi:10.1371/journal.ppat.1000683.g004

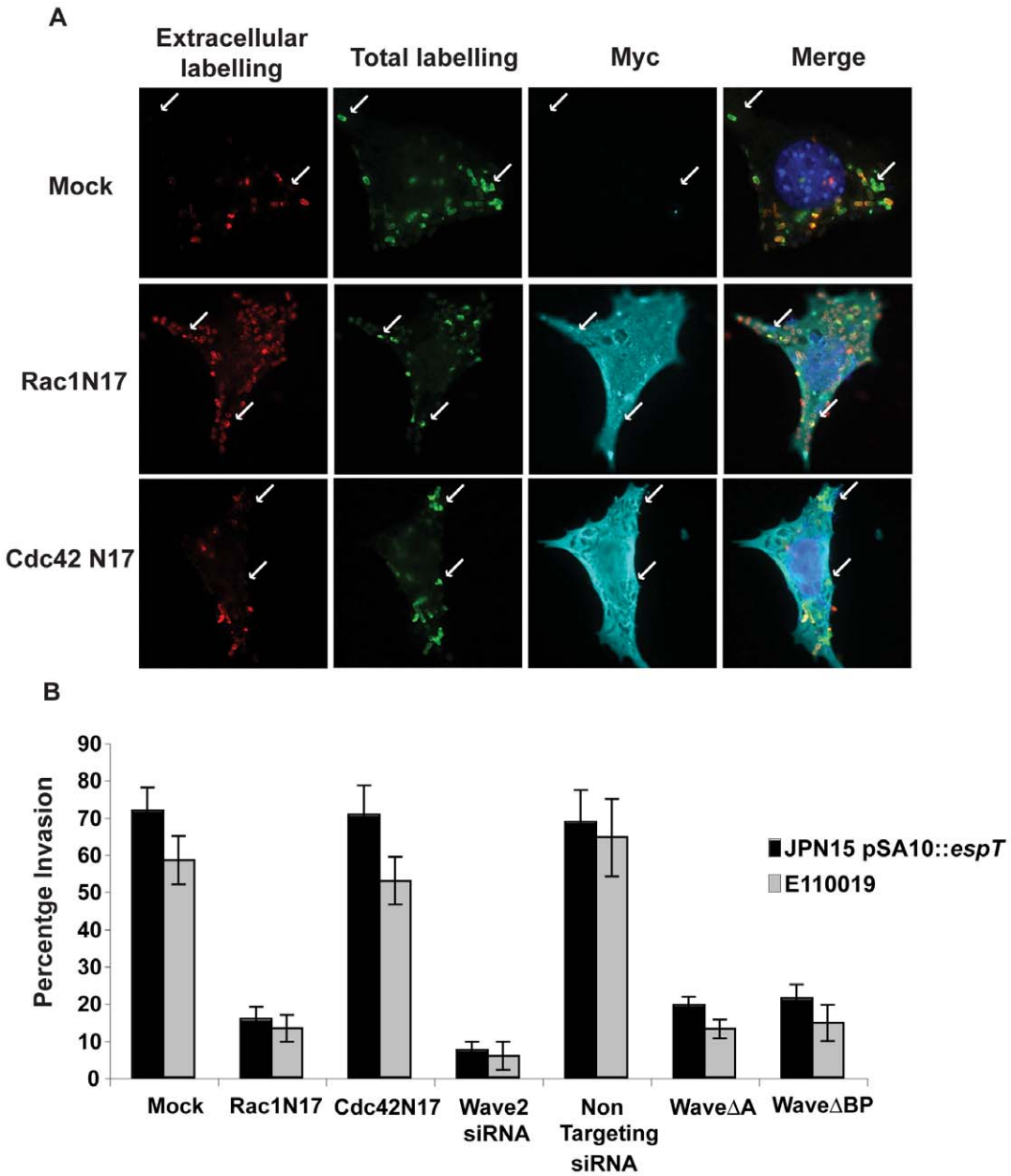


Figure 5. Rac1 and Wave2 are essential for EspT-mediated bacterial invasion. (A) Swiss 3T3 cells were left untransfected or transfected with Non Targeting (NT) or Wave2 siRNA olgos, the ectopic expression vector pDSRed encoding Wave2ΔA, Wave2ΔBP or pRK5 expressing dominant negative Rac1 and Cdc42 and infected with JPN15, JPN15 expressing EspT or E110019. Mock transfected cells or cells transfected with dominant negative Cdc42 were efficiently invaded by both JPN15 expressing EspT and E110019. Cells transfected with dominant negative Rac1 were significantly more resistant to bacterial invasion. The Wave2ΔA and Wave2ΔBP constructs also had a potent dominant negative effect on bacterial internalization. (B) Quantification of bacterial invasion; cells which had 3 or more internalized bacteria were scored as invaded. 100 cells were counted in triplicate in three independent experiments. Results are displayed as mean±SEM.
doi:10.1371/journal.ppat.1000683.g005

capacity of both JPN15 expressing EspT and E110019 compared to cells treated with non-targeting siRNA (Fig. 3A and 5B). Thus, Rac1, Wave2 and Abi1 are essential mediators of EspT-induced bacterial invasion.

Internalized EPEC are bound within a vacuole

After the initial invasion of host cells internalized bacteria are often bound within a vacuole which resembles early endosomes (reviewed in [46]). Intracellular bacteria either remain within the vacuole or rapidly escape to the cytoplasm [26]. In order to determine whether invasive EPEC are bound within a vacuole or free in the cytoplasm HeLa cells were infected with JPN15, JPN15 over expressing EspT (pICC461) and E110019 for 5 min up to 24 h and stained with various vacuolar markers including Early Endosome Antigen 1 (EEA1), Vacuolar ATPase (VATPase) and Lamp1. Internalized JPN15 expressing EspT and E110019 were labeled with EEA1 while external bacteria and JPN15 lacking EspT were not (Fig. 6 shows staining at 45 min post infection). EEA1 staining was apparent after 5 min and persists up to 1 h post infection (data not shown). At 3 h and up to 12 h post

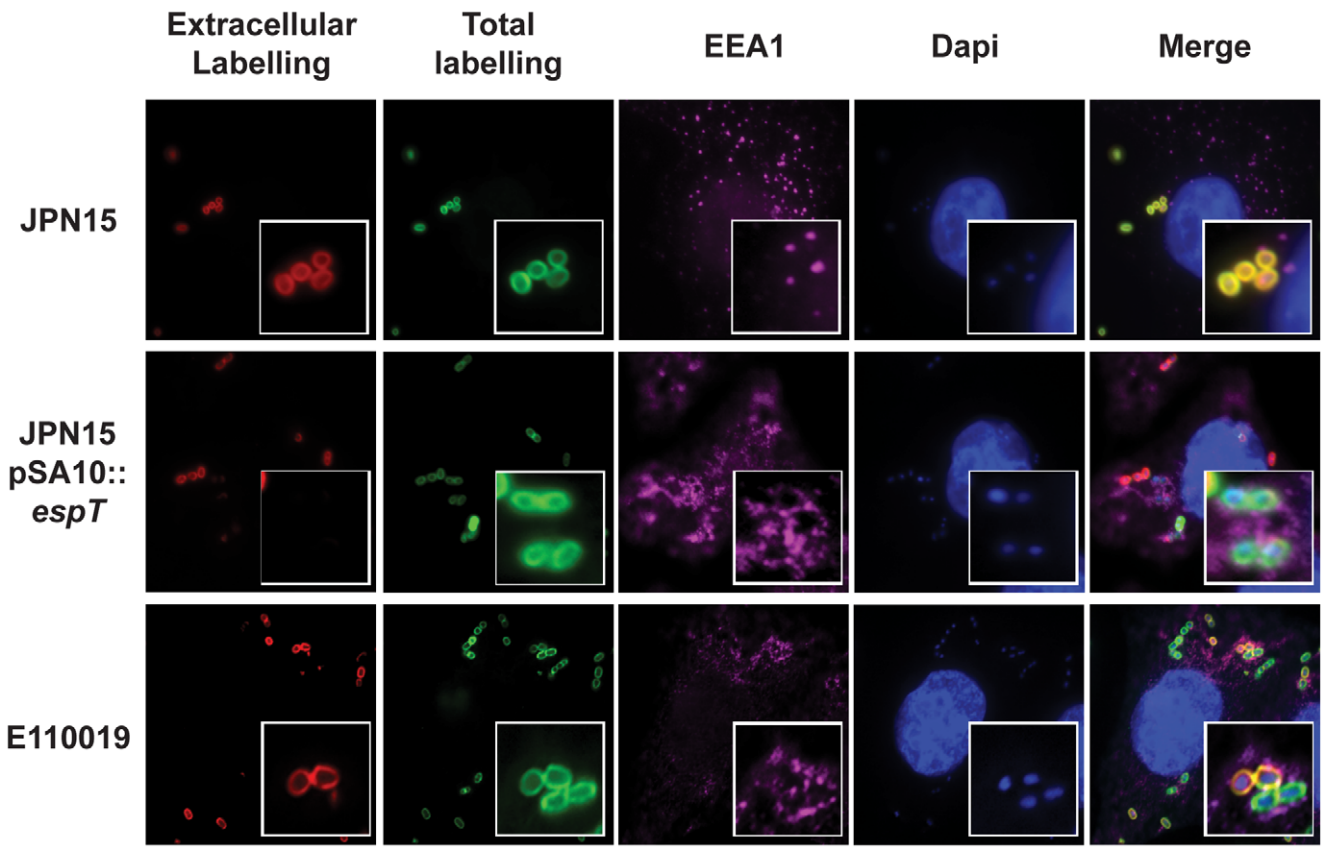


Figure 6. Internalized EPEC bacteria are enclosed within a vacuole. HeLa cells were infected with JPN15, JPN15 expressing EspT and E110019 for 45 min. Internalized bacteria bound within a vacuole were detected by anti EEA1 and a secondary antibody coupled to a CY5 (magenta). DNA was detected using Dapi staining. Extracellular JPN15 bacteria, which were detected by both the total stain and the extra-cellular probe, were not co-localized with EEA1. Intracellular JPN15 expressing EspT and E110019 which were detected by the total bacterial probe but not by the pre permeabilization stain were co localized within EEA1 rich structures indicative of early endosome like vacuoles.
doi:10.1371/journal.ppat.1000683.g006

infection the EPEC containing vacuole (ECV) was labeled with VATPase whilst external bacteria were not (Fig. 7B). Similarly to the *Salmonella* containing vacuole (SCV), a subset of ECVs became enriched with the lysosomal glycoprotein Lamp1 after 16 h (Fig. S7 and S8) and appear to adopt a perinuclear localization (Fig. 6B).

In order to determine if EPEC bacteria can multiply intracellularly we infected Swiss 3T3 cells with E110019 for 30 min before extracellular bacteria were killed by gentamycin. Infected cells were fixed for immuno-fluorescence microscopy at 2, 8, 16 and 24 h post infection. We observed a time dependent increase in the level of intracellular bacteria suggesting that internalized EPEC can multiply within host cells (Fig. S8).

Internalized EPEC and *C. rodentium* form intracellular actin pedestals

After escaping from the vacuole many intracellular pathogens such as *Shigella*, *Burkholderia* and *Listeria* utilize specialized outer membrane proteins to recruit actin nucleating factors in order to produce a propulsive force (reviewed in [26]). EPEC is synonymous with actin nucleation which leads to formation of Tir-dependent actin rich pedestals [12]. During the course of this study we observed that invasive EPEC were associated with filamentous actin comets reminiscent of pedestals. Confocal X-stacks confirmed that the intracellular EPEC bacteria were associated with pedestal-like filamentous actin structures (Fig. 7A). In order to determine if Tir was localized at the actin nucleation sites, we infected HeLa cells for 1 h with JPN15, JPN15 expressing EspT and E110019; following washes the cells were treated with gentamycin for a further 8 h. The cells were then stained with anti-VATPase and anti-Tir antisera in conjunction with phalloidin and Dapi staining. HeLa cells infected with JPN15 exhibited extracellular, pedestal-associated, bacteria which were associated with Tir but not with VATPase (Fig. 7B). In contrast, internalized JPN15 expressing EspT and E110019 bacteria were co-labeled with anti-VATPase, actin and Tir (Fig. 7B). Similarly, invasive *C. rodentium* also formed intracellular pedestals (Fig. S5), while *C. rodentium* Δ*tir* was invasive but failed to trigger actin polymerization (Fig. S8). In addition, the intracellular EPEC Δ*escN*, internalized by ectopically expressing EspT, were not associated with actin pedestals (Fig. S6). These results suggest that the actin filaments associated with EPEC contained within the ECV is nucleated in a Tir-dependent mechanism analogous to pedestal formation by extracellular bacteria.

In order to confirm this assertion we infected HeLa cells with E110019 for 2 h and processed the cells for transmission electron microscopy (TEM). The TEM confirmed that E110019 bacteria are internalized via ruffle formation (Fig. 7C). E110019 can also be seen forming multiple pedestals with the membrane on opposing surfaces during ruffle formation and closure (Fig. 7D). Moreover, internalized EPEC bacteria contained within the ECV are associated actin pedestals, which are strikingly similar to those normally associated with extracellular EPEC (Fig. 7C–E).

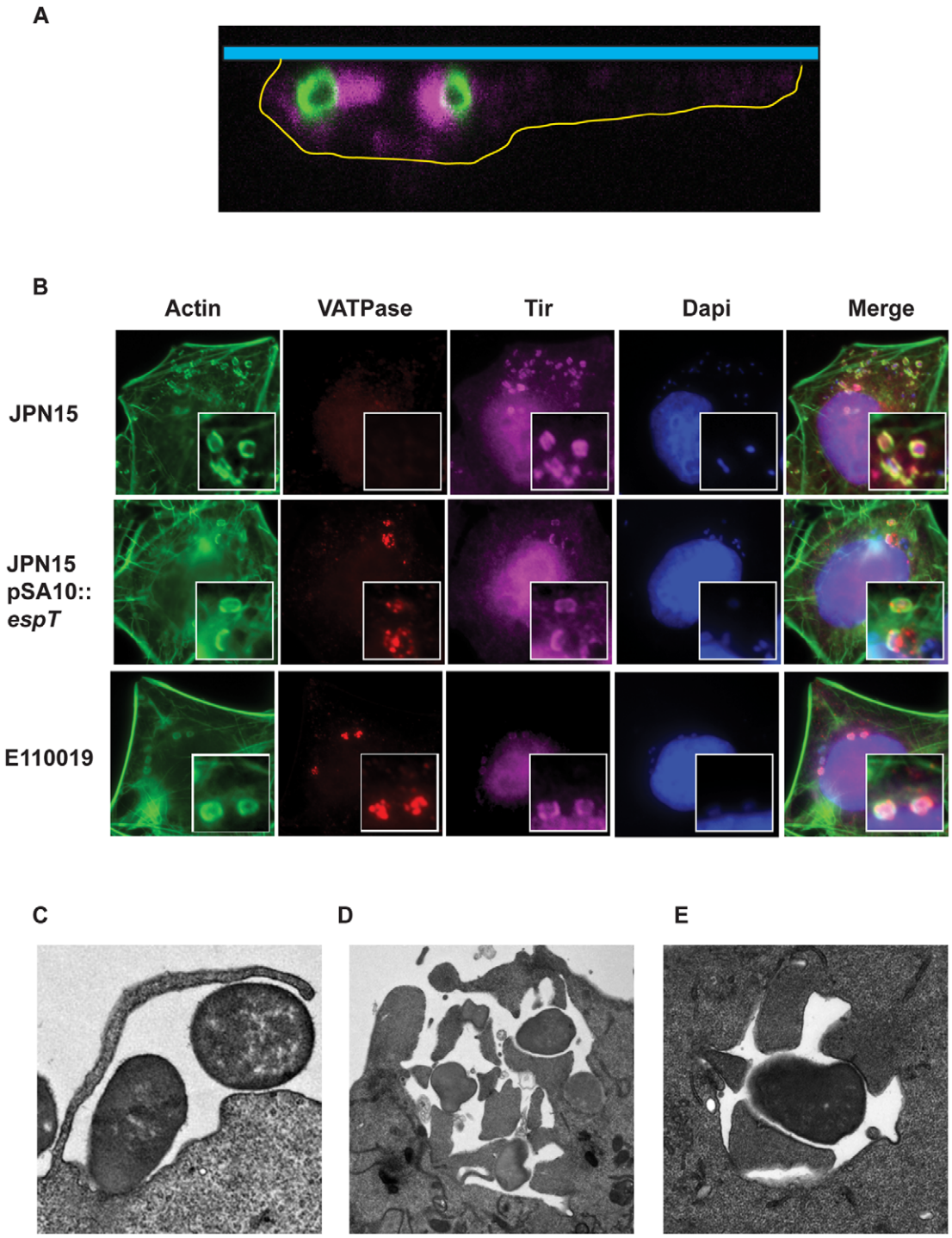


Figure 7. Internalized EPEC bacteria incorporate Tir into the vacuolar membrane which nucleates intracellular actin pedestals. (A) Swiss 3T3 cells were infected with E110019 and processed for immuno-fluorescence confocal microscopy. A series of confocal X-stacks were taken through the infected cells. The cell boundaries were defined based on actin staining and are marked by a yellow line, the coverslip is represented by the blue bar. The staining shows intracellular E110019 (Green) associated with actin pedestal-like structures (Magenta). (B) HeLa cells were infected for 60 min with JPN15, JPN15 expressing EspT, and E110019 were processed for immuno-fluorescence microscopy after 8 h gentamycin treatment. Actin was stained using Oregon Green phalloidin (Green), Tir was detected using polyclonal Tir antisera (Magenta), Vacuolar ATPase (VATPase) was detected using a monoclonal antibody (Red) and bacteria were detected using Dapi staining. Cells infected JPN15 recruited Tir to the site of bacterial attachment and form canonical actin rich pedestals but do not display any bacterial co-localization with the VATPase vacuolar marker. In cells infected with JPN15 expressing EspT or E110019 a proportion of bacteria were co-localized with VATPase, Tir and actin. (C) A TEM micrograph showing membrane ruffles engulfing E110019. (D) E110019 has the capacity to form multiple pedestals during ruffle formation and closure. (E) E110019 bacteria bound within a vacuole with intracellular pedestals formed around its circumference.
doi:10.1371/journal.ppat.1000683.g007

Interestingly, bacteria bound within ECVs can form multiple pedestals around their circumference (Fig. 7E).

In order to determine if the formation of intracellular pedestals by A/E pathogens plays a role in bacterial replication and survival within host cells we infected Swiss cells with wild type *C. rodentium* and *C. rodentium* Δ*tir* for 1.5 h and with E110019 for 30 min. Extracellular bacteria were then killed by a gentamycin wash and the cells incubated for a further 6, 12 or 24 h. We observed that both wild type *C. rodentium* and E110019 were capable of intracellular replication whereas the *C. rodentium* Δ*tir* mutant failed to replicate and instead exhibited a slow decline in bacterial numbers over time (Fig. S8). These results demonstrate that formation of pedestals by invasive A/E pathogens may play a functional role during intracellular survival.

Discussion

A/E pathogens have been long considered to be extracellular bacteria which do not invade mammalian cells [47]. However, sporadic reports have shown that atypical EPEC strains can invade non-phagocytic cells [36,48]. The invasive ability has been linked to intimin-Tir mediated tight association of EPEC with the host cell membrane which is hypothesized to produce immature phagocytosis cups leading to a passive push effect and inefficient internalization [35,36]. In this study we demonstrated for the first time that EPEC can actively invade non-phagocytic cells by inducing formation of membrane ruffles, defining a new category of invasive EPEC. Furthermore we demonstrate that this phenomenon is dependent on the T3SS effector EspT which has previously shown activate Rac1 and Cdc42 [23]. We also show that both actin remodeling and invasion is dependent upon a functional EspT as JPN15 expressing a $EspT^{W63A}$ failed to induce membrane ruffles or to invade. Importantly, in a previous report we indicated that expression of EspT might not confer bacterial invasion of epithelial cells [23]. However, these experiments were conducted using EPEC E2348/69, which in contrast to JPN15, *C. rodentium* and E110019, forms tight microclonies that mask the invasion phenotype (data not shown).

Intracellular pathogens have evolved a variety of mechanisms to promote invasion of mammalian cells, including the trigger (employed by *Salmonella* and *Shigella*) and zipper (employed by *Yersinia* and *Listeria*) mechanisms (reviewed in [26]). The trigger invasion mechanism is characterized by formation of actin rich membrane ruffles at the site of bacterial attachment, which are regulated by Rho GTPases, particularly Rac1 and Cdc42 and other cytoskeletal regulators such as PI3K [49]. *Shigella* and *Salmonella* utilize T3SS effector and translocator proteins such as IpgB1 and IpaC and SopB and SopE/2 to hijack host cell GTPase and phospho-inositol signaling to modulate membrane ruffling and formation of the macropinocytic pocket [28,29,30,37]. Importantly, although both IpgB1 and EspT belong to the WxxxE family of effectors and play a prominent role in bacterial invasion by inducing membrane ruffles, we have recently shown that they activate Rac1 by distinct mechanisms [23].

Downstream of Rho GTPase signaling, membrane ruffle formation is nucleated by the WASP super family proteins including N-WASP and Wave2. *Salmonella* invasion has been demonstrated to be at least in part dependent upon the Arp2/3 binding activity of Wave2 and also the association of Wave2 with Abi1 [50]. Wave2 cannot bind Rac1 directly; two different mechanisms have been proposed to describe how a Wave2-Rac1 complex is formed. Innocenti *et al* and Steffen *et al* demonstrate that Wave2 binds to Abi1 and two accessory proteins PIR121 and Nap1 which mediate Rac1 binding [42,51]. A report by Miki *et al* proposed that IRSp53 is the protein which links Rac1 to Wave2 [39]. In this study we demonstrate that EspT activation of Rac1 leads to a downstream recruitment of Wave2, Abi1 and IRSp53 to membrane ruffles. Depletion of endogenous Wave2 using siRNA resulted in a significant reduction in both the level of membrane ruffles induced by strains expressing EspT and their associated invasive capacity. We also show that the Arp2/3 and Abi1 binding regions of Wave2, but not N-WASP, are required for EspT-induced membrane ruffles and invasion. Furthermore, a construct of Wave2 which retained the IRSp53 and Arp2/3 binding regions but lacked the Abi1 interacting domain had a dominant negative effect on membrane ruffle formation, suggesting that IRSp53 is not required for, but may play an accessory role in, EspT-mediated actin rearrangements.

Once internalized *Shigella* and *Listeria* quickly escape the vacuole (reviewed in [52]). In contrast, *Salmonella* remains vacuole bound and utilizes different virulence factors to modify the vacuolar environment, position and interaction with the host endomembrane system in order to create an intracellular replicative SCV (reviewed in [53]). In this study we demonstrated that after invasion EPEC is bound within a vacuole (ECV) and remains vacuolated until at least 16 h post infection. We found that the ECV is EEA1 positive for up to 1 h post infection and progresses to being VATPase positive from 3 h to 12 h post infection. Furthermore, 12 h after infection the ECV appears to adopt a peri-nuclear position, which resembles the properties of the SCV. Similarly to the SCV (reviewed in [53]) we found that a subset of ECVs become enriched in the lysosomal glycoprotein Lamp1 (data not shown) indicating lysosomal fusion with the ECV. We also demonstrate that internalized EPEC bacteria can survive and replicate within host cells in a time dependent manner. Importantly and uniquely, we found that the ECV is associated with filamentous actin tails, which are reminiscent of the extracellular pedestals normally nucleated by EPEC stains. Formation of intracellular actin pedestal were essential for bacterial survival, as the intracellular population of invasive *tir* mutant declined over time.

Formation of extracellular pedestals is dependent upon the T3SS effector Tir [11]. The interaction of Tir with intimin triggers recruitment of the mammalian adaptor Nck which in turn recruits and activates N-WASP leading to Arp2/3 recruitment and actin polymerization [11,54,55,56]. In this study we found that internalized EPEC can localize Tir to the vacuolar membrane in a T3SS dependent manner and that the localization of Tir can promote actin nucleation. Furthermore, we found that a *C. rodentium* Δ*tir* mutant is still invasive but does not form intracellular pedestals, demonstrating that pedestal formation by internalized bacteria is a Tir-dependent process analogous to that of extracellular bacteria. Additionally using TEM we found that invasive EPEC bound within a vacuole are associated with intracellular pedestals around the circumference of the bacteria. Interestingly, membrane ruffles seen engulfing invading EPEC were occasionally associated with pedestals, suggesting the pedestals can be formed during or after internalization.

Canonically actin is recruited to the surface of intracellular pathogens which are non-vacuolated and this recruitment is mediated by outer-membrane proteins which are free to interact with host cell signaling molecules present in the cytoplasm. For example following escape from the vacuole *Shigella* and *Listeria* utilize IcsA/VirG and ActA, respectively, to trigger actin polymerization and motility (reviewed in [57]). The Vaccinia virus uses the viral membrane protein A36R in order to generate actin based motility in a similar manner to the extracellular EPEC pedestals [58]. Importantly, the SCV is also associated with an

Table 1. List of strains.

Strain	Description	Source/Reference
E110019	EPEC O111:H9 wild type	[22]
E2348/69	EPEC O127:H6 wild type	[66]
ICC192	EPEC O127:H6 Δ*escN*	[67]
JPN15	EPEC O127:H6 lacking the EAF plasmid encoding BFP	[38]
Salmonella Typhimurium	Strain SL1344	[68]
ICC169	*Citrobacter rodentium*	This study
ICC306	*Citrobacter rodentium ΔespT*	This study
ICC305	*Citrobacter rodentium Δtir*	R. Mundy

doi:10.1371/journal.ppat.1000683.t001

actin nest which is required to maintain the integrity of the vacuole and support the intracellular replication of *Salmonella* (reviewed in [59]).

Due to the positioning of the actin extensions around the entire circumference of EPEC it is unlikely these intracellular pedestals are involved in classical actin-based motility. However, there are reports suggesting that actin polymerization and depolymerization around the periphery of E-cadherin-coated beads can lead to directional movement in process referred to as flashing [60]; for this reason at this stage we cannot rule out the possibility that intracellular pedestals confer actin based motility. Furthermore, formation of intracellular pedestals by invasive EPEC may play a role in maintaining the vacuole integrity in a similar way to that described for other vacuolated pathogens [59]. To the best of our knowledge the current study demonstrates for the first time that an intracellular bacteria is able to recruit filamentous actin comets to the pathogen cell surface whilst encapsulated in a vacuole.

In order to survive within intracellular niche vacuolated bacteria must evade host cell lysosome mediated degradation. Interestingly, during the course of this study we observed that internalized EPEC, which were enclosed in ECVs, displaying strong actin staining around their circumference were rarely Lamp1 positive, whereas ECVs which had little or no actin polymerization associated with them were homogenously labeled with Lamp1 (data not shown). Furthermore, we observed that a *C. rodentium* Δ*tir* mutant was attenuated for intracellular replication. We propose that formation of actin rich intracellular pedestals around the circumference of the ECV by invasive EPEC may constitute a physical barrier to lysosome fusion protecting the enclosed bacteria from lysosomal degradation; however this hypothesis requires further testing. A similar phenomenon has been described for the trafficking of endosomes and lysosomes to wounded sites of plasma membrane. At sites of plasma membrane disruption lysosomes and endosomes are recruited to seal the breach, this process is inhibited if the cortical actin meshwork is stabilized and enhanced when it is disrupted [61]. Similarly the lysosome dependent internalization of *Trypanosoma cruzi* requires a depolymerization of the cortical actin network to allow lysosome transit to the plasma membrane [62].

Recently, while screen ca. 1000 clinical EPEC and EHEC isolates we found that none of the EHEC strains and only 1.8% of the EPEC strains contain *espT* [21]. Interestingly, *espT* was found in EPEC E110019 which was linked to a particularly sever outbreak of gastroenteritis in Finland [22]. E110019 was found to be particularly infectious and unusually for EPEC was associated with person to person spread and adult disease [22]. Although we have no clinical data of the other *espT* positive isolates it is tempting to speculate that the expression of EspT could be at least in part responsible for the hyper virulence of the E110019 strain. Further studies of the invasive EPEC category are needed to assess the risk they pose to human health.

Materials and Methods

Bacteria strains

Bacterial strains used in this study are listed in Table 1. The *C. rodentium* Δ*espT* were constructed using the using the one-step PCR λ-red-mediated mutation protocol [63] The O111:H2 E110019 strain was isolated from an outbreak in Finland [22]. All the strains were maintained on Luria–Bertani (LB) broth or agar supplemented with ampicilin (100μg/ml) or Kanamycin (50 μg/ml).

Plasmids and molecular techniques

Plasmids used in this study are listed in Table 2; primers are listed in Table 3. *espT* was amplified by PCR using E110019 genomic DNA as template and cloned into pSA10 [64] (primer pair 1 and 2). All constructs were verified by DNA sequencing. Site directed mutagenesis of EspT was carried out using a Quick-change® II kit (Stratagene) and primers 3 and 4 according to the manufacturers instructions. Plasmids pSA10::*espT* was used as template for the mutagenic reactions. The pCX340 vector encoding EspT-TEM fusion was constructed after amplification of *espT* from *C. rodentium* using primer pair 5 and 6.

The mammalian expression vector pRK5 containing one of Rac^{N17} or $Cdc42^{N17}$ dominant negatives used in the transfection

Table 2. List of plasmids.

Name	Description	Source/Reference
pSA10	pKK177-3 with Lac	[64]
pRK5::*myc-rac1N*^{17}	Dominant negative Rac1	[69]
pRK5::*myc-cdc42N*^{17}	Dominant negative Cdc42	[69]
pRK5:*myc-:wave2*	Wave2 full length	Gifted by Laura Machesky
pDSRED::*wave2ΔA*	Wave2 with truncated VCA	Gifted by Laura Machesky
pDSRED::*wave2ΔBP*	Wave2 with truncated WHD	Gifted by Laura Machesky
pICC228	pRK5::*espT-Myc*	[23]
pICC461	pSA10::*espT* E110019	This Study
pICC489	pACYC184::*espt C. rodentium*	This Study
pICC488	pCX340::*espT C. rodentium*	This Study
pICC490	pRK5::*espT*^{W63A}	This Study

doi:10.1371/journal.ppat.1000683.t002

Table 3. List of primers.

Primer	Name	Sequence
1	EspT-E110019-F	5′-ttgaattcatgccaggaacagtaaactcc-3′
2	EspT-E110019-R	5′-ccaatgcattggttctgcattaaacatattttaaatttctc-3′
3	EspTW63AF	5′-gaaaaacgaaggaaaaatgaatgaggcgatgagggaagaatgtatttgcttt-3′
4	EspTW63AR	5′-aaagcaaatacattcttccctcatcgcctcattcatttttccttcgtttttc-3′
5	EspTpCX340F	5′-ttcatatgccgggaacaataagctccag-3′
6	EspTpCX340R	5′-tgaattcggggttctctgcgcctcctgaa-3′

doi:10.1371/journal.ppat.1000683.t003

assays were a gift from Nathalie Lamarche-Vane. The pRK5 encoding Wave2, and the pDSRED Wave2ΔA and Wave2ΔBP were a kind gift from Laura Machesky via Ray Carabeo.

Infection of Swiss 3T3, HeLa and Caco2 cells

48 h prior to infection cells were seeded onto glass coverslips at a density of 5×10^5 cells per well and maintained in DMEM supplemented with 10% FCS at 37°C in 5% CO_2. Caco2 cells were grown in DMEM supplemented with 20% FCS at 37°C in 5% CO_2. The cells were washed in PBS and the media changed every 24 h for 12 days until the cells polarized. 3 h before infection, the cells were washed 3 times with PBS, the media replaced with fresh DMEM without FCS supplemented with 1% mannose and 500 µl of primed bacteria were added to each well, the plates were then centrifuged at 1000 rpm for 5 min at room temperature and infections were carried out at 37°C in 5% CO_2.

β Lactamase (TEM) T3SS dependent translocation assay

HeLa cells were seeded on to glass coverslips for infection as previously described above. Wild type EPEC E2348/69 and Δ*escN* T3SS null mutant were transformed with the pCX340 vector encoding EspT-TEM-1 fusion; an NleD-TEM fusion was used as a positive control. Translocation assay was performed as described previously [65].

Immunofluorescence staining and microscopy

Coverslips were washed 3 times in PBS and fixed with 3% Paraformaldehyde (PFA) for 15 min before washing 3 more times in PBS. For immuno-staining, the cells were permeabilized for 5 min in PBS 0.5% Triton X100, washed 3 times in PBS and quenched for 30 min with 50 mM NH_4Cl. Pre prermeabilized samples were not treated with triton X100. The coverslips were then blocked for 1 h with PBS 0.5% BSA before incubation with primary and secondary antibodies. The primary antibody mouse anti EEA1 (BD biosciences) and mouse anti VATPase (Gifted by Prof. D. Holden) were used at a dilution of 1:100, while rabbit anti O127, anti O111, anti O152, anti Tir and goat anti CSA-1 (salmonella LPS, gifted by Prof D. Holden) were used at a dilution of 1:500. Rabbit anti Wave2 (SantaCruz Biotechnology) and Mouse anti Abi1 (Abcam) were used at 1:200 dilutions. Coverslips were incubated with the primary antibody for 1 h, washed three times in PBS and incubated with the secondary antibodies. Donkey anti-rabbit IgG conjugated to a Cy2 or Cy3 fluorophore, donkey anti-mouse IgG conjugated to a Cy5 or Cy5 fluorophore, donkey anti goat IgG conjugated to a Cy2 or Cy3 fluorophore (Jackson laboratories) were used at a 1:200. Actin was stained using AlexaFluor 633 phalloidin, Oregon Green phalloidin or Rhodamine phalliodin (Invitrogen) at a 1:100 dilution. All dilutions were in PBS/0.5% BSA. Coverslips were mounted on slides using ProLong® Gold antifade reagent (Invitrogen) and visualized by Zeiss Axioimager immunofluorescence microscope using the following excitation wavelengths: Cy3 – 550nm, Cy5 – 650nm and Oregon Green – 488nm. All images were analyzed using the Axiovision Rel 4.5 software. Confocal X stacks were taken using a Leica Sp2 microscope. Cell boundaries were determined using actin staining and Abobe photoshop software.

Transfection

Swiss 3T3 cells or HeLa cells were transfected with pRK5 encoding EspT, $RhoA^{N19}$, Rac^{N17}, $Cdc42^{N17}$ dominant negatives fused to a Myc tag, pDSRED encoding Wave2, Wave2ΔA or Wave2ΔBP by lipofectamine 2000 (Invitrogen) according to the manufacturer's recommendations. The cells were incubated at 37°C in a humidified incubator with 5% CO_2 for 16 h, washed twice in PBS before having their media replaced with DMEM as described previously. Transfected cells were infected with the appropriate strain as described above.

siRNA of Wave2

HeLa cells were seeded at a density of approximatetly 5×10^6 cells per well 24 h prior to transfection of either Wave2 siRNA pool or a non-targeting pool supplied by Dharmacon using HiPerFect (Qiagen) according to the manufacturers instructions. The media was changed 16 h after transfection and the cells were allowed to recover for 12 h before being trypsinated and seeded at a density of 5×10^6 cells. The siRNA procedure was repeated for a total of 3 rounds before the cells were used. Levels of Wave2 and tubulin were then detected by western blotting using anti wave2 (Santa Cruz) and anti tubulin (Sigma) antibodies. Cells were then infected with the appropriate strain and processed for immuno-fluorescence microscopy as previously described.

Gentamycin protection assay

Cells seeded into the wells of a 24 well plate were infected as described above for 6 h at 37°C in 5% CO_2. The pre-gentamycin plates were washed 5 times in PBS and then permeabilzed for 15 minutes with 1% saponin in sterile water before plating in triplicate on LB plates in dilutions ranging from 10^0 to 10^{-7}. The post gentamycin samples were washed 5 times with PBS after the final wash the PBS was replaced with serum free DMEM containing 200µg/ml of gentmaycin and the cells incubated for 1 h at 37°C in 5% CO_2. The plates were then washed a further 5 times in PBS before permeabilization and plating as described above. The pre and post gentamycin plates were then incubated for 15 h in a static 37°C incubator and the colony forming units (cfu) were counted. The percentage of invasion was calculated based on the ratio of cfu on the pre and post gentamycin plates.

Scanning electron microscopy

Glass coverslips were seeded and infected for 2 h with the appropriate strains as described above. The cells were washed 3 times in phosphate buffer pH7.2 and then fixed with 2.5% Gluteraldehyde (Agar) in phosphate buffer pH7.2 for 15 min. The coverslips were then washed with phosphate buffer pH7.2 a further 3 times before being post fixed in 1% Osmium Tetroxide for 1 h. The cells were then washed 3 times in phosphate buffer before being washed for 15 min in graded ethanol solutions from 50% to 100% to dehydrate the samples. The cells were then transferred to an Emitech K850 Critical Point drier and processed according to the manufacturer's instructions. The coverslips were coated in gold/palladium mix using a Emitech Sc7620 minisputter to a thickness of approximately 370Å. Samples for scanning electron microscopy (SEM) were then examined blindly at an accelerating voltage of 25 kV using a Jeol JSM-6390.

Transmission electron microscopy

6 well plates were seeded and infected for 2 h with the appropriate strains. The cells were washed 3 times in phosphate buffer pH7.2 and then fixed with 2.5% Gluteraldehyde in phosphate buffer pH7.2 for 15 min. The plates were then washed with phosphate buffer pH7.2 a further 3 times before being removed from the plate using a Teflon scraper and subsequently harvested into in eppendorf tube. The eppendorfs were then centrifuged at 10,000 RPM to pellet the cells. The cell pellets were post fixed in 1% Osmium Tetroxide for 1 h, followed by 1% buffered tannic acid for 30 min and then a 1% aqueous sodium sulfate rinse for 10 min. The sample was dehydrated using an ethanol-propylene oxide series (with 2% uranyl acetate added at the 30% step) and embedded in Epon-araldite for 24 h at 60°C. Ultrathin sections (60 nm) were cut with a Leica EMUC6 ultramicrotome, contrasted with uranyl acetate and lead citrate, and viewed with an FEI 120-kV Spirit Biotwin TEM. Images were obtained with a Tietz F415 digital TemCam.

Supporting Information

Figure S1 EspT is translocated into host cells in a T3SS dependent manner. HeLa cells were infected with EPEC E2348/69 or E2348/69Δ*escN* containing the pCX340 β-lactamase fused to EspT. β-lactamase cleaves the CCF2/AM substrate, which fluoresces in green when uncleaved and in blue when cleaved, indicating translocation of the fusion protein. The T3SS effector NleD was used as a positive control.
Found at: doi:10.1371/journal.ppat.1000683.s001 (0.48 MB PDF)

Figure S2 IRSp53 is enriched in membrane ruffles induced by EspT. HeLa and Swiss cells were transfected with the ectopic expression vector pRK5 encoding EspT for 12 h. Actin was labeled with Oregon Green phalloidin (Green), Wave2 was detected with polyclonal rabbit antiserum (Red) and IRSp53 was detected using a monoclonal mouse antibody (Yellow). Transfection of EspT resulted in formation of membrane ruffles and lamellipodia in HeLa and Swiss cells respectively. Wave2 was localized to membrane ruffles and lamellipodia induced by EspT. IRSp53 was recruited to EspT dependent ruffles in HeLa cells but was not present in lamellipodia induced on Swiss 3T3 cells.
Found at: doi:10.1371/journal.ppat.1000683.s002 (1.52 MB PDF)

Figure S3 Wave2 WHD and VCA domains are needed for EspT-induced membrane remodeling. (A) Swiss cells were left untransfected or transfected with pDSRed encoding wild type Wave2 and Wave2ΔA (lacking the acidity Arp2/3 interacting region) or Wave2ΔBP (lacking the WHD needed for Abi1 binding). Transfected cells were infected with JPN15 expressing EspT for 2 h and processed for immuno-fluorescence microscopy. Actin was stained with Oregon green phalloidin (Green), the Wave constructs were detected with a polyclonal rabbit Wave2 antibody (Red) and JPN15 expressing EspT were visualized by Dapi. Mock transfected cells or cell transfected with wild type Wave2 displayed lamellipodia in 80–90% of transfected cells. Cells transfected with Wave2ΔA or Wave2ΔBP were severely attenuated in lamellipodia formation compared to the mock or Wave2 wild type transfected cells. (B) Quantification of lamellipodia and membrane ruffles on Swiss and HeLa cells respectively after 2 h infection with JPN15 expressing EspT. 100 cells were counted in triplicate in three independent experiments. Results are displayed as mean±SEM.
Found at: doi:10.1371/journal.ppat.1000683.s003 (2.59 MB PDF)

Figure S4 EspT mediated membrane remodeling and invasion is dependent on the conserved WxxxE motif. HeLa cells infected with JPN15, JPN15 expressing wild type EspT, or JPN15 expressing $EspT^{W63A}$ for 3 h were fixed and stained with phalliodin (green) to detect actin and Dapi stain to label bacteria (blue). In cells infected with JPN15 and JPN15 expressing $EspT^{W63A}$ there was no significant induction of membrane ruffling. Infection of HeLa cells with JPN15 expressing wild type EspT resulted in the formation of characteristic membrane ruffles. (B) Gentamycin protection assay of HeLa cells infected JPN15 and JPN15 expressing EspT or $EspT^{W63A}$. Results are representative of 3 independent experiments carried out in duplicate and are displayed as mean±SEM.
Found at: doi:10.1371/journal.ppat.1000683.s004 (0.92 MB PDF)

Figure S5 EspT is an essential mediator of *C. rodentium* invasion of epithelial cells. HeLa cells infected with *C. rodentium*, *C. rodentium* Δ*espT* or complemented *C. rodentium* Δ*espT* were fixed and stained prior to permeabilization (extracellular labeling) (Red). The cells were then washed, permeabilized, re-labeled (Total labeling) (Green) along with Alexaflour 633 Phalloidin (Cyan) and Dapi (Blue). In cells infected with *C. rodentium* Δ*espT* all bacterial cells detected by the total stain were also labeled with the extracellular stain indicating that this strain was not invasive (highlighted with arrows). In cells infected with *C. rodentium* or *C. rodentium* Δ*espT* expressing EspT a significant proportion of bacteria labeled with the total probe were not strained with the extracellular probe demonstrating cells invasion (highlighted with arrows).
Found at: doi:10.1371/journal.ppat.1000683.s005 (1.73 MB PDF)

Figure S6 Ectopic expression of EspT can facilitate invasion of epithelial cells by a T3SS null mutant. HeLa cells were transfected with pRK5 encoding EspT and subsequently infected with a Δ*escN* T3SS mutant. The cells were then fixed and processed for immuno-fluorescence microscopy. Actin was stained using Alexa-fluor 633 phalloidin (Cyan), external and internal bacteria were labeled in red and green respectively. Ectopic expression of EspT led to the formation of actin rich membrane ruffles and a significant proportion of Δ*escN* bacteria became internalized (highlighted with arrows).
Found at: doi:10.1371/journal.ppat.1000683.s006 (0.90 MB PDF)

Figure S7 ECVs become Lamp1 positive at late time points of infection. HeLa cells were infected with E110019 for 30 min before the cells were washed with gentamycin to eliminate non invasive-bacteria. The infected cells were then incubated for a further 16 h. The cells were fixed and processed for immuno-fluorescence microscopy Lamp1 was detected with a monoclonal antibody (Cyan), actin was labelled with phalliodin (Red) and bacteria were detected with Dapi. There was accumulation of Lamp1 staining on ECVs at 16 h post infection, which was not apparent at earlier time points.

Found at: doi:10.1371/journal.ppat.1000683.s007 (0.75 MB PDF)

Figure S8 (A) Internalized EPEC survive and replicate in epithelial cells. HeLa cells were infected with E110019 for 30 min before the cells were washed with gentamycin to eliminate non invasive-bacteria. The cells were then incubated for 2, 8, 16 and 24 h in the presence of gentamycin. Cells were processed for immuno-fluorescence microscopy, bacteria were detected with Dapi (Dlue) and actin was labeled with phalliodin (Red). There was a time dependent increase in the level of intracellular bacteria. (B) Quantitative gentamycin protection assay of intracellular growth. HeLa cells were infected for 3 h with *C. rodentium*, *C. rodentium* Δ*tir* and E110019 before extracellualr bacteria were eliminated with gentamycin. Cells were then incubated in the presence of gentamycin for 6, 12 or 24 h before the cells were lysed and plated for CFU counting. Results are representative of 3 independent experiments and are presents as mean±SEM.

Found at: doi:10.1371/journal.ppat.1000683.s008 (1.92 MB PDF)

Acknowledgments

We thank Prof. David Holden for his kind gift of CSA-1, Lamp1 and VATPase antibodies, Prof. Laura Machesky, Dr. Ray Carabeo and Dr. Nathalie Lamarche-Vane for generously providing the dominant negative constructs and Wave2 reagents and Prof. James Kaper for providing E110019. We thank Rosana Mundy for constructing the *C. rodentium* Δ*tir* mutant and Georgina MacKenzie for technical help.

Author Contributions

Conceived and designed the experiments: RB AA BR GF. Performed the experiments: RB AA DG VFC BR. Analyzed the data: RB AA GD GF. Wrote the paper: RB AA GD GF.

References

1. Nataro JP, Kaper JB (1998) Diarrheagenic Escherichia coli. Clin Microbiol Rev 11: 142–201.
2. Mundy R, MacDonald TT, Dougan G, Frankel G, Wiles S (2005) Citrobacter rodentium of mice and man. Cell Microbiol 7: 1697–1706.
3. Frankel G, Phillips AD (2008) Attaching effacing Escherichia coli and paradigms of Tir-triggered actin polymerization: getting off the pedestal. Cell Microbiol 10: 549–556.
4. Knutton S, Lloyd DR, McNeish AS (1987) Adhesion of enteropathogenic Escherichia coli to human intestinal enterocytes and cultured human intestinal mucosa. Infect Immun 55: 69–77.
5. Frankel G, Phillips AD, Rosenshine I, Dougan G, Kaper JB, et al. (1998) Enteropathogenic and enterohaemorrhagic Escherichia coli: more subversive elements. Mol Microbiol 30: 911–921.
6. Garmendia J, Frankel G, Crepin VF (2005) Enteropathogenic and enterohemorrhagic Escherichia coli infections: translocation, translocation, translocation. Infect Immun 73: 2573–2585.
7. Tobe T, Beatson SA, Taniguchi H, Abe H, Bailey CM, et al. (2006) An extensive repertoire of type III secretion effectors in Escherichia coli O157 and the role of lambdoid phages in their dissemination. Proc Natl Acad Sci U S A 103: 14941–14946.
8. Iguchi A, Thomson NR, Ogura Y, Saunders D, Ooka T, et al. (2009) Complete genome sequence and comparative genome analysis of enteropathogenic Escherichia coli O127:H6 strain E2348/69. J Bacteriol 191: 347–354.
9. Galan JE, Wolf-Watz H (2006) Protein delivery into eukaryotic cells by type III secretion machines. Nature 444: 567–573.
10. Coburn B, Sekirov I, Finlay BB (2007) Type III secretion systems and disease. Clin Microbiol Rev 20: 535–549.
11. Kenny B, DeVinney R, Stein M, Reinscheid DJ, Frey EA, et al. (1997) k. Cell 91: 511–520.
12. Frankel G, Phillips AD, Trabulsi LR, Knutton S, Dougan G, et al. (2001) Intimin and the host cell–is it bound to end in Tir(s)? Trends Microbiol 9: 214–218.
13. Matsuzawa T, Kuwae A, Yoshida S, Sasakawa C, Abe A (2004) Enteropathogenic Escherichia coli activates the RhoA signaling pathway via the stimulation of GEF-H1. Embo J 23: 3570–3582.
14. Kenny B, Jepson M (2000) Targeting of an enteropathogenic Escherichia coli (EPEC) effector protein to host mitochondria. Cell Microbiol 2: 579–590.
15. Arbeloa A, Bulgin RR, MacKenzie G, Shaw RK, Pallen MJ, et al. (2008) Subversion of actin dynamics by EspM effectors of attaching and effacing bacterial pathogens. Cell Microbiol 10: 1429–1441.
16. Alto NM, Shao F, Lazar CS, Brost RL, Chua G, et al. (2006) Identification of a bacterial type III effector family with G protein mimicry functions. Cell 124: 133–145.
17. Berger CN, Crepin VF, Jepson MA, Arbeloa A, Frankel G (2009) The mechanisms used by enteropathogenic Escherichia coli to control filopodia dynamics. Cell Microbiol 11: 309–322.
18. Jaffe AB, Hall A (2002) Rho GTPases in transformation and metastasis. Adv Cancer Res 84: 57–80.
19. Etienne-Manneville S, Hall A (2002) Rho GTPases in cell biology. Nature 420: 629–635.
20. Jaffe AB, Hall A (2005) Rho GTPases: biochemistry and biology. Annu Rev Cell Dev Biol 21: 247–269.
21. Arbeloa A, Blanco M, Moreira FC, Bulgin R, Lopez C, et al. (2009) Distribution of espM and espT among enteropathogenic and enterohaemorrhagic Escherichia coli. J Med Microbiol 58: 988–995.
22. Viljanen MK, Peltola T, Junnila SY, Olkkonen L, Jarvinen H, et al. (1990) Outbreak of diarrhoea due to Escherichia coli O111:B4 in schoolchildren and adults: association of Vi antigen-like reactivity. Lancet 336: 831–834.
23. Bulgin RR, Arbeloa A, Chung JC, Frankel G (2009) EspT triggers formation of lamellipodia and membrane ruffles through activation of Rac-1 and Cdc42. Cell Microbiol 11: 217–229.
24. Buccione R, Orth JD, McNiven MA (2004) Foot and mouth: podosomes, invadopodia and circular dorsal ruffles. Nat Rev Mol Cell Biol 5: 647–657.
25. Chhabra ES, Higgs HN (2007) The many faces of actin: matching assembly factors with cellular structures. Nat Cell Biol 9: 1110–1121.
26. Cossart P, Sansonetti PJ (2004) Bacterial invasion: the paradigms of enteroinvasive pathogens. Science 304: 242–248.
27. Yoshida S, Sasakawa C (2003) Exploiting host microtubule dynamics: a new aspect of bacterial invasion. Trends Microbiol 11: 139–143.
28. Hardt WD, Chen LM, Schuebel KE, Bustelo XR, Galan JE (1998) S. typhimurium encodes an activator of Rho GTPases that induces membrane ruffling and nuclear responses in host cells. Cell 93: 815–826.
29. Patel JC, Galan JE (2006) Differential activation and function of Rho GTPases during Salmonella-host cell interactions. J Cell Biol 175: 453–463.
30. Tran Van Nhieu G, Caron E, Hall A, Sansonetti PJ (1999) IpaC induces actin polymerization and filopodia formation during Shigella entry into epithelial cells. Embo J 18: 3249–3262.
31. Mounier J, Popoff MR, Enninga J, Frame MC, Sansonetti PJ, et al. (2009) The IpaC carboxyterminal effector domain mediates Src-dependent actin polymerization during Shigella invasion of epithelial cells. PLoS Pathog 5: e1000271. doi:10.1371/journal.ppat.1000271.
32. Burton EA, Plattner R, Pendergast AM (2003) Abl tyrosine kinases are required for infection by Shigella flexneri. Embo J 22: 5471–5479.
33. Handa Y, Suzuki M, Ohya K, Iwai H, Ishijima N, et al. (2007) Shigella IpgB1 promotes bacterial entry through the ELMO-Dock180 machinery. Nat Cell Biol 9: 121–128.
34. Drucker MM, Polliack A, Yeivin R, Sacks TG (1970) Immunofluorescent demonstration of enteropathogenic Escherichia coli in tissues of infants dying with enteritis. Pediatrics 46: 855–864.
35. Donnenberg MS, Kaper JB (1992) Enteropathogenic Escherichia coli. Infect Immun 60: 3953–3961.
36. Hernandes RT, Silva RM, Carneiro SM, Salvador FA, Fernandes MC, et al. (2008) The localized adherence pattern of an atypical enteropathogenic Escherichia coli is mediated by intimin omicron and unexpectedly promotes HeLa cell invasion. Cell Microbiol 10: 415–425.
37. Ohya K, Handa Y, Ogawa M, Suzuki M, Sasakawa C (2005) IpgB1 is a novel Shigella effector protein involved in bacterial invasion of host cells. Its activity to promote membrane ruffling via Rac1 and Cdc42 activation. J Biol Chem 280: 24022–24034.
38. Jerse AE, Yu J, Tall BD, Kaper JB (1990) A genetic locus of enteropathogenic Escherichia coli necessary for the production of attaching and effacing lesions on tissue culture cells. Proc Natl Acad Sci U S A 87: 7839–7843.
39. Miki H, Yamaguchi H, Suetsugu S, Takenawa T (2000) IRSp53 is an essential intermediate between Rac and WAVE in the regulation of membrane ruffling. Nature 408: 732–735.
40. Legg JA, Bompard G, Dawson J, Morris HL, Andrew N, et al. (2007) N-WASP involvement in dorsal ruffle formation in mouse embryonic fibroblasts. Mol Biol Cell 18: 678–687.
41. Machuy N, Campa F, Thieck O, Rudel T (2007) c-Abl-binding protein interacts with p21-activated kinase 2 (PAK-2) to regulate PDGF-induced membrane ruffles. J Mol Biol 370: 620–632.
42. Innocenti M, Zucconi A, Disanza A, Frittoli E, Areces LB, et al. (2004) Abi1 is essential for the formation and activation of a WAVE2 signalling complex. Nat Cell Biol 6: 319–327.
43. Suetsugu S, Kurisu S, Oikawa T, Yamazaki D, Oda A, et al. (2006) Optimization of WAVE2 complex-induced actin polymerization by membrane-bound IRSp53, PIP(3), and Rac. J Cell Biol 173: 571–585.

44. Suetsugu S, Miki H, Takenawa T (1999) Identification of two human WAVE/SCAR homologues as general actin regulatory molecules which associate with the Arp2/3 complex. Biochem Biophys Res Commun 260: 296–302.
45. Takenawa T, Miki H (2001) WASP and WAVE family proteins: key molecules for rapid rearrangement of cortical actin filaments and cell movement. J Cell Sci 114: 1801–1809.
46. Kumar Y, Valdivia RH (2009) Leading a sheltered life: intracellular pathogens and maintenance of vacuolar compartments. Cell Host Microbe 5: 593–601.
47. Celli J, Deng W, Finlay BB (2000) Enteropathogenic Escherichia coli (EPEC) attachment to epithelial cells: exploiting the host cell cytoskeleton from the outside. Cell Microbiol 2: 1–9.
48. Donnenberg MS, Donohue-Rolfe A, Keusch GT (1989) Epithelial cell invasion: an overlooked property of enteropathogenic Escherichia coli (EPEC) associated with the EPEC adherence factor. J Infect Dis 160: 452–459.
49. Ladwein M, Rottner K (2008) On the Rho'd: the regulation of membrane protrusions by Rho-GTPases. FEBS Lett 582: 2066–2074.
50. Shi J, Scita G, Casanova JE (2005) WAVE2 signaling mediates invasion of polarized epithelial cells by Salmonella typhimurium. J Biol Chem 280: 29849–29855.
51. Steffen A, Rottner K, Ehinger J, Innocenti M, Scita G, et al. (2004) Sra-1 and Nap1 link Rac to actin assembly driving lamellipodia formation. Embo J 23: 749–759.
52. Schroeder GN, Hilbi H (2008) Molecular pathogenesis of Shigella spp.: controlling host cell signaling, invasion, and death by type III secretion. Clin Microbiol Rev 21: 134–156.
53. Steele-Mortimer O (2008) The Salmonella-containing vacuole: moving with the times. Curr Opin Microbiol 11: 38–45.
54. Campellone KG, Giese A, Tipper DJ, Leong JM (2002) A tyrosine-phosphorylated 12-amino-acid sequence of enteropathogenic Escherichia coli Tir binds the host adaptor protein Nck and is required for Nck localization to actin pedestals. Mol Microbiol 43: 1227–1241.
55. Gruenheid S, DeVinney R, Bladt F, Goosney D, Gelkop S, et al. (2001) Enteropathogenic E. coli Tir binds Nck to initiate actin pedestal formation in host cells. Nat Cell Biol 3: 856–859.
56. Lommel S, Benesch S, Rottner K, Franz T, Wehland J, et al. (2001) Actin pedestal formation by enteropathogenic Escherichia coli and intracellular motility of Shigella flexneri are abolished in N-WASP-defective cells. EMBO Rep 2: 850–857.
57. Cossart P (1995) Actin-based bacterial motility. Curr Opin Cell Biol 7: 94–101.
58. Frischknecht F, Moreau V, Rottger S, Gonfloni S, Reckmann I, et al. (1999) Actin-based motility of vaccinia virus mimics receptor tyrosine kinase signalling. Nature 401: 926–929.
59. Guiney DG, Lesnick M (2005) Targeting of the actin cytoskeleton during infection by Salmonella strains. Clin Immunol 114: 248–255.
60. Yam PT, Theriot JA (2004) Repeated cycles of rapid actin assembly and disassembly on epithelial cell phagosomes. Mol Biol Cell 15: 5647–5658.
61. Miyake K, McNeil PL, Suzuki K, Tsunoda R, Sugai N (2001) An actin barrier to resealing. J Cell Sci 114: 3487–3494.
62. Rodriguez A, Rioult MG, Ora A, Andrews NW (1995) A trypanosome-soluble factor induces IP3 formation, intracellular Ca2+ mobilization and microfilament rearrangement in host cells. J Cell Biol 129: 1263–1273.
63. Datsenko KA, Wanner BL (2000) One-step inactivation of chromosomal genes in Escherichia coli K-12 using PCR products. Proc Natl Acad Sci U S A 97: 6640–6645.
64. Schlosser-Silverman E, Elgrably-Weiss M, Rosenshine I, Kohen R, Altuvia S (2000) Characterization of Escherichia coli DNA lesions generated within J774 macrophages. J Bacteriol 182: 5225–5230.
65. Charpentier X, Oswald E (2004) Identification of the secretion and translocation domain of the enteropathogenic and enterohemorrhagic Escherichia coli effector Cif, using TEM-1 beta-lactamase as a new fluorescence-based reporter. J Bacteriol 186: 5486–5495.
66. Levine MM, Bergquist EJ, Nalin DR, Waterman DH, Hornick RB, et al. (1978) Escherichia coli strains that cause diarrhoea but do not produce heat-labile or heat-stable enterotoxins and are non-invasive. Lancet 1: 1119–1122.
67. Garmendia J, Phillips AD, Carlier MF, Chong Y, Schuller S, et al. (2004) TccP is an enterohaemorrhagic Escherichia coli O157:H7 type III effector protein that couples Tir to the actin-cytoskeleton. Cell Microbiol 6: 1167–1183.
68. Hueck CJ, Hantman MJ, Bajaj V, Johnston C, Lee CA, et al. (1995) Salmonella typhimurium secreted invasion determinants are homologous to Shigella Ipa proteins. Mol Microbiol 18: 479–490.
69. Pelletier S, Julien C, Popoff MR, Lamarche-Vane N, Meloche S (2005) Cyclic AMP induces morphological changes of vascular smooth muscle cells by inhibiting a Rac-dependent signaling pathway. J Cell Physiol 204: 412–422.

Nature Reviews Microbiology | AOP, published online 11 January 2010; doi:10.1038/nrmicro2302

BACTERIAL PATHOGENICITY

A closer look at intracellular EPEC

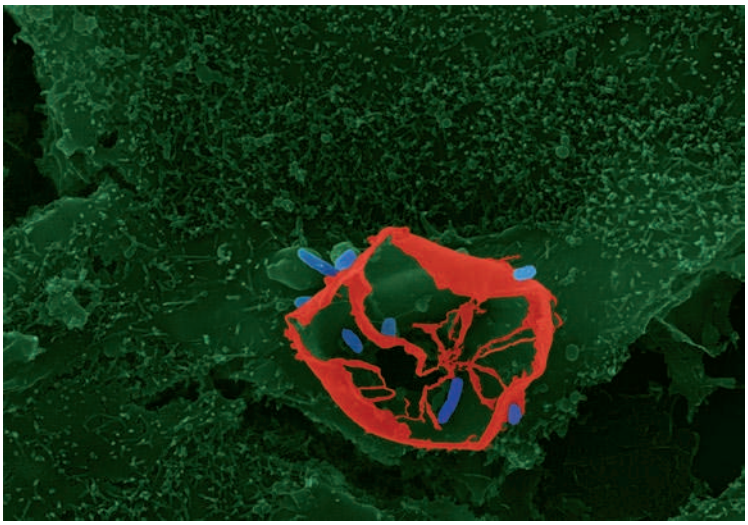
A rare subset of enteropathogenic *Escherichia coli* (EPEC) isolates that can actively invade non-phagocytic host cells by inducing the formation of membrane ruffles has been characterized in detail in a recent publication in *PLoS Pathogens*.

EPEC is a member of the group of attaching and effacing (A/E) bacterial pathogens, which attach tightly to host cells, efface the microvilli and subvert host cell actin to form characteristic pedestals beneath the attachment site. Although A/E pathogens are known to be extracellular, there have been isolated reports over the years that atypical EPEC isolates can invade non-phagocytic host cells.

Bulgin and colleagues were interested in following up their earlier work delineating the function of the type III secreted effector protein EspT, which belongs to the WXXXE family of effector proteins and which they had found could trigger the formation of membrane ruffles. *Salmonella* spp. and *Shigella* spp. induce membrane ruffles to facilitate entry into host cells in what is known as the trigger mechanism of entry. Using the EspT-expressing EPEC str. E110019, Bulgin *et al*. demonstrated that EspT promotes EPEC invasion of non-phagocytic cells by the trigger mechanism and that invasion is dependent on the WXXXE motif. RAC1 and WAVE2 (also known as WASF2) were identified as downstream host proteins that are essential for EspT-mediated invasion. Analysis of the behaviour of EPEC str. E110019 within host cells showed that the bacterium can replicate intracellularly and is contained in a vacuole. Intriguingly, transmission electron microscopy analysis showed that intracellular actin pedestals form around the circumference of the bacterium in the vacuole. The function of these pedestals remains to be investigated, but the authors speculate that they may form a physical barrier that prevents lysosomal fusion.

So, the expression of EspT allows EPEC isolates to actively invade non-phagocytic host cells. EspT is found in only a very small proportion of clinical isolates, but these rare isolates, such as EPEC str. E110019, can cause severe disease, and the authors conclude with the suggestion that this hypervirulence could be at least partly a result of the invasive phenotype.

Sheilagh Molloy



An EspT-induced ruffle (red) during enteropathogenic *Escherichia coli* (blue) invasion into Caco2 cells (green). Image courtesy of R. Bulgin, Imperial College, London, UK.

> “EspT promotes EPEC invasion of non-phagocytic cells by the trigger mechanism”

ORIGINAL RESEARCH PAPER Bulgin, R. *et al.* The T3SS effector EspT defines a new category of invasive enteropathogenic *E. coli* (EPEC) which form intracellular actin pedestals. *PLoS Pathog.* **5**, e1000683 (2009)

FURTHER READING Croxen, M. A. & Finlay, B. B. Molecular mechanisms of *Escherichia coli* pathogenicity. *Nature Rev. Microbiol.* **8**, 26–38 (2010)

© 2010 Macmillan Publishers Limited. All rights reserved

Cellular Microbiology (2010) **12**(5), 654–664
doi:10.1111/j.1462-5822.2009.01423.x
First published online 5 February 2010

EspM2 is a RhoA guanine nucleotide exchange factor

Ana Arbeloa,[1] James Garnett,[2†] James Lillington,[3,4†] Richard R. Bulgin,[1] Cedric N. Berger,[1] Susan M. Lea,[3] Steve Matthews[2] and Gad Frankel[1*]
[1]*Centre for Molecular Microbiology and Infection and* [2]*Division of Molecular Biosciences, Imperial College London, London, UK.*
[3]*Sir William Dunn School of Pathology and* [4]*Inorganic Chemistry Laboratory, University of Oxford, Oxford, UK.*

Summary

We investigated how the type III secretion system WxxxE effectors EspM2 of enterohaemorrhagic *Escherichia coli*, which triggers stress fibre formation, and SifA of *Salmonella enterica* serovar Typhimurium, which is involved in intracellular survival, modulate Rho GTPases. We identified a direct interaction between EspM2 or SifA and nucleotide-free RhoA. Nuclear Magnetic Resonance Spectroscopy revealed that EspM2 has a similar fold to SifA and the guanine nucleotide exchange factor (GEF) effector SopE. EspM2 induced nucleotide exchange in RhoA but not in Rac1 or H-Ras, while SifA induced nucleotide exchange in none of them. Mutating W70 of the WxxxE motif or L118 and I127 residues, which surround the catalytic loop, affected the stability of EspM2. Substitution of Q124, located within the catalytic loop of EspM2, with alanine, greatly attenuated the RhoA GEF activity *in vitro* and the ability of EspM2 to induce stress fibres upon ectopic expression. These results suggest that binding of SifA to RhoA does not trigger nucleotide exchange while EspM2 is a unique Rho GTPase GEF.

Introduction

Pathogenic bacteria use a variety of strategies to subvert cellular and immunological functions to facilitate colonization, multiplication and survival within the host. Several Gram-negative pathogens, e.g. *Salmonella enterica*, *Shigella* spp. and enteropathogenic and enterohaemorragic *Escherichia coli* (EPEC and EHEC), encode a type III secretion system (T3SS) which is central for their infection strategy. T3SS are molecular syringes that allow translocation of effector proteins directly from the bacteria to the cytoplasm of the host cell. Once translocated the effectors subvert cellular processes to facilitate the particular infection style of the pathogen (Mota and Cornelis, 2005). To this end bacterial T3SS effectors often display sequence, structural or functional similarities to eukaryotic proteins.

Rho GTPases react to a range of intrinsic and extrinsic stimuli in order to regulate a plethora of host cell signalling networks most notably those involved in remodelling the eukaryotic actin cytoskeleton and, as such, are prominent targets of T3SS effectors (Finlay, 2005). RhoA, Cdc42 and Rac1, the most studied Rho GTPases, induce formation of stress fibres, filopodia and lamellipodia respectively (Jaffe and Hall, 2005). To exert their control on these cellular processes Rho GTPases act as molecular switches cycling between GTP-bound 'on' and GDP-bound 'off' conformations. Rho GTPases have well-defined nucleotide and magnesium binding pocket, constituted mainly by two polypeptides called Switch I and II and by the phosphate-binding loop or P-loop. Mg^{2+} ions are required for high-affinity binding of guanine nucleotides to Rho GTPases. The Switch I and II regions define the major conformational differences between the GDP and GTP bound forms; only the GTP-bound conformation allows interactions of the Rho GTPases with their downstream effectors. The activation state of Rho GTPases is modulated by three main categories of regulatory proteins: (i) guanine nucleotide dissociation inhibitors (GDI) that sequester GTPases in the cytosol in a GDP-bound state, (ii) guanine nucleotide exchange factors (GEFs) that catalyse the GDP/GTP exchange, and (iii) GTPase activating proteins (GAPs) that inactivate the Rho GTPases by stimulating their intrinsic GTPase activity.

Type III secretion system effectors use different mechanisms to subvert Rho GTPases. For example, EPEC and EHEC EspG and EspG2 indirectly activate RhoA by disrupting microtubules, which leads to liberation of a RhoA-specific GEF, GEF-H1 (Matsuzawa *et al*., 2004). Other T3SS effectors modulate Rho GTPase directly as they function as either GEFs or GAPs. For example, the *Salmonella* effector SopE directly activates Rac1 and Cdc42 leading to lamellipodia formation and promoting bacterial invasion into non-phagocytic cells (Hardt *et al*., 1998). In contrast, *Salmonella* uses the GAP T3SS effector SptP to

Received 10 August, 2009; revised 30 November, 2009; accepted 2 December, 2009. *For correspondence. E-mail g.frankel@imperial.ac.uk; Tel. (+44) 2075945253; Fax (+44) 02057943069.
†These authors are equal contributors.
Re-use of this article is permitted in accordance with the Terms and Conditions set out at http://www3.interscience.wiley.com/authorresources/onlineopen.html

© 2010 Blackwell Publishing Ltd

stimulate the intrinsic Rho GTPase activity to restore cell architecture following bacterial internalization (Fu and Galan, 1999). SopE and SptP homologues have been identified in different species including *Burkholderia pseudomallei* (BopE), *Yersinia pseudotuberculosis* (YopE) and *Pseudomonas aeruginosa* (ExoS) (Goehring *et al*., 1999; Von Pawel-Rammingen *et al*., 2000; Stevens *et al*., 2003). By modulating the actin cytoskeleton via Rho GTPases, YopE and ExoS inhibit bacterial uptake by macrophages (Black and Bliska, 2000; Deng and Barbieri, 2008).

Based on a conserved motif comprising an invariant tryptophan (W) and a glutamic acid (E) separated by three variable amino acids, Alto *et al.* (2006) grouped together a number of known T3SS effectors from *Shigella* (IpgB1 and IpgB2), *Salmonella* (SifA and SifB) and EPEC and EHEC (Map) and termed them WxxxE effectors. Recently, we identified new WxxxE effectors encoded by EPEC and EHEC, EspM (Tobe *et al*., 2006) and EspT (Bulgin *et al*., 2009). Ectopic expression of Map leads to filopodia formation (Alto *et al*., 2006), IpgB2 and EspM trigger stress fibres (Alto *et al*., 2006; Arbeloa *et al*., 2008) and IpgB1 and EspT induce membrane ruffles and lamellipodia (Alto *et al*., 2006; Bulgin *et al*., 2009). These phenotypes are typically associated with activated Cdc42, RhoA and Rac1 (Hall *et al*., 1993) respectively.

Alto *et al.* suggested that the WxxxE effectors, which play important roles in cell invasion (IpgB proteins) and intracellular survival (SifA), mimic the function of Rho GTPases. Handa *et al.* (2007) subsequently demonstrated that IpgB1 stimulates formation of membrane ruffles by activating Rac1 through recruitment of the Rac1-specific ELMO–Dock180 GEF complex. Moreover, the structure of SifA in complex with the PH domain of SKIP has shown that its C-terminus domain, which includes the WxxxE motif, adopts a fold similar to SopE (Ohlson *et al*., 2008). However, neither direct binding to the Rho GTPases nor GEF activity was detected in this study. Furthermore, we have recently reported that Map (Berger *et al*., 2009), EspM (Arbeloa *et al*., 2008) and EspT (Bulgin *et al*., 2009) activate the Rho GTPases Cdc42, RhoA and Rac1. The aim of this study was to determine the mechanism through which EspM2 activates RhoA.

Results

EspM2 binds RhoA

We used His-EspM2 to investigate if activation of RhoA involves a direct interaction. Although highly soluble, His-EspM2 was unstable and appeared in two distinct bands corresponding to the full-length effector and a spontaneous degradation product; N-terminal sequencing revealed that the latter corresponds to EspM2 lacking the first 28 amino acids ($EspM2^{29–196}$) (Appendix S1 and Fig. S1). Ectopic expression of $EspM2^{29–196}$ in Swiss 3T3 cells resulted in stress fibre formation at the same level as full-length EspM2 (Fig. S2), confirming that it retained full biological activity. Consequently we have used $EspM2^{29–196}$ throughout this study.

Surface plasmon resonance was used to probe the interaction between His-$EspM2^{29–196}$ and His-RhoA. This technique allows binding to be observed in real time by the change in mass over the derivatized surface of a sensor chip. RhoA was flowed (sequential injections ranging from 0.05 μM to 50 μM) over an $EspM2^{29–196}$-bound surface and displayed an increased rate of binding with concentration confirming a specific interaction (Fig. 1A). Free GDP or GTP added to the running buffer inhibited formation of an $EspM2^{29–196}$–RhoA complex in a nucleotide concentration-dependent manner (Fig. 1B). GDP and GTP have the same effect as one another (within experimental error), reducing the binding affinity of $EspM2^{29–196}$ to RhoA by up to 67% in the nucleotide concentration range 0.5–8 μM.

As a control, Rac1 was flowed over the same $EspM2^{29–196}$ surface and for any given GTPase concentration showed substantially less binding (Fig. 1C), confirming the specificity of $EspM2^{29–196}$ for RhoA over other GTPases. As recent data suggested that SifA might bind RhoA (Ohlson *et al*., 2008), their direct interaction was also tested. We found that His-SifA and His–RhoA bound in a concentration-dependent manner (Fig. 1D), and was inhibited by free GDP or GTP (data not shown). Although high RhoA concentrations (μM range) were required to see an interaction, $EspM2^{29–196}$–RhoA binding was found to be long-lived. The interaction response was followed for 1000 s after each injection, by which time the rate of dissociation appeared to have fallen to zero in an incompletely dissociated state. Dissociation of the pre-formed $EspM2^{29–196}$–RhoA, as well as SifA–RhoA, complexes could not be brought about by addition of 500 μM free GDP in running buffer (in the presence or absence of 5 mM $MgCl_2$, data not shown) in contrast to the rapid dissociation of SopE–Cdc42 reported by Rudolph *et al.* (1999). Dissociation of $EspM2^{29–196}$–RhoA proved to be more difficult than that of SifA–RhoA, requiring high pH conditions (25 mM NaOH, pH 12.4), where high ionic strength (1 M NaCl) would suffice for the latter to bring the response back to the pre-experiment level.

EspM2 stimulates guanine nucleotide exchange in RhoA

We next investigated the ability of $EspM2^{29–196}$ to stimulate guanine nucleotide exchange in RhoA and other

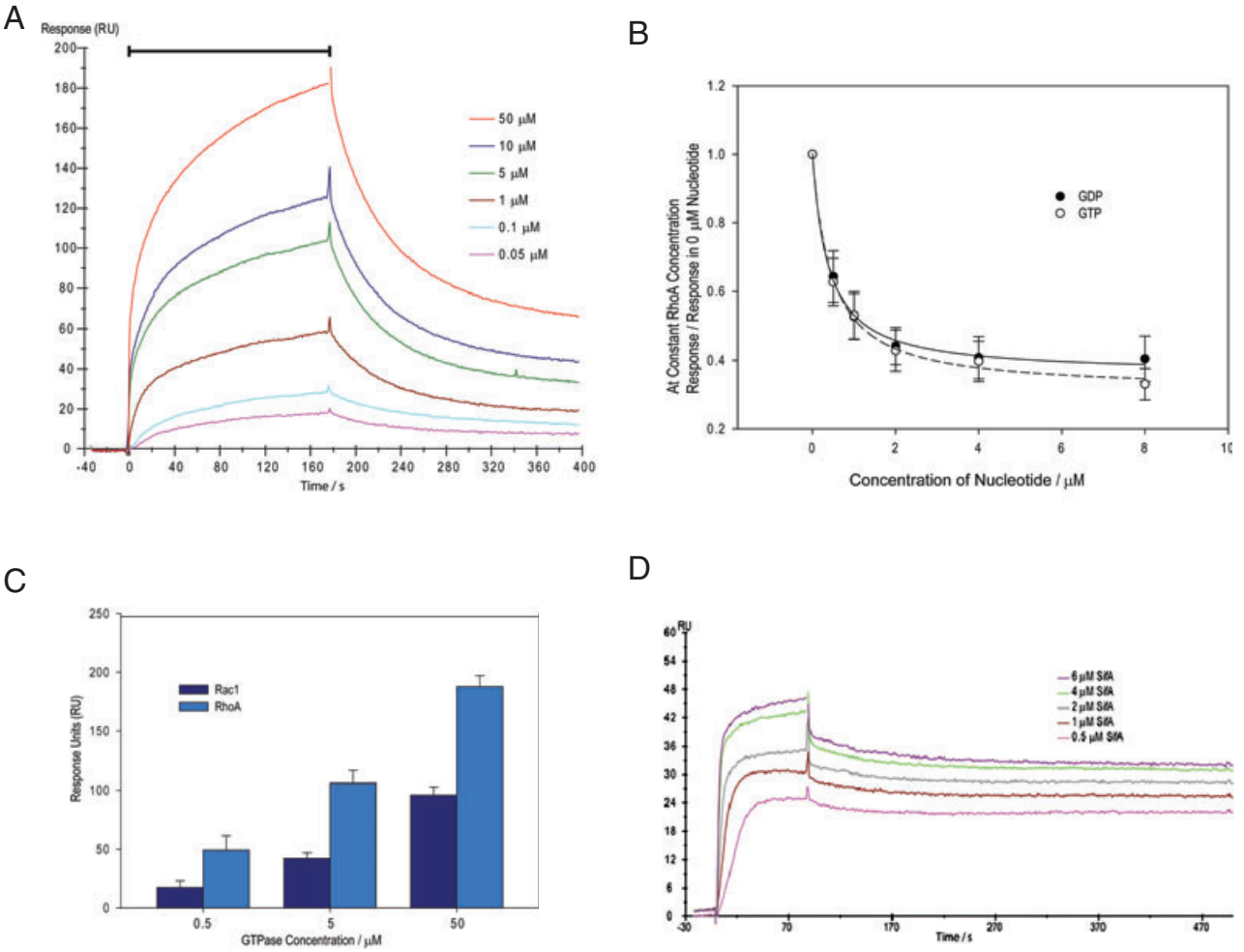


Fig. 1. RhoA binds directly to EspM2 and SifA.
A. Surface plasmon resonance showing concentration-dependent binding of RhoA to EspM2$^{29–196}$. Concentrations of RhoA varying from 0.05 µM to 50 µM were flowed at 50 µl min^{-1} (duration indicated by black bar) over a CM5 sensor chip with EspM2$^{29–196}$ covalently bound to the surface. Control substituted signals are shown.
B. Inhibition of EspM2$^{29–196}$–RhoA interaction by GDP or GTP. For RhoA (4 µM) flowing over an EspM2$^{29–196}$-bound surface in buffer containing GDP/GTP, the response maxima relative to response maxima in the absence of nucleotide are plotted with respect to GDP/GTP concentration.
C. Binding of EspM2$^{29–196}$ to RhoA and Rac1. Averaged response maxima for three representative concentrations compare the strength of EspM2 binding with the two GTPases.
D. Surface plasmon resonance demonstrates RhoA concentration dependence for binding SifA. Concentrations of SifA varying from 0.5 µM to 6 µM were flowed at 50 µl min^{-1} over a CM5 sensor chip with RhoA covalently bound to the surface.

GTPases *in vitro* using a RhoGEF exchange assay. This spectroscopic assay measures fluorescent emission upon insertion of *N*-methylanthraniloyl(mant)-GTP into the nucleotide binding pocket of the GTPases (Rossman *et al.*, 2002). As shown in Fig. 2 inclusion of 250 mM EDTA (positive control) in the assay induced efficient nucleotide exchange in RhoA, Cdc42, Rac1 and H-Ras, indicating that these proteins were biologically functional, while a slow intrinsic nucleotide exchange activity was detected in the presence of buffer alone (negative control). The fluorescence intensity rose dramatically and in a concentration-dependent manner when increasing amounts of purified EspM2$^{29–196}$ were added to RhoA (Fig. 2A). In contrast, EspM2$^{29–196}$ showed a weak exchange activity in Cdc42 (Fig. 2B), whereas it had no effect on Rac-1 and H-Ras (Fig. 2C and data not shown). No change in fluorescence emission was detected when EspM2 was incubated in the absence of any of the small GTPases (Fig. 2D). Testing the GEF activity of SifA revealed that it did not stimulate nucleotide exchange in any of the tested Rho GTPases or H-Ras (Fig. 2E). These results demonstrate that EspM2$^{29–196}$ is a specific RhoA GEF, and that although SifA can bind RhoA it cannot induce nucleotide exchange.

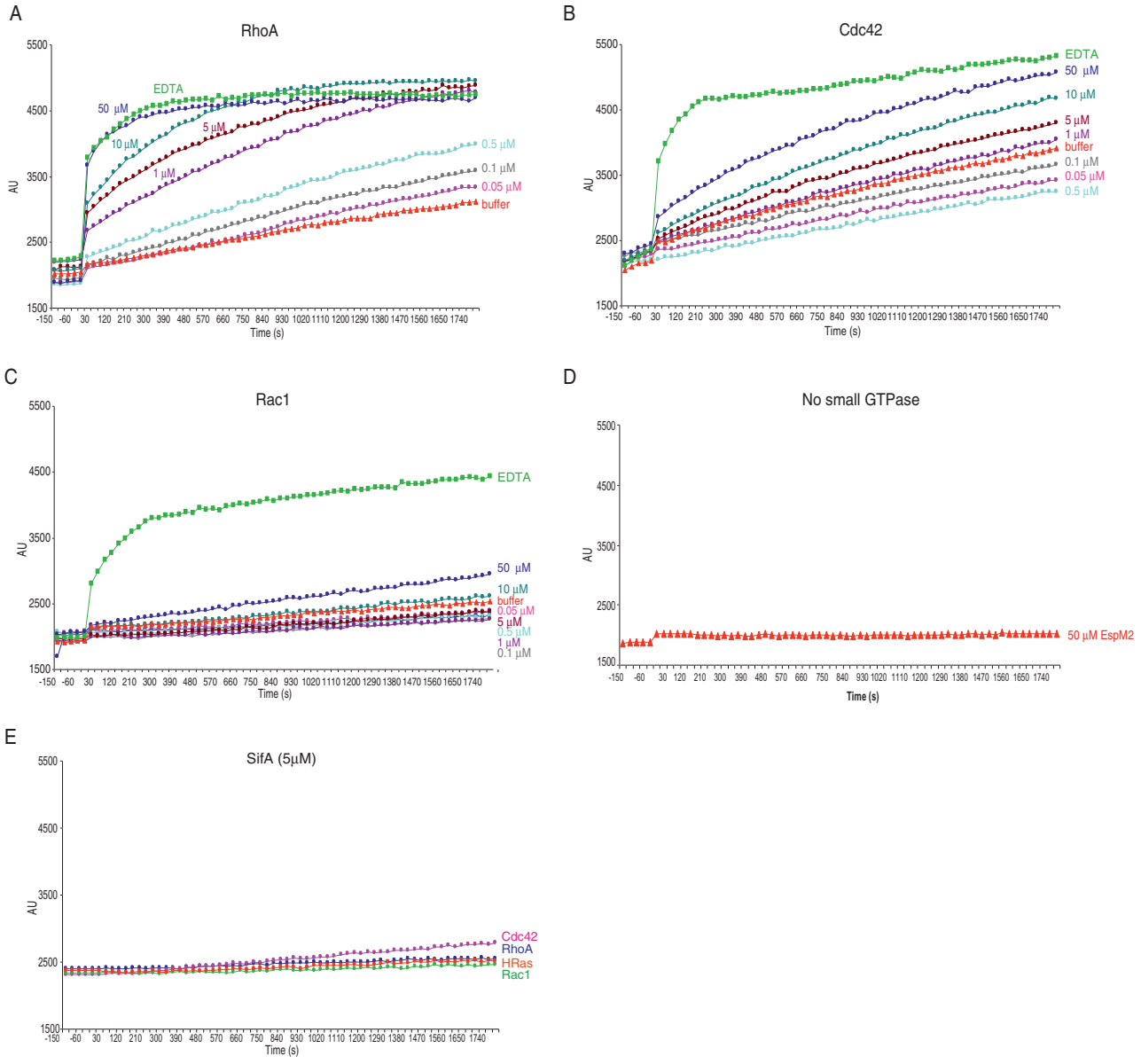


Fig. 2. EspM2 is a RhoA GEF.
A. EspM2$^{29–196}$ mediates loading of mant-GTP into RhoA. mant-GTP (0.5 μM) was incubated with 2 μM RhoA in presence of 250 mM EDTA (squares), or 0.05–50 μM EspM2$^{29–196}$ (circles) or in presence of buffer only (triangles). The insertion of the mant-GTP into the nucleotide binding pocket of RhoA in presence of EspM2$^{29–196}$ detected by an increase in the fluorescent emission was found to be concentration dependent.
B. EspM2$^{29–196}$ weakly induces loading of mant-GTP into Cdc42. mant-GTP (0.5 μM) was incubated with 2 μM Cdc42 in presence of 250 mM EDTA (squares), or 0.05–50 μM EspM2$^{29–196}$ (circles) or in presence of buffer only (triangles). Slow loading of mant-GTP into Cdc42 was only detected when high concentrations of EspM2$^{29–196}$ were added.
C. EspM2$^{29–196}$ does not induce nucleotide exchange for Rac1. mant-GTP (0.5 μM) was incubated with 2 μM Rac1 in presence of 250 mM EDTA (squares), or 0.05–50 μM EspM2$^{29–196}$ (circles) or in presence of buffer only (triangles). No efficient loading of man-GTP into Rac1 was observed after incubation with up to 50 μM EspM2$^{29–196}$.
D. Incubation of 50 μM EspM2$^{29–196}$ in the exchange buffer alone did not change the fluorescence intensity.
E. SifA does not induce nucleotide exchange in RhoA, Cdc42, Rac1 or H-Ras. mant-GTP (0.5 μM) was incubated with 2 μM RhoA (blue circles), Cdc42 (pink circles), Rac1 (green circles) or H-Ras (orange circles) in presence of 5 μM SifA. No loading of man-GTP into any of the small GTPases tested was observed in these conditions. Results shown are the average of three independent experiments.

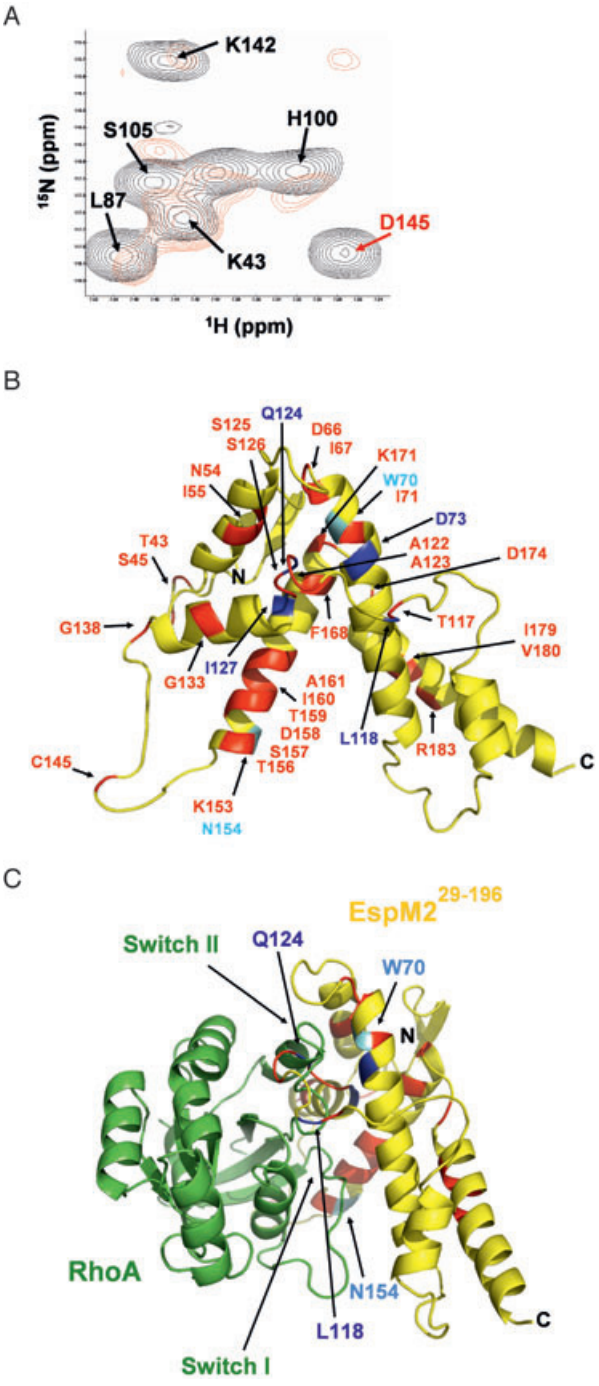


Fig. 3. Model of EspM2$^{29–196}$ and the EspM2$^{29–196}$–RhoA complex.
A. ^{1}H ^{15}N TROSY-HSQC titration of RhoA against EspM2$^{29–196}$. Black peaks show no addition of RhoA while red peaks show fourfold molar excess of RhoA. Chemical shift changes were deemed significant if the peak intensity was reduced by more than 80% (i.e. D145).
B. Homology model of EspM2$^{29–196}$ created with SWISS-MODEL (Arnold *et al*., 2006). Data from the RhoA NMR titration (red) and alanine mutations (blue) have been mapped onto the model. Those residues with chemical shift changes in the NMR titrations and which have also been mutated to alanines are coloured cyan.
C. Model of the EspM2$^{29–196}$–RhoA complex created by superimposing the EspM2$^{29–196}$ model and the crystal structure of RhoA (pdb:1xcg; Derewenda *et al*., 2004) onto the crystal structure of the SopE–Cdc42 complex (pdb:1gzs; Buchwald *et al*., 2002). All residues identified by the RhoA titration appear at the interface except for those within the C-terminal helix. In this model the intimate contacts with EspM2 are through the switch regions I and II of RhoA.

Mapping the EspM2 interface of the EspM2–RhoA complex

Although EspM2$^{29–196}$ is significantly more stable than full length, it has a proposenity to aggregate that can only be alleviated by high salt concentrations and pH values. These factors make EspM2 particularly unsuitable for structural study by either NMR or crystallography. Indeed, despite exhaustive attempts EspM2$^{29–196}$ and full-length EspM2 proved refractory to crystallization (see Appendix S1). Although deuteration of EspM2 was not possible, ~70% of the backbone resonances could be confidently assigned using standard triple resonance NMR methodology on a ^{15}N ^{13}C-labelled sample. NMR was then used to monitor the interaction of RhoA with EspM2$^{29–196}$ at a residue-specific level. At 1:1 molar ratio significant changes in ^{1}H ^{15}N TROSY-HSQC spectra of EspM2 were detectable; and it was possible to determine which assigned EspM2 residues were within intimate proximity of RhoA upon complex formation (Fig. 3A). After the addition of sevenfold molar excess RhoA, peaks corresponding to structured regions of EspM2$^{29–196}$ had broadened to such an extent that many were no longer visible and furthermore, addition of 5 mM GTP to the sample did not result in dissociation of the complex.

The chemical shift index based on NMR data for $^{13}C^{\alpha}$, $^{13}C^{\beta}$ and $^{13}C'$ resonances (Wishart *et al*., 1993) reveals that EspM2 is primarily helical (albeit for an unstructured ~30 residue region at the N-terminus), which is consistent with secondary structure prediction with PSIPRED (Jones, 1999) (Fig. S1). The helical content and locations are similar to that of the C-terminal domain of SifA whose crystal structure has been recently determined (Fig. S3) (pdb:3cxb; Ohlson *et al*., 2008). Based on these data we created a sequence alignment between EspM2$^{29–196}$ and SifA, and together with the crystal structure we computed a homology model of EspM2$^{29–196}$ using SWISS-MODEL (Arnold *et al*., 2006). NMR chemical shift data from RhoA titration was then mapped onto the model of EspM2$^{29–196}$ (Fig. 3B). Furthermore, a model of the complex with RhoA was created by superposing the EspM2$^{29–196}$ homology model and the crystal structure of RhoA (pdb:1xcg; Derewenda *et al*., 2004) onto the crystal structures of SopE and Cdc42, respectively, within the SopE–Cdc42 complex (pdb:1gzs; Buchwald *et al*., 2002) (Fig. 3C). In this model of the EspM2–RhoA complex, almost all of the perturbed

residues identify from NMR titration experiments lie within the interface and are situated at both of the switch sites of RhoA.

Site-directed mutagenesis of interface EspM2 residues

We introduced alanine substations in EspM2 residues L118A, Q124A and I127A, which are located within the EspM2 loop equivalent to the catalytic domain of SopE, D73, which located within the WxxxE motif and N154, which based on our RhoA-EspM2 model makes a hydrogen bond with the RhoA backbone. EspM2 W70A was used as a control. The EspM2$^{29–196}$ derivatives were expressed ectopically in Swiss 3T3 cells and formation of stress fibres was assessed microscopically (Fig. 4). While the W70A substitution completely abolished function, Q124A substitution attenuated stress fibre formation (seen in 35% of transfected cells compared with cells transfected with wild-type EspM2) while L118A and I127A reduced stress fibre formation by 56% and 65% respectively (Fig. 4). N154A only had a minor effect on stress fibres formation by EspM2 while no effect was detected for D73A (Fig. 4). We tested representative EspM2 mutants delivered form E2348/69 by infection. Consistent with the transfection data W70A and I127A did not trigger stress fibres while D73A, N154A and Q124A triggered stress fibres at levels comparable to the wild-type EspM2 (data not shown).

We next cloned *espM2* W70A, L118A, Q124A and I127A into pET28a for expression as 6His-tagged EspM2$^{29–196}$. Despite repeated attempts we were unable to purified EspM2 W70A and I127A, while the yield of EspM2 L118A was very low. These results suggest that these amino acids play an important structural role, which is consistent with the 3D model (Fig. 3). The Q124A mutant, purified at the same efficiency as the wild-type EspM2, was used in SPR and GEF assays. No significant difference in binding to RhoA was observed between wild-type EspM2 and EspM2 Q124A (Fig. 4). Importantly, EspM2 Q124A was attenuated in its ability to induce loading of GTP into RhoA as 50 μM protein was needed to achieve GTP loading equivalent to that induced by 1 μM wild-type EspM2 (Fig. 4).

Discussion

When first described the WxxxE effectors were thought to be molecular mimics of Rho GTPases (Alto *et al*., 2006). Recent data have shown that IpgB1 activates the Rac1 GEF complex ELMO/Dock180 (Handa *et al*., 2007), and Map, EspT and EspM activate Rho GTPases (Arbeloa *et al*., 2008; Berger *et al*., 2009; Bulgin *et al*., 2009) by an unknown mechanism. In this study we have investigated the mechanism by which EspM2 activates RhoA.

Using surface plasmon resonance we found that EspM2$^{29–196}$ forms a stable complex with nucleotide-free RhoA. The dissociation of the EspM2–RhoA complex was very slow and as a consequence we were unable to measure the dissociation rate constant. We found that the affinity of EspM2$^{29–196}$ to RhoA in presence of GDP or GTP was lower than in absence of nucleotide, which is similar to eukaryotic GEFs that also exhibit higher affinity and form stable complexes with the nucleotide-free Rho GTPases.

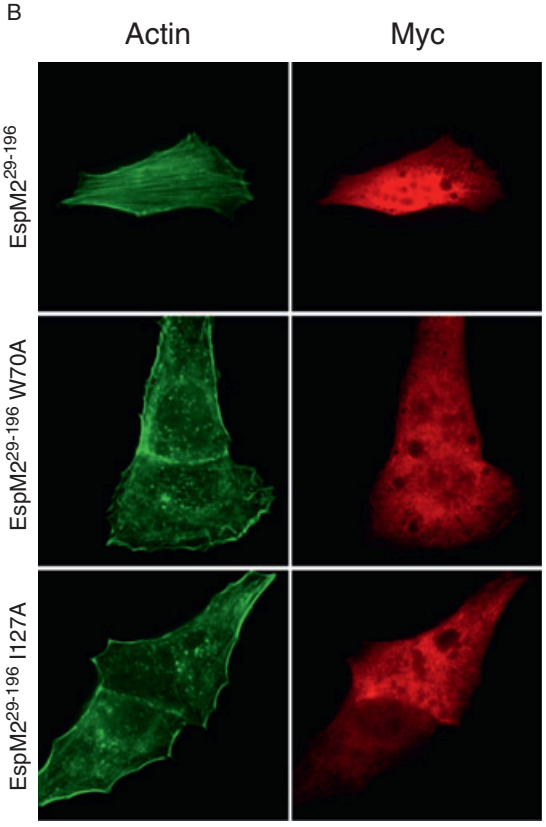
The initial step in nucleotide exchange is the formation of a low-affinity complex between the GEF and the GDP-bound Rho GTPase via recognition of the Switch I and II regions (Klebe *et al*., 1995), which favours GDP and Mg^{2+} release. This is then rapidly converted into a high-affinity GEF–GTPase binary complex (Lai *et al*., 1993); loading with free GTP leads to dissociation of the GEF and formation of a high-affinity Rho GTPase–GTP complex, which binds subsequently downstream effectors (Milburn *et al*., 1990). To test if EspM2 has a GEF activity we incubated RhoA with mant-GTP and increasing concentrations of EspM2$^{29–196}$. We found that EspM2$^{29–196}$ induced loading of GTP into RhoA in a concentration-dependent manner. This activity was specific for RhoA as EspM2$^{29–196}$ induced weak nucleotide exchange in Cdc42, while no nucleotide exchange was seen for Rac1 and the distant GTPase H-Ras. Interestingly, the *Salmonella* WxxxE effector SifA, which also binds RhoA, did not exhibit a detectable GEF activity. It is not currently known why binding to RhoA does not lead to nucleotide exchange or if SifA can induce nucleotide exchange in other small GTPases (e.g. Rab).

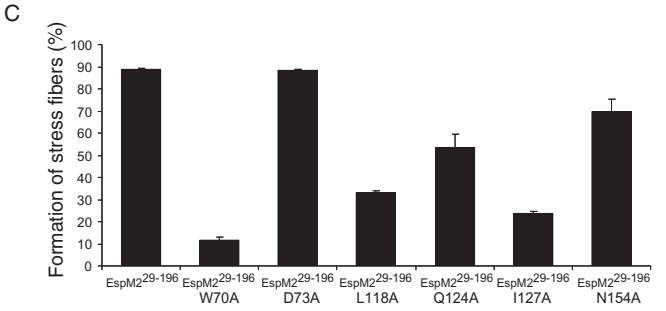
SopE from *Salmonella* was the first T3SS effector described as a GEF (Hardt *et al*., 1998). SopE activates Cdc42 and Rac1 leading to formation of membrane ruffles and bacterial invasion. The crystal structure of the SopE–Cdc42 complex illuminated the mechanism by which SopE functions as GEF. SopE is composed of six α-helices arranged in two three-helix bundles forming a V-shape. The junction connecting the two arms consists on small β sheet followed by a loop consisting of the GAGA motif, which is proposed to be the catalytic loop of SopE. Insertion of the GAGA motif between the switch regions of Cdc42 induces a push and pull type movement and release of GDP. Although SopE does not share sequence or structural similarity with eukaryotic GEFs, they induce similar conformational changes in the Rho GTPases. Recently, the crystal structure of SifA in complex with SKIP was solved (Ohlson *et al*., 2008). While the N-terminal SifA domain binds SKIP, the C-terminal domain, which shares no sequence similarity with SopE and harbours the WxxxE motif, adopts a SopE-like fold. NMR analysis of EspM2$^{29–196}$ combined with homology modelling revealed that it likely contains six to

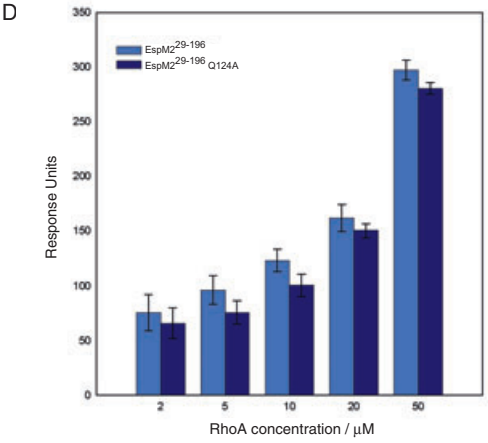
A

```
                                                  *     *  *
EspM2     96   AKISTEERQRVFFLVSQENQ---LTLDVKAAQSSINHVIM-GSASFGKKMDALCDG-MSR
IpgB2     91   RKIGDNLRKQIFKQVEKDYR---ISLDINAAQSSINHLVS-GSSYFKKKMDELCEG-MNR
EspT      89   TTIPGCVRERVFQRASFHCG---FSLDVRCAQTSTHHMIL-NSLYFQKKMDTLFGS-ADV
Map      100   SAISKETKCRIFKEVESAIQ---QPLDMNCAQSSISHFLQ-SNKYFNQKVDEQCGKGVDP
IpgB1    101   VVLTSDNKKNIFAAIEKKFPD--IKLDEKSAQTSISHTALNEIASSGLRAKILKRYSSDM
SifB     218   TAIDDAIKNKIAAKVIENTNLKNAAFEPNYAQSSVTQIVY--SCLFKNEILMNM-LEESS
SifA     224   ANISESTQQNAFLETMAMCGLKQLEIPPPHTHIPIEKMVK--EVLLADKTFQAF-LVTDP

SopE     139   PFLQEIGEAAKNAGLPGTTKNDVFTPSGAGANPFITPLISSANSKYPRMFINQHQQASFK
```







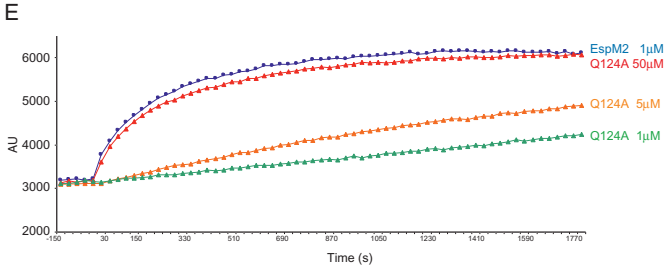


Fig. 4. Activity of EspM2$^{29–196}$ mutants.
A. Multiple sequence alignment of the putative catalytic loop and flanking regions of the WxxxE proteins: EspM2 of EHEC O157:H7 Sakai, IpgB1 and IpgB2 of *Shigella flexneri*, EspT of *Citrobacter rodentium*, Map of EPEC E2348/69 and SifA and SifB of *S.* Typhimurium. The loop region of SopE was added for comparison, with the catalytic region highlighted. Similar residues are highlighted in grey. A stretch of residues in the putative catalytic loop of SifA that is different from the other WxxxE effectors is highlighted. EspM2 residues selected for mutagenesis are indicated by a star.
B. Swiss 3T3 cells were transfected with pRK5 encoding myc-tagged EspM2$^{29–196}$, EspM2$^{29–196}$ W70A and EspM2$^{29–196}$ I127A. Actin was stained with Oregon green phalloidin and the myc tag was detected with monoclonal antibody.
C. Quantification of stress fibres formation in cell transfected with different EspM2$^{29–196}$ mutants. Results are displayed as mean ± SEM.
D. SPR comparison of RhoA binding to wild-type EspM2 and EspM2 Q124A. No significant difference in binding was detected over a range of RhoA concentrations. Shown is the averaged response of three repeats.
E. EspM2$^{29–196}$ Q124A is impaired in loading mant-GTP into RhoA. mant-GTP (0.5 µM) was incubated with 2 µM RhoA in presence of 1 µM EspM2$^{29–196}$ (blue circles) or 1 µM (green triangles), 5 µM (orange triangles) and 50 µM (red triangles) EspM2$^{29–196}$ Q124A.

seven α-helices arranged in a V-shape structure similar to SopE and SifA and a loop connecting the two arms (Fig. S3). Interestingly, the sequence of this putative catalytic loop is conserved between EspM2$^{29–196}$ and the other WxxxE effectors, but not SifA (Fig. 4A), which might provide an explanation as for why SifA cannot induce nucleotide exchange in RhoA.

The tryptophan and glutamic acid of the WxxxE motif have been shown to be essential as replacement of W or E by alanine completely abolished the effectors' function (Alto *et al*., 2006; Arbeloa *et al*., 2008). However, we recently found that conservative substitutions of the W and E residues in EspM2 had little effect on stress fibre formation, suggesting that they have a structural role. In our model the W70 and E74 residues in EspM2 are positioned around the junction of the two three-helix bundles. Consistently, the role proposed for these residues in SifA was to maintain the conformation of the putative catalytic loop through hydrophobic contacts with surrounding residues. Among these residues I258, the equivalent of I127 in EspM2, forms hydrophobic contacts with the tryptophan and hydrophobic contacts and a hydrogen bond with the glutamic acid (Ohlson *et al*., 2008). We observed that alanine substitutions of W70 and I127 of EspM2 abolished almost completely its ability to induce formation of stress fibres. Despite repeated attempts we were unable to purify His-tagged EspM2 W70 and I127 suggesting that these residues play a role in maintaining the global structure, which is consistent with the 3D model of EspM2.

We use NMR to investigate how formation of a complex with RhoA affects the conformation of EspM2$^{29–196}$. Titrating RhoA into ^{15}N ^{13}C-labelled EspM2$^{29–196}$ revealed specific protein interaction with most of the shifted peaks being located either in the penultimate helix or in the putative catalytic loop. Other than I127, substituting the putative EspM catalytic loop residue L118 by alanine also had a substantial effect on stress fibres formation; however, the recombinant protein was highly unstable.

While this project was reaching conclusion, Huang *et al.* (2009) published the crystal structure of the Map–Cdc42 complex and showed that Map induces guanine nucleotide exchange in Cdc42 while IpgB2 and IpgB1 induce nucleotide exchange in RhoA and Rac1 respectively. In this study it was shown that Map Q128, located within the catalytic loop, makes a hydrogen bond with Cdc42 Phe37, which fortifies the interaction between these two proteins. Moreover Map Q128Y does not bind to, or induce nucleotide exchange in, Cdc42. Interestingly, while not affecting the interaction of EspM2 with RhoA, EspM2 Q124A (equivalent to Map Q128) was attenuated in stress fibre formation by transfection and RhoA GEF activity; 50 μM EspM2 Q124A was needed to achieve the same GEF activity as 1 μM wild-type EspM2. Importantly, while mutations affecting protein stability were inactive when delivered either by transfection or by infection, we did not detect a significant effect on stress fibre formation when EspM2 Q124A (or D73A and N154A) were delivered by infection. This suggests that upon translocation the local effector concentration is high enough to induce nucleotide exchange, compared with ectopic expression which leads to global cytosolic distribution, low effector concentration and hence an attenuated stress fibre formation.

The high-affinity complexes formed between GEFs and their cognate Rho GTPases are quickly dissociated upon addition of GTP or GDP. Unexpectedly we found that the EspM2$^{29–196}$–RhoA and SifA–RhoA complexes did not dissociate in the presence of exogenous nucleotides. This result suggests that EspM2 could activate RhoA by a unique mechanism, involving constitutive activation, which allows recruitment of ROCK to the EspM2–RhoA complex. Supporting this hypothesis is our finding that upon infection of Swiss 3T3 cells with EPEC overexpressing EspM2 the induced stress fibres were stable for at least 5 h after the adherent bacteria were killed by gentamicin (not shown). Moreover, Alto *et al.* (2006) have shown that IpgB2 is co-immunoprecipitated with ROCK, possibly via mutual interaction with RhoA.

In conclusion, our work shows that EspM2 is a RhoA GEF. Importantly, a large screen of over 900 clinical EPEC and EHEC isolates revealed that *espM* is found in *c*. 50% of the strains (Arbeloa *et al*., 2009). It is now well documented that while 21 core effector genes are conserved in all EPEC and EHEC strains, the distribution of the non-conserved, accessory, effector genes varies from strain to strains (Iguchi *et al*., 2009). This suggests that EPEC and EHEC strains can employ different infection strategies. Although the role of EspM2 during infection is not yet known, a recent study by Simovitch *et al.* (2009) showed that it is involved in delocalization of the thigh junctions (TJ). Importantly, the TJ alterations induced by EspM2 did not interfere with their functionality; on the contrary, increased TER values were observed upon EspM2 expression. These results suggest that EspM2 might play a role in maintaining TJ during infection. Moreover, EspM2 might modulate additional cellular pathways, as IpgB2 was recently implicated in activation of NF-kB in a RhoA-ROCK-dependent manner (Fukazawa *et al*., 2008). Further studies are needed in order to determine the role played by EspM *in vivo*.

Experimental procedures

Bacterial strains and cell culture

Bacteria were grown from single colonies in Luria–Bertani (LB) broth in a shaking incubator at 37°C or maintained on LB plates. Culture medium was supplemented with ampicillin (100 μg ml^{-1}) or kanamycin (25 μg ml^{-1}) as appropriate.

Swiss 3T3 cells were maintained in DMEM with 4500 mg ml^{-1} glucose and supplemented with 10% fetal calf serum (Gibco) and 4 mM Glutamax (Gibco).

Plasmids and molecular techniques

Plasmids used in this study are listed in Table S1 in *Supporting information*; primers are listed in Table S2. *espM2* and *espM2*$^{29–196}$ were amplified by PCR using genomic EHEC O157:H7 strain Sakai DNA as template and cloned into pET28 with non-cleavable N-terminal 6His tag or into the mammalian expression vector pRK5 with an N-terminal myc tag. *sifA* was amplified by PCR using genomic *S.* Typhimurium SL1344 DNA as template and cloned into pET28 with an N-terminal 6His tag. All constructs were verified by DNA sequencing.

The vector pMW172-His expressing RhoA or Rac1 fused to a 6His Tag was a gift from Michael Way.

Site-directed mutagenesis

Site-directed mutagenesis was carried out using a Quickchange II kit (Stratagene) according to the manufacturer's instructions. Primers were designed using the Quickchange mutagenic primer design program (Stratagene). Plasmids pRK5:*espM2*$^{29–196}$, pET28:*espM2*$^{29–196}$ and pSA10:*espM2* were used as template for the mutagenic reactions. All constructs were verified by DNA sequencing.

Preparation of recombinant proteins

Escherichia coli B834 containing pET28a (NdeI/BamHI inserted *espM2*$^{29–196}$ or *SifA*) were grown at 310 K in LB broth containing 25 mg ml^{-1} kanamycin until an A_{600} of 0.6 was reached. Protein overexpression was induced by the addition of 1.0 mM IPTG. Cells were harvested after incubation at 293 K overnight (4500 *g*, 20 min, 277 K). Cell pellets were re-suspended in lysis buffer (20 mM Tris pH 8, 500 mM NaCl, 1 mM DTT), complete EDTA-free protease inhibitor cocktail (Roche) and homogenized. After centrifugation (14 000 *g*, 30 min, 277 K), the soluble fraction was applied to a 5 ml His trap FF Column (GE Healthcare) in a gradient of 0–300 mM imidazole. EspM2 fractions were pooled and purified using a Superdex 75 26/60 equilibrated in 20 mM Tris pH 8, 500 mM NaCl, 10 mM DTT, high salt due to the instability of the protein. Protein was Liquid Nitrogen flash cooled and frozen at 193 K on the same day, after experiencing protein precipitation in samples kept at 277 K over 2–3 days.

Preparation of His-RhoA and His-Rac-1 was identical with the following exceptions: expression was constitutive; cells were harvested after incubation at 310 K overnight. Lysis buffer was 20 mM Tris, 500 mM NaCl, 20 mM imidazole, 5 mM $MgCl_2$. Size exclusion buffer was 20 mM Tris, 200 mM NaCl, 3 mM $MgCl_2$, 1 mM DTT.

Surface plasmon resonance

Experiments were carried out using a BIAcore™ 2000 System (Biacore AB, Sweden) at 20°C. EspM2$^{29–196}$ was coupled to a CM5 sensor chip leading to a rise of 2000 Response Units using standard amine coupling protocols (BIAcore Amine Coupling Kit BR-1000-50). Hepes-buffered saline containing 5 mM $MgCl_2$ was flowed throughout the experiment at 50 μl min^{-1}. Samples of RhoA/Rac-1 were injected (in the same buffer) for 180 s duration over the EspM2$^{29–196}$ channel and over a RhoA control channel. Dissociation was followed for 1000 s from the end of injection after which regeneration of the surface was carried out with 25 mM NaOH. No loss of activity was seen after regeneration. Experiments (repeated three times) were carried out with (i) varying concentrations of RhoA ($\varepsilon = 18\,825\ M^{-1}\ cm^{-1}$) and Rac-1 ($\varepsilon = 23\,295\ M^{-1}\ cm^{-1}$) (concentration determined by Nanodrop Spectrophotometer, 0.005–50 μM), and with (ii) fixed 4 μM RhoA but varying concentrations of GDP/GTP (0.5–8 μM) added to the buffer. RhoA control channel subtracted signals are presented (BIAEvaluation software). The same conditions were used to analyse the SifA–RhoA interaction.

Guanine nucleotide exchange analysis

In vitro GEF activity assay was carried out using RhoGEF exchange assay biochem kit (Cytoskeleton Denver) according to the manufacturer's instructions. Briefly, exchange reaction assay mixtures contained 20 mM Tris pH 7.5, 50 mM NaCl, 10 mM $MgCl_2$, 50 μg ml^{-1} bovine serum albumin (BSA), 0.75 μM *N*-methylanthraniloyl(mant)-GTP, and 2 μM Rac1-His, Cdc42-His, H-Ras-His or RhoA-His GTPase. Fluorescence spectroscopic analysis of mant-GTP was carried out using Fluostar Optima spectrometer. The fluorescence measurements were taken every 30 s with excitation and emission wavelengths of 360 nm and 440 nm respectively. After five readings (150 s), purified EspM2$^{29–196}$ was added and the relative mant fluorescence was monitored every 30 s for a total time of 30 min. Experiments were performed in triplicate.

NMR sample preparation and backbone assignment of EspM2$^{29–196}$

Uniformly ^{15}N ^{13}C-labelled EspM2$^{29–196}$ was expressed in ^{15}N ^{13}C-labelled rich media (Cambridge isotopes). After purification as described above the sample was dialysed against NMR buffer [50 mM $NaPO_4$ pH 7.5, 150 mM NaCl, 5 mM DTT, 10% (v/v) D_2O] and concentrated to 0.9 mM. Backbone assignment for ~65% of EspM2$^{29–196}$ was achieved using standard double- and triple-resonance assignment experiments (Sattler *et al.*, 1999) at 295 K.

NMR titration of RhoA against EspM2$^{29–196}$

^{15}N ^{13}C-labelled EspM2$^{29–196}$ was mixed with unlabelled His-RhoA (dialysed in NMR buffer) ranging from 0x to 7x molar excess and ^{1}H ^{15}N TROSY-HSQC experiments were performed at each increment at 298 K. GTP (5 mM) was added to the sample of EspM2$^{29–196}$ saturated with RhoA and a final ^{1}H ^{15}N TROSY-HSQC was carried out.

Transfection

Swiss 3T3 cells were transfected with pRK5 encoding EspM2, EspM2$^{29–196}$ and derivatives fused to a myc tag by lipofectamine 2000 (Invitrogen), according to the manufacturer's recommenda-

tions. The cells were incubated at 37°C in a humidified incubator with 5% CO_2 for 19 h, washed twice in PBS before having their media replaced with DMEM as described previously (Arbeloa *et al*., 2008).

Infection of Swiss 3T3

Forty-eight hours prior to infection cells were seeded onto glass coverslips at a density of 5×10^5 cells per well and maintained in DMEM supplemented with 10% FCS at 37°C in 5% CO_2. Three hours before infection the cells were washed three times with PBS, the media replaced with fresh DMEM without FCS and 500 µl of primed bacteria were added to each well and infections were carried out for 90 min at 37°C in 5% CO_2.

Immunofluorescence staining and microscopy

Swiss 3T3 cells on coverslips were washed three times in PBS and fixed with 3% paraformaldehyde for 20 min before washing three more times with PBS. For immunostaining, the cells were permeabilized for 4 min in PBS 0.5% Triton X-100, washed three times with PBS and quenched for 30 min with 50 mM NH_4Cl. The coverslips were then blocked for 1 h with 10% donkey serum (Jackson laboratories) before incubation with primary and secondary antibodies. The primary antibody mouse anti-myc (Millipore) was used at a dilution of 1:500. Coverslips were incubated with the primary antibody for 1 h, washed three times in PBS and incubated with the secondary antibody for 1 h. Donkey anti-mouse IgG conjugated to a Cy3 fluorophore (Jackson laboratories) was used at a 1:200. Actin was stained using Oregon Green phalloidin (Invitrogen) at a 1:100 dilution. All dilutions were in 10% donkey serum. Coverslips were mounted on slides using ProLong Gold antifade reagent (Invitrogen) and visualized by Zeiss Axioimager immunofluorescence microscope using the following excitation wavelengths: Cy3 – 550 nm, Cy5 – 650 nm and Oregon Green – 488 nm. All images were analysed using the Axiovision Rel 4.5 software.

Acknowledgements

We thank Michael Way for pMW172 derivatives expressing RhoA or Rac1. We thank Clare Harding for cloning pET28:*sifA* and Leah Ensell for technical assistance. This work was supported by grants from the Wellcome Trust and the MRC.

References

Alto, N.M., Shao, F., Lazar, C.S., Brost, R.L., Chua, G., Mattoo, S., *et al.* (2006) Identification of a bacterial type III effector family with G protein mimicry functions. *Cell* **124:** 133–145.

Arbeloa, A., Bulgin, R.R., MacKenzie, G., Shaw, R.K., Pallen, M.J., Crepin, V.F., *et al.* (2008) Subversion of actin dynamics by EspM effectors of attaching and effacing bacterial pathogens. *Cell Microbiol* **10:** 1429–1441.

Arbeloa, A., Blanco, M., Moreira, F.C., Bulgin, R., Lopez, C., Dahbi, G., *et al.* (2009) Distribution of *espM* and *espT* among enteropathogenic and enterohaemorrhagic *Escherichia coli*. *J Med Microbiol* **58:** 988–995.

Arnold, K., Bordoli, L., Kopp, J., and Schwede, T. (2006) The SWISS-MODEL workspace: a web-based environment for protein structure homology modelling. *Bioinformatics* **22:** 195–201.

Berger, C.N., Crepin, V.F., Jepson, M.A., Arbeloa, A., and Frankel, G. (2009) The mechanisms used by enteropathogenic *Escherichia coli* to control filopodia dynamics. *Cell Microbiol* **11:** 309–322.

Black, D.S., and Bliska, J.B. (2000) The RhoGAP activity of the *Yersinia pseudotuberculosis* cytotoxin YopE is required for antiphagocytic function and virulence. *Mol Microbiol* **37:** 515–527.

Buchwald, G., Friebel, A., Galan, J.E., Hardt, W.D., Wittinghofer, A., and Scheffzek, K. (2002) Structural basis for the reversible activation of a Rho protein by the bacterial toxin SopE. *EMBO J* **21:** 3286–3295.

Bulgin, R.R., Arbeloa, A., Chung, J.C., and Frankel, G. (2009) EspT triggers formation of lamellipodia and membrane ruffles through activation of Rac-1 and Cdc42. *Cell Microbiol* **11:** 217–229.

Deng, Q., and Barbieri, J.T. (2008) Modulation of host cell endocytosis by the type III cytotoxin, *Pseudomonas* ExoS. *Traffic* **9:** 1948–1957.

Derewenda, U., Oleksy, A., Stevenson, A.S., Korczynska, J., Dauter, Z., Somlyo, A.P., *et al.* (2004) The crystal structure of RhoA in complex with the DH/PH fragment of PDZRhoGEF, an activator of the Ca(2+) sensitization pathway in smooth muscle. *Structure* **12:** 1955–1965.

Finlay, B.B. (2005) Bacterial virulence strategies that utilize Rho GTPases. *Curr Top Microbiol Immunol* **291:** 1–10.

Fu, Y., and Galan, J.E. (1999) A *Salmonella* protein antagonizes Rac-1 and Cdc42 to mediate host-cell recovery after bacterial invasion. *Nature* **401:** 293–297.

Fukazawa, A., Alonso, C., Kurachi, K., Gupta, S., Lesser, C.F., McCormick, B.A., and Reinecker, H.C. (2008) GEF-H1 mediated control of NOD1 dependent NF-kappaB activation by *Shigella* effectors. *PLoS Pathog* **4:** e1000228.

Goehring, U.M., Schmidt, G., Pederson, K.J., Aktories, K., and Barbieri, J.T. (1999) The N-terminal domain of *Pseudomonas aeruginosa* exoenzyme S is a GTPase-activating protein for Rho GTPases. *J Biol Chem* **274:** 36369–36372.

Hall, A., Paterson, H.F., Adamson, P., and Ridley, A.J. (1993) Cellular responses regulated by rho-related small GTP-binding proteins. *Philos Trans R Soc Lond B Biol Sci* **340:** 267–271.

Handa, Y., Suzuki, M., Ohya, K., Iwai, H., Ishijima, N., Koleske, A.J., *et al.* (2007) *Shigella* IpgB1 promotes bacterial entry through the ELMO–Dock180 machinery. *Nat Cell Biol* **9:** 121–128.

Hardt, W.D., Chen, L.M., Schuebel, K.E., Bustelo, X.R., and Galan, J.E. (1998) *S. typhimurium* encodes an activator of Rho GTPases that induces membrane ruffling and nuclear responses in host cells. *Cell* **93:** 815–826.

Huang, Z., Sutton, S.E., Wallenfang, A.J., Orchard, R.C., Wu, X., Feng, Y., *et al.* (2009) Structural insights into host GTPase isoform selection by a family of bacterial GEF mimics. *Nat Struct Mol Biol* **16:** 853–860.

Iguchi, A., Thomson, N.R., Ogura, Y., Saunders, D., Ooka, T.,

Henderson, I.R., *et al.* (2009) Complete genome sequence and comparative genome analysis of enteropathogenic *Escherichia coli* O127:H6 strain E2348/69. *J Bacteriol* **191:** 347–354.
Jaffe, A.B., and Hall, A. (2005) Rho GTPases: biochemistry and biology. *Annu Rev Cell Dev Biol* **21:** 247–269.
Jones, D.T. (1999) Protein secondary structure prediction based on position-specific scoring matrices. *J Mol Biol* **292:** 195–202.
Klebe, C., Prinz, H., Wittinghofer, A., and Goody, R.S. (1995) The kinetic mechanism of Ran-nucleotide exchange catalyzed by RCC1. *Biochemistry* **34:** 12543–12552.
Lai, C.C., Boguski, M., Broek, D., and Powers, S. (1993) Influence of guanine nucleotides on complex formation between Ras and CDC25 proteins. *Mol Cell Biol* **13:** 1345–1352.
Matsuzawa, T., Kuwae, A., Yoshida, S., Sasakawa, C., and Abe, A. (2004) Enteropathogenic *Escherichia coli* activates the RhoA signaling pathway via the stimulation of GEF-H1. *EMBO J* **23:** 3570–3582.
Milburn, M.V., Tong, L., Vos, A.M., Brunger, A., Yamaizumi, Z., Nishimura, S., and Kim, S.H. (1990) Molecular switch for signal transduction: structural differences between active and inactive forms of protooncogenic ras proteins. *Science* **247:** 939–945.
Mota, L.J., and Cornelis, G.R. (2005) The bacterial injection kit: type III secretion systems. *Ann Med* **37:** 234–249.
Ohlson, M.B., Huang, Z., Alto, N.M., Blanc, M.P., Dixon, J.E., Chai, J., and Miller, S.I. (2008) Structure and function of *Salmonella* SifA indicate that its interactions with SKIP, SseJ, and RhoA family GTPases induce endosomal tubulation. *Cell Host Microbe* **4:** 434–446.
Rossman, K.L., Worthylake, D.K., Snyder, J.T., Siderovski, D.P., Campbell, S.L., and Sondek, J. (2002) A crystallographic view of interactions between Dbs and Cdc42: PH domain-assisted guanine nucleotide exchange. *EMBO J* **21:** 1315–1326.
Rudolph, M.G., Weise, C., Mirold, S., Hillenbrand, B., Bader, B., Wittinghofer, A., and Hardt, W.D. (1999) Biochemical analysis of SopE from *Salmonella typhimurium*, a highly efficient guanosine nucleotide exchange factor for RhoGTPases. *J Biol Chem* **274:** 30501–30509.
Sattler, M., Schleucher, J., and Griesinger, C. (1999) Heteronuclear multidimensional NMR experiments for the structure determination of proteins in solution employing pulsed field gradients. *Prog NMR Spectrosc* **34:** 93–158.
Simovitch, M., Sason, H., Cohen, S., Zahavi, E.E., Melamed-Book, N., Weiss, A., *et al.* (2009) EspM inhibits pedestal formation by EHEC and EPEC and disrupts the architecture of a polarized epithelial monolayer. *Cell Microbiol* Doi: 10.1111/j.1462-5822.2009.01410.x.
Stevens, M.P., Friebel, A., Taylor, L.A., Wood, M.W., Brown, P.J., Hardt, W.D., and Galyov, E.E. (2003) A *Burkholderia pseudomallei* type III secreted protein, BopE, facilitates bacterial invasion of epithelial cells and exhibits guanine nucleotide exchange factor activity. *J Bacteriol* **185:** 4992–4996.
Tobe, T., Beatson, S.A., Taniguchi, H., Abe, H., Bailey, C.M., Fivian, A., *et al.* (2006) An extensive repertoire of type III secretion effectors in *Escherichia coli* O157 and the role of lambdoid phages in their dissemination. *Proc Natl Acad Sci USA* **103:** 14941–14946.
Von Pawel-Rammingen, U., Telepnev, M.V., Schmidt, G., Aktories, K., Wolf-Watz, H., and Rosqvist, R. (2000) GAP activity of the *Yersinia* YopE cytotoxin specifically targets the Rho pathway: a mechanism for disruption of actin microfilament structure. *Mol Microbiol* **36:** 737–748.
Wishart, D.S., Sykes, B.D., and Richards, F.M. (1993) Improved synthetic methods for the selective deuteration of aromatic amino acids: applications of selective protonation towards the identification of protein folding intermediates through nuclear magnetic resonance. *Biochim Biophys Acta* **1164:** 36–46.

Supporting information

Additional Supporting Information may be found in the online version of this article:

Appendix S1. Supplementary results.
Fig. S1. ^{1}H ^{15}N HSQC spectra of EspM2 constructs at 295 K.
A. Full-length EspM2 where the overlapping peaks within the centre of the spectra are due to resonances from highly flexible regions of the protein.
B. The much increased resolution of the spectra of $EspM2^{29–196}$ shows that this truncated form is a compact structure with an appropriate number of amide peaks.
Fig. S2. Activity of $EspM2^{29–196}$.
A. Serum-starved Swiss 3T3 cells were mock transfected or transfected with the mammalian expression vector pRK5 encoding myc-tagged EspM2 and $EspM2^{29–196}$ for 19 h. Actin was stained with Oregon green phalloidin and the myc tag was detected with monoclonal antibody. Transfection of EspM2 and $EspM2^{29–196}$ induces the formation of parallel stress fibres to the same extent.
B. Quantification of stress fibres on Swiss 3T3 after 19 h transfection with EspM2 and $EspM2^{29–196}$. Fifty cells were counted in duplicate in three independent experiments. Results are displayed as mean ± SEM.
Fig. S3. Secondary structure of $EspM2^{29–196}$. From the NMR chemical shift index (CSI) (Wishart *et al.*, 1993), predictions with PSIPRED (Jones, 1999) and a model based on the crystal structure of the C-terminal domain of SifA (pdb:3cxb; Ohlson *et al.*, 2008) $EspM2^{29–196}$ most likely contains between six and seven helices and two short N-terminal helices. Helices are shown as red rectangles, sheets as blue arrows, coils and loops are grey lines while regions in the CSI which have not been assigned are left blank.
Table S1. List of plasmids.
Table S2. List of primers.

Please note: Wiley-Blackwell are not responsible for the content or functionality of any supporting materials supplied by the authors. Any queries (other than missing material) should be directed to the corresponding author for the article.

IAI Accepts, published online ahead of print on 1 February 2010
Infect. Immun. doi:10.1128/IAI.01250-09
Copyright © 2010, American Society for Microbiology and/or the Listed Authors/Institutions. All Rights Reserved.

IAI Accepts published online ahead of print

The bacterial guanine nucleotide exchange factors SopE-like and WxxxE effectors

Running title: The SopE and WxxxE effector GEFs

Richard Bulgin[1], Benoit Raymond[1], James A. Garnett[2], Gad Frankel[1*], Valerie F. Crepin[1], Cedric N. Berger[1], Ana Arbeloa[1]

[1]Centre for Molecular Microbiology and Infection, Division of Cell and Molecular Biology and [2]Division of Molecular Biosciences, Imperial College, London, United Kingdom

*Correspondence: Gad Frankel, Flowers building, Imperial College, London, SW7 2AZ. Telephone: +44 20 7594 3070; Fax: +44 20 7594 3069; Email: g.frankel@imperial.ac.uk

Downloaded from iai.asm.org at IMPERIAL COLLEGE LONDON on February 25, 2010

IAI Accepts published online ahead of print

Abstract

Subversion of Rho family small GTPases, which control actin dynamics, is a common infection strategy used by bacterial pathogens. In particular, *Salmonella*, *Shigella*, enteropathogenic (EPEC) and enterohemorrhagic (EHEC) *Escherichia coli* translocate type III secretion system (T3SS) effector proteins to modulate the Rho GTPases RhoA, Cdc42 and Rac1 that trigger formation of stress fibers, filopodia and lamellipodia/ruffles, respectively. The *Salmonella* effector SopE is a guanine nucleotide exchange factor (GEF) that activates Rac1 and Cdc42, which induce 'the trigger mechanism of cell entry'. Based on a conserved Trp-xxx-Glu motif the T3SS effector proteins IpgB1 and IpgB2 of *Shigella*, SifA and SifB of *Salmonella* and Map of EPEC and EHEC were grouped together into a WxxxE family; recent studies identified the T3SS EPEC and EHEC effectors EspM and EspT as new family members. Recent structural and functional studies have shown that representatives of the WxxxE effectors share with SopE a 3D fold and a GEF activity. In this minireview we summarize contemporary findings related to the SopE and WxxxE GEFs in the context of their role in subverting general host cell signaling pathways and infection.

Downloaded from iai.asm.org at IMPERIAL COLLEGE LONDON on February 25, 2010

IAI Accepts published online ahead of print

Downloaded from iai.asm.org at IMPERIAL COLLEGE LONDON on February 25, 2010

Introduction

Colonization, multiplication and dissemination are the key steps of an infectious cycle. To persist within the hostile *in vivo* environments bacterial pathogens utilize sophisticated virulence strategies to subvert and hijack cellular and systemic functions. A common infection strategy used by Gram-negative pathogens involves injection of virulence factors, known as effectors, by the type III secretion system (T3SS), from the bacterial cell directly into the eukaryotic cell (reviewed in (26)). The injected effectors target different cellular compartments and subvert numerous signalling pathways for the benefit of the invaded or attached bacteria. Due to their essential role in regulating key cellular functions Rho-family small G proteins are common targets of T3SS bacterial effectors (reviewed in (23)).

To date, 22 members of the Rho GTPase family, belonging to the small GTPase protein superfamily, have been identified (54). Cdc42, Rac1 and RhoA, which trigger formation of filopodia, lamellipodia/ruffles and stress fibers, respectively, are the best characterized (29). The Rho GTPases share a conserved structure consisting of two flexible domains called Switch I and Switch II and a phosphate binding loop (P-loop) which together form a Mg^{2+} and nucleotide-binding pocket (reviewed in (22)). The small GTPases are modified post-transcriptionally by the addition of a lipid moiety to the C-terminus (farnesyl, geranyl, palmitoyl or methyl), signalled by the carboxyl-terminal CAAX motif (55), which targets them to different membranous compartments.

The function of the small GTPases is strictly regulated. By binding the two switch domains and the lipid moiety, the Guanine nucleotide Dissociation Inhibitors (GDIs) prevent membrane localization and maintain the GTPases in an inactive state in the cytosol (35, 59). Small GTPases act as molecular switches cycling between GTP bound (active) and GDP bound (inactive) conformations. Switching a GTPase on is mediated by Guanine nucleotide

IAI Accepts published online ahead of print

Exchange Factors (GEFs) that facilitate exchange of GDP for GTP. The intrinsically low GTP hydrolysis activity of Rho GTPases is greatly increased by interaction with GTPase-Activating Proteins (GAPs), leading to recycling of the G protein to its GDP-bound, inactive form. The Rho GTPases transmit signals in a GTP-dependent manner by activating and/or recruiting downstream effector proteins to their sites of action (reviewed in (38)).

Rho GTPases GEFs belong mainly to the Dbl family and contain a catalytic Dbl homology domain (DH) and a pleckstrin homology domain (PH), which mediates membrane association, modulates the activity of the DH domain and probably determines substrate specificity (39). The DH domain is involved in the exchange of the GDP to GTP by a mechanism called "push and pull". It interacts specifically with the Rho GTPases Switch I and Switch II regions leading to a conformational change and ejection of GDP and Mg^{2+}. This in turn leads to loading with GTP, which is present in the cytosol at a high concentration (72). Loading of Rho GTPase with GTP-Mg^{2+} triggers the dissociation of the GEF Rho GTPase complex and allows interaction of the latter with its effectors.

In order to subvert the Rho GTPase pathways, pathogenic bacteria inject into eukaryotic cells effector proteins that mimic GEF, GAP, or RhoGDI. For example *Salmonella* inject equivalent amounts of the T3SS effector proteins SopE and SptP that control the activity of Cdc42 and Rac1. Although sharing no sequence or structural similarities with eukaryotic GEFs (56), SopE triggers nucleotide exchange, which induces 'the trigger mechanism of cell entry' (32). SopE is then poly-ubiquitinated and targeted to the proteosome before SptP, which has a GAP activity and exhibits much slower degradation kinetics, helps the cell to recover from the SopE-induced membrane ruffling (42).

Recently, Alto *et al*. (1) assembled several known T3SS effectors into a single family that share the common motif Trp-xxx-Glu (WxxxE). This family originally included the

Downloaded from iai.asm.org at IMPERIAL COLLEGE LONDON on February 25, 2010

IAI Accepts published online ahead of print

Salmonella SifA and SifB, the *Shigella* IpgB2 and IpgB1 and the enteropathogenic *Escherichia coli* (EPEC) and enterohemorrhagic *E. coli* (EHEC) Map. Since the original classification new family members, EspM (3) and EspT (16), were discovered in EPEC, EHEC and *Citrobacter rodentium* (Fig. 1). Although initially thought to be Rho GTPase mimics (1), recent structural, biochemical and functional data show that the WxxxE effectors, like SopE, are Rho GTPases GEFs, which are the focus of this review.

The WxxxE effectors: from Rho GTPase mimics to Rho GTPase GEFs

The Rho GTPase mimicking hypothesis

In 2006 Alto *et al.* have shown that when expressed ectopically several of the WxxxE effectors subvert actin dynamics (1). IpgB2 induced formation of stress fibers, Map induced filopodia and IpgB1 induced formation of membrane ruffles, phenotypes which correspond to those induced by the activated forms of RhoA, Cdc42 and Rac1 respectively (Fig. 2). In order to determine if formation of stress fibers induced by IpgB2 was epistatic to RhoA, the activity of endogenous RhoA was inhibited either by dominant negative or by the bacterial toxins YopT and C3. In these conditions, IpgB2-induced stress fiber formation was not affected, suggesting that IpgB2 was acting independently of the small GTPase. Concordantly, IpgB2 was shown to interact with the Rho coiled coil p160 (ROCK) serine/threonine kinase and the RhoA binding motif of the formin mDia, the two canonical RhoA effectors involved in stress fiber formation (1). *In vitro* ROCK kinase assays showed that IpgB2 directly stimulated the activity of ROCK. Furthermore, inhibition of ROCK by the chemical inhibitor Y-27632 abolished IpgB2-induced stress fiber formation (1). Together these findings led Alto and colleagues to conclude that IpgB2 acts as a RhoA mimic, triggering the RhoA pathway by directly activating the RhoA effectors ROCK and mDia. This mechanism was extended to other WxxxE family members and in the absence of sequence similarities and structural data

Downloaded from iai.asm.org at IMPERIAL COLLEGE LONDON on February 25, 2010

IAI Accepts published online ahead of print

the results from the seminal paper of Alto *et al* (1) supported the hypothesis that the WxxxE effectors function as small GTPases mimics.

Before the WxxxE effectors were grouped together, Ohya *et al.* showed that IpgB1 induces formation of membrane ruffles which was dependent on Rac1 and to a lesser extent on Cdc42 (52). A follow-up study by Handa *et al.* has shown that IpgB1 binds the N-terminal region of the engulfment and motility protein (ELMO) in a similar manner to RhoG (30). Formation of membrane ruffles by IpgB1 was dependent on the ability of ELMO to bind the atypical Rac1 GEF Dock180. Cells transfected with truncated ELMO, which cannot bind Dock180, or Dock180, which cannot bind Rac1, failed to induce formation of IpgB1-dependent membrane ruffles upon *Shigella* infection (30). Translocation of ELMO-Dock 180 complex to the membrane is mediated by activated RhoG. Likewise, expression of IpgB1 induces translocation of the ELMO-Dock180 complex to the membrane where it induces membrane ruffles (30). Together these results led the authors to conclude that IpgB1 activates Rac1 by binding the ELMO-Dock180 bipartite GEF (30). These results extended the mimicking paradigm as Handa *et al.* have shown that IpgB1 was mimicking RhoG (30).

The ability of Map to induce formation of filopodia at the EPEC attachment sites during the early stages of infection was originally described by Kenny and co-workers in 2002 (41). Using dominant negative constructs Kenny *et al*. showed that Map induces filopodia in a Cdc42-dependent but Rac1-independent manner. These results were confirmed by Berger *et al.* that furthermore demonstrated that Map induces activation of Cdc42 (7). Similarly to IpgB2, transfection or translocation of the EspM effectors resulted in formation of stress fibers in a ROCK-dependent manner (3) (Fig. 2). Production of stress fibers by EspM required active RhoA, since inhibition of this GTPase by dominant negative constructs abolished stress fiber formation (3). Moreover, pull-down experiments have shown that expression of EspM induced activation of RhoA (3). EspT induces formation of membrane

Downloaded from iai.asm.org at IMPERIAL COLLEGE LONDON on February 25, 2010

IAI Accepts published online ahead of print

ruffles, similar in morphology to those induced by IpgB1, and lamellipodia (Fig. 2) (16), that facilitate EPEC invasion (15). The function of EspT was dependent on cellular GTPases as EspT enriches the GTP bound cellular fractions of Rac1 and Cdc42 in *in vitro* pull-down assays, while inhibition of Rac1, and to a lesser extent Cdc42, blocked EspT-induced formation of membrane ruffle and lamellipodia (16) and invasion (15). Despite the similarity between the phenotypes induced by EspT and IpgB1 the mechanism by which membrane ruffles and lamellipodia are formed by these two WxxxE effectors is distinct as EspT induces cytoskeletal re-arrangements independently of ELMO or Dock180 (16, 30); these results are consistent with the low sequence similarity between IpgB1 and EspT (Fig. 1). Moreover, siRNA and dominant negatives showed that formation of membrane ruffles by EspT is dependent on the Rac1 effector Wave2 (15).

WxxxE structure and function

The publication of the crystal structure of SifA in complex with the PH domain of its effector SKIP (SifA and kinesin–interacting protein) (51), represents a turning point in our understanding of the WxxxE effectors. SifA and SifB, which contrary to the other WxxxE effectors do not appear to affect actin dynamics, are particular in that they consist of two domains (51). Ohlson *et al.* have shown that while the N-terminal domain of SifA binds SKIP, the C-terminal domain, harbouring the WxxxE motif, contains two three helix bundles that form a V shape structure (51). This structure is surprisingly highly similar to that of SopE (14). The crystal structure of Cdc42 in complex with the biologically active catalytic fragment of SopE (residues 78-240) highlighted the mechanism by which SopE mediates guanine nucleotide exchange (32, 14) and as a result formation of membrane ruffles (Fig. 2). Although SopE does not share sequence or structural similarity with known eukaryotic GEFs, it locks the Switch I and II regions of Cdc42 in the same conformation as that observed in the equivalent regions of Rac1 or Cdc42 bound to the eukaryotic GEFs Tiam or Dbs, respectively.

Downloaded from iai.asm.org at IMPERIAL COLLEGE LONDON on February 25, 2010

IAI Accepts published online ahead of print

SopE is composed of six α-helices forming two three-helix bundles arranged in a V-shaped fashion. Connecting the two arms of the V is a small two-stranded β-sheet followed by a peptide segment harbouring a GAGA motif. Binding of SopE induces conformational changes in the Switch regions of Cdc42, which are mostly due to insertion of the catalytic GAGA motif between Switch I and Switch II. This leads to exertion of a push and pull type movement, which induces the release of the guanine nucleotide. Consistently, replacement of the first glycine of the GAGA motif by alanine abolishes SopE activity *in vitro* (14). The two GEF homologues of SopE, SopE2 (*Salmonella*) and BopE2 (*Burkholderia pseudomallei*) share with SopE a similar catalytic loop sequence and structure, suggesting a common nucleotide exchange mechanism (5, 65, 66, 70). Interestingly, several of the Cdc42-interacting residues of SopE are conserved in SifA. Moreover, although not similar in sequence, the chemical properties of the residues within the putative catalytic loop of SifA are comparable to those found in SopE (51). Nonetheless, despite the similarities with SopE and the ability to bind RhoA no GEF activity has yet demonstrated for SifA (4, 51).

Two recent independent reports have shown that several WxxxE effectors are RhoGTPase GEFs (4, 36). First, Huang *et al.* demonstrated that Map specifically binds nucleotide free Cdc42 and is able to induce release of GDP and incorporation of GTP (36). Moreover, the crystal structure of Map in complex with Cdc42 showed a similar structure to that of SopE and SifA, which is composed of seven α-helices arranged into one three-helix bundle and one four-helix bundle forming a V shaped structure; a putative catalytic loop connects the two V shaped arms. Furthermore, comparing the complexes of Cdc42 with Map, SopE, and the human GEF ITSN1 revealed that despite lacking sequence homology these three GEFs induce similar conformational changes in Cdc42, suggesting a common mechanism of nucleotide exchange. Importantly, although the sequences of the catalytic loops are somewhat different between SopE and Map, it was shown that an alanine and a glutamine residues

Downloaded from iai.asm.org at IMPERIAL COLLEGE LONDON on February 25, 2010

IAI Accepts published online ahead of print

cement the interaction of Map with the Switch I region of Cdc42 by making a hydrophobic contact and a hydrogen bond, respectively (36). Concordantly, deletion of the catalytic loop or substitution of either of these two residues inhibited the GEF activity of Map *in vitro* and compromised host signalling functions of Map during infection (36). Furthermore, GEF activity assays using recombinant IpgB1 and IpgB2 have shown that the former triggers nucleotide exchange in Rac1 and to a lower extent in Cdc42 (but not in RhoA) while the latter induces strong activation of RhoA and weak activation of Cdc42 and Rac1 (36). This Rho GTPase specificity of the WxxxE effectors appears to be governed by a complementary paring between residues at the α4-α6 "selective epitope" of the effectors and the β2-3 intersiwtch strand of the GTPases.

In a parallel study, EspM2 has been shown to bind tightly and irreversibly to RhoA *in vitro* and to specifically facilitate loading of GTP into purified RhoA (4). Moreover, modelling the structure of EspM2 aided by NMR, showed that it also adopts a SopE-like conformation (4). As it was shown for Map, mutagenesis of the equivalent glutamine within the catalytic loop impaired the ability of EspM2 to induce loading of GTP into RhoA and formation of stress fibers during ectopic expression (4).

Alto *et al.* have shown that substituting the tryptophan or glutamic acid residues within the WxxxE motif with alanine was detrimental for function (1). As conservative substitutions (replacing the tryptophan and glutamic acid residues with tyrosine and aspartic acid respectively) in EspM2 did not result in any significant loss of function (3), the conserved W and E residues were hypothesized to have mainly a structural role. Indeed, the 3D structures of SifA and Map and the EspM2 model have shown that the W and E residues are positioned around the junction of the two three-helix bundles, maintaining the conformation of the putative catalytic loop through hydrophobic contacts with surrounding residues (36, 51). Consistently, an EspM2 W70A was highly unstable (4). Interestingly, although sharing

Downloaded from iai.asm.org at IMPERIAL COLLEGE LONDON on February 25, 2010

IAI Accepts published online ahead of print

similar 3D structures with the WxxxE effectors, SopE has neither a W nor an E equivalent (Fig. 3). Nonetheless, taken together these results show that the WxxxE effectors belong to a large family of bacterial Rho GTPase GEFs, which also includes SopE, SopE2 and BopE2.

Regulation of the WxxxE effector activities

As it is now apparent that the WxxxE effectors, as is SopE, are Rho GTPase GEFs, there is a need to discuss this activity in the context of previously published data. For example Alto *et al.* (1) have shown that IpgB2 interacts with the RhoA effectors ROCK and mDia. It is possible that by binding simultaneously the Rho GTPase and its effectors IpgB2 amplify the transmitted signal, as was shown for eukaryotic GEFs (37). This might suggest a mechanism of nucleotide exchange by the WxxxE effectors involving formation of a tripartite complex consisting of GEF-Rho GTPase-effector as was suggested for EspM2 (4). Handa *et al.* have shown that IpgB1 forms a complex with ELMO-Dock180, which is essential for activation of Rac1 *in vivo* (30). Furthermore, Map contains a carboxy terminal PSD-95/Disk-large/ZO-1 (PDZ)-binding motif (DTRL), which mediates interaction between Map and PDZ1 of the scaffold protein sodium/hydrogen exchanger regulatory factor-1 (NHERF1) (1, 63). Alto *et al.* have shown that depleting cells of NHERF1 abolished Map-induced filopodia formation (1) while Simpson *et al.* (63) have shown that cells infected with EPEC expressing $Map_{\Delta TRL}$ exhibited no filopodia at 30 min post infection. Recently, Berger *et al.* have shown that maintenance of filopodia on the cell surface is dependent on the Map PDZ-binding motif, ezrin and the RhoA/ROCK pathway (7). These results suggest that the intrinsic GEF activity of these effectors is regulated by formation of large signalling complexes, as was also described for few eukaryotic GEFs, which were linked to activation of Rho GTPases in distinct cellular localizations and pathways (6, 60, 71).

Downloaded from iai.asm.org at IMPERIAL COLLEGE LONDON on February 25, 2010

IAI Accepts published online ahead of print

Role of SopE and the WxxxE effector GEFs in pathogenesis

SopE and the WxxxE effectors are central to the EPEC, EHEC, *Shigella* and *Salmonella* infection as they control cell invasion, intracellular survival and modulation of the host immune responses (Summarized in Fig. 4). Most of these activities are dependent on the GEF activity of these effectors.

SopE and the WxxxE effectors - invasion and intracellular survival

The virulence strategy used by *Shigella* and *Salmonella* involves invasion of enterocytes and macrophages. To invade non-phagocytyic cells *Shigella* and *Salmonella* use their T3SS to deliver effectors, which subvert actin dynamics leading to formation of membrane ruffles and macropinocytic pockets. *Shigella* invasion is dependent on T3SS effectors IpgB1, IpaC, IpaA, VirA and IpgD (49, 68, 69, 73), while *Salmonella* invasion requires several SPI-1 effectors including SopE, SopE2 and SopB (5, 32, 50). Cell invasion by *B. pseudomallei* is mediated by BopE (66).

In addition to playing a role in invasion, SopE has been suggested to affect intracellular bacterial survival by promoting fusion between the *Salmonella* containing vacuole (SCV) and early endosomes via recruitment and activation of the GTPase Rab5 (45). The SPI-2 effector SifA plays an important role in intracellular survival and virulence (8); while little is currently know of the function of SifB (9, 24). SifA contains a carboxyl-terminal CAAX motif, commonly found in the small GTPases, which when prenylated, facilitate membrane localization and activity (9, 53). SifA is involved in formation of the *Salmonella*-induced filaments (Sifs), which play a role in maintaining the integrity of the SCV (8, 58, 64). To achieve this SifA controls membrane dynamics and finely coordinates the equilibrium between the molecular motors kinesin and dynein. Indeed, by binding the host protein SKIP SifA inhibits recruitment of kinesin to the SCV (10), while by interacting with activated Rab7

Downloaded from iai.asm.org at IMPERIAL COLLEGE LONDON on February 25, 2010

IAI Accepts published online ahead of print

it inhibits recruitment of dynein (33). The role played by the WxxxE domain of SifA in these activities is not currently known.

In contrast with the other bacteria encoding SopE or the WxxxE effectors, the attaching and effacing pathogens (A/E) EPEC, EHEC and *C. rodentium* were considered to be exclusively extracellular, although sporadic reports have shown that atypical EPEC strains can invade non-phagocytic cells (21, 34). This invasive ability has been linked to the adherence pattern and tight association of EPEC with the host cell membrane, which was hypothesized to produce a passive push effect leading to internalization. Recently EspT has been shown to play an analogous role during EPEC and *C. rodentium* infections to that of IpgB1, SopE, SopE2 and BopE by promoting invasion into non-phagocytic cells via the triggered mechanism. EPEC and *C. rodentium* invasion requires Rac1 and Wave2 and to a lesser extent Cdc42 (15). Invaded EPEC resides in an *E. coli* containing vacuole (ECV) and induces formation of intracellular actin comets which appear to promote intracellular replication/survival (15). Screening for the presence of *espT* among clinical EPEC and EHEC strains has shown that it is a rare effector present only in 1.8 % of the EPEC strains and missing from all the O157 and non-O157 EHEC isolates (2). EspT defines a new rare category of invasive EPEC (15).

SopE and the WxxxE effectors - modulation of host responses

S. Typhimurium is able to modulate innate immune responses in cultured epithelial cell models independently of the classical TLRs (Toll-like) or NLRs (NOD-like) receptors but via mechanisms involving SopE, SopE2, and SopB (13). By stimulating the Rho GTPases these effectors activate the MAP kinase and NF-kB signalling pathways (13). Moreover, in a Cdc42 and Rac1 dependent manner, SopE stimulates Caspase-1 activation *in vitro* which is needed for induction of mucosal inflammation *in vivo* (46). As similarly to SopE the WxxxE effectors are Rho GTPase GEFs they might also modulate innate immune response. Indeed,

Downloaded from iai.asm.org at IMPERIAL COLLEGE LONDON on February 25, 2010

IAI Accepts published online ahead of print

activation of Rac1 by IpgB1-ELMO-Dock180 complex increases the cellular level of phosphorylated JNK, a MAP kinase involved in host responses (30). Moreover, a recent study by Fukazawa *et al.* (25) suggested that IpgB2, and to a minor extent IpgB1, activate NF-kB. IpgB2 was shown to activate NF-kB via a unique pathway involving GEF-H1, RhoA and NOD1.

SopE and the WxxxE effectors – subversion of intestinal barrier functions and diarrhea

Shigella, *Salmonella*, EPEC and EHEC diarrheal pathogens. Although other T3SS effectors are involved in disruption of the intestinal barrier functions and alteration of tight junctions (TJ), SopE and the WxxxE family members play an important role in this process.

SopE and SopE2 disrupt TJ structure and function (11). In contrast to wild type *S.* Typhimurium, the double *sopE/sopE2* mutant did not increase the permeability of polarized epithelial cell monolayers and was unable to cause redistribution of ZO-1 and occludin, or to alter cell polarity. As these phenotypes are dependent on host protein prenylation (geranylgeranylation) it was suggested that SopE and SopE2 utilize their ability to stimulate Rho family GTPases to disrupt TJ (11).

Recently, EspM2 has been shown to play a role in the disruption of the architecture of the polarized epithelial monolayer (62). Translocation or ectopic expression of EspM2 affected localization of ZO-1 that migrated towards the basal side of the polarized epithelial monolayer. This in turn led to cell rounding and extrusion form the monolayer. However the TJ alterations induced by EspM2 did not interfere with their functionality, in fact increased TER values were observed upon EspM2 expression suggesting that this effector might play a role in maintaining TJ during infection (62).

Map has been shown to play a role in reducing transepithelial electrical resistance (TER) in polarized Caco-2 cells (17, 43), although this was not reproduced in a subsequent study (63).

Downloaded from iai.asm.org at IMPERIAL COLLEGE LONDON on February 25, 2010

IAI Accepts published online ahead of print

Furthermore, in 2006 Dean *et al.* reported a role for Map, together with the T3SS effectors EspF and Tir and intimin in the effacement of absorptive microvilli and inactivation of the sodium-D-glucose cotransporter (SGLT-1), EPEC phenotypes which are directly correlated with watery diarrhea (18).

In vivo functions of SopE and the WxxxE effectors

Despite major advances in our understanding of SopE and the WxxxE effectors *in vitro*, a complete picture of the function of these effectors in pathogenesis is yet to be obtained. However, several *in vivo* studies provided some information about the role played by these effectors during infection.

The most dramatic *in vivo* phenotype associated with a WxxxE family member was observed with a *sifA* mutant. Consistent with the fact that SifA is required for *Salmonella* replication in macrophages *in vitro*, a *Salmonella sifA* mutant was severely attenuated during single or mixed mouse infections (8, 12, 24, 57). In contrast, a *sifB* mutant had little effect on virulence (24, 57). Using murine models of intestinal inflammation it was shown that SopE, and to a lesser extent SopE2, contribute to colitis (31) and virulence (40); SopE2 also induces diarrhoea in calves (74). It is worth noting that while SopE is absent from most of the *S.* Typhimurium isolates, SopE2 is conserved in all pathogenic strains (5, 65). Similarly to SopE, BopE has also been shown to play a role in *B. speudomallei* virulence as *bopE* mutants were attenuated when tested in a mouse model (67).

The role of IpgB2 and IpgB1 in *Shigella* virulence was investigated using both the Sereny test (61) and the murine pulmonary model (44). An *ipgB1/ipgB2* double mutant was highly attenuated as it did not induce any keratoconjunctivitis and was associated with reduced mortality (28). However, no particular phenotype was associated with a single *ipgB2* mutant (28), and the ability of *Shigella* to induce keratoconjunctivitis using the Sereny test was

Downloaded from iai.asm.org at IMPERIAL COLLEGE LONDON on February 25, 2010

IAI Accepts published online ahead of print

strongly enhanced in an *ipgB1* mutant (28). The precise role of IpgB1 and IpgB2 in pathogenesis *in vivo* needs to be clarified.

The role played in pathogenesis by Map, and more recently by EspM2 and EspT, has been investigated using the mouse-specific pathogen *C. rodentium*, the etiological agent of transmissible colonic hyperplasia, commonly used as a model for human EPEC and EHEC infections (reviewed in (47)). Single infection studies reported a subtle role for Map in colonization of the mouse colon (19, 48), while a mixed infection of wild type and *map* mutant revealed that the latter is extensively out competed (48). In addition, intestinal mitochondrial structure disruption and impaired mitochondrial cellular metabolism observed following *C. rodentium* infection were shown to be Map-dependent (43). Map was reported to have a role in TER disruption *in vivo* (43), although it had no role in maintaining colon water content at day 7 post infection (27). However, an independent study which compared stools water content in mice colonized at similar levels by wild type *C. rodentium* and a *map* mutant showed higher water content in the former group over a 12 days infection course, suggesting a possible role of Map in diarrhoea (63). This phenotype is consistent with binding of Map to NHERFs (63), which regulate ion channels activities. Recently, mouse infections have shown that while a *C. rodentium espT* mutant did not exhibit a significant difference in terms of bacterial shedding compared to wild type *C. rodentium*, an *espM2* mutant was shed at significantly lower levels, and caused less mortality in the highly susceptible CH3/HeJ mouse strain (20).

Conclusions and perspectives

SopE and the WxxxE effectors constitute an example of convergent evolution in bacterial virulence. Although exhibiting little sequence homology the WxxxE effectors and SopE share similar structure and function. Their mechanism of nucleotide exchanges appear to be similar to that employed by eukaryotic GEFS. While WxxxE effectors can trigger nucleotide

Downloaded from iai.asm.org at IMPERIAL COLLEGE LONDON on February 25, 2010

exchange *in vitro*, once translocated it appears that they function in the context of large signalling complexes, which are likely to regulate their activity. Importantly, while sharing 3D structure with the other family members and capable of binding RhoA (4, 51), no GEF activity was thus far associated with SifA. Extensive research over many years has shown that SopE and the WxxxE effectors are involved in divers aspects of infection, including cell invasion, intracellular survival and replication, modulation of host responses and subversion of the intestinal barrier function (Fig. 4). Contrasting the rapid characterization of the *in vitro* phenotypes of SopE and the WxxxE effectors, our understanding of their role in virulence is lagging. Translating the fascinating cell biology surrounding these effectors to pathogenesis is the challenge of future studies.

IAI Accepts published online ahead of print

Downloaded from iai.asm.org at IMPERIAL COLLEGE LONDON on February 25, 2010

IAI Accepts published online ahead of print

Acknowledgements

This work was supported by grants from the MRC (A.A and G.F.) and the Wellcome Trust (R.B., B.R., J.G., V.F.C., C.B and G.F.).

Downloaded from iai.asm.org at IMPERIAL COLLEGE LONDON on February 25, 2010

IAI Accepts published online ahead of print

References

1. **Alto, N. M., F. Shao, C. S. Lazar, R. L. Brost, G. Chua, S. Mattoo, S. A. McMahon, P. Ghosh, T. R. Hughes, C. Boone, and J. E. Dixon.** 2006. Identification of a bacterial type III effector family with G protein mimicry functions. Cell **124:**133-145.

2. **Arbeloa, A., M. Blanco, F. C. Moreira, R. Bulgin, C. Lopez, G. Dahbi, J. E. Blanco, A. Mora, M. P. Alonso, R. C. Mamani, T. A. Gomes, J. Blanco, and G. Frankel.** 2009. Distribution of espM and espT among enteropathogenic and enterohaemorrhagic *Escherichia coli*. J. Med. Microbiol. **58:**988-895.

3. **Arbeloa, A., R. R. Bulgin, G. MacKenzie, R. K. Shaw, M. J. Pallen, V. F. Crepin, C. N. Berger, and G. Frankel.** 2008. Subversion of actin dynamics by EspM effectors of attaching and effacing bacterial pathogens. Cell. Microbiol. **10:**1429-1441.

4. **Arbeloa, A., J. Garnett, J. Lillington, R. R. Bulgin, C. Berger, S. M. Lea, S. Matthews, and G. Frankel.** 2010. EspM2 is a RhoA guanine nucleotide exchange factor. Cell. Microbiol. DOI: 10.1111/j.1462-5822.2009.01423.x

5. **Bakshi, C. S., V. P. Singh, M. W. Wood, P. W. Jones, T. S. Wallis, and E. E. Galyov.** 2000. Identification of SopE2, a *Salmonella* secreted protein which is highly homologous to SopE and involved in bacterial invasion of epithelial cells. J. Bacteriol. **182:**2341-2344.

6. **Bellanger, J. M., C. Astier, C. Sardet, Y. Ohta, T. P. Stossel, and A. Debant.** 2000. The Rac1- and RhoG-specific GEF domain of Trio targets filamin to remodel cytoskeletal actin. Nat. Cell Biol. **2:**888-892.

Downloaded from iai.asm.org at IMPERIAL COLLEGE LONDON on February 25, 2010

IAI Accepts published online ahead of print

7. **Berger, C. N., V. F. Crepin, M. A. Jepson, A. Arbeloa, and G. Frankel.** 2009. The mechanisms used by enteropathogenic *Escherichia coli* to control filopodia dynamics. Cell. Microbiol. **11:**309-322.

8. **Beuzon, C. R., S. Meresse, K. E. Unsworth, J. Ruiz-Albert, S. Garvis, S. R. Waterman, T. A. Ryder, E. Boucrot, and D. W. Holden.** 2000. *Salmonella* maintains the integrity of its intracellular vacuole through the action of SifA. EMBO J. **19:**3235-3249.

9. **Boucrot, E., C. R. Beuzon, D. W. Holden, J. P. Gorvel, and S. Meresse.** 2003. *Salmonella typhimurium* SifA effector protein requires its membrane-anchoring C-terminal hexapeptide for its biological function. J. Biol. Chem. **278:**14196-14202.

10. **Boucrot, E., T. Henry, J. P. Borg, J. P. Gorvel, and S. Meresse.** 2005. The intracellular fate of *Salmonella* depends on the recruitment of kinesin. Science **308:**1174-1188.

11. **Boyle, E. C., N. F. Brown, and B. B. Finlay.** 2006. *Salmonella enterica* serovar Typhimurium effectors SopB, SopE, SopE2 and SipA disrupt tight junction structure and function. Cell. Microbiol. **8:**1946-1957.

12. **Brumell, J. H., C. M. Rosenberger, G. T. Gotto, S. L. Marcus, and B. B. Finlay.** 2001. SifA permits survival and replication of *Salmonella typhimurium* in murine macrophages. Cell. Microbiol. **3:**75-84.

13. **Bruno, V. M., S. Hannemann, M. Lara-Tejero, R. A. Flavell, S. H. Kleinstein, and J. E. Galan.** 2009. *Salmonella* Typhimurium type III secretion effectors stimulate innate immune responses in cultured epithelial cells. PLoS Pathog. **5:**e1000538.

Downloaded from iai.asm.org at IMPERIAL COLLEGE LONDON on February 25, 2010

IAI Accepts published online ahead of print

14. **Buchwald, G., A. Friebel, J. E. Galan, W. D. Hardt, A. Wittinghofer, and K. Scheffzek.** 2002. Structural basis for the reversible activation of a Rho protein by the bacterial toxin SopE. EMBO J. **21:**3286-3295.

15. **Bulgin, R., A. Arbeloa, D. Goulding, G. Dougan, F. V. Crepin, B. Raymond, and G. Frankel. 2009.** The T3SS effector EspT defines a new category of invasive enteropathogenic *E. coli* (EPEC) which form intracellular actin pedestals. PLoS Pathog. **5**:e1000683.

16. **Bulgin, R. R., A. Arbeloa, J. C. Chung, and G. Frankel.** 2009. EspT triggers formation of lamellipodia and membrane ruffles through activation of Rac-1 and Cdc42. Cell. Microbiol. **11:**217-229.

17. **Dean, P., and B. Kenny.** 2004. Intestinal barrier dysfunction by enteropathogenic *Escherichia coli* is mediated by two effector molecules and a bacterial surface protein. Mol. Microbiol. **54:**665-675.

18. **Dean, P., M. Maresca, S. Schuller, A. D. Phillips, and B. Kenny.** 2006. Potent diarrheagenic mechanism mediated by the cooperative action of three enteropathogenic *Escherichia coli*-injected effector proteins. Proc. Natl. Acad. Sci. U. S. A. **103:**1876-1881.

19. **Deng, W., J. L. Puente, S. Gruenheid, Y. Li, B. A. Vallance, A. Vazquez, J. Barba, J. A. Ibarra, P. O'Donnell, P. Metalnikov, K. Ashman, S. Lee, D. Goode, T. Pawson, and B. B. Finlay.** 2004. Dissecting virulence: systematic and functional analyses of a pathogenicity island. Proc. Natl. Acad. Sci. U. S. A. **101:**3597-3602.

20. **Deng, W., C. L. de Hoog, H. B.Yu, Y. Li, M., A. Croxen, N. A. Thomas, J. L. Puente, L. J. Foster, and B. B. Finlay.** 2010**.** A comprehensive proteomic analysis

Downloaded from iai.asm.org at IMPERIAL COLLEGE LONDON on February 25, 2010

IAI Accepts published online ahead of print

of the type III secretome of *Citrobater rodentium*. J. Biol. Chem. Published on December 24, 2009 as Manuscript M109.086603

21. **Donnenberg, M. S., and J. B. Kaper.** 1992. Enteropathogenic *Escherichia coli*. Infect. Immun. **60:**3953-3961.

22. **Dvorsky, R., and M. R. Ahmadian.** 2004. Always look on the bright site of Rho: structural implications for a conserved intermolecular interface. EMBO Rep **5:**1130-6.

23. **Finlay, B. B.** 2005. Bacterial virulence strategies that utilize Rho GTPases. Curr. Top. Microbiol. Immunol. **291:**1-10.

24. **Freeman, J. A., M. E. Ohl, and S. I. Miller.** 2003. The *Salmonella enterica* serovar typhimurium translocated effectors SseJ and SifB are targeted to the Salmonella-containing vacuole. Infect. Immun. **71:**418-427.

25. **Fukazawa, A., C. Alonso, K. Kurachi, S. Gupta, C. F. Lesser, B. A. McCormick, and H. C. Reinecker.** 2008. GEF-H1 mediated control of NOD1 dependent NF-kappaB activation by *Shigella* effectors. PLoS Pathog. **4:**e1000228.

26. **Galan, J. E., and H. Wolf-Watz.** 2006. Protein delivery into eukaryotic cells by type III secretion machines. Nature **444:**567-573.

27. **Guttman, J. A., Y. Li, M. E. Wickham, W. Deng, A. W. Vogl, and B. B. Finlay.** 2006. Attaching and effacing pathogen-induced tight junction disruption *in vivo*. Cell. Microbiol. **8:**634-645.

28. **Hachani, A., L. Biskri, G. Rossi, A. Marty, R. Menard, P. Sansonetti, C. Parsot, G. T. Van Nhieu, M. L. Bernardini, and A. Allaoui.** 2008. IpgB1 and IpgB2, two homologous effectors secreted via the Mxi-Spa type III secretion apparatus, cooperate

Downloaded from iai.asm.org at IMPERIAL COLLEGE LONDON on February 25, 2010

IAI Accepts published online ahead of print

to mediate polarized cell invasion and inflammatory potential of *Shigella flexenri*. Microbes Infect. **10:**260-268.

29. **Hall, A.** 1998. Rho GTPases and the actin cytoskeleton. Science **279:**509-514.

30. **Handa, Y., M. Suzuki, K. Ohya, H. Iwai, N. Ishijima, A. J. Koleske, Y. Fukui, and C. Sasakawa.** 2007. *Shigella* IpgB1 promotes bacterial entry through the ELMO-Dock180 machinery. Nat. Cell Biol. **9:**121-128.

31. **Hapfelmeier, S., and W. D. Hardt.** 2005. A mouse model for *S. typhimurium*-induced enterocolitis. Trends Microbiol. **13:**497-503.

32. **Hardt, W. D., L. M. Chen, K. E. Schuebel, X. R. Bustelo, and J. E. Galan.** 1998. *S. typhimurium* encodes an activator of Rho GTPases that induces membrane ruffling and nuclear responses in host cells. Cell **93:**815-826.

33. **Harrison, R. E., J. H. Brumell, A. Khandani, C. Bucci, C. C. Scott, X. Jiang, B. B. Finlay, and S. Grinstein.** 2004. *Salmonella* impairs RILP recruitment to Rab7 during maturation of invasion vacuoles. Mol. Biol. Cell **15:**3146-3154.

34. **Hernandes, R. T., R. M. Silva, S. M. Carneiro, F. A. Salvador, M. C. Fernandes, A. C. Padovan, D. Yamamoto, R. A. Mortara, W. P. Elias, M. R. da Silva Briones, and T. A. Gomes.** 2008. The localized adherence pattern of an atypical enteropathogenic *Escherichia coli* is mediated by intimin omicron and unexpectedly promotes HeLa cell invasion. Cell. Microbiol. **10:**415-425.

35. **Hoffman, G. R., N. Nassar, and R. A. Cerione.** 2000. Structure of the Rho family GTP-binding protein Cdc42 in complex with the multifunctional regulator RhoGDI. Cell **100:**345-356.

Downloaded from iai.asm.org at IMPERIAL COLLEGE LONDON on February 25, 2010

IAI Accepts published online ahead of print

36. **Huang, Z., S. E. Sutton, A. J. Wallenfang, R. C. Orchard, X. Wu, Y. Feng, J. Chai, and N. M. Alto.** 2009. Structural insights into host GTPase isoform selection by a family of bacterial GEF mimics. Nat. Struct. Mol. Biol. **16:**853-860.

37. **Hussain, N. K., S. Jenna, M. Glogauer, C. C. Quinn, S. Wasiak, M. Guipponi, S. E. Antonarakis, B. K. Kay, T. P. Stossel, N. Lamarche-Vane, and P. S. McPherson.** 2001. Endocytic protein intersectin-l regulates actin assembly via Cdc42 and N-WASP. Nat. Cell. Biol. **3:**927-932.

38. **Jaffe, A. B., and A. Hall.** 2005. Rho GTPases: biochemistry and biology. Annu. Rev. Cell De.v Biol. **21:**247-269.

39. **Joseph, R. E., and F. A. Norris.** 2005. Substrate specificity and recognition is conferred by the pleckstrin homology domain of the Dbl family guanine nucleotide exchange factor P-Rex2. J. Biol. Chem. **280:**27508-27512.

40. **Karasova, D., A. Sebkova, V. Vrbas, H. Havlickova, F. Sisak, and I. Rychlik.** 2009. Comparative analysis of *Salmonella enterica* serovar Enteritidis mutants with a vaccine potential. Vaccine **27:**5265-5670.

41. **Kenny, B., S. Ellis, A. D. Leard, J. Warawa, H. Mellor, and M. A. Jepson.** 2002. Co-ordinate regulation of distinct host cell signalling pathways by multifunctional enteropathogenic *Escherichia coli* effector molecules. Mol. Microbiol. **44:**1095-1107.

42. **Kubori, T., and J. E. Galan.** 2003. Temporal regulation of *salmonella* virulence effector function by proteasome-dependent protein degradation. Cell **115:**333-342.

43. **Ma, C., M. E. Wickham, J. A. Guttman, W. Deng, J. Walker, K. L. Madsen, K. Jacobson, W. A. Vogl, B. B. Finlay, and B. A. Vallance.** 2006. *Citrobacter rodentium* infection causes both mitochondrial dysfunction and intestinal epithelial

Downloaded from iai.asm.org at IMPERIAL COLLEGE LONDON on February 25, 2010

IAI Accepts published online ahead of print

barrier disruption in vivo: role of mitochondrial associated protein (Map). Cell. Microbiol. **8:**1669-1686.

44. **Mallett CP, V. L., Collins HH, Hale TL.** 1993. Evaluation of *Shigella* vaccine safety and efficacy in an intranasally challenged mouse model. Vaccine. **11:**190-196.

45. **Mukherjee, K., S. Parashuraman, M. Raje, and A. Mukhopadhyay.** 2001. SopE acts as an Rab5-specific nucleotide exchange factor and recruits non-prenylated Rab5 on *Salmonella*-containing phagosomes to promote fusion with early endosomes. J. Biol. Chem. **276:**23607-23615.

46. **Muller, A. J., C. Hoffmann, M. Galle, A. Van Den Broeke, M. Heikenwalder, L. Falter, B. Misselwitz, M. Kremer, R. Beyaert, and W. D. Hardt.** 2009. The *S.* Typhimurium effector SopE induces caspase-1 activation in stomal cells to inititate gut inflammation. Cell Host Microbe. **6:**125-136.

47. **Mundy, R., T. T. MacDonald, G. Dougan, G. Frankel, and S. Wiles.** 2005. *Citrobacter rodentium* of mice and man. Cell. Microbiol. **7:**1697-1706.

48. **Mundy, R., L. Petrovska, K. Smollett, N. Simpson, R. K. Wilson, J. Yu, X. Tu, I. Rosenshine, S. Clare, G. Dougan, and G. Frankel.** 2004. Identification of a novel *Citrobacter rodentium* type III secreted protein, EspI, and roles of this and other secreted proteins in infection. Infect. Immun. **72:**2288-2302.

49. **Niebuhr, K., S. Giuriato, T. Pedron, D. J. Philpott, F. Gaits, J. Sable, M. P. Sheetz, C. Parsot, P. J. Sansonetti, and B. Payrastre.** 2002. Conversion of PtdIns(4,5)P(2) into PtdIns(5)P by the *S. flexneri* effector IpgD reorganizes host cell morphology. EMBO J. **21:**5069-5078.

Downloaded from iai.asm.org at IMPERIAL COLLEGE LONDON on February 25, 2010

IAI Accepts published online ahead of print

50. **Norris, F. A., M. P. Wilson, T. S. Wallis, E. E. Galyov, and P. W. Majerus.** 1998. SopB, a protein required for virulence of *Salmonella dublin*, is an inositol phosphate phosphatase. Proc. Natl. Acad. Sci. U. S. A. **95:**14057-14069.

51. **Ohlson, M. B., Z. Huang, N. M. Alto, M. P. Blanc, J. E. Dixon, J. Chai, and S. I. Miller.** 2008. Structure and function of *Salmonella* SifA indicate that its interactions with SKIP, SseJ, and RhoA family GTPases induce endosomal tubulation. Cell Host Microbe **4:**434-446.

52. **Ohya, K., Y. Handa, M. Ogawa, M. Suzuki, and C. Sasakawa.** 2005. IpgB1 is a novel *Shigella* effector protein involved in bacterial invasion of host cells. Its activity to promote membrane ruffling via Rac1 and Cdc42 activation. J. Biol. Chem. **280:**24022-24034.

53. **Reinicke, A. T., J. L. Hutchinson, A. I. Magee, P. Mastroeni, J. Trowsdale, and A. P. Kelly.** 2005. A *Salmonella typhimurium* effector protein SifA is modified by host cell prenylation and S-acylation machinery. J. Biol. Chem. **280:**14620-14627.

54. **Ridley, A. J.** 2006. Rho GTPases and actin dynamics in membrane protrusions and vesicle trafficking. Trends Cell Biol. **16:**522-529.

55. **Roberts, P. J., N. Mitin, P. J. Keller, E. J. Chenette, J. P. Madigan, R. O. Currin, A. D. Cox, O. Wilson, P. Kirschmeier, and C. J. Der.** 2008. Rho Family GTPase modification and dependence on CAAX motif-signaled posttranslational modification. J. Biol. Chem. **283:**25150-25163.

56. **Rudolph, M. G., C. Weise, S. Mirold, B. Hillenbrand, B. Bader, A. Wittinghofer, and W. D. Hardt.** 1999. Biochemical analysis of SopE from *Salmonella typhimurium*, a highly efficient guanosine nucleotide exchange factor for RhoGTPases. J. Biol. Chem. **274:**30501-30509.

Downloaded from iai.asm.org at IMPERIAL COLLEGE LONDON on February 25, 2010

IAI Accepts published online ahead of print

57. **Ruiz-Albert, J., X. J. Yu, C. R. Beuzon, A. N. Blakey, E. E. Galyov, and D. W. Holden.** 2002. Complementary activities of SseJ and SifA regulate dynamics of the *Salmonella typhimurium* vacuolar membrane. Mol. Microbiol. **44:**645-661.

58. **Salcedo, S. P., M. Noursadeghi, J. Cohen, and D. W. Holden.** 2001. Intracellular replication of *Salmonella typhimurium* strains in specific subsets of splenic macrophages in vivo. Cell. Microbiol. **3:**587-597.

59. **Scheffzek, K., I. Stephan, O. N. Jensen, D. Illenberger, and P. Gierschik.** 2000. The Rac-RhoGDI complex and the structural basis for the regulation of Rho proteins by RhoGDI. Nat Struct. Biol. **7:**122-126.

60. **Seipel, K., S. P. O'Brien, E. Iannotti, Q. G. Medley, and M. Streuli.** 2001. Tara, a novel F-actin binding protein, associates with the Trio guanine nucleotide exchange factor and regulates actin cytoskeletal organization. J. Cell Sci. **114:**389-399.

61. **Serény B, T. C., Rácz P.** 1971. Immunogenicity of living attenuated *shigellae*. Acta Microbiol. Acad Sci. Hung. **18:**239-245.

62. **Simovitch, M., H. Sason, S. Cohen, E. E. Zahavi, N. Melamed-Book, A. Weiss, B. Aroeti, and I. Rosenshine.** EspM inhibits pedestal formation by EHEC and EPEC and disrupts the architecture of a polarized epithelial monolayer. Cell. Microbiol. In press.

63. **Simpson, N., R. Shaw, V. F. Crepin, R. Mundy, A. J. FitzGerald, N. Cummings, A. Straatman-Iwanowska, I. Connerton, S. Knutton, and G. Frankel.** 2006. The enteropathogenic *Escherichia coli* type III secretion system effector Map binds EBP50/NHERF1: implication for cell signalling and diarrhoea. Mol. Microbiol. **60:**349-363.

Downloaded from iai.asm.org at IMPERIAL COLLEGE LONDON on February 25, 2010

IAI Accepts published online ahead of print

64. **Stein, M. A., K. Y. Leung, M. Zwick, F. Garcia-del Portillo, and B. B. Finlay.** 1996. Identification of a *Salmonella* virulence gene required for formation of filamentous structures containing lysosomal membrane glycoproteins within epithelial cells. Mol. Microbiol. **20:**151-164.

65. **Stender, S., A. Friebel, S. Linder, M. Rohde, S. Mirold, and W. D. Hardt.** 2000. Identification of SopE2 from *Salmonella typhimurium*, a conserved guanine nucleotide exchange factor for Cdc42 of the host cell. Mol. Microbiol. **36:**1206-1221.

66. **Stevens, M. P., A. Friebel, L. A. Taylor, M. W. Wood, P. J. Brown, W. D. Hardt, and E. E. Galyov.** 2003. A *Burkholderia pseudomallei* type III secreted protein, BopE, facilitates bacterial invasion of epithelial cells and exhibits guanine nucleotide exchange factor activity. J. Bacteriol. **185:**4992-4996.

67. **Stevens, M. P., A. Haque, T. Atkins, J. Hill, M. W. Wood, A. Easton, M. Nelson, C. Underwood-Fowler, R. W. Titball, G. J. Bancroft, and E. E. Galyov.** 2004. Attenuated virulence and protective efficacy of a *Burkholderia pseudomallei* a type III secretion mutant in murine models of melioidosis. Microbiology **150:**2669-2676.

68. **Tran Van Nhieu, G., A. Ben-Ze'ev, and P. J. Sansonetti.** 1997. Modulation of bacterial entry into epithelial cells by association between vinculin and the *Shigella* IpaA invasin. ENBO J. **16:**2717-2729.

69. **Tran Van Nhieu, G., E. Caron, A. Hall, and P. J. Sansonetti.** 1999. IpaC induces actin polymerization and filopodia formation during *Shigella* entry into epithelial cells. EMBO J. **18:**3249-3262.

70. **Upadhyay, A., H. L. Wu, C. Williams, T. Field, E. E. Galyov, J. M. van den Elsen, and S. Bagby.** 2008. The guanine-nucleotide-exchange factor BopE from *Burkholderia pseudomallei* adopts a compact version of the Salmonella SopE/SopE2

Downloaded from iai.asm.org at IMPERIAL COLLEGE LONDON on February 25, 2010

fold and undergoes a closed-to-open conformational change upon interaction with Cdc42. Biochem. J. **411:**485-493.

71. **Vanni, C., A. Parodi, P. Mancini, V. Visco, C. Ottaviano, M. R. Torrisi, and A. Eva.** 2004. Phosphorylation-independent membrane relocalization of ezrin following association with Dbl in vivo. Oncogene **23:**4098-4106.

72. **Vetter, I. R., and A. Wittinghofer.** 2001. The guanine nucleotide-binding switch in three dimensions. Science **294:**1299-1304.

73. **Yoshida, S., E. Katayama, A. Kuwae, H. Mimuro, T. Suzuki, and C. Sasakawa.** 2002. *Shigella* deliver an effector protein to trigger host microtubule destabilization, which promotes Rac1 activity and efficient bacterial internalization. EMBO J. **21:**2923-2935.

74. **Zhang, S., R. L. Santos, R. M. Tsolis, S. Stender, W. D. Hardt, A. J. Baumler, and L. G. Adams.** 2002. The *Salmonella enterica* serotype typhimurium effector proteins SipA, SopA, SopB, SopD, and SopE2 act in concert to induce diarrhea in calves. Infect. Immun. **70:**3843-3855.

IAI Accepts published online ahead of print

Downloaded from iai.asm.org at IMPERIAL COLLEGE LONDON on February 25, 2010

IAI Accepts published online ahead of print

Figures legends

Figure 1. SopE and the WxxxE effectors. Multiple sequence alignment with hierarchical clustering of IpgB1 and IpgB2 from *S. flexneri* 2a, EspM2 from EHEC O157:H7, EspT from *C. rodentium*, Map from EPEC E2348/69, the C-terminal, WxxxE-containing motif of SifA and SifB, and SopE and SopE2 from *S.* Typhimurium and BopE from *B. pseudomallei*. Similar and identical residues are highlighted in grey. The WxxxE motif and the catalytic loops are boxed.

Figure 2. SopE and WxxxE effectors subvert actin dynamics. Serum-starved Swiss 3T3 cells were mock transfected or transfected with the mammalian expression vector pRK5 encoding myc-tagged IpgB2, EspM2 (not shown), Map, IpgB1, EspT or the catalytic domain of SopE (residues 78-240) for 16 h. Ectopic expression of IpgB2 and EspM2 induced formation of stress fibers, Map induced filopodia formation, IpgB1 induced formation of membrane ruffle while EspT and SopE induce membrane ruffles and lamelipodia. Actin was stained with Oregon Green phalloidin, the myc tag was detected with monoclonal antibody.

Figure 3: Structure of SopE and the WxxxE effectors. A. Overlay of the crystal structure of Map (yellow; pdb:3gcg; (36)), the crystal structure of the WxxxE-containing domain of SifA (green; pdb:3cxb; (51)), the model of EspM2 (purple; (4)) and the crystal structure of the GEF domain of SopE (cyan; pdb:1gzs; (14)). Although these structures generally superimpose well, there are differences between the helical arrangements within the corresponding WxxxE region of SopE (red box). Moreover differences in the orientation of the catalytic loop between SopE and Map and SifA and EspM2 could be accounted to the fact that crystal structures of SopE and Map are solved in complex with Cdc42, while the SifA

Downloaded from iai.asm.org at IMPERIAL COLLEGE LONDON on February 25, 2010

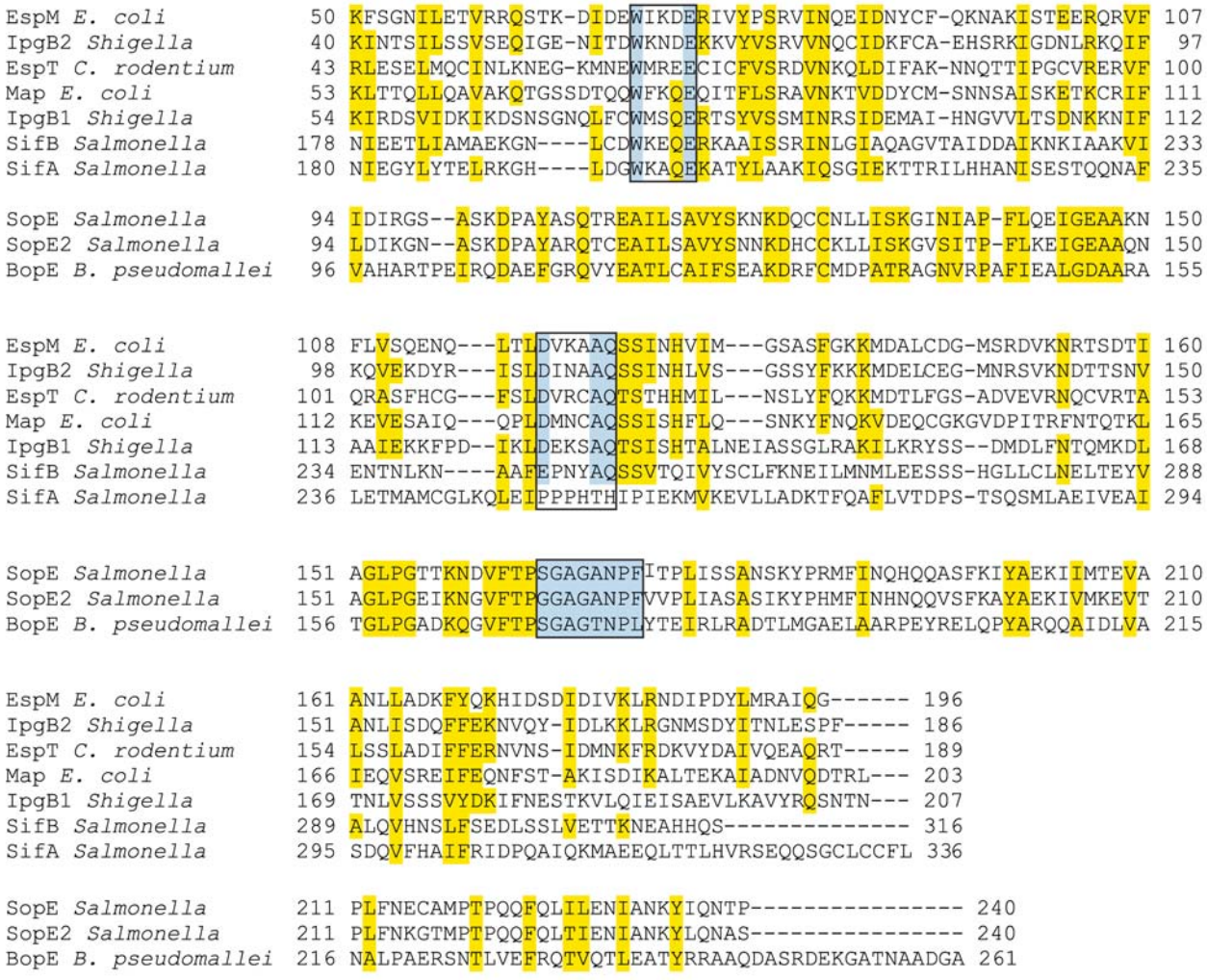
IAI Accepts published online ahead of print

structure is of Rho GTPase free effector. EspM2 was modelled on the SifA structure. B. Within the WxxxE motif of Map E78 makes 2 hydrogen bonds via the carboxyl oxygen to the backbone nitrogen of S130 (in helix 4), whilst the ring nitrogen of W74 makes a single hydrogen bond to the hydroxyl group of S130. The side chain of W74 is also buried away from the solvent in a hydrophobic pocket containing L58 and V62. The combination of these interactions orientates the catalytic loop (N-terminal to helix 4) correctly with respect to forming a complex with Cdc42. In SopE, Y106 and T110 are in equivalent positions to W74 and E78 in Map; however, they are not involved in inter-helical contacts.

Figure 4. SopE and the WxxxE bacterial effectors subvert host-cell pathways. Using the T3SS *Shigella* (A), EPEC/EHEC (B), and *Salmonella* (C) inject the effectors IpgB1/IpgB2, EspT/Map/EspM and SopE/SopE2/SifA/SifB, respectively. Except for SifA and SifB, these effectors activate a cascade of signal transduction pathways starting with activation of Rho GTPases (either Rac1, RhoA or Cdc42), which lead to actin polymerization. Membrane ruffles induced by IpgB1, EspT, SopE and SopE2 allow bacterial engulfment and subsequent internalization into a bacterial containing vacuole (BCV). Invasive EPEC and *Salmonella* remain in the BCV and induce the formation of intracellular actin comets, and *Salmonella*-induced filaments (Sifs), respectively, while *Shigella* escapes to the cytosol where it forms actin tails. In parallel to subversion of actin dynamics IpgB1, IpgB2, SopE and SopE2 induce inflammatory response; EspM, Map, SopE and SopE2 induce tight junction alteration and Map induces mitochondrial dysfunction. SopE and SifA, which is translocated across the SCV via the Spi2 T3SS, play a role in maintaining the SCV. The activity of SifB remains unknown.

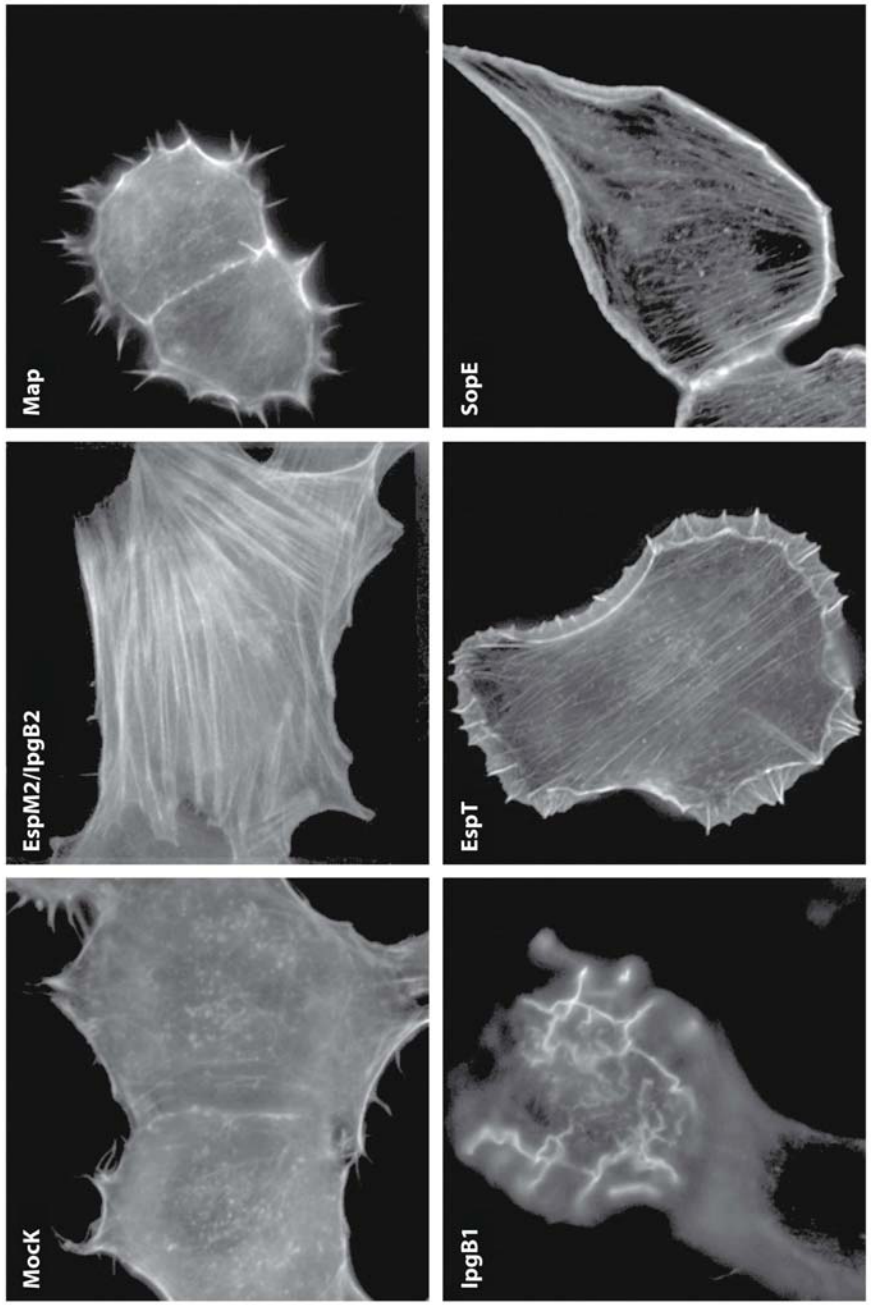
Downloaded from iai.asm.org at IMPERIAL COLLEGE LONDON on February 25, 2010

IAI Accepts published online ahead of print



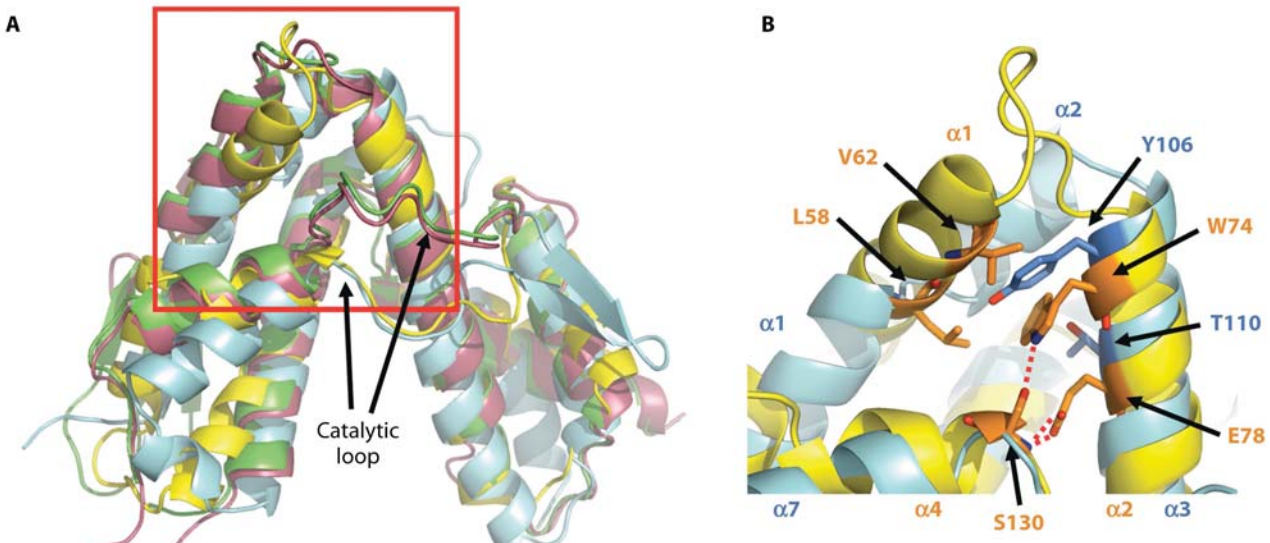
Downloaded from iai.asm.org at IMPERIAL COLLEGE LONDON on February 25, 2010

Downloaded from iai.asm.org at IMPERIAL COLLEGE LONDON on February 25, 2010



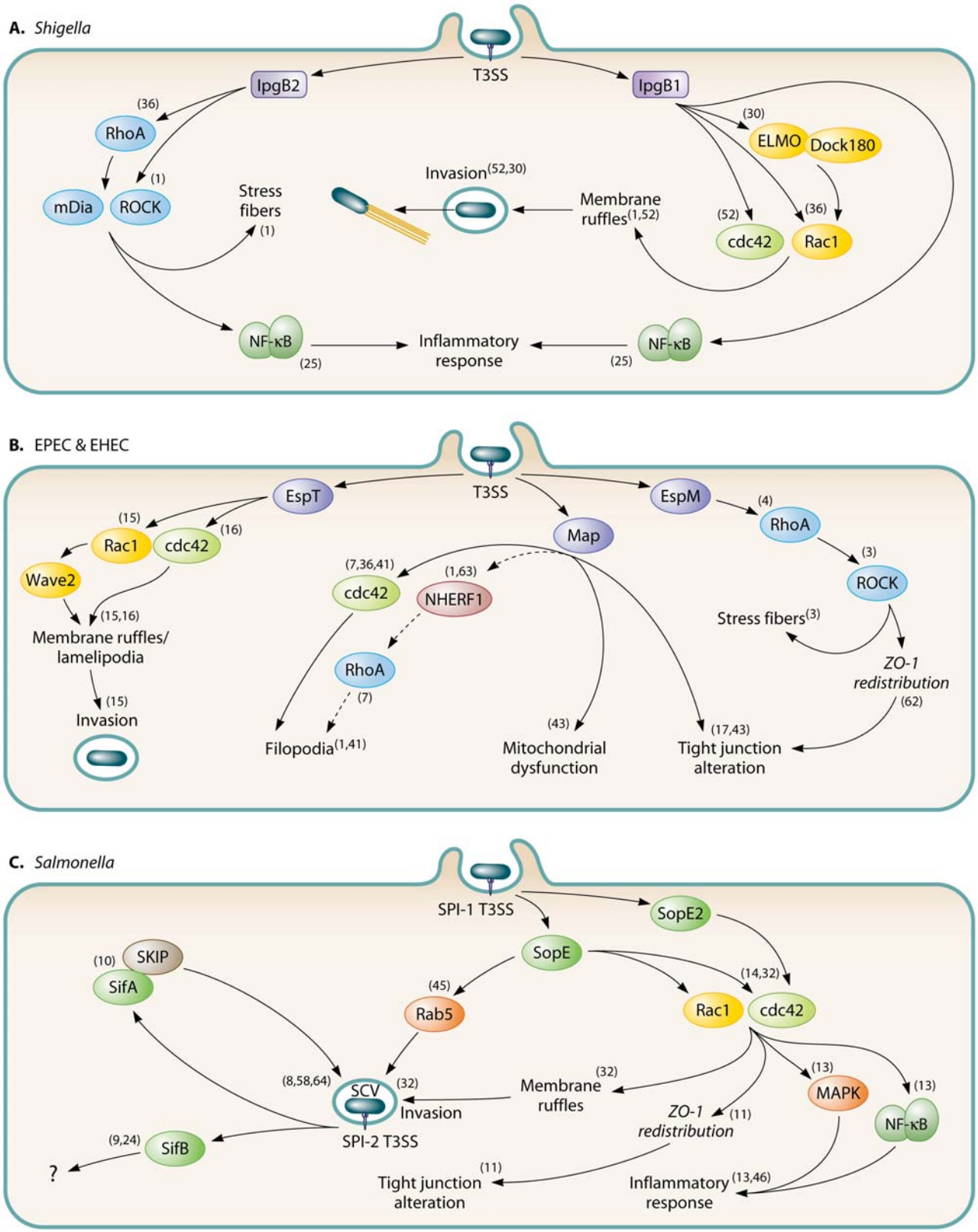
IAI Accepts published online ahead of print

IAI Accepts published online ahead of print



Downloaded from iai.asm.org at IMPERIAL COLLEGE LONDON on February 25, 2010

IAI Accepts published online ahead of print



Downloaded from iai.asm.org at IMPERIAL COLLEGE LONDON on February 25, 2010

JOURNAL OF BACTERIOLOGY, Jan. 2010, p. 525–538 Vol. 192, No. 2
0021-9193/10/$12.00 doi:10.1128/JB.01144-09
Copyright © 2010, American Society for Microbiology. All Rights Reserved.

The *Citrobacter rodentium* Genome Sequence Reveals Convergent Evolution with Human Pathogenic *Escherichia coli*▽†‡

Nicola K. Petty,[1] Richard Bulgin,[2] Valerie F. Crepin,[2] Ana M. Cerdeño-Tárraga,[1] Gunnar N. Schroeder,[2] Michael A. Quail,[1] Nicola Lennard,[1] Craig Corton,[1] Andrew Barron,[1] Louise Clark,[1] Ana L. Toribio,[1] Julian Parkhill,[1] Gordon Dougan,[1] Gad Frankel,[2] and Nicholas R. Thomson[1]*

Pathogen Genomics, The Wellcome Trust Sanger Institute, Wellcome Trust Genome Campus, Hinxton, Cambridge, CB10 1SA, United Kingdom,[1] and Centre for Molecular Microbiology and Infection, Division of Cell and Molecular Biology, Imperial College London, London SW7 2AZ, United Kingdom[2]

Received 27 August 2009/Accepted 28 October 2009

Citrobacter rodentium **(formally *Citrobacter freundii* biotype 4280) is a highly infectious pathogen that causes colitis and transmissible colonic hyperplasia in mice. In common with enteropathogenic and enterohemorrhagic *Escherichia coli* (EPEC and EHEC, respectively), *C. rodentium* exploits a type III secretion system (T3SS) to induce attaching and effacing (A/E) lesions that are essential for virulence. Here, we report the fully annotated genome sequence of the 5.3-Mb chromosome and four plasmids harbored by *C. rodentium* strain ICC168. The genome sequence revealed key information about the phylogeny of *C. rodentium* and identified 1,585 *C. rodentium*-specific (without orthologues in EPEC or EHEC) coding sequences, 10 prophage-like regions, and 17 genomic islands, including the locus for enterocyte effacement (LEE) region, which encodes a T3SS and effector proteins. Among the 29 T3SS effectors found in *C. rodentium* are all 22 of the core effectors of EPEC strain E2348/69. In addition, we identified a novel *C. rodentium* effector, named EspS. *C. rodentium* harbors two type VI secretion systems (T6SS) (CTS1 and CTS2), while EHEC contains only one T6SS (EHS). Our analysis suggests that *C. rodentium* and EPEC/EHEC have converged on a common host infection strategy through access to a common pool of mobile DNA and that *C. rodentium* has lost gene functions associated with a previous pathogenic niche.**

The mouse has been utilized extensively as a model for studies of infection and immunity (11, 25, 41, 44). Mice can be housed in relatively simple facilities and can be maintained under controlled pathogen- or germ-free conditions. Further, the availability of inbred or genetically manipulated mice greatly enhances the potential of any studies (35, 80). Although murine infection systems are used extensively, relatively few pathogens have been exploited that are naturally virulent for the species.

Spontaneous disease outbreaks in mouse colonies in the United States and Japan in the 1960s and 1970s were associated with infections by the Gram-negative pathogens *Escherichia coli* (Ex30, also known as murine pathogenic *E. coli* [MPEC]), *Citrobacter freundii* ANL, and *C. freundii* biotype 4280 (3, 9, 25, 43, 64). On the basis of DNA relatedness, these pathogenic strains were subsequently assigned to a separate species, *Citrobacter rodentium* (54, 84). *C. rodentium* is highly infectious, causing colitis and transmissible colonic hyperplasia (61). Following ingestion, *C. rodentium* colonizes the intestines of mice, residing predominantly in the cecum and colon (91), where in some inbred strains it can drive hyperplasia or overgrowth of the epithelium. *C. rodentium*-mediated colonic hyperplasia is highly infectious in poorly managed mouse facilities, spreading between mice via contaminated feces and environments (93). Some mouse strains are relatively resistant to clinical disease, but in such strains, *C. rodentium* lives in the intestine as a component of the microbiota; younger mice are generally more susceptible to infection (89).

C. rodentium is genetically related to *Escherichia coli* and is a member of the *Enterobacteriacae*. An extracellular pathogen, *C. rodentium* colonizes the lumen of the mouse gut mucosa by formation of so-called attaching/effacing (A/E) lesions on the apical surfaces of the enterocytes (82; reviewed in references 30 and 61). A/E lesions, which are characterized by effacement of the brush border microvilli and intimate bacterial attachment to pedestal-like structures, are also classically associated with the pathogenesis of enteropathogenic *E. coli* (EPEC), a leading cause of pediatric diarrhea, and enterohemorrhagic *E. coli* (EHEC), which causes diarrhea, hemorrhagic colitis, and hemolytic uremic syndrome (HUS) (reviewed in reference 45). In this respect, *C. rodentium*, EPEC, and EHEC share a common virulence strategy.

A/E lesion formation is dependent on the expression of intimin, a type III secretion system (T3SS) (reviewed in reference 31) and effector proteins encoded on a specific pathogenicity island (PI) known as the locus for enterocyte effacement (LEE) (57). The LEE of *C. rodentium*, and those of EPEC and EHEC, are horizontally acquired sections of DNA, and although not identical, they are highly related in terms of overall

* Corresponding author. Mailing address: Pathogen Genomics, The Wellcome Trust Sanger Institute, Wellcome Trust Genome Campus, Hinxton, Cambridge, CB10 1SA, United Kingdom. Phone: 44 (0)1223 494740. Fax: 44 (0)1223 494919. E-mail: nrt@sanger.ac.uk.

† Supplemental material for this article may be found at http://jb.asm.org/.

▽ Published ahead of print on 6 November 2009.

‡ The authors have paid a fee to allow immediate free access to this article.

TABLE 1. Bacterial strains, plasmids and primers used in this study

Strain, plasmid, or primer	Description	Reference
Strains		
ICC169	Spontaneous Nal^r derivative of ICC168	92
ICC304	Δ*espA*::AphT in ICC169	This study
E2348/69	Wild-type EPEC O127:H6	50
Plasmids		
pCX340	Expression vector for TEM fusion protein	14
pICC453	pCX340-EspS, expressing *C. rodentium* EspS fused to TEM	This study
pICC454	pCX340-EspH, expressing E2348/69 EspH fused to TEM	This study
pACYC184	Bacterial expression vector	New England Biolabs
pICC490	pACYC184 expressing *espA* from the *tet* promoter	This study
Primers		
NdeI-EspS-Fw	5′-AAACTCGAGCATATGTTTAGTATAAAAGGATACCTACC-3′	
EcoRI-EspS-Rv	5′-CCGGAATTCTCGTCAATATCTGTTGGTTGTGTCC-3′	
NdeI-EspH-Fw	5′-CCCGAGCATATGCGTTATATAGGGAGGTGTATG-3′	
EcoRI-EspH-Rv	5′-CGGAATTCCCAACTGTCACACCTGATAAAGAG −3′	
EspA-Fw	5′-TTATTAGGTGAGGATGATTGGG-3′	
BamHI-EspA-Rv	5′-CGGGATCCCTGATGTCATAGTTGATGTATCC-3′	
BamHI-EspA-Fw	5′-CGGGATCCAACTGTTTCAGCAATACCCATTG-3′	
EspA-Rv	5′-ATCATTATTAAGCACAGTTGTACC-3′	
EcoRV-rbsEspA-Fw	5′-TTTGATATCAAGAAGGAGATATACCATGGATACATCAACTATGACAT CAGTTGC-3′	
BamHI-EspA-Rv	5′-CGCGGATCCTTATTTGCCAATGGGTATTGCTGAAACAG-3′	

genetic organization and gene function (19, 26, 75). The fact that mice are resistant to EPEC and EHEC infection (60) makes *C. rodentium* an ideal animal model to study the roles of conserved genes in pathogenesis in vivo.

Aside from the role of the LEE in pathogenesis, a number of other genes have been shown to contribute to *C. rodentium* disease, including type IV pili (63) and various T3SS effector proteins (33, 39, 46, 55, 62, 86). However, direct comparisons between the virulence gene repertoires of *C. rodentium* and other enteric pathogens have been limited. Whole-genome sequencing has proved to be a powerful approach to defining the genetic structure of bacteria, providing a genomewide blueprint to guide genetic analysis. A fully annotated genome sequence can guide targeted mutagenesis and transcriptomic or proteomic studies. Here, we report the fully annotated genome sequence of a murine virulent strain of *C. rodentium*, ICC168, and make comparisons with the genomes of EPEC, EHEC, and other enteric bacteria.

MATERIALS AND METHODS

Bacterial strains and sequencing. The strain of *C. rodentium* sequenced, strain ICC168, was obtained in 1993 from S. W. Barthold's original stocks, previously known as *Citrobacter freundii* biotype 4280 (ATCC 51459) (3, 4), and subjected to minimal passages. The bacterial strains, plasmids, and primers used in the biological studies are shown in Table 1. Ten μg genomic DNA was fragmented by multiple passages through a 30-gauge needle and end repaired with a mixture of Klenow polymerase, T4 DNA polymerase, and polynucleotide kinase before size selection by preparative electrophoresis through a 0.8% agarose gel. The recovered sized fractions were subjected to a second round of end repair and size selection. Two- to 2.2-kb and 2.2- to 4-kb fractions were ligated into pUC19_smaI, and 4- to 5-, 5- to 6-, 6- to 9-, and 9- to 10-kb fractions were ligated into the low-copy-number vector pMAQ1b_smaI. Two bacterial artificial chromosome (BAC) libraries containing 15- to 25- and 25- to 40-kb inserts were constructed as previously described (69). End sequences obtained from 672 clones from each library were used to scaffold the assembly. The whole-genome shotgun was sequenced to approximately 9× coverage on ABI3730 automated sequencers using BigDye terminator chemistry.

The sequence was assembled, finished, and annotated as previously described (72). The program Artemis (81) was used to collate data and facilitate annotation. Base 1 of the *C. rodentium* genome matched that of *E. coli* K-12 MG1655 to aid whole-genome alignments, making the first gene *thrL*. The origin of replication is located between positions 4232946 and 4233181.

Pseudogenes were defined as coding sequences (CDS)s that had one or more possible inactivating mutations based on similarity with intact CDSs in related bacteria. Each single frameshift mutation or premature stop codon within a CDS was confirmed by checking the original sequencing data.

In addition, in order to provide a robust whole-genome phylogenetic species tree for *Citrobacter*, we sequenced the whole genome of *Citrobacter freundii* ballerup 7851 using 454 FLX pyrosequencing, assembled using the 454/Roche Newbler assembly program into 357 contigs (N50 contig size, 60,237 bp) from 410,057 sequence reads with an average read length of 177 bp to give a total sequence length of 4,904,659 bp.

Bioinformatics analyses. The following genome sequences were used in genome comparisons with *C. rodentium* ICC168: *E. coli* K-12 MG1655 (K-12; accession number U00096), *E. coli* E2348/69 (EPEC; accession number FM180568), *E. coli* O157:H7 Sakai (EHEC; accession number BA000007), *Salmonella enterica* subspecies *enterica* serovar Typhi CT18 (accession number AL513382), *S. enterica* subspecies *enterica* serovar Typhimurium LT2 (accession number AE006468), *S. enterica* subspecies *enterica* serovar Enteritidis P125109 (accession number AM933172), *Citrobacter koseri* ATCC BAA-895 (accession number CP000822), *Yersinia enterocolitica* 8081 (accession number AM286415), *Pectobacterium atrosepticum* SCRI1043 (accession number BX950851), *Klebsiella pneumoniae* 342 (accession number CP000964), *Enterobacter sakazakii* ATCC BAA-894 (accession number CP000783), and *Serratia marcescens* Db11 (http://www.sanger.ac.uk/Projects/S_marcescens/).

Pairwise whole-genome comparisons of *C. rodentium* with a range of enteric bacteria were performed using TBLASTX and visualized using the Artemis Comparison Tool (13). Circular diagrams were made using DNAplotter (12). Average nucleotide identities (ANI) were calculated from BLASTN matches over the entire lengths of the bacterial chromosomes. Orthologues in *C. rodentium* ICC168 and the three *E. coli* genomes (K-12, EPEC, and EHEC) were identified using an all-against-all reciprocal FASTA comparison of translated DNA with at least 40% identity over 80% of the length.

Phylogenetic analyses. The sequences for each of seven housekeeping genes (*adk*, *fumC*, *gyrB*, *icd*, *mdh*, *purA*, and *recA*) were extracted from the whole-genome sequences of several enteric bacteria, individually aligned using MUSCLE (24), and then concatenated. FindModel (77) was used to identify the best phylogenetic model to fit the data. Phylogenetic trees were constructed by the

TABLE 2. Genome features of *C. rodentium* ICC168

Parameter	Value				
	Chromosome	pCROD1	pCROD2	pCROD3	pCRP3
Genome size (bp)	5,346,659	54,449	39,265	3,910	3,172
G+C content (%)	54.7	47.2	41.8	51.0	46.8
No. of CDSs[a]	4,984 (182)	60 (5)	56 (1)	3	8
CDS density (%)	88.5	82.5	86.2	79.6	72.6
No. of tRNAs	86	0	0	0	0
No. of rRNA operons	7	0	0	0	0
No. of miscellaneous RNAs	56	1	0	0	1
No. of prophage regions	10	0	0	0	0
No. of genomic islands	17	0	0	0	0
No. of IS elements[b]	109 (31)	3 (2)	1	0	0

[a] The numbers in parentheses indicate the numbers of pseudogenes.
[b] The numbers in parentheses indicate partial/disrupted IS elements.

maximum-likelihood method using the General Time Reversible (GTR) plus Gamma model with PhyML (34) and Bayesian likelihood using GTR plus Gamma with 100,000 generations, sampling every 1,000, and a burn-in of 1,000 using MrBayes, and gave consistent results.

Strain and plasmid construction. *C. rodentium* strain ICC169 Δ*espA* (ICC304) was constructed using a modified version of the lambda red-based mutagenesis system (18). The *espA* gene and flanking regions were PCR amplified from wild-type *C. rodentium* ICC169 genomic DNA using the primers EspA-Fw/BamHI-EspA-Rv and BamHI-EspA-Fw/EspA-Rv (Table 1). The two fragments were digested with BamHI, ligated to each other, and cloned into pGEMT, and the nonpolar *aphT* cassette was then inserted into the BamHI site between the two fragments. After verification for correct orientation of the kanamycin resistance gene cassette, the insert was PCR amplified using the EspA-Fw and EspA-Rv primers (Table 1). The PCR product was electroporated into ICC169 containing pKD46 encoding the lambda red recombinase (18). Transformants were selected on kanamycin plates, and the correct insertion of the kanamycin resistance gene cassette was confirmed by PCR.

Full-length *espA* was amplified using *C. rodentium* ICC169 genomic DNA as a template and the primer pair EcoRV-rbsEspA-Fw and BamHI-EspA-Rv (Table 1). The PCR product was digested and ligated into the EcoRV/BamHI sites of pACYC184 to produce plasmid pICC490, which constitutively expresses *espA* from the tetracycline promoter (Table 1). The construction was confirmed by DNA sequencing.

Genes encoding EspS and EspH fusions to TEM-1 β-lactamase were constructed by PCR amplification using ICC169 or E2348/69 genomic DNA and the primer sets NdeI-EspS-Fw/EcoRI-EspS-Rv and Nde-EspH-Fw/EcoRI-EspH-Rv, respectively (Table 1). The plasmids resulting from the ligation of the digested PCR products into pCX340 were called pICC453 and pICC454, respectively.

The Role of EspA in vivo. Pathogen-free male C3H/Hej mice, 6 to 8 weeks old, were purchased from Harlan Olac (Bichester, United Kingdom). All animals were housed in individually HEPA-filtered cages with sterile bedding and free access to sterilized food and water. All animal experiments were performed in accordance with the Animals Scientific Procedures (Act 1986) and were approved by the local ethical review committee. Independent single-infection experiments were performed twice using four mice per group. The mice were inoculated by oral gavage with 200 ml of overnight LB-grown *C. rodentium* suspension in phosphate-buffered saline (PBS) ($\sim 5 \times 10^9$ CFU). The number of viable bacteria used as an inoculum was determined by retrospective plating on LB agar containing antibiotics. Stool samples were recovered aseptically at various time points after inoculation, and the number of viable bacteria per gram of stool was determined by plating them on LB agar (93). The experiment was terminated at day 8 postinoculation by sacrificing the mice.

T3SS translocation assay. The translocation assay is an adaptation of the assay described previously (14). The Swiss 3T3 cell line was grown in Dulbecco's modified Eagle's medium (DMEM) containing 4,500 mg liter glucose^{-1} supplemented with 10% fetal calf serum and 2 mM glutamine at 37°C in 5% CO_2. Two hundred μl of cells was seeded in black-wall/clear-bottom 96-well plates at a density of 2×10^4 cells per well to obtain 100% confluence on the day of infection. *C. rodentium* strains were grown for 8 h in LB broth and then transferred into fresh, sterile DMEM containing 1,000 mg liter glucose^{-1} and incubated statically at 37°C in 5% CO_2 overnight prior to infection. Each well was infected with 40 μl of the static overnight culture of either *C. rodentium* ICC169 or ICC304 carrying either pICC453 or pICC454. This was then centrifuged at 1,000 rpm for 5 min at room temperature. The infection was carried out at 37°C in 5% CO_2 for 2 h, followed by induction of the TEM-1 β-lactamase fusion protein for 1 h 30 min in the presence of 1 mM IPTG (isopropyl-β-D-thiogalactopyranoside). The cells were washed three times with Hanks' buffered salt solution (HBSS) and incubated for a minimum of 1 h 30 min in the dark at room temperature in 100 μl of 6 mM probenecid in HBSS-20 mM HEPES buffer supplemented with 20 μl of 6× CCF2/AM solution freshly prepared with the CCF2/AM loading kit (Invitrogen). The cells were washed in HBSS, and the fluorescence was quantified on a Fluostar Optima reader with excitation at 410 nm (10-nm band-pass), and emission was detected via 450-nm (blue fluorescence) and 520-nm (green fluorescence) filters. The translocation rate was expressed as the 450/520-nm emission ratio. Experiments were performed in triplicate.

Nucleotide sequence accession numbers. The annotated genome sequence of *C. rodentium* ICC168 has been deposited in the public databases under accession numbers FN543502 (chromosome), FN543503 (pCROD1), FN543504 (pCROD2), and FN543505 (pCROD3). The sequence of the fourth plasmid was identical to that of the previously sequenced plasmid pCRP3 (accession number AF311902). The raw sequence data generated for *Citrobacter freundii* ballerup 7851 has been deposited in the trace archive under accession number ERA000106 (ftp://ftp.era.ebi.ac.uk/vol1/ERA000/).

RESULTS

Genome structure and general features. The genome of *C. rodentium* ICC168 consists of a 5.3-Mb circular chromosome and four plasmids (pCROD1 to -3 and pCRP3) that range in size from 54 to 3 kb (Table 2; see Table S1 in the supplemental material). The genome of *C. rodentium* ICC168 shares significant synteny with those of *E. coli* K-12 and other members of the *Enterobacteriaceae*; however, there is evidence of repeated mediated recombination events (see below and data not shown). The chromosome is predicted to contain 4,984 CDSs, including 182 pseudogenes, 86 tRNAs, and 7 rRNA operons. We identified a total of 10 prophage-like regions, including five complete prophages, which were mainly Mu- or P2-like, and four putative lambdoid prophage remnants (Table 3). Seventeen genomic islands (GIs) were also identified within the chromosome (GI1 to GI16 and the LEE) as regions of aberrant GC content carrying mobility functions or showing evidence of integration, such as being flanked by direct repeats or insertion sequence (IS) elements. The exceptions are GI2, GI6, and GI13, which were identified on the basis of similarity to *Salmonella* pathogenicity islands 4 and 9. Many of the known and putative virulence factors of *C. rodentium* are encoded on the GIs (Table 3).

TABLE 3. Prophages and genomic islands of *C. rodentium* ICC168

Name	Start position	End position	Length (bp)	Insertion site	Flanking repeat (bp)[a]	Type	Virulence-related and other notable factors encoded
Prophages							
CRP28	285,573	325,997	40,425	*lfiG-lfiI*	ND	Mu-like prophage; intact	Dam
CRP99	990,424	1,027,608	37,185	ROD_08971	ND	Mu-like prophage; intact	Dam
CRPr11	1,143,137	1,151,111	7,975	ROD_t18 ($tRNA^{Ser}$)	70 DR	Putative lambdoid prophage; remnant	
CRPr13	1,304,879	1,315,433	10,555	*potC-potB*	12 DR	Putative lambdoid prophage; remnant	Three T3SS effectors (EspX7, EspN1[c], EspK)
CRPr17	1,762,632	1,769,107	6,476	*uspF-ttcA*	25 DR (2 MM)	putative lambdoid prophage; remnant	Three T3SS effectors (NleC, NleB2[c], NleG1)
CRPr20	2,096,166	2,115,165	19,000	*fliC*	8 DR	P2-like prophage; remnant	Dam
phiNP	2,730,430	2,775,336	44,907	*ssrA* (tmRNA)	25 DR	Untypeable prophage; intact	Five DNA methyltransferases (3 Dam, 1 Dcm, 1 unknown), DinI
CRPr33	1,304,879	1,315,433	3,912	ROD_31701-ROD_31781	ND	Putative lambdoid prophage; remnant	Three T3SS effectors (NleG2[c], NleG[c], EspM3)
CRP38	3,838,308	3,875,066	36,759	ROD_36451	ND	P2-like prophage; intact	HokA
CRP49	4,945,776	4,986,231	40,460	*gatD*	28 IR (8 MM) 4 DR	Mu-like prophage; intact	$tRNA^{Arg}$
Genomic islands							
GI1	363,963	378,377	14,415	ROD_t04($tRNA^{Thr}$)-ROD_03491	40 IR (2 MM)	Genomic island; no integrase; previously IS flanked	Two T3SS effectors (EspS, NleA/EspI), Aap-like protein, $tRNA^{Thr}$
GI2	981,787	1,036,635	17,664	ROD_t17($tRNA^{Ser}$)	ND	Putative genomic island; no integrase	T1SS and large repetitive protein[c]
GI3	1,151,112	1,154,180	3,069	ROD_t18($tRNA^{Ser}$)	70 DR (1 D, 3 MM)	Genomic island; integrase[c]	
GI4	1,185,005	1,194,883	9,879	ROD_t19($tRNA^{Ser}$)	18 DR (1 MM)	Genomic island; integrase[c]	Three T3SS effectors (EspL2, NleB1 and NleE)
GI5	2,147,048	2,164,244	17,197	ROD_t28($tRNA^{Ser}$)	19 DR (1 MM)	Genomic island; integrase	Two H-NS
GI6	2,712,024	2,730,042	18,019	*smpB_ssrA*	ND	Putative genomic island; no integrase	T1SS and large repetitive protein
GI7	2,775,891	2,794,475	18,585	ROD_26351-ROD_26491	ND	Genomic island; no integrase; IS flanked	LifA
GI8	3,124,334	3,142,596	18,263	ROD_29461-ROD_29651	ND	Genomic island; no integrase; IS flanked	CroR/I, T1SS, and large repetitive protein
LEE	3,142,637	3,183,242	40,606	ROD_29641-ROD_30191	ND	Genomic island; no integrase; IS flanked	T3SS, intimin, seven T3SS effectors (EspG, EspF, EspB, Tir, Map, EspH, EspZ)
GI9	3,340,622	3,370,076	29,455	ROD_t53($tRNA^{Phe}$)	ND	Genomic island; integrase[c]	LifA-like protein, one T3SS effector (EspN2-1[c])
GI10	3,517,032	3,557,418	40,387	ROD_t56($tRNA^{Leu}$)	51 DR (1MM)	Degenerate ICE element (ICECr1); integrase[c]	T1 RM system (M^+,S^+,R^-)
GI11	4,316,630	4,333,192	16,563	ROD_40761-ROD_41011	ND	Genomic island; no integrase; IS flanked	Intimin-like protein[c], five T3SS effectors (EspM1[c], EspO, EspT, NleG8. and EspM2)
GI12	5,017,131	5,037,202	20,072	ROD_47721-ROD_47851	ND	Genomic island; no integrase; IS flanked	LifA-like protein, one T3SS effector (EspN2-2)
GI13	5,064,524	5,087,409	22,886	ROD_48131-ROD_48201	ND	Putative genomic island, no integrase	T1SS and large repetitive protein[c]
GI14	5,146,469	5,158,968	12,500	*yjjG-prfC*	22 DR (4 MM)	Genomic island; integrase[c]	Four T3SS effectors (NleH, NleF, NleG7, and EspJ)
GI15	5,207,322	5,212,668	5,347	ROD_t85(tRNA-gly)	21 DR	Genomic island; integrase	
GI16	5,218,554	5,271,734	53,181	ROD_t86($tRNA^{Phe}$)	17 DR	Genomic island[b]; integrase	AIDA-like protein, hemolysin, PagC-like protein

[a] ND, none detected; DR, direct repeat; IR, inverted repeat; MM, mismatch; D, deletion.
[b] Also known as GI*pheV*-CR_{ICC168} (32).
[c] Pseudogene.

A total of 113 IS elements comprising 29 different types were found within the genome of *C. rodentium* ICC168, six of which (IS*Cro1* to *-6*) were newly identified in this study. The most abundant element, IS*Cro1*, which had 22 intact copies in the genome sequence, was previously referred to as IS*679* (19) but is actually a novel IS element. IS*Cro1* was found to be very similar to the single IS*679* element in *C. rodentium* (59%, 97%, and 98% amino acid identity to transposases A, B, and C, respectively), and it is possible, therefore, that one is a derivative of the other. It has been suggested that IS*679*-like elements may be involved in the horizontal transfer of virulence determinants (32), and it is notable that both GI7, which encodes the virulence factor LifA (47), and the LEE are flanked by intact copies of IS*Ec14* at one end and IS*Cro1* at the other end.

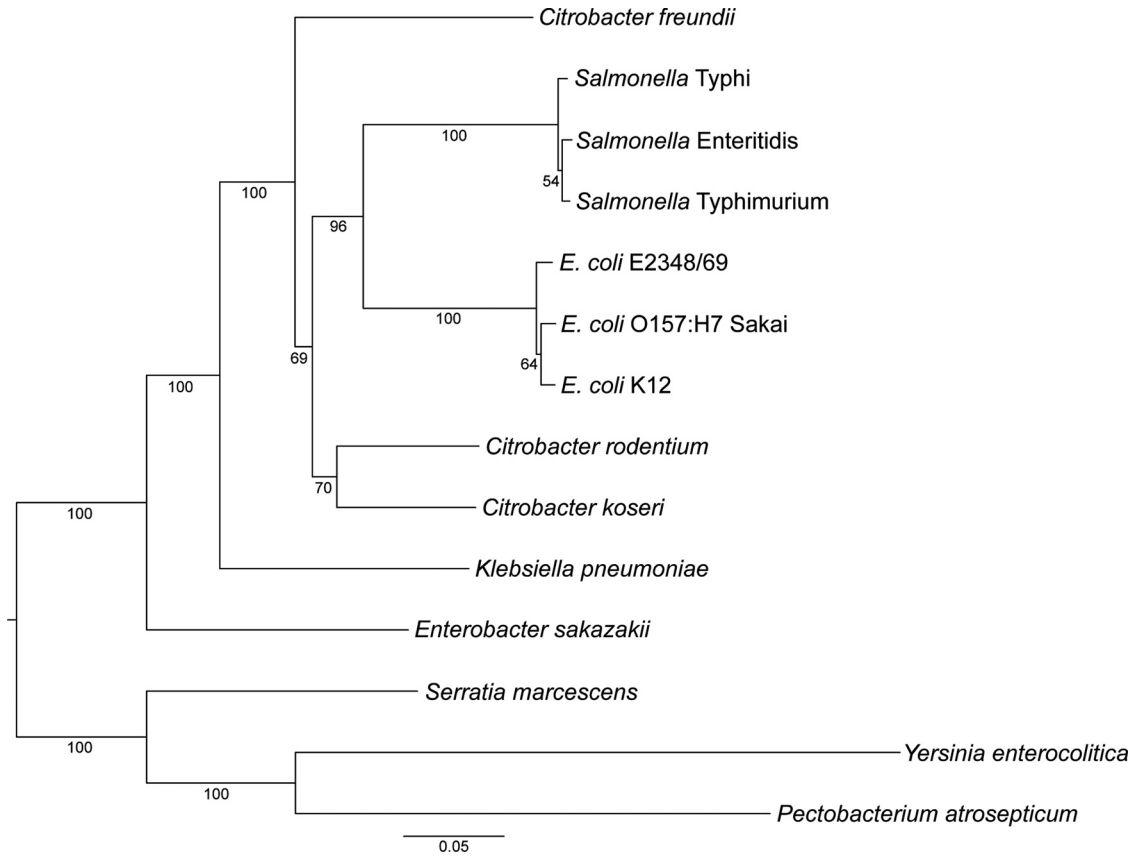


FIG. 1. Phylogeny of *C. rodentium* showing the phylogenetic relationship of *C. rodentium* to various enteric bacteria based on the nucleotide sequences of seven housekeeping genes (*adk*, *fumC*, *gyrB*, *icd*, *mdh*, *purA*, and *recA*). The tree shows bootstrap values (percentages of 1,000 replicates) below the branches and was rooted using an outgroup comprising *Yersinia*, *Serratia*, and *Pectobacterium*. The posterior probability for each node was 1 in every case and thus is not shown on the tree. The scale bar represents the number of substitutions per site.

Relationship between *C. rodentium* and other *Enterobacteriaceae*. To determine the relationship between *C. rodentium*, *E. coli*, and other enteric bacteria, a phylogenetic tree was constructed, based on the DNA sequences of seven conserved backbone genes located in core regions of the genome (Fig. 1). Figure 1 shows that *C. rodentium* clusters within the tree between other members of the *Enterobacteriaceae*. However, even though *C. rodentium* and *C. koseri* appear to cluster, the branch lengths separating them are almost as long as those separating *E. coli* and *Salmonella*, and *C. freundii* is more distantly related. These data indicate that *Citrobacter* as a genus is polyphyletic. This is consistent with the whole-genome ANI shared between *C. rodentium* and *C. koseri* (92.2%), *E. coli* K-12 (90.7%), *Salmonella* Typhi CT18 (90.7%), and *C. freundii* (88.9%).

Genome comparison with EPEC E2348/69 and EHEC Sakai. Reciprocal FASTA comparisons showed that the number of genes shared between *C. rodentium*, EPEC O127:H6 E2348/69 (referred to here as EPEC) (42), and EHEC O157:H7 Sakai (referred to here as EHEC) (37) is 2,940 (Fig. 2). This compares to 3,305 shared between *E. coli* strains K-12 MG1655 (referred to here as K-12) (6), EPEC, and EHEC.

The numbers of CDSs unique to *C. rodentium* and those shared exclusively between *C. rodentium* and either EPEC or EHEC were also high: 1,585, 230, and 229 CDSs, respectively

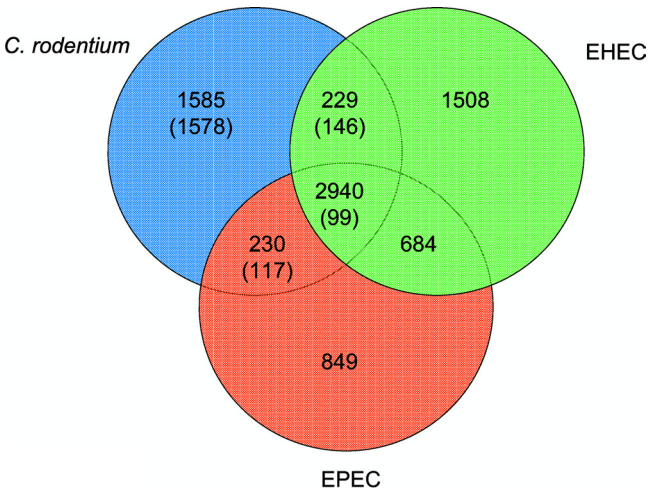


FIG. 2. Orthologous CDSs in *C. rodentium* ICC168, *E. coli* E2348/69 (EPEC), and *E. coli* O157:H7 Sakai (EHEC). The Venn diagram shows the number of genes that are unique to one strain, or shared between two or three of the strains, based on the results of reciprocal FASTA analysis with a minimum similarity of 40% identity over 80% of the CDSs. The numbers in parentheses indicate the numbers of *C. rodentium* genes in that category that have no orthologue in *E. coli* K-12 strain MG1655.

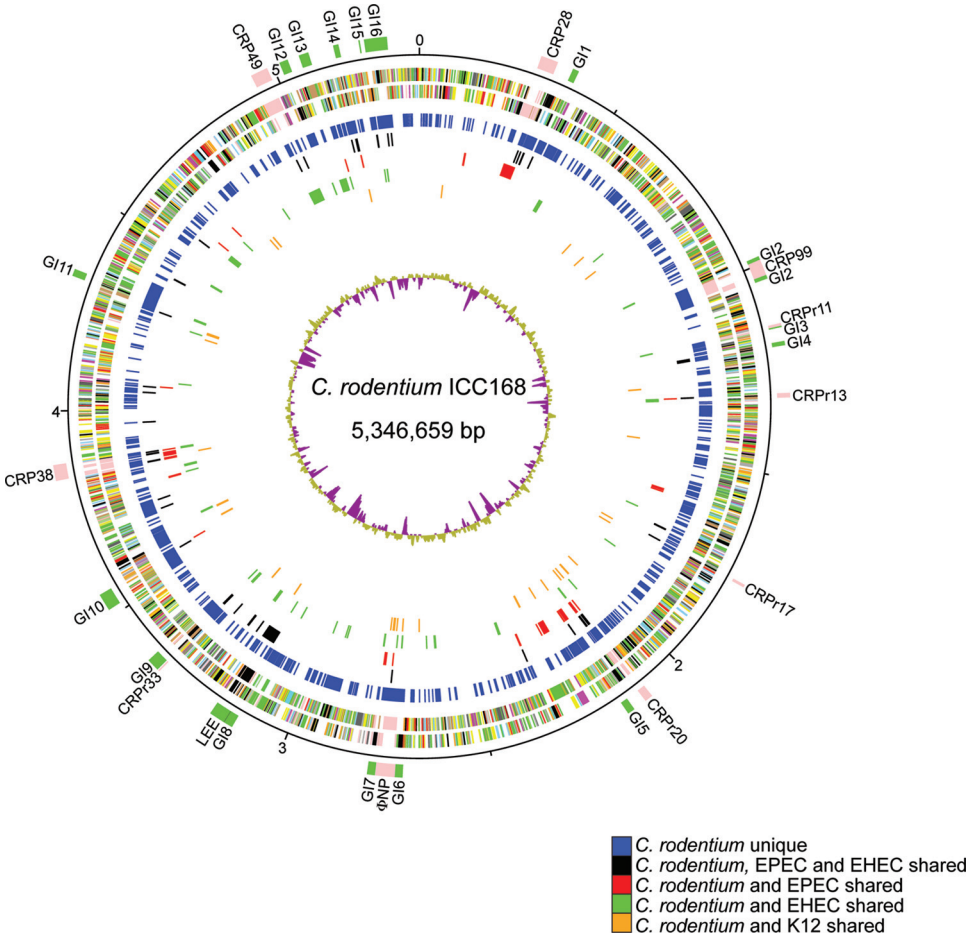


FIG. 3. Circular map of the *C. rodentium* ICC168 chromosome. From the outside in, the first circle shows the positions of genomic islands and prophages (detailed in Table 3). The second circle shows the genomic positions in Mbp. The third and fourth circles show the CDSs transcribed clockwise and counterclockwise, respectively (color coded according to the predicted functions of their gene products: black, pathogenicity or adaptation; gray, energy metabolism; red, information transfer; green, membrane or surface structure; yellow, central or intermediary metabolism; cyan, degradation of macromolecules; cerise, degradation of small molecules; pale blue, regulator; pink, prophage or IS element; orange, conserved hypothetical; pale green, unknown; and brown, pseudogene). The fifth circle shows *C. rodentium* CDSs (dark blue) that lack orthologues (by reciprocal FASTA analysis) in EPEC E2348/69, EHEC Sakai, or K-12 MG1655. The sixth circle shows *C. rodentium* CDSs (black) that have orthologues (by reciprocal FASTA analysis) in both EPEC and EHEC but not K-12. Circles 7, 8, and 9 show the positions of *C. rodentium* CDSs that have orthologues (by reciprocal FASTA analysis) in EPEC (red), EHEC (green), or K-12 (orange) (excluding those CDSs that also had orthologues in one or both of the other *E. coli* strains). The innermost circle shows a plot of G+C content.

(Fig. 2). We analyzed these three CDS groups in more detail. We subtracted from the groups those genes that were also shared with K-12 (Fig. 2). This comparison has been used previously to differentiate core *E. coli* genes from pathotype-specific functions (42). Almost half of the CDSs *C. rodentium* shares with either EPEC (75/117 CDSs) or EHEC (67/146 CDSs), but without an orthologue in K-12, were found to be clustered and located on GIs or prophages (Fig. 3). Of the genes shared with either EPEC or EHEC that were in the "backbone" of *C. rodentium*, many had putative functions associated with metabolism and sugar transport and utilization. Of particular note, *C. rodentium* carries all of the genes in the propanediol utilization operon, which are also found in EPEC but are absent in many other *E. coli* strains, including EHEC and K-12 (42). This supports the suggestion that the *cob-pdu* locus originated in a common ancestor of the *Enterobacteriaceae* and has been lost repeatedly by different lineages (42, 79). Also, among the genes shared only with EHEC was a urease gene cluster. The lack of urease production in EHEC has been linked to a premature stop codon in *ureD* (38, 65); however, *C. rodentium* encodes the full-length UreD and can produce urease (84). Interestingly, also among the EHEC and *C. rodentium* shared genes were those encoding the clustered regularly interspaced short palindromic repeats (CRISPR)-associated proteins, which were absent from EPEC and divergent from those found in K-12. The *C. rodentium* genome sequence also contains two CRISPRs, located in genomic locations equivalent to those in EHEC but which contain different numbers of repeats and spacers. No CRISPRs were apparent within the genome of EPEC. Figure 3 shows that *C. rodentium*-specific genes were located throughout the chromosome, although 414 of the 1,578 unique genes (genes not shared with EPEC, EHEC, or K-12) were located on genomic islands or prophages and are likely to have been acquired by recent horizontal gene transfer.

Of the 2,940 core genes present in *C. rodentium*, EPEC, and EHEC, only 99 had no orthologues in K-12 (see Table S2 in the supplemental material), and of these 76 were located on GIs and prophages. Over half (49) of these 76 genes were associated with virulence and included those found on the LEE, as well as other non-LEE-encoded T3SS effectors. Of note, among the remaining shared genes was a cluster with a putative role in the production of 4-hydroxybenzoate decarboxylase, which is found sporadically in other members of the *Enterobacteriaceae*, as well as elsewhere, and may be involved in metabolism of aromatic compounds under anaerobic conditions (20, 53, 56).

Patterns of functional gene loss. The genome of *C. rodentium* ICC168 has 188 pseudogenes, 43% of which are found in prophages, GIs, or plasmids (summarized in Table S3 in the supplemental material). Almost a quarter of the pseudogenes (42/188 CDSs) have been caused by prophage- or IS-mediated insertional inactivation, including disruption of flagellum biogenesis genes and other core and accessory functions (see Table S3 in the supplemental material). The remainder of the pseudogenes are truncated by frameshift mutations or premature stop codons or are gene remnants identified by similarity to full-length genes in other bacteria. Fifty-six of 188 pseudogenes had only a single frameshift mutation or premature stop codon, indicating that these inactivating mutations were relatively recent events. There are a number of sugar uptake and energy generation pseudogenes (see Table S3 in the supplemental material), which may be indicative of metabolic streamlining. Also, a number of pseudogenes are associated with virulence factors, including several T3SS effector proteins and essential functions within three distinct fimbrial operons (Table 4; see Tables S3 and S4 in the supplemental material).

Virulence determinants. Through targeted investigations and comparison with EPEC and EHEC, a number of factors have previously been shown to be important for *C. rodentium* virulence. Here, we describe the full repertoire of the known and potential virulence-associated determinants that were identified in the genome sequence of ICC168 (summarized in Table S4 in the supplemental material).

T2SS. *C. rodentium* has a type II secretion system (T2SS) encoded in a single locus (ROD_44871 to ROD_45001). Nine putative substrates for this secretion system were also identified, including four likely polysaccharide-degrading enzymes with similarity to chitinases encoded adjacent to the T2SS itself and four additional similar enzymes (including one encoded by a pseudogene) encoded elsewhere in the *C. rodentium* genome. *C. rodentium* also carries an orthologue of *yodA*, the product of which has been shown to be secreted by the pO157-encoded T2SS and to promote virulence in EHEC (40).

LEE-encoded T3SS. The LEE pathogenicity island, along with its associated T3SS, is conserved among the genomes of EPEC, EHEC, and *C. rodentium*, but with some notable differences. While the LEEs of EPEC and EHEC are inserted into the SelC tRNA locus, the *C. rodentium* LEE is in a nonsynonymous location flanked by IS elements, adjacent to another genomic island (GI8). Moreover, in relation to EPEC and EHEC, the *rorf1* and *espG* genes of *C. rodentium* are located at the opposite end of the LEE (19).

The *C. rodentium* T3SS translocated-protein repertoire. *C. rodentium* possesses a repertoire of 35 genes (including six pseudogenes) (Table 4) encoding proteins that show significant sequence homology to known T3SS effector proteins in other systems or that we have shown to be translocated by the *Citrobacter* T3SS. In comparison, EPEC E2348/69 encodes 27 T3SS effectors (42), EPEC B171 has 40 (42), and EHEC Sakai has 62 effector proteins (88) (Table 4). All of the *C. rodentium* effectors are encoded in regions thought to have been laterally acquired. Of the 29 intact *C. rodentium* effectors, seven are encoded on the LEE; five are present on the prophage remnants denoted CPRr13, CPRr17, and CPRr33; and 14 effector proteins are encoded on five GIs (GI1, GI2, GI4, GI11, and GI14) (Table 3). The three remaining effectors are located within regions with low GC content. The three prophage-like elements, CRPr13, CRPr17, and CRPr33, each consist of two genes encoding putative phage-related functions, along with three different T3SS effectors each. It is notable that these regions share similarity with and are integrated at the same sites as lambdoid prophages identified within the genomes of EPEC and EHEC (Table 3) (37, 42). CRPr13 encodes the effectors EspX7, EspN1, and EspK, which are homologues of effectors encoded on EHEC prophage Sp6. CRPr17 encodes an Sp10-like integrase and homologues of the effectors NleC, NleB, and NleG, which are found encoded on different lambdoid prophages in EPEC and EHEC, and CRPr33 shares sim-

TABLE 4. *C. rodentium* T3SS effectors and their homologues in EPEC and EHEC

Effector	No. in[a]:			
	C. rodentium ICC168	O127:H6 E2348/69	O111:NM B171	O157:H7 Sakai
Cif	0	1 (1)	1	0
EspB	1	1	1	1
EspF	1	1	1	1
EspG	1	2	1	1
EspH	1	1	1	1
EspJ	1	1	0	1
EspK	1	0	0	1
EspL	1	3 (2)	3 (2)	4 (1)
EspM	3 (1)	0	3 (1)	2
EspN	3 (2)	0	1	1
EspO	1	1 (1)	0	2
EspR	0	0	0	4 (1)
EspS	1	0	0	0
EspT	1	0	0	0
EspV	1	0	1 (1)	1 (1)
EspW	0	0	1	1
EspX	1	0	0	6 (1)
EspY	0	0	0	5 (1)
EspZ	1	1	1	1
Map	1	1	1	1
NleA	1	1	1	1
NleB	2 (1)	3 (1)	3 (2)	3 (1)
NleC	1	1	2 (2)	1
NleD	2	1	0	1
NleE	1	2	1	1
NleF	1	1	1	1
NleG	5 (2)	1	6	14 (5)
NleH	1	3 (1)	2 (1)	2
Ibe	0	0	2 (1)	0
TccP	0	0	1	2 (1)
Tir	1	1	1	1
Total	35 (6)	27 (6)	40 (12)	62 (12)

[a] The numbers in parentheses indicate pseudogenes.

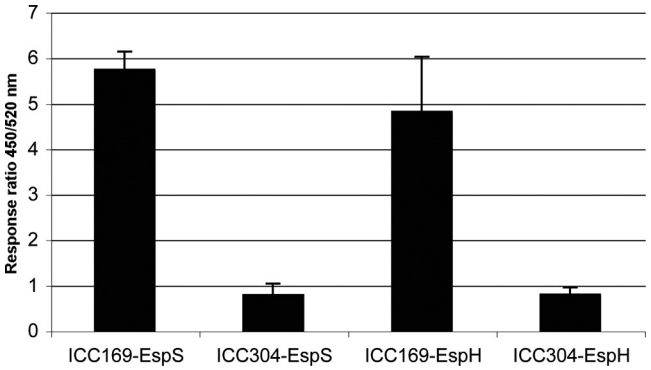


FIG. 4. EspS is a T3SS translocated protein. Translocation of EspS–TEM-1 and the control EspH–TEM-1 from wild-type (ICC169) and Δ*espA* (ICC304) *C. rodentium* was quantified using a Fluostar Optima reader with excitation at 410 nm (10-nm band-pass). Emission was detected via 450-nm (blue fluorescence) and 520-nm (green fluorescence) filters. The translocation rate was expressed as the 450/520-nm emission ratio. EspS and EspH were translocated from wild-type *C. rodentium*, but not from the Δ*espA* mutant. The error bars represent mean standard deviations (SD).

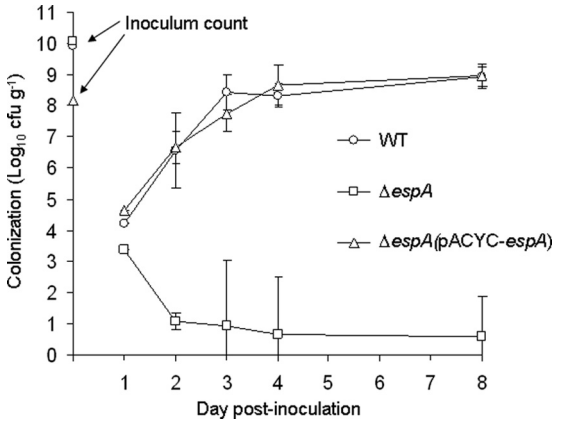


FIG. 5. Colonization dynamic of wild-type, Δ*espA* (ICC304), and Δ*espA*(pACYC-*espA*) *C. rodentium* strains after oral inoculation of C3H/Hej mice. Mice inoculated with wild-type (WT) and Δ*espA* (pACYC-*espA*) *C. rodentium* exhibited similar colonization dynamics, whereas Δ*espA C. rodentium* was unable to colonize. The inoculum count is the number of viable bacteria in 200 ml used to inoculate mice by oral gavage. The data are represented as means ± SD.

ilarities with prophage Sp17 and encodes homologues of three of the four effectors found on this prophage. It therefore seems likely that these three regions are remnants of lambdoid prophages and that the nine associated effector proteins have been carried into the *C. rodentium* genome on these phages by specialized transduction.

T3SS effector families. *C. rodentium* genes encode at least one intact member of each of the core set of effector families, consisting of the seven LEE-encoded effectors plus the non-LEE-encoded NleA/EspI, NleB, NleE, NleF, NleG, NleH, and EspL, previously suggested to represent the minimum set required to facilitate infection (42), as they are common to all LEE-encoding species sequenced to date. All the effector families that are not represented in the *C. rodentium* genome are also absent from at least one of the other sequenced A/E pathogens, E2348/69, B171, and Sakai (Table 4).

In addition to homologues of EPEC and EHEC effectors, we identified a new T3SS translocated protein in *C. rodentium*, named EspS, which has some similarity to OspB of *Shigella*. Using a β-lactamase fusion, we showed that EspS is translocated in an EspA-dependent manner (Fig. 4). Mouse inoculation showed that a Δ*espA* mutant was severely attenuated in virulence (Fig. 5). *C. rodentium* also encodes the effector EspT, found only rarely in EPEC (1), which subverts the eukaryotic cytoskeleton by activating the small Rho GTPases Rac1 and Cdc42 (10), and an intact copy of EspV, which is considered to be a pseudogene in EHEC Sakai due to an N-terminal truncation (88). Interestingly, two identical copies of NleD are encoded within the genome of *C. rodentium* adjacent to identical transposases, and three EspN family members are present (though two of these are encoded by pseudogenes), whereas E2348/69, B171, and Sakai have only one or no representatives from these four families (Table 4). This indicates that there has been an expansion of the NleD-like gene repertoire in *C. rodentium*.

T6SS. A new class of secretion system, the type VI secretion system (T6SS), has recently been described in a variety of bacterial species. T6SS gene clusters commonly consist of between 15 and 25 genes and were initially identified based on the presence of a gene encoding a homologue of the *Legionella pneumophila* type IV secretion system (T4SS) protein IcmF (17). A contribution to virulence was shown for T6SSs of several pathogenic bacteria (28). The T6SS apparatus is not well characterized yet, but recent studies indicate that several core components resemble bacteriophage tail proteins (49). The Hcp and VgrG proteins have been demonstrated to be secreted in several organisms; however, a possible dual role of these proteins as a structural part of the T6SS and secreted effector molecules is becoming evident (78).

There are two distinct T6SS gene clusters in the genome of *C. rodentium*, which we have designated *Citrobacter rodentium* type *s*ix secretion system cluster 1 (CTS1) and 2 (CTS2). CTS1 is composed of 39 genes, 18 of which are conserved components of the T6SS (Fig. 6). CTS1 is almost identical to a T6SS gene cluster carried by *Enterobacter cancerogenus* and also shows limited similarity to components of SPI-6 (also known as *Salmonella enterica* centisome 7 genomic island [*sci*]) (29). Like the T6SS cluster encoded by *E. cancerogenus* and the *sci* locus, CTS1 also carries a chaperone-usher fimbrial biogenesis operon (29). CTS1 contains all of the components that have been determined to be necessary for a functional T6SS in other bacteria (95). Interestingly, the *icmF* homologue in CTS1 has a frameshift at a region containing a polyadenosine tract, which may allow regulation of the gene via transcriptional slippage in an manner analogous to that of *mixE* of *Shigella* or the *pyrBI* locus in *E. coli* (52, 74).

CTS2 consists of 16 genes, 13 of which are conserved within other T6SS clusters (Fig. 6). Although CTS2 encodes all the components required for assembly of a functional T6SS, the *icmF* homologue in this cluster has a bona fide frameshift, which makes it unlikely that CTS2 is sufficient to produce a functional T6SS. CTS2 is highly similar to a putative T6SS in *C. freundii*, which has conserved gene order and an intact *icmF* homologue in a single frame (data not shown). CTS2 also

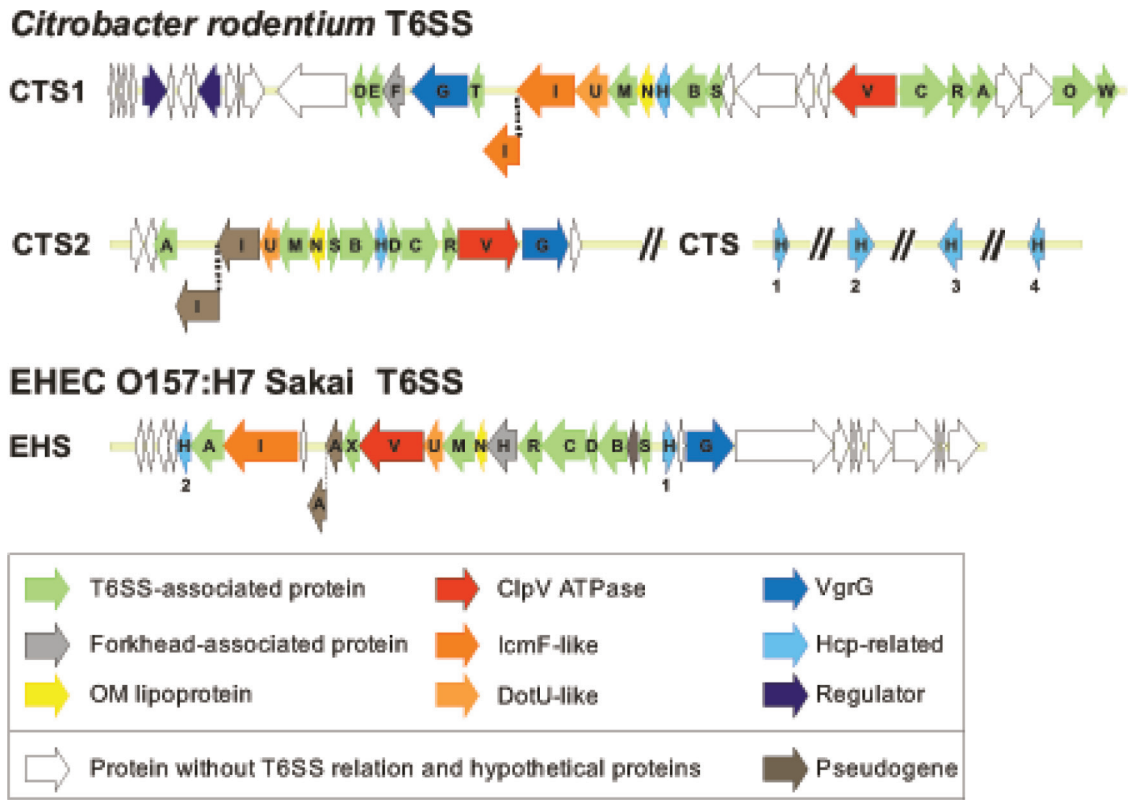


FIG. 6. T6SSs in *C. rodentium* and EHEC. Shown is a schematic representation of the *C. rodentium* ICC168 T6SS gene clusters CTS1 and CTS2 and the EHEC O157:H7 Sakai T6SS cluster EHS. Conserved T6SS components are highlighted. The differing architectures and lack of homology between CTS1, CTS2, and EHS suggest that these T6SS clusters have distinct evolutionary histories.

shares limited similarity with components of the T6SS clusters in *Pseudomonas* species (59, 85).

The differing architectures and lack of homology between CTS1 and CTS2 suggest that these two T6SS clusters have distinct evolutionary histories. In addition to CTS1 and CTS2, which each encode one Hcp family protein, there are four other Hcp homologues encoded in the *C. rodentium* chromosome, which share little homology to each other and thus may also have been acquired independently.

EHEC also encodes a T6SS, which we have designated the *e*ntero*h*emorrhagic *E. coli* type *s*ix secretion system cluster (EHS), which is encoded in O island 7 and has high homology to the *Shigella sonnei* T6SS (85). EHS is distinct from both *C. rodentium* T6SSs and consists of 33 genes, 18 of which are conserved components of the T6SS (Fig. 6). Unlike in CTS1 and CTS2, the *icmF* gene in the EHS operon is not interrupted by a frameshift. Additionally, downstream of *ehsG* there is a region including genes that are associated with Rhs proteins (51, 90). EHEC encodes only two Hcp homologues, EhsH1 and EhsH2, which are both encoded in the EHS cluster and have very limited similarity to each other. In contrast to the T3SS, which is conserved in all A/E pathogens and is essential for virulence, the overall lack of homology between EHS, CTS1, and CTS2 suggests that the T6SS may facilitate more subtle strain-specific adaptations to divergent host or environmental niches.

Other secretion systems. Type I secretion systems (T1SS) are involved in the transport of a wide range of substrates, and in common with many other enteric bacteria, *C. rodentium* encodes multiple T1SSs. Of particular note are four genomic islands (GI2, GI6, GI8, and GI13) (Table 3) that are predicted to each encode T1SS apparatus, as well as a presumptive secreted substrate, a large (1,637- to 5,979-amino-acid [aa]) repetitive protein (Table 3). The gene products forming the T1SSs share ~50% amino acid identity with each other. The associated repetitive proteins show higher variation in protein length and lower overall sequence conservation, with ~25% amino acid identity between ROD_08971, ROD_25701, ROD_29581, and ROD_48171.

The arrangement, nature, and proposed functions of CDSs seen in the four *C. rodentium* T1SS genomic islands appear to suggest that they are functional modules that have been laterally acquired. Wider comparisons also showed that these GIs are similar in gene content, arrangement, and, in some instances, sequence to GIs previously seen in other enteric bacteria. Comparisons with these other loci showed that the large repetitive protein encoded by GI6 shares 47% identity over 3,790 aa with the large repetitive protein of *S.* Typhi encoded on SPI-9. Both GIs are inserted in the same intergenic region between *ssrA* and *smpB*.

GI2, GI8, and GI13 also have some similarity to SPI-9 and the related SPI-4; however, GI13 has a high degree of similarity to O island 28 in EHEC EDL933 (51% identity over 5,392 aa to the large repetitive protein), and the large repetitive protein of GI2 is similar to a putative hemagglutinin/hemolysin-related protein in *Ralstonia solanacearum*. SPI-9 has been

TABLE 5. Fimbrial biosythesis operons identified in *C. rodentium*

Operon	CDS ID	Genes	Description[c]	EPEC orthologue	Sakai orthologue
1	ROD_01101–01121	*hofCB-ppdD*	Type IV fimbriae	E2348_C_0109–0111	ECs0110–0112
2	ROD_03641–03671		Chaperone-usher γ4 fimbriae		
3	ROD_03351, 10951–11021	*crl csgGFEDBAC*	Curli fimbriae	E2348_C_0233, 1129–1136	ECs0267, 1414–1412
4	ROD_11771–11781		Chaperone-usher β fimbriae[e]		
5	ROD_18141–18181	*lpfEDCBA*	Long polar fimbriae (chaperone-usher γ1 fimbriae)		
6	ROD_19341–19381		Chaperone-usher σ fimbriae		
7	ROD_22311–22341		Chaperone-usher γ4 fimbriae		
8	ROD_27771–27801		Chaperone-usher γ4 fimbriae		
9	ROD_29101–29191	*fimBEAICDFGHK*	Chaperone-usher γ1 fimbriae	E2348_C_4619–4627[a]	ECs5271–5279[a]
10	ROD_29201–29241		Alternate chaperone-usher (α) fimbriae	E2348_C_0247–0249[b]	ECs0321–0323[b]
11	ROD_29351–29391		Chaperone-usher γ4 fimbriae[d]		
12	ROD_34961–35021		Chaperone-usher π fimbriae		
13	ROD_41241–41291	*kfcHGFEDC*	Kfc (K99-like factor involved in *Citrobacter* colonization) chaperone-usher κ fimbriae		
14	ROD_41381–41551	*flp1 rcpCA tadZABCD tadVEFG*	Tight adherance (*tad*) locus (type IV fimbriae)		
15	ROD_44281–44321	*hofMNOPQ*	Type IV fimbriae	E2348_C_3635–3639	ECs4233–4237
16	ROD_46461–46571	*cfcABCDEFGHIJPV*	CFC (colonization factor *Citrobacter*) type IV fimbriae		
17	ROD_50611–50651		Chaperone-usher γ4 fimbriae[d]		
18	ROD_p1161–p1201		Chaperone-usher κ fimbriae		
19	ROD_p1291–p1301		Chaperone-usher γ1 fimbriae[d,e]		

[a] *fimK* is missing in EPEC and EHEC.
[b] No orthologues of ROD_29231 or ROD_29241.
[c] Chaperone-usher fimbrial operons have been grouped into clades and subclades according to the fimbrial usher protein classification scheme (68).
[d] Contains pseudogenes.
[e] Part of operon is missing.

shown to be required for intestinal colonization in mice and in vitro biofilm formation in *S.* Enteritidis (48); therefore, GI2, GI6, and GI13 may encode factors that play roles in the virulence of *C. rodentium*. However, transcription of the large repetitive protein of GI2 is unlikely to be due to the insertion of prophage CRP99 in the middle of the CDS. In addition, the CDS for the large repetitive protein on GI13 has been truncated by a premature stop codon; however, as it is located close to the C terminus, it is possible that a 5,884-aa protein may be expressed as opposed to the 5,979-aa full-length protein.

There are 20 putative type V secretion systems, or autotransporters, encoded in the *C. rodentium* genome. Fourteen of these, including one encoded by a pseudogene, were identified as putative autotransporter adhesins and were related to AIDA-I, TibA, or pertactin, which are involved in virulence in EPEC, enterotoxigenic *E. coli* (ETEC), and *Bordetella pertussis*, respectively (5, 8, 27). Two other autotransporters were predicted to belong to the serine protease autotransporter of the *Enterobacteriaceae* (SPATE) family of proteins, members of which have been shown to contribute to virulence in other pathogens (7, 23, 70). The majority of the autotransporters are located in the chromosomal backbone; however, one, AdcA, which was shown to function as an adhesin but had no obvious role in colonization of mice (36), is encoded on a genomic island. In addition, the two SPATE autotransporters are encoded by genes on the large plasmid pCROD1, along with a TibA-like autotransporter adhesin and its associated glycosyltransferase.

Adhesins. *C. rodentium* carries a total of 19 fimbrial biogenesis operons, including four incomplete operons (Table 5). Of the intact operons, the product of the Kfc chaperone-usher fimbrial operon and CFC type IV fimbriae were previously determined to be involved in gastrointestinal colonization (36, 63), whereas long polar fimbriae had no discernible role in the virulence of *C. rodentium* (87).

Of the nonfimbrial adhesins encoded by *C. rodentium* genes, LifA (47) and intimin (83) are essential for colonization. We also found two LifA homologues that are divergent from LifA at the N terminus but almost identical at the C terminus and that had 97% amino acid identity to each other. In addition, two intact genes and one pseudogene encoding intimin-like proteins were identified outside of the LEE (see Table S4 in the supplemental material).

Other potential virulence factors. Other predicted proteins encoded by *C. rodentium* genes that are potentially involved in virulence include homologues of the dispersin Aap of enteroaggrative *E. coli* (EAEC) (58) and virulence factor CexE of ETEC (76), the virulence-related outer membrane protein PagC (66), and the *Yersinia enterocolitica* porin required for colonization, SpfA (36).

Other factors previously reported to be important for the virulence of *C. rodentium* include the transcription factors Ler,

GrlA, GrlR, RegA, and RpoS (2, 19, 21, 36); the quorum-sensing locus (CroIR); and the Pho regulon (15, 16). In addition, *C. rodentium* genes encode three putative hemolysin expression regulatory proteins, two on the chromosome and the third on pCROD2, and the putative hemolysin activator HlyBC, which is presumably involved in the regulation of the putative hemolysin/hemagglutinin encoded by the downstream ROD_49941.

Plasmids. *C. rodentium* carries four plasmids (Table 2), the largest of which, pCROD1, is nonconjugative; encodes two toxin/antitoxin (TA) addiction systems, PemIK and CcdAB; and has a replication locus similar to those of plasmids belonging to the incompatibility group IncFII, such as the *E. coli* plasmid R100 (NR1) (94). In addition to functions associated with plasmid replication and maintenance, pCROD1 genes, including a colicin S4-like biosynthesis operon and one intact and one degenerate chaperone-usher fimbrial operon, encode proteins associated with virulence, including three putative autotransporters (Table 5).

The backbone of the 39-kb plasmid, pCROD2, is syntenic with those of plasmids R6K (IncX1) and pOLA52 (IncX2) (67), sharing 22 CDSs (average 47% amino acid identity) with the former and 31 CDSs (average 59% amino acid identity) with the latter out of the 51 pCROD2 CDSs. Included in the shared regions is the plasmid replication locus, suggesting that pCROD2 also belongs to incompatibility group IncX. pCROD2 carries a 16-kb conjugative plasmid transfer locus (ROD_p2371-ROD_p2531); however, transfer of this plasmid might be impaired due to the disruption of *triD* (ROD_p2461) by IS*102*. Two addiction systems are likely to be involved in the stability of this plasmid, the TA system *stbDE* and the putative TA locus *hicAB*. pCROD2 also encodes a putative H-NS DNA-binding protein (ROD_p2271) that has been linked to mitigating the impact of low-G+C DNA acquired by lateral gene transfer in other systems (22).

Plasmids pCROD3 and pCROD4 are small (3.9 and 3.2 kb, respectively) and nonconjugative. The sequence of the smallest plasmid is identical to that of the previously sequenced 3,172-bp pCRP3 from *C. rodentium* strain DBS100 (19).

DISCUSSION

The data that we have described here highlight several clear messages. The phylogenetic analysis of *C. rodentium* showed that although it clusters with members of the *Enterobacteriaceae*, *C. rodentium* is more distantly related to *E. coli* than *E. coli* is to *Salmonella*. Moreover, the genomic evidence we have presented also shows that the sequenced species currently within the genus *Citrobacter* do not cluster, and our analysis indicates that the genus is in fact polyphyletic.

It is apparent from the comparisons of the gene sets of *C. rodentium*, EPEC, and EHEC that a large percentage (~32%) of the *C. rodentium* genome is unique. These distinguishing functions include those known to be important for virulence in other systems, including T6SSs and associated effectors and multiple fimbrial operons, as well as other exported adhesins. Also included in this group are some novel T3SS effector proteins.

The majority of functions shared between *C. rodentium*, EPEC, and EHEC are also found in the nonpathogenic K-12, which suggests that these genes encode core enterobacterial functions. However, there are a significant number of genes found in *C. rodentium*, EPEC, and EHEC that are absent from K-12. The majority of these are located on mobile genetic elements and are also recognizable as key virulence determinants, including *lifA*, LEE, and many of the *C. rodentium* T3SS effector proteins. It is the acquisition of these factors that is likely to have been responsible for their convergently evolved common virulence strategy.

Specialized transduction by lambdoid phages has been shown to be important for the acquisition of virulence determinants by both EPEC and EHEC (88). It is clear from this analysis that this is also the likely mechanism by which many of the *C. rodentium* effectors have been acquired. It is important to note that although the cargo genes are found at analogous sites in the genome, comparisons of the phage genes thought to have brought these shared effectors into the genome show that they probably came from distinct phages and so are likely to be part of a large pool of temperate phages disseminating a related set of effector genes to a diverse set of hosts, underscoring their importance in pathogen evolution. It is access to this gene pool that has allowed *C. rodentium*, at least in part, to convergently evolve with the pathogenic *E. coli* strains.

It is likely that the acquisition of the LEE and its associated effector proteins had a dramatic effect on the pathogenic potential of *C. rodentium* in the mouse and perhaps even the niche it occupies within this host. Certainly the presence of such a large number of pseudogenes and IS elements in other bacteria, such as *S.* Typhi and *Yersinia pestis*, has been tightly linked to a change in lifestyle associated with the occupation of a new niche (71, 73). Although the numbers of pseudogenes in *C. rodentium* and EPEC are comparable, 60% of EPEC pseudogenes are in regions that are thought to have been laterally acquired. The inverse is true of *C. rodentium*, where 57% of pseudogenes fall in the core regions.

It is not just the relative number of pseudogenes lost by *C. rodentium* that draws parallels with *S.* Typhi and *Y. pestis*; *C. rodentium* has also lost metabolic, colonization, and virulence-associated functions. If there had been a change of niche, it would be expected that genes important for the previous lifestyle would be lost. Certainly the observation that the majority of pseudogenes lie in the *C. rodentium* backbone is consistent with this. A specific example that illustrates this point is the loss of function in the fimbrial genes that has occurred exclusively in operons unique to *C. rodentium* compared to EPEC and EHEC.

C. rodentium is the etiological agent of transmissible colonic hyperplasia in mice. It colonizes the gut mucosa via A/E lesions and may also reach deeper tissues (e.g., the liver and spleen). We have recently shown that *espT* can mediate invasion of *C. rodentium* into mammalian cells (10a); it is not yet known if EspT plays a role in in vivo dissemination or in the hyperplastic or immunological responses. *C. rodentium* is nontoxigenic, using an infection strategy that appear to rely mainly on its T3SS effector repertoire. Although we have shown that *C. rodentium* is genetically distinct from EPEC and EHEC and does not share the same host, the three bacteria have similar infection strategies and share virulence genes that are found on mobile genetic elements. Accordingly, it is unlikely that *C. rodentium* acquired the virulence loci directly from EPEC or EHEC, and

the data point to the existence of a common ancestral source. Nonetheless, the availability of the complete *C. rodentium* genome annotation will enhance future studies of virulence mechanisms in A/E pathogens using a natural and unique host-pathogen interaction model.

ACKNOWLEDGMENTS

We thank Simon Harris for assistance with the phylogenetic analyses. We thank the core sequencing and informatics teams at the Sanger Institute for their assistance and the Wellcome Trust for its support of the Sanger Institute Pathogen Genomics group.

REFERENCES

1. **Arbeloa, A., M. Blanco, F. Moreira, R. Bulgin, C. Lapez, G. Dahbi, J. Blanco, A. Mora, M. P. Alonso, R. C. Mamani, T. A. Gomes, J. Blanco, and G. Frankel.** 2009. Distribution of espM and espT among enteropathogenic and enterohemorrhogic *Escherichia coli*. J. Med. Microbiol. **58:**988–995.
2. **Barba, J., V. H. Bustamante, M. A. Flores-Valdez, W. Deng, B. B. Finlay, and J. L. Puente.** 2005. A positive regulatory loop controls expression of the locus of enterocyte effacement-encoded regulators Ler and GrlA. J. Bacteriol. **187:**7918–7930.
3. **Barthold, S. W., G. L. Coleman, P. N. Bhatt, G. W. Osbaldiston, and A. M. Jonas.** 1976. The etiology of transmissible murine colonic hyperplasia. Lab Anim. Sci. **26:**889–894.
4. **Barthold, S. W., G. W. Osbaldiston, and A. M. Jonas.** 1977. Dietary, bacterial, and host genetic interactions in the pathogenesis of transmissible murine colonic hyperplasia. Lab Anim. Sci. **27:**938–945.
5. **Benz, I., and M. A. Schmidt.** 1989. Cloning and expression of an adhesin (AIDA-I) involved in diffuse adherence of enteropathogenic *Escherichia coli*. Infect. Immun. **57:**1506–1511.
6. **Blattner, F. R., G. Plunkett III, C. A. Bloch, N. T. Perna, V. Burland, M. Riley, J. Collado-Vides, J. D. Glasner, C. K. Rode, G. F. Mayhew, J. Gregor, N. W. Davis, H. A. Kirkpatrick, M. A. Goeden, D. J. Rose, B. Mau, and Y. Shao.** 1997. The complete genome sequence of *Escherichia coli* K-12. Science **277:**1453–1474.
7. **Boisen, N., F. Ruiz-Perez, F. Scheutz, K. A. Krogfelt, and J. P. Nataro.** 2009. Short report: high prevalence of serine protease autotransporter cytotoxins among strains of enteroaggregative *Escherichia coli*. Am. J. Trop. Med. Hyg. **80:**294–301.
8. **Brennan, M. J., Z. M. Li, J. L. Cowell, M. E. Bisher, A. C. Steven, P. Novotny, and C. R. Manclark.** 1988. Identification of a 69-kilodalton nonfimbrial protein as an agglutinogen of *Bordetella pertussis*. Infect. Immun. **56:**3189–3195.
9. **Brennan, P. C., T. E. Fritz, R. J. Flynn, and C. M. Poole.** 1965. *Citrobacter freundii* associated with diarrhea in laboratory mice. Lab Anim. Care **15:**266–275.
10. **Bulgin, R. R., A. Arbeloa, J. C. Chung, and G. Frankel.** 2009. EspT triggers formation of lamellipodia and membrane ruffles through activation of Rac-1 and Cdc42. Cell Microbiol. **11:**217–229.

10a. **Bulgin, R., A. Arbeloa, D. Goulding, G. Dougan, V. Crepin, B. Raymond, and G. Frankel.** The T3SS effector EspT defines a new category of invasive enteropathogenic *E. coli* (EPEC) which form intracellular actin pedestals. PLoS Pathogens, in press.

11. **Carter, P. B.** 1975. Animal model of human disease. Yersinia enteritis. Animal model: oral Yersinia enterocolitica infection of mice. Am. J. Pathol. **81:**703–706.
12. **Carver, T., N. Thomson, A. Bleasby, M. Berriman, and J. Parkhill.** 2009. DNAPlotter: circular and linear interactive genome visualization. Bioinformatics **25:**119–120.
13. **Carver, T. J., K. M. Rutherford, M. Berriman, M. A. Rajandream, B. G. Barrell, and J. Parkhill.** 2005. ACT: the Artemis Comparison Tool. Bioinformatics **21:**3422–3423.
14. **Charpentier, X., and E. Oswald.** 2004. Identification of the secretion and translocation domain of the enteropathogenic and enterohemorrhagic *Escherichia coli* effector Cif, using TEM-1 beta-lactamase as a new fluorescence-based reporter. J. Bacteriol. **186:**5486–5495.
15. **Cheng, C., S. M. Tennant, K. I. Azzopardi, V. Bennett-Wood, E. L. Hartland, R. M. Robins-Browne, and M. Tauschek.** 2009. Contribution of the *pst-phoU* operon to cell adherence by atypical enteropathogenic *Escherichia coli* and virulence of *Citrobacter rodentium*. Infect. Immun. **77:**1936–1944.
16. **Coulthurst, S. J., S. Clare, T. J. Evans, I. J. Foulds, K. J. Roberts, M. Welch, G. Dougan, and G. P. Salmond.** 2007. Quorum sensing has an unexpected role in virulence in the model pathogen *Citrobacter rodentium*. EMBO Rep. **8:**698–703.
17. **Das, S., and K. Chaudhuri.** 2003. Identification of a unique IAHP (IcmF associated homologous proteins) cluster in *Vibrio cholerae* and other proteobacteria through *in silico* analysis. In Silico Biol. **3:**287–300.
18. **Datsenko, K. A., and B. L. Wanner.** 2000. One-step inactivation of chromosomal genes in *Escherichia coli* K-12 using PCR products. Proc. Natl. Acad. Sci. USA **97:**6640–6645.
19. **Deng, W., Y. Li, B. A. Vallance, and B. B. Finlay.** 2001. Locus of enterocyte effacement from *Citrobacter rodentium*: sequence analysis and evidence for horizontal transfer among attaching and effacing pathogens. Infect. Immun. **69:**6323–6335.
20. **Dodd, C. E., and D. Jones.** 1982. A numerical taxonomic study of the genus Shigella. J. Gen. Microbiol. **128:**1933–1957.
21. **Dong, T., B. K. Coombes, and H. E. Schellhorn.** 2009. Role of RpoS in the virulence of *Citrobacter rodentium*. Infect. Immun. **77:**501–507.
22. **Doyle, M., M. Fookes, A. Ivens, M. W. Mangan, J. Wain, and C. J. Dorman.** 2007. An H-NS-like stealth protein aids horizontal DNA transmission in bacteria. Science **315:**251–252.
23. **Dutta, P. R., R. Cappello, F. Navarro-Garcia, and J. P. Nataro.** 2002. Functional comparison of serine protease autotransporters of enterobacteriaceae. Infect. Immun. **70:**7105–7113.
24. **Edgar, R. C.** 2004. MUSCLE: multiple sequence alignment with high accuracy and high throughput. Nucleic Acids Res. **32:**1792–1797.
25. **Ediger, R. D., R. M. Kovatch, and M. M. Rabstein.** 1974. Colitis in mice with a high incidence of rectal prolapse. Lab Anim. Sci. **24:**488–494.
26. **Elliott, S. J., L. A. Wainwright, T. K. McDaniel, K. G. Jarvis, Y. K. Deng, L. C. Lai, B. P. McNamara, M. S. Donnenberg, and J. B. Kaper.** 1998. The complete sequence of the locus of enterocyte effacement (LEE) from enteropathogenic *Escherichia coli* E2348/69. Mol. Microbiol. **28:**1–4.
27. **Elsinghorst, E. A., and J. A. Weitz.** 1994. Epithelial cell invasion and adherence directed by the enterotoxigenic *Escherichia coli tib* locus is associated with a 104-kilodalton outer membrane protein. Infect. Immun. **62:**3463–3471.
28. **Filloux, A., A. Hachani, and S. Bleves.** 2008. The bacterial type VI secretion machine: yet another player for protein transport across membranes. Microbiology **154:**1570–1583.
29. **Folkesson, A., S. Lofdahl, and S. Normark.** 2002. The *Salmonella enterica* subspecies I specific centisome 7 genomic island encodes novel protein families present in bacteria living in close contact with eukaryotic cells. Res. Microbiol. **153:**537–545.
30. **Frankel, G., and A. D. Phillips.** 2008. Attaching effacing *Escherichia coli* and paradigms of Tir-triggered actin polymerization: getting off the pedestal. Cell Microbiol. **10:**549–556.
31. **Garmendia, J., G. Frankel, and V. F. Crepin.** 2005. Enteropathogenic and enterohemorrhagic *Escherichia coli* infections: translocation, translocation, translocation. Infect. Immun. **73:**2573–2585.
32. **Girardeau, J. P., Y. Bertin, and C. Martin.** 2009. Genomic analysis of the PAI ICL3 locus in pathogenic LEE-negative Shiga toxin-producing *Escherichia coli* and *Citrobacter rodentium*. Microbiology **155:**1016–1027.
33. **Gruenheid, S., I. Sekirov, N. A. Thomas, W. Deng, P. O'Donnell, D. Goode, Y. Li, E. A. Frey, N. F. Brown, P. Metalnikov, T. Pawson, K. Ashman, and B. B. Finlay.** 2004. Identification and characterization of NleA, a non-LEE-encoded type III translocated virulence factor of enterohaemorrhagic *Escherichia coli* O157:H7. Mol. Microbiol. **51:**1233–1249.
34. **Guindon, S., F. Lethiec, P. Duroux, and O. Gascuel.** 2005. PHYML Online—a web server for fast maximum likelihood-based phylogenetic inference. Nucleic Acids Res. **33:**W557–W559.
35. **Harrison, J. A., B. Villarreal-Ramos, P. Mastroeni, R. Demarco de Hormaeche, and C. E. Hormaeche.** 1997. Correlates of protection induced by live Aro$^-$ Salmonella typhimurium vaccines in the murine typhoid model. Immunology **90:**618–625.
36. **Hart, E., J. Yang, M. Tauschek, M. Kelly, M. J. Wakefield, G. Frankel, E. L. Hartland, and R. M. Robins-Browne.** 2008. RegA, an AraC-like protein, is a global transcriptional regulator that controls virulence gene expression in *Citrobacter rodentium*. Infect. Immun. **76:**5247–5256.
37. **Hayashi, T., K. Makino, M. Ohnishi, K. Kurokawa, K. Ishii, K. Yokoyama, C. G. Han, E. Ohtsubo, K. Nakayama, T. Murata, M. Tanaka, T. Tobe, T. Iida, H. Takami, T. Honda, C. Sasakawa, N. Ogasawara, T. Yasunaga, S. Kuhara, T. Shiba, M. Hattori, and H. Shinagawa.** 2001. Complete genome sequence of enterohemorrhagic *Escherichia coli* O157:H7 and genomic comparison with a laboratory strain K-12. DNA Res. **8:**11–22.
38. **Heimer, S. R., R. A. Welch, N. T. Perna, G. Posfai, P. S. Evans, J. B. Kaper, F. R. Blattner, and H. L. Mobley.** 2002. Urease of enterohemorrhagic Escherichia coli: evidence for regulation by fur and a trans-acting factor. Infect. Immun. **70:**1027–1031.
39. **Hemrajani, C., O. Marches, S. Wiles, F. Girard, A. Dennis, F. Dziva, A. Best, A. D. Phillips, C. N. Berger, A. Mousnier, V. F. Crepin, L. Kruidenier, M. J. Woodward, M. P. Stevens, R. M. La Ragione, T. T. MacDonald, and G. Frankel.** 2008. Role of NleH, a type III secreted effector from attaching and effacing pathogens, in colonization of the bovine, ovine, and murine gut. Infect. Immun. **76:**4804–4813.
40. **Ho, T. D., B. M. Davis, J. M. Ritchie, and M. K. Waldor.** 2008. Type 2 secretion promotes enterohemorrhagic *Escherichia coli* adherence and intestinal colonization. Infect. Immun. **76:**1858–1865.
41. **Hormaeche, C. E.** 1979. Natural resistance to Salmonella typhimurium in different inbred mouse strains. Immunology **37:**311–318.
42. **Iguchi, A., N. R. Thomson, Y. Ogura, D. Saunders, T. Ooka, I. R. Henderson,**

D. Harris, M. Asadulghani, K. Kurokawa, P. Dean, B. Kenny, M. A. Quail, S. Thurston, G. Dougan, T. Hayashi, J. Parkhill, and G. Frankel. 2009. Complete genome sequence and comparative genome analysis of enteropathogenic *Escherichia coli* O127:H6 strain E2348/69. J. Bacteriol. **191:**347–354.

43. **Itoh, K., K. Maejima, K. Ueda, and K. Fujiwara.** 1978. Effect of intestinal flora on megaenteron of mice. Microbiol. Immunol. **22:**661–672.
44. **Jones, B. D., N. Ghori, and S. Falkow.** 1994. Salmonella typhimurium initiates murine infection by penetrating and destroying the specialized epithelial M cells of the Peyer's patches. J. Exp. Med. **180:**15–23.
45. **Kaper, J. B., J. P. Nataro, and H. L. Mobley.** 2004. Pathogenic *Escherichia coli*. Nat. Rev. Microbiol. **2:**123–140.
46. **Kelly, M., E. Hart, R. Mundy, O. Marches, S. Wiles, L. Badea, S. Luck, M. Tauschek, G. Frankel, R. M. Robins-Browne, and E. L. Hartland.** 2006. Essential role of the type III secretion system effector NleB in colonization of mice by *Citrobacter rodentium*. Infect. Immun. **74:**2328–2337.
47. **Klapproth, J. M., M. Sasaki, M. Sherman, B. Babbin, M. S. Donnenberg, P. J. Fernandes, I. C. Scaletsky, D. Kalman, A. Nusrat, and I. R. Williams.** 2005. *Citrobacter rodentium lifA/efa1* is essential for colonic colonization and crypt cell hyperplasia in vivo. Infect. Immun. **73:**1441–1451.
48. **Latasa, C., A. Roux, A. Toledo-Arana, J. M. Ghigo, C. Gamazo, J. R. Penades, and I. Lasa.** 2005. BapA, a large secreted protein required for biofilm formation and host colonization of *Salmonella enterica* serovar Enteritidis. Mol. Microbiol. **58:**1322–1339.
49. **Leiman, P. G., M. Basler, U. A. Ramagopal, J. B. Bonanno, J. M. Sauder, S. Pukatzki, S. K. Burley, S. C. Almo, and J. J. Mekalanos.** 2009. Type VI secretion apparatus and phage tail-associated protein complexes share a common evolutionary origin. Proc. Natl. Acad. Sci. USA **106:**4154–4159.
50. **Levine, M. M., J. P. Nataro, H. Karch, M. M. Baldini, J. B. Kaper, R. E. Black, M. L. Clements, and A. D. O'Brien.** 1985. The diarrheal response of humans to some classic serotypes of enteropathogenic *Escherichia coli* is dependent on a plasmid encoding an enteroadhesiveness factor. J. Infect. Dis. **152:**550–559.
51. **Lin, R. J., M. Capage, and C. W. Hill.** 1984. A repetitive DNA sequence, rhs, responsible for duplications within the *Escherichia coli* K-12 chromosome. J. Mol. Biol. **177:**1–18.
52. **Liu, C., L. S. Heath, and C. L. Turnbough, Jr.** 1994. Regulation of *pyrBI* operon expression in *Escherichia coli* by UTP-sensitive reiterative RNA synthesis during transcriptional initiation. Genes Dev. **8:**2904–2912.
53. **Liu, J., X. Zhang, S. Zhou, and P. Tao.** 2007. Purification and characterization of a 4-hydroxybenzoate decarboxylase from Chlamydophila pneumoniae AR39. Curr. Microbiol. **54:**102–107.
54. **Luperchio, S. A., J. V. Newman, C. A. Dangler, M. D. Schrenzel, D. J. Brenner, A. G. Steigerwalt, and D. B. Schauer.** 2000. *Citrobacter rodentium*, the causative agent of transmissible murine colonic hyperplasia, exhibits clonality: synonymy of *C. rodentium* and mouse-pathogenic *Escherichia coli*. J. Clin. Microbiol. **38:**4343–4350.
55. **Ma, W., F. F. Dong, J. Stavrinides, and D. S. Guttman.** 2006. Type III effector diversification via both pathoadaptation and horizontal transfer in response to a coevolutionary arms race. PLoS Genet. **2:**e209.
56. **Matsui, T., T. Yoshida, T. Hayashi, and T. Nagasawa.** 2006. Purification, characterization, and gene cloning of 4-hydroxybenzoate decarboxylase of Enterobacter cloacae P240. Arch. Microbiol. **186:**21–29.
57. **McDaniel, T. K., K. G. Jarvis, M. S. Donnenberg, and J. B. Kaper.** 1995. A genetic locus of enterocyte effacement conserved among diverse enterobacterial pathogens. Proc. Natl. Acad. Sci. USA **92:**1664–1668.
58. **Monteiro, B. T., L. C. Campos, M. P. Sircili, M. R. Franzolin, L. F. Bevilacqua, J. P. Nataro, and W. P. Elias.** 2009. The dispersin-encoding gene (aap) is not restricted to enteroaggregative Escherichia coli. Diagn. Microbiol. Infect. Dis. **65:**81–84.
59. **Mougous, J. D., M. E. Cuff, S. Raunser, A. Shen, M. Zhou, C. A. Gifford, A. L. Goodman, G. Joachimiak, C. L. Ordonez, S. Lory, T. Walz, A. Joachimiak, and J. J. Mekalanos.** 2006. A virulence locus of *Pseudomonas aeruginosa* encodes a protein secretion apparatus. Science **312:**1526–1530.
60. **Mundy, R., F. Girard, A. J. FitzGerald, and G. Frankel.** 2006. Comparison of colonization dynamics and pathology of mice infected with enteropathogenic *Escherichia coli*, enterohaemorrhagic *E. coli* and *Citrobacter rodentium*. FEMS Microbiol. Lett. **265:**126–132.
61. **Mundy, R., T. T. Macdonald, G. Dougan, G. Frankel, and S. Wiles.** 2005. *Citrobacter rodentium* of mice and man. Cell. Microbiol. **7:**1697–1706.
62. **Mundy, R., L. Petrovska, K. Smollett, N. Simpson, R. K. Wilson, J. Yu, X. Tu, I. Rosenshine, S. Clare, G. Dougan, and G. Frankel.** 2004. Identification of a novel *Citrobacter rodentium* type III secreted protein, EspI, and roles of this and other secreted proteins in infection. Infect. Immun. **72:**2288–2302.
63. **Mundy, R., D. Pickard, R. K. Wilson, C. P. Simmons, G. Dougan, and G. Frankel.** 2003. Identification of a novel type IV pilus gene cluster required for gastrointestinal colonization of *Citrobacter rodentium*. Mol. Microbiol. **48:**795–809.
64. **Muto, T., M. Nakagawa, Y. Isobe, M. Saito, and T. Nakano.** 1969. Infectious megaenteron of mice. I. Manifestation and pathological observation. Jpn. J. Med. Sci. Biol. **22:**363–374.
65. **Nakano, M., T. Iida, and T. Honda.** 2004. Urease activity of enterohaemorrhagic *Escherichia coli* depends on a specific one-base substitution in *ureD*. Microbiology **150:**3483–3489.
66. **Nishio, M., N. Okada, T. Miki, T. Haneda, and H. Danbara.** 2005. Identification of the outer-membrane protein PagC required for the serum resistance phenotype in Salmonella enterica serovar Choleraesuis. Microbiology **151:**863–873.
67. **Norman, A., L. H. Hansen, Q. She, and S. J. Sorensen.** 2008. Nucleotide sequence of pOLA52: a conjugative IncX1 plasmid from *Escherichia coli* which enables biofilm formation and multidrug efflux. Plasmid **60:**59–74.
68. **Nuccio, S. P., and A. J. Baumler.** 2007. Evolution of the chaperone/usher assembly pathway: fimbrial classification goes Greek. Microbiol. Mol. Biol. Rev. **71:**551–575.
69. **Osoegawa, K., P. Y. Woon, B. Zhao, E. Frengen, M. Tateno, J. J. Catanese, and P. J. de Jong.** 1998. An improved approach for construction of bacterial artificial chromosome libraries. Genomics **52:**1–8.
70. **Parham, N. J., S. J. Pollard, M. Desvaux, A. Scott-Tucker, C. Liu, A. Fivian, and I. R. Henderson.** 2005. Distribution of the serine protease autotransporters of the Enterobacteriaceae among extraintestinal clinical isolates of *Escherichia coli*. J. Clin. Microbiol. **43:**4076–4082.
71. **Parkhill, J., G. Dougan, K. D. James, N. R. Thomson, D. Pickard, J. Wain, C. Churcher, K. L. Mungall, S. D. Bentley, M. T. Holden, M. Sebaihia, S. Baker, D. Basham, K. Brooks, T. Chillingworth, P. Connerton, A. Cronin, P. Davis, R. M. Davies, L. Dowd, N. White, J. Farrar, T. Feltwell, N. Hamlin, A. Haque, T. T. Hien, S. Holroyd, K. Jagels, A. Krogh, T. S. Larsen, S. Leather, S. Moule, P. O'Gaora, C. Parry, M. Quail, K. Rutherford, M. Simmonds, J. Skelton, K. Stevens, S. Whitehead, and B. G. Barrell.** 2001. Complete genome sequence of a multiple drug resistant *Salmonella enterica* serovar Typhi CT18. Nature **413:**848–852.
72. **Parkhill, J., B. W. Wren, K. Mungall, J. M. Ketley, C. Churcher, D. Basham, T. Chillingworth, R. M. Davies, T. Feltwell, S. Holroyd, K. Jagels, A. V. Karlyshev, S. Moule, M. J. Pallen, C. W. Penn, M. A. Quail, M. A. Rajandream, K. M. Rutherford, A. H. van Vliet, S. Whitehead, and B. G. Barrell.** 2000. The genome sequence of the food-borne pathogen *Campylobacter jejuni* reveals hypervariable sequences. Nature **403:**665–668.
73. **Parkhill, J., B. W. Wren, N. R. Thomson, R. W. Titball, M. T. Holden, M. B. Prentice, M. Sebaihia, K. D. James, C. Churcher, K. L. Mungall, S. Baker, D. Basham, S. D. Bentley, K. Brooks, A. M. Cerdeno-Tarraga, T. Chillingworth, A. Cronin, R. M. Davies, P. Davis, G. Dougan, T. Feltwell, N. Hamlin, S. Holroyd, K. Jagels, A. V. Karlyshev, S. Leather, S. Moule, P. C. Oyston, M. Quail, K. Rutherford, M. Simmonds, J. Skelton, K. Stevens, S. Whitehead, and B. G. Barrell.** 2001. Genome sequence of *Yersinia pestis*, the causative agent of plague. Nature **413:**523–527.
74. **Penno, C., P. Sansonetti, and C. Parsot.** 2005. Frameshifting by transcriptional slippage is involved in production of MxiE, the transcription activator regulated by the activity of the type III secretion apparatus in *Shigella flexneri*. Mol. Microbiol. **56:**204–214.
75. **Perna, N. T., G. F. Mayhew, G. Posfai, S. Elliott, M. S. Donnenberg, J. B. Kaper, and F. R. Blattner.** 1998. Molecular evolution of a pathogenicity island from enterohemorrhagic *Escherichia coli* O157:H7. Infect. Immun. **66:**3810–3817.
76. **Pilonieta, M. C., M. D. Bodero, and G. P. Munson.** 2007. CfaD-dependent expression of a novel extracytoplasmic protein from enterotoxigenic Escherichia coli. J. Bacteriol. **189:**5060–5067.
77. **Posada, D., and K. A. Crandall.** 1998. MODELTEST: testing the model of DNA substitution. Bioinformatics **14:**817–818.
78. **Pukatzki, S., S. B. McAuley, and S. T. Miyata.** 2009. The type VI secretion system: translocation of effectors and effector-domains. Curr. Opin. Microbiol. **12:**11–17.
79. **Rasko, D. A., M. J. Rosovitz, G. S. Myers, E. F. Mongodin, W. F. Fricke, P. Gajer, J. Crabtree, M. Sebaihia, N. R. Thomson, R. Chaudhuri, I. R. Henderson, V. Sperandio, and J. Ravel.** 2008. The pangenome structure of Escherichia coli: comparative genomic analysis of E. coli commensal and pathogenic isolates. J. Bacteriol. **190:**6881–6893.
80. **Robson, H. G., and S. I. Vas.** 1972. Resistance of inbred mice to Salmonella typhimurium. J. Infect. Dis. **126:**378–386.
81. **Rutherford, K., J. Parkhill, J. Crook, T. Horsnell, P. Rice, M. A. Rajandream, and B. Barrell.** 2000. Artemis: sequence visualization and annotation. Bioinformatics **16:**944–945.
82. **Schauer, D. B., and S. Falkow.** 1993. Attaching and effacing locus of a *Citrobacter freundii* biotype that causes transmissible murine colonic hyperplasia. Infect. Immun. **61:**2486–2492.
83. **Schauer, D. B., and S. Falkow.** 1993. The *eae* gene of *Citrobacter freundii* biotype 4280 is necessary for colonization in transmissible murine colonic hyperplasia. Infect. Immun. **61:**4654–4661.
84. **Schauer, D. B., B. A. Zabel, I. F. Pedraza, C. M. O'Hara, A. G. Steigerwalt, and D. J. Brenner.** 1995. Genetic and biochemical characterization of *Citrobacter rodentium* sp. nov. J. Clin. Microbiol. **33:**2064–2068.
85. **Shrivastava, S., and S. S. Mande.** 2008. Identification and functional characterization of gene components of Type VI secretion system in bacterial genomes. PLoS One **3:**e2955.
86. **Simpson, N., R. Shaw, V. F. Crepin, R. Mundy, A. J. FitzGerald, N. Cummings, A. Straatman-Iwanowska, I. Connerton, S. Knutton, and G. Frankel.**

2006. The enteropathogenic *Escherichia coli* type III secretion system effector Map binds EBP50/NHERF1: implication for cell signalling and diarrhoea. Mol. Microbiol. **60:**349–363.

87. **Tatsuno, I., R. Mundy, G. Frankel, Y. Chong, A. D. Phillips, A. G. Torres, and J. B. Kaper.** 2006. The *lpf* gene cluster for long polar fimbriae is not involved in adherence of enteropathogenic *Escherichia coli* or virulence of *Citrobacter rodentium*. Infect. Immun. **74:**265–272.
88. **Tobe, T., S. A. Beatson, H. Taniguchi, H. Abe, C. M. Bailey, A. Fivian, R. Younis, S. Matthews, O. Marches, G. Frankel, T. Hayashi, and M. J. Pallen.** 2006. An extensive repertoire of type III secretion effectors in *Escherichia coli* O157 and the role of lambdoid phages in their dissemination. Proc. Natl. Acad. Sci. USA **103:**14941–14946.
89. **Vallance, B. A., W. Deng, K. Jacobson, and B. B. Finlay.** 2003. Host susceptibility to the attaching and effacing bacterial pathogen *Citrobacter rodentium*. Infect. Immun. **71:**3443–3453.
90. **Wang, Y. D., S. Zhao, and C. W. Hill.** 1998. Rhs elements comprise three subfamilies which diverged prior to acquisition by *Escherichia coli*. J. Bacteriol. **180:**4102–4110.
91. **Wiles, S., S. Clare, J. Harker, A. Huett, D. Young, G. Dougan, and G. Frankel.** 2004. Organ specificity, colonization and clearance dynamics in vivo following oral challenges with the murine pathogen *Citrobacter rodentium*. Cell Microbiol. **6:**963–972.
92. **Wiles, S., S. Clare, J. Harker, A. Huett, D. Young, G. Dougan, and G. Frankel.** 2005. Organ-specificity, colonization and clearance dynamics *in vivo* following oral challenges with the murine pathogen *Citrobacter rodentium*. Cell Microbiol. **7:**459.
93. **Wiles, S., G. Dougan, and G. Frankel.** 2005. Emergence of a 'hyperinfectious' bacterial state after passage of Citrobacter rodentium through the host gastrointestinal tract. Cell Microbiol. **7:**1163–1172.
94. **Williams, L. E., C. Detter, K. Barry, A. Lapidus, and A. O. Summers.** 2006. Facile recovery of individual high-molecular-weight, low-copy-number natural plasmids for genomic sequencing. Appl. Environ. Microbiol. **72:**4899–4906.
95. **Zheng, J., and K. Y. Leung.** 2007. Dissection of a type VI secretion system in *Edwardsiella tarda*. Mol. Microbiol. **66:**1192–1206.